



# **Multifunctional oligopyridines for application in biological and materials chemistry**

Inauguraldissertation

zur

Erlangung der Würde eines Doktors der Philosophie

vorgelegt der

Philosophisch-Naturwissenschaftlichen Fakultät

der Universität Basel

Von

**Valérie Chaurin**

aus Cloyes sur le Loir, France

Basel, 2007

Genehmigt von der Philosophisch-Naturwissenschaftlichen Facultät

Auf Antrag von

Prof. Dr. Edwin Constable

Prof. Dr. Wolf-Dietrich Woggon

Basel, den 27. September 2007

Prof. Dr. Hans-Peter Hauri

*A mes parents Rosa et François*

*A mes petites sœurs Nathalie et Céline*

*A mes grand-parents Suzanne et Gérard*

*“Live as if you were to die tomorrow.  
Learn as if you were to live forever”*

*Mahatna Gandhi*

## Acknowledgements

I would like to thank my supervisor Prof. Ed Constable for giving to me the opportunity to join his group and give me interest with chemistry; thanks for his help and great support during these three last year. He gave me the opportunity to work in so many disciplines, to learn so much and develop independent thinking. I will be grateful all my life.

I would like to thank Prof. Catherine Housecroft, my second supervisor, for her help, support, encouragement and patience.

Grateful acknowledgements to my scientific collaborator in Bern: Jean-Paul Bianké and Prof. Häner and in Nantes: Maxim Ergov and Prof. Jacques Lebreton.

I would like to thanks Dr. Maria Schwarz who give me the opportunity to discover Capillary Electrophoresis and to Dr. Alexandra Stettler for the Capillary Electrophoresis measurements.

Thanks to Markus and Silvia for their expertise in X-ray crystallography.

I would like to thanks all the Constable/Housecroft group members, past and present, for their help, in particularly, thanks so much to Conor, Stefan and Kevin.

I want to thank as well Markus Hauri and Franz Stehlin for the orderings and fixing all my technical problems as good as possible. Thanks to Beatrice for all the administration stuff.

Thanks to all my friends, especially to Tiphaine and Xavier, always present for me. I would like to thanks William M for his support and Antoine, the best flatmate!!!

The University of Basel and the Swiss National Science Foundation for the financial support.

Et le plus important pour moi, merci a toute ma famille, en particulier merci à mes parents, Rosa et François, sans qui je ne serais pas là aujourd'hui. Je les remercie de tout mon cœur pour leur amour, pour leur éternel soutien et encouragements.

## Chapter 1 Introduction

1.1 Coordination chemistry .....	9
1.2 Supramolecular assembly .....	10
1.3 1,10-phenanthroline and 2,2'-bipyridine ligands .....	13
1.4 copper(I) polypyridine complexes .....	15
1.5 Introduction to DNA .....	19
1.5.1 Discovery of DNA .....	19
1.5.2 Physical and chemical properties .....	21
1.5.2.1 Hydrogen bonding and stability .....	21
1.5.2.2 $\pi$ - $\pi$ Stacking Interactions .....	22
1.5.3 Transition metal-oligonucleotide systems:.....	22
1.6 Metal complexes in Medicine .....	27
1.7 Aim of the work .....	29
1.8 References .....	32

## chapter 2 Synthesis, electrochemical and photochemical investigation of 6,6'-disubstituted-2,2'-bipyridine and 2,9'-disubstituted-1,10-phenanthroline copper(I) complexes

2.1 Introduction .....	37
2.2 6,6'-Disubstituted-2,2'-bipyridine and 2,9'-disubstituted-1,10-phenanthroline ligands derivatives. ....	38
2.2.1 Syntheses of some 2,9- disubstituted -1,10-phenanthroline.....	38
2.2.2 Synthesis of some asymmetrical 2,9-difunctionalized-1,10-phenanthrolines.....	50
2.2.3 Synthesis of some 6,6'-disubstituted-2,2'-bipyridines.....	52
2.2.4 Synthesis of some mono- $\alpha$ -functional 6,6'-dimethyl-2,2'-bipyridines. ....	56
2.2.5 Synthesis of some 6,6'-disubstituted-2,2'-bipyridine and and 2,9-disubstituted-1,10-phenanthroline with triphenylamine substituents.....	60
2.2.5.1 Non conjugated ligands.....	61
2.2.5.2 Conjugated ligands.....	64
2.3 6,6'-Disubstituted-2,2'-bipyridine and 2,9-disubstituted-1,10-phenanthroline copper(I) complexes.....	73
2.3.1 General method for the synthesis of copper(I) 1,10-phenanthroline and 2,2'-bipyridine complexes.....	73
2.3.2 Description of crystal structures of the copper(I) complexes obtained.....	73

2.3.2.1 Crystal structure of bis[6,6'-bis(chloromethyl)-2,2'-bipyridine]copper(I) hexafluorophosphate .....	75
2.3.2.2 Crystal structure of bis[6,6'-bis(hydroxymethyl)-2,2'-bipyridine]copper(I) hexafluorophosphate. ....	76
2.3.2.3 Crystal structure of bis[6,6'-di(chloromethyl)-1,10-phenanthroline]copper(I) hexafluorophosphate. ....	79
2.3.2.4 Crystal structure of bis[2-methyl-9-(tert-butyl dimethylsilyl)methyl]-1,10-phenanthroline]copper(I) hexafluorophosphate dichloromethane solvate .....	81
2.3.2.5 Crystal structure of bis[6-(4-( <i>N,N</i> -diphenylamino)phenoxy)methyl]-6'-methyl-2,2'-bipyridine]copper(I) hexafluorophosphate.....	85
2.3.2.6 Crystal structure of bis[6,6'-bis(4-( <i>N,N</i> -diphenylamino)phenoxy)methyl]-2,2'-bipyridine]copper(I) hexafluorophosphate.....	87
2.3.2.7 Crystal structure of the bis[6,6'-bis(2-(4-( <i>N,N</i> -diphenylamino)phenyl)ethenyl)-2,2'-bipyridine]copper(I) hexafluorophosphate.....	89

### **Chapter 3 DNA Hybridization Assisted by Metal Complex Formation**

3.1 Introduction .....	114
3.1 .....Synthesis of 2,2'-bipyridine and 1,10-phenanthroline phosphoramidite building blocks .....	119
3.1.1 Background .....	119
3.1.1 Synthesis of the 6'-methyl-2,2'-bipyridine phosphoramidite building block .....	119
3.1.2 Synthesis of the 9-methyl-1, 10-phenanthroline phosphoramidite building block: ..	121
3.2 Synthesis of oligonucleotide conjugates .....	123
3.3 Effect of bpy and phen metal-binding domains on the duplex stability in the absence of metal ions. ....	125
3.4 Effect of metal-coordination on duplex stability.....	126
3.5 Effect of mixed-ligand complexes on hybrid stability.....	130
3.6 Effect of EDTA on the duplex stabilisation .....	131
3.7 Influence of gap size at the site of metal-complex formation .....	133
3.8 Conclusions .....	137
3.9 References .....	138

<b>Chapter 4</b>	<b>Affinity capillary electrophoresis</b>	
4.1	Introduction .....	141
4.2	Tetranucleotides—specific interactions between DNA and metal cations .....	164
4.3	Interactions of bpy or phen derivatives, DNA and bpy-DNA with metal ions .....	171
4.4	Conclusions .....	174
4.5	Experimental .....	174
4.5.1	Materials and Methods .....	174
4.5.1.1	Chemicals and Reagents .....	174
4.5.1.2	Apparatus .....	175
4.5.1.3	Capillaries .....	175
4.5.1.4	Methods .....	176
4.6	References .....	178
<b>Chapter 5</b>	<b>Conclusions and outlook</b> .....	182
<b>Chapter 6</b>	<b>General Experimental</b>	
6.1	General .....	183
6.1.1	Instrument .....	183
6.1.1	Abbreviations .....	184
6.1.1.1	general .....	184
6.1.1.2	NMR assignments .....	185
6.2	Synthesis and characterizations .....	186
6.2.1	Synthesis and characterizations of Ligands .....	186
6.2.2	Copper(I) complexes: synthesis and characterisation .....	224
6.3	Characterisation of oligonucleotides .....	238
6.4	References .....	241
<b>Appendices</b>	.....	236
CV	Valérie Chaurin .....	323



## Introduction

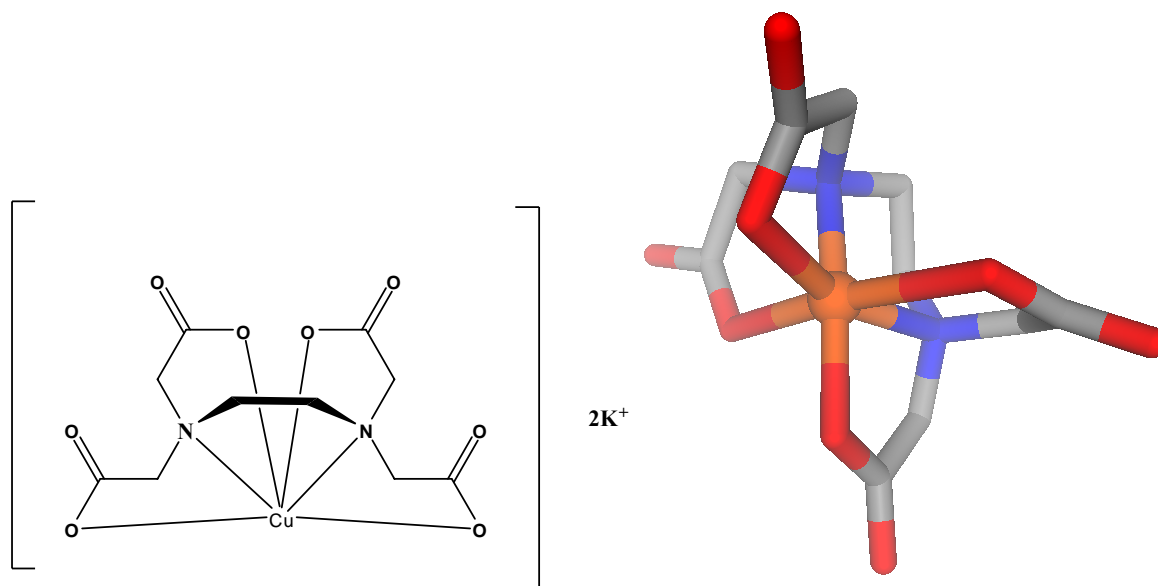
### 1.1 Coordination chemistry

Coordination chemistry was pioneered by Nobel Prize winner Alfred Werner (1866-1919), a professor at the University of Zurich <sup>[1]</sup>. He received the first Nobel Prize in inorganic chemistry in 1913 for his coordination theory of transition metal-ammine complexes. At the start of the 20<sup>th</sup> century, inorganic chemistry was not an important field until Werner studied metal-ammine complexes such as  $[\text{Co}(\text{NH}_3)_6\text{Cl}_3]$ . He recognized the existence of several forms of cobalt-ammonia chloride. These compounds have different colours and other characteristics. The chemical formula has three chloride ions per metal ion, but the number of chloride ions that precipitate with  $\text{Ag}^+$  ions per formula is not always three. He thought only ionized chloride ions will form a precipitate with silver ion. To distinguish ionized chloride from the coordinated chloride, Werner formulated the “Complex Formula” and explained the structure of the cobalt complexes.

Today we are defining coordination compounds (or complexes) as an important subclass of inorganic compounds. They consist of any molecules with a central metal atom (usually a transition element) surrounded by non-metallic atoms or groups of atoms, called ligands, joined to it by chemical bonds (coordinate covalent bond) in which, formally, both electrons come from the ligand. Purely carbon-donor ligands are considered as “organometallic” rather than coordination compounds. Coordination compounds are often intensely coloured. Coordination compounds include such substances as vitamin B12, hemoglobin, and chlorophyll, dyestuffs, pigments and catalysts used in preparing organic substances.

The metal atom in a coordination compound may be an electrically neutral atom or an ion. The ligands may also be neutral or charged. A ligand forms a chemical bond with the metal atom by sharing a pair of electrons with it. A ligand can attach to the atom by one bond (unidentate) or several bonds (multidentate). The latter configuration is cyclic, because it

contains a ring of atoms. Multidentate compounds are called chelates (for example  $\text{H}_4\text{EDTA}$ ) (Figure 1.1) and comprise an important group of compounds.



**Figure 1.1** Example of  $\text{EDTA}^{4-}$  coordinating a copper(II) centre in  $\text{K}_2[\text{Cu}(\text{edta})]^{[2]}$ .

Many coordination compounds have distinct geometric structures. Two common forms are the square planar, in which four ligands are arranged at the corners of a hypothetical square around the central metal atom, and octahedral, in which six ligands are arranged, four in a plane and one each above and below the plane. Altering the position of the ligands relative to one another can produce different compounds with the same chemical formula.

## 1.2 Supramolecular assembly

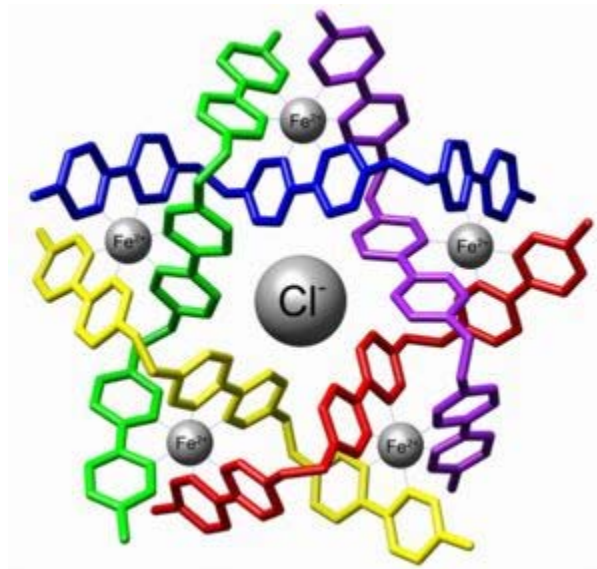
Supramolecular chemistry is related on the Werner's coordination chemistry, being defined by Jean-Marie Lehn in 1978: "Just as there is a field of molecular chemistry based on the covalent bond, there is a field of supramolecular chemistry, the chemistry of molecular assemblies and of the intermolecular bond" <sup>[3-4]</sup>. In fact, supramolecular chemistry is the part of chemistry which involved non covalent bonding interactions between molecules. These could be  $\pi$ - $\pi$  interactions, hydrogen bonding, electrostatic, Van der Waals forces, hydrophobic or solvent effects. Supramolecules are formed by the association of several chemical species held together by non covalent bonds <sup>[5]</sup>. Because of the reversibility of the non-covalent

bonds, J.-M. Lehn described it as a dynamic chemistry <sup>[6]</sup>. This dynamic characteristic makes it extremely resourceful in creating a large diversity of supramolecules.

The importance of supramolecular chemistry was recognized in 1987 when Donald J. Cram, Jean-Marie Lehn and Charles J. Pedersen received a Nobel Prize for their work in this area.

Self-assembly appears as the main point of supramolecular chemistry; metal ion-self-assembly has been extensively developed as a powerful tool for the spontaneous and efficient generation of complex inorganic architectures <sup>[7-13]</sup>.

There are two types of molecular self-assembly: intramolecular self-assembly and intermolecular self-assembly. Intramolecular self-assembly often involves complex polymers with the capacity to adopt stable structures with conformations well defined (for example the protein folding). But the self-assembly which often interests the supramolecular chemist is the intermolecular self-assembly which permits the development of quaternary structure. Characteristic examples of supramolecular assembly were developed by Jean-Marie Lehn and coworkers. They described, for instance, the self assembly of the circular helicate  $[(Fe_5L_5)Cl]^{9+}$  from five tris-bpy ligand strands and five equivalents of  $FeCl_2$  (figure 1.2) <sup>[14-16]</sup>.



**Figure 1.2** Self-assembly of a circular double helicate <sup>[14]</sup>.

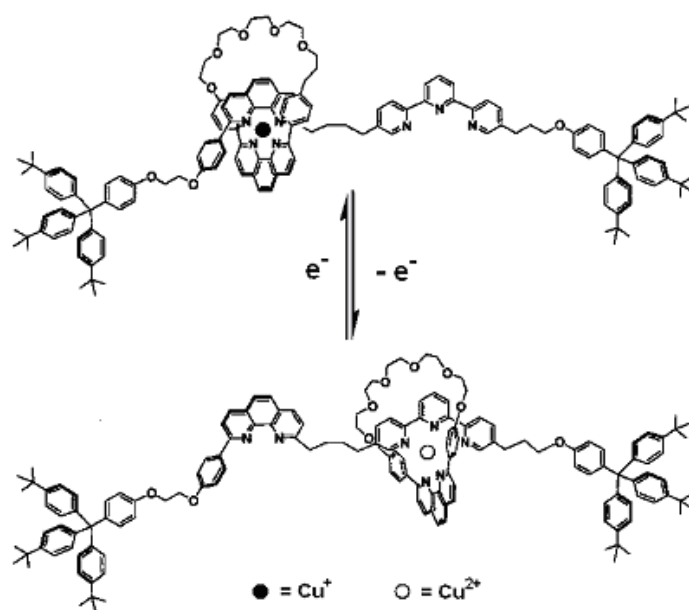
Other examples of such systems are seen in the inventive work of Sauvage and coworkers, who show the importance of metal ion coordination number, geometry, and the number of coordination sites of the ligand <sup>[17-18]</sup>.

The coordination properties of the transition metal are essential for the assembly of supramolecular systems but as well because they give the possibility to create functional

supramolecular systems, where reversible motion within the supramolecule can be induced electrochemically or photochemically.

Indeed, for instance, since the stereoelectronic requirement of a metal center can be strongly modified by changing its oxidation state, redox-active transition metal complexes are expected to undergo electrochemically induced arrangement of the coordination sphere. This is particularly true for copper complexes: Cu(I) is usually low coordinate (coordination number  $CN \leq 4$ ), whereas Cu(II) is preferably square planar or higher coordinate ( $CN = 5$  or  $6$ ) [17].

In the system shown in Figure 1.3, Sauvage showed that the Cu(I) complex achieved its preferred coordination environment with two bidentate 1,10-phenanthroline ligands. However, when Cu(I) is oxidized to Cu(II), the ring must glide along the rodlike component to reach a five-coordinate environment.



**Figure 1.3** The copper rotaxane: the four-coordinate arrangement and the five-coordinate arrangement [17].

Innovation and application of supramolecular assemblies have reached impressive new heights. For example, organizations involving nucleic acids have been used for drug or DNA delivery, and can also be efficient as sensors for detection purposes [19]. It is a period of great promise in the area of self-assembly and supramolecular systems involving DNA, RNA, or more generally, systems capable of information storage. If recent scientific progress is a fair

indicator, the future promises remarkable new developments in molecular recognition elements with a vast array of applications.

### 1.3 1,10-Phenanthroline and 2,2'-bipyridine ligands

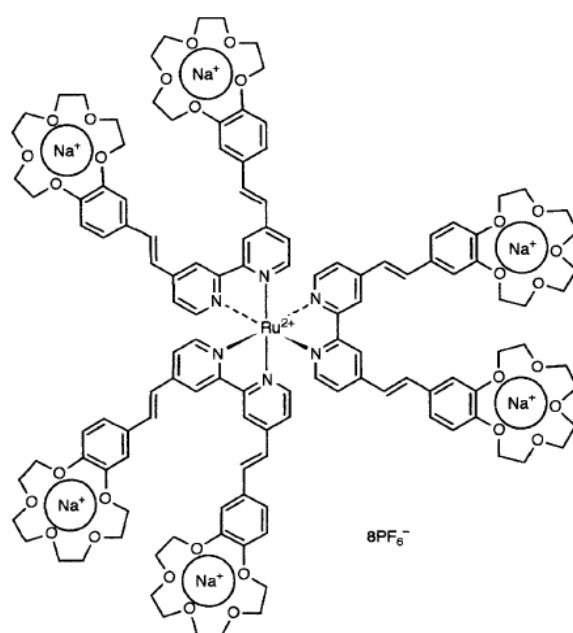
2,2'-Bipyridines have been known since 1888 when F. Blau synthesized the first 2,2'-bipyridine-iron complex<sup>[20]</sup>. One year later, Blau synthesized and analyzed 2,2'-bipyridine by dry distillation of copper picolinate<sup>[21]</sup>. He also briefly reported the preparation of 1,10-phenanthroline in 1888<sup>[20]</sup> and described this in more detail later<sup>[22]</sup>. Smith et al. greatly improved the preparation of this ligand<sup>[23]</sup>. The first studies of 1,10-phenanthroline coordination chemistry by Walden, Hammet and Chapman focused on its oxidative properties. They developed the phenanthroline-ferrous complex as a nearly ideal, high potential, redox indicator<sup>[24-25]</sup>.

Since then 2,2'-bipyridine and 1,10-phenanthroline have been continuously and intensively used in both analytical and preparative coordination chemistry<sup>[26-27]</sup>.

The ligands 2,2'-bipyridine (bpy), 1,10-phenanthroline (phen) and their derivatives (NN) have become fundamental building blocks in supramolecular chemistry<sup>[28]</sup>. This is due to their versatility in coordinating to almost any metal in the periodic table<sup>[29]</sup> through both  $\sigma$  and  $\pi$ -bonding. The unoccupied  $\pi^*$ -orbitals of the aromatic rings overlap with occupied orbitals of the metal while the nitrogen atom donates a lone pair to form a  $\sigma$ -bond with the metal ion.

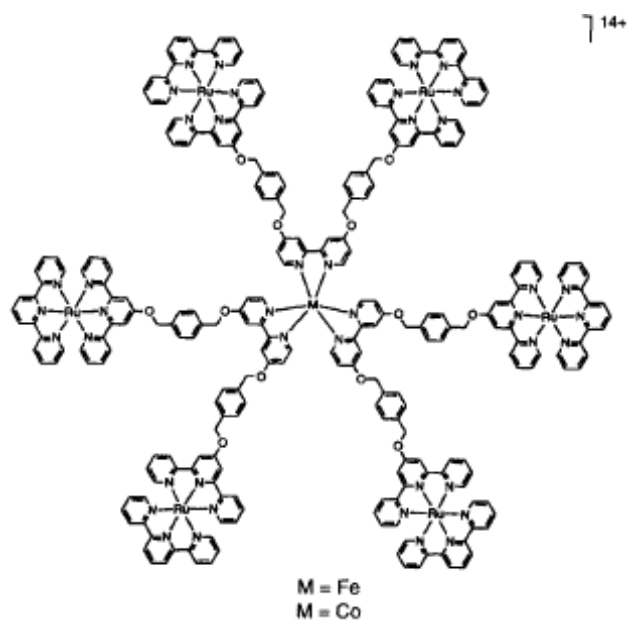
2,2'-Bipyridine and 1,10-phenanthroline-metal complexes have very interesting photo- and electro-chemical properties, which make them attractive candidates for technological applications, such as solar energy conversion<sup>[30]</sup>. These interesting physical properties in turn have lead researchers to study the potential of bpy and phen ligands in the formation of supramolecular coordination complexes<sup>[31-32]</sup>. There are many examples in the literature of 1,10-phenanthroline and 6,6'-disubstituted-2,2'-bipyridine ligands being used as precursors for large supramolecular architectures.

2,2'-Bipyridine has been used for example in the core of metallodendrimers<sup>[33]</sup>. Beer et al. reported in 1991 a "starlike" supramolecular system with a tris(bipyridine)ruthenium(II) core and six benzo- or azacrown ether units on the surface<sup>[33]</sup> (Figure 1.4).



**Figure 1.4** Alkali and alkaline-earth metals can be recognized by the benzocrown ether with a [Ru(bpy)<sub>3</sub>] core synthesized by Beer et al <sup>[33]</sup>.

Other examples of dendrimers with a tris(bipyridine)ruthenium(II) core were reported by Constable et al <sup>[34-35]</sup> (Figure 1.5).

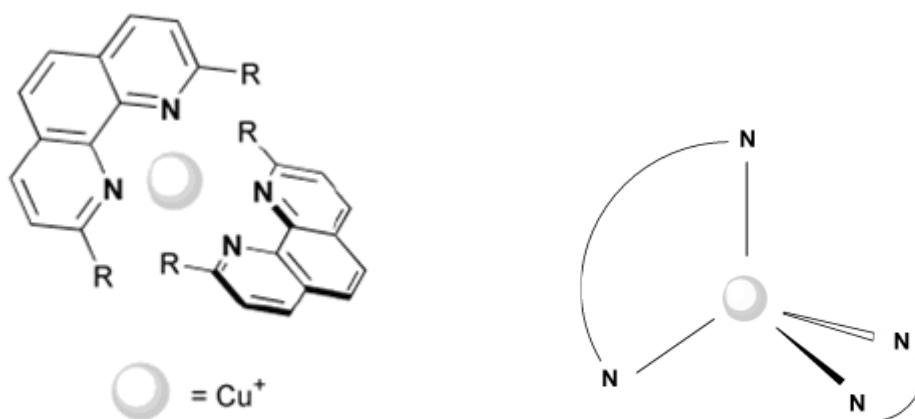


**Figure 1.5** The dendrimer synthesized by Constable et al. with a tris(bipyridine)ruthenium(II) core <sup>[34]</sup>.

## 1.4 Copper(I) polypyridine complexes

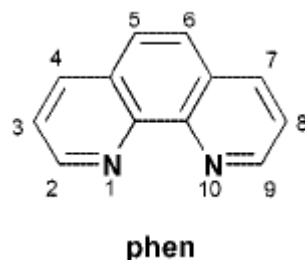
Over the past three decades, the field of inorganic photochemistry has focused on molecular systems that possess low-lying metal-to-ligand charge-transfer (MLCT) excited states capable of electron and/or energy transfer. Although complexes of ruthenium(II), osmium(II) and rhenium(I) have been by far the most studied in this area, certain copper(I) polypyridine complexes  $[\text{Cu}(\text{NN})_2]^+$  also have been found to possess suitable photochemical characteristics [36-43].

The unsubstituted  $[\text{Cu}(\text{phen})_2]^+$  complex ion is not luminescent in solution. However, in 1980 Blaskie and McMillin observed the room temperature luminescence of a disubstituted complex,  $[\text{Cu}(\text{dmp})_2]^+$  (dmp = 2,9-dimethyl-1,10-phenanthroline) in dichloromethane upon excitation into the visible MLCT band [36]. After this important discovery the studies of  $[\text{Cu}(\text{NN})_2]^+$  complexes have typically focused on substituted phenanthrolines [44] (Figure 1.6).



**Figure 1.6** Coordination geometry of Cu(I)-phenanthroline  $[\text{Cu}(\text{NN})_2]^+$  [44].

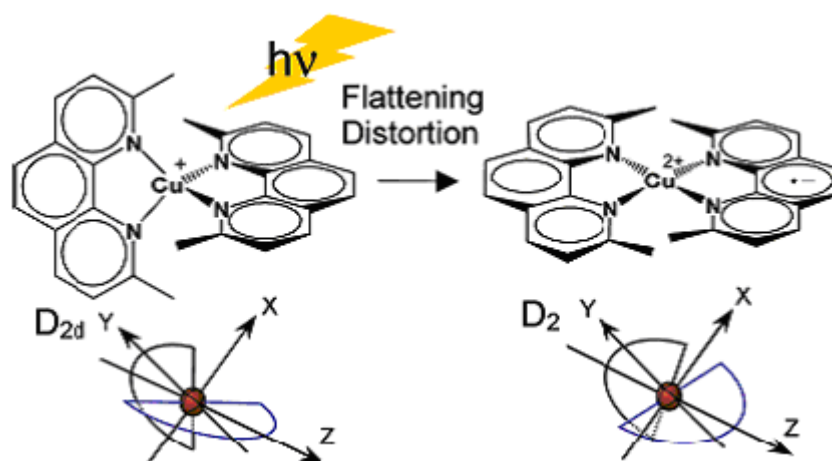
Most of the copper(I) photochemical research has focused on complexes of 2,9-disubstituted phenanthrolines. The numeration of the 1,10-phenanthroline ring atoms is shown in the figure 1.7



**Figure 1.7** Numeration of the 1,10-phenanthroline ring atoms.

A significant characteristic of  $[\text{Cu}(\text{NN})_2]^+$  complexes is the high luminescence quantum efficiency of their absorption and luminescence properties, which are higher than those observed among the analogous  $\text{Ru}(\text{II})$ -polypyridines. The photophysical properties of  $[\text{Cu}(\text{NN})_2]^+$  are associated with the chemical nature, the size and the position of the substituents of the 1,10-phenanthroline ring. These chemical perturbations can greatly alter the geometry of the ground and excited states, thus influencing the photophysical properties.

One of the peculiar aspects of  $[\text{Cu}(\text{NN})_2]^+$  photochemistry is the change in geometry upon photoexcitation. For instance, the ground state geometry of  $\{\text{Cu}(\text{phen})_2\}^+$  complexes can range from nearly tetrahedral ( $D_{2d}$  symmetry) to flattened tetrahedral ( $D_2$  symmetry), with the degree of distortion being dictated by the steric effect of the ligand substituents <sup>[44]</sup> (Figure 1.8).



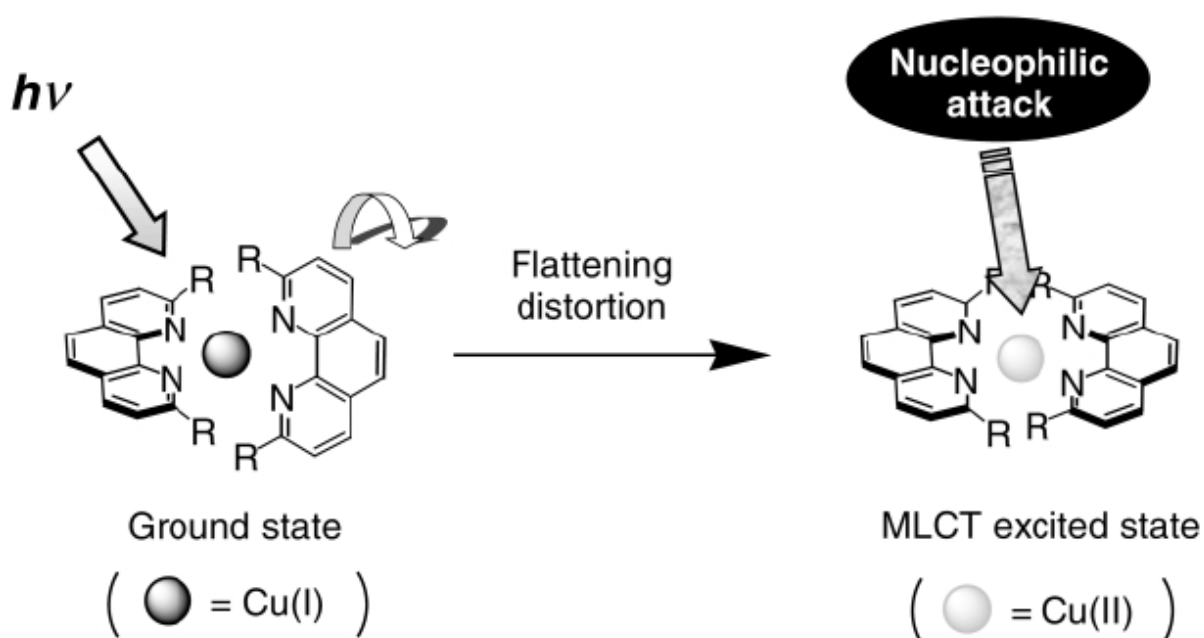
**Figure 1.8** Photoinduced flattening distortion of  $[\text{Cu}(\text{dmp})_2]^+$  <sup>[44]</sup>.

$[\text{Cu}(\text{dmp})_2]^+$  exhibits intense ligand-centred (LC) bands in the ultraviolet region typical of the  $\pi\text{-}\pi^*$  transitions of the free phen ligand <sup>[45]</sup>. The bands in the visible spectral region are much weaker and are assigned to metal-to-ligand charge-transfer (MLCT) electronic transitions <sup>[46]</sup>.



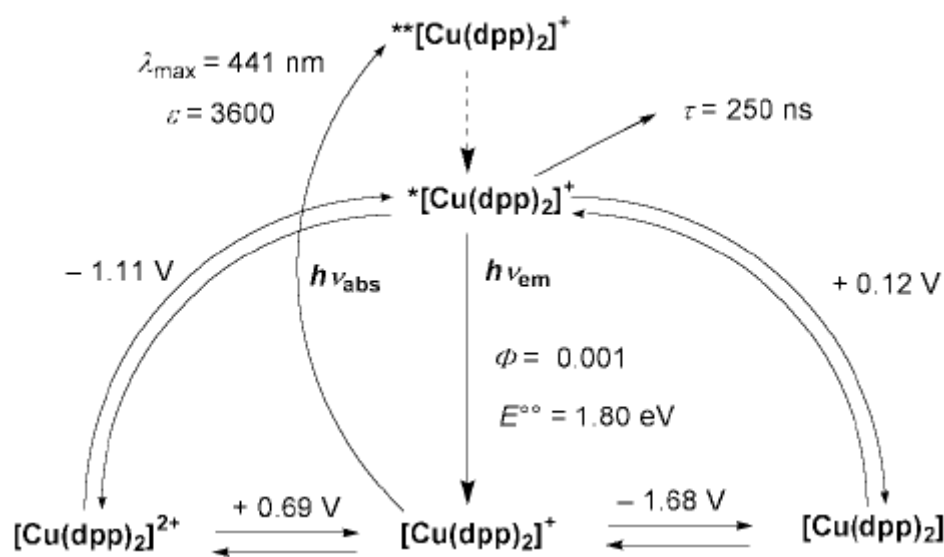
These occur at low energy because the  $\text{Cu}^+$  ion can be easily oxidized and the unsubstituted or substituted phen ligands possess low energy  $\pi^*$  orbitals [47-48]. Spectral intensities are strictly related to the symmetry of the complex that depends of the distortion from the tetrahedral geometry [37; 49-53].

The luminescence of  $[\text{Cu}(\text{NN})_2]^+$  in fluid solution was first reported in 1980 by Blaskie and McMillin. They observed luminescence, upon excitation into the MLCT band of  $[\text{Cu}(\text{dmp})_2]^+$  that peaked around 700 nm with an excited state lifetime of 54 ns in  $\text{CH}_2\text{Cl}_2$ . The luminescence from Cu(I)-phenanthrolines arises from two MLCT excited states in thermal equilibrium: a singlet ( $^1\text{MLCT}$ ) and a triplet ( $^3\text{MLCT}$ ) [50]. The energy gap between these states is about  $2000\text{ cm}^{-1}$ . The population of the lower lying  $^3\text{MLCT}$  level largely exceeds that of  $^1\text{MLCT}$ , although the minority  $^1\text{MLCT}$  excited responsible for most of the observed luminescence [44, 50]. Upon light excitation into the lowest  $^3\text{MLCT}$  excited state the metal centre is reduced from Cu(I) to Cu(II). The Cu(II) complex undergoes a Jahn-Teller distortion to assume a more flattened coordination geometry [43]. This flattened geometry reveals a new fifth coordination site for the  $d^9$  ion, that can be attacked by nucleophiles, including solvent, molecules and counterions (Figure 1.9) [44].



**Figure 1.9** Flattening distortion and subsequent nucleophilic attack by solvent, counterion or other molecules following light excitation in Cu(I)-phenanthrolines [44].

The electrochemistry of Cu(I)-phenanthrolines has received little attention compared to the photophysics, and the electrochemical potentials of many complexes are not available. One extensive study of the electrochemical properties deals with the ground and excited state electrochemistry of  $[\text{Cu}(\text{dpp})_2]^+$ , (dpp = 2,9-diphenyl-1,10-phenanthroline). Figure 1.10 show a series of photophysical properties and electrochemical parameters for  $[\text{Cu}(\text{dpp})_2]^+$  in its ground and excited states. It is evident from the results summarized in figure 1.10 that the complex is a better oxidant and reductant in the excited state than in the ground state.



**Figure 1.10** Photophysical and electrochemical properties of  $[\text{Cu}(\text{dpp})_2]^+$ . Two asterisks denote species with spin-allowed MLCT excited states populated by exciting in correspondence of the absorption maxima; one asterisk indicates the species with lowest-lying luminescent MLCT excited states <sup>[44, 55-56]</sup>.

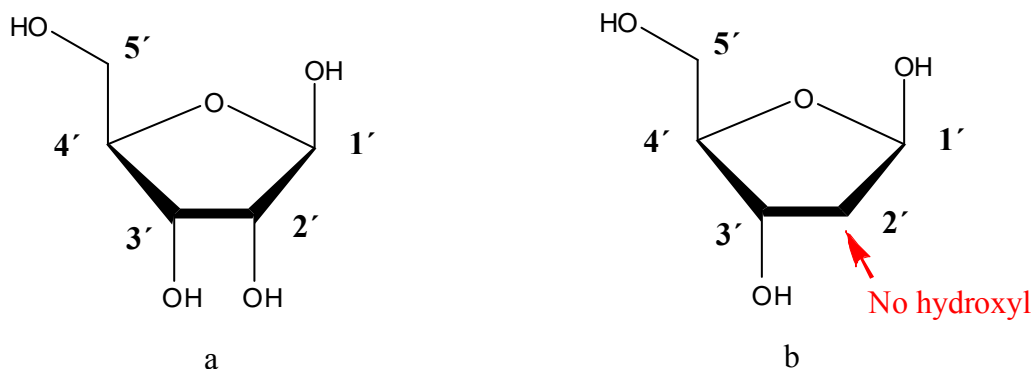
Many comparisons were made between  $[\text{Cu}(\text{NN})_2]^+$  and Ru(II)-polypyridine (absorption, emission and chemical properties) <sup>[44]</sup>. At the present state, the ruthenium complexes seem more attractive but it will not be surprising if in the near future the use of copper complexes will receive more attention of large abundance, low cost and environmental benignity, etc.

## 1.5 Introduction to DNA

Deoxyribonucleic acid (DNA) is the material that carries genetic information in all organisms, except some viruses that use ribonucleic acid (RNA), and is capable of self-replication and the synthesis of RNA. It is a nucleic acid that consists of two long chains of nucleotides twisted together into a double helix and joined by hydrogen bonds between complementary bases adenine and thymine or cytosine and guanine.

### 1.5.1 Discovery of DNA

In the 19<sup>th</sup> century DNA and RNA were isolated as a mixture but not separated. At this time the scientists discovered the polymeric nature of their “nucleic acid” and only later observed the two different types of nucleotides: with ribose or with deoxyribose. They began also to distinguish the two substances: DNA and RNA (figure 1.11)



**Figure 1.11 a.** Structure of Ribose (in RNA). **b.** structure of Deoxyribose (in DNA).

In 1869 *Friedrich Miesche* (1844-1895), a Swiss biologist, discovered in the sperm of salmon a substance he called “nuclein”<sup>[57]</sup>, a nucleoprotein containing an acidic portion, known today as DNA. *Richard Altmann* named it “nucleic acid” in 1889. He discovered that this substance exists only in the chromosomes.

In 1929 *Phoebus Levene* identified the components of DNA: the four bases, the sugar and the phosphate chain. He understood that these components are linked in the order phosphate-sugar-base and named each of these units a nucleotide<sup>[58]</sup>. *William Astbury* produced the first X-ray diffraction patterns from DNA in 1937 and showed that DNA has a regular structure but did not propose a correct structure. In 1952 *Edwin Chargaff* observed that the proportion

of purines (adenine and guanine) and of pyrimidines (cytosine and thymine) is always equal [59, 60]. During this time Lord Todd understood that the primary structure of DNA is a linear polymer of deoxyribonucleosides linked by 3' to 5' phosphodiester bonds [61].

*Rosalind Franklin* and *Maurice Wilkins* discovered from their X-ray diffraction studies that DNA strands have two periodicities: a major one of 0.34 nm and a secondary one of 3.4 nm. Based on these results *James D. Watson* and *Francis Crick* elucidated in 1953 the structure of DNA and proposed in their article “the molecular structure of nucleic acids” [62-64] their famous models that we now use. *Watson* built a model that incorporated two helices, paired bases, and the sugar structure recommended by *Franklin*. *Crick* did calculations. *Wilkins* and *Franklin* produced X-ray diffraction calculations that confirmed the structure. *Pauling* agreed with the proposed structure as, the true nature of DNA had finally been discovered. In 1962, *Watson*, *Crick* and *Wilkins* received the Nobel Prize for physiology and medicine, for their determination of the structure of DNA.

Maurice Wilkins explained in his Nobel-lecture that the generation of X-ray diffraction data was critically dependent on the high-quality DNA provided by Rudolf Signer who was a Professor of organic chemistry in Bern. In addition to his contribution to the elucidation of the DNA structure, his important work established DNA as a high molecular weight macromolecule. Furthermore, Rudolf Signer was an unselfish and generous personality, as he offered his high-quality DNA samples to anyone interested within the scientific community [65-66].

Only in 1956 was the first synthesis of a nucleobase (thymidine) achieved by *Khorama* and co-workers [67].



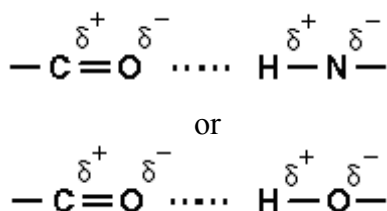
**Figure 1.12** “We have discovered the secret of life”-Watson and Crick in 1953 and 2003.

## 1.5.2 Physical and chemical properties

There are two major factors responsible for the formation and the stability of DNA: the hydrogen bonding and the  $\pi$ - $\pi$  stacking interactions.

### 1.5.2.1 Hydrogen bonding and stability

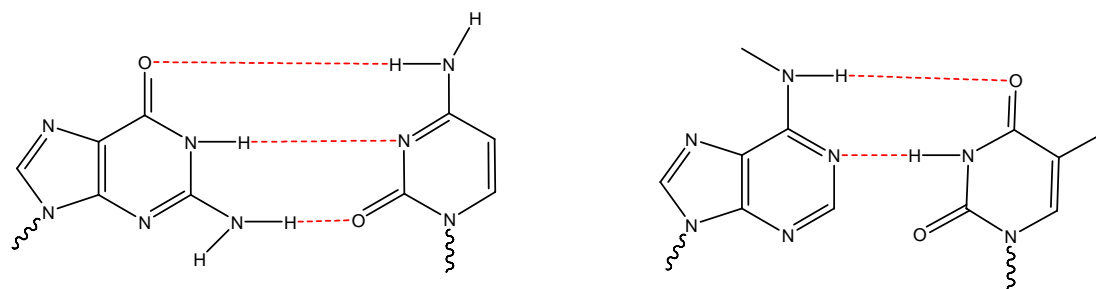
The hydrogen bond is a type of interaction that exists between two partial electric charges of opposite polarity (figure 1.13). One part of the bond involves a hydrogen atom. The hydrogen atom must be attached to a relatively electronegative element. The molecule or moiety including the hydrogen bonded to an electronegative atom is called the hydrogen-bond *donor*. The most electronegative elements, oxygen, nitrogen, and fluorine, are most commonly involved as part of hydrogen bond donors. The electronegative atom attracts the electron cloud from around the hydrogen nucleus and, by decentralizing the cloud, leaves the atom with a partial positive charge. Because of the small size of hydrogen relative to other atoms and molecules, the resulting charge, though only partial, nevertheless represents a large charge density. A hydrogen bond results when this strong positive charge density attracts a lone pair of electrons on another heteroatom, which becomes the hydrogen-bond *acceptor*.



**Figure 1.13** Partial charges.

Although stronger than van der Waals forces, the typical hydrogen bond is much weaker than both the ionic bond and the covalent bond. However, when several hydrogen bonds are formed between two molecules or parts of the same molecule, the resulting interaction can be quite stable (figure 1.14).

Hydrogen bonds have an essential role in the structure of nucleic acid. In the model of *Watson* and *Crick*, the hydrogen bonds are responsible for the AT and GC pairing in duplex <sup>[68]</sup>. The GC base pair has three hydrogen bonds, whereas the AT base pair has only two hydrogen bonds. Consequently the GC pair is more stable.



**Figure 1.14** Watson - Crick base pairs: hydrogen bonds between G-C and A-T.

### 1.5.2.2 $\pi$ - $\pi$ Stacking Interactions

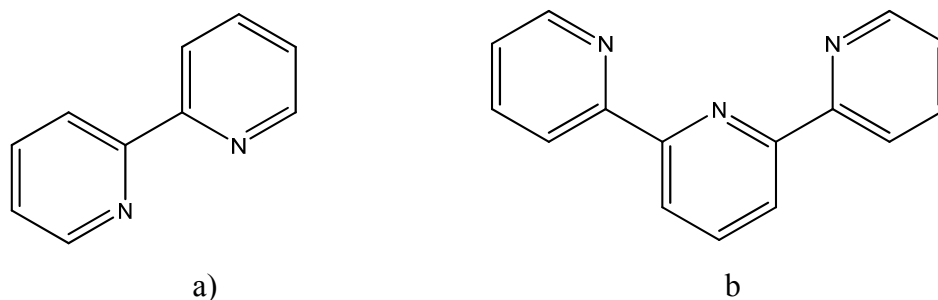
$\pi$ - $\pi$ -stacking occurs between adjacent nucleotides and stabilizes the double helical structure of DNA. The nitrogenous bases of the nucleotides are made from either purine or pyrimidine rings, consisting of planar aromatic rings. Within the DNA molecule, the aromatic rings are positioned nearly perpendicular to the length of the DNA strands. As a consequence, the faces of the aromatic rings are arranged parallel to each other, allowing the bases to participate in aromatic interactions.

Though a non-covalent bond is weaker than a covalent bond, the sum of all the  $\pi$ -stacking interactions within the double-stranded DNA molecule creates a strong net stabilizing effect.

Many interactions contribute to the  $\pi$ - $\pi$ -stacking between the DNA base pairs<sup>[69-71]</sup>. First, the Van der Waals interactions which is the sum of the dispersion and repulsion energies. The second contribution is an electrostatic interaction between partial atomic charges. The third contribution is an electrostatic interaction between the charge distribution associated with the out-of-plane  $\sigma$ -electron density. There is as well a fourth distribution: an electrostatic interaction between the charge distributions associated with out-of-plane  $\sigma$ -electron density and the partial atomic charges, contribution quite sensitive to geometry. The last contribution is an interaction of aromatic residues and solvent<sup>[72-75]</sup>.

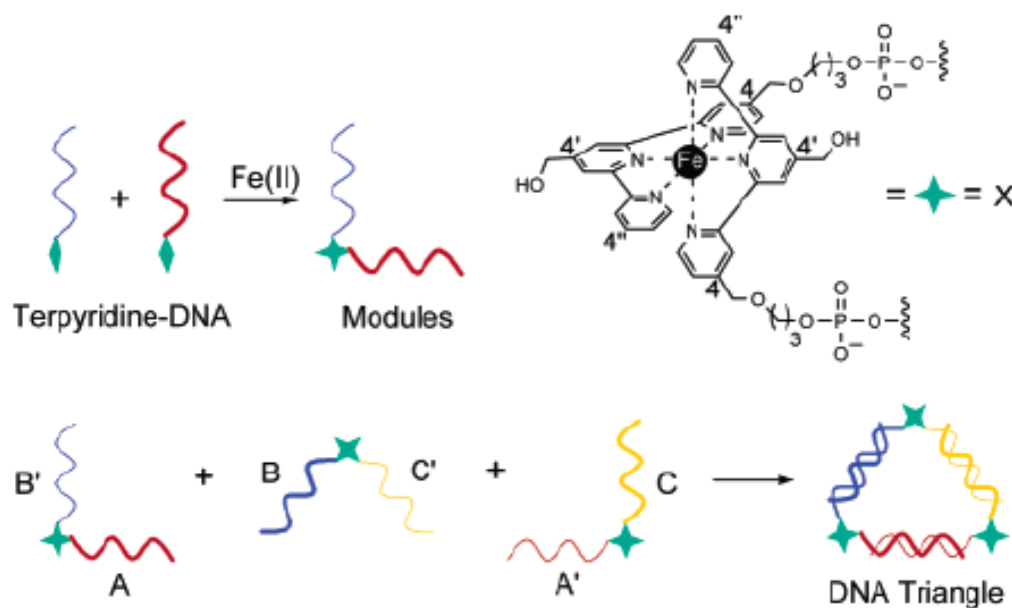
### 1.5.3 Transition metal-oligonucleotide systems:

$\{\text{Fe}(\text{tpy})_2\}$  (tpy = 2,2':6',2''-terpyridine) (Figure 1.15) and  $\{\text{Ru}(\text{bpy})_3\}$  (bpy = 2,2'-bipyridine) (Figure 1.15) complexes have recently been introduced for example as stable vertexes into oligonucleotides to direct the assembly of DNA nanostructure by duplex formation<sup>[76]</sup>.



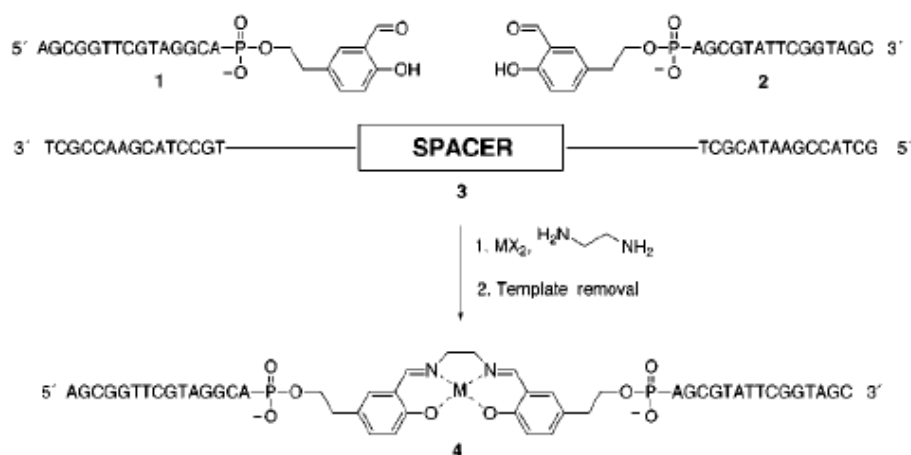
**Figure 1.15** a) 2,2'-bipyridine; b) 2,2':6',2''-terpyridine.

Han and coworkers report the synthesis of a 2,2':6',2''-terpyridine derivative whose dimeric metal complexes can be used as an alternative to the Holliday junction (figure 1.16). This 2,2':6',2''-terpyridine derivative allowed the preparation of 2,2':6',2''-terpyridine-DNA conjugates that formed two-way branched metal-organic modules upon reaction of 2,2':6',2''-terpyridine ligands in the presence of Fe(II) ions. These modules self-assembled into DNA triangles in which each vertex and side consisted of a  $\{\text{Fe}(\text{tpy})_2\}$  unit and a DNA duplex, respectively <sup>[76, 77]</sup>.



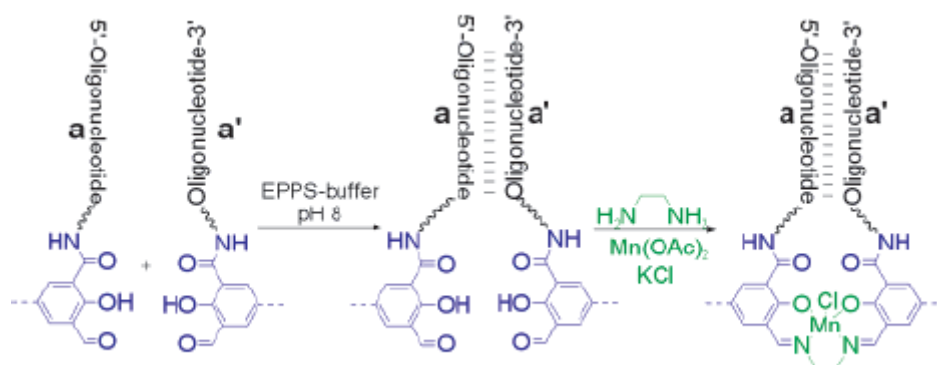
**Figure 1.16** Terpyridine-DNA conjugated for two-way branched metal-organic modules capable of self assembly into DNA triangles <sup>[76]</sup>.

Czlapinski and Sheppard have shown, that metal-salen complexation between two salicylaldehydes attached to short oligonucleotides can be controlled by a DNA template (figure 1.17) <sup>[78]</sup>.



**Figure 1.17** Template directed metallosalen-DNA assembly [78].

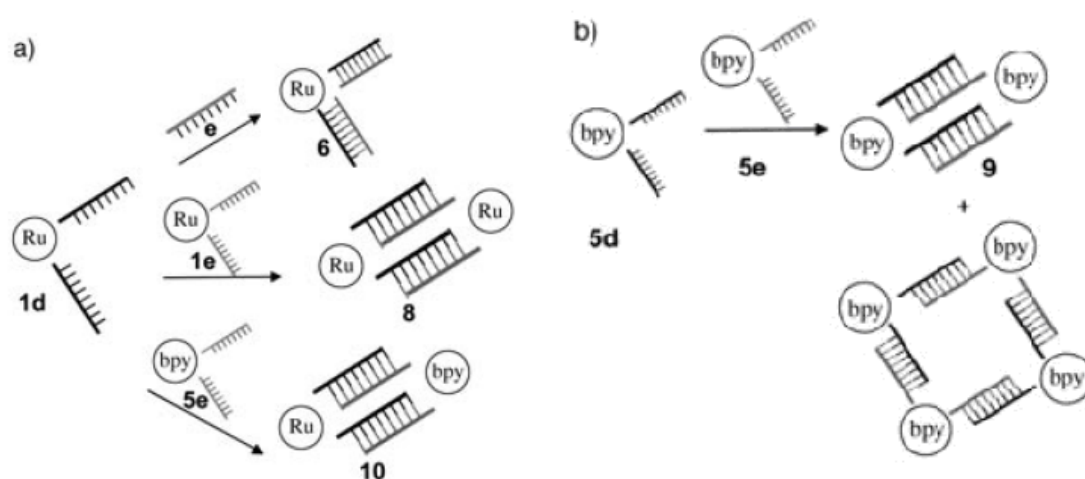
Brown developed a modular DNA-programmed assembly of linear and branched conjugated nanostructures. In his molecular engineering strategy, two or three salicylaldehyde groups are contained within the same compound, enabling the assembly and covalent coupling of multiple modules. Furthermore, no additional DNA template is needed because the oligonucleotides attached on either side of salicylaldehyde group act as clamps to hold the organic modules in a predetermined arrangement. The metal-salen forming coupling was deliberately chosen, because the linkages between the individual headgroups of the modules will be essentially linear due to the stereochemistry of the manganese-salen complex formed (figure 1.18) [79]. The salen ligand adopts a locked coplanar geometry by chelating a manganese ion [80].



**Figure 1.18** DNA-controlled formation of a covalent manganese-salen link between two salicylaldehyde termini linked to complementary DNA sequences [79].

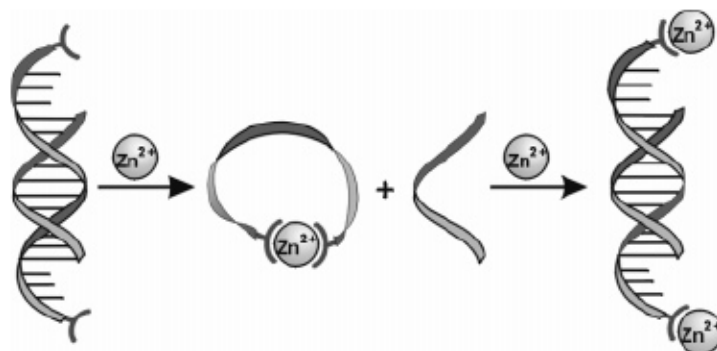


Sleiman reported the synthesis and properties of a branched ruthenium(II)-DNA complex, in which two parallel DNA strands are linked to a relatively rigid  $\{\text{Ru}(\text{bpy})_3\}$  center. Self-assembly of this molecule leads to the formation of a discrete metal-DNA cyclic nanostructure, which contains two DNA duplexes and two redox- and photoactive  $[\text{Ru}(\text{bpy})_3]^{2+}$  centers. Furthermore, he showed that branched oligonucleotides based on the non-metalead ligand undergo less selective association, which illustrates the role of the transition metal in this self-assembly process (figure 1.19) <sup>[81]</sup>.



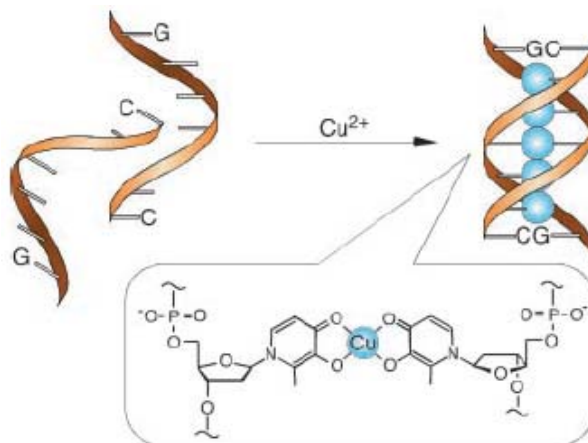
**Figure 1.19** Self-assembly of cyclic metal-DNA nanostructures using ruthenium tris(bipyridine)-branched oligonucleotide<sup>[81]</sup>.

Roland Kramer and co-workers described a chemically modified single-stranded DNA which displays a unique response behaviour towards  $\text{Fe}^{2+}$  or  $\text{Zn}^{2+}$ : A Bis(terpyridine) modified single-stranded DNA smoothly forms a stable cycle by  $\text{Fe}^{2+}$  or  $\text{Zn}^{2+}$  assisted ring closure (figure 1.20), presenting an allosteric control of oligonucleotide hybridisation by metal-induced cyclisation <sup>[82]</sup>.



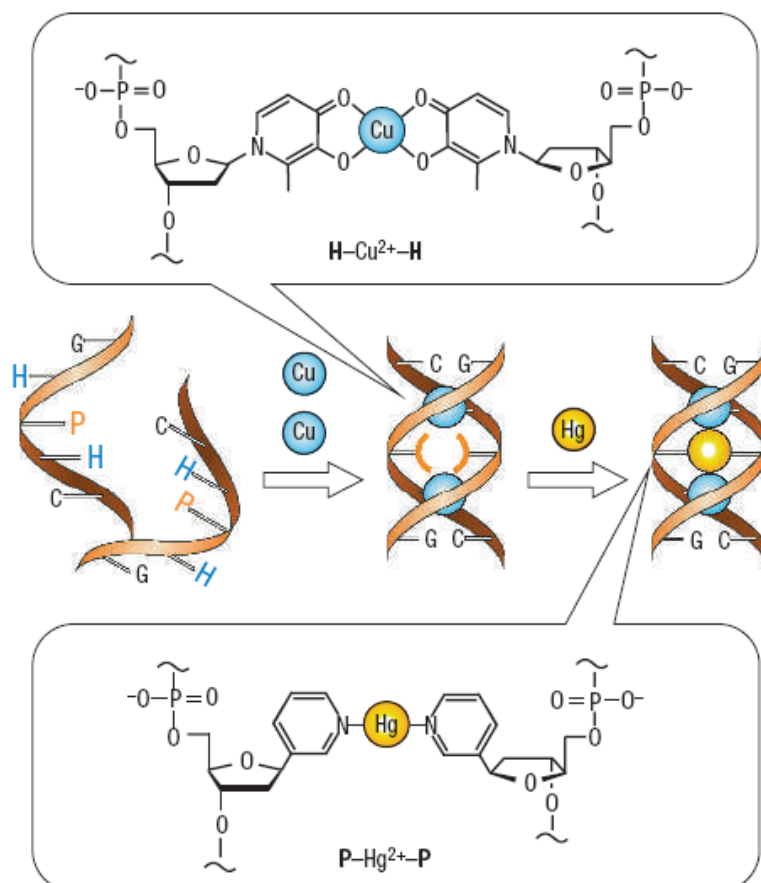
**Figure 1.20** Cyclization and control of hybridization of bis(tpy) modified DNA by  $\text{Zn}^{2+}$  <sup>[82]</sup>.

Taking advantage of metal binding nucleobases or base-pairing mediated by metal chelation, Shionoya and coworkers double stranded DNA mimic with metal ions placed throughout the helix (figure 1.21) <sup>[83]</sup>.



**Figure 1.21** Schematic representation of  $\text{Cu}^{2+}$  mediated duplex formation between two artificial DNA strands in which hydroxypyridone nucleobases replace natural base pairs <sup>[83]</sup>.

Recently, they presented another beautiful self-assembly system of metal ions inside artificial DNA. They reported a heterogeneous metal assembly through  $\text{Cu}^{2+}$  and  $\text{Hg}^{2+}$  mediated base pairing in addition to natural hydrogen-bonded between two artificial DNA strands, in which two hydroxypyridone nucleobases (H) and one pyridine nucleobase (P) are included in place of natural nucleobases ( figure 1.22) <sup>[84]</sup>.

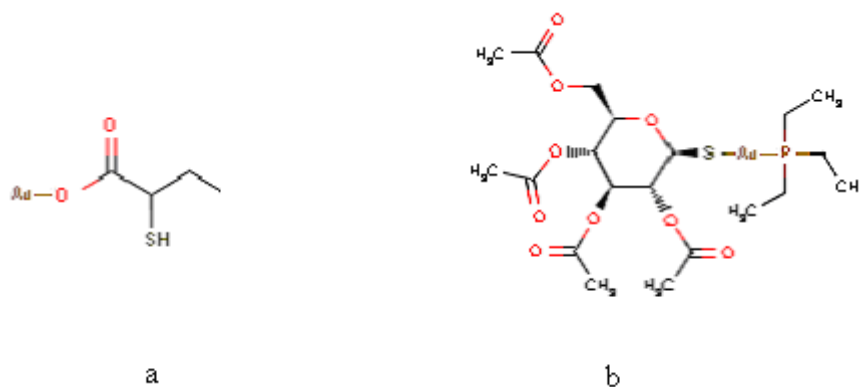


**Figure 1.22** Self-assembly of metal ions inside artificial DNA duplexes <sup>[84]</sup>.

## 1.6 Metal complexes in Medicine

Many metal compounds are already in clinical use <sup>[85-93]</sup>. These include mineral supplements containing metals fundamental for human life, such as Fe, Zn, Mn, Cu, Mo, Ca or Mg.

At the beginning of last century, a gold complex,  $\text{K}[\text{Au}(\text{CN})_2]$ , was introduced for the treatment of tuberculosis. Today several injectable gold(I) thiolates (e.g. aurothiomalate, aurothiopropionol sulfonate) and also the orally active drug auranofin, (2,3,4,6-tetra-O-acetyl-1-thio-1- $\beta$ -D-glucopyranosatotriethylphosphinegold(I)) (figure 1.23) are used for the treatment of rheumatoid arthritis <sup>[86,87,89]</sup>.



**Figure 1.23** a) Structure of aurothiomalate. b) Structure of auranofin.

The most celebrated pharmaceutical metal complexes are cis-[PtCl<sub>2</sub>(NH<sub>3</sub>)<sub>2</sub>] (cisplatin) (figure 1.24) and cis-[Pt<sup>II</sup>(CBDCA)(NH<sub>3</sub>)<sub>2</sub>] (where CBDCA is 1,2-dicarboxycyclobutane). The platinum(II) complexes have considerably improved the success rate for the treatment of certain types of cancer, notably testicular cancer. These types of complexes are used in cancer chemotherapy because they bind to DNA and cause cell death<sup>[93-100]</sup>.



**Figure 1.24** a. Cisplatin. b. Carboplatin, cis-[Pt<sup>II</sup>(CBDCA)(NH<sub>3</sub>)<sub>2</sub>].

Although platinum(II) complexes have been the most intensively investigated, research has been extended to practically all metals, among which the coordination compounds of Ga, Ti, Fe, Ru, Rh, Pd, Cu and organometallic compounds of Ge, Ti, V, Fe and Rh seem to be the most promising<sup>[93, 101, 102]</sup>. For instance, the antimetastatic activity of a range of Ru(III) complexes is well established<sup>[101]</sup>.

Simple inorganic salts are also in clinical use. For example, lithium salts are used in psychiatry for the treatment of manic depression, silver salts are used as antibacterial agent<sup>[103]</sup> and iron(II) sulfate is used to treat hypochromic anemia caused by iron deficiency<sup>[102]</sup>. Dermatology also uses metal compounds of Zn, Ag, Hg, Sb or Al.

Indeed, James Cowan and his colleagues have made new metal coordination complexes that mimic the activity of natural enzymes that break apart DNA, RNA and protein in the body. They made different complexes to break apart portions of RNA that enable HIV and Hepatitis

C viruses to function, as well as the angiotensin converting enzyme (ACE) that constricts blood vessels in the body. The difference between most drugs and metal complexes is that the drugs are designed to inhibit. They will bind to a protein molecule and just block its function but with metals it is possible to destroy completely the target.

## 1.7 Aim of the work

Nucleic acids are vital components of living systems that act as the genetic information pool for individuals and by extension for species and the entire biosphere. Apart from the inherent chemical interest in nucleic acids as supramolecules and the desire to understand their precise roles and regulation in the development of individual organism, there are forceful medical and socio-economic reasons for their study.

Many disease states are genetically linked, are associated with nucleic acid damage or are a direct consequence of invasion of the parent organism by other pathogenic organisms whose behaviour and action is controlled by their own nucleic acids.

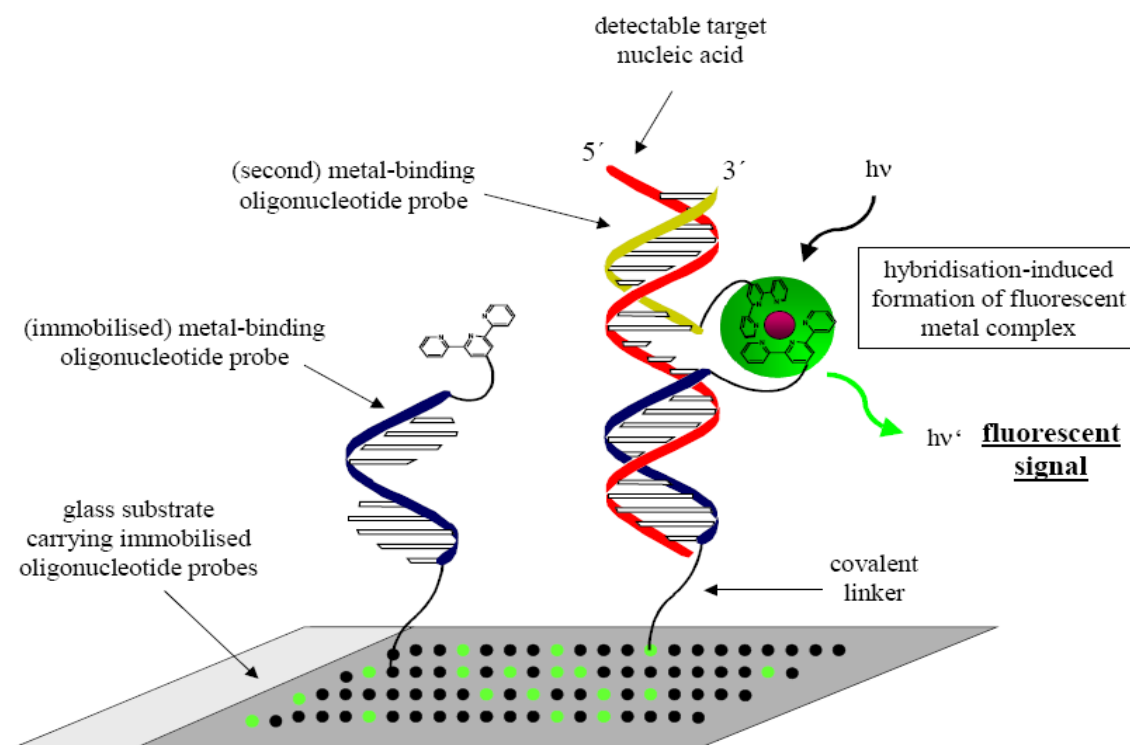
From a medical view point, it is a high priority to develop methods for switching individual genes on or off, for detecting and deleting damaged nucleic acid and for targeting the nucleic acids of specific pathogenic species.

Our interests in nucleic acids originate in our ongoing research in supramolecular chemistry and nanoscale devices and are expressed in a synthetic programme leading to the preparation of nucleic acids in which metal complexes are covalently linked to the oligonucleotide backbone.

The project is aimed at the preparation and investigation of novel types of arrays containing oligonucleotide metal conjugates. Arrays of this type should allow the direct detection and quantification of nucleic acid (DNA) single strands that is without the need of generating a labelled analyte. Currently, oligonucleotide microarrays are designed and used for the detection of labelled nucleic acids. Therefore, a DNA sequence of interest must first be transformed into a labelled form before to be analysed.

The basic concept consists of the generation of a fluorescent metal complex upon hybridisation of analyte nucleic acid to substrate bound oligonucleotides containing metal binding ligands in the presence of a second, oligonucleotide-ligand conjugate and appropriate metal ion.

Such a direct detection can be achieved through the generation of a detectable signal, which is induced by the hybridisation of nucleic acid to the oligonucleotide array. We propose to achieve this goal by the hybridisation-induced formation of a fluorescent metal complex. The principle is illustrated in the figure 1.25.

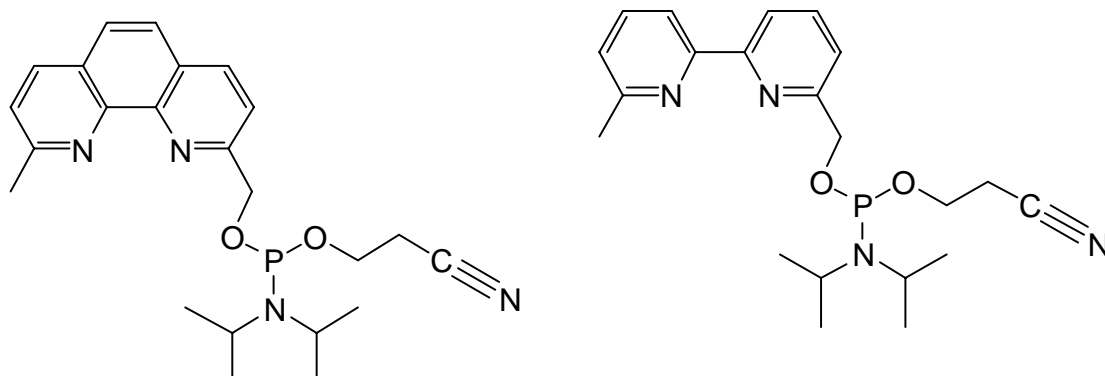


**Figure 1.25** Formation of a fluorescent metal complex by formation of a ternary hybrid composed of two metal ligand containing oligonucleotides and a nucleic acid

The first part of this work consisted of synthesis, X-ray diffraction, electrochemical and fluorescence studies of new Cu(I) complexes with bipyridine and phenanthroline ligands.

The next phase of this project consisted of the study of metal complex-assisted duplex formation. For this study several types of oligopyridine ligand (bipyridine and phenanthroline) were terminally linked to oligonucleotides (figure 1.26). The effect of metal complex formation on the hybridisation of the oligonucleotides was evaluated by thermal denaturation and UV spectroscopy.

The last phase of this project was based on the detection and quantification of nucleic acids with chip electrophoresis.



**Figure 1.26** Representative examples of the systems studied in this project.

## 1.8 References

- [1] Werner, A., *Z. Anorg. Chem.*, **1893**, 3, 267.
- [2] Porai-Koshits, M. A., Novozhilova, N. V., Polynova, T. N., Filippova, T. V. Martynenko, L. I., *Kristallografiya*, **1973**, 18, 89.
- [3] Lehn, J. M., *Acc. Chem. Res.*, **1978**, 11, 49.
- [4] Lehn, J. M., *Pure Appl. Chem.*, **1978**, 50, 871.
- [5] Lehn, J. M., *Supramolecular Chemistry: Concepts and Perspectives*, VCH, Weinheim, Germany, **1995**.
- [6] Lehn, J. M., *Science*, **2002**, 295, 2400.
- [7] Constable, E. C., *Prog. Inorg. Chem.*, **1994**, 42, 67.
- [8] Lawrence, D. S., Jiang, T., Levett, M., *Chem. Rev.*, **1995**, 95, 2229.
- [9] Fujira, M., *Chem. Soc. Rev.*, **1998**, 27, 417.
- [10] Caulder, D. L., Raymond, K. N., *J. Chem. Soc. Dalton Trans.*, **1999**, 8, 1185.
- [11] Holliday, B. J., Mirkin, C. A., *Angew. Chem. Int. Ed. Engl.*, **2001**, 40, 2022.
- [12] Funeriu, D. P., Lehn, J.-M., Baum, G., Fenske, D., *Chem. Eur. J.*, **1997**, 3, 99.
- [13] Funeriu, D. P., Fromm, K. M., Lehn, J.-M., Fenske, D., *Chem. Eur. J.*, **2000**, 6, 2103.
- [14] Hasenknopf, B., Lehn, J.-M., Baum, G., Kneisel, B. O., Fenske, D., *Angew. Chem. Int. Ed. Engl.*, **1996**, 35, 1838.
- [15] Hasenknopf, B., Lehn, J.-M., Boumediene, N., Dupont-Gervais, A., Van Dorsselaer, A., Kneisel, B., Fenske, D., *J. Am. Chem. Soc.*, **1997**, 119, 10956.
- [16] Hasenknopf, B., Lehn, J.-M., Boumediene, N., Leize, E., Van Dorsselaer, A., *Angew. Chem. Int. Ed. Engl.*, **1998**, 37, 3265.
- [17] Armaroli, N., Balzani, V., Collin, J. P., Gavina, P., Sauvage, J.-P., Ventura, B., *J. Am. Chem. Soc.*, **1999**, 121, 4397.
- [18] Livoreil, A., Sauvage, J.-P., Armaroli, N., Balzani, V., Flamigni, L., Ventura, B., *J. Am. Chem. Soc.*, **1997**, 119, 12114.
- [19] Ardeshirpour, Y., Deen, M. J., Shirani, S., *Can. J. Elect. Comput. Eng.*, **2004**, 29, 231.
- [20] Blau, F., *Ber. Dtsch. Chem. Ges.*, **1888**, 21, 1077.
- [21] Blau, F., *Monatsch. Chem.*, **1889**, 10, 375.
- [22] Blau, F., *Monatsch. Chem.*, **1889**, 19, 647.
- [23] Smith, G. F., Getz, C. A., *Chem Rev.*, **1935**, 16, 113.



- [24] Walden, G. H., Hammett, L. P., Chapman, R. P., *J. Am. Chem. Soc.*, **1931**, 53, 3908.
- [25] Walden, G. H., Hammett, L. P., Chapman, R. P., *J. Am. Chem. Soc.*, **1933**, 55, 2649.
- [26] Reedijk, J., in *Comprehensive Coordination Chemistry*, Wilkinson, G., Gillard, R. D., McCleverty, J. A. (Eds.), Vol. 2, Pergamon, Oxford, **1987**, p. 73.
- [27] Constable, E. C., Steel, P. J., *Coord. Chem. Rev.*, **1989**, 93, 205.
- [28] Steel, P. J., *Molecules*, **2004**, 9, 440.
- [29] Constable, E. C., Steel, P. J., *Coord. Chem. Rev.*, **1989**, 93, 205.
- [30] Kalyanasundaran, K., *Coord. Chem. Rev.*, **1982**, 46, 159.
- [31] Rehahn, M., *Acta Polymer.*, **1998**, 49, 201.
- [32] Schubert, U. S., Eschbaumer, C., *Angew. Chem. Int. Ed.*, **2002**, 41, 2892.
- [33] Beer, P. D., Kocian, O., Mortimer, R. J., Ridgway, C., *J. Chem. Soc. Chem. Commun.* **1991**, 1460.
- [34] Constable, E. C., Harverson, P., Oberholzer, M., *Chem. Comm.*, **1996**, 1821.
- [35] Constable, E. C., Housecroft, C. E., *Chimia*, **1999**, 53, 187.
- [36] Blaskie, M. W., McMillin, D. R., *Inorg. Chem.*, **1980**, 19, 3519.
- [37] Ichinaga, A. K., Kirchhoff, J. R., McMillin, D. R., Dietrich-Buchecker, C. O., Marnot, P. A., Sauvage, J.-P., *Inorg. Chem.*, **1987**, 26, 4290.
- [38] Kirchhoff, J. R., Gamache, R. E. Jr., Blaskie, M. W., Del Paggio, A. A., Lengel, R. K., McMillin, D. R., *Inorg. Chem.*, **1983**, 22, 2380.
- [39] Dietrich-Buchecker, C. O., Marnot, P. A., Sauvage, J.-P., Kirchhoff, J. R., McMillin, D. R., *J. Chem. Soc. Chem. Commun.*, **1983**, 513.
- [40] Gamache, R. E. Jr., Rader, R. A., McMillin, D. R., *J. Am. Chem. Soc.*, **1985**, 107, 1141.
- [41] Palmer, C. E. A., McMillin, D. R., Kirmaier, C., Holten, D., *Inorg. Chem.*, **1987**, 26, 3167.
- [42] Crane, D. R., DiBenedetto, J., Palmer, C. E. A., McMillin, D. R., Ford, P. C., *Inorg. Chem.*, **1988**, 27, 3698.
- [43] Miller, M. T., Gantzel, P. K., Karpishin, T. B., *Inorg. Chem.*, **1998**, 37, 2285.
- [44] Armaroli, N., *Chem. Soc. Rev.*, **2001**, 30, 113.
- [45] Armaroli, N., De Cola, L., Balzani, V., Sauvage, J.-P., Dietrich-Buchecker, C. O., Kern, J.-M., *J. Chem. Soc. Faraday Trans.*, **1992**, 88, 553.
- [46] McMillin, D. R., Buckner, M. T., Ahn, B. T., *Inorg. Chem.*, **1977**, 16, 943.
- [47] Gordon, K. C., McGarvey, J. J., *Inorg. Chem.*, **1991**, 30, 2986.

- [48] Armaroli, N., Rodgers, M. A. J., Ceroni, P., Balzani, V., Dietrich-Buchecker, C. O., Kern, J.-M., Bailal, A., Sauvage, J.-P., *Chem. Phys. Lett.*, **1995**, *241*, 555.
- [49] Phifer, C. C., McMillin, D. R., *Inorg. Chem.*, **1986**, *25*, 1329.
- [50] Everly, R. M., McMillin, D. R., *J. Phys. Chem.*, **1991**, *95*, 9071.
- [51] Cunningham, C. T., Cunningham, K. L. H., Michalec, J. F., McMillin, D. R., *Inorg. Chem.*, **1999**, *38*, 4388.
- [52] Miller, M. T., Gantzel, P. K., Karpishin, T. B., *Inorg. Chem.*, **1999**, *38*, 3414.
- [53] Miller, M. T., Karpishin, T. B., *Inorg. Chem.*, **1999**, *38*, 5246.
- [54] Ferderlin, P., Kern, J.-M., Rastegar, A., -Buchecker, C. O., Marnot, P. A., Sauvage, *New J. Chem.*, **1990**, *14*, 9.
- [55] Meyer, T. J., *Pure Appl. Chem.*, **1986**, *58*, 1193.
- [56] Juris, A., Balzani, V., Barigelletti, F., Campagna, S., Belser, P., von Zelewsky, A., *Coord. Chem. Rev.*, **1988**, *84*, 85.
- [57] Mirsky, A. E., *Scientific American*, **1978**, *218*, 78.
- [58] Leven, P.A., *J. Biol. Chem.*, **1919**, *40*, 415.
- [59] Chargaff, E., *Journal of Cellular and Comparative Physiology*, **1951**, *38*, 41.0c.
- [60] Chargaff, E., *Federation Proceeding*, **1951**, *10*, 654.
- [61] Todd, A. R., Brown, D. M., *J. Chem. Soc.*, 1952, 52.
- [62] Watson, J., Crick, F., *Nature*, **1953**, *171*, 737.
- [63] Watson, J., Crick, F., *Nature*, **1953**, *171*, 964.
- [64] Crick, F., Watson, J., *Proc. Roy. Soc.*, **1954**, *A223*, 80.
- [65] Meilis, M., *Chimia*, **2003**, *57*, 735.
- [66] Schmitz, L., *Chimia*, **2004**, *58*, 51.
- [67] Khorana, H. G., Tener, G. M., Moffatt, J. G., Pol, E. H., *chem Ind (London)*, **1956**, 1523.
- [68] Saenger, W., *Principles of Nucleic Acid Structure*, Springer-Verlag, New York, **1984**.
- [69] Chessari, G., Hunter, C. A., Blanco, J. L. J., Low, C. R., Vinter, J. G., *NATO ASI Series, Series C: Mathematical and Physical Sciences*, **1999**, *526*, 331.
- [70] Hunter, C. A., *J. Mol. Biol.*, **1993**, *230*, 1025.
- [71] Hunter, C. A., *Phil. Trans. Roy. Soc. Lon., Ser. A: Math., Phys. Eng. Sci.*, **1993**, *345*, 77.
- [72] Diederich, F., Smithrud, D. B., Sanford, E. M., Wyman, T. B., Ferguson, S. B., Carcanague, D. R., Chao, I., Houk, K. N., *Acta Chem. Scand.*, **1992**, *46*, 205.
- [73] Smithrud, D. B., Diederich, F., *J. Am. Chem. Soc.*, **1990**, *112*, 339.

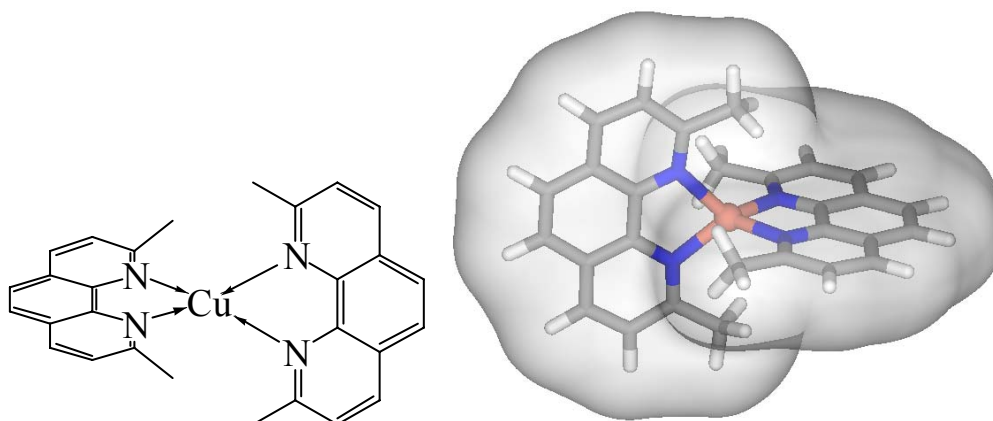
- [74] Smithrud, D. B., Wyman, T. B., Diederich, F., *J. Am. Chem. Soc.*, **1991**, *113*, 5420.
- [75] Meyer, E. A., Castellano, R. K., Diederich, F., *Angew. Chem. Int. Ed. Engl.*, **2003**, *42*, 1210.
- [76] Choi, J. S., Kang, C. W., Jung, K., Yang, J. W., Kim, Y.-G., Han, H., *J. Am. Chem. Soc.*, **2004**, *126*, 8606.
- [77] Mitra, D., Di Cesare, N., Sleiman, H. F., *Angew. Chem.*, **2004**, *116*, 5928.
- [78] Czapinski, J.L., Sheppard, T. L., *J. Am. Chem. Soc.*, **2001**, *123*, 8618.
- [79] Gothelf, K. V., Thomsen, A., Nielsen, M., Clo, E., Brown, R. S., *J. Am. Chem. Soc.*, **2004**, *126*, 1044.
- [80] Pospisil, P. J., Carsten, D. H., Jacobsen, E. N., *Chem. Eur. J.*, **1996**, *2*, 974.
- [81] Mitra, D., Di Cesare, N., Sleiman, H. F., *Angew. Chem. Int. Ed. Engl.*, **2004**, *43*, 5804.
- [82] Göritz, M., Krämer, R., *J. Am. Chem. Soc.*, **2005**, *127*, 18016.
- [83] Tanaka, K., Tengeiji, A., Kato, T., Toyama, N., Shionoya, M., *Science*, **2003**, *299*, 1212.
- [84] Tanaka, K., Clever, G. H., Takezawa, Y., Yamada, Y., Kaul, C., Shionoya, M., Carell, T., *nature nanotechnology*, **2006**, *1*, 190.
- [85] Stochel, G., Wanat, A., Kulis, E., Stasicka, Z., *Coord. Chem. Rev.*, **1998**, *171*, 203.
- [86] Martell, A. E., Hancock, R. D., *Modern Inorganic Chemistry*, Fackler, J. P. (Ed), *Plenum*, New York, **1996**.
- [87] Howard-Lock, H. H., Lock, C. J. L., *Comprehensive Coordination Chemistry*, Wilkinson, G., McCleverty, J. A. (Ed), Pergamon, Oxford, **1987**, vol 6. p. 755.
- [88] Hugues, M. N., Wilkinson, G. (Ed), *Comprehensive Coordination Chemistry*, Pergamon, Oxford, **1987**, p. 541.
- [89] Bertini, J., Gray, H. B., Lippard, S. J., Valentine, J. S., *Bioinorganic chemistry*, University Books, Mill Valley, CA, **1994**, p. 505.
- [90] Sadler, P. J., *Adv. Inorg. Chem.*, **1991**, *36*, 1.
- [91] Keppler, B. K., Lipponer, K. G., Stenzel, B., Kratz, F., *Metal Complexes in Cancer Chemotherapy*, Keppler, B. K. (Ed), VCH, Weinheim, **1993**.
- [92] Berners-Price, S. J., Sadler, P. J., *Coord. Chem. Rev.*, **1996**, *151*, 1.
- [93] Talley, R. W., O'Bryan, R. M., Brownlee, R. W., Gastesi, R. A., *Proc. Am. Ass. Cancer. Res.*, **1970**, *11*, 78.
- [94] Roberts, J. J., Pascoe, J. M., *Nature*, **1972**, *235*, 282.
- [95] Stone, P. J., Kelman, A. D., Sinex, F. M., *Nature*, **1974**, *251*, 736.
- [96] Ling, E. C. H., Allen, G.W., Hambley, T.W., *J. Am. Chem. Soc.*, **1994**, *116*, 2673.

- [97] Ellis, L. T., Er and, H. M., Hambley, T. W., *Aust. J. Chem.*, **1995**, *48*, 793.
- [98] Hambley, T. W., *Coord. Chem. Rev.*, **1997**, *166*, 181.
- [99] T.W. Hambley, *J. Chem. Soc. Dalton Trans.*, **2001**, *120*, 2711-2718.
- [100] Alston, D. R., Lilley, T. H., Stoddart, J. F., *J. Chem. Soc. Chem. Commun.*, **1985**, 1600.
- [101] Nagy, L., Csintalan, G., Kalman, E., Sipos, P., Szvetnik, A., *Acta. Pharm. Hung.*, **2003**, *73*, 221.
- [102] Murgel, G. A., *Rev. Bras. Med.*, **1969**, *26*, 375.
- [103] Lee, D., Cohen, R. E., Rubner, M. F., *Langmuir*, **2005**, *21*, 9651.

## **Chapter 2 : Synthesis, electrochemical and photochemical investigation of 6,6'-disubstituted-2,2'-bipyridine and 2,9'-disubstituted-1,10-phenanthroline copper(I) complexes**

### 2.1 Introduction

Coordination chemistry was born in the pioneering research of Werner at the end of the 19<sup>th</sup> and the beginning of the 20<sup>th</sup> Centuries <sup>[1]</sup>. For the first 60-70 years, the emphasis was upon understanding the bonding in coordination compounds and in developing models to describe the metal-ligand interactions in qualitative and quantitative terms. Over the last 50 years, the photochemical and electrochemical properties of coordination compounds have been investigated in detail.<sup>[2]</sup> One of the initial driving forces was the impetus in the 1970's and 1980's to develop novel photocatalysts which might offer alternative strategies for energy generation that did not rely upon fossil fuels. This need has returned at the beginning of the 21<sup>st</sup> Century. One of the most investigated structures in this context is the {Ru(bpy)<sub>3</sub>} motif (bpy = 2,2'-bipyridine) which has remarkable photophysical properties. From the late 1970s, the photochemical and electrochemical properties of a family of copper(I) 1,10-phenanthroline complexes ([Cu(NN)<sub>2</sub>]<sup>+</sup>) with similar photophysical properties have been the centre of much research and have reported in many publications<sup>[3-5]</sup>. One of the features of these types of complexes in comparison to {Ru(bpy)<sub>3</sub>} is their lower coordination number (4) and coordination geometry do to (tetrahedral) (Figure 2.1). However, the prime motivation for studying these {Cu(NN)<sub>2</sub>}<sup>+</sup> is their possible practical application in the field of energy conversion and storage<sup>[6-8]</sup>. In inorganic photochemistry, the bulk of activity has centred upon metal complexes of the ruthenium(II)-oligopyridine family<sup>[9]</sup>, species which have proved to be exceptionally useful for the design of supramolecular systems with controlled excitation energy transduction and storage<sup>[10-12]</sup> and they are also of interest in the synthesis of sensors based upon luminescence enhancement or quenching<sup>[13]</sup>.



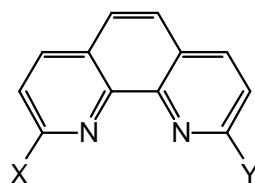
**Figure 2.1** Coordination geometry of the  $\{\text{Cu}(\text{NN})_2\}^+$  moiety as exemplified by  $[\text{Cu}(2,9\text{-dimethyl-1,10-phenanthroline})_2]^+$ .

In this chapter, the synthesis of some 6,6'-disubstituted-2,2'-bipyridine and 2,9'-disubstituted-1,10-phenanthroline ligands will be described and the electrochemical and photophysical properties of their copper(I) complexes will be reported.

## 2.2 6,6'-Disubstituted-2,2'-bipyridine and 2,9'-disubstituted-1,10-phenanthroline ligands derivatives.

### 2.2.1 Syntheses of some 2,9- disubstituted -1,10-phenanthroline.

A series of symmetrically disubstituted compounds ( $X = Y$ ) (Figure 2.2), with substituents linked to the ring through a carbon atom, have been prepared from 2,9-dimethyl-1,10-phenanthroline.



X = Y = CH<sub>3</sub> (**1**)

X = Y = CH<sub>2</sub>OH (**4**)

X = Y = CH<sub>2</sub>TES (**7**)

X = Y = CHO (**2**)

X = Y = CH<sub>2</sub>Br (**5**)

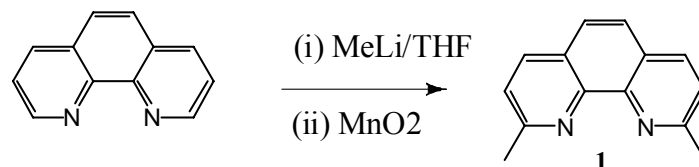
X = Y = C<sub>5</sub>H<sub>4</sub>OCH<sub>3</sub> (**8**)

X = Y = COOH (**3**)

X = Y = CH<sub>2</sub>Cl (**6**)

**Figure 2.2** Symmetrical 2,9-disubstituted-1,10-phenanthroline compounds synthesized.

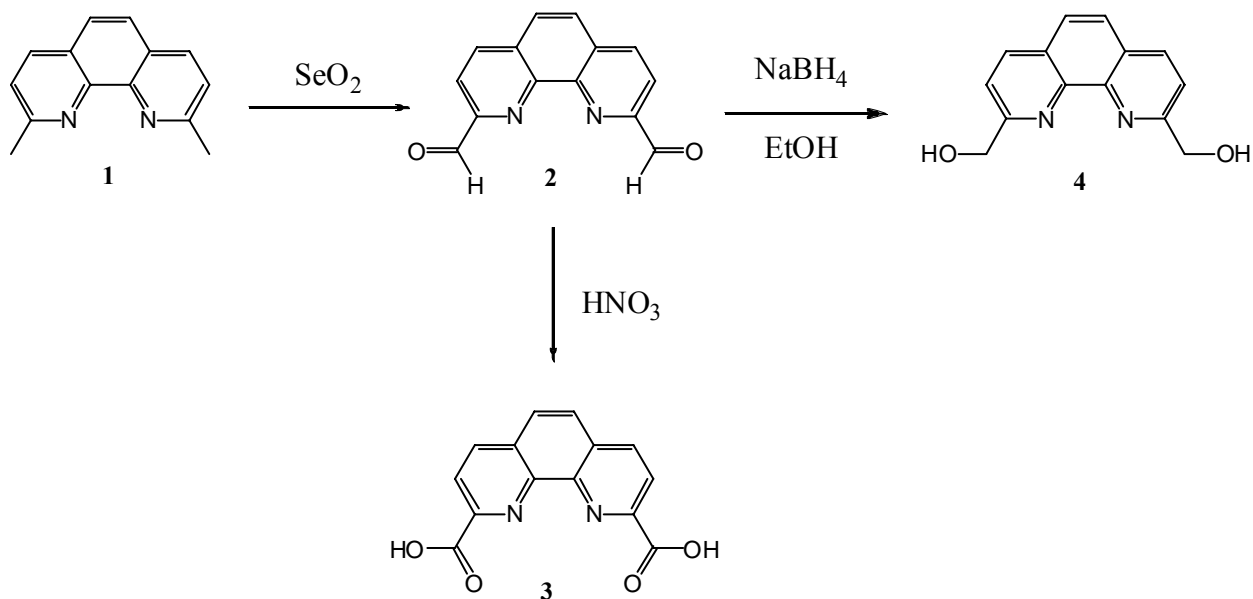
First, the starting material 2,9-dimethyl-1,10-phenanthroline **1** was synthesized by the direct dimethylation of 1,10-phenanthroline with methyllithium in dry THF followed by oxidation of the tetrahydroderivative with MnO<sub>2</sub>. Simple separation of the MnO<sub>2</sub> by filtration over celite gave the desired product in good yield (88%)<sup>[14-16]</sup>. (Figure 2.3)



**Figure 2.3** Synthesis of 2,9-dimethyl-1,10-phenanthroline **1**.

Following the known syntheses of 1,10-phenanthroline derivatives, the dialdehyde **2**, dialcohol **4** and dicarboxylic acid **3** derivatives were prepared<sup>[17]</sup>. The 2,9-dimethyl-1,10-phenanthroline **1** was oxidised to the 1,10-phenanthroline-2,9-dicarbaldehyde **3** with selenium dioxide in dioxan containing 4% water<sup>[17-23]</sup>. The <sup>1</sup>H NMR spectrum revealed the -CHO singlet at δ 10.30 ppm. Further oxidation with nitric acid gave 1,10-phenanthroline-2,9-dicarboxylic acid **3** in excellent yield (96%)<sup>[17,22]</sup>. The dialdehyde **2** was also reduced with sodium borohydride to the corresponding alcohol, 2,9-bis(hydroxymethyl)-1,10-phenanthroline, **4** in 68% yield (Figure 2.4)<sup>[14;17;18]</sup>. The <sup>1</sup>H NMR spectrum revealed the -CH<sub>2</sub>

group as a singlet at  $\delta$  4.86 ppm and the  $^{13}\text{C}$  NMR spectrum showed the high symmetry and exhibited only six signals in the aromatic region and one for the methylene.



**Figure 2.4** Synthesis of some 2,9-disubstituted-1,10-phenanthrolines.

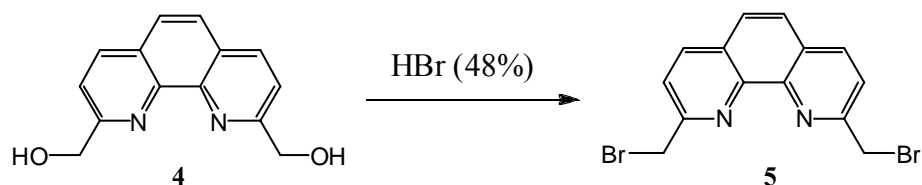
Various methods for the synthesis of 2,9-dibromomethyl-1,10-phenanthroline **5** and of 2,9-dichloromethyl-1,10-phenanthroline **6** are known <sup>[24-26]</sup> but unrestricted access to these two compounds are either poor yield or involve too many synthetic steps (up to four) with intermediates which have proved hard to purify. The dibromo-compound **5** has been prepared by bromination of the dimethyl-compound **1** with *N*-bromosuccinimide (NBS) <sup>[24]</sup>, reaction of the diol **4** <sup>[17;27]</sup> or its acetate <sup>[25]</sup> with HBr. The dichloro compound has been prepared by the reaction of the diol with  $\text{SOCl}_2$  <sup>[28]</sup>.

We first investigated the direct methods for the synthesis of 2,9-dibromomethyl-1,10-phenanthroline **5**. Bromination of 2,9-dimethyl-1,10-phenanthroline **1** was carried out under a variety of conditions in an attempt to directly prepare the desired compound, but without marked success. In our hands, the free-radical halogenation of 2,9-dimethyl-1,10-phenanthroline **1** with excess *N*-bromosuccinimide (NBS) afforded 2,9-bis(tribromomethyl)-1,10-phenanthroline in good yield.

Therefore, the reported synthesis in three steps was investigated. In our hands, the bromination of bis(hydroxymethyl)-1,10-phenanthroline **4** with hydrobromic acid, gave the



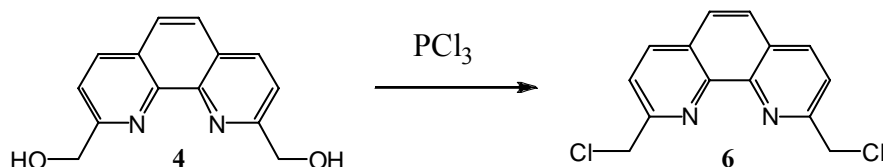
desired compound, 2,9-dibromomethyl-1,10-phenanthroline **5**, in 42 % yield (Figure 2.5). The  $^1\text{H}$  NMR spectrum showed a shift in the resonance of the methylene group to  $\delta$  4.97 ppm<sup>[17]</sup>.



**Figure 2.5** Synthesis of 2,9-dibromomethyl-1,10-phenanthroline **5**.

Attempts to prepare 2,9-dichloromethyl-1,10-phenanthroline **6** by reacting 2,9-dimethyl-1,10-phenanthroline **1** with excess *N*-chlorosuccinimide (NCS) were also unsuccessful.

The desired compound was obtained in poor yield by treatment of the bis(hydroxymethyl)-1,10-phenanthroline **4** with  $\text{PCl}_3$  (Figure 2.6). The  $^1\text{H}$  NMR spectrum showed a shift in the methylene resonance to  $\delta$  4.96 ppm.



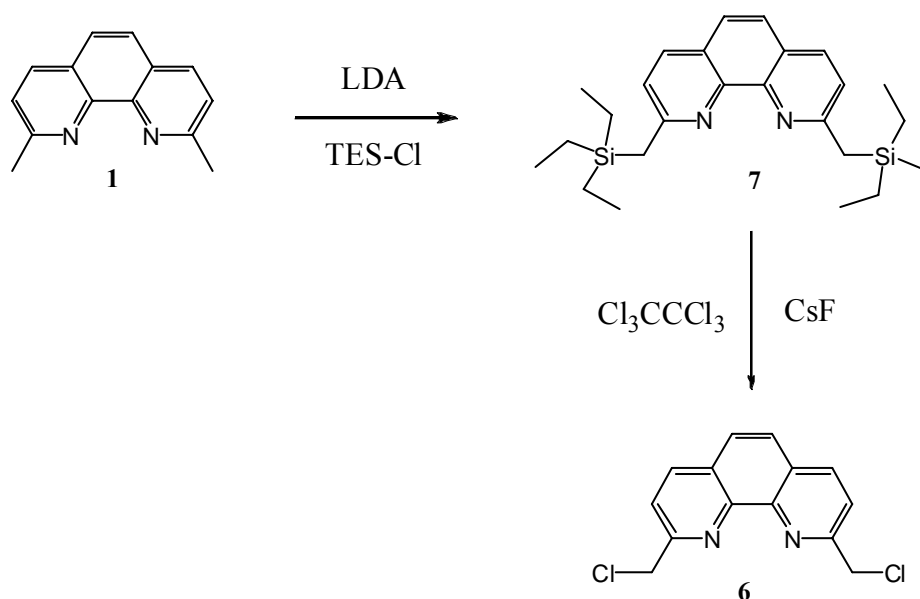
**Figure 2.6** Synthesis of 2,9-dichloromethyl-1,10-phenanthroline **6** using the bis(hydroxymethyl)-1,10-phenanthroline **4** intermediate.

This disappointing result inspired the search for a more efficient synthetic route to access 2,9-dichloromethyl-1,10-phenanthroline **6** and bis(bromomethyl)-1,10-phenanthroline **5**.

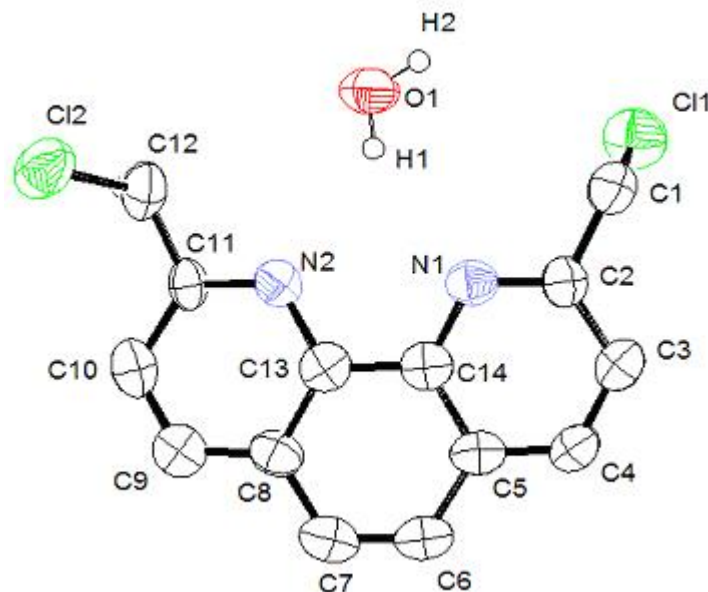
A recent paper reported the synthesis of the dibromo compound with an overall yield of 60%. Compound **5** was synthesised in only two steps while additionally avoiding polar, notoriously sparingly soluble compounds, by varying a literature method for the 2,2'-bipyridine analogues<sup>[29]</sup>. The compound 2,9-dimethyl-1,10-phenanthroline **1** was doubly deprotonated with three

equivalents of LDA per methyl group (the excess of LDA being required due to the presence of unremovable water in purchased 2,9-dimethyl-1,10-phenanthroline). The resulting dianion was then quenched with chlorotriethylsilane (TES-Cl) to give the disilylated intermediate in 84% yield. The silyl groups were then exchanged for bromine by treatment with dibromotetrafluoroethane and caesium fluoride in DMF while applying ultrasound. After only 2 h, 71% of the dibromo-species **5** could be isolated <sup>[30]</sup>.

Because of the difficulties in obtaining the commercially available dibromotetrafluoroethane, a variation was attempted to obtain 2,9-dichloromethyl-1,10-phenanthroline **6**, using the dichlorotetrafluoromethane. In two steps, this way gave the dichloride **6** in excellent yield (88%) (Figure 2.7). The <sup>1</sup>H NMR spectrum of disilylated intermediate revealed the –CH<sub>2</sub> singlet at  $\delta$  2.80 ppm and that of the 2,9-dichloromethyl-1,10-phenanthroline showed a shift in the methylene resonance to  $\delta$  4.96 ppm.



**Figure 2.7** Synthesis of 2,9-dichloromethyl-1,10-phenanthroline **6** using 2,9-bis[(triethylsilyl)methyl]-1,10-phenanthroline **7** as an intermediate.



**Figure 2.8** ORTEP representation of 2,9-dichloromethyl-1,10-phenanthroline monohydrate **6**. Hydrogen atoms are omitted for clarity.

Bond	Distance/ Å	Bond	Distance/ Å
Cl(2)-C(12)	1.795(7)	C(1)-C(2)	1.488(11)
C(12)-C(11)	1.489(10)	C(11)-N(2)	1.298(8)
Cl(1)-C(1)	1.750(8)	C(2)-N(1)	1.311(9)

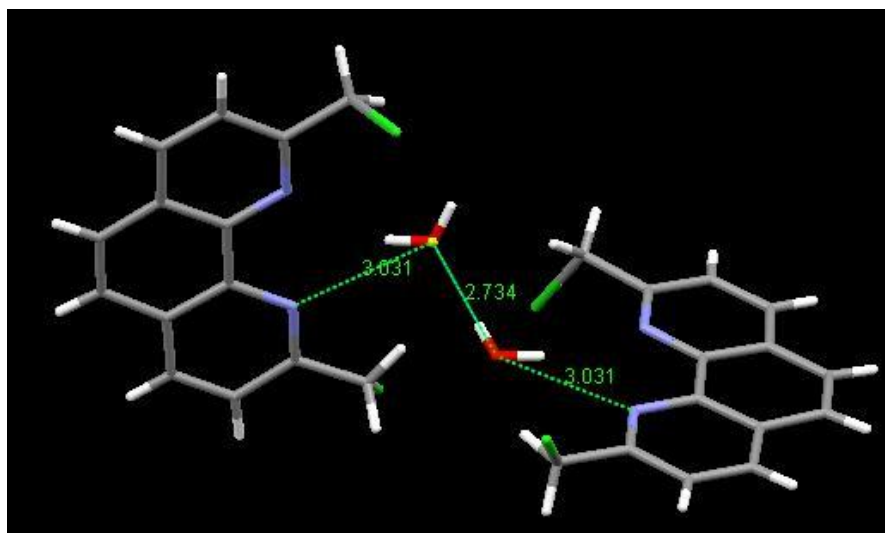
Bond	Angles/ °	Bond	Angles/ °
Cl(2)-C(12)-C(11)	113.1(5)	C(1)-C(2)-N(1)	117.1(6)
C(12)-C(11)-N(2)	115.2(6)	C(2)-N(1)-C(14)	119.3(6)
Cl(1)-C(1)-C(2)	111.8(6)	C(13)-N(2)-C(11)	119.0(6)

N(1)-C(14)-C(13)-N(2)	-176.03	
-----------------------	---------	--

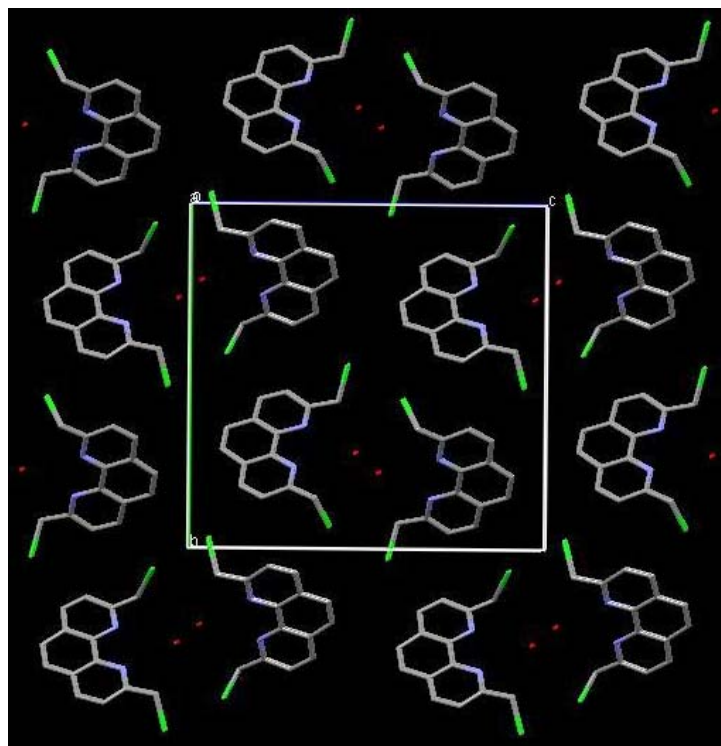
**Table 2.1** Selected bonds lengths (Å), angles (°), and torsion angle (°) for the 2,9-dichloromethyl-1,10-phenanthroline **6**.

We have obtained X-ray quality crystals of 2,9-dichloromethyl-1,10-phenanthroline **6** as a monohydrate. It is well-known that 1,10-phenanthroline ligands have a tendency to crystallise as monohydrates. The 1,10-phenanthroline ring system is almost planar, with an N1-C14-C13-N2 torsion angle of 4.53°. There is an interesting hydrogen-bonding system in the lattice. Both of the nitrogen atoms N1 and N2 are hydrogen-bonded to the water, with N...O donor-acceptor distances of 3.098Å and 3.031Å respectively. (N(1)-H(1) 2.368Å ;N(2)-H(1) 2.357Å

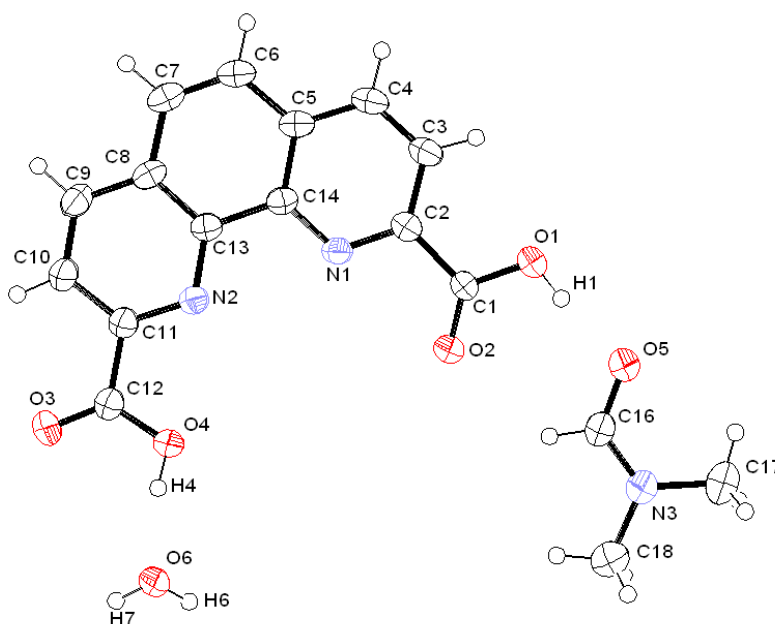
; N(1)-H(2) 3.221 Å; N(2)-H(2) 3.730 Å; H(2)-H'(2) 2.375 Å). This water is in turn hydrogen-bonded to the adjacent water molecule in the lattice, which gives an isolated dimeric system with adjacent 1,10-phenanthrolines connected to each other via the hydrogen-bonded water molecules (Figure 2.9). The 1,10-phenanthroline units are arranged in columns, with alternating configurations, as shown in Figure 2.10.



**Figure 2.9** The dimeric hydrogen-bonded system in 2,9-dichloromethyl-1,10-phenanthroline monohydrate **6**.



**Figure 2.10** Packing in 2,9-dichloromethyl-1,10-phenanthroline monohydrate **6**, as viewed along the a axis.



**Figure 2.11** ORTEP representation of the 1,10-phenanthroline-2,9-dicarboxylic acid **3** molecule as the mixed solvate containing one water and one DMF molecule.

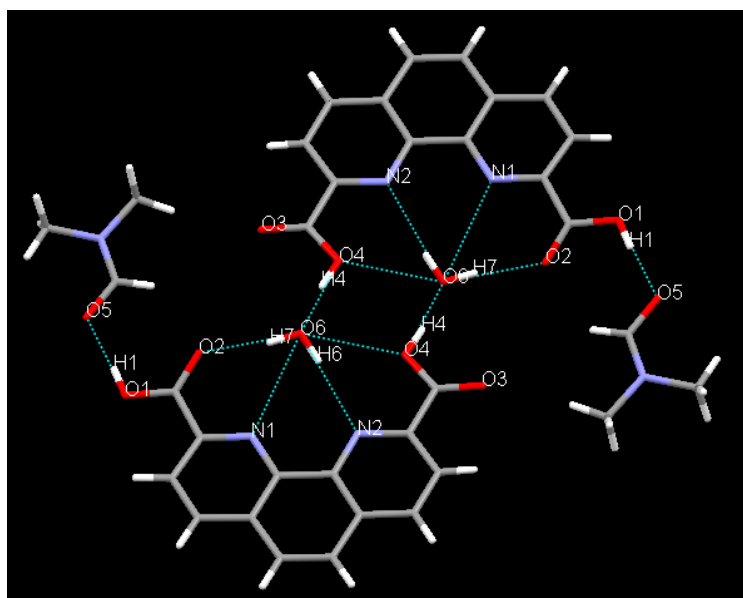
Bond	Distance/ Å	Bond	Distance/ Å
C(1)-C(2)	1.501(4)	C(11)-C(12)	1.501(4)
C(1)-O(1)	1.299(3)	C(11)-N(2)	1.338(3)
C(1)-O(2)	1.211(3)	C(12)-O(3)	1.210(3)
C(2)-N(1)	1.331(3)	C(12)-O(4)	1.298(3)

Bond	Angles/°	Bond	Angles/°
C(2)-C(1)-O(1)	114.6(2)	C(11)-C(12)-O(3)	121.6(2)
C(2)-C(1)-O(2)	122.3(2)	C(11)-C(12)-O(4)	113.4(2)
O(1)-C(1)-O(2)	123.0(3)	O(3)-C(12)-O(4)	124.9(3)
C(1)-C(2)-C(3)	121.3(2)	C(8)-C(13)-N(2)	122.8(2)
C(1)-C(2)-N(1)	114.9(2)	C(14)-C(13)-N(2)	118.9(2)
C(3)-C(2)-N(1)	123.7(2)	C(13)-C(14)-N(1)	118.5(2)
C(10)-C(11)-C(12)	118.6(2)	C(5)-C(14)-N(1)	121.7(2)
C(10)-C(11)-N(2)	123.5(2)	C(14)-N(1)-C(11)	118.3(2)
C(12)-C(11)-N(2)	117.9(2)		

N(1)-C(14)-C(13)-N(2)	0.47	
-----------------------	------	--

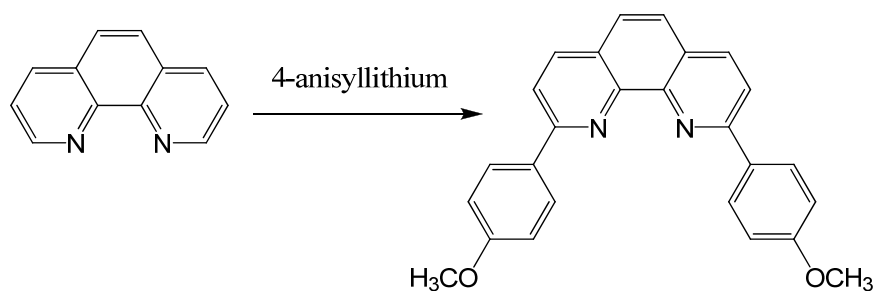
**Table 2.2** Selected bonds lengths (Å), angles (°), and torsion angles (°) for the 1,10-phenanthroline-2, 9-dicarboxylic acid **3** in the **3**.H<sub>2</sub>O.DMF.

We have also structurally characterised the dicarboxylic acid **3** obtained from aqueous DMF as a mixed solvate with one water molecule and one DMF molecule in the lattice. There is hydrogen-bonding between the OH group of the carboxylic acid and the DMF carbonyl group (H...O, 1.668 Å;  $\angle$ O...H-O 173.18°, O...O, 2.504 Å). The water molecule is involved in a hydrogen bond to N2 and O2 of the carboxylic acid. The carboxylic acid that is not involved in the hydrogen bond to the DMF is hydrogen-bonded to the water molecule of a second **3**.H<sub>2</sub>O.DMF moiety and the entire assembly forms a dimeric assembly as shown in Figure 2.12. The 1,10-phenanthroline ring system is planar, with an N1-C14-C13-N2 torsion angle of 0.47°. The 1,10-phenanthrolines are arranged in columns, with  $\pi$ - $\pi$  interactions between the central rings. The 1,10-phenanthrolines are not superimposed directly, but are arranged in two orientations, offset by an angle of 42.86°. Although adjacent 1,10-phenanthroline columns can be orientated so as to be viewed in a plane, there are no Desiraju-type ribbons in the lattice, due to the lack of opportunity for direct ligand-to-ligand hydrogen-bonding.

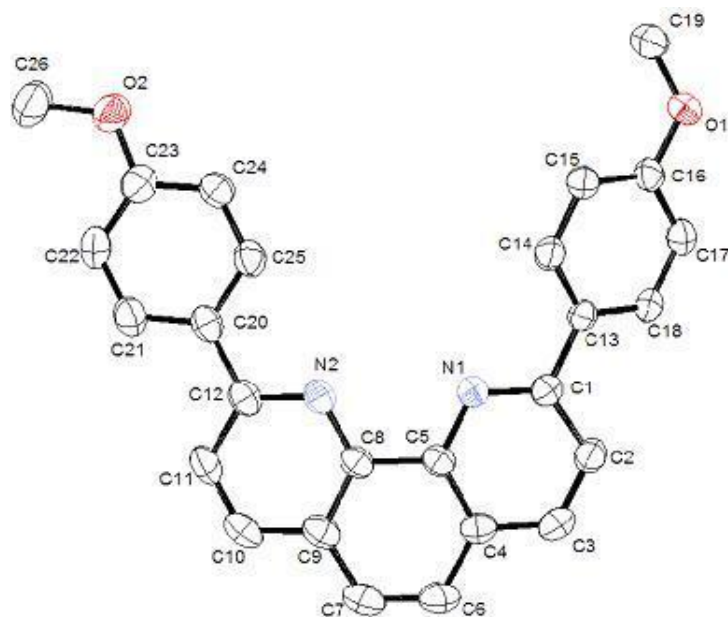


**Figure 2.12** The hydrogen bonding network in the dimeric assembly in the lattice of **3**.H<sub>2</sub>O.DMF.

We have also considered the introduction of phenylene spacers at the 2- and 9-position of the 1,10-phenanthroline. The key intermediate is 2,9-bis(4-methoxyphenyl)-1,10-phenanthroline **8** was obtained using the literature method<sup>[31]</sup> in good yield (70%) from the reaction of 1,10-phenanthroline with 4-anisyllithium (Figure 2.13)



**Figure 2.13** Synthesis of 2,9-bis(4-methoxyphenyl)-1,10-phenanthroline **8**



**Figure 2.14** ORTEP representation of the 2,9-bis(4-methoxyphenyl)-1,10-phenanthroline **8** molecule in the dichloromethane solvate. Hydrogen atoms have been omitted for clarity.

Bond	Distance/ Å	Bond	Distance/ Å
C(26)-O(2)	1.427(4)	C(19)-O(1)	1.418(3)
O(2)-C(23)	1.374(3)	O(1)-C(16)	1.362(3)
C(12)-O(20)	1.492(3)	C(13)-C(1)	1.487(3)
C(12)-N(2)	1.334(3)	N(1)-C(1)	1.329(3)

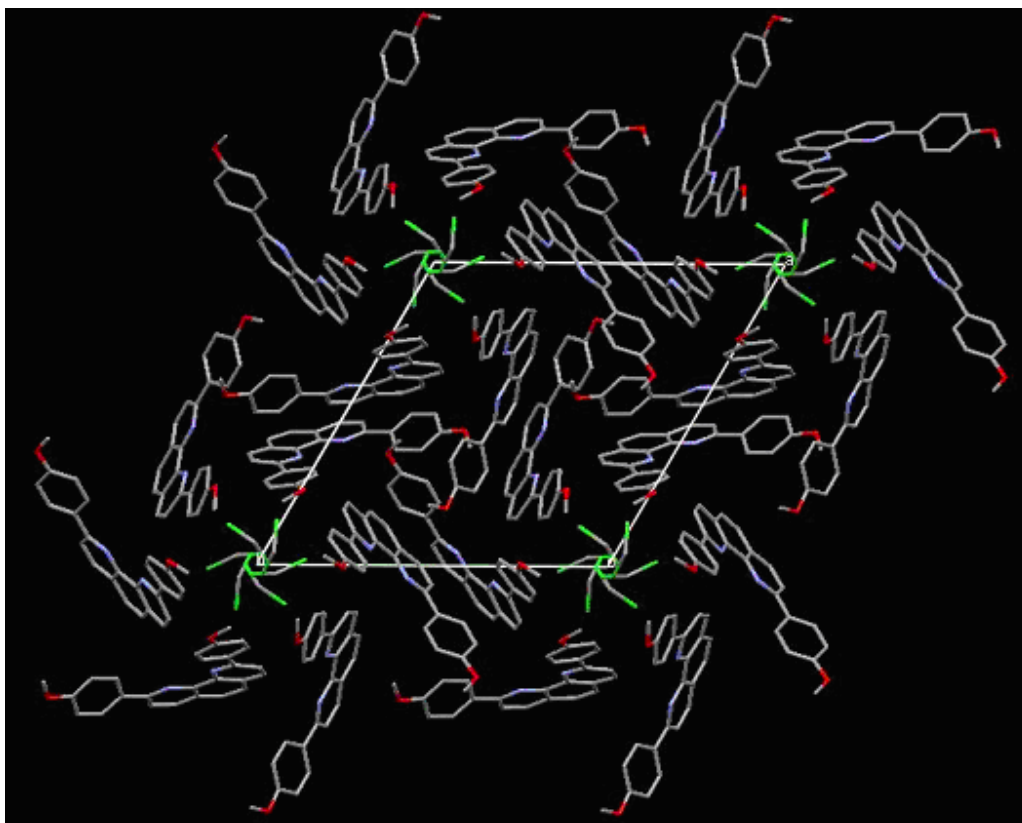
Bond	Angles/°	Bond	Angles/°
C(26)-O(2)-C(23)	117.5(2)	C(22)-C(23)-O(2)	124.6(2)
C(19)-O(1)-C(16)	117.5(2)	C(24)-C(23)-O(2)	115.8(2)
C(13)-C(1)-N(2)	116.88(18)	C(17)-C(16)-O(1)	116.0(2)
C(20)-C(12)-N(3)	116.0(2)	C(15)-C(16)-O(1)	124.5(2)

N(1)-C(5)-C(8)-N(2)	-1.57	
---------------------	-------	--

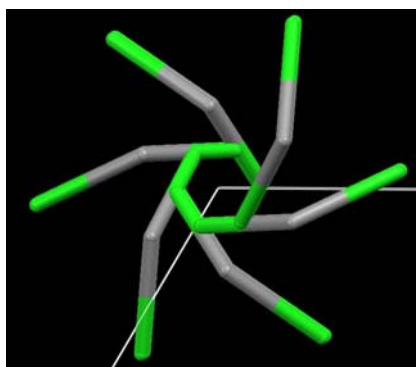
**Table 2.3** Selected bonds lengths (Å), angles (°), and torsion angles (°) for the 2,9-bis(4-methoxyphenyl)-1,10-phenanthroline **8** in the dichloromethane solvate.

We have determined the solid state structure of the dichloromethane solvate of 2,9-bis(4-methoxyphenyl)-1,10-phenanthroline **8**. The 1,10-phenanthroline moiety is almost planar, with an N1-C5-C8-N2 torsion angle of 1.57°. The best least squares planes of the anisyl substituents make angles of 5.48 and 29.27° with the least squares plane through the 1,10-phenanthroline. The packing in the lattice has a number of interesting features, but the symmetry of the system is illustrated best by viewing along the c axis (Figure 2.15). Here, the arrangement of the molecules can be most clearly seen. The dichloromethane molecules lie along the unit cell axes and in this perspective they form attractive hexagon patterns at each corner of the unit cell (Figure 2.16).



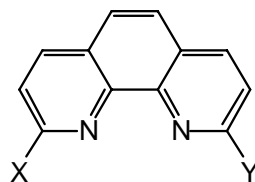


**Figure 2.15** Packing in 2,9-bis(4-methoxyphenyl)-1,10-phenanthroline dichloromethane hydrate, as viewed along the c axis.



**Figure 2.16** The view of "stacked dichloromethane" molecules along the c-axis

## 2.2.2 Synthesis of some asymmetrical 2,9-difunctionalized-1,10-phenanthrolines.

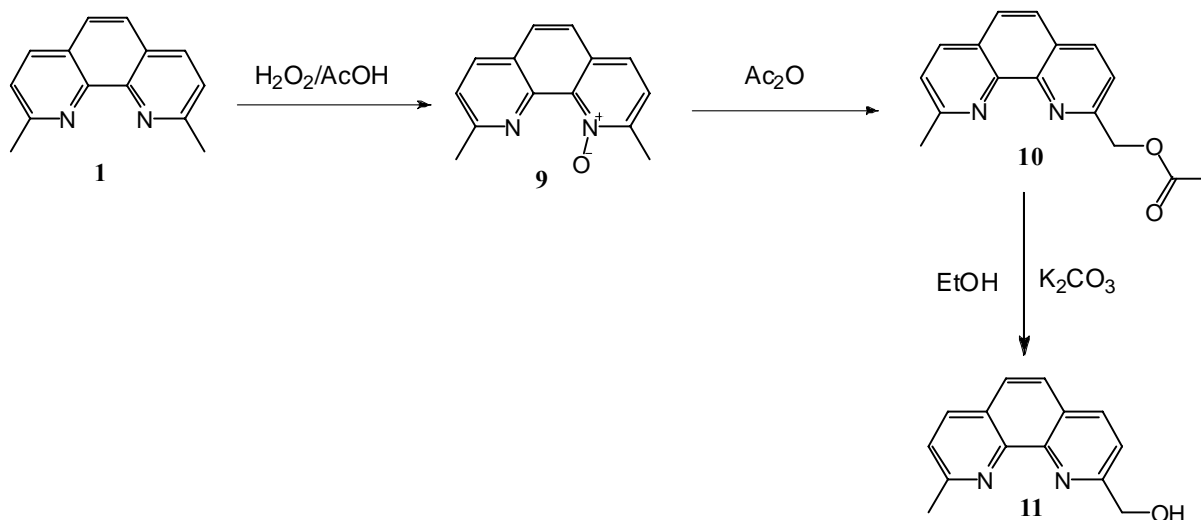


X = CH <sub>3</sub>	Y = CH <sub>3</sub>	<b>(1)</b>	X = CH <sub>3</sub>	Y = CH <sub>2</sub> Cl	<b>(11)</b>
X = CH <sub>3</sub>	Y = CH <sub>3</sub> OCOCH <sub>3</sub>	<b>(9)</b>	X = CH <sub>3</sub>	Y = CH <sub>2</sub> Br	<b>(12)</b>
X = CH <sub>3</sub>	Y = CH <sub>2</sub> OH	<b>(10)</b>			

**Figure 2.17** Asymmetrical 2,9-difunctionalized-1,10-phenanthrolines.

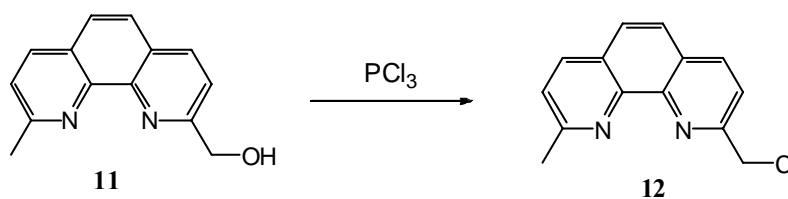
The direct halogenation of 2,9-dimethyl-1,10-phenanthroline **1** by free-radical halogenation using either *N*-chlorosuccinimide (NCS) <sup>[13;29]</sup> or *N*-bromosuccinimide (NBS) <sup>[32]</sup> under diverse reaction conditions <sup>[33]</sup> gave the monohalo product **12** or **13** in extremely poor yield (2%). Therefore, we have used an alternative route for the monofunctionalization of **1** by initial mono *N*-oxide. The *N*-oxide is an ideal intermediate for the synthesis of unsymmetrical 2-functionalised-9-methyl-1,10-phenanthroline derivatives <sup>[34]</sup>. The mono *N*-oxide **9** was obtained by oxidation of **6** with 30% of hydrogen peroxide in glacial acetic acid <sup>[35-36]</sup> at 65°C. The temperature of the reaction is critical. If the temperature is less than 60°C the reaction is not complete and at 70°C the yield diminishes due to the formation of products such as 6,6'-dimethyl-3,3'-diformyl-2,2'-bipyridine *N*-oxide.

This was followed by the Boekelheide rearrangement <sup>[37]</sup> by heating in acetic anhydride to give 2-(acetoxymethyl)-9-methyl-1-10-phenanthroline **10**. Hydrolysis with ethanol and potassium carbonate gave the desired 2-(hydroxymethyl)-9-methyl-1-10-phenanthroline **11** in excellent yield (Figure 2.18) <sup>[34]</sup>. The <sup>1</sup>H NMR spectrum reveals a singlet at δ 5.13 ppm assigned to the methylene group.



**Figure 2.18** Synthesis of 2-(hydroxymethyl)-9-methyl-1,10-phenanthroline **11**.

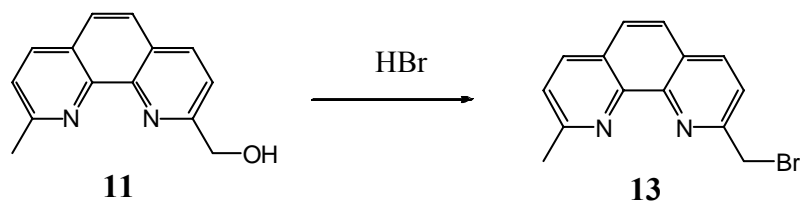
Phosphorus trichloride in  $\text{CHCl}_3$  smoothly transformed 2-(hydroxymethyl)-9-methyl-1,10-phenanthroline **11** into the chloromethyl derivative: 2-(chloromethyl)-9-methyl-1,10-phenanthroline **12** (Figure 2.19) <sup>[34]</sup>. The  $^1\text{H}$  NMR spectrum showed a shift in the resonance of the methylene group from  $\delta$  5.13 ppm in the alcohol to  $\delta$  4.97 ppm in the chloromethyl compound.



**Figure 2.19** Synthesis of 2-(chloromethyl)-9-methyl-1,10-phenanthroline **12**.

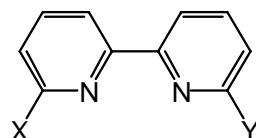
Attempts to obtain the analogous 2-(bromomethyl)-9-methyl-1,10-phenanthroline **13** by reaction with  $\text{PBr}_3$  resulted in reduction to 2,9-dimethyl-1,10-phenanthroline **1** in yields up to 70% and only gave the desired 2-(bromomethyl)-9-methyl-1,10-phenanthroline **13** in 20% yield <sup>[34]</sup>. However, refluxing 2-(hydroxymethyl)-9-methyl-1,10-phenanthroline **11** with hydrobromic acid gave 2-(bromomethyl)-9-methyl-1,10-phenanthroline **13**, in a better yield of

55% (Figure 2.20). The  $^1\text{H}$  NMR spectrum showed a shift in the resonance of the methylene group to  $\delta$  5.06 shift.



**Figure 2.20** Synthesis of 2-(bromomethyl)-9-methyl-1,10-phenanthroline **13**.

### 2.2.3 Synthesis of some 6,6'-disubstituted-2,2'-bipyridines.



$X = Y = \text{CH}_3$	<b>(14)</b>	$X = Y = \text{CH}_2\text{Br}$	<b>(18)</b>
$X = Y = \text{CH}_3\text{OCOCH}_3$	<b>(16)</b>	$X = Y = \text{CH}_2\text{TES}$	<b>(19)</b>
$X = Y = \text{CH}_2\text{OH}$	<b>(17)</b>	$X = Y = \text{CH}_2\text{Cl}$	<b>(20)</b>

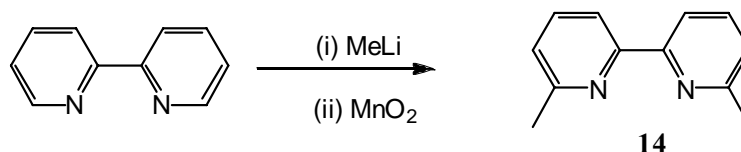
**Figure 2.21** Symmetrical 6,6'-disubstituted-2,2'-bipyridine compounds synthesized.

The first synthesis was that of 6,6'-dimethyl-2,2'-bipyridine **14**. Despite the importance of this ligand in coordination chemistry <sup>[38]</sup>, its synthesis can be a problem, attested by the numerous preparations that have been reported. These involve organometallic, and/ or toxic and unpleasant reagents, low yields, or high temperatures <sup>[13-14; 39-49]</sup>

One of the simplest methods for the synthesis is based upon the coupling of simpler pyridine derivatives <sup>[50-61]</sup>

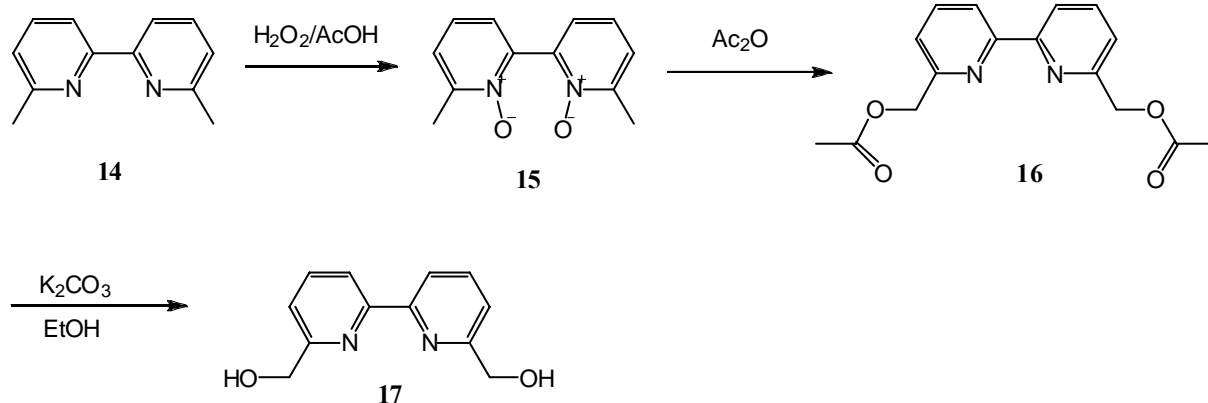
Our first approach to the synthesis of 6,6'-dimethyl-2,2'-bipyridine **14** was the reductive homocoupling of 6-bromo-2-methylpyridine <sup>[49]</sup> with a  $\text{Pd}(\text{OAc})_2$  catalyst. The desired compound was obtained in a relatively low yield (51%) and the reaction involved expensive starting materials and reagents. This result inspired the search for a more efficient synthetic

route and this was found through the direct dimethylation of 2,2'-bipyridine with methyllithium<sup>[14]</sup> in dry THF followed by oxidation of the intermediate tetrahydro compound with MnO<sub>2</sub>. Simple filtration of MnO<sub>2</sub> through celite gave the product in good yield (86%) (Figure 2.22). This reaction is analogous to that used for the preparation of 2,9-dimethyl-1,10-phenanthroline **1** but there only appears to be a single previous report of the direct methylation of 2,2'-bipyridine<sup>[14]</sup>.



**Figure 2.22** Synthesis of 6,6'-dimethyl-2,2'-bipyridine **14**.

In order to further derivatise the 2,2'-bipyridine, we converted the 6,6'-dimethyl-2,2'-bipyridine **1** to 6,6'-dimethyl-2,2'-bipyridine *N,N*-dioxide **15** by treatment with excess of hydrogen peroxide (30%) in acetic acid<sup>[62]</sup>. The compound has previously been prepared using 3-chloroperbenzoic acid as the oxidizing agent<sup>[62]</sup>. The <sup>1</sup>H NMR spectrum of 6,6'-dimethyl-2,2'-bipyridine **14**, is well known from the literature and is a simple first order spectrum. Upon conversion to the bis(*N*-oxide) **15** the <sup>1</sup>H NMR spectrum of the aromatic region is transformed into an ill-defined multiplet. This reaction was followed by the one pot acetylation and Boekelheide rearrangement<sup>[37]</sup> by reflux in acetic anhydride to give 6,6'-bis(acetoxymethyl)-2,2'-bipyridine **16**<sup>[62]</sup>. Hydrolysis with ethanol and potassium carbonate gave the desired 6,6'-di(hydroxymethyl)-2,2'-bipyridine **17** in good yield (Figure 2.23). The <sup>1</sup>H NMR spectrum showed a methylene singlet at δ4.90 ppm and the <sup>13</sup>C NMR spectrum showed the high symmetry with only five signals in the aromatic region and the methylene at δ 65.60 ppm, in agreement with the literature assignments.<sup>[62]</sup>



**Figure 2.23** Synthesis of 6,6'-di(hydroxymethyl)-2,2'-bipyridine **17** from 6,6'-dimethyl-2,2'-bipyridine

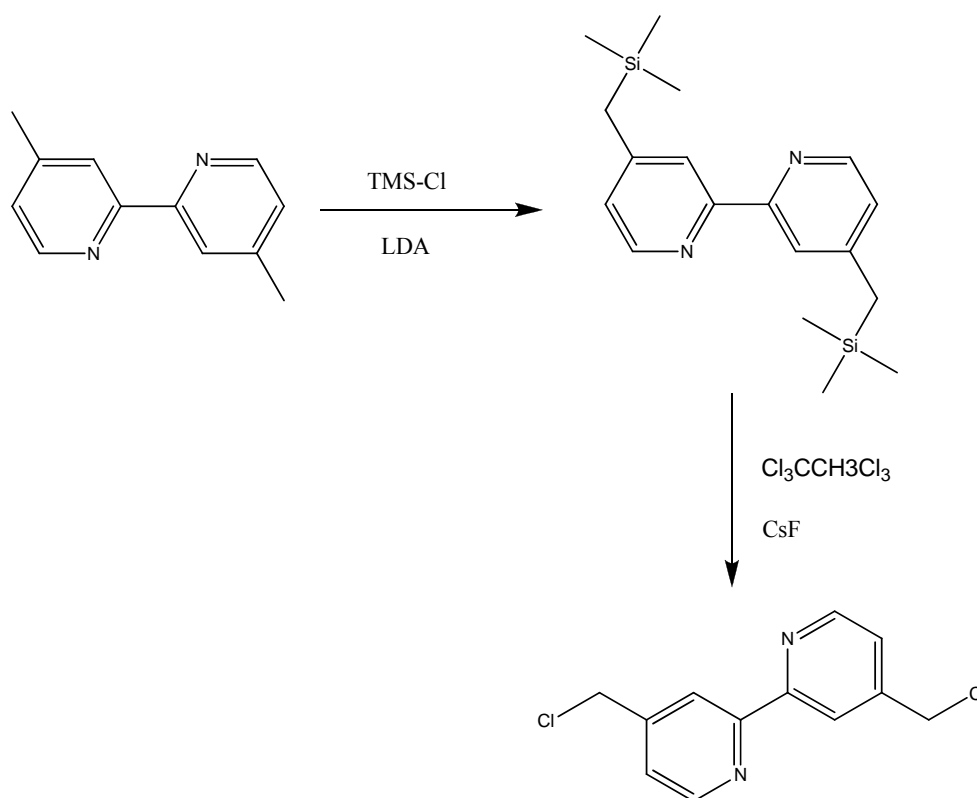
Many methods for the synthesis of simple  $\alpha$ -(halomethyl)pyridines have been reported <sup>[63-67]</sup>. The literature procedures are lengthy and often characterised by low or variable yields when extended to the functionalisation of oligopyridines. The compound 6,6'-di(hydroxymethyl)-2,2'-bipyridine **17** is a key intermediate for the synthesis of such 2,2'-bipyridine derivatives. The next step was the syntheses of 6,6'-bis(bromomethyl)-2,2'-bipyridine **18**. Refluxing of the diol **17** with hydrobromic acid gave the dibromo compound **18** in a yield of 42% (Figure 2.24). The  $^1\text{H}$  NMR spectrum showed a shift in the methylene resonance from  $\delta$  4.90 ppm in the diol due to  $\delta$  4.62 ppm.



**Figure 2.24** Synthesis of 6,6'-bis(bromomethyl)-2,2'-bipyridine **18**

In the literature, 6,6'-bis(chloromethyl)-2,2'-bipyridine has generally been derived from 6,6'-dibromo-2,2'-bipyridine via a lithiation, followed by addition of *N,N*-dimethylformamide to give 2,2'-bipyridine-6,6'-dicarbaldehyde <sup>[68-70]</sup>. Reduction with sodium borohydride in absolute methanol gave the diol **17**, which upon treatment with redistilled thionyl chloride afforded 6,6'-bis(chloromethyl)-2,2'-bipyridine **20** (45%). However, the net molecular weight loss (-2Br), the arduous large-scale lithiations and the poor yields are a good reason to choose alternative procedures for the synthesis of the bis(chloromethyl) derivative **20**. These results

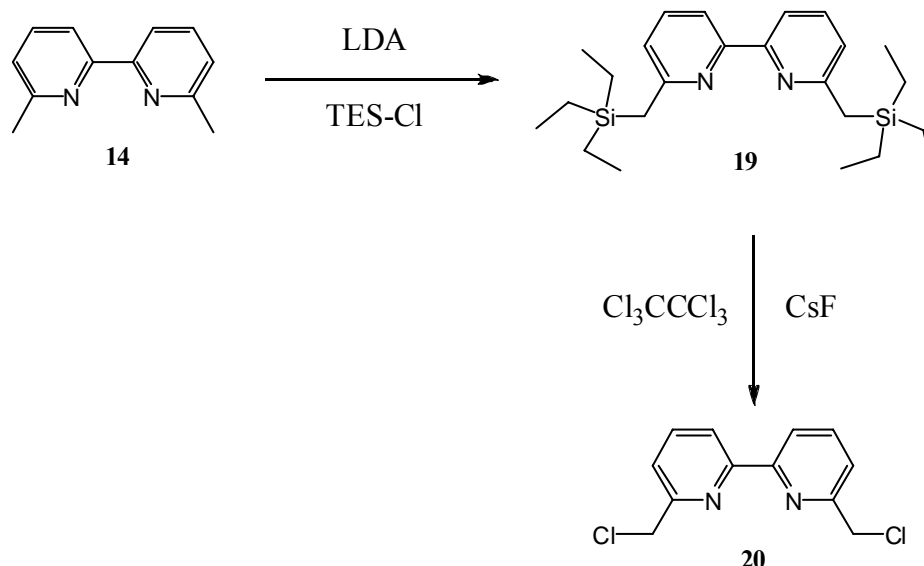
inspired us to search for a more efficient synthetic route to 6,6'-bis(chloromethyl)-2,2'-bipyridine **20**. A recent report described an efficient synthesis of 4,4'-bis(chloromethyl)-2,2'-bipyridine in only two steps in excellent yield (91 %). The 6,6'-dimethyl-2,2'-bipyridine **14** was doubly deprotonated with two equivalents of LDA per methyl group and the resulting dianion was then quenched with chlorotrimethylsilane (TMS-Cl) to give a disilylated intermediate in 97%. The silyl groups were then exchanged for chlorine by treatment with hexachloroethane ( $\text{Cl}_3\text{CCl}_3$ ) and caesium fluoride (CsF) in DMF (Figure 2.25) [71]. We find the bis(trimethylsilyl)ated intermediate to be relatively unstable and not suitable for scale-up.



**Figure 2.25** An efficient synthesis of 4,4'-bis(chloromethyl)-2,2'-bipyridine

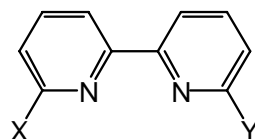
The next attempt was similar to the synthesis of 2,9-dichloromethyl-1,10-phenanthroline **6**, described previously. The 6,6'-dimethyl-2,2'-bipyridine **14** was doubly deprotonated with two equivalents of LDA per methyl group. The resulting dianion was then quenched with chlorotriethylsilane (TES-Cl) to give the bis(triethylsilyl)ated intermediate in 88% yield. The silyl groups were then exchanged for chlorine by treatment with hexachloroethane ( $\text{Cl}_3\text{CCl}_3$ ) and caesium fluoride (CsF) in DMF in 78% yield (Figure 2.26). The  $^1\text{H}$  NMR spectrum of the disilylated intermediate revealed a methylene resonance as a

singlet at  $\delta$  2.43 ppm and the  $^1\text{H}$  NMR spectrum of the 6,6'-dichloromethyl-2,2'-bipyridine **20** showed a shift of this signal to  $\delta$  4.75 ppm.



**Figure 2.26** Synthesis of 6,6'-bis(chloromethyl)-2,2'-bipyridine **20**.

#### 2.2.4 Synthesis of some mono- $\alpha$ -functional 6,6'-dimethyl-2,2'-bipyridines.



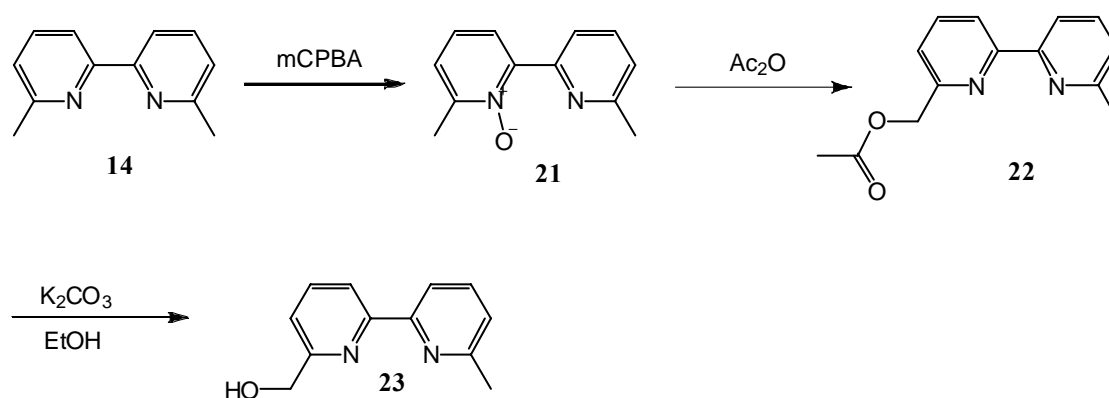
- |                     |  |             |                     |                        |             |
|---------------------|--|-------------|---------------------|------------------------|-------------|
| X = CH <sub>3</sub> | Y = CH <sub>3</sub>                    | <b>(14)</b> | X = CH <sub>3</sub> | Y = CH <sub>2</sub> Br | <b>(24)</b> |
| X = CH <sub>3</sub> | Y = CH <sub>3</sub> OCOCH <sub>3</sub> | <b>(22)</b> | X = CH <sub>3</sub> | Y = CH <sub>2</sub> Cl | <b>(25)</b> |
| X = CH <sub>3</sub> | Y = CH <sub>2</sub> OH                 | <b>(23)</b> |                     |                        |             |

**Figure 2.27** Some mono- $\alpha$ -functionalized derivatives of 6,6'-dimethyl-2,2'-bipyridines.

As described above, good methods were found for the synthesis of symmetrical 6,6'-difunctionalised 2,2'-bipyridines. Alternative methods were developed for the preparation of unsymmetrically 6,6'-difunctionalized 2,2'-bipyridines. The unsymmetrical alcohol **23** was prepared using *N*-oxide methodology. The treatment of 6,6'-dimethyl-2,2'-bipyridine **14** with exactly 1 equivalent of *m*-chloroperbenzoic acid (MCPBA) in chloroform at 0°C gave the



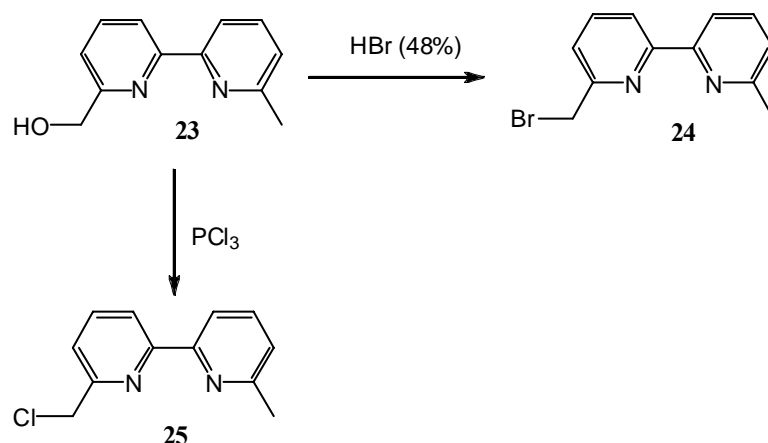
mono *N*-oxide in 72% yield. The Boekelheide rearrangement strategy <sup>[37]</sup> was then used to modify the 6 position. The *N*-oxide **21** was treated with acetic anhydride to give 6-(acetoxymethyl)-6'-methyl-2,2'-bipyridine **22** <sup>[62]</sup>. Subsequent treatment with potassium carbonate in ethanol gave the desired product, 6-(hydroxymethyl)-6'-methyl-2,2'-bipyridine **23** <sup>[62]</sup> in 98% yield (Figure 2.28). <sup>1</sup>H NMR spectroscopy revealed a spectrum characteristic of a non-symmetrical 2,2'-bipyridine: in the aliphatic region the methylene and methyl groups are observed as singlets at  $\delta$  4.81 ppm and  $\delta$  2.62 ppm respectively. The <sup>13</sup>C NMR spectrum revealed 12 peaks as expected for the unsymmetrical molecule.



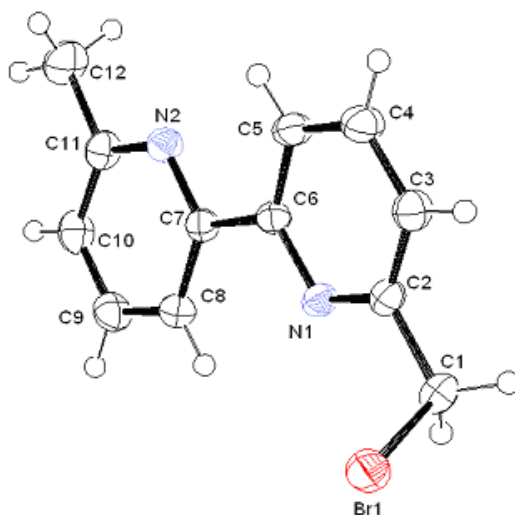
**Figure 2.28** Synthesis of 6-(hydroxymethyl)-6'-methyl-2,2'-bipyridine **23**.

The monobromo compound **24** was synthesized using the same conditions as the the monobromo phen **13** species, that is, by reacting the mono-alcohol **23** with hydrobromic acid, to give the desired product in a yield of 65% (Figure 2.29). Again, the methylene singlet is a characteristic indicator for this reaction and is observed in the product at  $\delta$  4.63 ppm shift.

Analogous to the preparation of the monochloro 1,10-phenanthroline derivative **12**, phosphorus trichloride in CHCl<sub>3</sub> smoothly transformed 6-(hydroxymethyl)-6'-methyl-2,2'-bipyridine **23** into the chloromethyl derivative **25** (Figure 2.29) <sup>[62]</sup>. The <sup>1</sup>H NMR spectrum showed a methylene singlet at  $\delta$  4.74 ppm as expected.



**Figure 2.29** Synthesis of 6-(bromomethyl)-6'-methyl-2,2'-bipyridine **24** and 6-(chloromethyl)-6'-methyl-2,2'-bipyridine **25**.



**Figure 2.30** ORTEP representation of the 6-(bromomethyl)-6'-methyl-2,2'-bipyridine **24**.

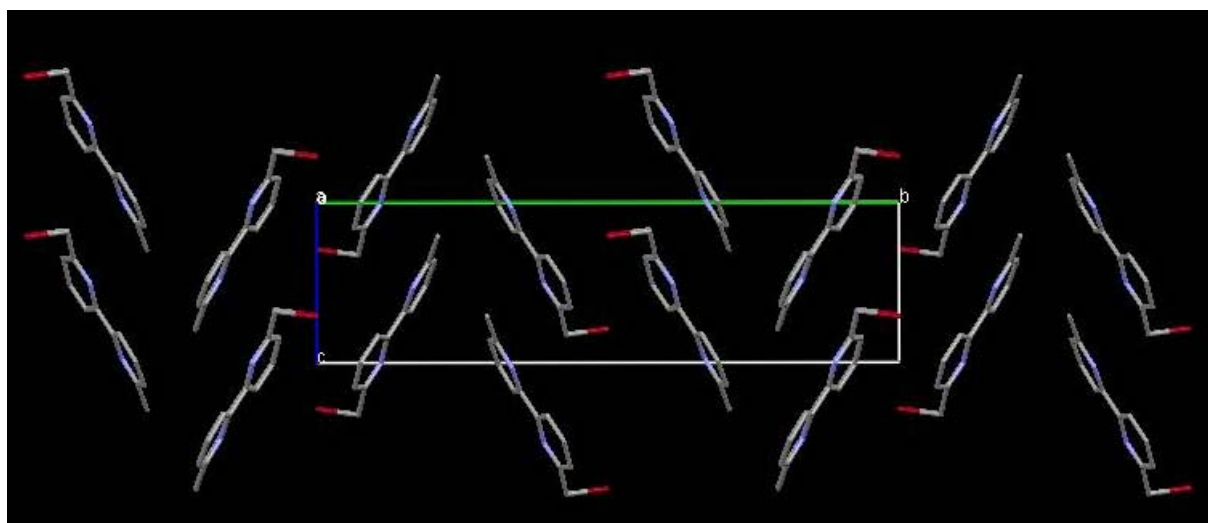
Bond	Distance/ Å	Bond	Distance/ Å
C(1)-C(2)	1.499(2)	C(11)-C(12)	1.502(2)
Br(1)-C(1)	1.9651(17)	N(1)-C(6)	1.3503(19)
N(1)-C(2)	1.336(2)	N(2)-C(7)	1.3491(19)
N(2)-C(11)	1.338(2)		

Bond	Angles/°	Bond	Angles/°
Br(1)-C(1)-C(2)	110.38(11)	C(6)-C(7)-N(2)	116.69(13)
C(1)-C(2)-N(1)	116.33(14)	N(2)-C(11)-C(12)	116.36(16)
N(1)-C(6)-C(7)	116.59(13)		

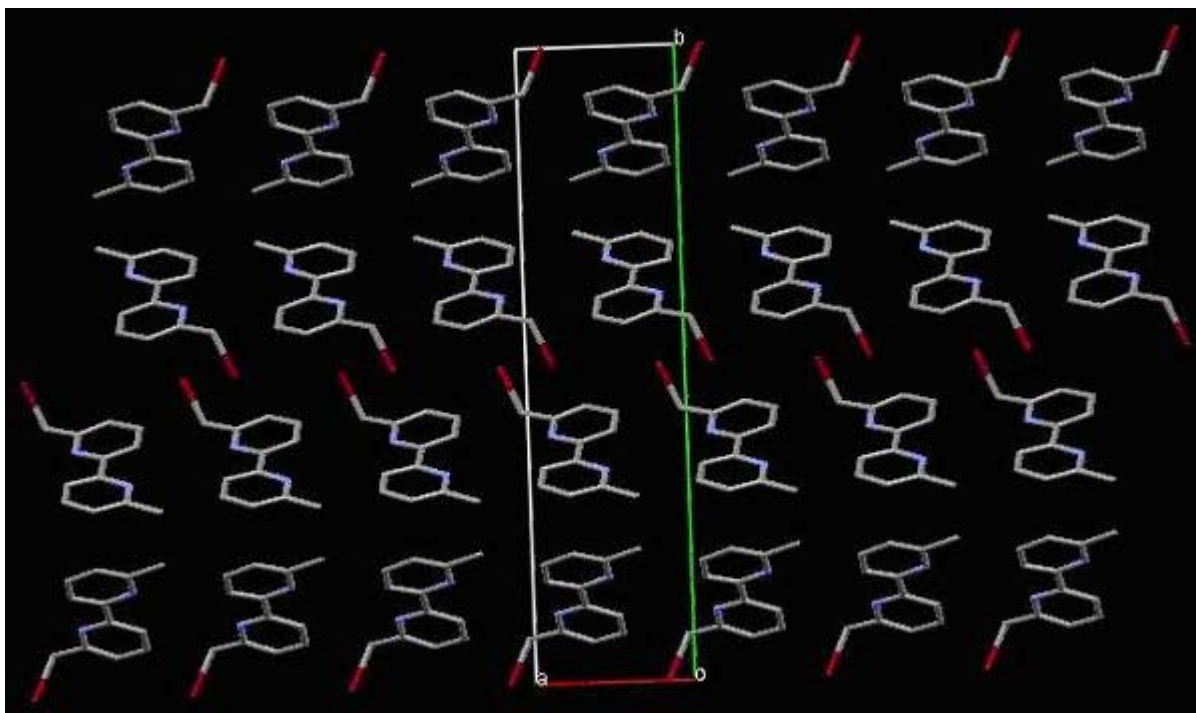
N(1)-C(6)-C(7)-N(2)	174.34	N(1)-C(6)-C(7)-C(8)	6.96
---------------------	--------	---------------------	------

**Table 2.4** Selected bonds lengths ( $\text{\AA}$ ), angles ( $^\circ$ ), and torsion angles ( $^\circ$ ) for the 6-(bromomethyl)-6'-methyl-2, 2'-bipyridine **24**.

We have obtained X-ray quality crystals of the bromomethyl compound and have determined the solid state structure of the compound. The compound adopts the expected trans conformation of the pyridine rings about the interannular C-C bond. The 2,2'-bipyridine is not absolutely planar, with an N1-C6-C7-N2 torsion angle of  $174.34^\circ$ . The packing is interesting, with the molecules arranged in ribbons packed in a type of double herringbone' arrangement. This is best viewed along the b axis. Steric, rather than electronic, considerations seem to dictate the packing in this system, as there is no convincing hydrogen-bonding evident (figure 2.31).



**Figure 2.31** Packing in 6-(bromomethyl)-6'-methyl-2, 2'-bipyridine, as viewed along the a axis, showing the 'herringbone' arrangement.



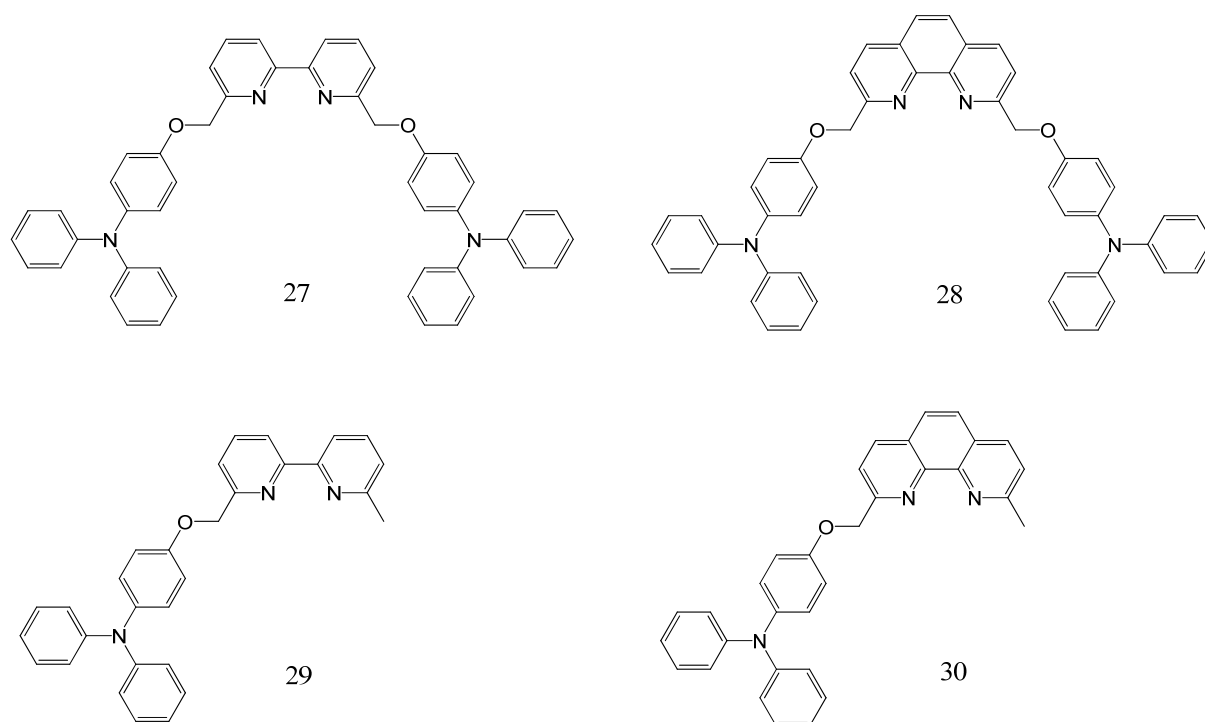
**Figure 2.32** Packing in 6-(bromomethyl)-6'-methyl-2,2'-bipyridine **24**, as viewed along the *c* axis

### 2.2.5 Synthesis of some 6,6'-disubstituted-2,2'-bipyridine and 2,9-disubstituted-1,10-phenanthroline with triphenylamine substituents.

Triphenylamine was used for several reasons:

- (1) The large steric size of the ligand should impose geometrical restrictions on the CuI coordination site which is very interesting from both an X-ray and luminescent lifetime point of view.
- (2) The fact that the triphenylamine is redox active and in the ground state a strong electron donor could influence the electrochemistry of the complexes greatly and that of the triphenylamine-ligand.
- (3) As triphenylamine complexes are widely used in OLED and DSSC application in ruthenium chemistry, these systems could also be used to gain an understanding of the complexes and therefore contribute to the development of CuI complexes in such applications.

## 2.2.5.1 Non conjugated ligands

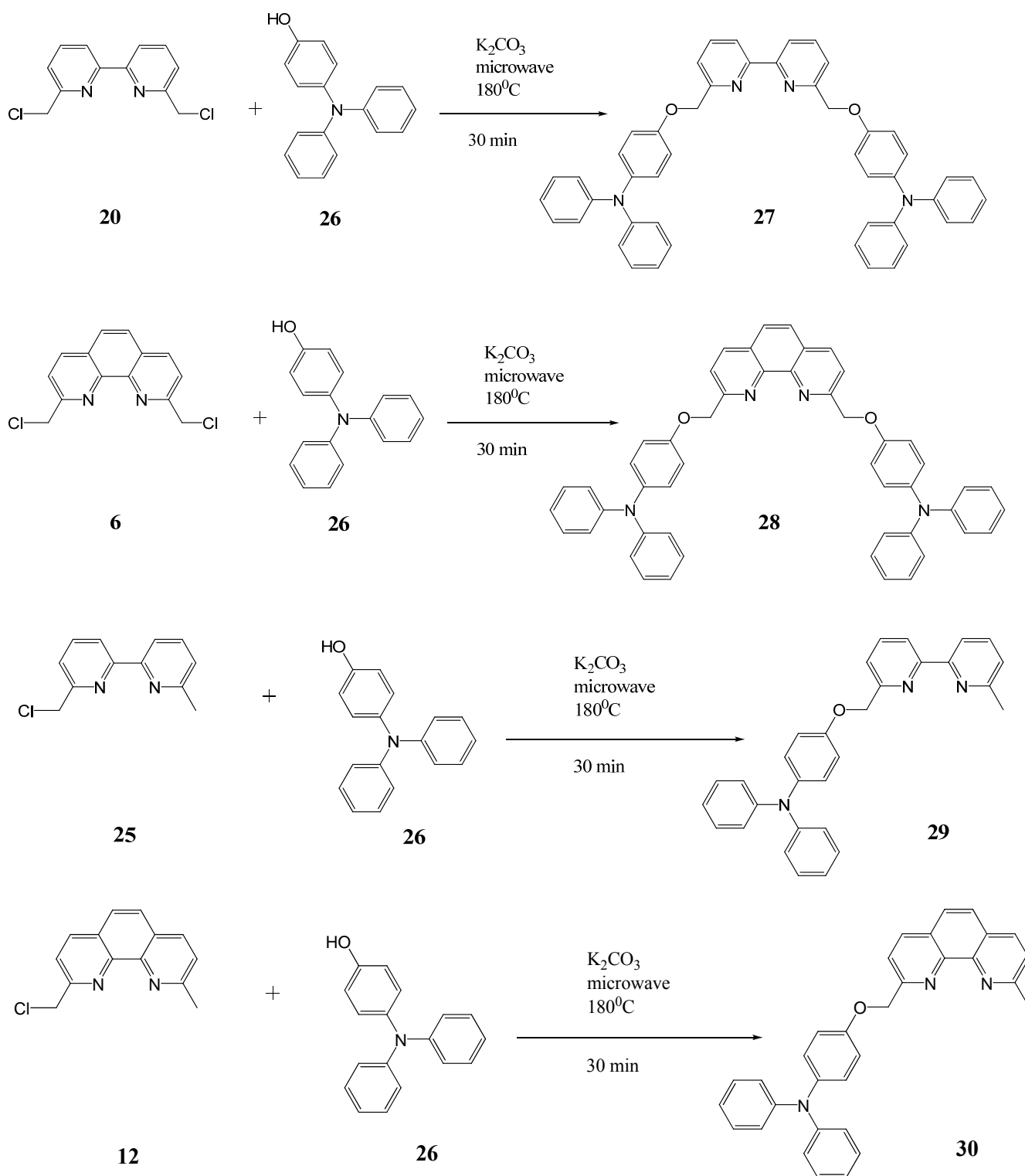


**Figure 2.33** Some 6,6'-disubstituted-2,2'-bipyridine and 2,9'-disubstituted-1,10-phenanthroline with triphenylamine substituents.

General synthetic scheme pathway.

The non-conjugated ligands were synthesised by condensation of the appropriate halomethyl-functionalised 2,2'-bipyridine or 1,10-phenanthroline derivatives and 4-(*N,N*-diphenylamino)phenol under microwave conditions in the presence of a base.

All microwave irradiation experiments were carried out using the *Biotage Synthesizer*. All experiments were carried out in sealed microwave process vials at 180<sup>0</sup>C for 30 minutes in acetonitrile solvent. The reaction involved 1 equivalent of the bischloromethyl derivative and 2.1 equivalents of the 4-(*N,N*-diphenylamino)phenol for the bis adducts and a 1:1.1 ratio for the mono adducts in the presence of 10 equivalents of K<sub>2</sub>CO<sub>3</sub>. After the reaction, the vessel was allowed to cool and the residue taken up in CH<sub>2</sub>Cl<sub>2</sub>, the solution washed with water, dried and filtered. The impure solids were then recrystallised from CH<sub>2</sub>Cl<sub>2</sub>/diethyl ether mixtures to yield pure off-white solids (Figure 2.34).

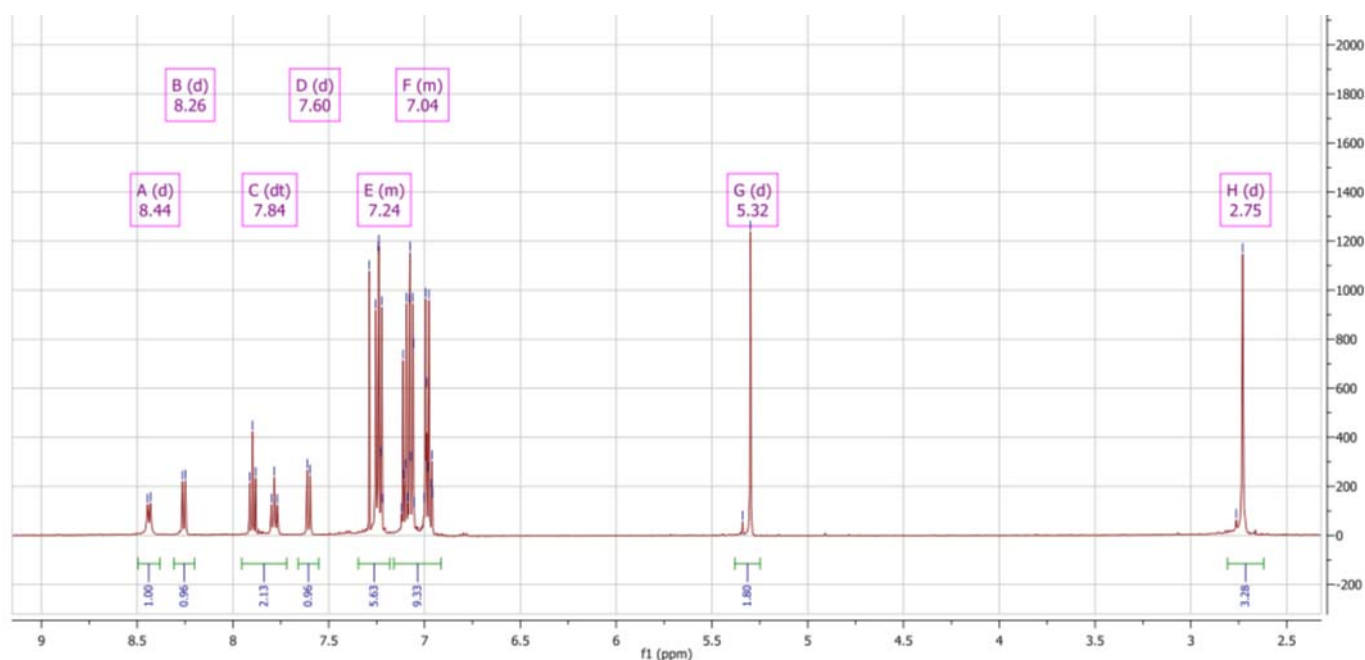


**Figure 2.34** Synthetic schemes of some 6,6'-disubstituted-2,2'-bipyridine and 2,9-disubstituted-1,10-phenanthrolines with triphenylamine substituents.

These compounds were analyzed by  $^1H$  and  $^{13}C$  NMR spectroscopy at 400 MHz in  $CDCl_3$ , ES mass spectrometry and elementary analysis.

The  $^1\text{H}$  NMR spectra of the four ligands showed a shift in the resonance of the methylene group.

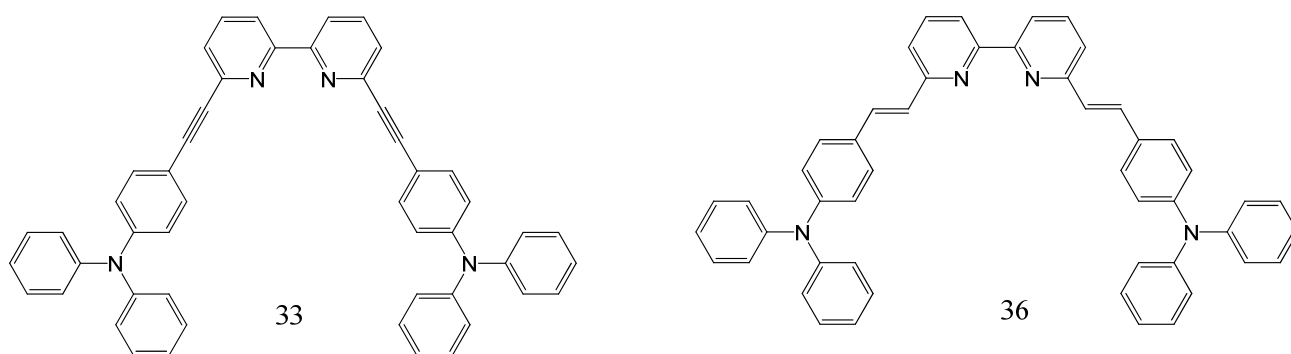
For example, the  $^1\text{H}$  NMR spectra of 6-(4-(*N,N*-diphenylamino)phenoxy)methyl)-6'-methyl-2,2'-bipyridine **29** showed 5 peaks between 7.60 and 8.44 ppm, characteristic of the pyridine protons of the unsymmetric bpy ligands (A, B, C D). The spectrum showed a shift in the resonance of the methylene group from  $\delta$  4.74 ppm in the chloromethyl compound **25** to  $\delta$  5.30 ppm in the compound **29** (Figure 2.35). The  $^{13}\text{C}$  NMR spectrum revealed 20 peaks as expected.



**Figure 2.35**  $^1\text{H}$  NMR spectrum of 6-(4-(*N,N*-diphenylamino)phenoxy)methyl)-6'-methyl-2,2'-bipyridine **29** in  $\text{CDCl}_3$  at 400 MHz.

The  $^1\text{H}$  NMR spectrum of 2,9-bis(4-(*N,N*-diphenylamino)phenoxy)methyl)-1,10-phenanthroline **28** showed 3 peaks between 7.83 and 8.33 ppm, 2 doublets and a singlet, characteristic of the pyridine protons of the symmetric phen ligands. The spectrum showed a shift in the resonance of the methylene group from  $\delta$  4.96 ppm in the chloromethyl compound **36** to  $\delta$  5.59 ppm in the compound **28**. The  $^{13}\text{C}$  NMR spectrum revealed 15 peaks as expected.

## 2.2.5.2 Conjugated ligands

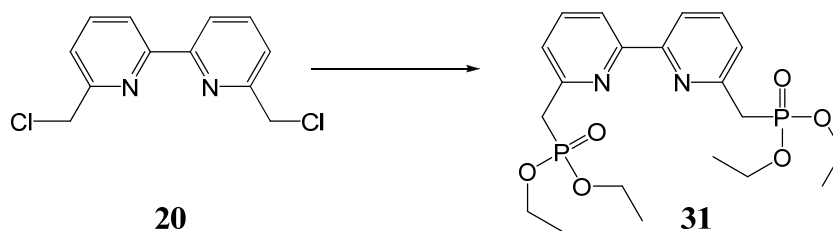


**Figure 2.36** Conjugated bipyridines with triphenylamine substituents.

**(1) Synthesis of ethenyl ligand: 6,6'-bis(2-(4-(*N,N*-diphenylamino)phenyl)ethenyl)-2,2'-bipyridine **33**:**

6,6'-Bis(phosphonate)-2,2'-bipyridine **31** was synthesized quantitatively by means of an Arbuzov reaction from the 6,6'-bis(chloromethyl)-2,2'-bipyridine precursor **20** (Figure 2.37). 6,6'-Bis(chloromethyl)-2,2'-bipyridine and triethylphosphite were heated at 80 °C for 6 h. The solution was then allowed to cool to room temperature, and triethylphosphite were removed under reduced pressure. The oily brown residue was taken up with pentane (20 mL). The residue was redissolved in CH<sub>2</sub>Cl<sub>2</sub> and purified by column chromatography. The fractions containing the pure product were combined and evaporated to dryness to give a white solid in 90 % yield.

The <sup>1</sup>H NMR spectrum showed a shift in the resonance of the methylene group from δ 4.75 ppm to δ 3.48 ppm and the <sup>31</sup>P NMR spectrum at 162 MHz showed a peak at δ 22.17 ppm.

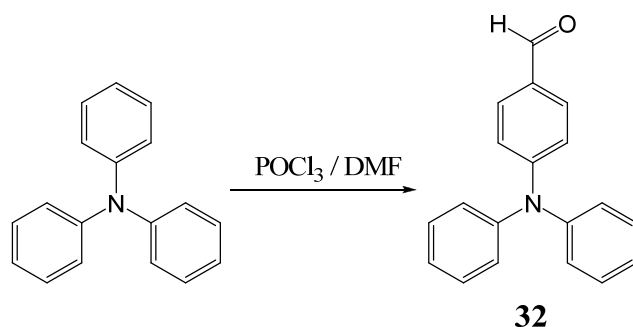


**Figure 2.37** Synthesis of 6,6'-Bis(phosphonate)-2,2'-bipyridine **31**



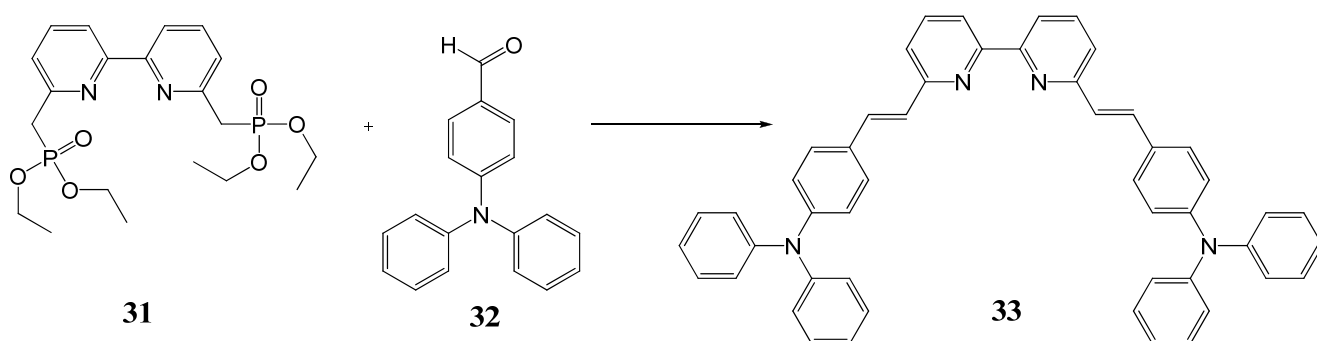
4-(Diphenylamino)benzaldehyde **32** was prepared via formylation of triphenylamine.

Triphenylamine was dissolved in DMF. POCl<sub>3</sub> was added dropwise to the mixture at 0°C. The reaction was next heated to 145°C for 2 h. After cooling, the mixture was poured into an ice-bath with stirring and later neutralized with sodium carbonate. Pale yellow solids were collected by filtering and recrystallized in ethanol in 66 % yield (Figure 2.38). The <sup>1</sup>H NMR spectrum revealing the CHO singlet at 9.79 ppm.



**Figure 2.38** Synthesis of the 4-(diphenylamino)benzaldehyde **32**

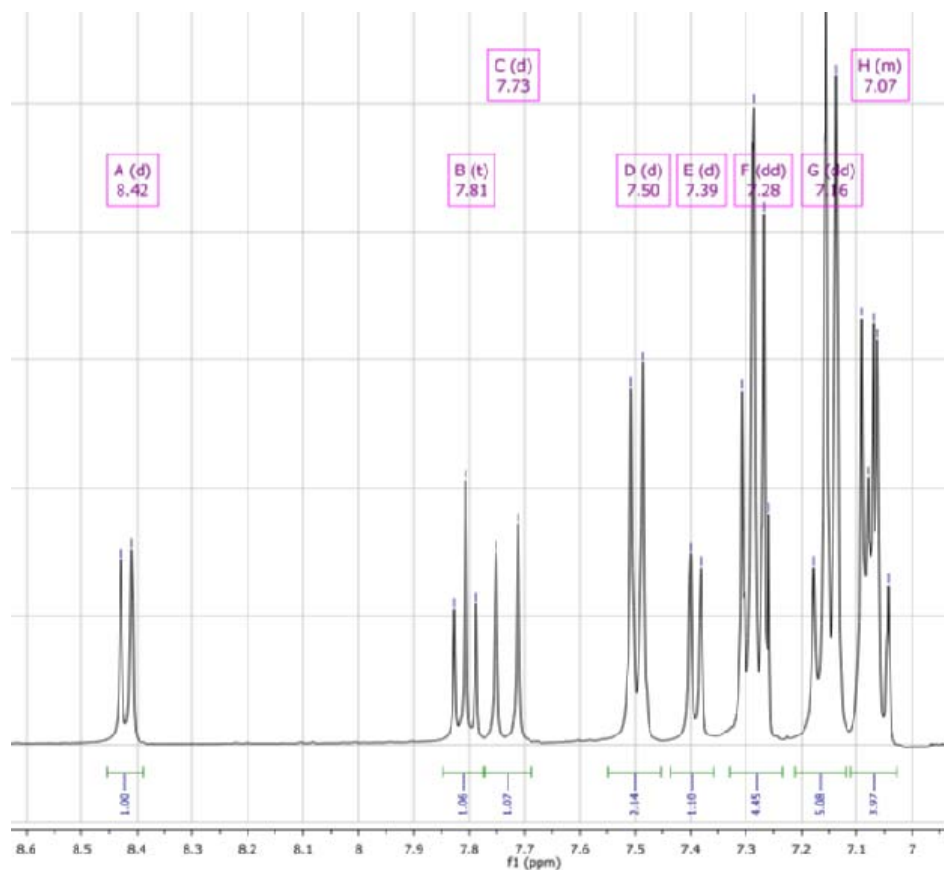
Finally, treatment of **31** with the aldehydes **32** under normal Wittig conditions gave the desired ethenyl ligand **33** (Figure 2.39):



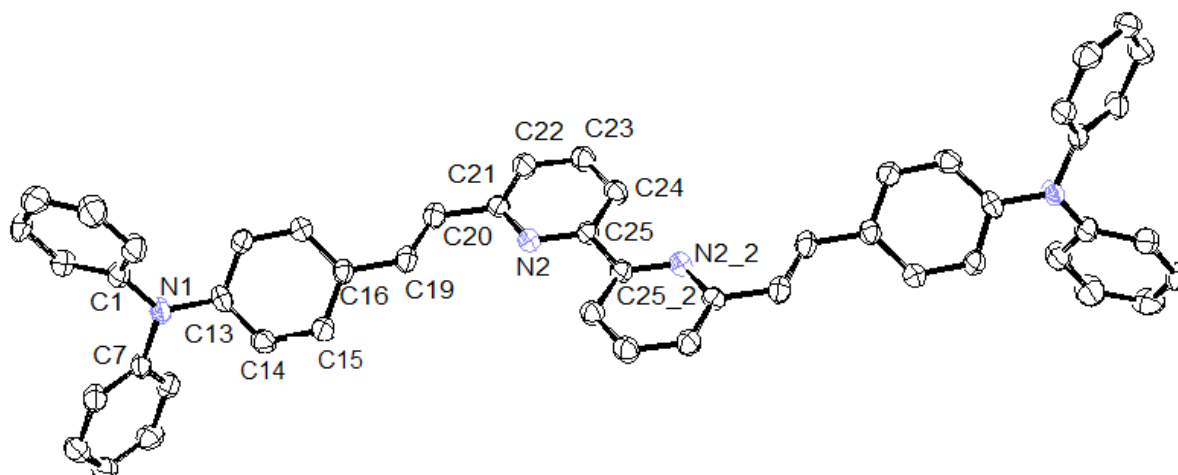
**Figure 2.39** Synthesis of the ethenyl ligand: 6,6'-bis(2-(4-(*N,N*-diphenylamino)phenyl)ethenyl)-2,2'-bipyridine **33**.

Potassium *tert*-butoxide was added to a solution of **31** and **32** in THF. The reaction mixture was stirred for 2 h at room temperature. After addition of water, THF was removed under reduced pressure, and the aqueous residue was extracted with CH<sub>2</sub>Cl<sub>2</sub>. The collected organic layers were washed with brine and water, dried over magnesium sulfate, and filtered. After

evaporation of the solvent, precipitation from  $\text{CH}_2\text{Cl}_2$ /pentane afforded the desired ethenyl ligand: 6,6'-bis(2-(4-(*N,N*-diphenylamino)phenyl)ethenyl)-2,2'-bipyridine **33** in 54 % yield (Figure 2.39).



**Figure 2.40**  $^1\text{H}$  NMR spectrum of 6,6'-bis(2-(4-(*N,N*-diphenylamino)phenyl)ethenyl)-2,2'-bipyridine **33** in  $\text{CDCl}_3$  at 400 MHz.



**Figure 2.41** ORTEP representation of the 6,6'-bis(2-(4-(*N,N*-diphenylamino)phenyl)ethenyl)-2,2'-bipyridine. Hydrogen atoms have been omitted for clarity.

Bond	Distance/Å	Bond	Distance/Å
C(21)-N(2)	1.341(5)	N(2)-C(25)	1.349(4)
C(21)-C(20)	1.477(5)	N(1)-C(13)	1.418(4)
C(20)-C(19)	1.337(5)	N(1)-C(1)	1.416(4)
C(19)-C(16)	1.461(5)	N(1)-C(7)	1.418(4)

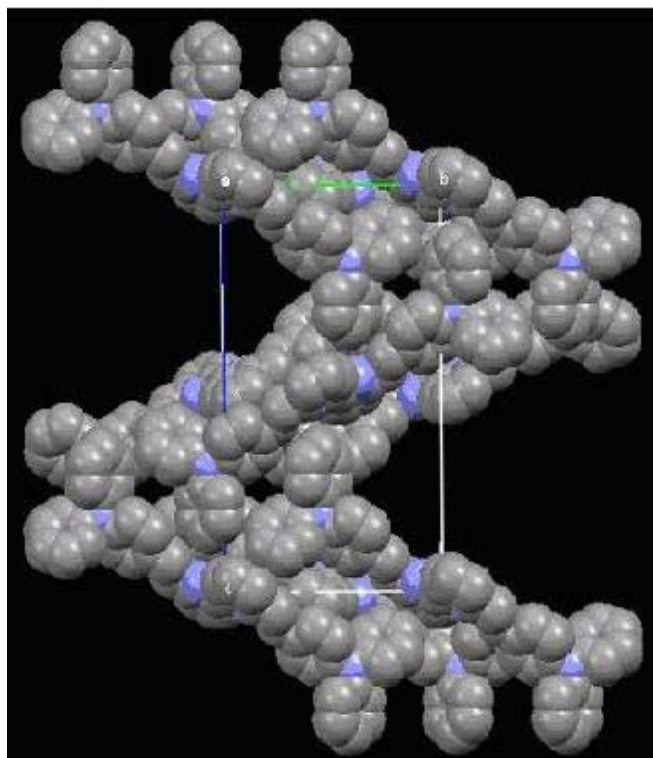
Bond	Angles/°	Bond	Angles/°
N(2)-C(21)-C(20)	117.5(3)	C(14)-C(13)-N(1)	119.2(3)
C(21)-C(20)-C(19)	123.7(3)	C(13)-N(1)-C(1)	120.9(3)
C(20)-C(19)-C(16)	127.3(3)	C(13)-N(1)-C(7)	118.6(3)
C(19)-C(16)-C(15)	123.6(3)	C(1)-N(1)-C(7)	119.4(3)

N(2)-C(25)-C'(25)-N'(2)	180.00	N(2)-C(25)-C'(25)-C'(24)	6.96
-------------------------	--------	--------------------------	------

**Table 2.5** Selected bonds lengths (Å), angles (°), and torsion angles (°) in 6,6'-bis(2-(4-(*N,N*-diphenylamino)phenyl)ethenyl)-2,2'-bipyridine **33**.

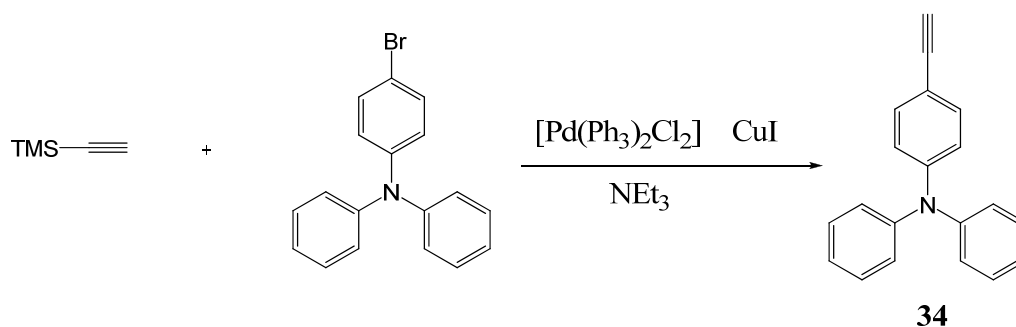
The compound, 6,6'-bis(2-(4-(*N,N*-diphenylamino)phenyl)ethenyl)-2,2'-bipyridine **33**, is a symmetrical 2,2'-bipyridine with the 4-ethenylphenyldiphenylamine substituent attached to the 6- and 6'- positions. The compound was obtained as X-ray quality crystals and the structure has been determined. The ligand adopts the expected trans conformation with respect to the orientation of the pyridyl rings about the interannular C-C bond. There is a centre of symmetry between the 2- and 2'- carbons. The central 2,2'-bipyridine unit is perfectly planar. The ethenyl groups has the trans-arrangement as expected in the basis of the <sup>1</sup>H NMR spectrum (H-H coupling constant  $J = 15.9$  Mz). The packing has a number of features of interest. The ligands are arranged in corrugated layers, as apparent by viewing along the *c* axis. Viewing along the *a* axis affords an elegant perspective of the system, as shown in Figure 2.42. Surprisingly for a system with so many rings, there is a dearth of face-to-face  $\pi$ - $\pi$  interactions, with none being found by this researcher. This is primarily a function of the non-planar and sterically demanding triphenylamine moieties. The three aromatic substituents on the amine nitrogen describe a flattened trigonal arrangement with the least squares planes through the phenyl rings making an interplanar angle of 64.68° and angles of 71.53° and 69.56° with the 4-substituted phenyl ring. There are extensive edge-to-face interactions between aromatic rings.



**Figure 2.42** Packing in the lattice of 6,6'-bis(2-(4-(*N,N*-diphenylamino)phenyl)ethynyl)-2,2'-bipyridine **33**, as viewed along the *a* axis.

**(2) Synthesis of the ethynyl ligand: 6,6'-bis(2-(4-(*N,N*-diphenylamino)phenyl)ethynyl)-2,2'-bipyridine **36**:**

First, (4-Bromophenyl)diphenylamine, commercially available, was functionalized with TMS-acetylene and subsequent removal of the TMS group gave 4-(ethynylphenyl)diphenylamine **4** in 56 % yield<sup>[72]</sup>.

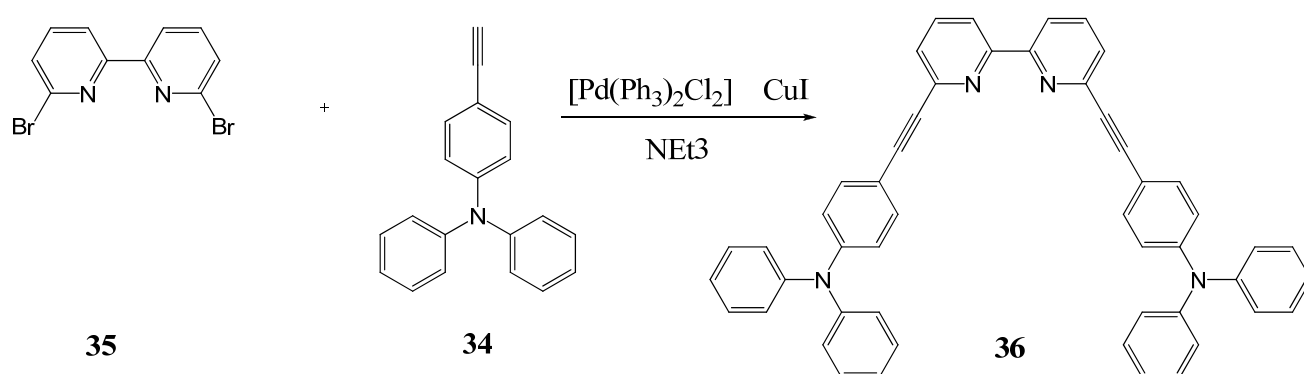


**Figure 2.43** Synthesis of the 4-(ethynylphenyl)diphenylamine **4**

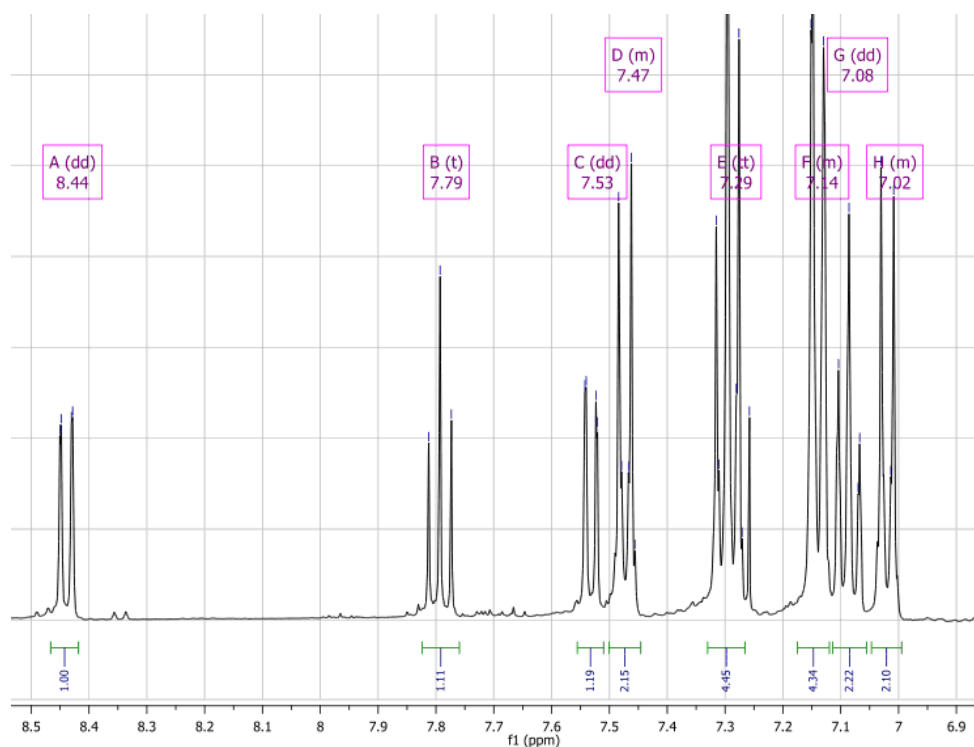
Finally, treatment of **34** with the 6,6'-dibromo-2,2'-bipyridine **35** under normal Sonogashira conditions gave the desired ethynyl ligand **36** (Figure 2.44).

To a mixture of 6,6'-dibromo-2,2'-dipyridine, CuI, triphenylphosphine and  $[\text{Pd}(\text{PPh}_3)_2\text{Cl}_2]$  was added triethylamine under  $\text{N}_2$ . 4-(Ethynylphenyl)diphenylamine was introduced portion wise, and the reaction mixture was allowed to stir at room temperature overnight after which the reaction was quenched by pouring over distilled water. The aqueous layer was extracted with  $\text{CH}_2\text{Cl}_2$ , and the combined organic phases were dried and concentrated. The residue was chromatographed on silica gel (elution with 1:1  $\text{CH}_2\text{Cl}_2$ /hexane) to provide a yellow solid (94 mg, 42%), the desired compound **36**.

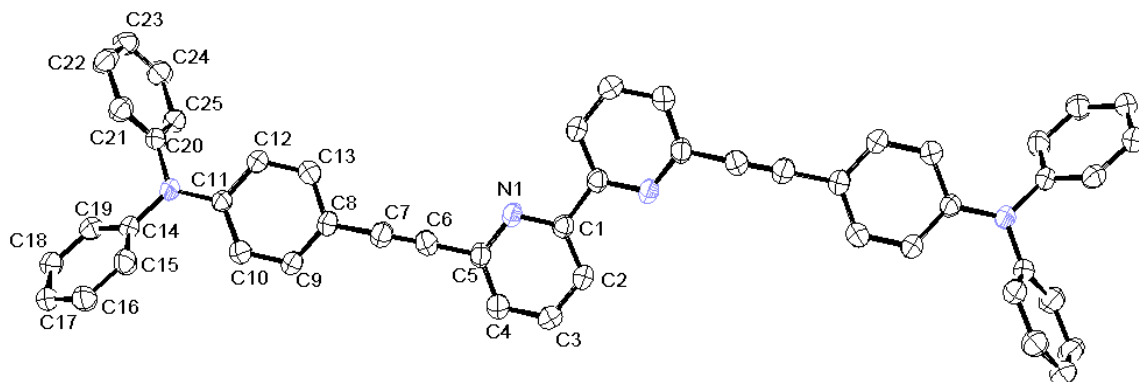
The  $^{13}\text{C}$  NMR spectrum revealed 15 peaks as expected.



**Figure 2.44** Synthesis of the ethynyl ligand: 6,6'-bis(2-(4-(N,N-diphenylamino)phenyl)ethynyl)-2,2'-bipyridine **36**.



**Figure 2.45**  $^1\text{H}$  NMR spectrum of 6,6'-bis(2-(4-(*N,N*-diphenylamino)phenyl)ethynyl)-2,2'-bipyridine **36** in  $\text{CDCl}_3$  at 400 MHz.



**Figure 2.46** ORTEP representation of the ethynyl ligand: 6,6'-bis(2-(4-(*N,N*-diphenylamino)phenyl)ethynyl)-2,2'-bipyridine **36**.

Bond	Distance/ Å	Bond	Distance/ Å
C(1)-C(1)#1	1.483(4)	C(7)-C(8)	1.430(3)
C(4)-C(5)	1.383(3)	C(11)-N(8)	1.395(2)
C(5)-C(6)	1.442(3)	C(14)-N(8)	1.427(2)
C(6)-C(7)	1.195(3)	C(20)-N(8)	1.434(2)
C(5)-N(1)	1.345(2)		

Bond	Angles/°	Bond	Angles/°
C(4)-C(5)-N(1)	122.92(17)	C(7)-C(8)-C(9)	121.24(18)
C(5)-N(1)-C(1)	117.56(16)	C(7)-C(8)-C(13)	120.86(18)
C(6)-C(5)-N(1)	117.14(1)	C(20)-N(8)-C(14)	116.91(14)
C(5)-C(6)-C(7)	177.6(2)	C(20)-N(8)-C(11)	120.27(15)
C(4)-C(5)-C(6)	119.92(18)	C(14)-N(8)-C(11)	122.75(15)
C(6)-C(7)-C(8)	177.9(2)		

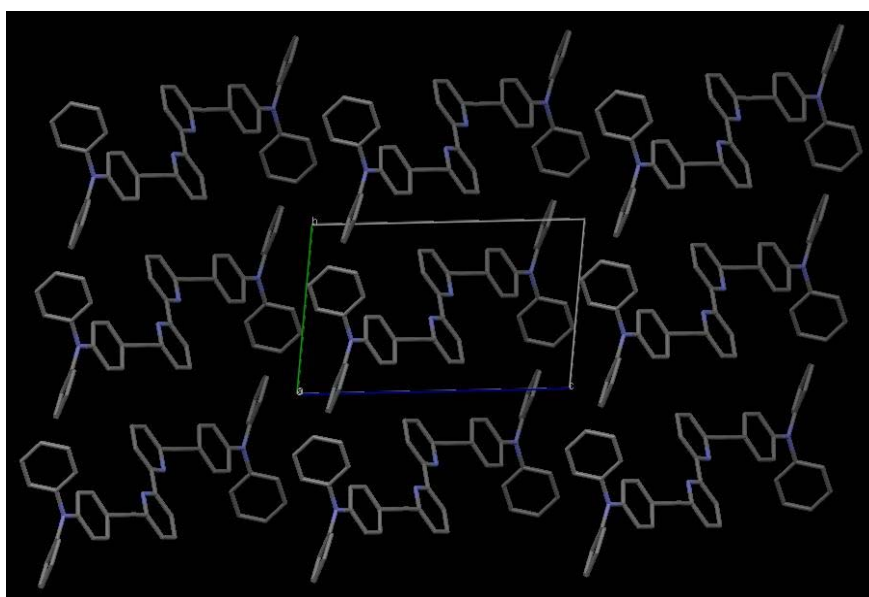
  

N(1)-C(1)-C'(1)-N'(1)	180°	N(1)-C(1)-C'(1)-C'(2)	0.31°
-----------------------	------	-----------------------	-------

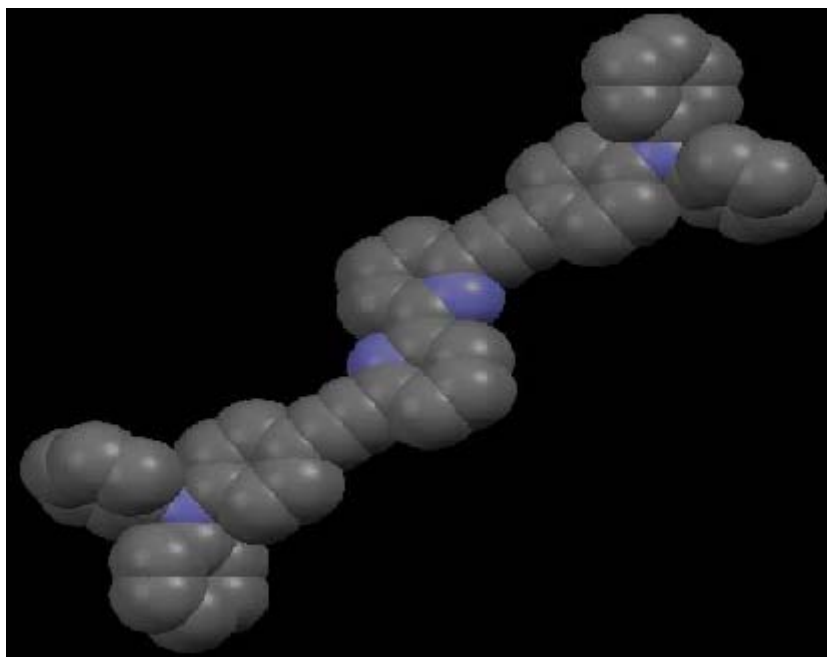
**Table 2.6** Selected bonds lengths (Å), angles (°), and torsion angles (°) in 6,6'-bis(2-(4-(*N,N*-diphenylamino)phenyl)ethynyl)-2,2'-bipyridine **36**.

X-ray quality crystals of ligand **36** were grown from a CH<sub>2</sub>Cl<sub>2</sub> solution of **36**. The title compound is a triphenylamine *N,N'*-disubstituted bipyridine, with the asymmetric unit being half of one molecule. The bipyridyl unit adopts a *trans* conformation and is necessarily planar, with an N1-C1-C1'-N1' torsion angle of 0.00°. The triple-bond environment is almost linear, with both C5-C6-C7 and C6-C7-C8 angles being 178°.

The packing is very efficient, with adjacent molecules being superimposed as one looks along a, b and c axes (Figure 2.47). The distance between the centroid of ring C8-C9-C10-C11-C12-C13 and that of N1'-C1'-C2'-C3'-C4'-C5' is 3.893 Å, with a C3'-centroid-centroid angle of 109.2°. These values are typical for a  $\pi$ - $\pi$  stacking interaction.



**Figure 2.47** View of the packing of **36** along a axis.



**Figure 2.48** 6,6'-Bis(2-(4-(*N,N*-diphenylamino)phenyl)ethynyl)-2,2'-bipyridine **36**.



## 2.3 6,6'-Disubstituted-2,2'-bipyridine and 2,9-disubstituted-1,10-phenanthroline copper(I) complexes.

### 2.3.1 General method for the synthesis of copper(I) 1,10-phenanthroline and 2,2'-bipyridine complexes.

A solution of one equivalent of  $[\text{Cu}(\text{MeCN})_4][\text{PF}_6]$  in degassed acetonitrile was treated with two equivalents of the 1,10-phenanthroline or 2,2'-bipyridine ligand and the mixture was ultrasonicated for 1h at room temperature. The mixtures turned dark red instantaneously, indicating the formation of the complexes. The complete dissolution of the ligand marked the end of complexation. Any unreacted  $[\text{Cu}(\text{MeCN})_4][\text{PF}_6]$  was removed by filtration over celite. The solvent was concentrated in vacuo to give a red solid. The complexes were recrystallised from  $\text{CH}_2\text{Cl}_2/\text{Et}_2\text{O}$ .

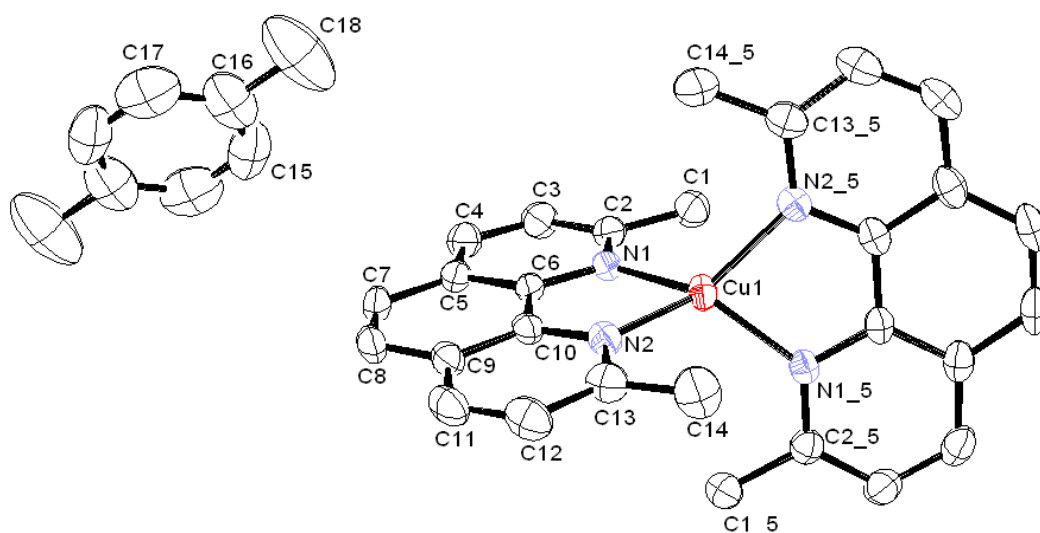
### 2.3.2 Description of crystal structures of the copper(I) complexes obtained.

The  $\{\text{Cu}(\text{phen})_2\}^+$  coordination motif has long been championed as a viable alternative to  $\{\text{Ru}(\text{bpy})_3\}^{2+}$  domains in the design of photoactive devices <sup>[73-74]</sup>. In order to stabilise the copper(I) centre it is necessary to introduce substituents at the 2- or 2,9-positions of the 1,10-phenanthroline. The most common derivatives have methyl or aryl substituents at these positions and 2,9-dimethyl-1,10-phenanthroline **1** (neocuproin or neocuproine) was rapidly identified as one of the reagents of choice for the spectrophotometric analysis of copper <sup>[75-78]</sup>. The useful photophysical properties of  $[\text{Cu}(\mathbf{1})_2]^+$  were first reported by McMillin and coworkers <sup>[79]</sup> and since that time numerous publications have dealt with this cation and derivatives with different substitution patterns on the 1,10-phenanthroline ligands. Numerous experimental <sup>[80-85]</sup> and calculational <sup>[86-87]</sup> investigations have confirmed that the photophysical properties of the  $\{\text{Cu}(\text{phen})_2\}$  complexes depend critically upon the geometry and specifically upon the degree of flattening of the ideal  $D_{2d}$  structure.

To date, structural analyses of  $[\text{CuL}_2]\text{X}\cdot\text{Y}$  (L = 2,9-dimethyl-1,10-phenanthroline; X = anion; Y = solvent) have been reported for complexes with X = 2,9-dimethyl-1,10-phenanthroline <sup>[88]</sup>, X = Br, Y =  $\text{H}_2\text{O}$  <sup>[89]</sup>, X =  $\text{ClO}_4$  <sup>[90-91]</sup>, X =  $\text{NO}_3$  <sup>[92]</sup>, X =  $\text{BF}_4$  <sup>[93]</sup>, X =  $\text{BF}_4$ ,

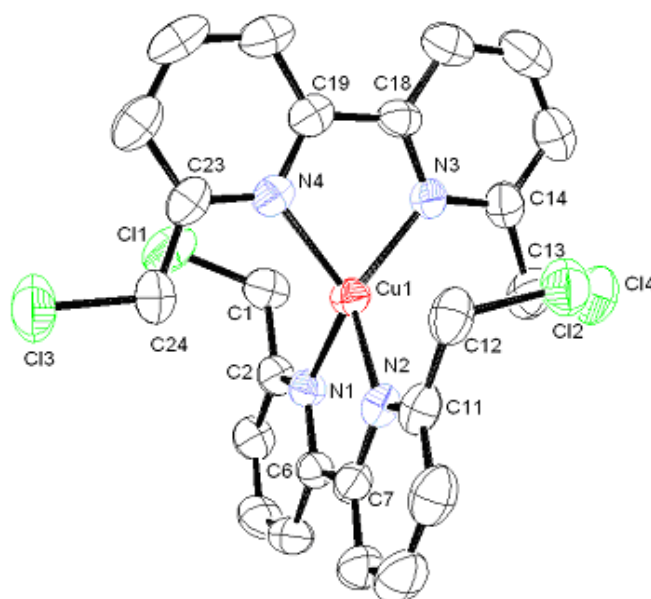
Y =  $\frac{1}{2}$  Me<sub>2</sub>CO [93], X = BF<sub>4</sub>, Y =  $\frac{1}{2}$  MeCN,  $\frac{1}{2}$  L [93], X = PF<sub>6</sub> [93], X = PF<sub>6</sub> L =  $\frac{1}{2}$  CH<sub>2</sub>Cl<sub>2</sub> [93], X = calix(4)arenate [93], X = tosylate [93], X = 9,10-anthraquinone-2-sulfonate, L = MeCN [93], X = 9,10-anthraquinone-2-sulfonate, L =  $\frac{3}{2}$  H<sub>2</sub>O [93], X = picrate, L = MeCN [93], X = Cu(hfacac)<sub>3</sub> [94], X = NO<sub>3</sub> Y = 2H<sub>2</sub>O [89;93;95], X = BF<sub>4</sub> Y = toluene [96], X = BF<sub>4</sub> Y = CH<sub>2</sub>Cl<sub>2</sub> [96], X = PF<sub>6</sub> Y =  $\frac{1}{4}$  bis(4-pyridylmethylidene),  $\frac{1}{2}$  MeCN [97] X = dicyanamide [97], and X = squarate, Y =  $\frac{1}{2}$  H<sub>2</sub>O [98]. The least-squares planes angles between the 2,9-dimethyl-1,10-phenanthroline ligands vary between 67.61° and 89.05° in these complexes; 82.94° [88], 77.60° [89], 80.06°, 82.16° [90-91], 67.61° [92], 89.05° [93], 79.80° [93], 83.35° [93], 76.10° [93], 70.99° [93], 74.14° [93], 87.47° [93], 86.59° [93], 82.13,81.11° [93], 68.71° [93], 74.98° [94], 85.69, 85.89, 84.67° [89;93;95], 82.66° [96], 88.89° [96], 78.56° [97] 82.66° [97], 78.32° [98].

In view of the large number of polymorphs and pseudopolymorphs observed in these systems we have determined the structures of the compounds [CuL<sub>2</sub>][PF<sub>6</sub>], [CuL<sub>2</sub>][PF<sub>6</sub>].CH<sub>2</sub>Cl<sub>2</sub> and [CuL<sub>2</sub>][PF<sub>6</sub>].toluene. The first two compounds (a = 13.36680(10) Å, b = 10.73200(10) Å, c = 18.6048(2) Å, α = 90°, β = 92.7576°(6), γ = 90°; a = 10.7084(2) Å, b = 11.1148(3) Å, c = 13.3808(3) Å, α = 69.2651°(12), β = 72.5084°(14), γ = 72.5205°(13)) are identical to the literature reports (IPIDEQ [93], a = 13.2144(4) Å, b = 10.7139(3) Å, c = 18.4938(5) Å, α = 90°, β = 92.449°(1) γ = 90°; IPIDIU [93], a = 10.5250(3) Å, b = 11.1161(3) Å, c = 13.3764(3) Å, α = 69.721°(1), β = 72.974°(1), γ = 72.455°(1)). The pseudopolymorph [CuL<sub>2</sub>][PF<sub>6</sub>].toluene is a new compound (a = 16.7294(3) Å, b = 15.3450(3) Å, c = 13.3089(3) Å, α = 90°, β = 108.0749°(10), γ = 90°) (Figure 4.49).



**Figure 4.49** ORTEP representation of the cation present in bis(2,9-dimethyl-1,10-phenanthroline)copper(I) complexes. Hydrogen atoms are omitted for clarity.

2.3.2.1 Crystal structure of bis[6,6'-bis(chloromethyl)-2,2'-bipyridine]copper(I) hexafluorophosphate



**Figure 4.50** ORTEP representation of the cation present in bis[6,6'-bis(chloromethyl)-2,2'-bipyridine]copper(I) hexafluorophosphate. Hydrogen atoms are omitted for clarity.

Bond	Distance/ Å	Bond	Distance/ Å
N(1)-Cu(1)	2.018(3)	C(1)-Cl(1)	1.798(4)
N(2)-Cu(1)	2.026(3)	C(12)-Cl(2)	1.795(4)
N(3)-Cu(1)	2.014(3)	C(24)-Cl(3)	1.773(4)
N(4)-Cu(1)	2.026(3)	C(13)-Cl(4)	1.784(4)

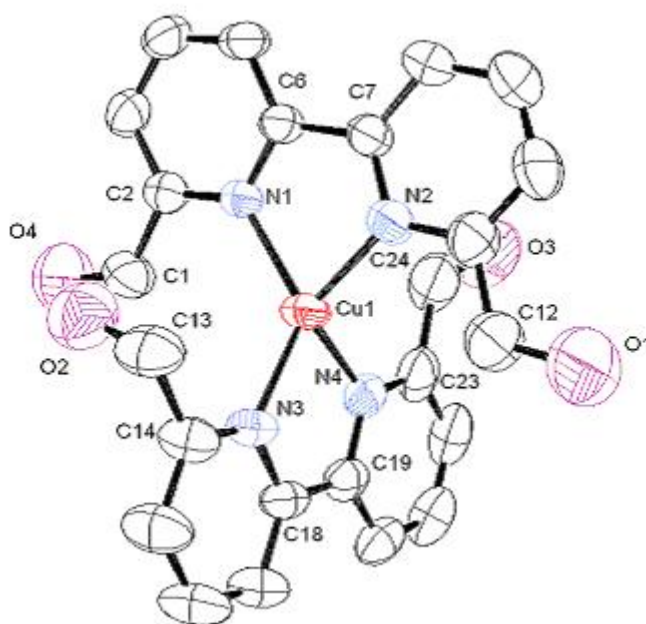
Bond	Angles/°	Bond	Angles/°
N(1)-Cu(1)-N(2)	81.66(12)	Cu(1)-N(3)-C(18)	113.0(3)
N(1)-Cu(1)-N(3)	126.47(12)	Cu(1)-N(4)-C(19)	113.0(3)
N(2)-Cu(1)-N(3)	127.47(12)	Cu(1)-N(4)-C(23)	126.7(3)
N(1)-Cu(1)-N(4)	123.29(12)	N(1)-C(2)-C(3)	122.1(3)
N(2)-Cu(1)-N(4)	121.68(12)	N(2)-C(11)-C(12)	116.9(4)
N(3)-Cu(1)-N(4)	82.15(13)	C(13)-C(14)-N(3)	114.6(4)
Cu(1)-N(1)-C(2)	127.0(2)	N(4)-C(23)-C(24)	113.8(3)
Cu(1)-N(1)-C(6)	114.2(2)	C(2)-C(1)-Cl(1)	108.6(3)
Cu(1)-N(2)-C(7)	113.4(2)	C(11)-C(12)-Cl(2)	110.5(3)
Cu(1)-N(2)-C(11)	126.9(3)	C(23)-C(24)-Cl(3)	114.9(3)
Cu(1)-N(3)-C(14)	127.4(3)	C(14)-C(13)-Cl(4)	112.9(4)

N(1)-C(6)-C(7)-N(2)	-4.44	N(3)-C(18)-C(19)-N(4)	3.66
---------------------	-------	-----------------------	------

**Table 2.7** Selected bonds lengths (Å), angles (°), and torsion angles (°) for the bis[6,6'-bis(chloromethyl)-2,2'-bipyridine]copper(I) hexafluorophosphate.

The title complex is bis[6,6'-bis(chloromethyl)-2,2'-bipyridine]copper(I) hexafluorophosphate, with a single disordered hexafluorophosphate anion. The geometry about the copper is predictably distorted tetrahedral. The N-Cu-N bond angles are 82.14° and 81.66°. The group N1-C6-C7-N2 has a torsion angle of 4.44°, and that of N3-C18-C19-N4 is 3.61°. There are few interesting features, with no convincing intermolecular hydrogen-bonding. The cations are arranged into columns when viewed down the c axis, with each complex superimposable on its neighbour in that direction. Additionally, each cation is separated from its neighbour with a hexafluorophosphate anion. There is also a short contact of 3.747 Å between C12 and its adjacent symmetry equivalent representing a face-to-face  $\pi$ -stacking interaction between 1,10-phenanthroline ligands of adjacent cations with a least-squares planes distance of 3.451 Å. The least squares plane between the 1,10-phenanthroline ligands in the cation is 89.81°.

### 2.3.2.2 Crystal structure of bis[6,6'-bis(hydroxymethyl)-2,2'-bipyridine]copper(I) hexafluorophosphate.



**Figure 4.51** ORTEP representation of the cation present in bis[6,6'-bis(hydroxymethyl)-2,2'-bipyridine]copper(I) hexafluorophosphate. Hydrogen atoms are omitted for clarity.

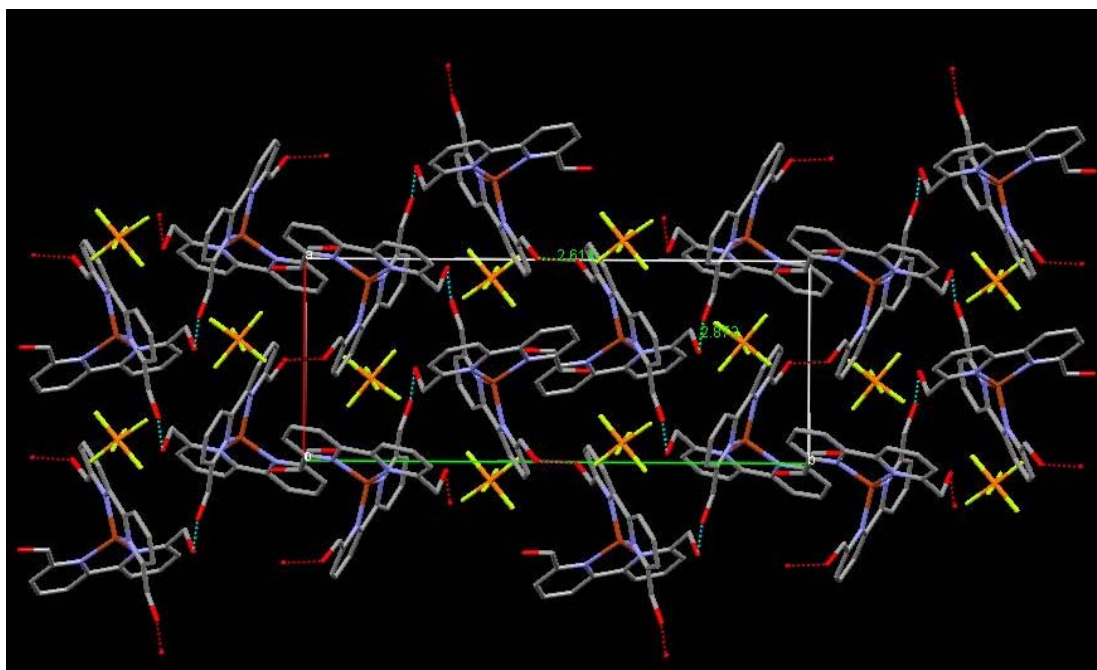
Bond	Distance/ Å	Bond	Distance/ Å
N(1)-Cu(1)	2.023(3)	C(1)-O(4)	1.392(9)
N(2)-Cu(1)	2.042(3)	C(12)-O(1)	1.382(7)
N(3)-Cu(1)	2.014(3)	C(13)-O(2)	1.422(10)
N(4)-Cu(1)	2.045(4)	C(24)-O(3)	1.365(7)

Bond	Angles/°	Bond	Angles/°
N(1)-Cu(1)-N(2)	81.52(12)	Cu(1)-N(3)-C(18)	114.0(3)
N(1)-Cu(1)-N(3)	128.38(13)	Cu(1)-N(4)-C(19)	114.2(3)
N(2)-Cu(1)-N(3)	127.83(13)	Cu(1)-N(4)-C(23)	126.5(3)
N(1)-Cu(1)-N(4)	128.86(13)	C(1)-C(2)-N(1)	115.8(3)
N(2)-Cu(1)-N(4)	115.97(14)	N(2)-C(11)-C(12)	115.5(4)
N(3)-Cu(1)-N(4)	81.02(13)	N(3)-C(14)-C(15)	121.9(4)
Cu(1)-N(1)-C(2)	127.6(2)	N(4)-C(23)-C(24)	113.2(5)
Cu(1)-N(1)-C(6)	113.7(2)	C(2)-C(1)-O(4)	123.7(8)
Cu(1)-N(2)-C(7)	113.0(2)	C(11)-C(12)-O(1)	118.2(6)
Cu(1)-N(2)-C(11)	127.4(3)	C(14)-C(13)-O(2)	107.1(8)
Cu(1)-N(3)-C(14)	126.5(3)	C(23)-C(24)-O(3)	120.5(6)

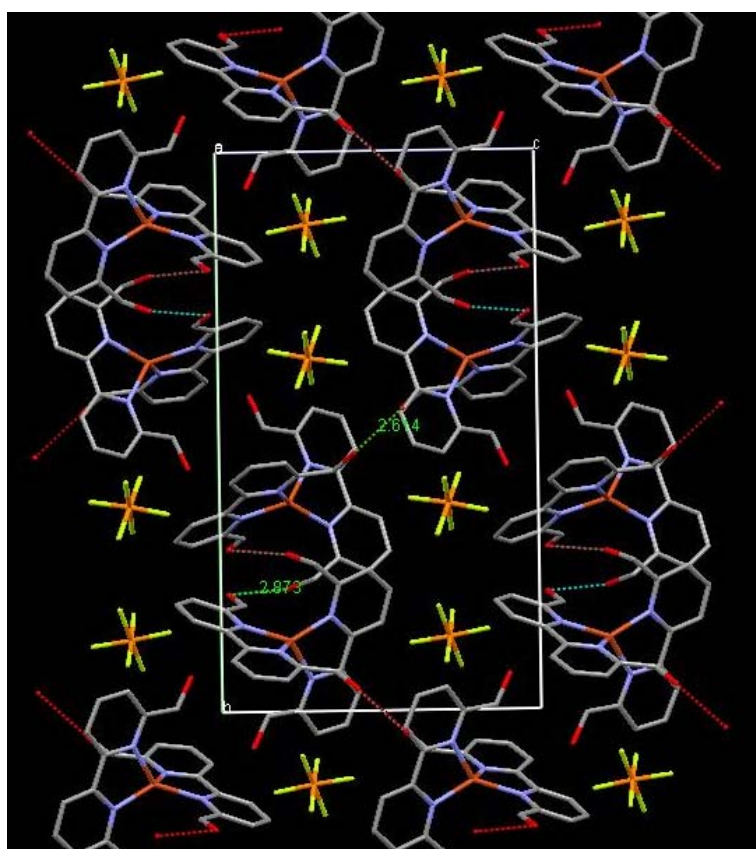
N(1)-C(6)-C(7)-N(2)	-10.18	N(3)-C(18)-C(19)-N(4)	2.38
---------------------	--------	-----------------------	------

**Table 2.8** Selected bonds lengths (Å), angles (°), and torsion angles (°) for the bis[6,6'-bis(hydroxymethyl)-2,2'-bipyridine]copper(I) hexafluorophosphate.

The title complex, bis[6,6'-bis(hydroxymethyl)-2,2'-bipyridine]copper(I) hexafluorophosphate, is a Cu(I) complex coordinated to two 6,6'-bis(hydroxymethyl)-2,2'-bipyridine ligands, with a hexafluorophosphate counterion. The N1-Cu1-N2 and N3-Cu1-N4 bond angles are 81.52° and 81.01° respectively. The bond distances are between 2.01Å and 2.05Å. These parameters are as expected for a complex of this type. Selected bond lengths and angles are in table 4.7 The torsion angle of the N3-C18-C19-N4 group is an unremarkable 2.38°, but that of the N1-C6-C7-N2 group is 10.18°, which is remarkable. Three of the four hydroxy groups are broadly in the plane of the bipyridine, but O2 is at an angle of 78.71° to the N3-C14-C13 group. It should be noted here that O2 is hydrogen-bonded to the O4 of an adjacent cation, with an O2-O4 distance of 2.837Å. O1 is also hydrogen-bonded, to the O1' of an adjacent cation, with an O1-O1' distance of 2.614Å. Due to the hydrogen-bonding in this system, the packing is quite interesting. The extent of the intermolecular interactions is best seen by viewing along the c axis (see figure 4.52) and the a axis, (see figure 4.53).

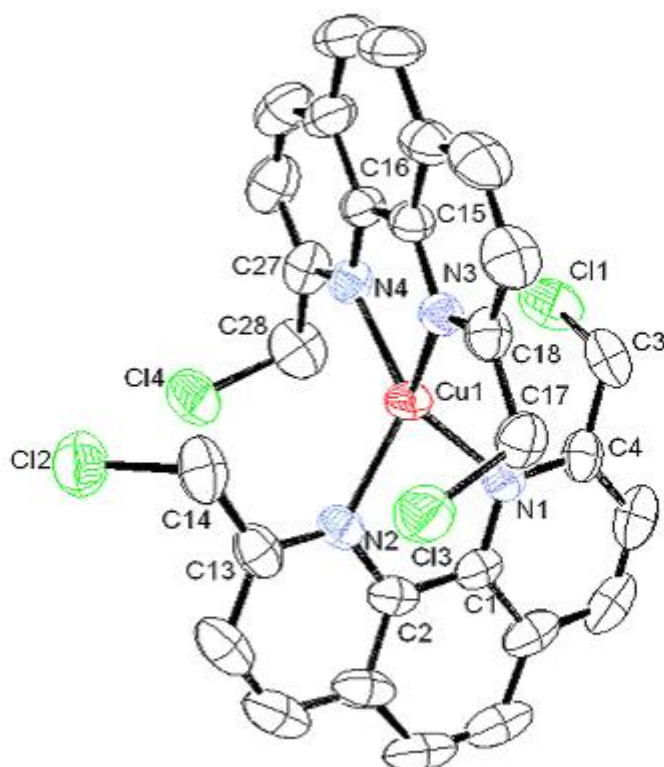


**Figure 4.52** View along c axis of the packing in bis[6,6'-bis(hydroxymethyl)-2,2'-bipyridine]copper(I) hexafluorophosphate.



**Figure 4.53** View along a axis of the packing in bis[6,6'-bis(hydroxymethyl)-2,2'-bipyridine]copper(I) hexafluorophosphate.

2.3.2.3 Crystal structure of bis[6,6'-di(chloromethyl)-1,10-phenanthroline]copper(I) hexafluorophosphate.



**Figure 4.54** ORTEP representation of the bis[6,6'-di(chloromethyl)-1,10-phenanthroline]copper(I) cation in bis[6,6'-di(chloromethyl)-1,10-phenanthroline]copper(I) hexafluorophosphate. Hydrogen atoms are omitted for clarity.

Bond	Distance/ Å	Bond	Distance/ Å
N(1)-Cu(1)	2.043(2)	C(3)-Cl(1)	1.787(4)
N(2)-Cu(1)	2.042(2)	C(14)-Cl(2)	1.776(4)
N(3)-Cu(1)	2.042(2)	C(17)-Cl(3)	1.794(3)
N(4)-Cu(1)	2.046(2)	C(28)-Cl(4)	1.785(4)

Bond	Angles/°	Bond	Angles/°
N(1)-Cu(1)-N(2)	82.13(10)	Cu(1)-N(3)-C(18)	130.1(2)
N(1)-Cu(1)-N(3)	123.00(9)	Cu(1)-N(4)-C(16)	111.36(19)
N(2)-Cu(1)-N(3)	122.53(9)	Cu(1)-N(3)-C(27)	130.1(2)
N(1)-Cu(1)-N(4)	126.77(9)	C(3)-C(4)-N(1)	116.6(3)
N(2)-Cu(1)-N(4)	126.18(10)	N(2)-C(13)-C(14)	115.5(3)
N(3)-Cu(1)-N(4)	82.08(9)	C(15)-C(16)-N(4)	117.6(2)
Cu(1)-N(1)-C(1)	111.59(19)	C(17)-C(18)-N(3)	116.9(3)

Cu(1)-N(1)-C(4)	129.9(2)	C(4)-C(3)-Cl(1)	108.0(2)
Cu(1)-N(2)-C(2)	111.30(19)	C(13)-C(14)-Cl(2)	113.7(3)
Cu(1)-N(1)-C(13)	130.3(2)	C(18)-C(17)-Cl(3)	110.4(2)
Cu(1)-N(3)-C(15)	111.65(18)	C(27)-C(28)-Cl(4)	103.7(3)
N(1)-C(1)-C(2)-N(2)	2.03	N(3)-C(15)-C(16)-N(4)	0.05

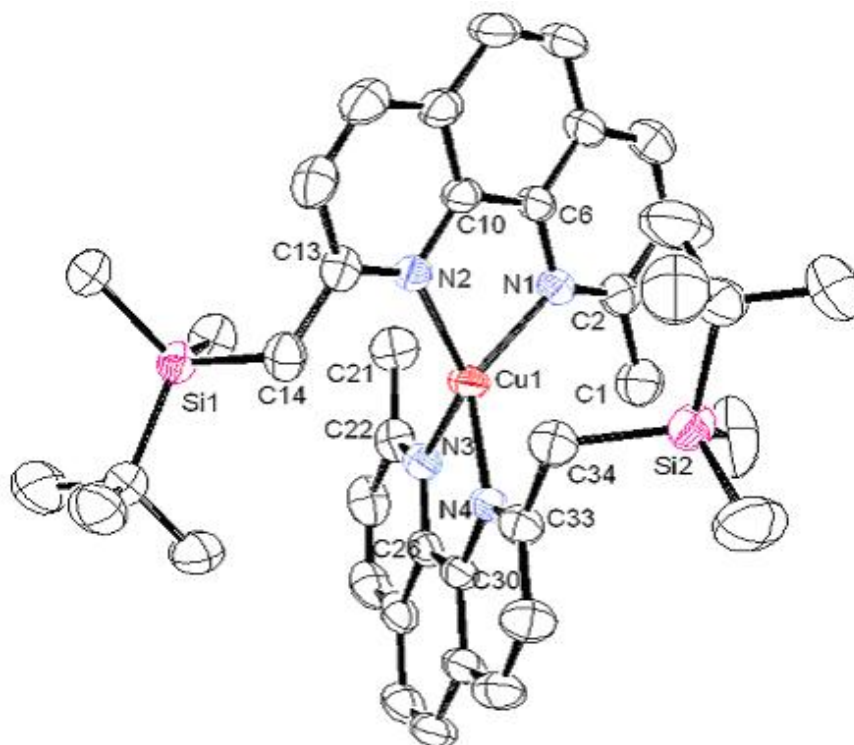
**Table 2.9** Selected bonds lengths (Å), angles (°), and torsion angles (°) for the bis[6,6'-di(chloromethyl)-1,10-phenanthroline]copper(I) hexafluorophosphate.

The title complex is bis[6,6'-di(chloromethyl)-1,10-phenanthroline]copper(I) hexafluorophosphate. The geometry around the metal centre is highly distorted tetrahedral, with significant deviations from 109.47° as can be seen from table 4.8. The 1,10-phenanthroline retains its planarity, with an N1-C1-C2-N2 torsion angle of 2.03° and an N3-C15-C16-N4 torsion angle of 0.05°.

The packing is unremarkable, with few obvious intermolecular interactions. There are certainly  $\pi$ - $\pi$  face to face interactions between ring C1C2C7C8C9C10 and the adjacent symmetry equivalent, with a centroid-centroid distance of 3.753 Å and a C1-centroid-centroid angle of 93.1°. A similar interaction is evident with ring C15C16C21C22C23C24 and the ring that is symmetry related to it, but with an inter-ring distance of 3.746 Å, and a C15-centroid-centroid angle of 98.2°.



2.3.2.4 Crystal structure of bis[2-methyl-9-(tert-butyl dimethylsilyl)methyl]-1,10-phenanthroline]copper(I) hexafluorophosphate dichloromethane solvate



**Figure 4.55** ORTEP representation of bis[2-methyl-9-(tert-butyl dimethylsilyl)methyl]-1,10-phenanthroline]copper(I) cation in bis[2-methyl-9-(tert-butyl dimethylsilyl)methyl]-1,10-phenanthroline]copper(I) hexafluorophosphate dichloromethane solvate. Hydrogen atoms are omitted for clarity.

Bond	Distance/ Å	Bond	Distance/ Å
N(1)-Cu(1)	2.0471(16)	N(3)-Cu(1)	2.0481(17)
N(2)-Cu(1)	2.0388(16)	N(4)-Cu(1)	2.0455(16)

Bond	Angles/°	Bond	Angles/°
Cu(1)-N(1)-C(2)	130.01(15)	N(1)-Cu(1)-N(4)	132.57(7)
Cu(1)-N(1)-C(6)	110.87(13)	N(2)-Cu(1)-N(4)	119.80(7)
Cu(1)-N(2)-C(10)	111.47(13)	N(3)-Cu(1)-N(4)	82.24(7)
Cu(1)-N(2)-C(13)	129.63(14)	C(1)-C(2)-N(1)	118.4(2)
Cu(1)-N(3)-C(2)	129.59(15)	N(2)-C(13)-C(14)	118.11(18)
Cu(1)-N(3)-C(26)	111.64(14)	C(21)-C(22)-N(3)	117.7(2)
Cu(1)-N(4)-C(30)	111.35(13)	N(4)-C(33)-C(34)	117.96(18)
Cu(1)-N(4)-C(33)	129.72(14)	C(13)-C(14)-Si(1)	113.89(15)
N(1)-Cu(1)-N(2)	82.55(7)	C(33)-C(34)-Si(2)	114.38(16)

N(1)-Cu(1)-N(3)	114.13(7)	
N(2)-Cu(1)-N(3)	132.76(7)	

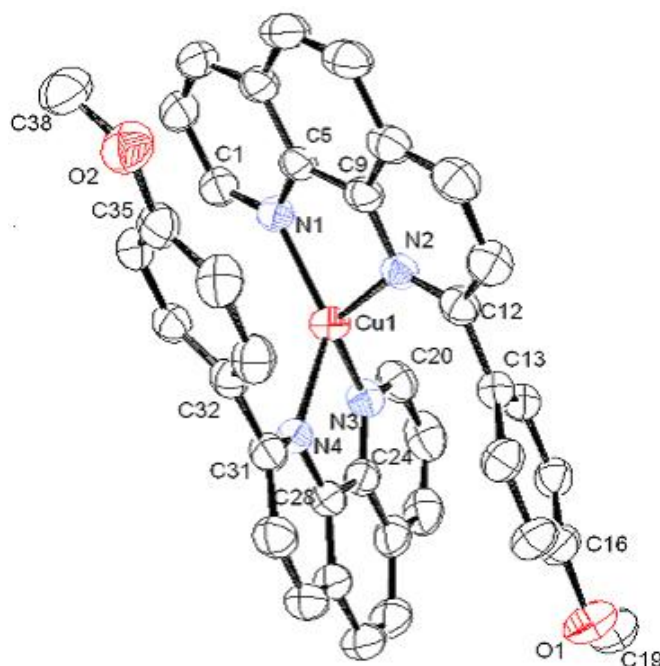
N(1)-C(6)-C(10)-N(2)	-3.10	N(3)-C(26)-C(30)-N(4)	-0.97
----------------------	-------	-----------------------	-------

**Table 2.10** Selected bonds lengths (Å), angles (°), and torsion angles (°) for bis[2-dimethyl-9-(tert-butyldimethylsilyl)methyl]-1-10-phenanthroline]copper(I) hexafluorophosphate.

This complex is a bis[2-dimethyl-9-(tert-butyldimethylsilyl)methyl]-1-10-phenanthroline]copper(I) hexafluorophosphate complex of a disubstituted phenanthroline ligand, with one dichloromethane solvent molecule and a disordered PF<sub>6</sub> counterion. The metal-ligand bond lengths are shown in table 4.9, and are as expected for a Cu(I) phenanthroline complex. The metal-ligand bond angles are 82.55° and 82.44°, again, typical for this type of complex.

What is remarkable about this system is evident in the packing. Despite the steric freedom inherent in the TBDMS group, there is a surprising degree of order. Each cation is directly superimposable upon its immediate neighbour. This applies whether looking along the a, b or c axes.

Crystal structure of bis[2-(4-methoxyphenyl)-1,10-phenanthroline]copper(I) hexafluorophosphate.



**Figure 4.56** ORTEP representation of the cation present in bis[2-(4-Methoxyphenyl)-1,10-phenanthroline]copper(I) hexafluorophosphate.. Hydrogen atoms are omitted for clarity.

Bond	Distance/ Å	Bond	Distance/ Å
N(1)-Cu(1)	1.9959(19)	C(16)-O(1)	1.367(3)
N(2)-Cu(1)	2.1046(18)	C(35)-O(2)	1.367(3)
N(3)-Cu(1)	1.9999(19)	C(19)-O(1)	1.424(4)
N(4)-Cu(1)	2.0968(18)	C(38)-O(2)	1.429(4)

Bond	Angles/°	Bond	Angles/°
N(1)-Cu(1)-N(2)	82.23(7)	Cu(1)-N(2)-C(12)	131.00(15)
N(1)-Cu(1)-N(3)	135.21(8)	Cu(1)-N(3)-C(20)	129.48(17)
N(2)-Cu(1)-N(3)	129.67(7)	Cu(1)-N(3)-C(24)	112.55(15)
N(1)-Cu(1)-N(4)	129.85(7)	Cu(1)-N(4)-C(28)	109.46(14)
N(2)-Cu(1)-N(4)	97.58(7)	Cu(1)-N(4)-C(31)	128.82(15)
N(3)-Cu(1)-N(4)	81.96(7)	N(2)-C(12)-C(13)	117.94(19)
Cu(1)-N(1)-C(1)	129.53(17)	N(4)-C(31)-C(32)	116.98(19)
Cu(1)-N(1)-C(5)	112.69(15)	C(19)-O(1)-C(16)	117.7(2)
Cu(1)-N(2)-C(9)	109.23(14)	C(38)-O(2)-C(35)	117.7(2)

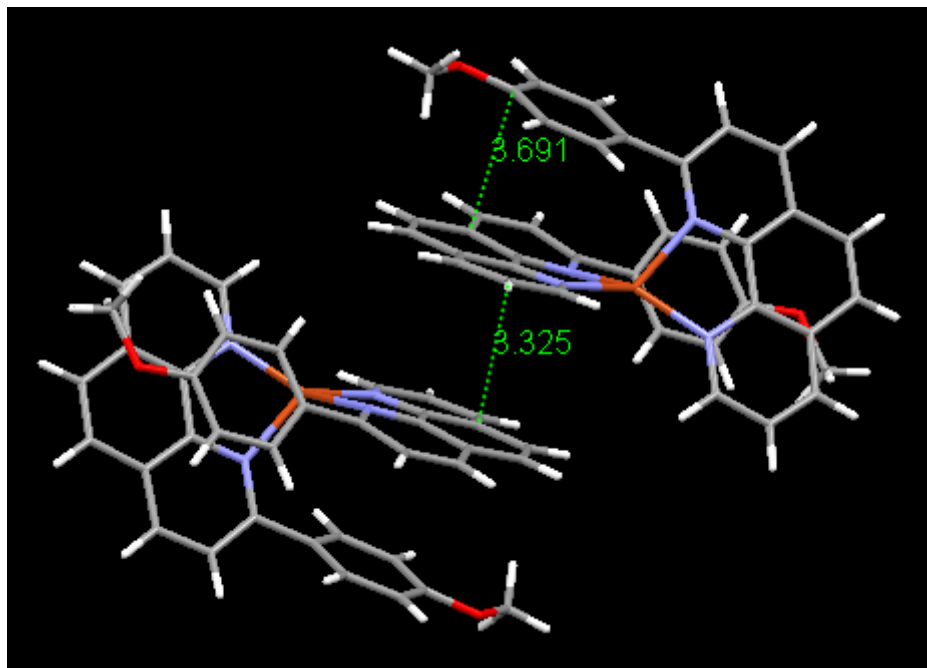
N(1)-C(5)-C(9)-N(2)	2.56	N(3)-C(24)-C(28)-N(3)	4.94
---------------------	------	-----------------------	------

**Table 2.11** Selected bonds lengths (Å), angles (°), and torsion angles (°) for the bis[2-(4-methoxyphenyl)-1,10-phenanthroline]copper(I) hexafluorophosphate.

In bis[2-(4-methoxyphenyl)-1,10-phenanthroline]copper(I) hexafluorophosphate, the copper(I) centre is coordinated to two 2-(4-methoxyphenyl)-1,10-phenanthroline ligands. The counterion is a disordered  $[\text{PF}_6]$ . What is remarkable about this complex is the geometry that the presence of the 4-methoxyphenyl groups impose on the metal centre. Although the copper to donor bond angles are typical for a copper(I) phenanthroline complex ( $\text{N1Cu1N2}$  at  $82.23^\circ$  and  $\text{N3Cu1N4}$  at  $81.96^\circ$ ), other angles show some deviation from typical complexes of this type. The  $\text{N1-Cu1-N3}$  angle is  $135.22^\circ$ , unusual for this type of system. Although there appears to be a  $\pi$ - $\pi$  interaction between the phenyl group and the phenanthroline (Figure 2.57), the rings are offset, and the orientation is probably a steric effect.

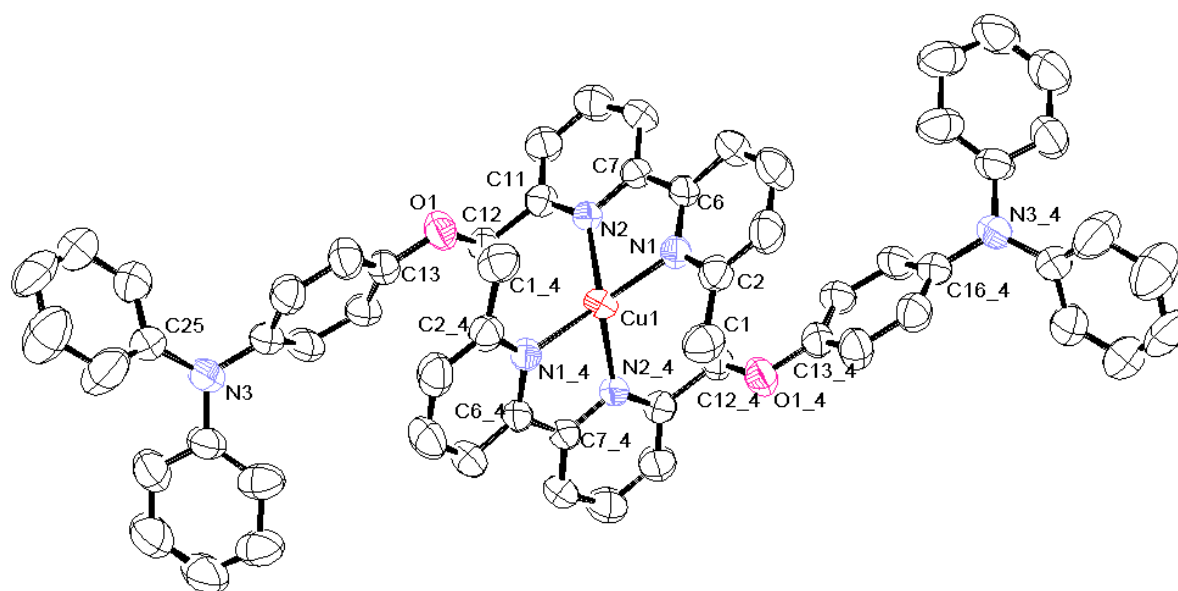
The packing in this system shows some nice features. The cations are arranged in columns, superimposable on their immediate neighbour when viewed along the *a* axis of the unit cell. The anions occupy the spaces between cations. There is some evidence of intramolecular  $\pi$ - $\pi$  stacking between ring C14-C15-C16-C17-C18 and ring C27-C28-C29-C30-C31-N4, with a centroid-centroid distance of  $3.695\text{\AA}$ , and a C31-centroid-centroid angle of  $103.86^\circ$ . These values are within the range of accepted  $\pi$ - $\pi$  stacking parameters. In addition, there is an intermolecular  $\pi$ - $\pi$  stacking between ring C20-C21-C22-C23-C24-N3 and its adjacent symmetry equivalent. Centroid-centroid distance is  $3.572\text{\AA}$ , and N3-Centroid-Centroid angle is  $111.75^\circ$ , again typical of a slightly offset  $\pi$ - $\pi$  stacking system.

The phenanthroline and phenyl groups are not coplanar, there being an angle of  $52.63^\circ$  between the mean phenyl plane and the mean phenanthroline plane.



**Figure 2.57**  $\pi$ - $\pi$  interactions between the phenyl group and the phenanthroline in bis[2-(4-methoxyphenyl)-1,10-phenanthroline]copper(I) hexafluorophosphate.

2.3.2.5 Crystal structure of bis[6-(4-(*N,N*-diphenylamino)phenoxy)methyl)-6'-methyl-2,2'-bipyridine]copper(I) hexafluorophosphate.



**Figure 2.58** ORTEP representation of the cation present in bis[6-(4-(*N,N*-diphenylamino)phenoxy)methyl)-6'-methyl-2,2'-bipyridine]copper(I) hexafluorophosphate. Hydrogen atoms are omitted for clarity.

Bond	Distance/ Å	Bond	Distance/ Å
N(1)-Cu(1)	2.023(2)	C(1)-C(2)	1.492(5)
N(2)-Cu(1)	2.057(3)	C(12)-O(1)	1.438(4)
C(11)-C(12)	1.501(4)	C(13)-O(1)	1.374(4)

Bond	Angles/°	Bond	Angles/°
C(11)-C(12)-O(1)	105.3(3)	C(2)-N(1)-Cu(1)	125.9(2)
C(12)-O(1)-C(13)	117.5(3)	C(7)-N(2)-Cu(1)	112.9(2)
C(6)-N(1)-Cu(1)	114.4(2)	C(11)-N(2)-Cu(1)	128.2(2)
C(1)-C(2)-N(1)	116.4(3)		

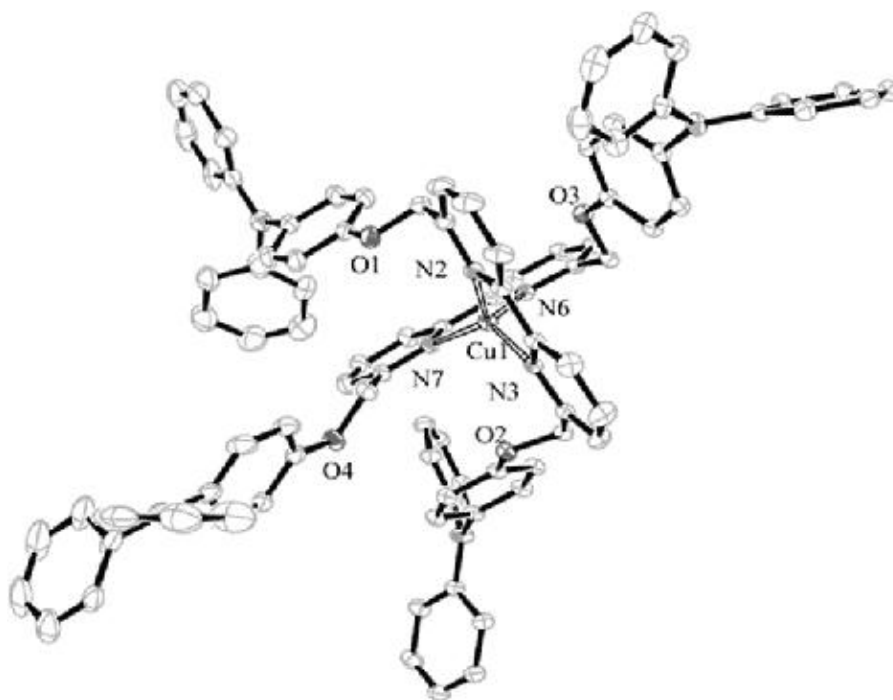
N(1)-C(6)-C(7)-N(2)	6.57	
---------------------	------	--

**Table 2.12** Selected bonds lengths (Å), angles (°), and torsion angles (°) for the bis[6-(4-(*N,N*-diphenylamino)phenoxy)methyl]-6'-methyl-2,2'-bipyridine]copper(I) hexafluorophosphate.

This complex is bis[6-(4-(*N,N*-diphenylamino)phenoxy)methyl]-6'-methyl-2,2'-bipyridine]copper(I) hexafluorophosphate with a single [PF<sub>6</sub>] counterion. The angles around the metal centre are in table 2.12 and are consistent with what is expected in Cu(I) complexes of bpy-type ligands. There is a centre of inversion through the copper centre. The bpy ligand has some slight torsional strain, with an N1-C6-C7-N2 torsion angle of 6.57°.

The packing in this system is very nice, due to the asymmetric ligand. Across the bc plane, the cations are arranged into corrugated in-phase sheets studded with anion molecules. Although there are no obvious intermolecular interactions, there is a close contact between the centroid of ring C7-C8-C9-C10-C11-N2 and an adjacent C29 (part of a triphenyl amine group) which may be an edge-to-face interaction.

2.3.2.6 Crystal structure of bis[6,6'-bis(4-(*N,N*-diphenylamino)phenoxy)methyl)-2,2'-bipyridine]copper(I) hexafluorophosphate.



**Figure 2.59** ORTEP representation of the cation present in bis[6,6'-bis(4-(*N,N*-diphenylamino)phenoxy)methyl)-2,2'-bipyridine]copper(I) hexafluorophosphate ether solvate. Hydrogen atoms are omitted for clarity.

Bond	Distance/ Å	Bond	Distance/ Å
N(2)-Cu(1)	2.058(3)	C(16)-O(1)	1.361(5)
N(3)-Cu(1)	2.036(2)	C(19)-O(1)	1.422(5)
N(6)-Cu(1)	2.047(2)	C(30)-O(2)	1.430(4)
N(7)-Cu(1)	2.037(2)	C(31)-O(2)	1.368(3)
C(78)-O(4)	1.422(4)	C(64)-O(3)	1.369(3)
C(79)-O(4)	1.372(4)	C(67)-O(3)	1.433(4)

Bond	Angles/°	Bond	Angles/°
N(2)-Cu(1)-N(3)	80.10(10)	Cu(1)-N(3)-C(29)	126.75(18)
N(2)-Cu(1)-N(6)	119.66(10)	Cu(1)-N(6)-C(68)	127.18(19)
N(3)-Cu(1)-N(6)	122.31(10)	Cu(1)-N(6)-C(72)	114.01(19)
N(2)-Cu(1)-N(7)	127.46(10)	Cu(1)-N(7)-C(73)	114.1(2)
N(3)-Cu(1)-N(7)	132.45(9)	Cu(1)-N(7)-C(77)	127(2)
N(6)-Cu(1)-N(7)	80.59(10)	C(16)-O(1)-C(19)	117.3(3)
Cu(1)-N(2)-C(20)	126.6(2)	C(30)-O(2)-C(31)	115.9(2)
Cu(1)-N(2)-C(24)	114.2(2)	C(64)-O(3)-C(67)	116.5(2)

Cu(1)-N(3)-C(25)	114.6(2)	C(78)-O(4)-C(79)	118.9(3)
C(29)-C(30)-O(2)	107.3(2)	O(1)-C(16)-C(17)	115.9(4)
O(2)-C(31)-C(32)	115.4(2)	O(1)-C(19)-C(20)	108.1(3)
O(2)-C(31)-C(36)	124.8(3)	C(63)-C(64)-O(3)	124.7(3)
C(15)-C(16)-O(1)	125.2(4)	O(3)-C(64)-C(65)	115.4(3)
C(77)-C(78)-O(4)	107.9(3)	O(3)-C(67)-C(68)	105.8(2)
O(4)-C(79)-C(80)	114.2(4)	O(4)-C(79)-C(84)	126.1(4)
N(7)-C(73)-C(72)-N(6)	-1.73	N(3)-C(25)-C(24)-N(2)	0.61

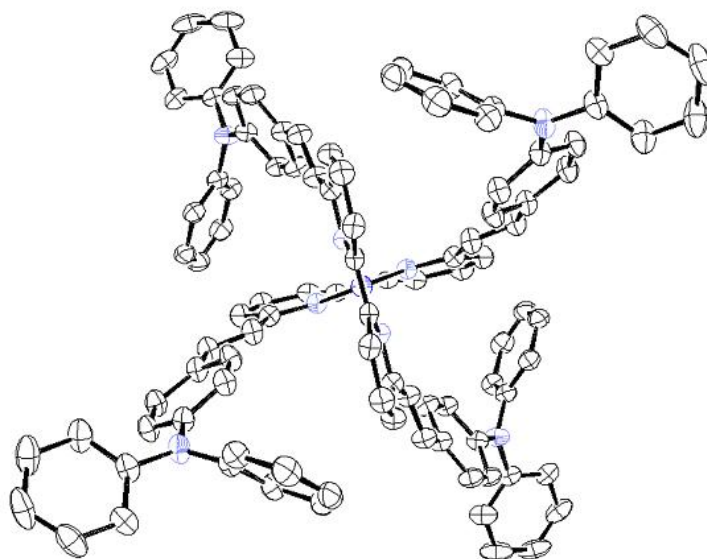
**Table 2.13** Selected bonds lengths (Å), angles (°), and torsion angles (°) for the cation present in bis[6,6'-bis(4-(*N,N*-diphenylamino)phenoxy)methyl]-2,2'-bipyridine]copper(I) hexafluorophosphate ether solvate.

The complex contains a copper(I) acceptor coordinated to two 6,6'-bis(4-(*N,N*-diphenylamino)phenoxy)methyl)-2,2'-bipyridine ligands with a hexafluorophosphate anion, and two disordered ether molecules per cation unit. A phenyl group on one of the triphenylamine groups is also disordered. The geometry around the metal centre is distorted tetrahedral, with an N2-Cu1-N3 angle of 80.1° and an N6-Cu1-N7 angle of 80.59°. There is barely any torsional strain on the bipyridyl N-C-C-N groups.

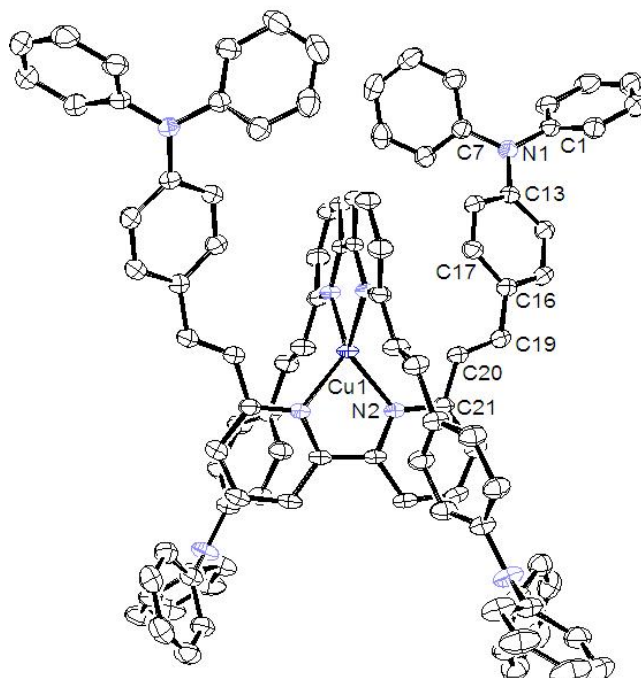
The packing of this complex shows some intermolecular  $\pi$ - $\pi$  interactions, notably the edge-to-face interaction between ring C6-C7-C8-C9-C10-C11-C12 and the C49-C50-C51-C52-C53-C54 ring of the adjacent molecule. The distance between the centroid of ring C6-C7-C8-C9-C10-C11-C12 and the (riding) hydrogen on C51 is 2.671 Å, with a C6-centroid-hydrogen angle of 99.34°. This is consistent with accepted phenyl edge-to-face parameters. The ring C49-C50-C51-C52-C53-C54 is in turn involved in a similar interaction with the edge of ring C91-C92-C93-C94-C95-C96 in another adjacent molecule. So there is an extensive network of edge-to-face interactions throughout the lattice.



2.3.2.7 Crystal structure of the bis[6,6'-bis(2-(4-(*N,N*-diphenylamino)phenyl)ethenyl)-2,2'-bipyridine]copper(I) hexafluorophosphate.



**Figure 2.60** ORTEP representation of the cation present in bis[6,6'-bis(2-(4-(*N,N*-diphenylamino)phenyl)ethenyl)-2,2'-bipyridine]copper(I) hexafluorophosphate. Hydrogen atoms are omitted for clarity.



**Figure 2.61** Alternative ORTEP representation of the cation present in bis[6,6'-bis(2-(4-(*N,N*-diphenylamino)phenyl)ethenyl)-2,2'-bipyridine]copper(I) hexafluorophosphate. Hydrogen atoms are omitted for clarity.

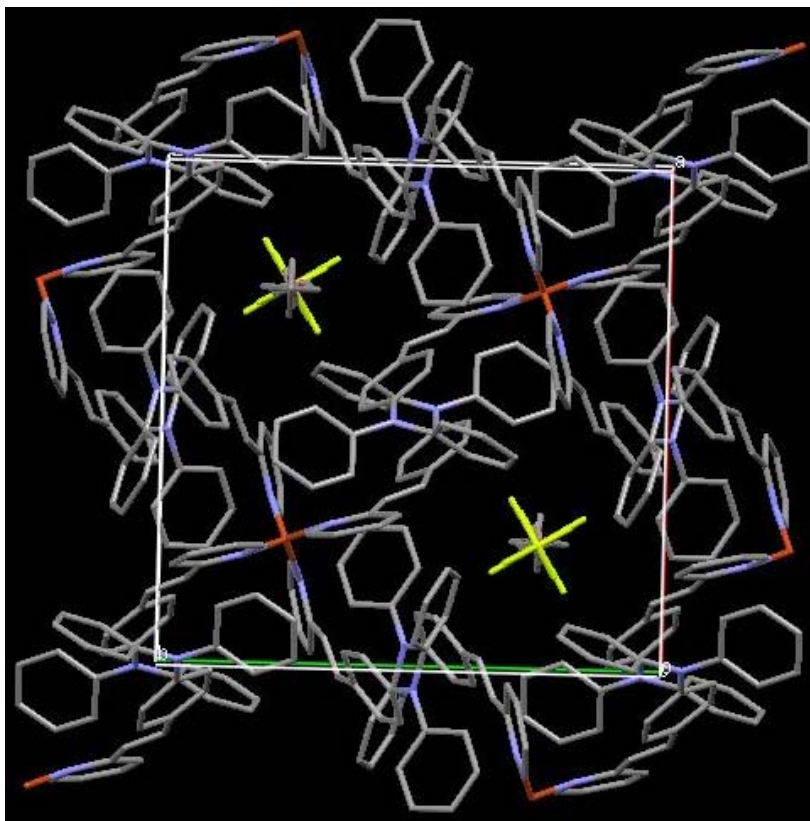
Bond	Distance/ Å	Bond	Distance/ Å
Cu(1)-N(2)	2.0401(13)	C(19)-C(16)	1.469(2)
N(2)-C(21)	1.339(2)	C(13)-N(1)	1.416(2)
C(20)-C(21)	1.456(2)	N(1)-C(1)	1.408(2)
C(20)-C(19)	1.323(3)	N(1)-C(7)	1.429(2)

Bond	Angles/°	Bond	Angles/°
N(2)#1-Cu(1)-N(2)#2	125.49(4)	C(1)-N(1)-C(7)	118.78(14)
N(2)#1-Cu(1)-N(2)#3	125.49(4)	C(1)-N(1)-C(13)	122.25(14)
N(2)#2-Cu(1)-N(2)#3	80.73(7)	C(7)-N(1)-C(13)	118.84(14)
N(2)#1-Cu(1)-N(2)	80.73(7)	C(15)-C(16)-C(19)	121.65(15)
N(2)#2-Cu(1)-N(2)	125.49(4)	C(17)-C(16)-C(19)	120.75(15)
N(2)#3-Cu(1)-N(2)	125.49(4)	C(20)-C(21)-N(2)	114.43(14)
Cu(1)-N(2)-C(21)	125.22(10)	C(19)-C(20)-C(21)	129.94(16)
Cu(1)-N(2)-C(25)	113.70(11)	C(16)-C(19)-C(20)	122.34(16)

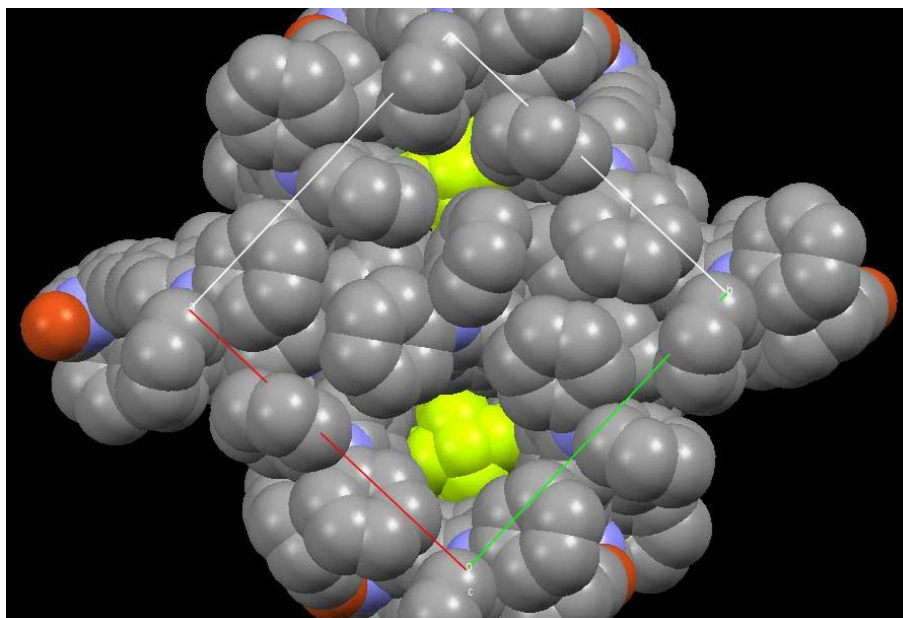
**Table 2.14** Selected bonds lengths (Å), angles (°), and torsion angles (°) for the cation present in bis[6,6'-bis(2-(4-(*N,N*-diphenylamino)phenyl)ethenyl)-2,2'-bipyridine]copper(I) hexafluorophosphate

The bis[bis(ethene-2,1-diyl)bis(*N,N*-diphenylaniline)(2,2'-bipyridine-6,6'-diyl)]copper(I) hexafluorophosphate is a Cu(I) acceptor coordinated to two substituted bipyridine ligands, with a disordered hexafluorophosphate anion and a disordered ethanol solvent molecule. With respect to the cation, the asymmetric unit consists of a quarter-occupancy Cu(I) and one half a ligand. The N1-Cu1-N1' bond angle is 80.73°, and the metal-ligand bond-length is 2.040Å, these are typical parameters for a complex of this type.

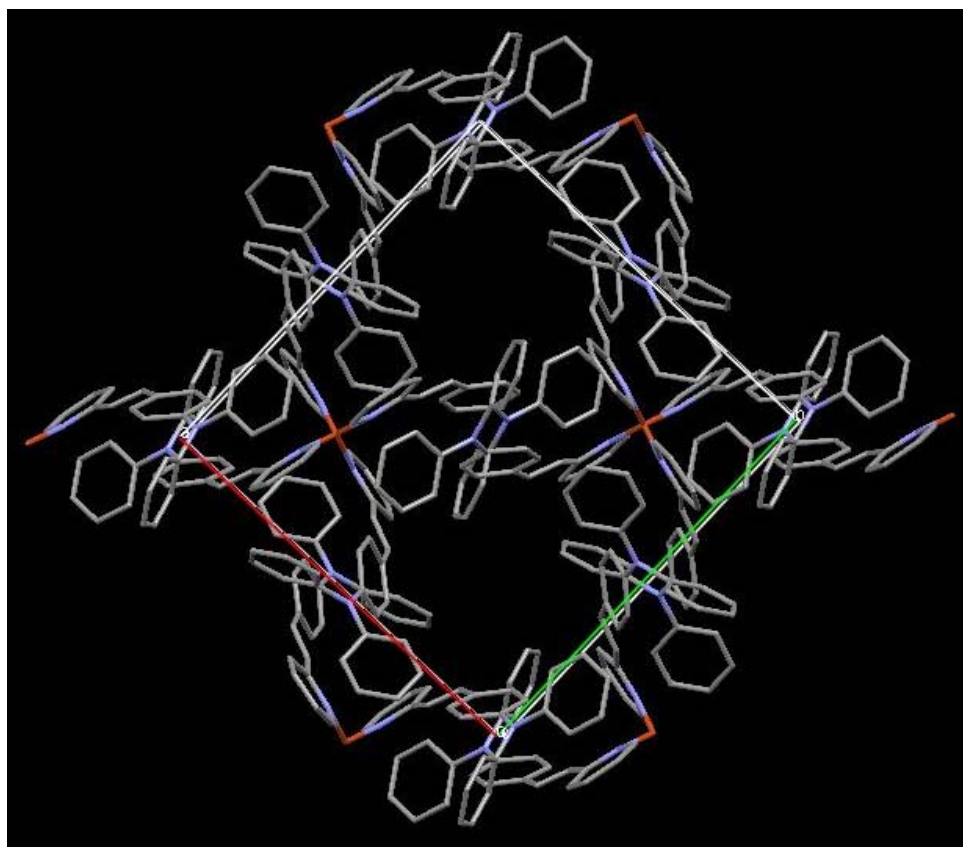
The packing is quite pretty in this system. The anions and solvent molecules are arranged in columns, with the cations arranged about them. This is best viewed down the *c* axis, as shown in figures 2.62 and 2.64 (in figure 2.64 solvent and anions are removed for illustrative purposes).



**Figure 2.62** Packing in bis[6,6'-bis(2-(4-(*N,N*-diphenylamino)phenyl)ethenyl)-2,2'-bipyridine]copper(I) hexafluorophosphate, as viewed along the *c* axis.

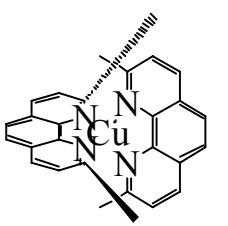
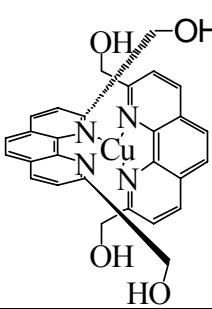
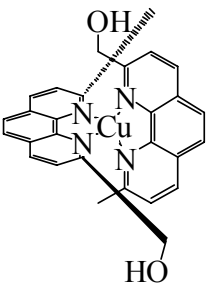
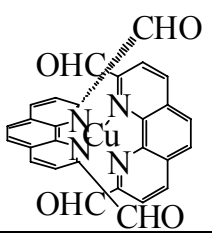
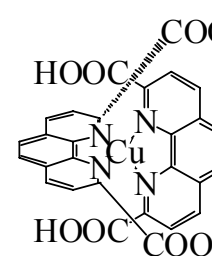


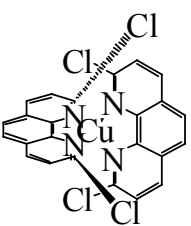
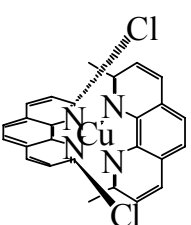
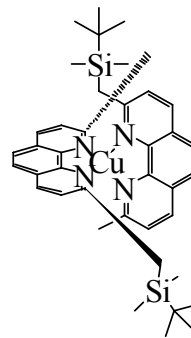
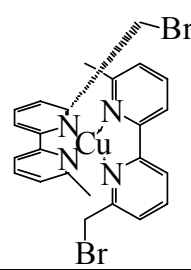
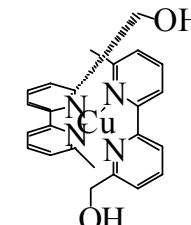
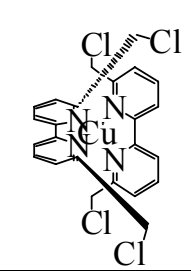
**Figure 2.63** Packing in bis[6,6'-bis(2-(4-(*N,N*-diphenylamino)phenyl)ethenyl)-2,2'-bipyridine]copper(I) hexafluorophosphate as viewed along the *c* axis.

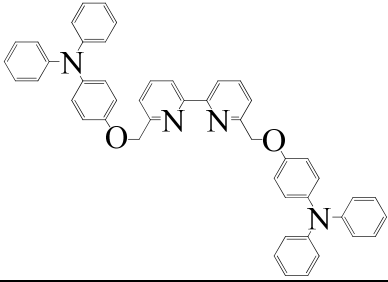
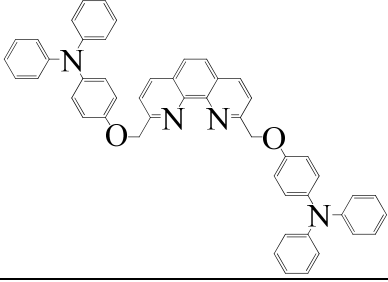
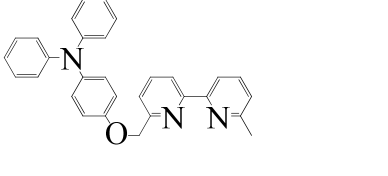
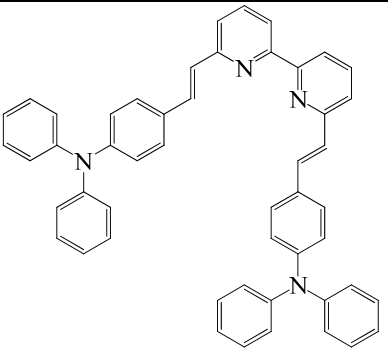
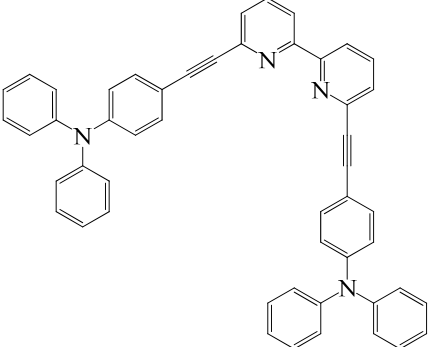


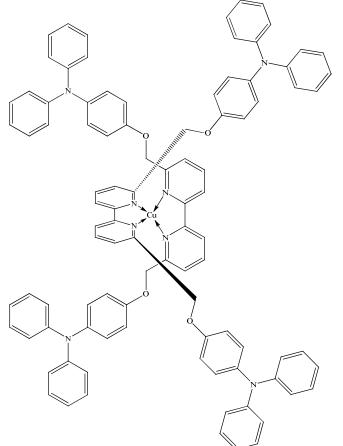
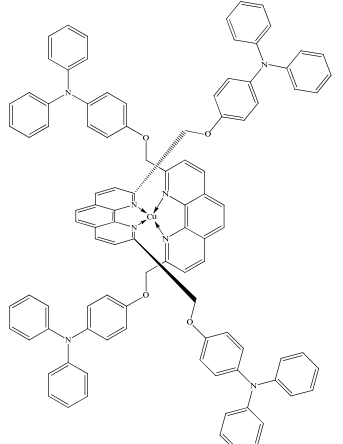
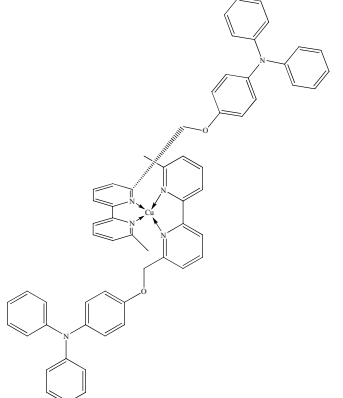
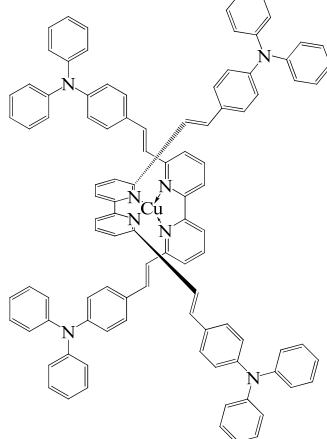
**Figure 2.64** Packing in bis[6,6'-bis(2-(4-(*N,N*-diphenylamino)phenyl)ethenyl)-2,2'-bipyridine]copper(I) hexafluorophosphate, as viewed along the *c* axis but with solvent molecules and cations removed.

Electrochemistry, UV-VIS and fluorescence of disubstituted-2,2'-bipyridine and 2,9'-disubstituted-1,10-phenanthroline copper(I) complexes

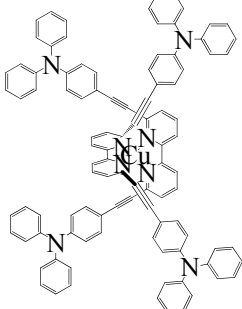
	ELECTROCHEMISTRY	
	$E_{1/2} / V$	$E_{1/2}^{red} / V$
 $PF_6$	0.332	-0.976
 $PF_6$	Not observed	-1.207
 $PF_6$	0.334	-0.878
 $PF_6$	0.915	-1.243
 $PF_6$	0.462 <sup>a</sup>	-1.087 <sup>a</sup>

 PF <sub>6</sub>	0.790	-1.302
 PF <sub>6</sub>	0.782	-1.372
 PF <sub>6</sub>	0.424	-1.201
 PF <sub>6</sub>	0.609	-0.990
 PF <sub>6</sub>	0.138	-1.362
 PF <sub>6</sub>	0.128	-1.087

	0.408 <sup>b, c</sup>	-1.567 <sup>b, c</sup>
	0.450 <sup>b, c</sup> 0.203 <sup>b, c</sup>	-1.483 <sup>b, c</sup>
	0.440 <sup>b, c</sup> 0.147 <sup>b, c</sup>	-1.532 <sup>b, c</sup>
	0.58 <sup>b, c</sup>	-1.518 <sup>b, c</sup>
	0.664 <sup>b, c</sup> 0.598 <sup>b, c</sup>	-1.645 <sup>b, c</sup>

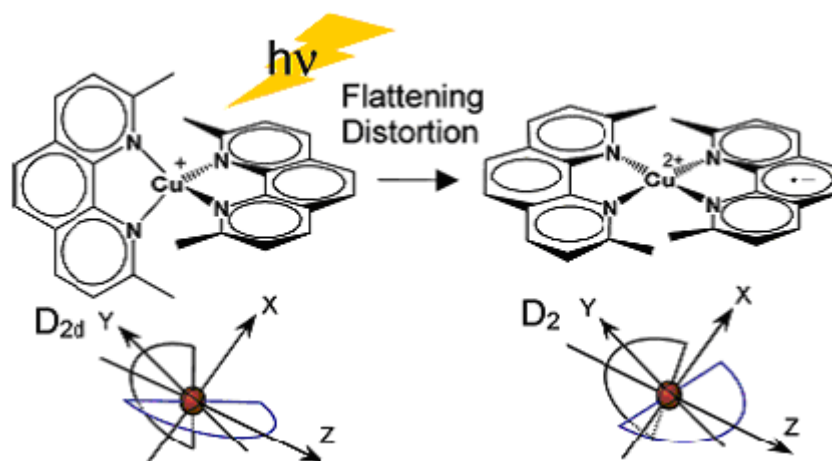
 <p style="text-align: right;">PF<sub>6</sub></p>	<p>0.853<sup>b, c</sup> 0.439<sup>b, c</sup> 0.145<sup>b, c</sup></p>	<p>-1.464<sup>b, c</sup></p>
 <p style="text-align: right;">PF<sub>6</sub></p>	<p>0.815<sup>b, c</sup> 0.605<sup>b, c</sup> 0.410<sup>b, c</sup> Non reversible</p>	<p>-1.862<sup>b, c</sup></p>
 <p style="text-align: right;">PF<sub>6</sub></p>	<p>-0.862<sup>b, c</sup> 0.492<sup>b, c</sup> 0.275<sup>b, c</sup></p>	<p>-1.534<sup>b, c</sup></p>
 <p style="text-align: right;">PF<sub>6</sub></p>	<p>0.559<sup>b, c</sup> 0.463<sup>b, c</sup></p>	<p>-1.566<sup>b, c</sup></p>



 <p style="text-align: right;">PF<sub>6</sub></p>	<p>0.621<sup>b, c</sup> 0.458<sup>b, c</sup></p>	<p>-1.520<sup>b, c</sup></p>
<p>Cyclic voltammograms unless otherwise stated of Cu<sup>I</sup>(ligands)<sub>2</sub><sup>+</sup> were recorded in CH<sub>3</sub>CN measured at 100 mV s<sup>-1</sup> with a common electrolyte, 0.1 M tetrabutylammonium hexafluorophosphate, a Ag wire reference electrode, a Pt gauze auxiliary electrode, and a glassy carbon working electrode. All values were referenced to <sup>a</sup> CV was run in DMSO <sup>b</sup> CV was run in DCM <sup>c</sup> versus Fc / Fc<sup>+</sup></p>		

**Table 2.15** Electrochemistry data.

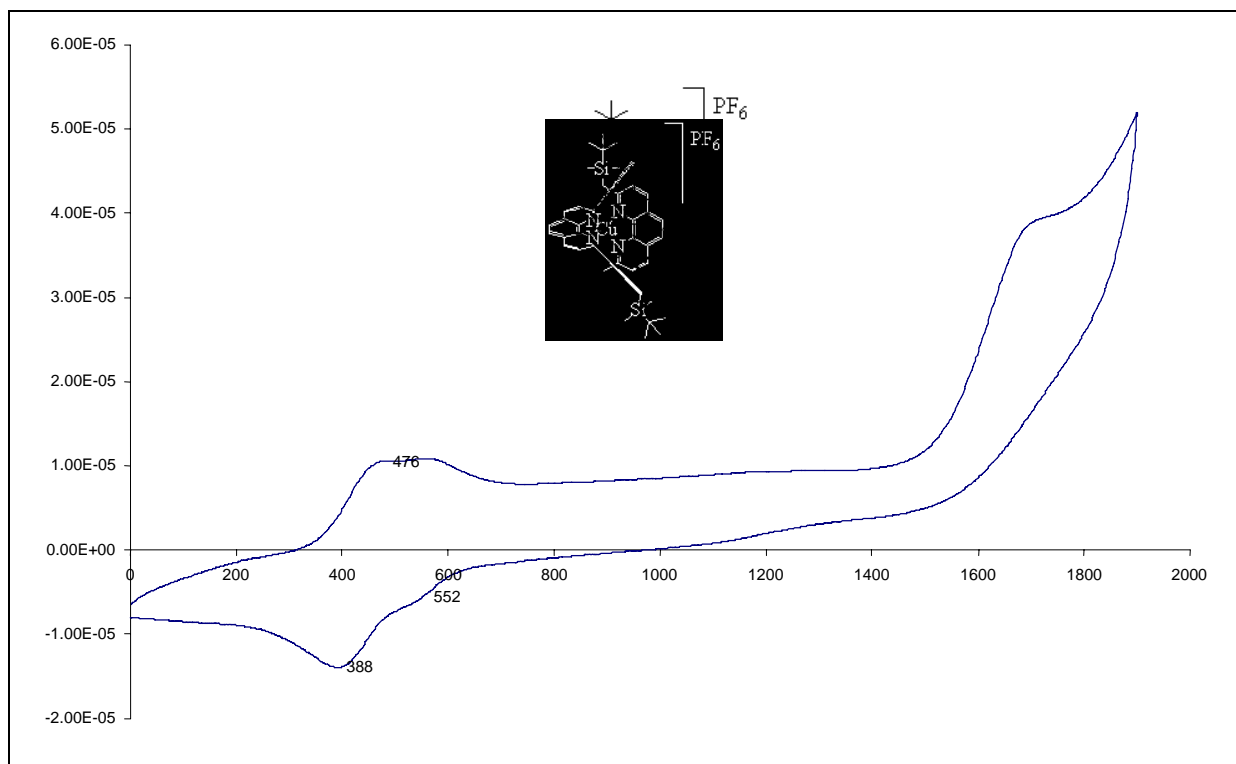
The copper(I) complex 2,9-dimethyl-1,10-phenanthroline [Cu(dmphen)<sub>2</sub>]<sup>+</sup> is a well-known prototypical metal complex that attracts much attention<sup>[99-100]</sup>. The most intriguing property of the [Cu(dmphen)<sub>2</sub>]<sup>+</sup> complex is that it undergoes photo-induced structural change<sup>[101-103]</sup>. With MLCT excitation, the central metal is formally oxidized from Cu(I) to Cu(II), and a structural change is induced as expected from the structural difference between Cu(I) complexes (tetrahedral-like) and Cu(II) complexes (square-planar-like) in the ground state. The dihedral angle between the two ligands becomes smaller with this “flattening” motion and the molecular symmetry of [Cu-(dmphen)<sub>2</sub>]<sup>+</sup> is reduced from *D*<sub>2d</sub> to *D*<sub>2</sub>, although the complex cannot reach the square planar structure because of the methyl groups at the 2 and 9 positions of the ligands (Figure 2.65).



**Figure 2.65** Photoinduced flattening distortion of  $[\text{Cu}(\text{dmphen})_2]^+$ <sup>[3]</sup>.

Such a structural change occurs not only with MLCT transition of  $[\text{Cu}(\text{dmphen})_2]^+$  but also in photochemical and electrochemical electronic conversion of  $\text{Cu}(\text{I})/\text{Cu}(\text{II})$  in general. Elucidation of the dynamics and mechanism of the structural change of copper complexes is very important not only for fundamental understanding but also for potential application of this series of metal complexes.

In an initial investigation we decided to study simple  $\text{Cu}(\text{I})$  complexes to try and ascertain the dependence on the  $\text{Cu}(\text{I})$  redox chemistry of the substituents on the ligands. The cyclic voltammograms of the "simple" complexes were recorded in acetonitrile (Table 2.15). Previous studies have shown that the potential of the  $\text{Cu}^{2+/+}$  couple in  $[\text{Cu}(\text{NN})_2]^+$  systems with 2 and 9 phenanthroline substituents is influenced to a large degree by the sterics of the substituents<sup>[104]</sup>. In general, as the steric bulk of the 2 and 9 substituents increases, the ligands are less able to rearrange to the preferred (square-planar) coordination geometry of  $\text{Cu}(\text{II})$  due to steric clashes with the opposing ligand. This stabilizes the  $\text{Cu}^+$  state and results in an increase in the  $\text{Cu}^{2+/+}$  redox potential. Thus, assuming there are no extreme changes in the electron-donating or -withdrawing properties of the ligands, this redox couple can be used to indicate the rigidity the ligands impart on the complex by observing the shift in the  $\text{Cu}^{2+/+}$  redox potentials. It can be seen in table 2.16 that the potentials are very much dependent on the nature of the substituent on the alpha carbon. A representative example is shown in figure 2.65 which clearly shows that  $\text{Cu}(\text{I})/\text{Cu}(\text{II})$  couple.

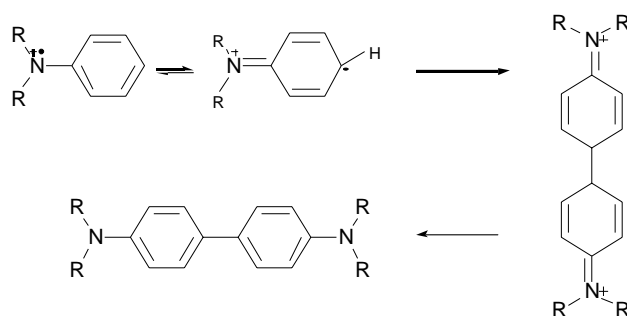


**Table 2.16** CV of bis[2-dimethyl-9-(tert-butyldimethylsilyl)methyl]-1-10-phenanthroline]copper(I) hexafluorophosphate in  $\text{CH}_3\text{CN}$ .

After establishing the electrochemistry of these simple systems we then examined the effect of placing a strongly electron donating redox active component on the oligopyridine ligand. The triarylamine moiety was chosen as it displays rich redox chemistry and possesses interesting properties in materials chemistry. The cyclic voltammograms (CVs) in dichloromethane of the bipyridine ligand bearing one triarylamine units and its corresponding Cu complex is shown in table 2.17. A small amount of ferrocene was added as an internal standard during the experiment. In the anodic scans, the ligand exhibits an oxidation process at +0.408 V that is reversible. This result means that the triarylamine moiety is electrochemically oxidized to the triarylaminium cationic radical and reversibly reduced to the starting amine and that the radical is chemically stable without any subsequent chemical side reactions. Also shown in figure 2.66 is the ligand bearing one triarylamine unit.

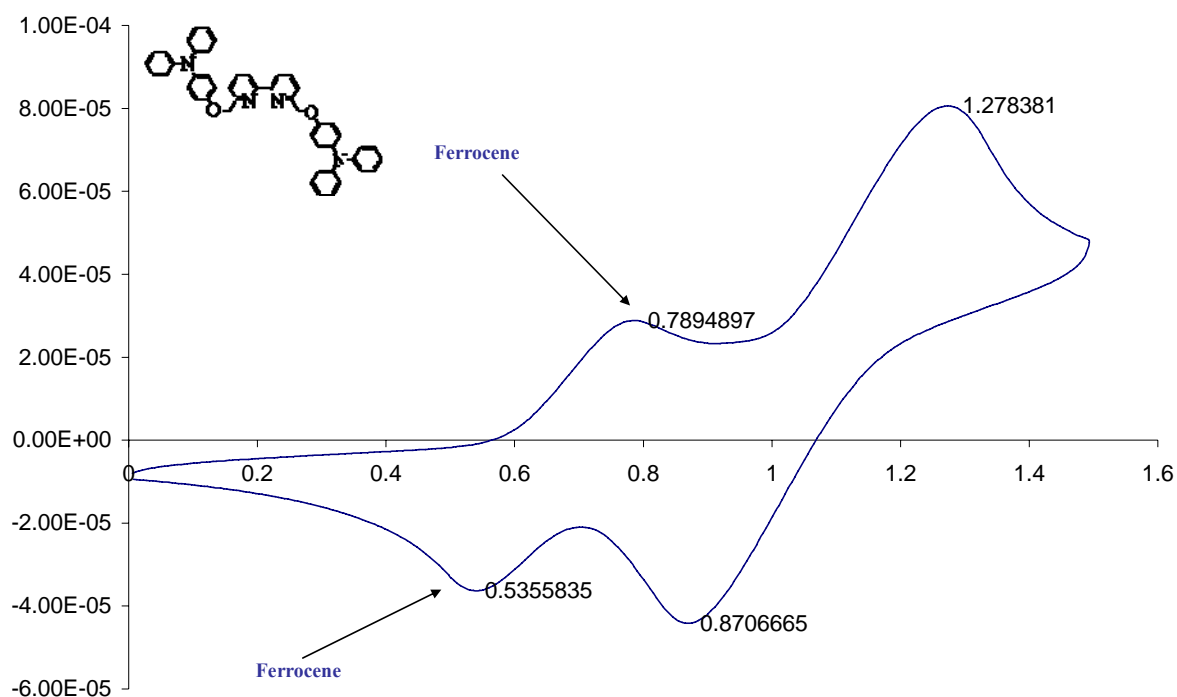
The Cu(I) complex shows markedly different electrochemistry the reversible oxidation peak at +0.408 V in the ligand now appears to have transformed to an irreversible oxidation process at a potential of +0.815 V. There are appears to be two other oxidation processes as determined by differential pulse voltammetry (DPV) which occur at +0.410 and +0.605 V. Therefore it is apparent that the radical cation is not stable upon incorporation into the Cu(I)

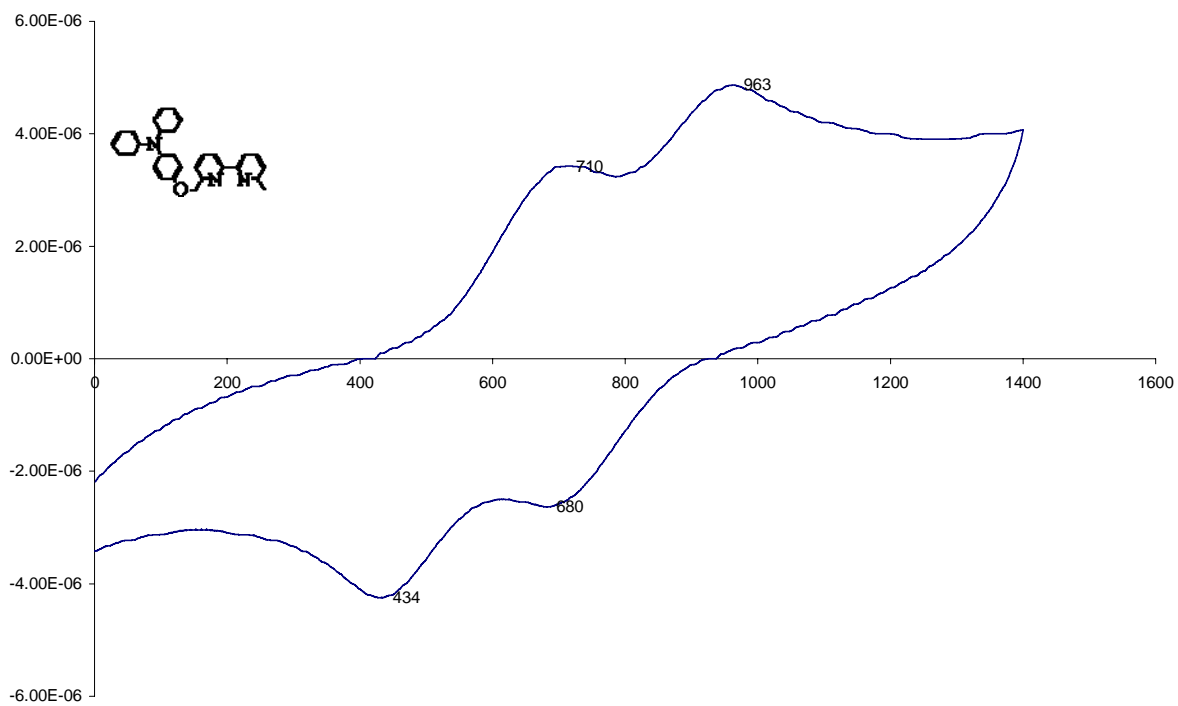
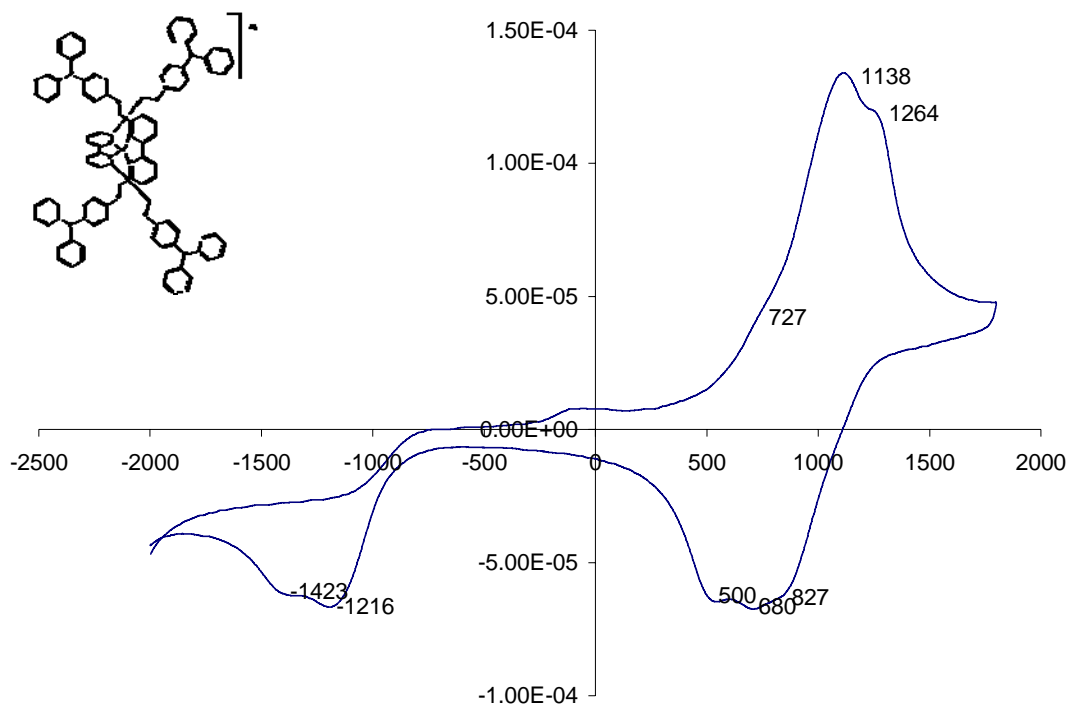
complex. The mechanism of decomposition of triarylamine radical cations has been well established and is shown in figure 2.66<sup>[105]</sup>. The difference in stability has been related to the ease of proton removal in compounds that bear an electron-withdrawing group. It has been

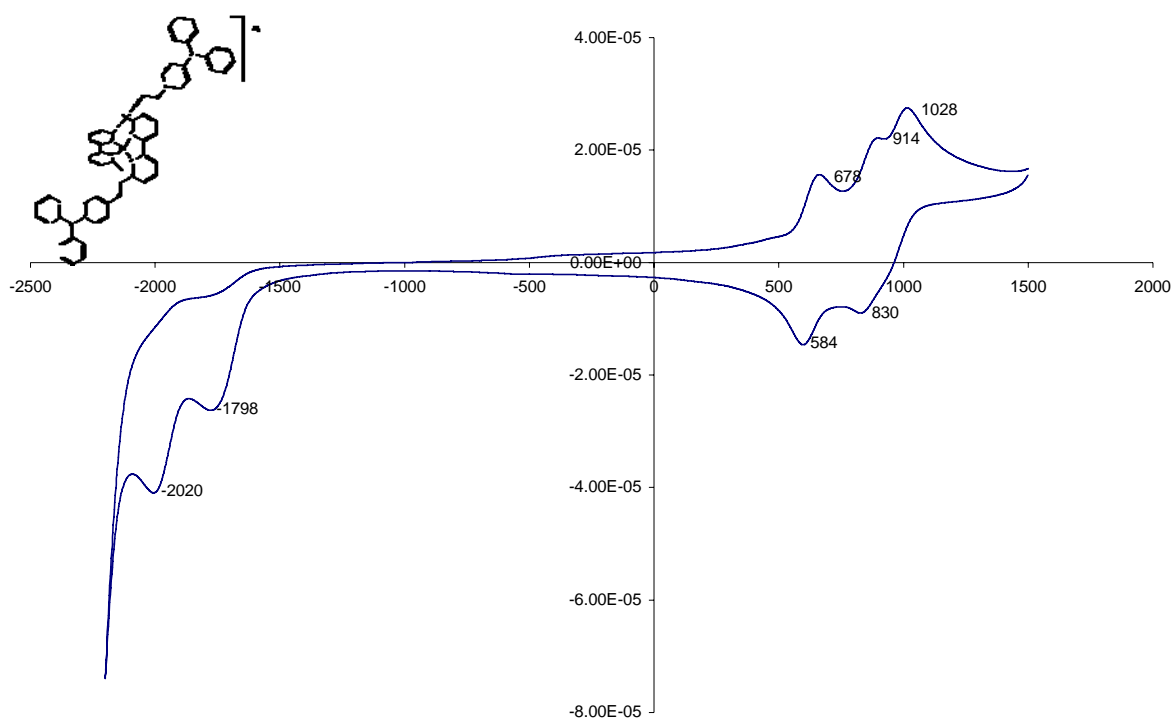


**Figure 2.66** Mechanism of decomposition of triarylamine radical cation<sup>[105]</sup>

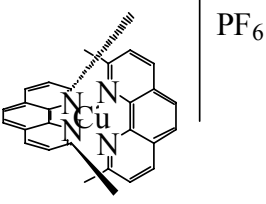
well established that incorporation of electron-donating substituents at the *para*-position of triarylamines affords stable radical cations<sup>[106]</sup>. Therefore we can postulate that in our system, due the electron withdrawing character of the metal centre, the radical cation is no longer stable when compared to the ligand and therefore the other redox processes may be the decomposition pathway of the radical cation overlapping with the Cu(I/II) couple.

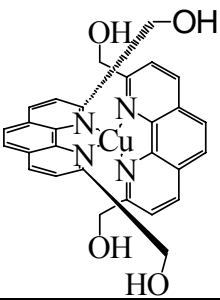
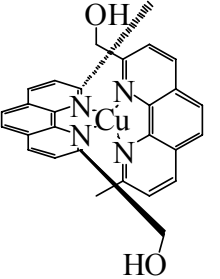
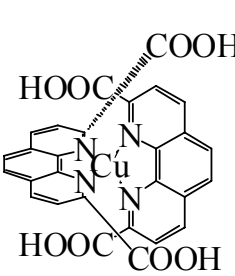
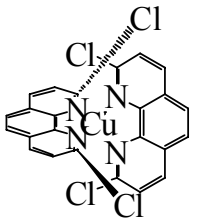
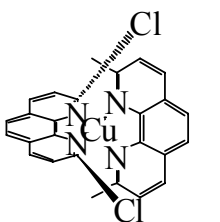


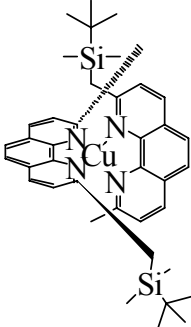
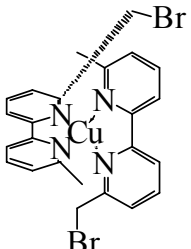
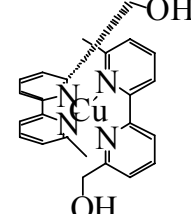
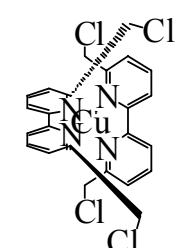
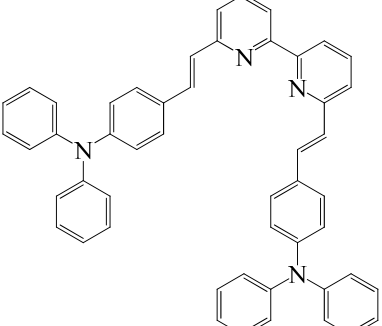




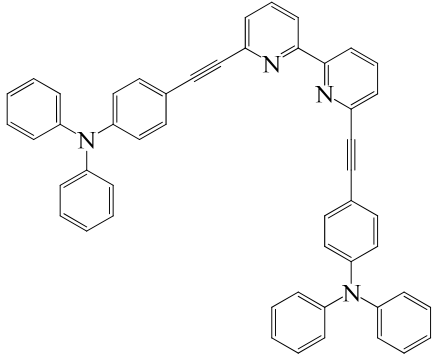
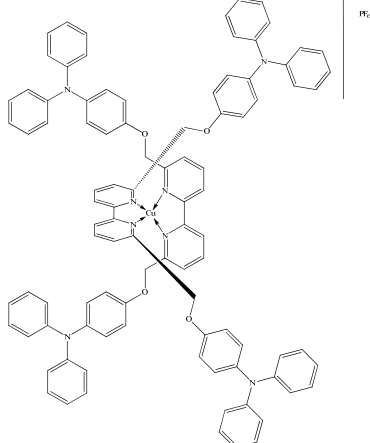
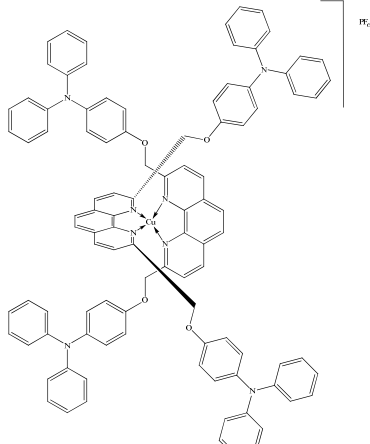
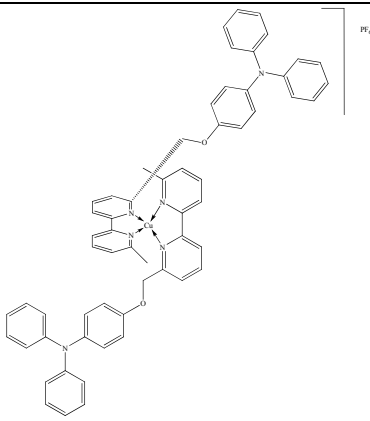
**Table 2.17** CV data for representative complexes.

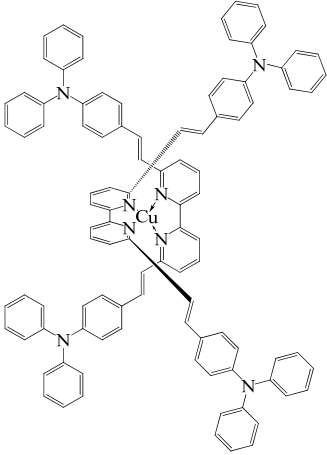
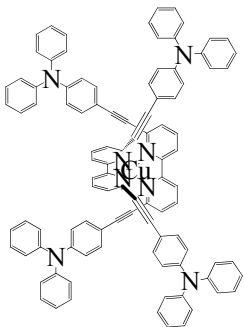
	UV vis	emission max
	$\lambda_{\max}$ nm ( $\epsilon$ , $M^{-1}$ , $cm^{-1}$ )	EM : nm
	457 (8620), 275 (62025).	EX: 457 nm EM: 660 nm

 <p>OH—OH PF<sub>6</sub> OH HO</p>	449 (6813), 278 (35320).	none
 <p>OH PF<sub>6</sub> HO</p>	449 (6813), 302 (35783).	none
 <p>COOH PF<sub>6</sub> HOOC HOOC COOH</p>	460 (2127), 333 sh (15992), 286 (47582).	none
 <p>Cl PF<sub>6</sub> Cl Cl Cl</p>	448 (7371), 279 (60909).	none
 <p>Cl PF<sub>6</sub> Cl</p>	452 (7642), 278 (69977).	none

 <p>PF<sub>6</sub></p>	437 (5036), 283 (49801).	EX: 437 nm EM: 680 nm
 <p>PF<sub>6</sub></p>	455 (5442), 304 (27738).	none
 <p>PF<sub>6</sub></p>	449 (6183), 302 (35783).	none
 <p>PF<sub>6</sub></p>	445 (4906), 302 (23649).	none
	299 (108000), 389 (189425).	EX: 389 nm EM: 473 nm



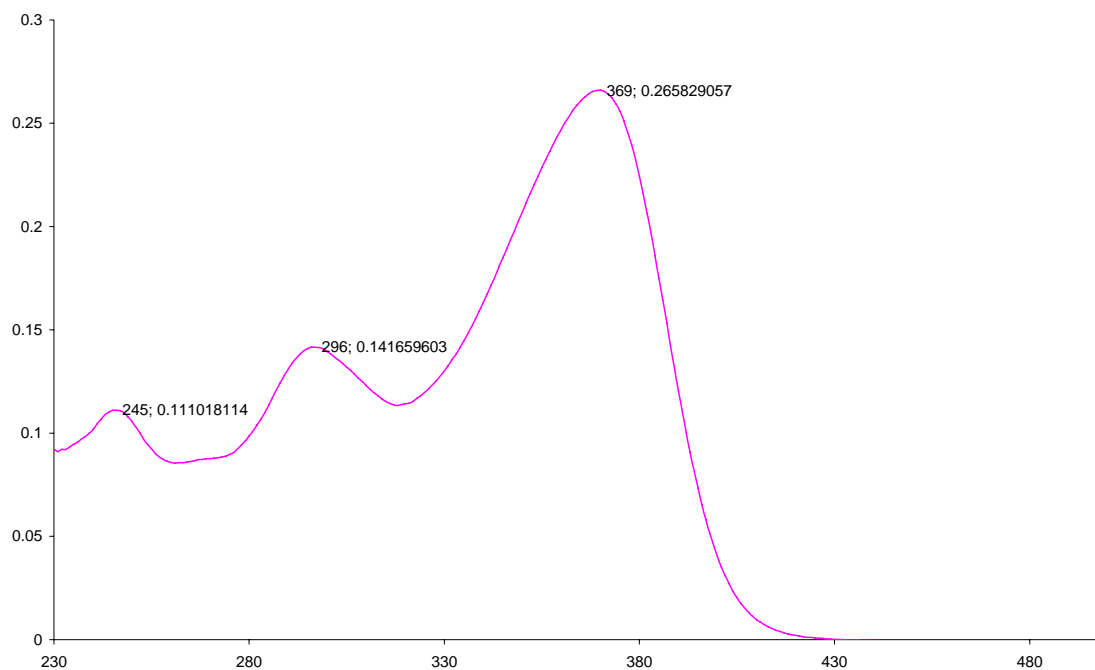
 <p>The structure shows a copper(I) center coordinated to two terphenyl ligands and one bis(pyridine) ligand. The terphenyl ligands are connected to the copper center via their central phenyl rings. The bis(pyridine) ligand is connected via one of its pyridine rings to the central phenyl ring of the second terphenyl ligand.</p>	245 (27754), 296 (35414), 369 (66457).	EX: 369 nm EM: 451 nm
 <p>The structure shows a copper(I) center coordinated to two terphenyl ligands and one bis(phenyl) ligand. The terphenyl ligands are connected to the copper center via their central phenyl rings. The bis(phenyl) ligand is connected via one of its phenyl rings to the central phenyl ring of the second terphenyl ligand.</p>	300 (120101), 450 (4573).	EX: 450 nm EM: 519 nm
 <p>The structure shows a copper(I) center coordinated to two terphenyl ligands and one bis(phenyl) ligand. The terphenyl ligands are connected to the copper center via their central phenyl rings. The bis(phenyl) ligand is connected via one of its phenyl rings to the central phenyl ring of the second terphenyl ligand.</p>	296 (112660), 446 (6053).	EX: 446nm EM: 518 nm
 <p>The structure shows a copper(I) center coordinated to two terphenyl ligands and one bis(phenyl) ligand. The terphenyl ligands are connected to the copper center via their central phenyl rings. The bis(phenyl) ligand is connected via one of its phenyl rings to the central phenyl ring of the second terphenyl ligand.</p>	301 (77622), 450 (6382).	EX: 450 nm EM: 525 nm

 <p style="text-align: right;">PF<sub>6</sub></p>	299 (180500) 398 (231750).	EX: 398 nm EM: 483 nm
 <p style="text-align: right;">PF<sub>6</sub></p>	297 (102052), 383 (115415).	EX: 338 nm EM: 440 nm

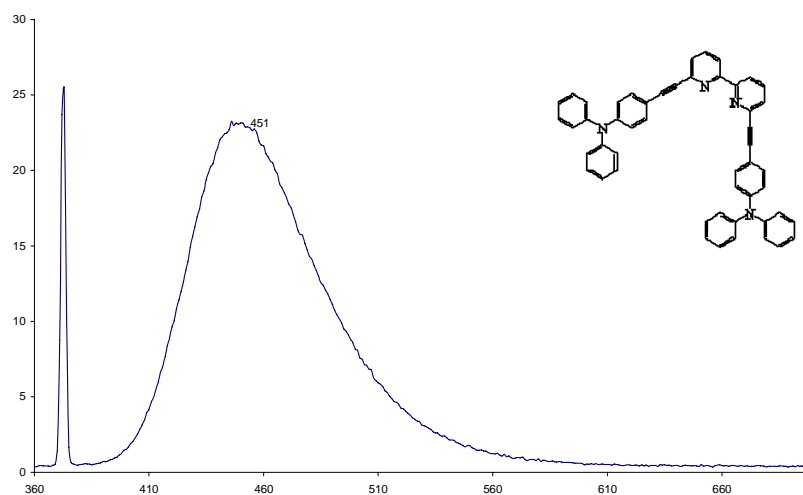
**Table 2.18** UV-Vis data and fluorescence data.

The conjugated compounds with triphenylamine substituents are much more fluorescent than the other complexes.

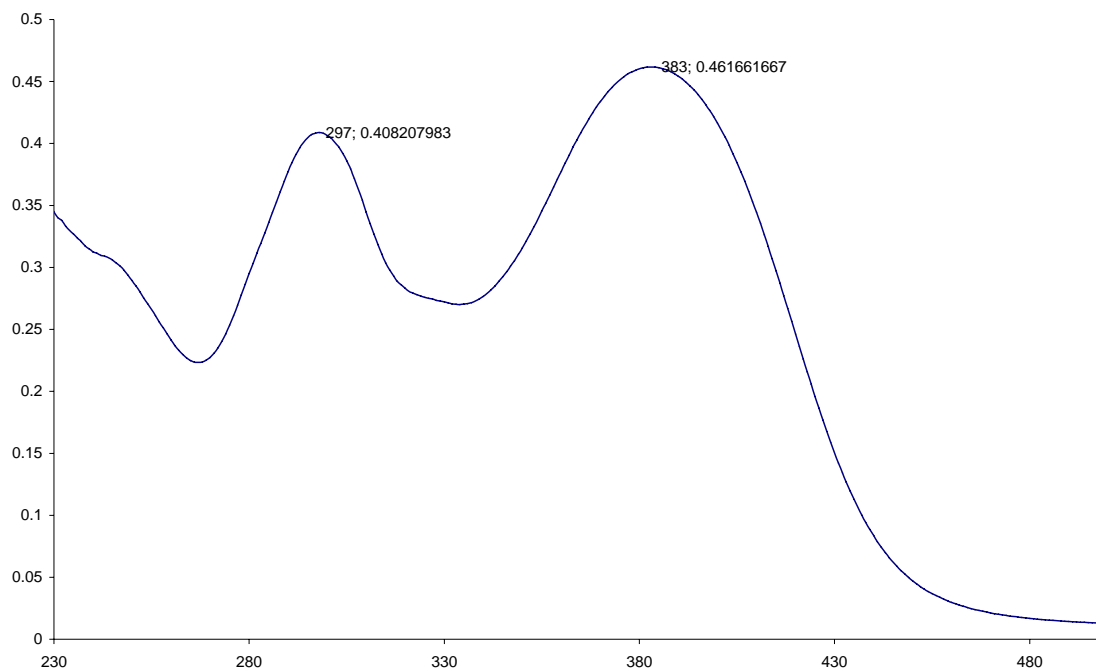
Examples of absorbance and emission spectra are shown in figures 2.67-2.70.



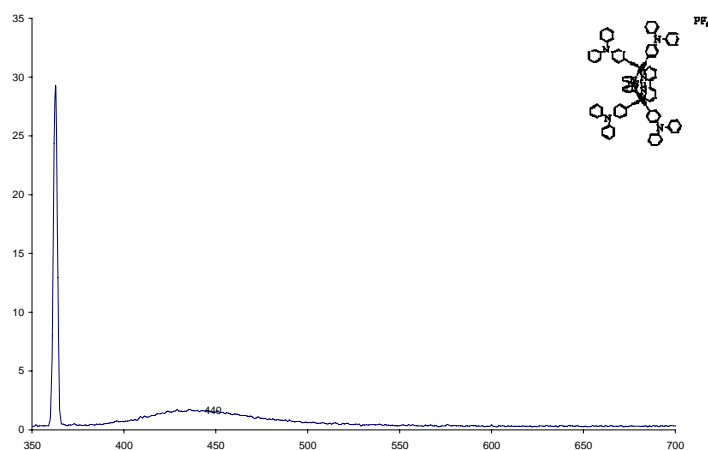
**Figure 2.67** Absorbance spectra of 6,6'-bis(4-(*N,N*-diphenylamino)phenylethynyl)-2,2'-bipyridine:



**Figure 2.68** Emission spectra of 6,6'-bis(4-(*N,N*-diphenylamino)phenylethynyl)-2,2'-bipyridine, excitation : 369 nm. Emission : 451 nm



**Figure 2.69** Absorbance spectra of bis[4,4'-(2,2'-bipyridine-6,6'-diylbis(ethyne-2,1-diyl))bis(*N,N*-diphenylaniline)]copper(I) hexafluorophosphate.



**Figure 2.70** Emission spectra of bis[4,4'-(2,2'-bipyridine-6,6'-diylbis(ethyne-2,1-diyl))bis(*N,N*-diphenylaniline)]copper(I) hexafluorophosphate. Excitation . 383 nm. Emission: 440 nm

## 4-5 References

- [1] Werner, A., *Founder of Coordination Chemistry*, G.B. Kauffman, Springer-Verlag, Berlin, **1966**.
- [2] Roundhill, D. M., *Photochemistry and Photophysics of Metal Complexes*, Plenum Press, New York, **1994**.
- [3] Armaroli, N., *Chem. Soc. Rev.*, **2001**, 30, 113.
- [4] Scaltrito, D. V., Thompson, D. W., O'Callaghan, J. A., Meyer, G. J., *Coord. Chem. Rev.*, **2000**, 208, 243.
- [5] McMillin, D. R., McNett, K. M., *Chem. Rev.*, **1998**, 98, 1201.
- [6] Bignozzi, C. A., Argazzi, R., Kleverlaan, C. J., *Chem. Soc. Rev.*, **2000**, 29, 87.
- [7] Schwab, P. F. H., Levin, M. D., Michl, J., *Chem. Rev.*, **1999**, 99, 1863.
- [8] Balzani, V., Campagna, S., Denti, G., Juris, A., Serroni, S., Venturi, M., *Acc. Chem. Res.*, **1998**, 31, 26.
- [9] Juris, A., Balzani, V., Barigelletti, F., Campagna, S., Belser, P., von Zelewsky, A., *Coord. Chem. Rev.*, **1988**, 84, 85.
- [10] Barigelletti, F., Flamigni, L., *Chem. Soc. Rev.*, **2000**, 29, 1.
- [11] Harriman, A., Ziessel, R., *Chem. Commun*, **1996**, 1707.
- [12] Balzani, V., Juris, A., Venturi, M., Campagna, S., Serroni, S., *Chem. Rev.*, **1996**, 96, 759.
- [13] Bignozzi, C. A., Argazzi, R., Kleverlaan, C. J., *Chem. Soc. Rev.*, **2000**, 29, 87
- [14] Shaul, M., Cohen, Y., *J. Org. Chem.*, **1999**, 64, 9358.
- [15] Pijper, P. J., Goot, H. v. d., Timmerman, H., Nauta, W. Th., *Eur. J. Med. Chem. Chim. Ther.*, **1984**; 19, 399.
- [16] Arai, S., Ishikura, M., Sato, K., Yamagishi, T., *J. Heterocycl. Chem.*, **1995**; 32, 1081.
- [17] Chandler, J. C., Deady, L. W., Reiss, J. A., *J. Heterocyclic chem.*, **1981**, 18, 599.
- [18] Goswami, S., Mukherjee, R., Ray, J., *Org. Lett.*, **2005**, 7, 1283.
- [19] Goswami, S., Adak, A. K., *Synth. Commun.*, **2003**; 33, 475.
- [20] Kaye, P. T.; Wellington, K. W., *Synth. Commun.*; **2001**; 31, 2405.
- [21] Linnane, P., James, T. D., Imazu, S., Shinkai, S., *Tetrahedron Lett.*, **1995**; 36, 8833.
- [22] Wang, T., Bradshaw, J. S.; Huszthy, P., Kou, X., Dalley, N. Kent; Izatt, R. M., *J. Heterocycl. Chem.*; **1994**, 31, 1.
- [23] Abushamleh, A. S., Goodwin, H. A., *Aust. J. Chem.*, **1980**, 33, 2171.

- [24] Mukkula, V.-M., Sund., C., Kwiatkowski, M., Pasanen, P., Högberg, M., Kankare, J., Takalo, H., *Helv. Chim. Acta*, **1992**, 75, 1621.
- [25] Esposito, V., Galeone, A., Mayol, L., Oliviero, G., Randazzo, A., Varra, M., *Eur. J. Org. Chem.*, **2002**, 4228.
- [26] Newkome, G. R., Kiefer, G. E., Puckett, W. E., *J. Org. Chem.*, **1983**, 48, 5112.
- [27] Bates, G. B., Cole, E., Parker, D., Katakya, R., *J. Chem. Soc. Dalton Trans.*, **1996**, 2693.
- [28] Weijnen, J. G. J., Engbersen, J. F. J., *Recl. Trav. Chim. Pays-Bas*, **1993**; 112, 351.
- [29] Newkome, G. R., Kiefer, G. E., Xia, Y.-J., Gupta, V. K., *Synthesis*, **1984**, 676.
- [30] Eggert, J. P. W., Harrofield, J., Lüning, U., Skelton, B. W., White, A. H., Löffler, F., Konrad, S., *Eur. J. Org. Chem.*, **2005**, 1348.
- [31] Dietrich-Buchecker, C. O.; Sauvage, J.-P., *Tetrahedron Lett.*, 1983, 24, 5091.
- [32] Newkome, G. R., Gupta, V. K., Fronczek, F. R., *Inorg. Chem.*, **1983**, 22, 171.
- [33] Offermann, W., Vogtle, F., *Angew. Chem. Int. Ed. Engl.*, **1980**, 19, 464.
- [34] Newkome, G. R., Theriot, K. J., Gupta, V. K., Fronczek, F. R., Baker, G. R., *J. Org. Chem.*, **1989**, 54, 1766.
- [35] Maerker, G., Case, F. H., *J. Am. Chem. Soc.*, **1958**, 80, 2745.
- [36] Corey, E. J., Borrer, A. L., Foglia, T., *J. Org. Chem.*, **1965**, 30, 288.
- [37] Boekelheide, V., Linn, W. J., *J. Am. Chem. Soc.*, **1954**, 76, 1286.
- [38] Reedijk, J., in *Comprehensive Coordination Chemistry*, Wilkinson, G., Gillard, R. D., McCleverty, J. A. (Eds.), Vol. 2, Pergamon, Oxford, **1987**, p. 73.
- [39] Oae, S., Inibushi, Y., Yoshihara, M., *Phosphorus, Sulfur Silicon*, **1995**, 103, 101.
- [40] Newkom, G. R., Pantaleo, D. C., Puckett, W. E., Ziefle, P. L., Deutsch, W. A., *J. Inorg. Nucl. Chem.*, **1981**, 43, 1529.
- [41] Fort, Y., Becker, S., Caubère, P., *Tetrahedron*, **1994**, 41, 11893.
- [42] Dietrich-Bicheker, C. O., Marnot, P. A., Sauvage, J.-P., *Tetrahedron Lett.*, **1982**, 23, 5291.
- [43] Parks, J. E., Wagner, B. E., Holm, R. H., *J. Organometal. Chem.*, **1973**, 56, 53.
- [44] Uchida, Y., Kajita, R., Kawasaki, Y., Oae, S., *Tetrahedron Lett.*, **1995**, 36, 4007.
- [45] Uenishi, J., Tanaka, T., Wakabayashi, S., Oae, S., *Tetrahedron Lett.*, **1990**, 31, 4625.
- [46] DeTar, D. R., *Org. React.*, **1957**, 9, 409.
- [47] Fabian, R. H., Klassen, D. M., Sonntag, R. W., *Inorg. Chem.*, **1980**, 19, 1977.
- [48] Rode, T., Breitmaier, E., *Synthesis*, **1987**, 574.

- [49] Cassol, T. M., Demnitz, F. W. J., Navarro, M., de Neves, E. A., *Tetrahedron Lett.*, **2000**, *41*, 8203.
- [50] Goswami, S., Adak, A. K., Mukherjee, R., Jana, S., Dey, S., Gallagher, J. F., *Tetrahedron*, **2005**, *61*, 4289.
- [51] Mathieu, J., Marsura, A., *Synth. Commun.*, **2003**, *33*, 409.
- [52] Cui, X.-L., Brown, R. S., *J. Org. Chem.*, **2000**, *65*, 5653.
- [53] Heller, M., Schubert, U. S., *J. Org. Chem.*, **2002**, *67*, 8269.
- [54] Galaup, C., Carrie, M.-C., Tisnes, P., Picard, C., *Eur. J. Org. Chem.*, **2001**, *11*, 2165.
- [55] Franca, K. W. R. De, Navarro, M., Leonel, E., Durandetti, M., Nedelec, J.-Y., *J. Org. Chem.*, **2002**, *67*, 1838.
- [56] De Franca, K. W. R., de Lira Oliveira, J., Florencio, T., Da Silva, A. P., Navarro, M., Leonel, E., Nedelec, J.-Y., *J. Org. Chem.*, **2005**, *70*, 10778.
- [57] Rajalakshmanan, E.; Alexander, V.; *Synth. Commun.*; **2005**; *35*, 891.
- [58] Laitinen, R. H., Csoban, K., Pursiainen, J., Huuskonen, J., Rissanen, K., *Acta Chem. Scand.*, **1997**; *51*, 462.
- [59] Wang, Z., Reibenspies, J., Motekaitis, R. J.; Martell, A. E.; *J. Chem. Soc. Dalton Trans.* **1995**; 1511.
- [60] Voegtle, F., Hochberg, R., Kochendoerfer, F., Windscheif, P.-M., Volkmann, M., Jansen, M., *Chem. Ber.*, **1990**, *11*, 2181.
- [61] Willink; W., *Recl. Trav. Chim. Pays-Bas*, **1935**, *54*, 275.
- [62] Newkom, G. R., Wallace, E., Puckett, Kiefer, G. E., Gupta, V. K., Xia, Y., Coreil, M., Hackney, M. M., *J. Org. Chem.*, **1982**, *47*, 4116.
- [63] Koenig, T.; Wiczorek, J. S., *J. Org. Chem.*, **1968**, *33*, 1530.
- [64] Vozza, J. F., *J. Chem. Soc.*, **1962**, 3856.
- [65] Traynelis, V. J., Martello, R. F., *J. Am. Chem.*, **1958**, *80*, 6590.
- [66] Baker, W., Buggle, K. M., McOmie, J. F. W., Watkins, *J. Chem. Soc.*, **1958**, 3594.
- [67] Mathes, W., Schuly, H., *Angew. Chem., Int. Ed. Engl.*, **1963**, *2*, 144.
- [68] Parks, J. E.; Wagner, B. E.; Holm, R. H., *J. Organomet. Chem.*, **1973**, *56*, 53.
- [69] Newkom, G. R., Masayoshi, O., Wallace, E., Puckett, W. E., Deutsch, W. A., *J. Am. Chem. Soc.*, **1980**, *102*, 4551.
- [70] Lehn, J.-M., Rigault, A., Siegel, J., Harrowfield, J., Chevrier, B., Moras, D., *Proc. Natl. Acad. Sci.*, **1987**, *84*, 2565.
- [71] Smith, A. P., Lamba, J. J. S., Fraser, C. L., *Org. Synth.*, **2002**, *48*, 82.

- [72] McIlroy, S. P., Clo, E., Nikolajsen, L., Frederiksen, P. K., Nielsen, C. B., Gothelf, K. V., Ogilby, P. R., *J. Org. Chem.*, **2005**, *70*, 1134.
- [73] Miller, M. T., Gantzel, P. K., Karpishin, T. B., *Inorg. Chem.* **1998**, *37*, 2285.
- [74] D. R. McMillin, K. M. McNett, *Chem. Rev.*, **1998**, *98*, 1201.
- [75] Gahler, A. R., *Anal. Chem.*, **1954**, *26*, 577.
- [76] Smith, G. F., McCurdy, W. H., *Anal. Chem.*, **1952**, *24*, 371.
- [77] Smith, G. F., *Anal. Chem.*, **1954**, *26*, 1534.
- [78] Wilkins, H., Schilt, A. A., Smith, G. F., *Anal. Chem.*, **1955**, *27*, 1574.
- [79] McMillin, D. R., Buckner, M. T., Ahn, B. T., *Inorg. Chem.*, **1977**, *16*, 943.
- [80] Everly, R. M., Ziessel, R., Suffert, J., McMillin, D. R., *Inorg. Chem.*, **1991**, *30*, 559.
- [81] Shinozaki, K., Kaizu, Y., *Bull. Chem. Soc. Jpn.*, **1994**, *67*, 2435.
- [82] Pallenberg, A. J., Koenig, K. S., Barnhart, D. M., *Inorg. Chem.*, **1995**, *34*, 2833.
- [83] Eggleston, M. K., McMillin, D. R., Koenig, K. S., Pallenberg, A. J., *Inorg. Chem.*, **1997**, *36*, 172.
- [84] Cunningham, C. T., Moore, J. J., Cunningham, K. L. H., Fanwick, P. E., McMillin, D. R., *Inorg. Chem.*, **2000**, *39*, 3638.
- [85] Kalsani, V., Schmittel, M., Listorti, A., Accorsi, G., Armaroli, N., *Inorg. Chem.*, **2006**, *45*, 2061.
- [86] Wang, X. J., Wang, W., Koyama, M., Kubo, M., Miyamoto, A., *J. Photochem. Photobiol. A-Chem.*, **2006**, *179*, 149.
- [87] Wang, X. J., Lv, C., Koyama, M., Kubo, M., Miyamoto, A., *J. Organomet. Chem.*, **2006**, *691*, 551.
- [88] Hoffmann, S. K., Corvan, P.J., Singh, P., Sethulekshmi, C. N., Metzger, R. M., Hatfield, W. E., *J. Am. Chem. Soc.*, **1983**, *105*, 4608.
- [89] Dobson, J. F., Green, B. E., Healy, P. C., Kennard, C. H. L., Pakawatchai, C., White, A. H., *Aust. J. Chem.*, **1984**, *37*, 649.
- [90] Dessy, G., Fares, V., *Cryst. Struct. Commun.*, **1979**, *8*, 507.
- [91] Kon, A. Yu., Burshtein, I. F., Proskina, N. N., Ibragimov, B. T., *Koord. Khim. (Russ.)*, **1987**, *13*, 260.
- [92] Hamalainen, R., Ahlgren, M., Turpeinen, U., Raikas, T., *Cryst. Struct. Commun.*, **1979**, *8*, 75.
- [93] Kovalevsky, A. Yu., Gembicky, M., Novozhilova, I. V., Coppens, P., *Inorg. Chem.*, **2003**, *42*, 8794.
- [94] Pawlowski, V., Kunkely, H., Zabel, M., Vogler, A., *Inorg. Chim. Acta*, **2004**, *357*, 824.

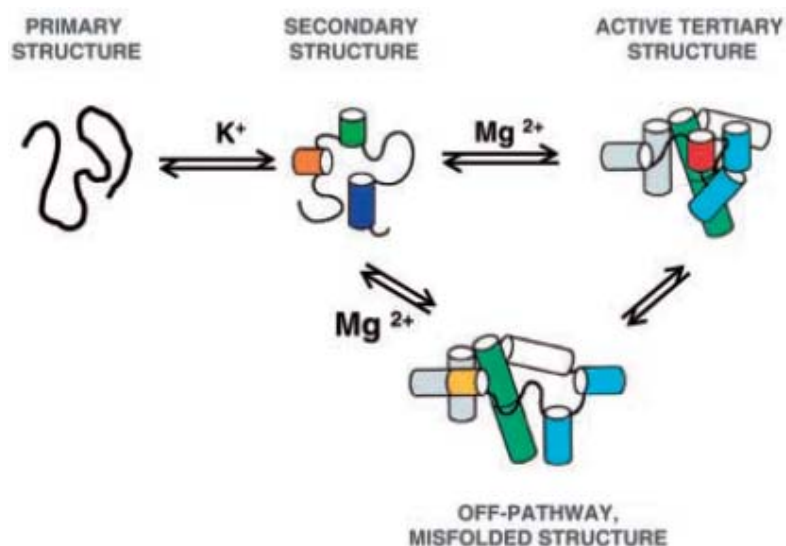


- [95] Hamalainen, R., Turpeinen, U., Ahlgren, M., Raikas, T., *Finn.Chem.Lett.*, **1978**, 199.
- [96] Blake, A. J., Hill, S. J., Hubberstey, P., Li, W.-S., *J.Chem.Soc.,Dalton Trans.*, **1998**, 909.
- [97] King, G., Gembicky, M., Coppens, P., *Acta Crystallogr., Sect.C:Cryst.Struct.Commun.*, **2005**, 61, m329.
- [98] Ucar, I., A.Bulut, Buyukgungor, O., *Acta Crystallogr.,Sect.C:Cryst.Struct.Commun.*, **2005**, 61, m266.
- [99] McMillin, D. R., Buckner, M. T., Ahn, B. T.,*Inorg. Chem.*, **1977**, 16, 943;
- [100] McMillin, D. R., Kirchhoff, I. R., Goodwin, K. V, *Coord. Chem. Rev.*, **1985**, 64, 83; C. Kotal. *Coord. Chem. Rev.*, 1990, **99**, 213.
- [101] Yao, Y., Perkovic, M. W., Rillema, D., Woods, C., *Inorg. Chem.*, **1992**, 31, 3956.
- [102] Armaroli, N., Balzani, V., Barigelletti, F., De Cola, L., Flamigni, L., Sauvage, J.-P., Hemmert, C., *J. Am. Chem. Soc.*, **1994**, 116, 5211.
- [103] Dietrich-Buchecker, C. O.,Nierengarten, J. F., Sauvage, J. P., Armaroli, N., Balzani, V., De Cola, L., *J. Am. Chem. Soc*, **1993**, 115, 11237.
- [104] Scaltrito, D. V., Thompson, D. W., O'Callaghan, J. A., Meyer, G. J., *Coord. Chem. Rev.*, **2000**, 208, 243.
- [105] Seto, E. T., Nelson, R. F., Fritsch, J. M., Marcoux, L.S., Leedy, D. W., Adams, R. N., *J. Am. Chem. Soc.*, **1966**, 88, 3498.
- [106] Nelson, R. F., Adams, R. N., *J. Am. Chem. Soc.*, **1968**, 90, 3925.

## Chapter 3: DNA Hybridization Assisted by Metal Complex Formation

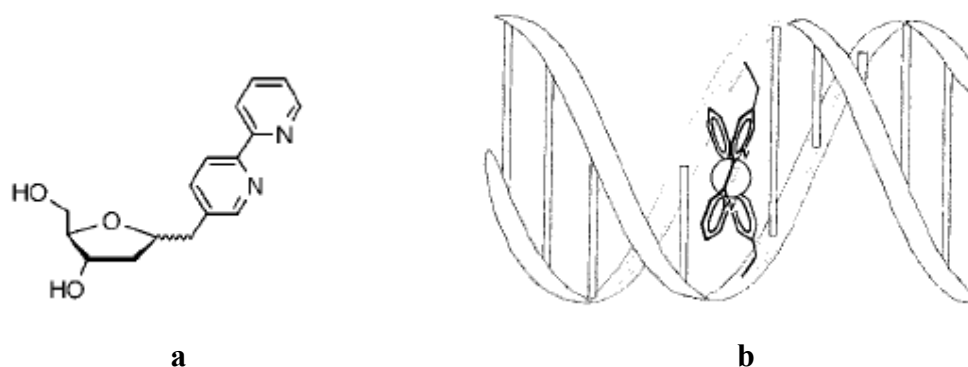
### 3.1 Introduction

There is currently significant interest in the development of short oligonucleotides, which bind to nucleic acid targets with a high selectivity as well as a high affinity <sup>[1-2]</sup>. Different strategies have been adopted for this purpose, including the conjugation of oligonucleotides with affinity enhancing moieties and the synthesis of oligonucleotide analogs with enhanced binding properties <sup>[3-4]</sup>. An additional approach consists of the use of molecular or supramolecular interactions in assisting the hybridization of nucleic acids <sup>[5-8]</sup>. One possible type of cooperativity is coordination to metal ions to produce metal-linked oligonucleotide strands. When two short oligonucleotide sequences are coupled by coordination to a single metal centre, the so-formed, metal-linked oligonucleotide will be capable of recognizing a longer complementary sequence with enhanced binding characteristics. The binding of metal ions, taking place concomitant with the hybridization process offers a powerful and selective methodology for nucleotide recognition. It is well known that metal ions can interact with donor atoms of both the backbone and the bases of nucleic acids and the importance of metal ions in controlling the structure and function of nucleic acids is well documented <sup>[9-12]</sup>. For example, for folded RNA molecules, the pathway for adopting proper tertiary structure and the stabilization of that structure, depends on specific and non-specific interactions with certain classes of ions (groups 1 and 2). Pills analysis of the folding process of RNA reveals happens in two steps. The first is the formation of secondary structure which is promoted by monovalent counter-ions (particularly  $K^+$ ). The second step consists of the formation of the ternary structure, for which divalent ions such as  $Mg^{2+}$  are required (figure 3.1) <sup>[11]</sup>.



**Figure 3.1** A simplified view of the complex folding pathway for RNA molecules and the involvement of metal ions <sup>[11]</sup>.

Transition metal ions are also of interest in controlling and developing the molecular architecture of nucleic acids and their analogs. Metal-mediated hybridization of various types of DNA analogs has been reported <sup>[13-18]</sup>. For instance, the placement of charged metal complexes at the center of the DNA helix as illustrated in the figure 3.2 has been extensively studied. The key of this approach was a nucleoside mimic, liganoside, where the heterocyclic base is replaced by a strong chelator (2,2'-bipyridine). The liganoside was incorporated into DNA oligonucleotides using solid-phase DNA synthesis, and next,  $\text{Cu}(\text{OAc})_2$  was added to the modified DNA duplex. With this work, Yitzhak Tor showed that metal coordination is typically stronger than hydrogen bonds, and unlike covalent bonds, can be easily denatured in the presence of competing ligands <sup>[14]</sup>.



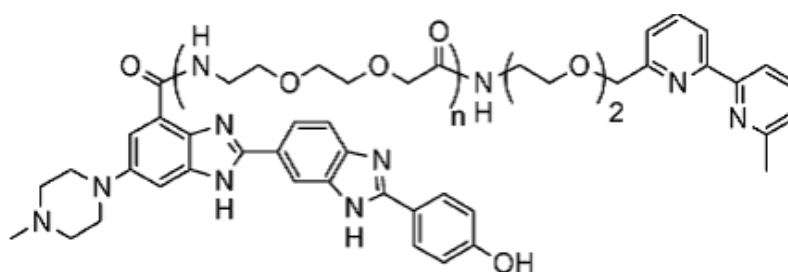
**Figure 3.2 a.** A liganoside. **b.** Schematic representation of interstrand metal complex within a DNA double helix <sup>[14]</sup>.

Specific modification through the incorporation of metal-binding domains has also been used for the synthesis of DNA-based nanostructures [19-22]. Furthermore, metal-derived hairpin mimics have been described [23-25] and different types of transition metal complexes have found application in the context of artificial ribonucleases [26-28]. Due to their compatibility with nucleic acids, metal ions are ideal candidates for the development of systems in which DNA hybridization and metal complex formation can act in a cooperative manner. The feasibility of metal cooperative complex formation in assisting nucleic acid hybridization has been demonstrated by *Balasubramanian* and coworkers, who reported that the coordination of gadolinium(III) to two short oligonucleotides modified with iminodiacetic acid donors leads to enhanced target affinity (figure 3.3) [8].

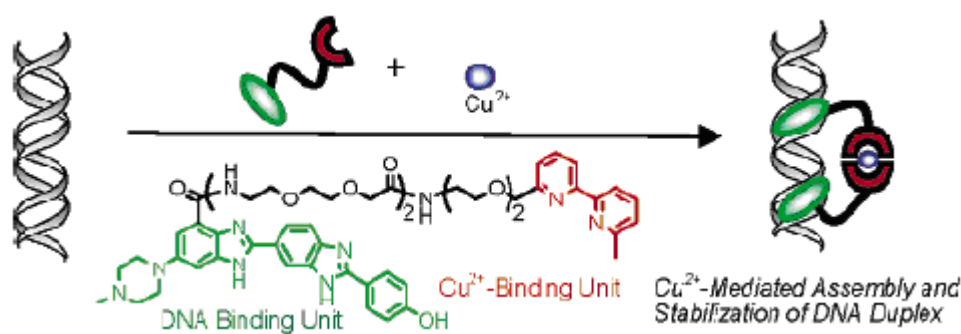


**Figure 3.3** Metal chelation to enhance oligonucleotide binding [8].

Important in this general context are the recent observations of *Sasaki and coworkers* [29], who showed that copper-induced dimerisation of a minor groove binding ligand increases its affinity to DNA. The principle of this experiment was to establish a new binding mode in which small molecular ligands may assemble on a DNA template by multidendate coordination with the metal cation. As a starting point for such an assembling system, a new Hoechst ligand having a 2,2'-bipyridine as a metal-chelating unit (bpy-H) was designed. First the ligand was incorporated into DNA oligonucleotides and next  $\text{CuCl}_2$  was added (figure 3.4 and 3.5) [29].

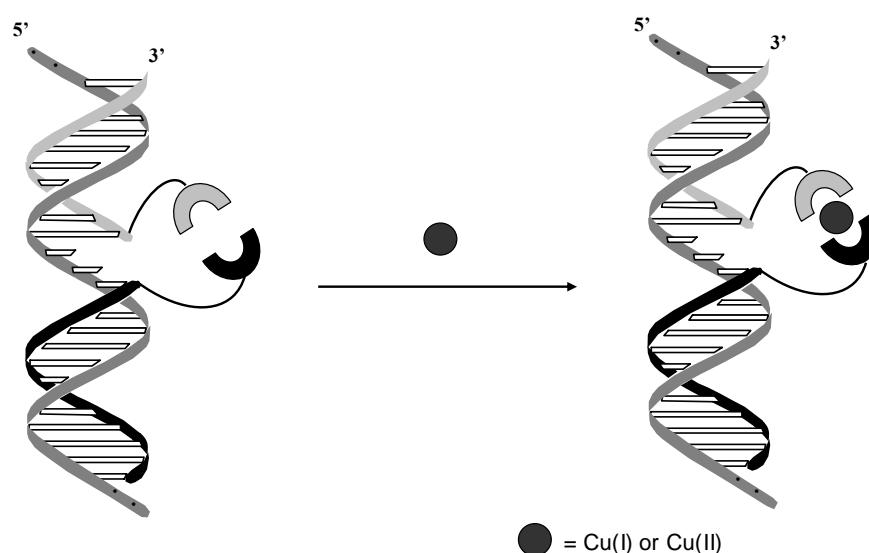


**Figure 3.4** Bpy-H ligand (n=2) [29].



**Figure 3.5** General concept of a self-assembling system on a DNA template by multiple coordination with a metal cation: the non-covalent assembly of Bpy-H is mediated by  $\text{Cu}^{2+}$  coordination on a DNA template <sup>[29]</sup>.

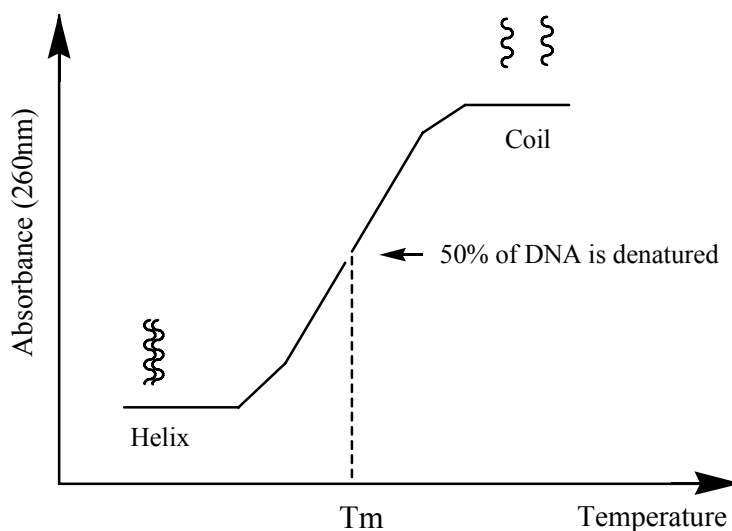
Stimulated by this work, we have studied the effect of copper ion complexation by metal-binding domains attached to complementary oligodeoxynucleotides in DNA hybridization. In this chapter, we describe the synthesis of oligonucleotide conjugates incorporating 2,2'-bipyridine (bpy) and 1,10-phenanthroline (phen) metal-binding domains and the influence on the structure and stability of duplexes formed with complementary target strands in the absence and presence of copper(I) and copper(II) (illustrated in Figure 3.6).



**Figure 3.6** Illustration of copper-complex assisted DNA hybridization.

In this study, the effect of metal complex formation on the hybridisation of the oligonucleotides was evaluated by thermal denaturation and UV spectroscopy.

The dissociation of a double stranded DNA molecule is often referred as melting because it occurs quickly once a certain temperature has been reached. The binding affinity between the oligonucleotide and its target sequence is generally characterized by the MELTING TEMPERATURE ( $T_m$ ) of the double stranded helix that is formed between sense and antisense sequence. The  $T_m$  conventionally reflects the temperature at which 50% of the double strand has dissociated into two single strands under equilibrium. The  $T_m$  depends on the length of the molecule and of the specific nucleotide sequence composition of that DNA molecule (figure 3.7).



**Figure 3.7** The  $T_m$  conventionally reflects the temperature at which 50% of the double strand has dissociated into two single strands under equilibrium.

In this study, the thermal denaturing was monitored by measuring the change in UV absorbance at 260nm and determining the melting temperature ( $T_m$ ) from the first derivative of the melting curve.

This part of the project was done in collaboration with the group of Prof. Robert Häner at the University of Bern (Switzerland) and the group of Prof. Jacques Lebreton at the University of Nantes (France).

## 3.1 Synthesis of 2,2'-bipyridine and 1,10-phenanthroline phosphoramidite building blocks

### 3.1.1 Background

In 1888, Blau first reported the preparation of 2,2'-bipyridine and described the first transition metal complex of this important ligand with this report of the red complex  $[\text{Fe}(\text{bpy})_3]^{2+}$  [30]. Since then, 2,2'-bipyridine and the related ligand 1,10-phenanthroline have been continuously and intensively used in both analytical and preparative coordination chemistry [31-32].

Today, 2,2'-bipyridine and 1,10-phenanthroline and their derivatives have become fundamental building blocks in supramolecular chemistry [33]. This is because of their versatility in coordinating to almost any metal in the periodic table [32] via  $\sigma$  and  $\pi$ -bonding. The unoccupied  $\pi^*$  orbitals of the aromatic rings overlap with occupied orbitals of the metal while the nitrogen atom donates a lone pair to form a  $\sigma$ -bond with the metal ion. These properties explain the importance of bpy and phen ligands in the formation of supramolecular coordination complexes [34].

In our work, 2,2'-bipyridine and 1,10-phenanthroline derivatives have not been selected as ligands only because of their high stability and affinity to numerous metal ions, but also, because they form complexes with comparable dimensions to a DNA base pair.

### 3.1.1 Synthesis of the 6'-methyl-2,2'-bipyridine phosphoramidite building block

The first synthesis was that of 6,6'-dimethyl-2,2'-bipyridine **14**. Despite the importance of this ligand for inorganic cations [31], its synthesis can be a problem, attested by the numerous preparations that have been reported. These involve organometallic, and/or toxic and unpleasant reagents, low yields, or high temperatures [35-47].

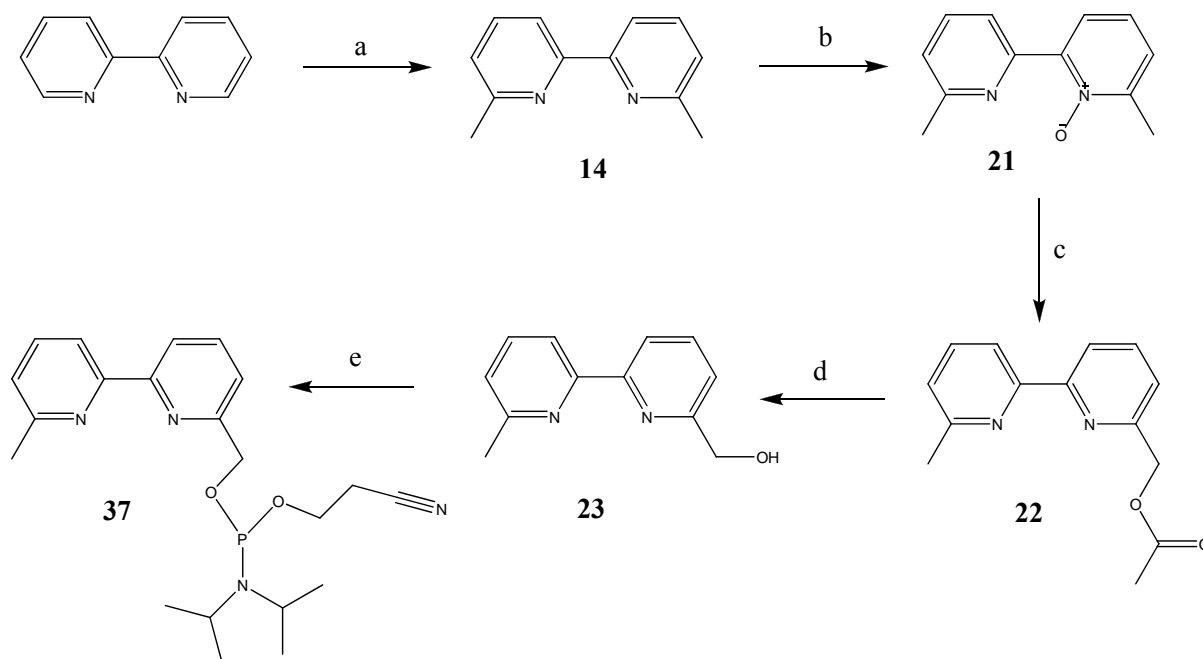
The first attempt for the synthesis of the 6,6'-dimethyl-2,2'-bipyridine **14** was the reductive homocoupling of 6-bromopicoline [47] with  $\text{Pd}(\text{OAc})_2$  catalyst. The desired compound was

obtained in a relatively low yield (51%) and the reaction was required expensive reagents, not compatible with multigram/kilogram scale preparation. This results inspired the search for a more efficient synthetic route and this was found through the direct dimethylation of 2,2'-bipyridine with methyllithium <sup>[39]</sup> in dry THF. Simple filtration through celite gave the product in good yield (86%) (figure 3.8).

The 6-(hydroxymethyl)-6'-methyl-2,2'-bipyridine **23** was synthesised as described in the literature <sup>[48-51]</sup>. The 6,6'- dimethyl-2,2'-bipyridine **14** was treated with one equivalent of 3-chloroperbenzoic acid (mCPBA) which afforded the 6,6'-dimethyl-2,2'-bipyridine-*N*-oxide **21**. The unreacted 6,6'- dimethyl-2,2'-bipyridine was separated by column chromatography. This was followed by acetylation and Boekelheide rearrangement (rearrangements of *N*-Oxide) <sup>[52]</sup> by heating in acetic anhydride to give 6-(acetoxymethyl)-6'-methyl-2,2'-bipyridine **22**. Treatment with potassium carbonate in ethanol gave the desired product, 6-(hydroxymethyl)-6'-methyl-2, 2'-bipyridine **23** (figure 3.8).

From this bpy derivativ, the phosphoramidite **37** was prepared by phosphorylation using (cyanoethyloxy)bis(*N,N*-diisopropylamino)phosphine in the presence of diisopropylammonium tetrazolide (figure 3.8) <sup>[53]</sup>.





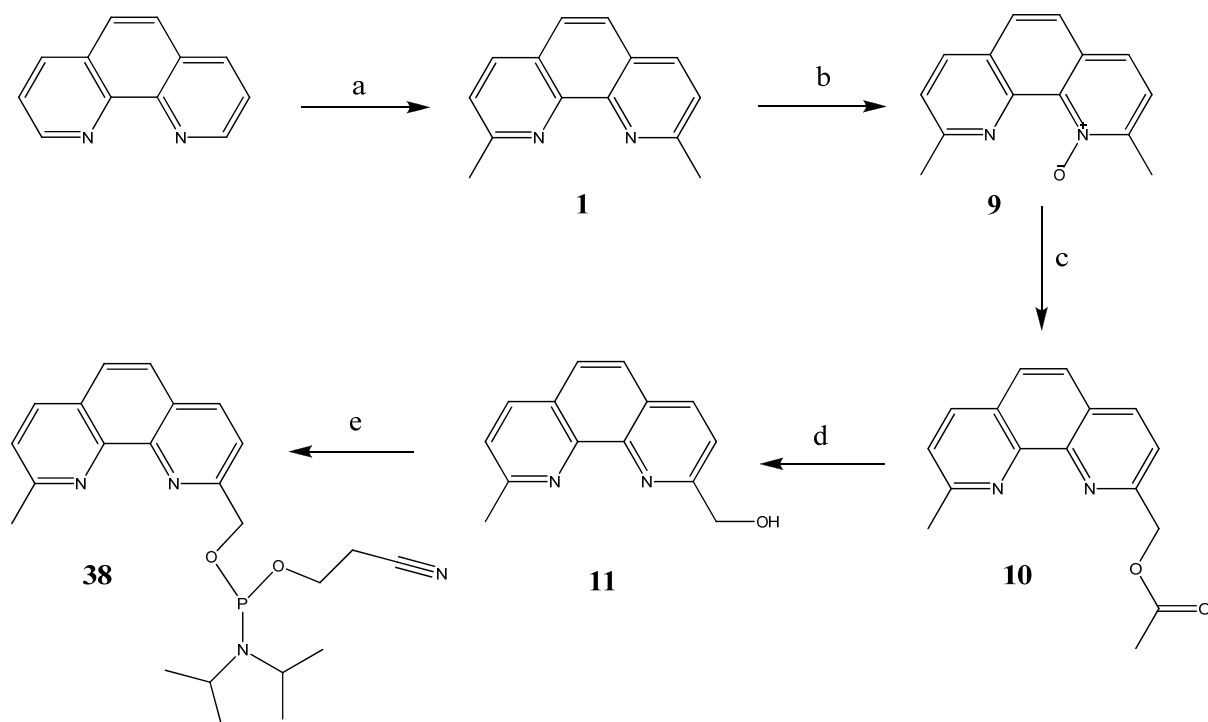
**Figure 3.8** Conditions: (a) MeLi at  $-78^{\circ}\text{C}$  for 1h, reflux for 3h,  $\text{MnO}_2$ , 4h, 86%; (b) m-chloroperbenzoic acid, rt., 1h, 69%; (c) acetic anhydride, reflux for 15 min, 71%; (d) ethanol,  $\text{K}_2\text{CO}_3$ , rt., 24h, 98%; (e)  $(\text{iPr}_2\text{N})_2\text{P}(\text{OCH}_2\text{CH}_2\text{CN})$ , *N,N*-diisopropylammonium 1*H*-tetrazolide,  $\text{CH}_2\text{Cl}_2$ , rt., 1h, 70%.

### 3.1.2 Synthesis of the 9-methyl-1,10-phenanthroline phosphoramidite building block

As for the bipyridine, the direct dimethylation of 2,2'-bipyridine with methyllithium<sup>[39]</sup> in dry THF was used to synthesise 2,9-dimethyl-1,10-phenanthroline in excellent yield (92%).

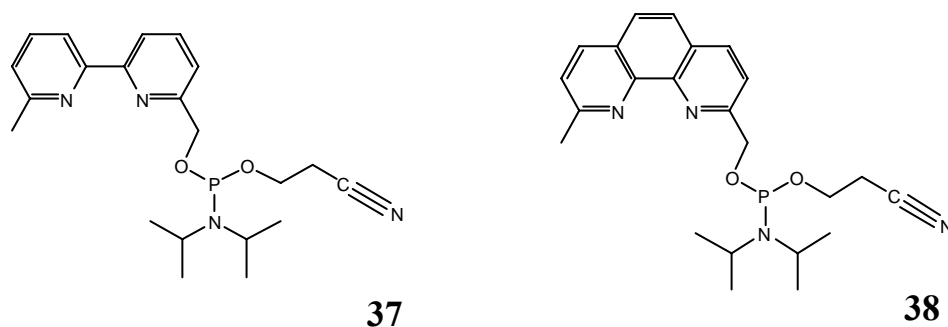
The 2-(hydroxymethyl)-9-methyl-1,10-phenanthroline was synthesised as described in the literature<sup>[48-51]</sup>. Oxidation using hydrogen peroxide in acetic acid afforded 2,9-dimethyl-1,10-phenanthroline-*N*-oxide **9** in good yield. This was followed by the Boekelheide rearrangement<sup>[52]</sup> by heating in acetic anhydride to give 2-(acetomethyl)-9-methyl-1,10-phenanthroline. Hydrolysis with ethanol and potassium carbonate gave the desired 2-(hydroxymethyl)-9-methyl-1,10-phenanthroline **11** in excellent yield.

As for the bipyridine, from this phenanthroline derivated, the phosphoramidite was prepared by phosphorylation using (2-cyanoethoxy)bis(*N,N*-diisopropylamino)phosphine in the presence of diisopropylammonium tetrazolide (Figure 3.9)<sup>[50]</sup>.



**Figure 3.9** Conditions: (a) MeLi at  $-78^{\circ}\text{C}$  for 1h, reflux for 3h,  $\text{MnO}_2$ , 4h, 92%;(b)acetic acid and  $\text{H}_2\text{O}_2$ , reflux, 24h, 80%; (c) acetic anhydride, reflux for 15 min, 65%; (d) ethanol,  $\text{K}_2\text{CO}_3$ , rt., 24h, 97%; (e)  $(\text{iPr}_2\text{N})_2\text{P}(\text{OCH}_2\text{CH}_2\text{CN})$ , N,N-diisopropylammonium 1H-tetrazolide,  $\text{CH}_2\text{Cl}_2$ , rt., 1h,75%.

### 3.2 Synthesis of oligonucleotide conjugates



**Figure 3.13** Phosphoramidite-ligands used in this study.

The phosphoramidites **37** and **38** (figure 3.13) were incorporated into the oligonucleotides (Table 1) using standard oligonucleotide technology<sup>[56-57]</sup>. The metal-binding domains were incorporated at the 5'-end of a 13-mer sequence (**C1-bpy** and **C1-phen**) and at the 3' end of an 8-mer sequence (**C2-bpy** and **C2-phen**) (table 3.1). For the synthesis of the **C1**-conjugates, conventional deoxynucleoside phosphoramidites were used. The **C2**-conjugates were synthesised using reverse phosphoramidites<sup>[58-59]</sup>. Standard conditions were applied, with the exception that prolonged (5 min) coupling time was allowed for the modified building blocks to ensure maximal coupling efficiency. The **C1**-conjugates were designed to be complementary to the 5'-end and the **C2**-conjugates complementary to the 3'-end of the target (**T0**) (table 3.2) Oligonucleotides **R0** - **R2** (table 3.3) were prepared as reference oligonucleotides. Detachment of the oligonucleotides from the solid support and deprotection involved standard conditions (conc. NH<sub>3</sub> solution, 55°C, and 16h). Oligonucleotides were purified using ion-exchange HPLC and characterized by *electrospray mass spectrometry*.

**Table 3.1.** Oligonucleotide ligand conjugates (sequences are given starting from the 3'-end to facilitate interpretation of the data, see below).

Oligomer	5'-conjugates	Found mass (g/mol)	Calculated mass (g/mol)
<b>C1-bpy</b>	3'-CGCCGCAGTTATT- <b>37</b> -5'	4187	4188

<b>C1-phen</b>	3'-CGCCGCAGTTATT- <b>38</b> -5'	4211	4213
----------------	---------------------------------	------	------

Oligomer	3'-conjugates	Found mass (g/mol)	Calculated mass (g/mol)
<b>C2-bpy</b>	3'- <b>37</b> -CGTCAGCG-5'	2672	2673
<b>C2-phen</b>	3'- <b>38</b> -CGTCAGCG-5'	2696	2698

The oligonucleotides modified with the different metal binding domains were designed to be complementary to the target sequence **T0** and its analogues **T1**, **T2**, and **T3** (table 2). Oligonucleotide target **T1**, **T2** and **T3** were derived from **T1** by sequential addition of 1, 2 and 3 cytosines at position 14 from the 5'-end, in order to investigate the influence of spacing between the two ligands on the metal-duplex stability.

**Table 3.2** Target oligonucleotides (**T**) used in this study:

	Sequence	Found mass (g/mol)	Calculated mass (g/mol)
<b>T0</b>	5'-GCGGCGTCAATAACGCTGACG-3'	6456	6456
<b>T1</b>	5'-GCGGCGTCAATAA <b>C</b> CGCTGACG-3'	6745	6745
<b>T2</b>	5'-GCGGCGTCAATAA <b>CC</b> CGCTGACG-3'	7034	7034
<b>T3</b>	5'-GCGGCGTCAATAA <b>CCC</b> CGCTGACG-3'	7322	7323

Oligonucleotide **R0** (fully complementary to **T0**), and oligonucleotides **R1** and **R2** (partially complementary to **T0**) which do not bear any metal-coordinating building block in their sequences were synthesized as reference sequences (table 3.3).



**Table 3.3.** Reference oligonucleotides (**R**) used in this study:

	Sequence	Found mass (g/mol)	Calculated mass (g/mol)
<b>R0</b>	3'-CGCCGCAGTTATTGCGACTGC-5'	6397	6398
<b>R1</b>	3'-GCGACTGC-5'	2410	2410
<b>R2</b>	3'-CGCCGCAGTTATT-5'	3925	3925

### 3.3 Effect of bpy and phen metal-binding domains on the duplex stability in the absence of metal ions.

The first experiment examined the influence on the stability of the duplex of the bpy- and phen-modified oligonucleotides with the target complementary strand **T0** in the absence of metal ions.  $T_m$ -values obtained from thermal denaturation experiments are shown in Table 3.4. When the target complement **T0** and the oligonucleotides **R1** and **R2** are bound together, we observed a  $T_m$  of 49°C (entry 4-1). When we put the target **T0** and the bpy conjugates **C1-bpy** and **C2-bpy** together we observed a  $T_m$  of 53.5°C and when the target **T0** is in the presence of **C1-phen** and **C2-phen**, the  $T_m$  is 56.5°C. The introduction of metal binding domains leads to an increase in stability in comparison to the native duplex (Table 3.4). Thus, an increase in the  $T_m$  value of 4°C and 7.5°C respectively for bpy- (entry 4-2), and phen-modified (entry 4-3) oligonucleotide hybrids with **T0** was observed. The incorporation of these building blocks has a positive effect on duplex stabilisation. The observed increase in the stability of the modified duplexes (in comparison to the unmodified duplex, which possesses a nicked sequence in the molecule structure) may be the result of stacking interaction between the two diimine ligands facing each other or between the diimine ligands and the adjacent nucleobases. We conclude that the presence of the two oligopyridine metals binding domains leads to an increase in duplex stability of ~ 5°C in the absence of transition metal ions.

**Table 3.4** The effect of terminal bpy and phen ligands on hybrid stability:

entry	hybrid <sup>a)</sup>	T <sub>m</sub> (°C)	ΔT <sub>m</sub> <sup>b)</sup> (°C)
4-1	5'-GCGGCGTCAATAACGCTGACG-3' 3'-CGCCGCAGTTATT-GCGACTGC-5'	<b>T0 + R1 + R2</b>	49 -
4-2	5'-GCGGCGTCAATAACGCTGACG-3' 3'-CGCCGCAGTTATT GCGACTGC-5' 	<b>T0 + C1-bpy + C2-bpy</b>	53.5 <b>+4.5</b>
4-3	5'-GCGGCGTCAATAACGCTGACG-3' 3'-CGCCGCAGTTATT GCGACTGC-5' 	<b>T0 + C1-phen + C2-phen</b>	56.5 <b>+7.5</b>

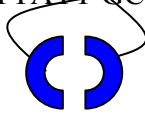

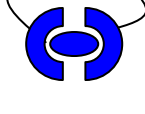

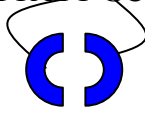

a) Conditions: Na<sub>2</sub>HPO<sub>4</sub> (10mM; pH = 7.5); NaCl (100mM); oligonucleotide (1.5μM); T<sub>m</sub> values were determined as the first derivative of the melting curve. <sup>b)</sup> Difference in T<sub>m</sub> relative to reference (entry 4-1).

### 3.4 Effect of metal-coordination on duplex stability.

We next investigated the influence of copper(I) and copper(II) salts on the stability of the modified duplexes. The thermal denaturing experiments with the modified duplex in the presence of these metal ions showed a further remarkable increase in the T<sub>m</sub>-values in the presence of copper(II) and/or copper(I) (Table 3.5). For the bpy conjugates (**C1-bpy** and **C2-bpy**, entries 5-2 and 5-3) an increase of approx. 7°C was observed upon addition of either of the two metals. In aqueous solution, simple copper(I) salts are unstable with respect to oxidation or disproportionation and copper(II) species are expected at equilibrium. However, in the case of bpy-ligands bearing substituents at the 6- or 6,6'- positions or phen-ligands bearing substituents at the 2- or 2,9-positions, copper(I) {CuL<sub>2</sub>}<sup>+</sup> complexes are stabilised by about 3 lgK units to give water stable copper(I) complexes<sup>[62-66]</sup>. Furthermore, with 6,6'-disubstituted 2,2'-bipyridine or 2,9-disubstituted 1,10-phenanthroline ligands, reaction with

copper(II) or copper(I) leads to the same copper(I) solution species. This phenomenon is discussed in detail elsewhere <sup>[67]</sup>. On the other hand, no effect was observed with zinc(II) (Table 3.5, entry 5-4) as expected from the observations that (i) zinc(II) complexes of bpy and phen ligands are less stable than copper(II) complexes following the Irving-Williams series and (ii) zinc(II) complexes of bpy-ligands bearing substituents at the 6- or 6,6'- positions or phen-ligands bearing substituents at the 2- or 2,9-positions are less stable than those with bpy and phen. These findings can be interpreted in terms of a common type of copper(I) complex and minimal binding of  $Zn^{2+}$  to conjugated ligands under the experimental conditions. The phen conjugates (**C2-phen**) showed an increase of 4.5°C in  $T_m$  upon addition of copper(I). The thermal denaturation curves for the hybrids in the absence and presence of copper(I) for both types of conjugates are shown in Figure 3.14. In all cases, a single transition is observed. Hyperchromicities in the presence and absence of the metals are comparable. Copper(I) and copper(II) ions interact with two bpy or phen ligands to form a stable tetrahedral  $\{CuL_2\}$  species <sup>[68-70]</sup>. The formation of these metal complexes leads to a linking of the two conjugate strands and the formation of a single metallonucleotide strand and, hence, an increase in hybrid stability. The addition of other transition metal salts had no experimentally significant influence on the  $T_m$  of any control duplex (figure 3.15). Thus, we can rule out that the effects observed in the case of modified-duplexes are due to non-specific metal coordination to any part of the nucleic acid - DNA and RNA are well-known to have a large variety of sites for metal interaction <sup>[58-62]</sup> but rather to specific complex formation between copper and the bpy or phen ligands. Formation of the copper(I) complex does not have an influence on the general B-form structure of the DNA as verified by the circular dichroism spectra (figure 3.16). (A representative selection of circular dichroism experiments is shown in Figure 3.16 and show that the introduction of metal coordinating ligands into oligonucleotide sequences does not alter the B-form of the DNA. Moreover, the addition of metal has not induced any changes in the typical spectrum. Thus, all results support the formation of a B-type hybrid between the three oligonucleotides (target and two conjugates) which is stabilized by the formation of a copper-complex).

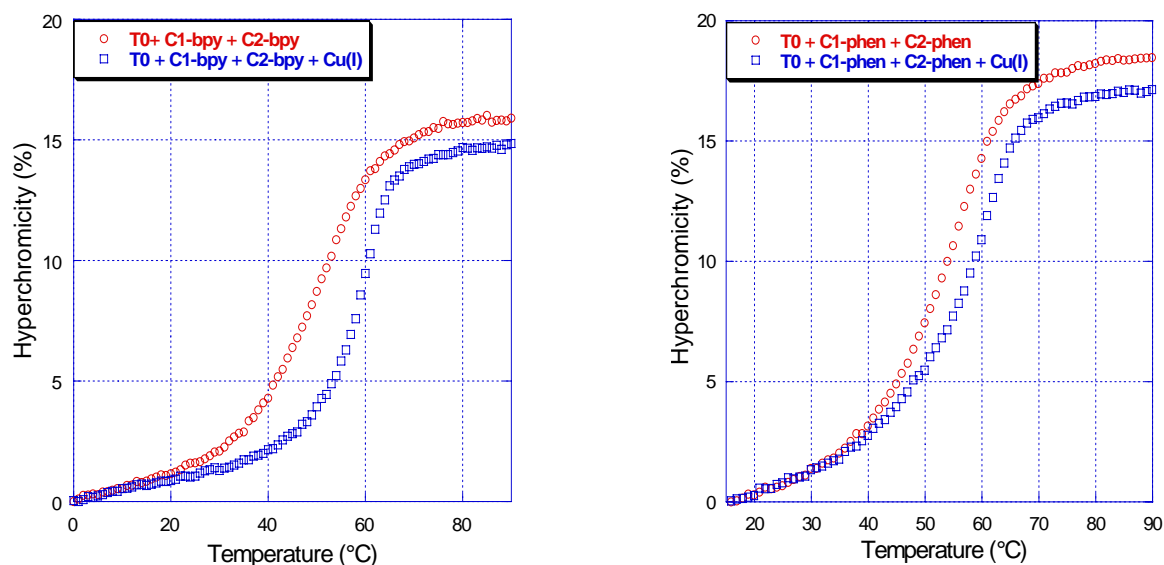
**Table 3.5** Thermal denaturing experiments with bpy and phen conjugates in the presence and absence of metals ions.

entry	hybrid <sup>a)</sup>	T <sub>m</sub> (°C)	ΔT <sub>m</sub> <sup>b)</sup> (°C)	
5-1	5'-GCGGCGTCAATAACGCTGACG-3' 3'-CGCCGCAGTTATT GCGACTGC-5' 	T <sub>0</sub> + C1-bpy + C2-bpy	53.5	-
5-2	5'-GCGGCGTCAATAACGCTGACG-3' 3'-CGCCGCAGTTATT GCGACTGC-5' 	T <sub>0</sub> + C1-bpy + C2-bpy + Cu(I)	61.0	+ 7.5
5-3	5'-GCGGCGTCAATAACGCTGACG-3' 3'-CGCCGCAGTTATT GCGACTGC-5' 	T <sub>0</sub> + C1-bpy + C2-bpy + Cu(II)	60.5	+ 7.0
5-4	5'-GCGGCGTCAATAACGCTGACG-3' 3'-CGCCGCAGTTATT GCGACTGC-5' 	T <sub>0</sub> + C1-bpy + C2-bpy + Zn(II)	52.5	- 1.0
5-5	5'-GCGGCGTCAATAACGCTGACG-3' 3'-CGCCGCAGTTATT GCGACTGC-5' 	T <sub>0</sub> + C1-phen + C2-phen	56.5	-
5-6	5'-GCGGCGTCAATAACGCTGACG-3' 3'-CGCCGCAGTTATT GCGACTGC-5' 	T <sub>0</sub> + C1-phenB + C2-phenB + Cu(I)	61.0	+ 4.5

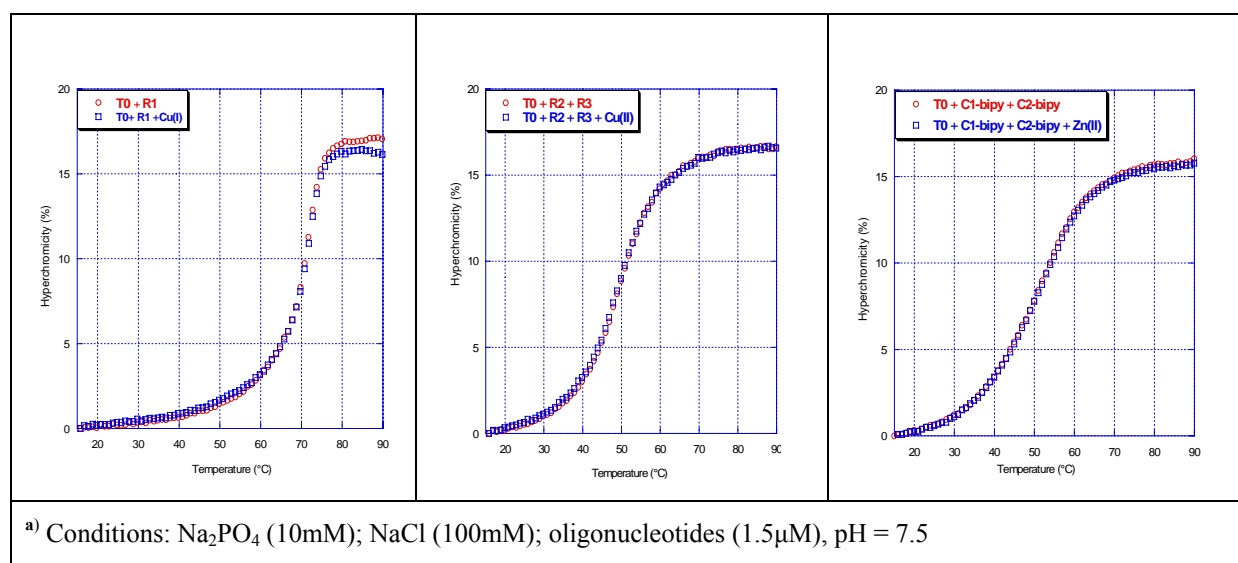


a) Conditions:  $\text{Na}_2\text{HPO}_4$  (10mM; pH = 7.5); NaCl (100mM); oligonucleotides (1.5 $\mu\text{M}$ );  $T_m$  values were determined as the first derivative of the melting curve. b) Difference in  $T_m$  relative to metal-free experiments.

Cu(I) come from  $\text{Cu}(\text{CH}_3\text{CN})_4\text{PF}_6$ , Cu(II) from  $\text{CuCl}_2$  and Zn(II) from  $\text{ZnCl}_2$



**Figure 3.14** Thermal denaturing curves of hybrids formed by target and conjugates in the presence and absence of copper ions. Conditions:  $\text{Na}_2\text{HPO}_4$  (10mM; pH = 7.5); NaCl (100mM); oligonucleotides (1.5 $\mu\text{M}$ ); heating and cooling rate: 0.5 $^\circ\text{C}/\text{min}$ ; each of the curves shown corresponds to the second of three ramps.



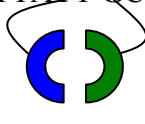



**Figure 3.15** Thermal denaturing curves of hybrids formed by target and conjugates in the presence and absence of copper ions.<sup>a)</sup>

### 3.5 Effect of mixed-ligand complexes on hybrid stability.

Mixed-ligand duplexes were formed by hybridizing one **bpy** and one **phen** oligonucleotide probe to the target **T0** (Table 3.6, entries 6-1 and 6-3). With a difference of 6°C between these two duplexes (57.0°C and 51°C, respectively) in the absence of metal, the stability of the mixed-ligand duplex depends considerably on the relative positions (3' or 5') of the bpy or phen metal-binding domains. Upon the addition of copper(I) (Table 3.6, entries 6-2 and 6-4) this difference between the two heteroleptic duplexes disappears ( $T_m = 61^\circ\text{C}$  in both cases) consistent with the formation of two very similar metal complexes. Furthermore, for both mixed-domain complexes, the hybrid stability is, not unexpectedly, very similar to that of the homo-complexes (table 3.5, entries 5-2 and 5-6), which also contain a single, metal-linked strand.

**Table 3.6** Thermal denaturing experiments with bpy and phen conjugate in the presence and absence of metal.

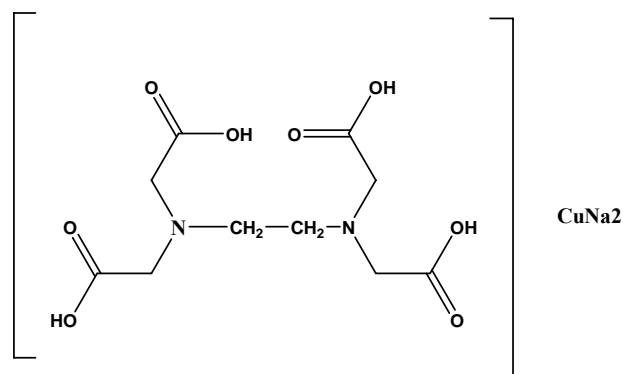
entry	hybrid <sup>a)</sup>	$T_m$ (°C)	$\Delta T_m^b)$ (°C)
6-1	5'-GCGGCGTCAATAACGCTGACG-3' 3'-CGCCGCAGTTATT GCGACTGC-5' 	<b>T0 + C1-phen + C2-bpy</b> 57.0	-
6-2	5'-GCGGCGTCAATAACGCTGACG-3' 3'-CGCCGCAGTTATT GCGACTGC-5' 	<b>T0 + C1-phen + C2-bpy + Cu(I)</b> 61.0	+ 4.0
6-3	5'-GCGGCGTCAATAACGCTGACG-3' 3'-CGCCGCAGTTATT GCGACTGC-5' 	<b>T0 + C1-bpy + C2-phen</b> 51.0	-

6-4	5'-GCGGCGTCAATAACGCTGACG-3' 3'-CGCCGCAGTTATT GCGACTGC-5' 	<b>T0 + C1-bpy + C2-phen + Cu(I)</b>	61.0	<b>+ 10.0</b>
-----	--	--------------------------------------	------	---------------

<sup>a)</sup> Conditions: Na<sub>2</sub>HPO<sub>4</sub> (10mM; pH = 7.5); NaCl (100mM); oligonucleotides (1.5μM); T<sub>m</sub> values were determined as the first derivative of the melting curve. <sup>b)</sup> Difference in T<sub>m</sub> relative to metal-free experiments.

### 3.6 Effect of EDTA on the duplex stabilisation

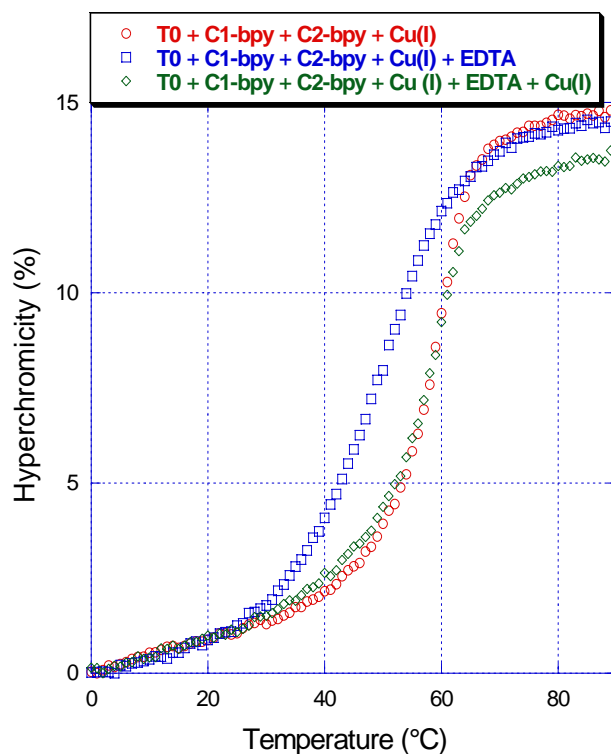
H<sub>4</sub>EDTA (ethylenediaminetetraacetic acid) is a chelating agent, forming coordination compounds with most monovalent, divalent, trivalent and tetravalent metal ions. H<sub>4</sub>EDTA contains four carboxylic acid and two tertiary amine groups that can participate in acid-base reactions. EDTA forms especially strong complexes with Mn, Cu, Fe(III), and Co(III) (figure 3.17).



**Figure 3.17** EDTA coordinating a Cu<sup>2+</sup>


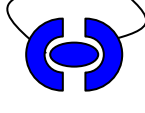
In our investigation, experiments involving H<sub>4</sub>EDTA were performed in order to test the strength of the bpy-metal complexes and the reversibility of metal-induced duplex formation. The denaturation curves are shown in figure 3.18. The addition of H<sub>4</sub>EDTA to the metalloduplex leads to a T<sub>m</sub> which is equal to the one obtained in the absence of metal - in

other words, the copper is removed quantitatively upon treatment with the chelating ligand EDTA. The  $T_m$  value of the metal-coordinated duplex is restored upon treatment with additional copper(I) or copper(II) establishing the complete reversibility of the formation of the metal linkage between the oligonucleotides (table 3.7).



**Figure 3.18** Thermal denaturing curves of hybrids formed by bpy conjugated duplex with consecutive metal and EDTA additions. Conditions: Conditions:  $\text{Na}_2\text{HPO}_4$  (10mM; pH = 7.5); NaCl (100mM); oligonucleotides (1.5mM); heating and cooling rate:  $0.5^\circ\text{C}/\text{min}$ ; each of the curves shown corresponds to the second of three ramps.

**Table 3.7** Thermal denaturing experiments with bipyridine conjugated.

entry	hybrid <sup>a)</sup>	Tm (°C)
7-1	5'-GCGGCGTCAATAACGCTGACG-3' 3'-CGCCGCAGTTATT GCGACTGC-5' 	61.0
7-2	<b>T0 + C1-bpy+ C2-bpy + Cu(I) +EDTA</b>	50.0
7-3	<b>T0 + C1-bpy + C2-bpy + Cu(I) +EDTA +Cu(I)</b>	60.0
7-4	5'-GCGGCGTCAATAACGCTGACG-3' 3'-CGCCGCAGTTATT GCGACTGC-5' 	61.0
7-5	<b>T0 + C1-bpy+ C2-bpy + Cu(I) +EDTA</b>	51.5
7-6	<b>T0 + C1-bpy + C2-bpy + Cu(II) +EDTA + Cu(II)</b>	59.5

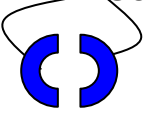
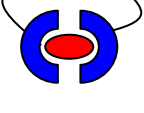
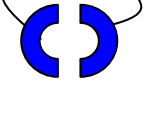
<sup>a)</sup> Oligonucleotides and reagents were added in the order indicated; Conditions: Na<sub>2</sub>HPO<sub>4</sub>(10mM; pH = 7.5); NaCl (100mM); oligonucleotide concentration: 1.5µM, pH=7.5.

### 3.7 Influence of gap size at the site of metal-complex formation

In order to investigate the influence of the gap between the two metal-binding domains facing each other – at the complexation site - on duplex stability, hybridisation to targets **T1 - T3**, containing one, two and three additional cytosines at the junction of the two complementary functionalised oligomers (Table 3.8) was examined. These oligonucleotides are formally derived from **T0** by sequential addition of the respective numbers of cytosines after position 13. In this way, the relative distance between the metal-binding bpy or phen domains was

gradually increased while the total number of base pairs formed in each hybrid was kept constant. Thermal denaturing experiments were performed with the bpy conjugates **C1-bpy** and **C2-bpy** and the results are summarised in Table 3.8. In the absence of copper, an elongation of the gap between the two ligands leads to a slight increase (2-3°C) in the  $T_m$  of the duplex. This stabilisation may well be attributed to the steric requirements of the bpy or phen substituents. With increasing gap size, the metal-free functionalised oligonucleotides are better accommodated with a reduction of repulsion between the metal binding domains, and hence hybrid stability increases. Upon the addition of the metal ion, however, formation of the metal-complex becomes the dominant aspect. Apparently, close proximity facilitates the coordination of the metal by the two terminal metal-binding domains. In this context, the relatively short and inflexible methylene linker further supports this interpretation of the data: the stability of the hybrids is highest if the gap is minimal, i.e. if the two metal-binding domains are juxtaposed, as is the case with target **T0**.

**Table 3.8** The influence of gap size between the metal ligands on hybrid strength. Gap size as varied by increasing the number (0-3) of cytidine nucleotides in the target strand.

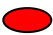

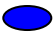
entry	Hybrid <sup>a)</sup>	Hybrid <sup>a)</sup>	$T_m$	$\Delta T_m$ b)
8-1	5'-GCGGCGTCAATAACGCTGACG-3' 3'-CGCCGCAGTTATT GCGACTGC-5' 	<b>T0 + C1bpy +C2bpy</b>	53	
8-2	5'-GCGGCGTCAATAACGCTGACG-3' 3'-CGCCGCAGTTATT GCGACTGC-5' 	<b>T0 + C1bpy +C2bpy + Cu(I)</b>	61	<b>+ 8</b>
8-3	5'-GCGGCGTCAATAA <b>A</b> CGCTGACG-3' 3'-CGCCGCAGTTATT GCGACTGC-5' 	<b>T1 + C1bpy +C2bpy</b>	55	<b>-</b>

8-4	5'-GCGGCGTCAATAAAACGCTGACG-3' 3'-CGCCGCAGTTAATTGCGACTGC-5'	<b>T1 + C1-bpy + C2-bpy + Cu(I)</b>	57	<b>+2</b>
8-5	5'-GCGGCGTCAATAAAACGCTGACG-3' 3'-CGCCGCAGTTAATTGCGACTGC-5'	<b>T2 + C1-bpyA + C2-bpyA</b>	55	<b>-</b>
8-6	5'-GCGGCGTCAATAAAACGCTGACG-3' 3'-CGCCGCAGTTAATTGCGACTGC-5'	<b>T2 + C1-bpyA + C2-bpyA + Cu(I)</b>	57	<b>+2</b>
8-7	5'-GCGGCGTCAATAAAAACGCTGACG-3' 3'-CGCCGCAGTTAATTGCGACTGC-5'	<b>T3 + C1-bpy + C2-bpy</b>	56	<b>-</b>
8-8	5'-GCGGCGTCAATAAAAACGCTGACG-3' 3'-CGCCGCAGTTAATTGCGACTGC-5'	<b>T3 + C1-bpy + C2-bpy + Cu(I)</b>	57	<b>+1</b>

<sup>a)</sup> Conditions: Na<sub>2</sub>HPO<sub>4</sub> (10mM, pH = 7.5); NaCl (100mM); oligonucleotides (1.5μM); T<sub>m</sub> values were determined as the first derivative of the melting curve. <sup>b)</sup> Difference in T<sub>m</sub> relative to the metal-free reference.

A series of control experiments was performed to ensure that the effect observed is due to the formation of metal complexes between the two conjugates. These controls are summarised in table 2.9. The addition of metal has no influence on the stability of reference duplexes with oligonucleotides **R1**, **R2**, **R3**. Thus we can rule out that the observed effects are due to non-specific metal coordination to any part of the nucleic acid, but rather to specific complex formation between the bpy or phen ligands (table 2.9).

**Table 3.9** Thermal denaturing experiments with control oligonucleotides in the absence and presence of metal

entry	hybrid <sup>a)</sup>		T <sub>m</sub> (°C)
9-1	5'-GCGGCGTCAATAACGCTGACG-3' 3'-CGCCGCAGTTATTGCGACTGC-5'	<b>T0+R1</b>	72
9-2	5'-GCGGCGTCAATAACGCTGACG-3' 3'-CGCCGCAGTTATTGCGACTGC-5' 	<b>T0+R1+CuI</b>	72.5
9-3	5'-GCGGCGTCAATAACGCTGACG-3' 3'-CGCCGCAGTTATT-5'	<b>T0+R3</b>	50.0
9-4	5'-GCGGCGTCAATAACGCTGACG-3' 3'-GCGACTGC-5'	<b>T0+R2</b>	- <sup>b)</sup>
9-5	5'-GCGGCGTCAATAACGCTGACG-3' 3'-CGCCGCAGTTATT GCGACTGC-5'	<b>T0+R2+R3</b>	49
9-6	5'-GCGGCGTCAATAACGCTGACG-3' 3'-CGCCGCAGTTATT GCGACTGC-5' 	<b>T0+R2+R3+CuI</b>	49.5
9-7	5'-GCGGCGTCAATAACGCTGACG-3' 3'-CGCCGCAGTTATT GCGACTGC-5' 	<b>T0+R2+R3+CuII</b>	49.0

<sup>a)</sup> Conditions: Na<sub>2</sub>HPO<sub>4</sub> (10mM); NaCl (100mM); oligonucleotides (1.5μM); pH = 7.5; T<sub>m</sub> values were determined as the first derivative of the melting curve. <sup>b)</sup> No cooperative melting observed.



### 3.8 Conclusions

The influence of metal complex formation on the hybridisation of oligodeoxynucleotides was investigated. Oligonucleotides containing 3'- and 5'- linked 6'-methyl-2,2'-bipyridine- and 2-methyl-1,10-phenanthroline-derived metal-binding domains were synthesized. Pairs of oligonucleotide conjugates were designed to hybridize to a target DNA sequence, such that the two copper-binding domains are arranged head-to-head in the ternary hybrid to create an  $N_4$  metal-binding site. Incorporation of the metal-binding domains had a positive influence on hybrid stability *per se* ( $\Delta T_m$  of 4.5 to 7.5°C). Addition of copper(I) or copper(II) sources results in the formation of metal complex and leads to substantial further stabilization (up to 10°C increase in  $T_m$ ). While the placement of the metal-free ligands had no influence on the extent of the stabilization, the stabilizing effect obtained by metal-coordination was found to be distance-dependent, i.e. the largest increase is observed upon placement of the ligands as close to each other as possible. While the stability of the hybrid is substantially influenced by metal-coordination, the overall B-form structure of the DNA is not affected. This study shows that hybridisation of relatively short (13- and 8-mer) oligonucleotides modified with bpy or phen metal-binding domains to a complementary target DNA is assisted by formation of metallonucleotides containing  $\{Cu(bpy)_2\}$ ,  $\{Cu(phen)_2\}$  or  $\{Cu(bpy)(phen)\}$  domains.

The results obtained with 6'-methyl-2,2'-bipyridine- and 2-methyl-1,10-phenanthroline-derived conjugated indicate that the methyl substituted as probably a important responsibility in the stabilisation of the metal complex.

### 3.9 References

- [1] Chan, J. H. P., Lim, S. H., Wong, W. S. F., *Clin. Exp. Pharmacol. Physiol.*, **2006**, *33*, 533.
- [2] Chen, X. L., Dudgeon, N., Shen, L., Wang, J. H., *Drug Discovery Today*, **2005**, *10*, 587.
- [3] Uhlmann, E., Peyman, A., *Chem. Rev.*, **1990**, *90*, 543.
- [4] De Mesmaeker, Häner, R., Martin, P., Moser, H. E., *Acc. Chem. Res.*, **1995**, *28*, 366.
- [5] Distefano, M. D., Shin, J. A., Dervan, P. B., *J. Am. Chem. Soc.*, **1991**, *113*, 5901.
- [6] Distefano, M. D., Dervan, P. B., *J. Am. Chem. Soc.*, **1992**, *114*, 11006.
- [7] Kandimalla, E. R., Manning, A., Lathan, C., Byrn, R. A., Agrawal, S., *Nucleic Acids Res.*, **1995**, *23*, 3578.
- [8] Horsey, I., Krishnan-Ghosh, Y., Balasubramanian, S., *Chem. Commun.*, **2002**, 1950.
- [9] Barton, J. K., Lippard, S. J., *Nucleic Acid-Metal Ion Interactions* (Spiro, T. G., Ed.), **1980**, pp 31-113, John Wiley & Sons, Princeton University.
- [10] Wilson, T. J., Lilley, D. M. J., *RNA*, **2002**, *8*, 587.
- [11] Pyle, A. M., *J. Biol. Inorg. Chem.*, **2002**, *7*, 679.
- [12] Göritz, M., Krämer, R., *J. Am. Chem. Soc.* **2005**, *127*, 18016.
- [13] Meggers, E., Holland, P. L., Tolman, W. B., Romesberg, F. E., Schultz, P. G., *J. Am. Chem. Soc.* **2000**, *122*, 10714.
- [14] Weizman, H., Tor, Y., *J. Am. Chem. Soc.*, **2001**, *123*, 3375.
- [15] Zimmermann, N., Meggers, E., Schultz, P. G., *J. Am. Chem. Soc.*, **2002**, *124*, 13684.
- [16] Tanaka, K., Yamada, Y., Shionoya, M., *J. Am. Chem. Soc.*, **2002**, *124*, 8802.
- [17] Tanaka, K., Tengeiji, A., Kato, T., Toyama, N., Shionoya, M., *Science* , **2003**, *299*, 1212.
- [18] Zhang, L. L., Meggers, *J. Am. Chem. Soc.*, **2005**, *127*, 74.
- [19] Stewart, K. M., Rojo, J., McLaughlin, L. W., *Angew. Chem. Int. Ed.*, **2004**, *43*, 5808.
- [20] Stewart, K. M., McLaughlin, L. W., *Chem. Commun.*, **2003**, 2934.
- [21] Choi, J. S., Kang, C. W., Jung, K., Yang, J. W., Kim, Y. G., Han, H. Y., *J. Am. Chem. Soc.*, **2004**, *126*, 8606.
- [22] Mitra, D., Di Cesare, N., Sleiman, H. F., *Angew. Chem. Int. Ed.*, **2004**, *43*, 5804.
- [23] Lewis, F. D., Helvoigt, S. A., Letsinger, R. L., *Chem. Commun.*, **1999**, 327.
- [24] Czapinski, J. L., Sheppard, T. L., *ChemBiochem*, **2004**, *5*, 127.

- [25] Bianké, G., Häner, R., *ChemBioChem*, **2004**, *5*, 1063.
- [26] Trawick, B. N., Daniher, A. T., Bashkin, J. K., *Chem. Rev.*, **1998**, *98*, 939.
- [27] Häner, R., Hall, J., *Antisense Nucleic Acid Drug Dev.*, **1997**, *7*, 423.
- [28] Niittymäki, T., Lonnberg, H., *Org. Biomol. Chem.*, **2006**, *4*, 15.
- [29] Tanada, M., Tsujita, S., Kataoka, T., Sasaki, S., *Org. Lett.*, **2006**, *8*, 2475.
- [30] Blau, F., *Ber. Dtsch. Chem. Ges.*, **1888**, *21*, 1077.
- [31] Reedijk, J., in *Comprehensive Coordination Chemistry*, Wilkinson, G., Gillard, R. D., McCleverty, J. A. (Eds.), Vol. 2, Pergamon, Oxford, **1987**, p. 73.
- [32] Constable, E. C., Steel, P. J., *Coord. Chem. Rev.*, **1989**, *93*, 205.
- [33] Steel, P. J., *Molecules*, **2004**, *9*, 440.
- [34] Vogtle, F., *Supramolecular Chemistry*, Wiley, Chichester, **1991**.
- [35] Newkome, G. R., Puckett, W. E., Kiefer, G. E., Gupta, V. K., Xia, Y., Coreil, M., Hackney, M. A., *J. Org. Chem.*, **1982**, *47*, 4116.
- [36] Oae, S., Inibushi, Y., Yoshihara, M., *Phosphorus, Sulfur Silicon*, **1995**, *103*, 101.
- [37] Newkom, G. R., Pantaleo, D. C., Puckett, W. E., Ziefle, P. L., Deutsch, W. A., *J. Inorg. Nucl. Chem.*, **1981**, *43*, 1529.
- [38] Fort, Y., Becker, S., Caubère, P., *Tetrahedron*, **1994**, *41*, 11893.
- [39] Shaul, M., Cohen, Y., *J. Org. Chem.*, **1999**, *64*, 9358.
- [40] Dietrich-Bicheker, C. O., Marnot, P. A., Sauvage, J.-P., *Tetrahedron Lett.*, **1982**, *23*, 5291.
- [41] Parks, J. E., Wagner, B. E., Holm, R. H., *J. Organometal. Chem.*, **1973**, *56*, 53.
- [42] Uchida, Y., Kajita, R., Kawasaki, Y., Oae, S., *Tetrahedron Lett.*, **1995**, *36*, 4007.
- [43] Uenishi, J., Tanaka, T., Wakabayashi, S., Oae, S., *Tetrahedron Lett.*, **1990**, *31*, 4625.
- [44] DeTar, D. R., *Org. React.*, **1957**, *9*, 409.
- [45] Fabian, R. H., Klassen, D. M., Sonntag, R. W., *Inorg. Chem.*, **1980**, *19*, 1977.
- [46] Rode, T., Breitmaier, E., *Synthesis*, **1987**, 574.
- [47] Cassol, T. M., Demnitz, F. W. J., Navarro, M., de Neves, E. A., *Tetrahedron Lett.*, **2000**, *41*, 8203.
- [48] Newkome, G. R.; Puckett, W. E.; Kiefer, G. E.; Gupta, V. D.; Xia, Y.; Coreil, M.; Hackney, M. A., *J. Org. Chem.*, **1982**, *47*, 4116.
- [49] Shaul, M., Cohen, Y., *J. Org. Chem.*, **1999**, *64*, 9358.
- [50] Schubert, U. S., Newkome, G. R., Goldel, A., Pemp, A., Kersten, J. L., Eisenbach, C. D., *Heterocycles*, **1998**, *48*, 2141.

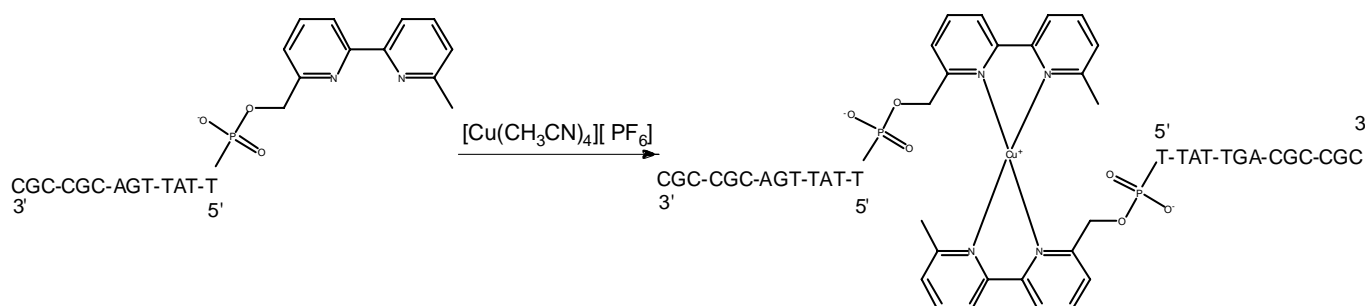
- [51] Newkome, G. R., Theriot, K. J., Gupta, V. K., Fronczek, F. R., Baker, G. R., *J. Org. Chem.*, **1989**, *54*, 1766.
- [52] Boekelheide, V., Linn, W. J., *J. Am. Chem. Soc.*, **1954**, *76*, 1286.
- [53] Bannwarth, W., Treciak, A., *Helv. Chim. Acta*, **1987**, *70*, 175.
- [54] Mosher, H. S., Yanko, W. H., Whitemore, F. C., *Org. Synth.*, **1947**, *27*, 48.
- [55] Pratt, Y. T., Drake, N. L., *J. Am. Chem. Soc.*, **1960**, *82*, 1155.
- [56] Chandler, C. J., Deady, L. W., Reiss, J. A., *J. Heterocycl. Chem.*, **1981**, *18*, 599.
- [57] Newkome, G. R., Kiefer, G. E., Puckett, W. E., Vreeland, T. J., *J. Org. Chem.*, **1983**, *48*, 5112.
- [58] Beaucage, S. L., Caruthers, M. H., *Tetrahedron Lett.*, **1981**, *22*, 1859.
- [59] Sinha, N. D., Biernat, J., McManus, J., Koster, H., *Nucleic Acids Res.*, **1984**, *12*, 4539.
- [60] Claeboe, C. D., Gao, R., Hecht, S. M., *Nucleic Acids Res.*, **2003**, *31*, 5685.
- [61] Pease, A. C., Solas, D., Sullivan, E. J., Cronin, M. T., Holmes, C. P., Fodor, S. P. A., *Proc. Nat. Acad. Sci. (USA)*, **1994**, *91*, 5022.
- [62] Smith, A. P., Fraser, C. L., *Comprehensive Coordination Chemistry II* (McCleverty, J. A. and Meyer, T. J., Eds.), **2004**, pp 1-23, Elsevier, Oxford.
- [63] Luman, C. R., Castellano, F. N., *Comprehensive Coordination Chemistry II* (McCleverty, J. A. and Meyer, T. J., Eds.), **2004**, pp 25, Elsevier, Oxford.
- [64] Kaes, C., Katz, A., Hosseini, M. W., *Chem. Rev.*, **2000**, *100*, 3553.
- [65] Brandt, W. W., Dwyer, F. P., Gyarfas, E. C., *Chem. Rev.*, **1954**, *54*, 959.
- [66] James, B. R., Williams, R. J., *J. Chem. Soc.*, **1961**, 2007.
- [67] Chaurin, V., Constable, E. C., Housecroft, C., E., *New J. Chem*, **2006**, *30*, 1740.
- [68] Siddique, Z. A., Yamamoto, Y., Ohno, T., Nozaki, K., *Inorg. Chem.*, **2003**, *42*, 6366.
- [69] Kickelbick, G., Reinohl, U., Ertel, T. S., Weber, A., Bertagnolli, H., Matyjaszewsky, K., *Inorg. Chem.*, **2001**, *40*, 6.
- [70] Garriba, E., Micera, G., Sanna, D., Strinna-Erre, L., *Inorg. Chim. Acta*, **2000**, *299*, 253.

## Chapter 4 : Affinity capillary electrophoresis

### 4.1 Introduction

The goal of this chapter was to investigate the formation of metal complexes of bpy-functionalised nucleic acids (Figure 4.1) using the versatile analytical technique of affinity capillary electrophoresis (ACE). The first part of this work was concerned studying the interactions between short oligonucleotides and different cations by ACE; in the second part, model studies of the complexation of 2,2'-bipyridine and copper(I) are reported and in the final section, we investigated the interactions between bpy-functionalised nucleic acids and Cu(I).

This project was done as part of a collaboration with the group of Dr Maria Schwarz at the University of Basel. Dr Alexandra Stettler performed the majority of the capillary electrophoresis measurements and the work is part of a joint project between the groups of Professor Constable and Dr Schwartz. Many of the results in this chapter have recently been published <sup>[1]</sup> and much of this chapter is based upon the recent joint publication.



**Figure 4.1** Illustration of the complexation of bpy-DNA with a copper(I) salt.

Electrophoretic methods are not so well known in the supramolecular community and a brief introduction is appropriate. The process of electrophoresis is defined as “the differential movement or migration of ions by attraction or repulsion in an electric field”. In practical terms, a positive (anode) and negative (cathode) electrode are placed in a solution containing

ions. Then, when a voltage is applied across the electrodes, solute ions of different charge, i.e., anions (negative) and cations (positive), will move through the solution in the direction of the electrode of opposite charge.

Capillary electrophoresis (CE) is the technique of performing electrophoresis in buffer-filled, narrow-bore capillaries, normally with 25 to 100  $\mu\text{M}$  internal diameter. This chapter begins with an introduction to capillary electrophoresis (CE).

## **Introduction capillary electrophoresis**

### ***Historical background***

Electrophoresis, defined as a migration of analytes within an electrolyte solution under the influence of an electric field, was introduced as a biochemical separation technique in the mid-1930's by Arne Tiselius. He developed the use of electrophoresis for the task of separating proteins in suspension on the basis of their electrical charges. For this work he was awarded his doctorate in 1930. In 1937, he used electrophoretic methods to separate chemically similar proteins in blood serum<sup>[2]</sup>. He continued his research into the separation of proteins and other substances by absorption chromatography. For his work, he received the Nobel Prize for Chemistry in 1948.

The original method of "free solution" electrophoresis was limited by the instability of the apparatus and by the effects of diffusion, aggravated by the heating effect of the electric field, which limited the resolution that could be obtained. The development of popularity began with the introduction of a "support medium" such as a gel or paper derivatives. The purpose of this "support medium" was to contain the electrolyte or "running buffer" and to give an obstacle to the free movement of the analyte, such that the random influence of diffusion was minimised<sup>[3]</sup>.

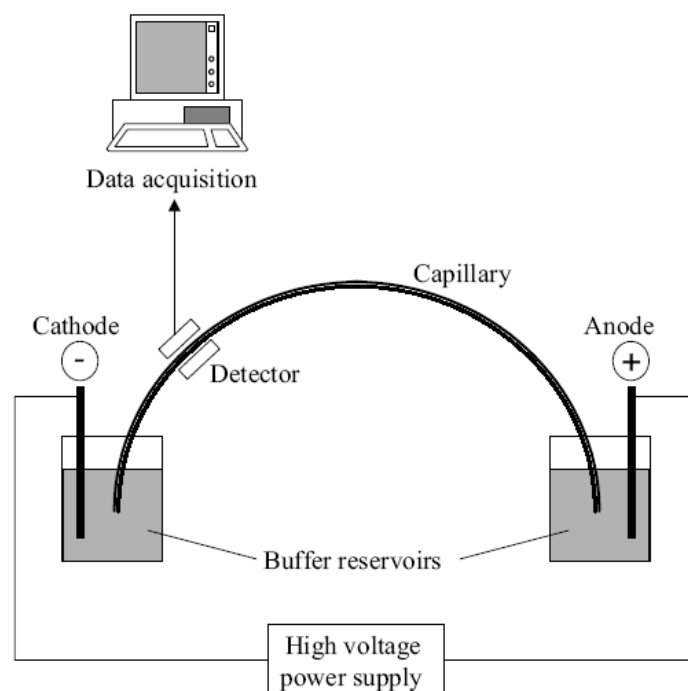
Capillary electrophoresis (CE) was developed as a technique in the early 1990's and has grown little by little in popularity. In its simplest and most commonly used form, it is close to the original Tiselius method, but it is not only popular because of the simplicity but also because of the additional advantages of speed, versatility and low running costs. It is a remarkable analytical method which has found application in the separation of biopolymers such as peptides, proteins and oligonucleotides as well as metal and other inorganic ions and is currently employed in the analysis of the pharmaceuticals and the monitoring of water

quality <sup>[4]</sup>. Although the basic methodology involves the separation of molecules based on their charge to mass ratio, there are simple modifications to the procedure, borrowed from existing well-established techniques, which allow separations based on size or isoelectric point, or which permit the separation of non-charged molecules, while the degree of resolution can result in the separation of optical isomers using appropriate mobile or static phases. There are many documented examples of the application of CE techniques to the separation of proteins <sup>[5]</sup>, DNA fragments <sup>[6]</sup>, carbohydrates <sup>[7,8]</sup> and drugs <sup>[9-12]</sup>.

### ***Instrumentation***

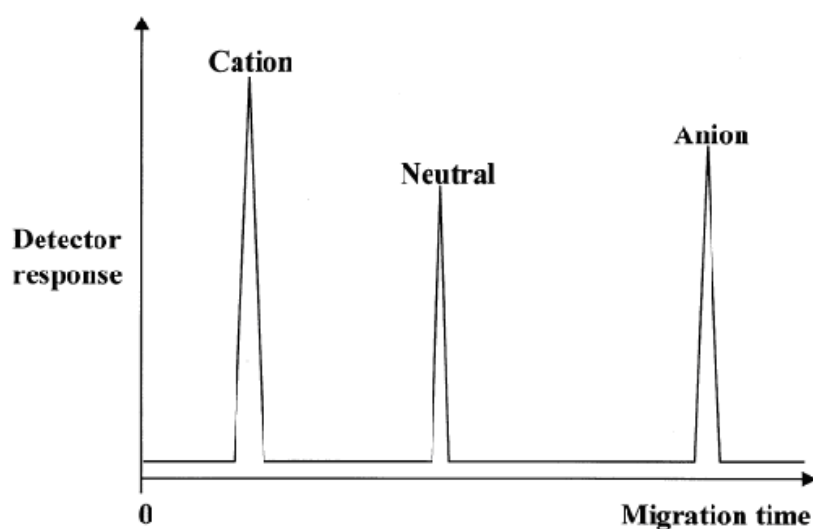
The instrumentation required for CE is relatively simple and is illustrated in Figure 4.2. The ends of a capillary are positioned in separate buffer reservoirs, each containing an electrode connected to a high voltage power supply capable of delivering up to 30kV potential. The sample is injected into the capillary by temporarily replacing one of the buffer reservoirs (normally the one at the anode) with a sample reservoir and applying either an electric potential or external pressure for a few seconds. After replacing the buffer reservoir, an electric potential is applied across the capillary and the separation is performed. Optical (UV-visible or fluorometric) detection of separated analytes can be achieved directly through the capillary wall near the opposite end (normally near the cathode) <sup>[13]</sup>.

The basic elements of a CE instrument include an autosampler, a detection module, a high-voltage power supply, the capillary and a computer to control the assembly and to collect the data.



**Figure 4.2** Diagram of a typical capillary electrophoresis system <sup>[13]</sup>.

The data output from CE is presented in the form of an electropherogram, which is analogous to a chromatogram. An electropherogram is a plot of migration time vs. detector response. The detector response is usually concentration dependant, such as a UV-visible absorbance or fluorescence intensity. The appearance of a typical electropherogram is shown in Figure 4.3 for the separation of a three-component mixture of cationic, neutral and anionic solutes <sup>[13]</sup>.



**Figure 4.3** A typical electropherogram showing the separation of a cation, a neutral species and an anion <sup>[13]</sup>.



### ***The buffer***

The electrophoretic separation of samples is performed in a buffer with a precise (and known) pH value and a constant ionic strength. The ionic strength should be as low as possible, so that the contribution of the sample ions to the total current and their speed will be maximised. During electrophoresis, the buffer ions are carried through the gel in the same way as the sample ions: in general, negatively charged ions migrate towards the anode, positively charged ones towards the cathode.

With the Second Law of electrophoresis by Michael Faraday – *the mass of the resulting separated elements are directly proportional to the atomic masses of the elements when an appropriate integral divisor is applied*- it is possible to calculate the amount of ions migrating in an electrophoresis experiment: The amount of electricity is equal to the amount of substances, which are eliminated from different electrolytes.

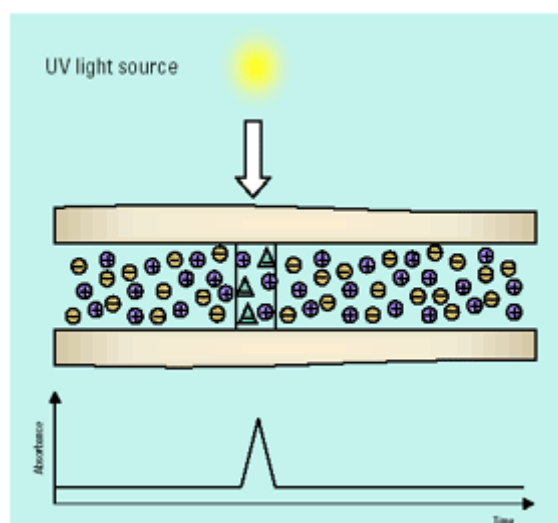
In capillary systems, the pH is usually set to a very high (or low) value, and then as many as possible sample molecules are negatively (or positively) charged, and thus migrate in the same direction.

### ***Methods of detection***

It is not only necessary to be able to separate the analytes, but it is also essential to be able to detect them as they move through the capillary. Many of the methods for detecting analytes in CE are similar to those used for other types of chromatography such as liquid chromatography (LC).

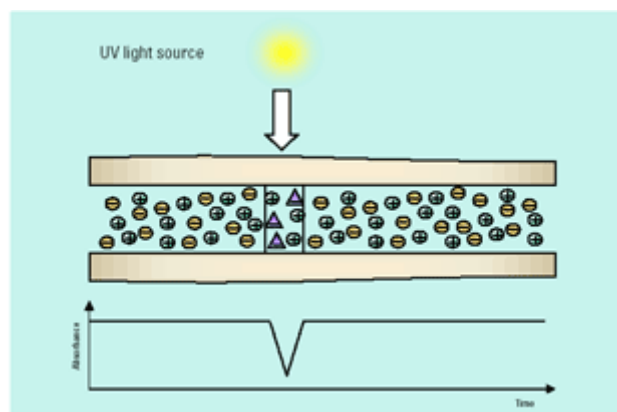
UV-visible absorption spectroscopy is the most common detection method because it is simple to use and most analytes can be observed with it. Figure 4.4 illustrates UV-visible detection for a CE system. Analytes passing the light source absorb UV-visible radiation resulting in a decrease in light reaching the detector. This is observed as a signal. The concentration of the analyte passing the detector is directly proportional to the decrease in signal following the Beer-Lambert law, so the concentration may be quantified after calibration with standards.

UV-visible spectroscopy is most sensitive when used at low wavelengths where typical  $\pi$ - $\pi^*$  and  $\pi$ -n absorptions have high extinction coefficients. In the absence of suitable conjugated groups, as, for example, in the cases of peptides and carbohydrates, it is necessary to observe at wavelengths below 200 nm where carbon - carbon bonds absorb. However, the use of such high energy radiation causes problems as it limits the buffers which can be used. To use vacuum UV wavelengths, it is necessary to use phosphate or borate buffers, which themselves absorb very little radiation. Organic buffers often contain chromophores themselves limiting their use in this range.



**Figure 4.4** Principle of UV detection (direct detection).

Another common method of quantification is by indirect UV-visible detection. This method involves using a buffer in the capillary which absorbs the radiation from the lamp along with analytes which do not absorb UV-visible radiation. As analytes move past the detector, the amount of light passing through the capillary increases as the concentration of the UV-visible is reduced. Indirect UV-visible detection is most commonly used for inorganic ions which do not absorb UV-visible radiation.



**Figure 4.5** Principle of UV detection (indirect detection).  
The following table summarizes the common detection methods.

Method	Mass detection limit (moles)	Concentration detection limit (molar)	Advantages/ disadvantages
<b>UV- Vis</b>	$10^{-13} - 10^{-16}$	$10^{-5} - 10^{-8}$	<ul style="list-style-type: none"> <li>• Universal</li> <li>• Diode array offers spectral information</li> </ul>
<b>Fluorescence</b>	$10^{-15} - 10^{-17}$	$10^{-7} - 10^{-9}$	<ul style="list-style-type: none"> <li>• Sensitive</li> <li>• Usually requires derivatisation</li> </ul>
<b>Laser induced fluorescence</b>	$10^{-18} - 10^{-20}$	$10^{-14} - 10^{-16}$	<ul style="list-style-type: none"> <li>• Extremely sensitive</li> <li>• Usually requires derivatisation</li> <li>• Expensive</li> </ul>
<b>Amperometry</b>	$10^{-18} - 10^{-19}$	$10^{-10} - 10^{-11}$	<ul style="list-style-type: none"> <li>• Sensitive</li> <li>• Selective but useful only for electroactive analytes</li> <li>• Requires special electronics and capillary modifications</li> </ul>
<b>Conductivity</b>	$10^{-15} - 10^{-16}$	$10^{-7} - 10^{-8}$	<ul style="list-style-type: none"> <li>• Universal</li> <li>• Requires special electronics and capillary modifications</li> </ul>
<b>Mass spectrometry</b>	$10^{-16} - 10^{-17}$	$10^{-8} - 10^{-9}$	<ul style="list-style-type: none"> <li>• Sensitive and offers structural information</li> </ul>
<b>Indirect UV, fluorescence, amperometry</b>	10 - 100 times less than direct method		<ul style="list-style-type: none"> <li>• Universal</li> <li>• Lower sensitivity than</li> </ul>

Method	Mass detection limit (moles)	Concentration detection limit (molar)	Advantages/ disadvantages
			direct methods

**Table 4.1** List common detection methods for CE experiments and their principal features.

### *Modes of capillary electrophoresis*

Capillary electrophoresis comprises a family of five techniques that have different operative and separative characteristics. The techniques are:

- Capillary zone electrophoresis
- Capillary gel electrophoresis
- Capillary isoelectric focusing
- Micellar electrokinetic chromatography
- Isotachopheresis

### *Capillary zone electrophoresis (CZE)*

CZE is the most widely-used mode of CE and is used for the separation of both anionic and cationic solutes in a single analysis <sup>[14]</sup>. In CZE the anions and cations migrate in different directions, but they are all swept towards the cathode because the electroosmotic flow (EOF) is usually significantly higher than the solute velocity due to migration (mobility). In a typical analysis, cations elute first because the direction of migration is the same as the direction of EOF. Neutral solutes elute next, but are unresolved because they have no mobility and move only with the EOF. Anions elute last because they migrate in the opposite direction to the EOF.

### *Capillary gel electrophoresis (CGE)*

CGE is the CE-analog of traditional slab-gel electrophoresis and is used for the size-based separation of biological macromolecules such as oligonucleotides, DNA restriction fragments and proteins <sup>[15]</sup>. The separation is performed by filling the capillary with a sieve-like matrix, for example, cross-linked polyacrylamide, agarose or even solutions of linear polymer. The

main advantages over slab-gel electrophoresis are a wider range of gel matrix and composition, online detection, improved quantification and automation.

### ***Capillary isoelectric focusing (CIEF)***

CIEF is used to separate biological molecules (mainly proteins); based on differences between the isoelectric points (pI). CIEF is performed by filling the capillary with a mixture of ampholytes and the sample, and then forming a pH gradient. By applying an electric field across the capillary with a basic solution at the cathode and an acidic solution at the anode, the ampholytes and solutes migrate until they reach a region where their overall charge is neutral ( $\text{pH}=\text{pI}$ ). The ampholyte and solute zones remain extremely narrow because diffusion to a zone of different pH results in the generation of charge and subsequent migration back to the proper zone.

### ***Micellar electrokinetic chromatography (MEKC)***

MEKC is a unique mode of CE because it can separate neutral as well as charged solutes. In MEKC ionic surfactants are added to the running buffer to form micelles<sup>[16]</sup>. Micelles have a three-dimensional structure with hydrophobic moieties of the surfactant in the interior and the charged moieties at the exterior. The separation of neutrals is based on the hydrophobic interaction of solutes with the micelles. The stronger the interaction, the longer the solutes migrate with the micelle. The selectivity of MEKC can be controlled by the choice of surfactant and also by the addition of modifiers to the buffer.

### ***Isotachopheresis (ITP)***

ITP uses two different buffer systems. The solutes are sandwiched between leading and trailing electrolytes, creating a steady state in which the solute zones migrate in order of decreasing mobility. Two unique aspects of ITP are that all solute zones migrate at the same velocity and that they all adopt the concentration of the leading electrolyte. The latter aspect makes ITP a very useful technique for the analysis of dilute solutions. Samples can be concentrated to many orders of magnitude.

### ***Capillary electrochromatography (CEC)***

CEC is a fusion of liquid chromatography (LC) and capillary electrophoresis. In CEC the capillary is packed with a stationary phase similar to those used in LC [17]. When an electric field is applied the EOF moves the mobile phase through the packed column. A uniform velocity profile is created which minimizes peak dispersion. The selectivity of the separation—as in LC—depends on the partition of analyte between the stationary and mobile phases. This allows the high efficiency separation of neutral compounds within very short analysis times.

CEC has three specific benefits:

- separation of closely related compounds
- shorter run times and increased sample throughput, and
- substitution of gradient HPLC methods by isocratic CEC.

CEC uses capillary columns packed with LC stationary phases. As in LC, CEC separations are achieved by the partition of a solute between the mobile and stationary phases. The additional separation by mobilities resolves charged and neutral components. In CEC, the pressure driven flow of LC is removed and replaced by an electrically driven flow—the electro-osmotic flow (EOF). This has the following advantages:

- no pump with moving mechanical parts or seals
- elimination of eddy diffusion, resulting in increased efficiency, and a column length and particle size that are not restricted by a pressure limit.

### **Electrophoresis: Theory - Generalities**

Separation by electrophoresis is based on differences in solute velocity in an electric field.

The velocity of an ion is given by:

$$v = \mu_e \cdot E \quad (1)$$

Where  $v$  = ion velocity (m/s)

$\mu_e$  = electrophoretic mobility ( $\text{m}^2/\text{Vs}$ )

$E$  = applied electric field (V/m)

The electric field is a function of an applied voltage and capillary length (in volts/cm). The mobility, for a given ion and medium, is a constant which is characteristic of that ion. The

mobility is determined by the electric force that the molecule experiences, balanced by its frictional drag through the medium. That is:

$$\mu_e \alpha = \frac{\text{Electric force}(F_E)}{\text{Frictional force}(F_F)} \quad (2)$$

The electric force can be given by:

$$F_E = q E \quad (3)$$

Where  $q$  = ion charge

and the frictional force (for a spherical ion) is given by:

$$F_F = -6 \pi \eta r v \quad (4)$$

Where  $\eta$  = solution viscosity

$r$  = ion radius

$v$  = ion velocity

A small ion will have less frictional drag and will move through the medium faster than a larger one. Similarly a multiply charged ion will experience more attraction to the electrode and also move through the medium faster. It is the difference in solute velocities that is responsible for the separating effect in electrophoresis.

During electrophoresis, a steady state, defined by the balance of these forces, is attained. At this point the forces are equal but opposite and

$$q E = 6 \pi \eta r v \quad (5)$$

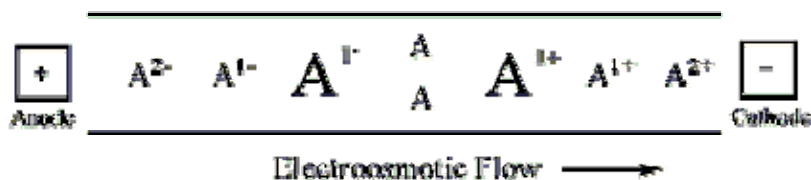
Solving for velocity and substituting equation (5) into equation (1) yields an equation that describes the mobility in terms of physical parameters.

$$\mu_e = \frac{q}{6\pi\eta r} \quad (6)$$

From this equation it is evident that small, highly charged species have high mobilities whereas large, minimally charged species have low mobilities<sup>[18, 19]</sup>.

### Electro-osmotic flow (EOF)

The velocity of migration of an analyte in capillary electrophoresis will also depend upon the rate of electro-osmotic flow (EOF) of the buffer solution. In a typical system, the electroosmotic flow is directed toward the negatively charged cathode so that the buffer flows through the capillary from the source vial to the destination vial. Separated by differing electrophoretic mobilities, analytes migrate toward the electrode of opposite charge. As a result, negatively charged analytes are attracted to the positively charged anode, against the EOF, while positively charged analytes are attracted to the cathode, in running in the same direction as the EOF as shown in Figure 4.6.



**Figure 4.6** Diagram of the separation of charged and neutral analytes (A) according to their respective electrophoretic and electroosmotic flow mobilities.

The velocity of the electro-osmotic flow  $V_{\text{EOF}}$  can be written as:

$$V_{\text{EOF}} = \mu_{\text{EOF}} \cdot E$$

Where  $\mu_{\text{EOF}}$  is the electro-osmotic mobility, which is defined as:

$$\mu_{\text{EOF}} = (\varepsilon \cdot \zeta) / \eta$$

Where  $\zeta$  is the zeta potential of the capillary wall,  $\varepsilon$  is the relative permittivity of the buffer solution and  $\eta$  is the solution viscosity. We note the independence of the mobility from the applied electric field.

Experimentally, the electro-osmotic mobility can be determined by measuring the retention time of a reference neutral analyte. The velocity (V) in an electric field can then be defined as:



$$V + V_{\text{EOF}} = (\mu_e + \mu_{\text{EOF}}) \cdot E$$

Since the electro-osmotic flow of the buffer solution is generally greater than that of the electrophoretic flow of the analytes, all analytes, regardless of charge, are carried along with the buffer solution toward the cathode. Even small, triply charged anions can have the direction of flow redirected towards the cathode by the relatively powerful EOF of the buffer solution.

Negatively charged anions analytes are retained longer in the capillary due to their conflicting electrophoretic mobilities. The order of migration seen by the detector is summarised in Figure 4.6: small multiply charged cations migrate quickly and small multiply charged anions are retained strongly <sup>[20]</sup>.

### **Introduction to CE analysis of nucleic acids**

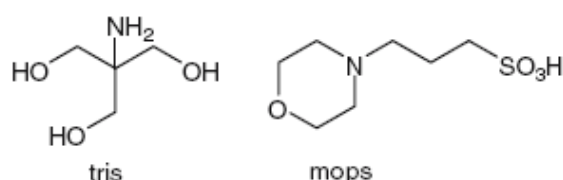
With the completion of the Human Genome Project in 2003 <sup>[21]</sup>, it became critical to understand in detail the mechanisms for the expression of the phenotype from the genotype. It is clear that the modulation and control of DNA expression is achieved through interactions both with large biomolecules and with small molecules or ions. Metal cations are ubiquitous and play an important regulatory role through specific and non-specific interactions with negatively charged nucleic acids and oligonucleotides <sup>[22-24]</sup>.

Solid-state structural characterization of DNA, RNA or oligonucleotide complexes provides unambiguous information about binding modes but caution is required in extending these results to equilibria in solution. There is a demand for rapid and precise analytical methods for the quantification of metal ion-nucleotide interactions under equilibrium conditions. Methods for the quantification of nucleotide-metal ion interactions can be classified as mixture-based (spectroscopy, densimetry, potentiometry and calorimetry)<sup>[25-27]</sup> or separation-based (ultrafiltration-centrifugation, chromatography and electrophoresis). Affinity capillary electrophoresis (ACE) is a powerful tool for studying DNA macromolecule interactions <sup>[28-30]</sup> and the simplicity, speed and sensitivity of measurement make it attractive for studying DNA-metal ion interactions. Although ACE investigations of metal ion-DNA interactions have been reported, only a few studies describe the quantification of complex equilibria. Apparent

equilibrium constants have been determined for the interactions of  $\text{Ag}^+$  [31],  $\text{Mg}^{2+}$  [32],  $\text{Ca}^{2+}$  [32] and  $\text{Fe}^{2+}$  [33] salts with double-stranded DNA.

Two different modes of capillary electrophoresis, electrophoretic mobility shift assay (EMSA) and peak area evaluation, are commonly used. EMSA is best suited to studying low-affinity complexes formed under conditions of rapid equilibration and should be ideal for measuring interactions of labile metal ions with DNA, although previous studies have utilized peak area analysis. The specific features that make EMSA appropriate to studying DNA-metal ion interactions are (1) the fast kinetics, (2) the moderate binding and (3) the fact that the ionic mobility of the complex is significantly different from that of the DNA itself.

The different techniques used for studying DNA-metal ion interactions have varying environmental conditions. Many buffers contain components (e.g. phosphate or amine) that can coordinate to metal ions and form ternary DNA-metal ion-buffer complexes. Most reported studies of DNA-metal ion interactions have been performed in tris(hydroxymethyl)aminomethane (tris) buffer, which is known to coordinate metal ions. As the ionic mobilities of DNA, DNA-metal ion complexes and DNA-metal ion-buffer ternary complexes will be different, EMSA is an ideal technique with which to probe these interactions in detail.



**Figure 4.7** Structures of tris and mops.

In this chapter, we specifically describe the use of ACE for investigating interactions between single-stranded DNA (ss-DNA) or oligonucleotides and metal ions. Apparent aggregation constant for the binding of metal ions by the oligonucleotide have been calculated and the role of the buffer components tris and 3-(*N*-morpholino)propanesulfonic acid (mops; Figure 4.7) investigated. Varying the oligonucleotide sequence has allowed us to investigate the selectivity of binding in detail.

### Theory of ACE

ACE is a resourceful analytical technique used to study a variety of biomolecular noncovalent interactions and in determining binding and dissociation constants of formed complexes. ACE has been successfully used to examine protein-drug, protein-DNA, peptide-carbohydrate, peptide-peptide, DNA-dye, carbohydrate-drug, antigen-antibody, and other biological interactions.

In a standard form of ACE a sample of receptor (or ligand) and non-interacting standard(s) is exposed to an increasing concentration of ligand (or receptor) in the electrophoresis buffer so causing a shift in the migration time of the ligand/receptor relative to the standard(s).

We derive here the general relationships between the mobility and equilibria for a system involving a solute L and a metal ion M that can form a 1:1 complex ML (Eq. 1):



Binding constants ( $K_B$ ) can be calculated from an evaluation of the net mobility of L with metal ion concentration in the running buffer <sup>[35]</sup>.

*Derivation of the relationship between  $K_B$  and  $\mu$*

The net mobility  $\mu$  is related to the mole fraction ( $x_L$ ) and mobility ( $\mu_L$ ) of the ligand L and the mole fraction ( $x_{ML}$ ) and mobility ( $\mu_{ML}$ ) of the complex ML (Eq. 2), where the mole fractions have the conventional definitions in terms of the equilibrium concentration of the ligand and the equilibrium concentration of the complex (Eqs. 3, 4).

$$\mu = x_L \mu_L + x_{ML} \mu_{ML} \quad (2)$$

$$x_L = \frac{[L]}{[L] + [ML]} \quad (3)$$

$$x_{ML} = \frac{[ML]}{[L] + [ML]} \quad (4)$$

Combining Eqs. 2, 3 and 4 yields Eq. 5 in which the net mobility is related to the equilibrium concentrations of the species L, M and ML:

$$\mu = \frac{[L]}{[L] + [ML]} \mu_L + \left( 1 - \frac{[L]}{[L] + [ML]} \right) \mu_{ML} \quad (5)$$

$$\mu = \frac{1}{1 + [ML]/[L]} \mu_L + \frac{[ML]}{[L] + [ML]} \mu_{ML}$$

For the 1:1 ML complex with stability constant  $K_B$  (Eq. 6), it follows that the net mobility is a function of the equilibrium concentration of the analyte M (Eq. 7).

$$K_B = \frac{[ML]}{[L][M]} \quad (6)$$

$$\mu = f([M]) = \frac{\mu_L + K_B [M] \mu_{ML}}{1 + K_B [M]} \quad (7)$$

In the case of more than one metal ion binding to the solute to give complexes  $M_nL$ , the experimental  $K_B$  will describe the macroscopic equilibrium and express the sum of every possible interaction between M and L. In the specific case of cooperative binding<sup>[35]</sup>, the net mobility is given by Eq. 8, and the mobility of the complex,  $\mu_{M_nL}$  and the apparent stability constant,  $K_B$ , can be obtained from nonlinear curve fitting:

$$\mu = \frac{\mu_L + K_B [M]^n \mu_{M_nL}}{1 + K_B [M]^n} \quad (8)$$

To obtain the net mobility,  $\mu$ , from capillary electropherograms, the time taken for the analyte and a reference molecule to reach a certain point on the capillary is determined (Eq. 9). Knowing the separation potential ( $U_{sep}$  in volts), the effective and total length of the capillary ( $l_{eff}$  and  $l_{tot}$  in centimetres) and the experimental migration times of the analyte and the electroosmotic flow (EOF in square centimetres per volts per second  $t_{sample}$  and  $t_{EOF}$  in seconds), we can calculate  $\mu$  using Eq. 9:

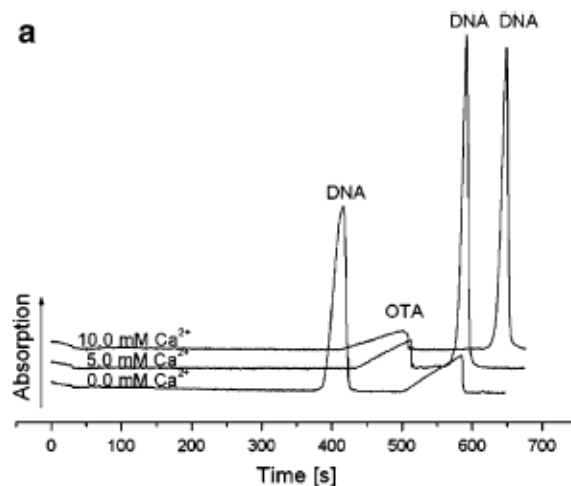
$$\mu = \frac{l_{eff} \cdot l_{tot}}{U_{sep}} \left( \frac{1}{t_{sample}} - \frac{1}{t_{EOF}} \right) \quad (9)$$

## **Interactions of DNA with metal ions**

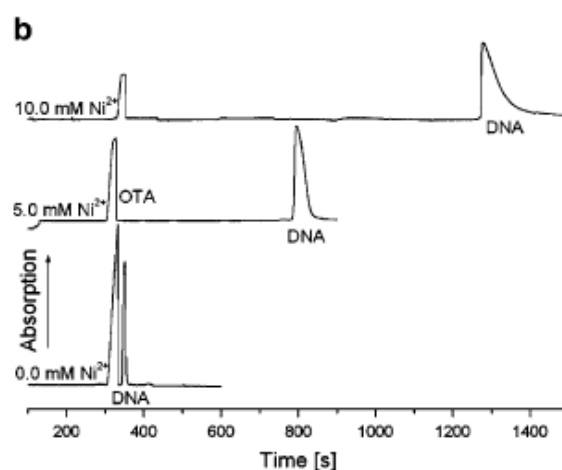
### **Migration pattern**

In this section, we comment on the empirical observations of the electropherograms of DNA and oligonucleotides in the presence of metal ions and buffers. All measurements were made at a constant total buffer concentration, although the ionic strength changes as the concentration of metal salt is varied. To calculate the true mobility of the DNA (or oligonucleotide), a noninteracting internal standard has to be added (an inert and preferably neutral molecule, e.g., DMSO).

The use of a PAA-coated capillary not only prevents wall absorption, but also suppresses the EOF. In Figures 4.8 and 4.9 the influence of added metal ions on the mobility of the reference molecule OTA and indirectly on the magnitude of the EOF is shown. With increasing concentrations of metal ions in the running buffer, the standard apparently migrates faster towards the anode (Figure 4.8). In an independent experiment with OTA and DMSO (an EOF marker) as analytes in the presence of various concentrations of metal ions, it was shown that the ionic mobility is not influenced by the metal ion concentration, despite a decrease in the EOF. The decrease in ionic mobility of the DNA or oligonucleotide induced by increased complexation to the metal ion is significantly greater. The reduction in the electrophoretic mobility of the DNA is a measurable quantity that reflects the change of the net DNA charge as a result of coordination to positively charged metal ions. As the metal ion concentration increases, the equilibrium tends towards saturation and the metal complex is the dominant DNA-containing species and the measured ionic mobility is equal to that of the fully complexed ss-DNA strand. Despite the short length of the oligonucleotide (four-base ss DNA) in Figure 4.9, the change in DNA charge compared with that of the reference molecule is significant.



**Figure 4.8** Capillary electropherogram in 50 mM tris(hydroxymethyl)aminomethane (*tris*), pH=7.4, 24-base single stranded DNA with  $\text{Ca}^{2+}$  in the running buffer



**Figure 4.9** Capillary electropherogram in 20 mM 3-(*N*-morpholino)propanesulfonic acid (*mops*), pH=7.4, 5'-d(TCAG) with  $\text{Ni}^{2+}$  in the running buffer. Separation voltage of -30 kV; *o*-toluic acid (OTA) was used as an internal standard; capillary, fused silica coated with 3% polyacrylamide (PAA).

### Buffer influence

Studies of DNA and oligonucleotides are always made in buffer solution; the buffer maintains the pH of the solution constant while other components in the reaction mixture are varied. Many of the buffers used to maintain neutral, physiological pH values are based on substituted amines. The assumption is generally made that the buffers do not interact with

DNA. However, the buffer components are not benign and can form adducts with DNA<sup>[36]</sup>, metal ions<sup>[37-39]</sup> or metal-DNA complexes<sup>[36-40]</sup>. For example, the electrophoretic mobility of DNA in free solution is 20% higher in tris-borate-EDTA (TBE)<sup>2</sup> buffer than in tris-acetate-EDTA (TAE) buffer<sup>[41]</sup>. The results mean that the effective charge of DNA is higher in TBE buffer than in TAE buffer, due to the formation of DNA-borate complexes<sup>[41-44]</sup>: DNA-borate complexes migrate faster than DNA alone because the borate ion has a higher charge/unit mass than a DNA base pair.

We initially considered tris as a buffer as it commonly used as a medium for studies of metal ion-DNA interactions with DNA<sup>[31, 32, 45]</sup> and is particularly suitable for capillary electrophoresis experiments owing to its low conductivity<sup>[46]</sup>. However, transition metal ions form complexes of reasonable stability with tris<sup>[40, 47-53]</sup> and ternary M(DNA)(tris) complexes with oligonucleotides or DNA<sup>[36, 40]</sup>. Measured macroscopic  $K_B$  values in the presence of a large excess of buffer will relate to mixtures of species. We therefore selected mops as our standard buffer for two reasons, firstly, it is known that complexes of mops with group 1 and group 2 metal ions are only of marginal stability in aqueous solution, although transition metal complexes are of similar or greater stability than those with tris<sup>[40, 54]</sup> and, secondly, although the zwitterionic or anionic character of mops stabilized the binary complexes with transition metal ion, it also destabilizes ternary complexes with negatively charged oligonucleotides or DNA (table 4.2). This prediction has been quantified for ternary complexes of mops or tris with AMP, ADP or ATP, where (1) compared where metal ion-nucleotide complexes, the ternary complexes with tris are an order of magnitude more stable than those with mops and (2) the larger the negative charge on the nucleotide, the less stable is the ternary complex with mops<sup>[40, 54]</sup>.

**Table 4.2** Binding constants of the 24mer nucleotide measured in 3-(N-morpholino)propanesulfonic acid (mops) and tris (hydroxymethyl)aminomethane (tris) buffers with various metal ions.

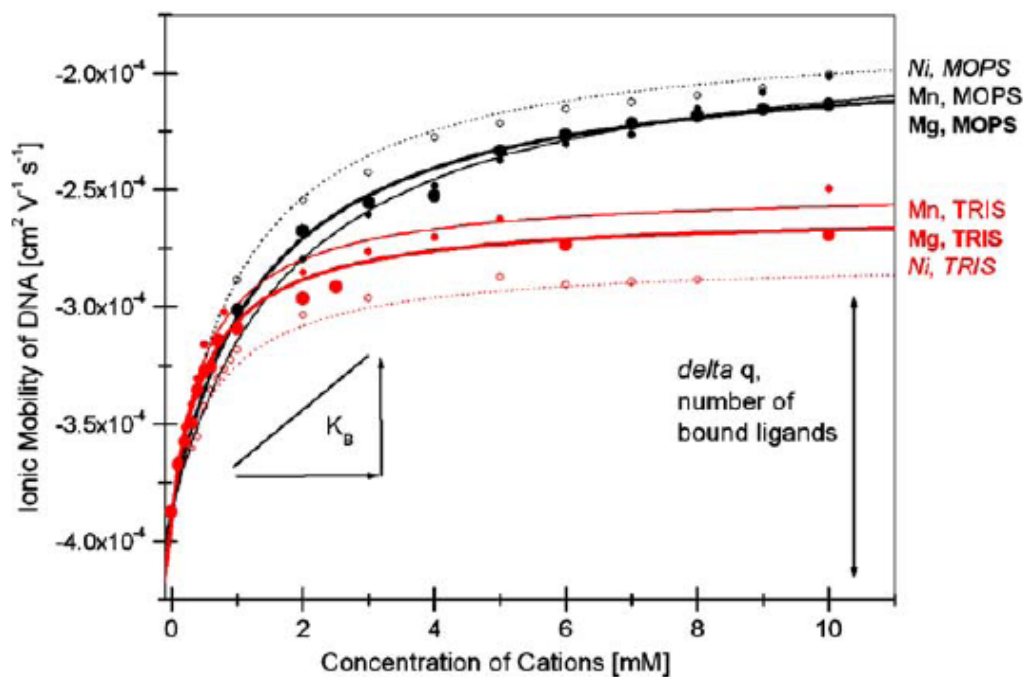
<b>metal cation</b>	<b>mops</b>	<b>TRIS</b>
	$K_B \times 10^5 \text{ (M}^{-2}\text{)}$	$K_B \times 10^3 \text{ (M}^{-1}\text{)}$
$\text{Ca}^{2+}$	$8.49 \pm 2.24$	$1.36 \pm 0.10$
$\text{Mg}^{2+}$	$7.75 \pm 1.75$	$1.75 \pm 0.10$
$\text{Mn}^{2+}$	$5.70 \pm 1.63$	$1.81 \pm 0.14$
$\text{Ni}^{2+}$	$9.85 \pm 1.75$	$1.41 \pm 0.92$

Running buffer: *red* 50mM tris buffer (pH 7.4), *black* 20 mM mops buffer (pH 7.4); sample 24mer ss-DNA, 5'-d(TTATTGACGCCGCTTTTTTTTTTTT); separation voltage  $-30\text{kV}$ ; capillary, fused silica coated with 3% PAA, 67 cm/ 54 cm/ 50  $\mu\text{M}$  (*red*; total length/ effective length/ diameter), 84 cm/ 33.5 cm/ 50  $\mu\text{M}$  (*back*).

The apparently large differences in stability are, in part, a function of the different dimensionality of the  $K_B$  value.

Figure 4.10 shows that the choice of buffer has a significant effect upon the ionic mobility of the DNA-metal ion solutions and that with a given buffer the behavior is further modulated by the specific metal ion present. The ionic mobility in the absence of metal salt is the same in both buffers, indicating that the same solution species are present- in other words, DNA-buffer complexes are not important under our experimental conditions. In the next section we present the analysis of the electrophoretic behavior in such system.





**Figure 4.10** Running buffer: *red* 50mM tris buffer (pH 7.4), *black* 20 mM mops buffer (pH 7.4); sample 24mer ss-DNA, 5'-d(TTATTGACGCCGCTTTTTTTTTTTT); separation voltage  $-30\text{kV}$ ; capillary, fused silica coated with 3% PAA, 67 cm/ 54 cm/ 50  $\mu\text{M}$  (*red*; total length/ effective length/ diameter), 84 cm/ 33.5 cm/ 50  $\mu\text{M}$  (*back*).

#### Detailed analysis and quantification of electrophoretic behavior

For a detailed interpretation of the differences between the two buffers, we need, in principle, to discuss the various possible equilibria in a solution containing DNA, metal and buffer (Eqs. 10, 11, 12, 13, 14,15, and 16):





Our experiments allow the determination of the overall stability constant  $K'_B$  for the formation of the ternary (or binary) complex (Eq. 17) and require no detailed knowledge of the speciation of the starting metal ion-buffer solution or the nature of DNA-buffer complexes. The overall stability constant  $K'_B$  is simply the product of the usually quoted stability constants for Eqs. 11 and 16<sup>[40, 54]</sup>:



$$K'_B = \frac{[M(DNA)(BUFF)]}{[M][DNA][BUFF]}$$

The mobility is given by Eq. 18 (cf. Eq. 2), with the assumption that DNA-buffer complexes make a minimal contribution<sup>[36]</sup>:

$$\mu = x_{(DNA)}\mu_{(DNA)} + x_{M(DNA)(BUFF)}\mu_{M(DNA)(BUFF)} \quad (18)$$

The overall binding constant  $K'_B$  (Eq. 16) is related to the mobility by Eq. 19, which is simply an extension of Eq. 7 to the ternary system. The buffer is in large excess and the concentration remains essentially constant at all concentration of the metal. For multiple metal binding sites it necessary to substitute  $[M]^n$  and  $[BUFF]^n$  in Eq. 19:

$$\mu = f([M]) = \frac{\mu_{DNA} + K'_B [M] \cdot [BUFF] \mu_{[(DNA)(M)(BUFF)]}}{1 + K'_B [M] \cdot [BUFF]} \quad (19)$$

We now consider the case of the binding of nickel(II) in detail and demonstrate the true stoichiometry of the reaction. At higher metal ion concentrations, the mobility in tris has reached a plateau value and in mops is close to this. The plateau mobility represents the mobility of the metal ion saturated DNA. Excess nickel(II) will be predominantly present as nickel-buffer complexes (10 mM Ni(II), 50 mM tris, 17% Ni(aq)<sup>2+</sup>, 46% Ni(tris)<sup>2+</sup>, 37 %

$\text{Ni}(\text{tris})^{2+}$  [40, 47, 48, 50, 52, 53], 10 mM Ni(II), 20mM mops, 7%  $\text{Ni}(\text{aq})^{2+}$ , 93 %  $\text{Ni}(\text{mops})^{2+}$  [54, 55]) and the nickel (II) complexes could be binary or ternary, with the former favored by mops and the latter by tris.

In the case of the tris buffer, the change in mobility from zero metal ion concentration to the plateau value  $\Delta\mu$  is  $1.0 \times 10^{-4} \text{ cm}^2 \text{ V}^{-1} \text{ s}^{-1}$ . The less negative value of  $\mu$  confirms that the nickel-DNA complex has a less negative charge than the DNA. The absolute value of the mobility is given by Eq.20 (where  $q$  is the charge,  $r$  is the hydrodynamic radius and  $\eta$  is the viscosity of the medium):

$$\mu = \frac{q}{6\pi \cdot r \cdot \eta} \quad (20)$$

The change in mobility is given in Eq.21, where  $\Delta q$  is the change in charge of the DNA between the metal-free and metal-saturated forms, making the assumptions that the viscosity of the solution remains the same [56] and that the hydrodynamic radii of the DNA and the DNA-nickel complexes are the same [57]:

$$\Delta\mu = \frac{\Delta q}{6\pi \cdot r \cdot \eta} \quad (21)$$

Solving Eq.21 using the experimental value for  $\Delta\mu$  in tris of  $1.0 \times 10^{-4} \text{ cm}^2 \text{ V}^{-1} \text{ s}^{-1}$  and  $0.9 \times 10^{-3} \text{ kg m}^{-1} \text{ s}^{-1}$  for  $\eta$  [58], we obtain Eq.22:

$$\Delta q = 1.7 * 10^{-10} r \cdot c \quad (22)$$

As tris is a neutral ligand, regardless of the formation of ternary or binary complexes the change in charge per nickel ion bound is +2 (at pH= 7.4, hydroxy complexes can be discounted) and  $\Delta q$  is simply  $2n$ , where  $n$  is the number of nickel ions bound. Using a value of 1.1 nm for the hydrodynamic radius of a single strand [57], we obtain  $\Delta q = 1.9 \times 10^{-19} \text{ C}$ , and dividing by the elementary charge of  $1.6 \times 10^{-19} \text{ C}$ , we obtain a difference between the DNA and nickel-DNA complex of 1.2 charge units. In view of the gross assumptions made in this calculation, together with the expectation that the ss-DNA conformation is likely to be complex, possibly with a minihairpin at the 5'-d(CGCCG) motif, this is a minimum value and

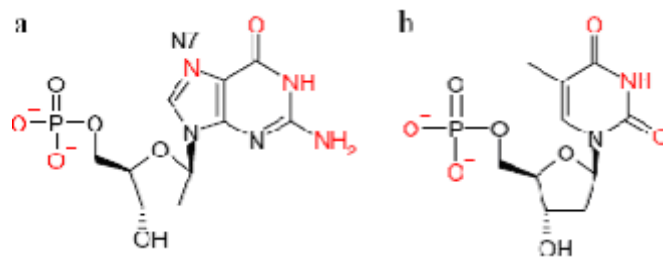
we can state that the nickel-DNA complex in tris buffer has a 1:1 metal-DNA stoichiometry, although we cannot state whether it is a binary or a ternary complex.

A comparison of the mobility shifts for the nickel-DNA system in tris and mops buffers is most informative. In mops buffer the plateau value for  $\Delta\mu$  is about twice that for tris buffer, which means that the change in charge is also twice that in tris. On the basis of a 1:1 complex in tris, we conclude that in mops either four  $\{\text{Ni(mops)}\}^+$  or two  $\text{Ni}^{2+}$  units are coordinated to the DNA. The former is unreasonable, in terms of both speciation and the known destabilisation of mops ternary complexes and we conclude that the saturated species in mops buffer is a  $\text{Ni}_2(\text{DNA})$  species although small amounts of the ternary species could be present. The difference in behavior is probably partly steric in origin—tris acts as a terdentate N,O,O donor<sup>[59, 60]</sup> and the molecular volume of a  $\{\text{Ni(tris)(H}_2\text{O)}_2\}$  moiety is  $158 \text{ \AA}^3$  compared with  $100 \text{ \AA}^3$  for  $\{\text{Ni(H}_2\text{O)}_5\}$ .

## 4.2 Tetranucleotides—specific interactions between DNA and metal cations.

In the previous section we discussed the behavior of a 24mer ss-DNA with metal ions and analysed the interactions with nickel(II) in detail. It is not appropriate to discuss the site of metal ion binding in detail. In an attempt to investigate metal-DNA interactions in a more systematic way, we studied the behavior of the tetranucleotides 5'-d(AAAA), 5'-d(GGGG), 5'-d(CCCC), 5'-d(TTTT) and 5'-d(TCAG). Rather surprisingly, very little is known about the solution or the solid-state conformation of tetranucleotides in the absence of a complementary strand. In particular, the tetranucleotides we selected are expected to be single-stranded and flexible in solution and certainly will not adopt a DNA duplex structure<sup>[61, 62]</sup>.

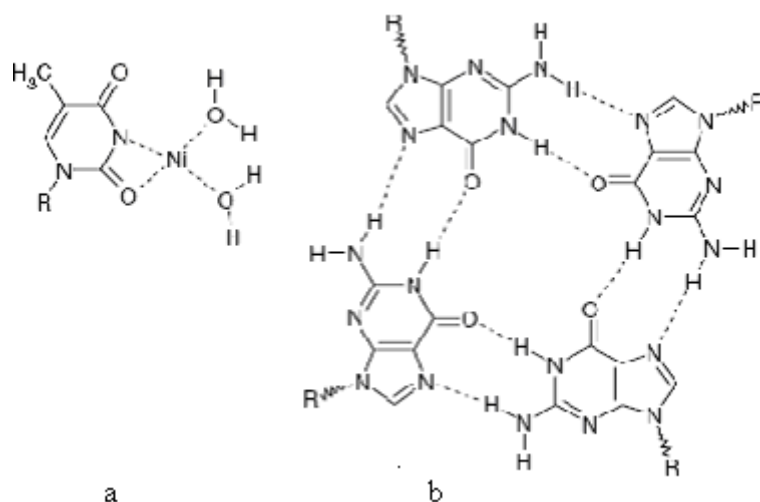
Metal ions can stabilize or destabilize the duplex forms of A-DNA or B-DNA<sup>[33]</sup>. There are a number of different potential binding sites for metal ions at the DNA: the most likely are the phosphate groups and N7 of the purine bases adenine and guanine (Figure 4.11 a, b)<sup>[27, 63]</sup>.



**Figure 4.11** **a** Guanosine monophosphate, **b** thymine monophosphate. The potential donor atoms are indicated in *red*.

The higher electronegativity of N7 of guanine is responsible for stronger interaction with cations than other nitrogen donors within the heterocycles [64, 65]. Hard cations prefer to bind to the phosphate group of the backbone, whereas softer cations, such as transition metal dications, preferentially interact with the nitrogen donor of the purine bases. Binding of the metal ions may be direct or indirect through water molecules, and coordinated water ligands can provide additional bridging interactions to other bases [27, 63, 66, 67]. It has been shown that nickel(II) has a particular preference for binding to the N7 terminal or outlooped guanine sites of B-form DNA [63, 68-77]. Although at  $\text{pH} > 8$ , transition metals can generate M-DNA in which cations replace the imino protons (Figure 4.12 a), this is not likely to be relevant under our experimental conditions [78].

Uniquely, in the case of 5'-d(GGGG), there is also the possibility of forming a guanine quadruplex (Figure 4.12 b) through Hoogsteen hydrogen bonding which can be further stabilized by binding a metal ion such as  $\text{K}^+$  [79]. The most stable structures are obtained with potassium or strontium ions and the stabilizing influence is in the sequence  $\text{K}^+ \gg \text{Na}^+ > \text{Rb}^+ > \text{Cs}^+ \gg \text{Li}^+$  and  $\text{Sr}^{2+} \gg \text{Ba}^{2+} > \text{Ca}^{2+} > \text{Mg}^{2+}$  [80]. It has been reported that  $\text{Li}^+$  [81] and transition metal dications [82] destabilize the quadruplex structure.



**Figure 4.12** a M-DNA (thymine), b guanine quadruplex.

We now describe the electrophoretic behavior of the tetranucleotides in the presence of various metal ions. Figure 4.13 gives an overview of the migration patterns of the various tetranucleotides in the presence of metal cations. The starting point for the discussion is the mobility in the absence of added metal ions (although, of course, sodium is present in the buffer). The four tetranucleotides 5'-d(AAAA), 5'-d(CCCC), 5'-d(TTTT) and 5'-d(TCAG) all have a mobility of  $-3.0 \pm 0.05 \text{ cm}^2 \text{ V}^{-1} \text{ s}^{-1}$ , whereas 5'-d(GGGG) has a mobility of  $-4.0 \text{ cm}^2 \text{ V}^{-1} \text{ s}^{-1}$ . The electrophoresis provides clear evidence for the presence of different species in the solution of 5'-d(GGGG) from the species in solutions of the other tetranucleotides ( $N_4$ ). However, it is possible to comment further on the nature of the solution species. The increased mobility of the 5'-d(GGGG) species results from an increase in the charge-to-hydrodynamic radius ratio compared with that of a single-stranded tetranucleotide. From Eq. 20 it follows that the ratio of the mobility of 5'-d(GGGG) ( $G_4$ ) to  $N_4$  is given by Eq.23 (assuming the viscosity of the solutions is constant):

$$\frac{\mu(G_4)}{\mu(N_4)} = \frac{q(G_4) \cdot r(N_4)}{q(N_4) \cdot r(G_4)} \quad (23)$$

For a  $G_n$  multiplex, assuming a common hydrodynamic radius of single-stranded  $G_4$  and  $N_4$ , we obtain Eq. 24:

$$\frac{\mu(G_4)}{\mu(N_4)} = \frac{4}{3} = n \frac{r(N_4)}{r(G_4)} \quad (24)$$

The best solution is for a quadruplex with  $n = 4$ , where the calculated ratio  $r(N_4)/r(G_4)$  of 1/3 is close to that calculated from a simple model based on cylinders of fixed radius (1/2.414) and that observed in solid-state structural determinations of sequences with guanine quadruplexes.

The pyrimidine tetranucleotides 5'-d(CCCC) and 5'-d(TTTT) show essentially similar behavior with extrapolated plateau values in the presence of  $Mg^{2+}$  or  $Ca^{2+}$  being reached at lower metal ion concentrations than with  $Ni^{2+}$ . Extrapolation to the final plateau mobilities is not reliable for  $Ni^{2+}$ , but the data (in particular the estimated  $\Delta q$ ) are compatible with the binding of a single metal ion per nucleotide. We suggest that the binding site is the phosphate, compatible with the higher stability of the complexes with the harder  $Mg^{2+}$  and  $Ca^{2+}$  ions.

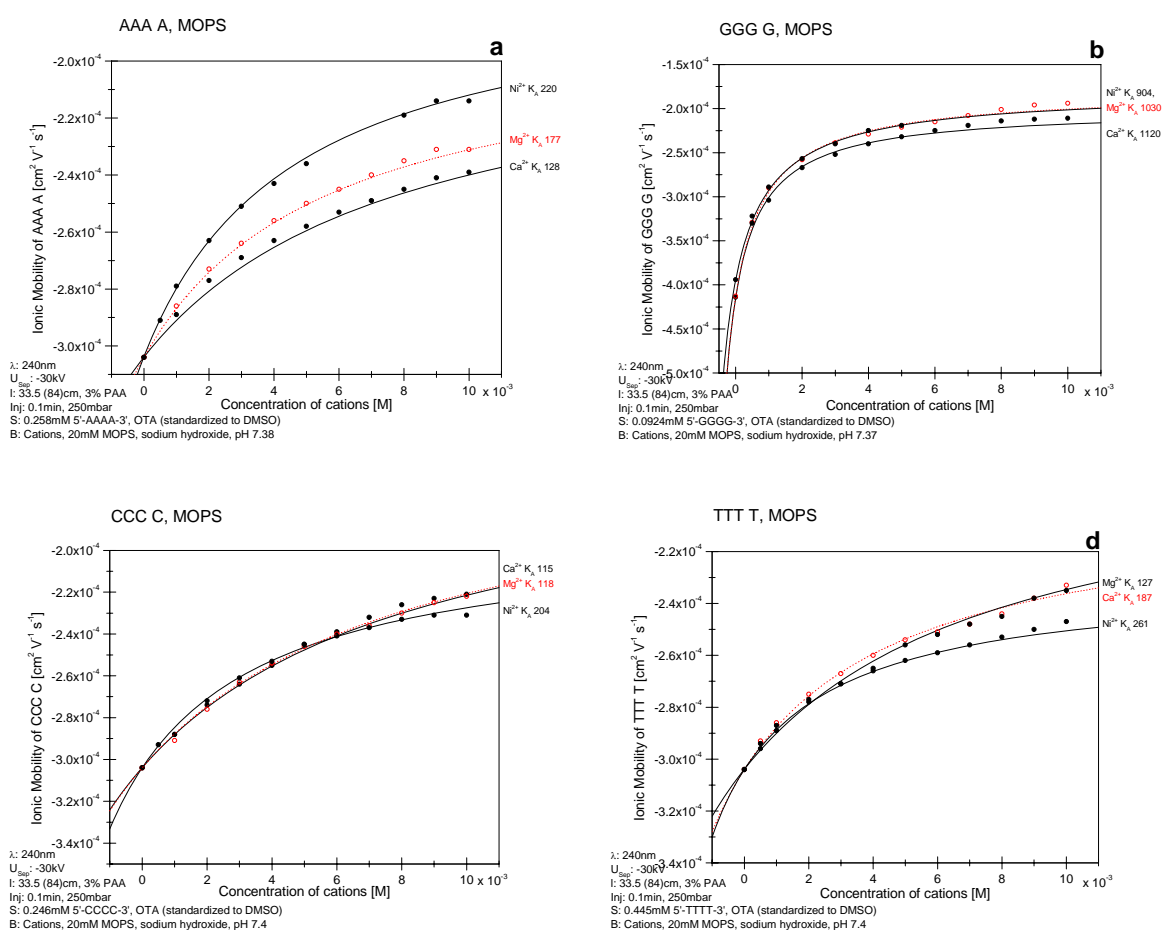
The trend for the pyrimidine tetranucleotides is reversed for 5'-d(AAAA), with the mobility reaching a plateau at lower metal ion concentrations in the presence of  $Ni^{2+}$ , indicating a greater stability for the nickel complex compared with the calcium and magnesium complexes. The curves for  $Mg^{2+}$  and  $Ca^{2+}$  are very similar to those for the pyrimidine tetranucleotides.

These observations are compatible with binding of calcium or magnesium at the phosphate and nickel at the purine although the  $K_b$  values are the same within experimental error (table 4.3). Very different behavior is observed for the tetranucleotide 5'-d(TCAG), where the change in mobility in the presence of  $Ni^{2+}$  is double that for  $Ca^{2+}$  and  $Mg^{2+}$  and the extracted stability constant for the nickel complex is significantly larger than for calcium or magnesium. As the mobility of 5'-d(TCAG) in the absence of added metal ion is the same as that of 5'-d(CCCC), 5'-d(AAAA), 5'-d(TTTT), the different behavior in the presence of nickel is not due to different starting structures of the tetranucleotides. This behavior is almost certainly associated with the binding of nickel to the N7 of the terminal guanine. We tentatively suggest that a second nickel is interacting with phosphate.

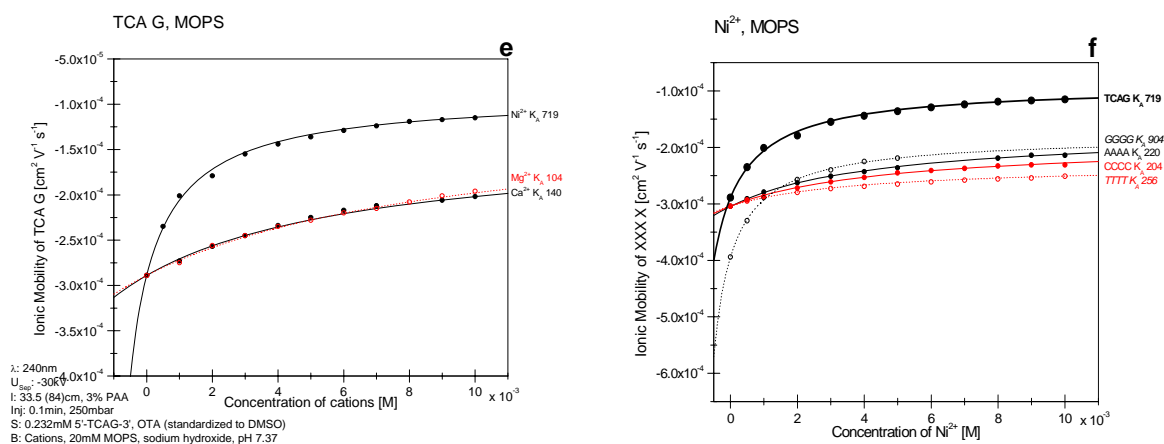
In the case of 5'-d(GGGG) the behavior is very different. We have already commented upon the difference in mobility in the absence of metal salt being compatible with the presence of the guanine quadruplex in solution. The three metal ions  $Ni^{2+}$ ,  $Mg^{2+}$  and  $Ca^{2+}$  all give very

similar changes in mobility and the change in charge to radius ratio is significantly larger than is observed with the other nucleotides. The change in mobility is  $2 \times 10^{-4} \text{ cm}^2 \text{ V}^{-1} \text{ s}^{-1}$  at the plateau value and using a value for the hydrodynamic radius of the quadruplex of  $3 \times 1.1 \text{ nm}$  (see earlier), the calculated  $\Delta q$  value is 4, strongly indicating that quadruplex binds a metal ion at each of the two termini.

Finally, it is useful to compare the behavior of the five tetranucleotides with the single metal ion,  $\text{Ni}^{2+}$  (Figure 4.13 f). This clearly shows that (1) the overall changes in mobility for the three tetranucleotides 5'-d(CCCC), 5'-d(TTTT) and 5'-d(AAAA) are very similar, (2) that the changes in mobility for 5'-d(TCAG) and 5'-d(GGGG) are very similar and (3) the overall change for 5'-d(TCAG) and 5'-d(GGGG) is twice that of 5'-d(CCCC), 5'-d(TTTT) or 5'-d(AAAA). These observations are in accord with the proposals above.







**Figure 4.13** Mobility shifts of tetranucleotides (0.3 mM) in the presence of various concentrations of metal salts (20 mM mops running buffer). a 5'-d(AAAA), b 5'-d(GGGG), c 5'-d(CCCC), d 5'-d(TTTT), and e 5'-d(TCAG) all in the presence of various concentrations of  $Mg^{2+}$  (red),  $Ca^{2+}$  (black) and  $Ni^{2+}$  (blue). f A comparison of the five tetranucleotides in the presence of  $Ni^{2+}$ .

**Table 4.3** Interactions between the single-stranded DNA and  $Ca^{2+}$ ,  $Mg^{2+}$ ,  $Ni^{2+}$ , with 20mM mops at pH=7.4.

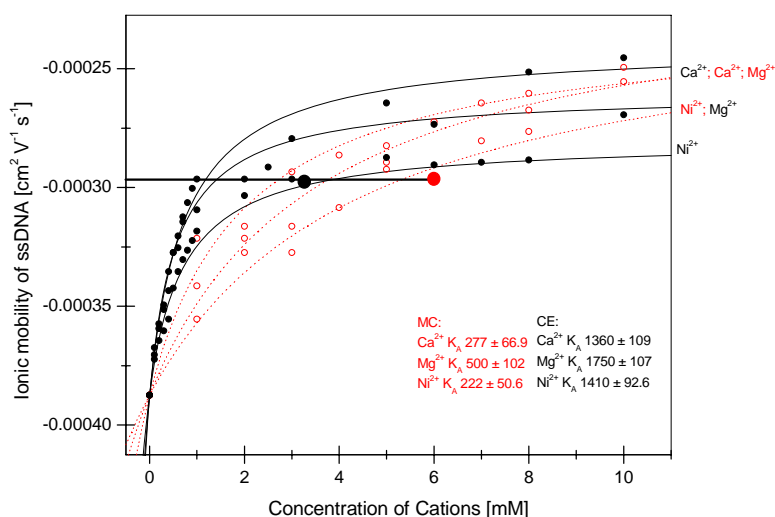
Single stranded	$Ca^{2+}$	$Mg^{2+}$	$Ni^{2+}$
3'-AAA A-5'	$128 \pm 14.5$	$177 \pm 8.58$	$220 \pm 10.1$
3'-CCC C-5'	$115 \pm 7.42$	$118 \pm 9.43$	$204 \pm 16.1$
3'-GGG G-5'	$1120 \pm 102$	$1030 \pm 63.4$	$904 \pm 47.9$
3'-TTT T-5'	$221 \pm 26.4$	$187 \pm 32.6$	$261 \pm 20.0$
3'-TCA G-5'	$140 \pm 13.3$	$104 \pm 8.93$	$719 \pm 37.7$

### Affinity electrophoresis on microchip

We now report very briefly on attempts to use microchip methods for investigating DNA-metal ion interactions. In contrast to the measurements using the capillary, detection on the microchip is realized over the whole length of the separation channel. Since the limit of detection on the chip is drastically lower (the optical path is 50  $\mu$ m) the sample concentrations have to be higher. This means that the change in the ionic mobility is

shallower, particularly at the early stages of the "titration" of metal salts into the DNA solution.

We have investigated the interactions of a 24-mer ss-DNA with a variety of metal salts (Figure 4.14, red line). On the graph there are two points marked on the  $\text{Ni}^{2+}$  curves for capillary and chip experiments. They indicate an analyte-ligand ratio of 1:24. For both points, the same ionic mobility can be measured. Above the marked concentration range of metal ions, no detection of the analyte was possible. Furthermore, only measurements with tris buffer were successful, since mops induced too high an electrophoretic current at a given separation voltage.



**Figure 4.14** Mobility shift of 24mer ss-DNA and various metal ions in tris buffer measured with capillary (*black*) and chip (*red*), experimental conditions: CE (see Figure 1), electric field of -280V/cm, Separation time of 15s.

Due to the incomplete measurement limited by insufficient UV sensitivity at the high metal ion concentrations needed to reach the mobility plateau, the calculated  $K_B$ -values have significantly higher deviations and for system with low  $K_B$  it is not realistic to calculate a value. Despite the lower magnitude of  $K_B$  on the chip compared to capillary measurements, the order of metal ions regarding their interacting strength with the DNA is comparable ( $K_B$ :  $\text{Ca}^{2+}$  ( $277 \pm 67 \text{ M}^{-1}$ )  $\approx$   $\text{Ni}^{2+}$  ( $222 \pm 51 \text{ M}^{-1}$ )  $<$   $\text{Mg}^{2+}$  ( $500 \pm 102 \text{ M}^{-1}$ )).

### 4.3 Interactions of bpy or phen derivatives, DNA and bpy-DNA with metal ions

The goal of this part of work was to study the phenomenon of metal complex formation between bpy-DNA and metal ions (copper(I) and copper(II)). This section only presents the preliminary results and the studies are ongoing. Copper is an essential element and its concentration in serum and tissues is under homeostatic control. The normal level of copper in human blood is approximately 16 $\mu$ M. Metal ions at these concentrations are expected to interact with a large variety of potential ligands within the biological environment. One possible binding site is a nucleic acid. The donor atoms in nucleic acids are hard and are expected to preferentially bind copper(II). In contrast, copper(I) is generally unstable with respect to disproportionation in aqueous conditions. Copper(I) species may be stabilised with respect to copper(II) in aqueous solution by coordination to good  $\pi$ -acceptor ligands such as 2,2'-bipyridines or 1,10-phenanthrolines [1]. The hybrid bpy-DNA species are, therefore, expected to bind both copper(I) and copper(II).

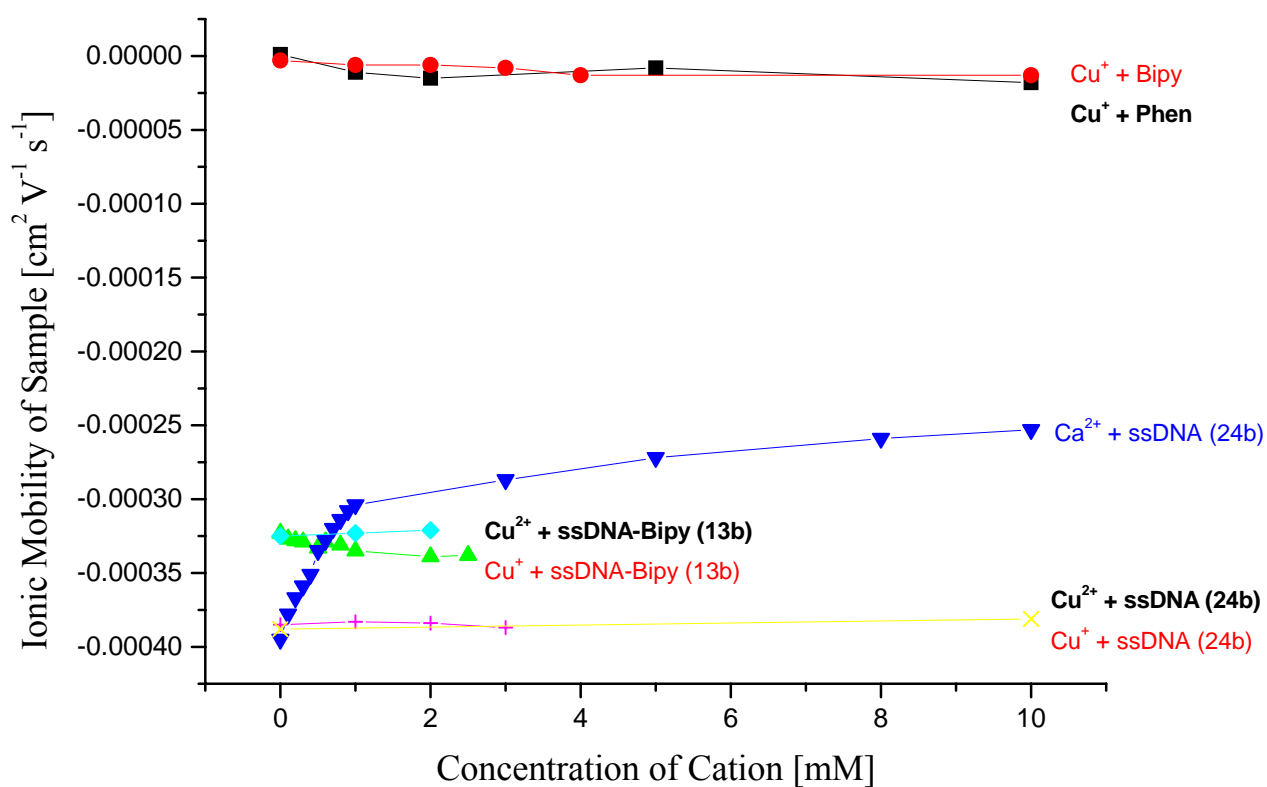
The first target was to investigate the interactions of copper(I) and copper(II) species with single-stranded DNA. Lamanna and coworkers studied the interaction of copper(II) with DNA. The results of their studies indicate that the double helix contains at least two kinds of binding site for copper. One site is present for every four nucleotides, has a high affinity for copper, and shows a cooperative effect. The other is an intercalating site for copper that is present every base pair. In single-stranded DNA, they found an average copper binding site every three nucleotides with a lower affinity than in double-stranded DNA [83].

Our first investigation was of interactions between copper(I) or copper(II) and DNA by capillary electrophoresis (Figure 4.15). We chose the 24-mer single-stranded DNA (5' TTA TTG ACG CCG CTT TTT TTT TTT 3') and investigated interactions with copper(II) chloride and  $[\text{Cu}(\text{CH}_3\text{CN})_4][\text{PF}_6]$ .

In this and subsequent experiments, the buffer was prepared by mixing a 50 mM solution of tris with boric acid to give a pH value of 7.4. An aqueous solution of the DNA (0.045 mM) and the internal standard OTA was used as the ligand source. The copper compounds were dissolved in the buffer solution to yield stock solutions of 10.0 mM. These were diluted

stepwise by the buffer solution to 0.1 mM. The copper(I) solution was prepared in deoxygenated buffer kept under argon; the final oxidation state is unclear.

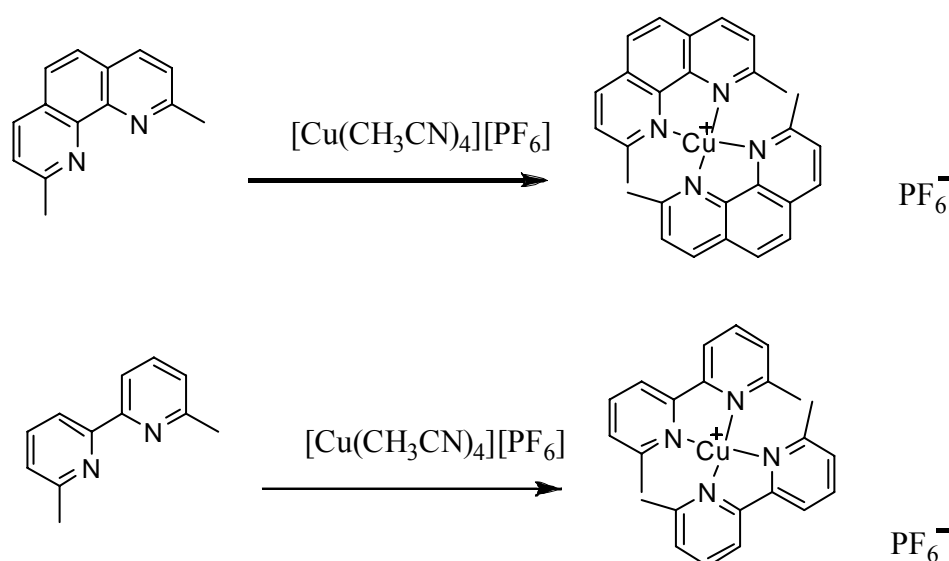
The mobility shift of the 24-mer DNA is independent of the concentration of copper(I) or copper(II) over the concentration range 0-10 mM suggesting that copper-buffer or copper-OTA interactions dominate and that copper-DNA interactions are very weak. For comparison, Figure 4.15 also shows the behaviour in the presence of varying concentrations of calcium(II) salts, which are expected to preferentially bind to the hard oxygen donors of the nucleic acid. The curve plateaus at a ratio of  $\text{Ca}^{2+}$ -DNA of 20:1 corresponding to the binding of a calcium at most phosphate groups.



**Figure 4.15** Mobility shift of different probes in the presence of various concentrations of metal salts.

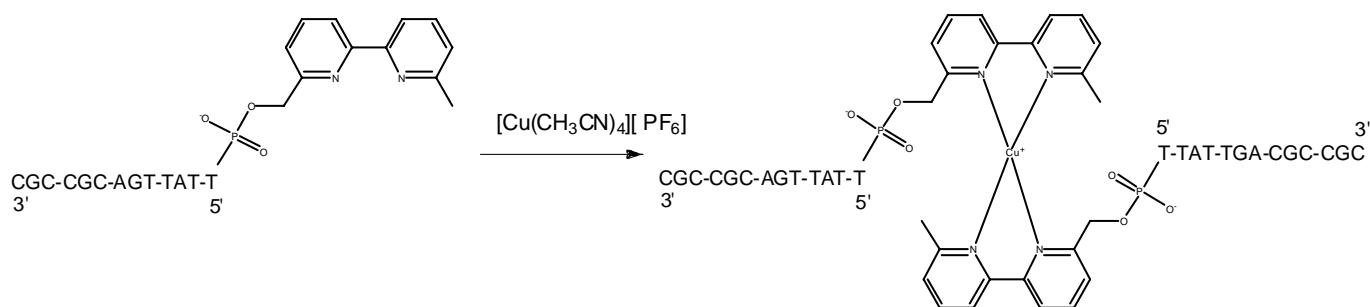
The second experiment studied the complexation of 6,6'-dimethyl-2,2'-bipyridine and 2,9-dimethyl-1,10-phenanthroline with copper(I). As we have demonstrated, the stability of the

$\{\text{Cu}^{\text{I}}\text{L}_2\}^+$  motif with these ligands is sufficient to make them the stable species in aqueous solution <sup>[1]</sup>. In preliminary experiments, little difference in mobility was observed at various concentrations of copper(I) or copper(II) (Figure 4.16). These experiments were performed under the same conditions as with copper salts and single-stranded-DNA. We believe that the copper-buffer interactions are also dominant in this case. The difference in absolute mobility of the DNA and the bpy or phen ligands is a function of the negative charge of the DNA.



**Figure 4.16** Illustration of the complexation of 2,9-dimethyl-1,10-phenanthroline and 6,6'-dimethyl-2,2'-bipyridine with copper(I).

The final experiment performed was the investigation of the interaction of bpy-DNA and copper(I) (Figure 4.15, Figure 4.17). The 13-mer conjugate shown in Figure 4.17 was selected as the test sequence. The experiments were performed in the same conditions as before.



**Figure 4.17** Illustration of the complexation of bpy-DNA with copper(I).

Figure 4.15 shows the electrophoresis experiments establishing an interaction between the bpy-DNA and Cu(I). We observe a clear difference in behaviour between copper(I) and copper(II) in this experiment which is a clear difference from those involving the simple bpy or phen ligands and the 24-mer ssDNA. Although detailed analysis on such preliminary data is hazardous, we note that the change in mobility is the opposite direction to that observed in the interaction of calcium(II) with the 24-mer DNA: This implies that the interaction of the bpy-DNA with the copper(I) results in a more negative species, compatible with the formation of the metallated species indicated in Figure 4.17.

## 4.4 Conclusions

ACE methods may be used to investigate the interactions of oligonucleotides and nucleic acids with metal ions. Initial studies indicate that the choice of buffer is critical and that the commonly used buffers such as tris and mops can act as ligands and bind transition metal ions, thereby introducing additional equilibria involving ternary complexes. The observed binding affinities of oligonucleotides for group 2 and transition metal ions may be rationalized in terms of a two-site binding model involving phosphate oxygen and heterocycle nitrogen donors in the nucleotide and can be quantified using limiting mobility values. Anomalous results with the tetranucleotide 5'-d(GGGG) are interpreted in terms of the formation of a quadruplex in the presence of metal ions.

To summarise, ACE methods provide a great deal of information on dynamic equilibria through rapid experimental procedures. We are currently investigating the environmental variables in detail to determine whether the method may be used for the extraction of "conventional" binding constants for metal ion-DNA interactions.

## 4.5 Experimental

### 4.5.1 Materials and Methods

#### 4.5.1.1 Chemicals and Reagents

All chemicals were of analytical grade. Acrylamide, boric acid,  $\text{CuCl}_2 \cdot 2\text{H}_2\text{O}$ ,  $\text{FeCl}_2 \cdot 4\text{H}_2\text{O}$ , and potassium persulfate were obtained from Acros (Geel, Belgium). dmsO,  $\text{MnCl}_2 \cdot 4\text{H}_2\text{O}$ , NaOH, o-toluic acid (OTA), 3-(trimethoxysilyl)propyl methacrylate, tris

(tris(hydroxymethyl)aminomethane), and zinc chloride were obtained from Fluka (Buchs, Switzerland).  $\text{FeCl}_3 \cdot 6\text{H}_2\text{O}$  was obtained from Riedel-de-Haën (Buchs, Switzerland). Magnesium chloride, (3-(*N*-morpholino)propanesulfonic acid) hemisodium salt (mops), and *N,N,N',N'*-tetramethylethylenediamine were obtained from Sigma (Buchs, Switzerland).  $\text{CaCl}_2 \cdot 2\text{H}_2\text{O}$  and  $\text{NiCl}_2 \cdot 6\text{H}_2\text{O}$  were obtained from Merck (Dietikon, Switzerland). The 24-mer single stranded DNA, 5'-TTA TTG ACG CCG CTT TTT TTT TTT-3' and the tetranucleotides AAAA, GGGG, TTTT, CCCC and TCAG were obtained from Microsynth (Balgach, Switzerland) and purified immediately before use by high performance liquid chromatography (HPLC).

#### 4.5.1.2 Apparatus

*Capillary affinity measurements:* For the measurements with the tris buffer, a Crystal ATI Unicam Model 310 from PrinCE Technology (Emmen, Netherlands) was used as CE system. The UV detector was a Spectra 100 from Thermo Separation Products (Egelsbach, Germany). Data were collected and analyzed with a  $\mu$ DAQ AD-modifier from Eagle Technology (Cape Town, South Africa).

For the measurements with the mops buffer, a PRINCE 500 autosampler 2-LIFT from PrinCE Technology (Emmen, Netherlands) was used as the CE system. The UV detector was a Spectra 100 from Thermo Separation Products (Egelsbach, Germany). Data were collected and analyzed with a PowerChrom 280 AD-modifier from eDAQ (Denistone East, Australia).

*Microchip affinity measurements:* Microchip experiments were performed on a commercial Shimadzu MCE-2010 instrument (Kyoto, Japan). The  $\text{D}_2$ -lamp based instrument possesses a diode array detector located along the separation channel. UV detection at a wavelength of 240 nm was used for all samples. All microchips were purchased from Shimadzu. The 35 mm x 12.5 mm x 2 mm quartz chip has a simple cross injector design; the separation channel is 25 mm long, 50  $\mu\text{m}$  deep and 110  $\mu\text{m}$  wide. Access holes are at the end of each channel and these reservoirs are labelled sample inlet (#1), sample waste (#2), buffer inlet (#3) and buffer waste (#4). All channels are coated with a polyacrylamide layer.

#### 4.5.1.3 Capillaries

Uncoated fused silica capillary tubing from BGB Analytik AG (Adliswil, Switzerland) with an internal diameter of 50  $\mu\text{m}$ , an effective length of 54 cm and a total length of 67 cm or effective 33.5 cm and total length 84 cm was used for all measurements. The procedure

reported by Hjertén<sup>[33]</sup> was utilized for preparing a covalently bound layer of 3% polyacrylamide on the surface of the silica capillary to prevent wall absorption.

#### 4.5.1.4 Methods

*Capillary affinity measurements:* Capillaries were conditioned daily before use by flushing with water for 10 min at 1000 mbar and 10 min with buffer at 1000 mbar. Between the measurements, the capillary was washed for 10 min, 1000 mbar with the plain buffer. The loading method consisted of three programs: Washing for 3 min at 1000 mbar with buffer, injection for 0.1 min at 250 mbar with the sample and separation for up to 20 min at a potential of -30 kV (cathode detection site) with buffer.

Two different buffers, tris and mops, were used. The tris buffer was prepared by mixing a solution of tris with boric acid (solid) to obtain a pH value of 7.4 and dilution to a final tris concentration of 50 mM. For the mops buffer, mops and 1M NaOH were mixed to obtain the same pH value of 7.4 and diluted to a final mops concentration of 20 mM. The DNA and the internal standard (OTA) were dissolved in water. The metal salts were dissolved in the buffer solution to yield stock solutions that were 10.0 mM in metal ion. These were diluted stepwise by the buffer solutions to 0.5 mM.

The detection method on the capillary was with UV light: at a wavelength of 240 nm (mops) or 260 nm (TRIS) respectively. It was a normal on-capillary method with detection on the anode-site. Each measurement was repeated three times.

*Microchip affinity measurements:* The entire procedure was performed at room temperature (25°C). Calculations and nonlinear fittings were carried out with the computer program Origin 6.0 from Microcal Software Inc. (Northampton, USA). Channels were flushed manually by means of a 2.5 mL syringe with a special flashing tip (Shimadzu). Before and after use, the chip was washed with double deionised water for at least for 30 s. The channels were dried using the vacuum from a water-pump. Before measuring, the channels were flushed with buffer solution and the four access holes cleaned with the vacuum (without emptying the channels). Finally, reservoirs #2-#4 were filled with buffer and #1 with the sample solution. This was also done manually using syringes. After setting the chip in the instrument, it was washed again under a potential for 90 s; voltages of 0.80 kV, 0.80 kV, 0.00 kV and 1.50 kV were applied to channels 1-4 respectively. The measurements were made as



pinched injections achieved by a two-step high-voltage program. In a first step (injection mode), a sample plug was introduced into the intersection. The applied voltages at the four reservoirs were 0.00 kV, 0.50 kV, 0.16 kV and 0.00 kV. After 15 s, the voltage was switched for a previously determined length of time (e.g. 15 s) to the separation mode with 0.80 kV, 0.80 kV, 0.00 kV and 1.50 kV, respectively.

On the microchip the detection method was with UV light of wavelength 240 nm. The detection took place over the whole separation channel. Measuring the anionic receptors the voltage program for the coated chips was the inverse of the normal method. The analytes migrated from anode through the whole separation channel towards the cathode. All measurements were reproduced three times.

## 4.6 References

- [1] Stettler, A. R., Chaurin, V., Constable, E. C., Housecroft, C. E., Schwarz, M. A., *J. Biol. Inorg. Chem.*, **2007**, *12*, 194.
- [2] Tiselius, A., *Trans. Faraday Soc.*, **1937**, *33*, 524.
- [3] Graham, K., *Biotechnol. Appl. Biochem.*, **1998**, *27*, 9.
- [4] Altria, K. D., Bryant, S. M., *LC/GC Int*, **1997**, *10*, 26.
- [5] Wijnen, P. A. H. M., Van Diejenvisser, M. P., *Eur. J. Clin. Chem. Clin. Biochem.*, **1996**, *7*, 535.
- [6] Righetti, P. G., Gelfi, C., *Anal. Biochem.*, **1997**, *244*, 195.
- [7] Weber, P. L., Lundte, S. M., *Electrophoresis*, **1996**, *17*, 302.
- [8] Paulus, A., Klockow, A., *J. Chromatogr.*, **1996**, *720*, 353.
- [9] Bressolle, F., Audran, M., Pham, T. N., Vallon, J. J., *J. Chromatogr.*, **1996**, *687*, 303.
- [10] Naylor, S., Benson, L. M., Tomlinson, A. J., *J. Chromatogr.*, **1996**, *735*, 415.
- [11] Nguyen, N. T., Siegler, R. W., *J. Chromatogr.*, **1996**, *735*, 123.
- [12] Riekkola, M. L., Jumppanen, J. H., *J. Chromatogr.*, **1996**, *735*, 151.
- [13] Frazier, R. A., Ames, J. M., Nursten, H. E., *Capillary electrophoresis for food analysis: method development monograph Narrow-bore*, Roy. Soc. Chem., ed 1, **2000**.
- [14] Bachmann, K., Haumann, F., Groh, T., *Fresenius J. Anal. Chem.*, **2004**, *343*, 901.
- [15] Guttman, A., Schwartz, H. E., *Anal. Chem.*, **1995**, *67*, 2279.
- [16] Landers, J. P. (ed), *Handbook of Capillary Electrophoresis*, CRC Press, Ann Arbor, Mich, **1994**.
- [17] Russel, W. B., Saville, D. A., Schowalter, W. R., *Colloidal dispersion*, Cambridge University Press, New York, **1989**.
- [18] Foret, F., Krivankova, L., Bocek, P., *Capillary Zone Electrophoresis*, Ed: Radola, B. J., **1993**.
- [19] *High performance capillary electrophoresis*, Ed: Agilent Technologies, **2000**.
- [20] Jandik, P., Bonn, G., Wiley-VCH Verlagsgesellschaft mbH, Weinheim, Germany, **2004**
- [21] Human Genome Program, **2003**, Genomics and its impact on science and society: a 2003 primer. US Department of Energy.

- [22] Sigel, H. (ed), **1979**, Metal ions in biological systems, Vol 8., Nucleotides and derivatives: their ligating ambivalency.
- [23] Sigel, A., Sigel, H. (eds), **1996**, Metal ions in biological systems, vol 32, Interactions of metal ions with nucleotides, nucleic acids, and their constituents.
- [24] Sigel, A., Sigel, H. (eds), **1996**, Metal ions in biological systems, vol 33, Probing of nucleic acids by metal ion complexes of small molecules.
- [25] de la Fuente, M., Hernanz, A., Navarro, R., *J. Biol. Inorg. Chem.*, **2004**, *9*, 973.
- [26] Kankia, B. I., *Biopolymers*, **2004**, *74*, 232.
- [27] Sigel, H., Griesser, R., *Chem. Soc. Rev.*, **2005**, *34*, 875.
- [28] He, X. Y., Ding, Y. S., Li, D. Z., Lin, B. C., *Electrophoresis*, **2004**, *25*, 697.
- [29] Heegaard, N. H. H., *Electrophoresis*, **2003**, *24*, 3879.
- [30] Guijt-van Duijn, R. M., Frank, J., van Dedem, G. W. K., Baltussen, E., Schalkhammer, T., *Electrophoresis*, **2001**, *22*, 1247.
- [31] Arakawa, H., Neault, J. F., Tajmir-Riahi, H. A., *Biophys. J.*, **2001**, *81*, 1580.
- [32] Ahmad, R., Arakawa, H., Tajmir-Riahi, H. A., *Biophys. J.*, **2003**, *84*, 2460.
- [33] Ouameur, A. A., Arakawa, H., Ahmad, Naoui, M., Tajmir-Riahi, H. A., *DNA Cell Biol.* **2005**, *24*, 394.
- [34] Hjertén, S., *J. Chromatogr. A.*, **1985**, *347*, 191.
- [35] Rüttinger, H.-H., In: Neubert, R. H. H., Rüttinger, H.-H., Affinity capillary electrophoresis in pharmaceuticals and biopharmaceuticals. Dekker, New York, **2003**, p 23.
- [36] Stellwagen, N. C., Bossi, A., Gelfi, C., Righetti, P. G., *Anal Biochem.*, **2000**, *287*, 167.
- [37] Sokolowska, M., Bal, W., *J. Inorg. Biochem.*, **2005**, *99*, 1653.
- [38] Taha, M., Khalil, M. M., Mohamed, S. A., *J. Chem. Eng. Data*, **2005**, *50*, 882.
- [39] Good, N. E., Winget, G. D., Connolly, T. N., Izana, S., Singh, R. M. M., *Biochemistry*, **1966**, *5*, 467.
- [40] Fischer, B. E., Haring, U. K., Tribolet, R., Sigel, H., *Eur. J. Biochem.*, **1979**, *94*, 523.
- [41] Stellwagen, N. C., Gelfi, C., Righetti, P. G., *Biopolymers*, **1997**, *42*, 687.
- [42] Olivera, B. M., Baine, P., Davidson, N., *Biopolymers*, **1964**, *2*, 245.
- [43] Manning, G., *Q. Rev. Biophys.*, **1978**, *11*, 179.
- [44] Stellwagen, N. C., Gelfi, C., Righetti, P. G., *Biopolymers*, **2000**, *54*, 137.
- [45] Ouameur, A. A., Tajmir-Riahi, H. A., *J. Biol. Chem.*, **2004**, *279*, 42041.
- [46] Shihabia, S. K., *Electrophoresis*, **2000**, *21*, 2872.
- [47] Hall, J. L., Liden, T. M., Swisher, J. A., Brannon, D. G., *Inorg. Chem.*, **1962**, *1*, 409.

- [48] Bai, K. S., Martell, A. E., *J. Inorg. Nucl. Chem.*, **1969**, *31*, 1697.
- [49] Brignac, P. J., Mo, C., *Anal. Chem.*, **1975**, *47*, 1465.
- [50] Bologni, L., Sabatini, A., Vacca, A., *Inorg. Chem. Acta*, **1983**, *69*, 71.
- [51] Canepari, S., Carunchio, V., Schina, R., *Polyhedron*, **1999**, *18*, 3263.
- [52] Rao, G. N., Muthy, G. S. R., Prakash, A., *Indian J. Chem. A.*, **1982**, *21*, 203.
- [53] Forsling, W., *Acta Chem. Scand. A.*, **1978**, *32*, 857.
- [54] Azab, H. A., Orabi, A. S., *J. Chem. Eng. Data*, **2001**, *46*, 346.
- [55] Anwar, Z., Azab, H., *J. Chem. Eng. Data*, **1999**, *44*, 1151.
- [56] Okafo, G. N., Brown, R., *J. Chem. Soc. Chem. Commun.*, **1991**, 867.
- [57] Fujimoto, B. S., Miller, J. M., Ribeiro, N. S., Schurr, J. M., *Biophys.*, **1994**, *67*, 304.
- [58] Kell, G. S., In: Franks F. (ed) *Water-a comprehensive treatise*. Plenum, New York, **1972**, p 406.
- [59] Ivarsson, G. J. M., *Acta Crystallogr. Sect. B.*, **1982**, *38*, 1829.
- [60] Zeng, M.-H., Liang, H., Zeng, R.-Y., Yi, X.-H., Yu, K.-B., *Acta Chim. Sin.*, **2002**, *60*, 784.
- [61] Packer, M. J., Dauncey, M. P., Hunter, C. A., *J. Mol. Biol.*, **2000**, *295*, 85.
- [62] Dixit, S. B., Beveridge, D. L., Case, D. A., Cheatham, T. E., Giudice, E., Lankas, F., Lavery, R., Maddocks, J. H., Osman, R., Sklenar, H., Thayner, K. M., Varnai, P., *Biophys. J.*, **2005**, *89*, 3721.
- [63] Egli, M., *Curr. Opin. Chem. Biol.*, **2004**, *8*, 580.
- [64] Abrescia, N. G. A., Huynh-Dinh, T., Subirana, J. A., *J. Biol. Inorg. Chem.*, **2002**, *7*, 195.
- [65] Spöner, J., Sabat, M., Gorb, L., Leszczynski, J., Lippert, B., Hobza, P., *J. Phys. Chem. B.*, **2000**, *104*, 7535.
- [66] Soler-Lopez, M., Malinina, L., Subirana, J. A., *J. Biol. Chem.*, **2000**, *275*, 23034.
- [67] Chiu, T. K., Dickerson, R. E., *J. Mol. Biol.*, **2000**, *301*, 915.
- [68] Valls, N., Uson, I., Gouyette, C., Subirana, J. A., *J. Am. Chem. Soc.*, **2004**, *126*, 7812.
- [69] Gao, Y. G., Sriram, K., Wang, A. H., *Nucl. Acid. Res.*, **1993**, *21*, 4093.
- [70] Abrescia, N. G. A., Malinina, L., Subirana, J. A., *J. Mol. Biol.*, **1999**, *294*, 657.
- [71] Subirana, J. A., Abrescia, N. G. A., *Biophys. Chem.*, **2000**, *86*, 179.
- [72] Abrescia, N. G. A., Malinina, L., Fernandez, L. G., Huynh-Dinh, T., Neidle, S., Subirana, J. A., *Nucleic Acid. Res.*, **1999**, *27*, 1593.
- [73] Yang, X. I., Robinson, H., Gao, Y. G., Wang, A. H.-J., *Biochemistry*, **2000**, *39*, 10950.

- [74] De Meester, P, Goodgame, D. M. L., Skapski, A. C., Smith, B. T., *Biochim. Biophys. Acta*, **1974**, 340, 113.
- [75] Collins, A. D., De Meester, P, Goodgame, D. M. L., Skapski, A. C., *Biochim. Biophys. Acta*, **1975**, 116, 2958.
- [76] Sigel, H., Massoud, S. S., Corfu, N. A., *J. Am. Chem. Soc.*, **1994**, 116, 2958.
- [77] Labiuk, S. L., Delbaere, L. T. J., Lee, J. S., *J. Biol. Inorg. Chem.*, **2003**, 8, 715.
- [78] Hartzell, B., McCord, B., *Electrophoresis*, **2005**, 26, 1046.
- [79] Simonsson, T., *Biol. Chem.*, **2001**, 382, 621.
- [80] Guschlbauer, W., Chantot, J. F., Thiele, D., *J. Biomol. Struct. Dyn.*, **1990**, 8, 491.
- [81] Sen, D., Gilbert, W., *Methods Enzymol.*, **1992**, 211, 191.
- [82] Blume, S. W., Guarcello, V., Zacharias, W., Miller, D. M., *Nucleic Acid. Res.*, **1997**, 25, 617.
- [83] Sagripanti, J.-L., Goering, P. L., Lamanna, A., *Toxicol. Appl. Pharmacol.*, **1991**, 110, 477.

## Chapter 5 Conclusions and outlook

The influence of a metal complex formation on the hybridisation of oligodeoxynucleotides was investigated. Incorporation of the metal-binding domains had a positive influence on the hybrid. Addition of copper(I) or copper(II) ions results in the formation of metal complexes and leads to substantial further stabilization. The placement of the metal-free ligands had no influence on the extent of the stabilization. The stabilizing effect obtained by metal-coordination was found to be distance-dependent.

This study showed that hybridisation of relatively short (13- and 8-mer) oligonucleotides modified with bpy or phen metal-binding domains to a complementary target DNA is assisted by formation of metallonucleotides containing  $\{\text{Cu}(\text{bpy})_2\}$ ,  $\{\text{Cu}(\text{phen})_2\}$  or  $\{\text{Cu}(\text{bpy})(\text{phen})\}$  domains.

The study of photochemistry of disubstituted-2,2'-bipyridine and 2,9'-disubstituted-1,10-phenanthroline copper(I) complexes showed that compound with triphenylamine substituents are very fluorescent.

We can imagine now the preparation and investigation of novel types of arrays containing oligonucleotide metal conjugates. Arrays of this type should allow the *direct* detection and quantification of nucleotic acids (DNA). The basic concept consists of the generation of a fluorescent metal complex upon hybridisation of analyte nucleic acid to substrate bound oligonucleotides containing metal binding ligands substituted with triphenylamine in the presence of a second, oligonucleotide-ligand conjugate and appropriate metal ion.

## Chapter 6 : General Experimental

### 6.1 General

#### 6.1.1 Instrument

##### **Mass spectrometry**

MALDI mass spectra were recorded using a PerSeptive Biosystems Voyager instrument, and ESI mass spectra were recorded using a Finnigan MAT LCQ spectrometer.

##### **$^1\text{H}$ NMR and $^{13}\text{C}$ NMR Spectroscopy**

$^1\text{H}$  NMR and  $^{13}\text{C}$  NMR spectra were recorded on a Bruker DRX400 spectrometer (University Basel).

##### **UV-vis spectroscopy**

UV-vis spectra were recorded on a Varian 5000 UV-VIS-NIR spectrometer.

##### **Fluorescence**

Fluorescence spectra were recorded using a Shimadzu RF-5301 PC spectrofluorophotometer.

##### **Electrochemistry**

Electrochemical measurements were performed with an Eco Chemie Autolab PGSTAG 20 system using glassy carbon working and platinum auxiliary electrodes with silver as reference using purified acetonitrile as solvent and 0.1M  $[\text{nBu}_4\text{N}][\text{BF}_4]$  as supporting electrolyte; ferrocene was added at the end of each experiment as an internal reference.

## 6.1.2 Abbreviations

### 6.1.2.1 general

A	adenosine
Ar	argon
bpy	2,2'-Bipyridine
C	cytosine
CD	circular dichroism
CE	capillary electrophoresis
CHCl <sub>3</sub>	chloroform
CH <sub>3</sub> CN	acetonitrile
<sup>13</sup> C-NMR	Carbon Magnetic Resonance Spectroscopy
CPBA	3-Chloroperoxybenzoic acid
DCM	Dichloromethane
DMF	N, N-Dimethylformamide
DMSO	Dimethylsulfoxide
DNA	Deoxyribonucleic acid
Et <sub>2</sub> O	Diethylether
Et <sub>3</sub> N	Triethylamine
EtOAc	Ethyl acetate
EtOH	Ethanol
Fc	Ferrocene
G	guanosine
g	gram(s)
h	hour
Hz	hertz
HPLC	High Pressure Liquid Chromatography
<sup>1</sup> H-NMR	Proton Magnetic Resonance Spectroscopy
H <sub>2</sub> O	water
H <sub>2</sub> SO <sub>4</sub>	sulfuric acid
LDA	Lithium diisopropylamine
n-hex	hexan



MALDI-TOF-MS	Matrix Assisted Laser Desorption Ionisation-Time of Flight-Mass Spectrometry
Na <sub>2</sub> CO <sub>3</sub>	Sodium carbonate
Na <sub>2</sub> SO <sub>4</sub>	sodium sulfate
MeLi	Methylithium
MeOH	Methanol
N <sub>2</sub>	nitrogen
PCl <sub>3</sub>	Phosphorus trichloride
Phen	1,10-phenanthroline
PhLi	Phenyllithium
R <sub>f</sub>	retention factor
RNA	ribonucleic acid
rt	room temperature
T	thymine
THF	Tetrahydrofuran
TLC	Thin layer chromatography
T <sub>m</sub>	melting temperature
Tpy	2,2':6',2''-Terpyridine
U	uridine

#### 6.1.2.2 NMR assignments

$\delta$	chemical shift, in ppm
$\Delta\delta$	change in chemical shift
J	coupling constant, in Hz
s	singlet
d	doublet
t	triplet
q	quartet
m	multiplet
br	broad

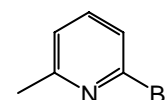
## 6.2 Synthesis and characterizations

### 6.2.1 Synthesis and characterizations of Ligands

#### 2-Bromo-6-methylpyridine (6-bromopicoline):

Formula: C<sub>6</sub>H<sub>6</sub>BrN

Molecular weight: 172.02



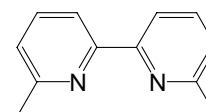
2-Amino-6-methyl-pyridine (4.0 g, 36.96 mmol) was added to HBr (48% aqueous, 25 mL) at room temperature and then cooled to -30 °C. Elemental bromine (5.30 mL, 103.2 mmol) was added dropwise to the thick orange/brown slurry while being stirred with a mechanical stirrer. Upon addition of the bromine, a yellow precipitate formed immediately. After stirring for 90 min at -30 °C a solution of NaNO<sub>2</sub> [(6.8 g, 98.4 mmol) in H<sub>2</sub>O (15 mL)] was added and a brown gas evolved. The dark brown mixture was brought to room temperature and stirred for 1 hour. It was then cooled back down to -30 °C and a solution of NaOH [(26.0 g, 670 mmol) in H<sub>2</sub>O (50 mL)] was added dropwise. The temperature was kept under 10 °C during the addition after which the mixture was brought to room temperature and extracted 5 times with Et<sub>2</sub>O. The combined organic layers were dried with Na<sub>2</sub>SO<sub>4</sub> and solvent evaporated to yield the desired product as a light brown solid (5.2 g, 81.7 %) <sup>[1]</sup>.

<sup>1</sup>H NMR (400 MHz, CDCl<sub>3</sub>): δ = 2.48 (s, 3H, H-7), 7.05 (d, 1H, J = 7.5 Hz, H-5), 7.23 (d, 1H, J = 7.8 Hz, H-3), 7.38 (t, 1H, J = 7.8 Hz, H-4).

#### 6,6'-Dimethyl-2,2'-bipyridine via homocoupling of 6-bromopicoline (14):

Formula: C<sub>12</sub>H<sub>12</sub>N<sub>2</sub>

Molecular weight: 184.24



A mixture of 6-bromopicoline (3.0 g, 17.44 mmol), *n*-Bu<sub>4</sub>NBr (2.81 g, 8.7 mmol, 0.5 eq.), Pd(OAc)<sub>2</sub> (196 mg, 0.87 mmol, 5 mol%) and K<sub>2</sub>CO<sub>3</sub> (2.41 g, 17.44 mmol, 1 eq.) in

DMF:H<sub>2</sub>O, 2.4:1 (2.4 mL) was heated to 110 °C under N<sub>2</sub>. Then isopropyl alcohol (1.34 mL) was added and the flask was tightly stoppered. Stirring was continued at 110 °C for 2 days. The cooled reaction mixture was diluted with water and extracted with EtOAc. Drying with Na<sub>2</sub>SO<sub>4</sub>, filtration and evaporation afforded a brown oil which was chromatographed (eluent: *n*-hex: EtOAc, 4:1) to give the desired 6,6'-dimethyl-2,2'-bipyridine as a yellow solid (1.0 g, 62 %) [2].

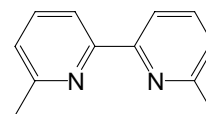
**<sup>1</sup>H NMR** (400 MHz, CDCl<sub>3</sub>): δ = 2.62 (s, 6H, H-7, 7'), 7.14 (d, 2H, J = 7.8 Hz, H-5, 5'), 7.67 (t, 2H, J = 7.8 Hz, H-4, 4'), 8.17 (d, 2H, J = 7.8 Hz, H-3, 3')

**ESI-MS** *m/z*: 185.0 ([M + H]<sup>+</sup>)

#### 6,6'-Dimethyl-2,2'-bipyridine (14):

Formula: C<sub>12</sub>H<sub>12</sub>N<sub>2</sub>

Molecular weight: 184.24



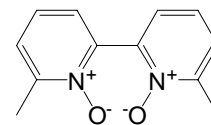
To a cold (-78 °C) solution of 2,2'-bipyridine (6.0 g, 0.038 mol) in dry THF (200 mL) was added methyllithium (1.6 M, 100 mL, 0.16 mol). The reaction was kept at -78 °C for 1 hour after which it was allowed to reach room temperature for an additional hour. The reaction mixture was then brought to reflux for 3 hours after which the MeLi was quenched with ice which resulted in the formation of a yellow precipitate. The mixture was condensed and the product was extracted using dichloromethane/water. The organic layer was dried with magnesium sulfate and manganese dioxide was then added (100 g) and the mixture was stirred for 1.5 hours. The mixture was then filtered through celite and the product was condensed. The final product was found to be a beige solid (6.05 g, 86 %) [3].

**<sup>1</sup>H NMR** (400 MHz, CDCl<sub>3</sub>): δ = 2.59 (s, 6H, H-7, 7'), 7.11 (d, 2H, J = 7.7 Hz, H-5, 5'), 7.65 (t, 2H, J = 7.8 Hz, H-4, 4'), 8.14 (d, 2H, J = 7.7 Hz, H-3, 3')

**ESI-MS** *m/z*: 185.0 ([M + H]<sup>+</sup>).

**6,6'-Dimethyl-2,2'-bipyridine *N,N'*-dioxide (15):**Formula: C<sub>12</sub>H<sub>12</sub>N<sub>2</sub>O<sub>2</sub>

Molecular weight: 216.24



6,6'-Dimethyl-2,2'-bipyridine (1.0 g, 6.52 mmol) was placed in 6 mL of glacial acetic acid. 2.0 mL of hydrogen peroxide (30%) was then added and the reaction was heated to 80 °C. After 4 hours, an additional 0.4 mL of hydrogen peroxide (30 %) was added and the reaction was maintained at 80 °C for 20 hours. The reaction mixture was then evaporated on the rotovap and dried on the high vacuum pump after which recrystallization from diethyl ether led to the pure desired product as a white solid (1.06 g, 90 %) <sup>[4]</sup>.

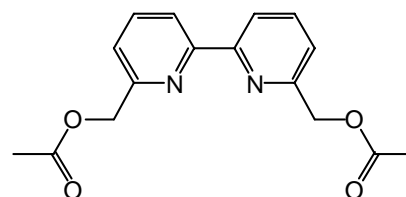
<sup>1</sup>H NMR (400 MHz, CDCl<sub>3</sub>): δ = 2.59 (s, 6H, H-7, 7'), 7.37 (m, 6H, H-3, 3', 4, 4', 5, 5').

<sup>13</sup>C NMR (100 MHz, CDCl<sub>3</sub>): δ = 18.15 (C-7, 7'), 125.12 (C-5, 5'), 125.88 (C-3, 3'), 127.16 (C-6, 6'), 143.69 (C-2, 2'), 150.02 (C-4, 4').

ESI-MS *m/z*: 217.0 ([M + H]<sup>+</sup>).

**6,6'-Bis(acetoxymethyl)-2,2'-bipyridine (16):**Formula: C<sub>16</sub>H<sub>16</sub>N<sub>2</sub>O<sub>2</sub>

Molecular weight: 300.31



6,6'-Dimethyl-2,2'-bipyridine-1,1'-bis-*N*-oxide (520 mg, 2.40 mmol) was dissolved in freshly distilled acetic anhydride (15 mL) and brought to reflux for 20 minutes. The dark brown reaction mixture was then evaporated and dried on the high vacuum pump. It was purified by column chromatography (Al<sub>2</sub>O<sub>3</sub>, dichloromethane: diethyl ether, 3:1) to give a beige solid (505 mg, 70 %) <sup>[4]</sup>.

**<sup>1</sup>H NMR** (400 MHz, CDCl<sub>3</sub>): δ = 2.18 (s, 6H, H-10, 10'), 5.29 (s, 4H, H-7, 7'), 7.35 (d, 2H, J = 6.9 Hz, H-5, 5'), 7.82 (t, 2H, J = 7.8 Hz, H-4, 4'), 8.35 (d, 2H, J = 7.8 Hz, H-3, 3')

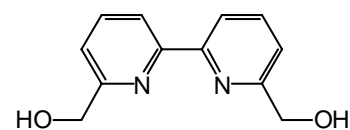
**<sup>13</sup>C NMR** (100 MHz, CDCl<sub>3</sub>): δ = 21.15 (C-10, 10'), 67.14 (C-7, 7'), 120.40 (C-3, 3'), 121.75 (C-5, 5'), 137.73 (C-4, 4'), 155.39 (C-2, 2'), 155.62 (C-6, 6'), 170.83 (C-9, 9').

**ESI-MS** *m/z*: 301.0 ([M + H]<sup>+</sup>).

### 6,6'-Bis (hydroxymethyl)-2,2'-bipyridine (17):

Formula: C<sub>12</sub>H<sub>12</sub>N<sub>2</sub>O<sub>2</sub>

Molecular weight: 216.24



Absolute ethanol (50 mL) was added to a mixture of 6,6'-bis(acetoxymethyl)-2,2'-bipyridine (500 mg, 1.68 mmol) and anhydrous K<sub>2</sub>CO<sub>3</sub> (750 mg, 5.45 mmol). The reaction mixture was stirred at room temperature for 24 hours and was then filtered through celite. The filtrate was evaporated and the product dried on the pump, yielding the desired product as a beige solid (355 mg, 98 %) [5].

**<sup>1</sup>H NMR** (400 MHz, CD<sub>3</sub>OD): δ = 4.90 (s, 4H, H-7, 7'), 7.50 (d, 2H, J = 7.6 Hz, H-5, 5'), 7.87 (t, 2H, J = 8.0 Hz, H-4, 4'), 8.20 (d, 2H, J = 7.6 Hz, H-3, 3')

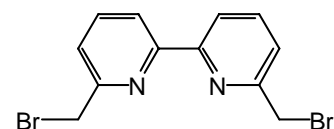
**<sup>13</sup>C NMR** (100 MHz, CD<sub>3</sub>OD): δ = 65.60 (C-7, 7'), 120.52 (C-3, 3'), 121.39 (C-5, 5'), 138.5 (C-4, 4'), 156.22 (C-2, 2'), 161.73 (C-6, 6').

**ESI-MS** *m/z*: 216.9 ([M + H]<sup>+</sup>)

### 6,6'-bis(bromomethyl)-2, 2'-bipyridine (18):

Formula: C<sub>12</sub>H<sub>10</sub>Br<sub>2</sub>N<sub>2</sub>

Molecular weight: 339.92



6,6'-Bis(hydroxymethyl)-2,2'-bipyridine (150 mg, 0.69 mmol) was brought to reflux in hydrobromic acid (2 mL) for 2 hours. The reaction mixture was then neutralized with 2 M NaOH to give a precipitate. After cooling the mixture in an ice-bath, the precipitate was filtered and washed (15 mL x 5) with water to yield the desired product as beige solid (99 mg, 42 %) [6].

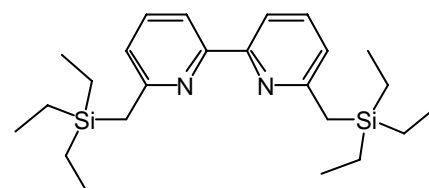
<sup>1</sup>H NMR (400 MHz, CDCl<sub>3</sub>): δ = 4.62 (s, 4H, H-7, 7'), 7.44 (d, 2H, J= 7.5 Hz, H-5, 5'), 7.80 (t, 2H, J=7.8, H-4, 4'), 8.38 (d, 2H, J= 7.8 Hz, H-3, 3').

ESI-MS *m/z*: 341.0 ([M + H]<sup>+</sup>)

### 6,6'-Bis(triethylsilylmethyl)-2,2'-bipyridine (19):

Formula: C<sub>24</sub>H<sub>40</sub>N<sub>2</sub>Si<sub>2</sub>

Molecular weight: 412.27

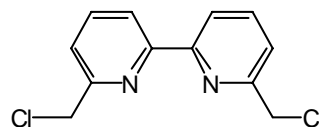


A solution of 6,6'-dimethyl-2,2'-bipyridine (0.92 g, 5.0 mmol) in dry THF (30 mL) was cooled to 0 °C under nitrogen. A 2M solution of lithium diisopropylamide (15.0 mL, 30.0 mmol) was added quickly, the cooling was removed and the reaction mixture was stirred for 1h at room temperature. Chlorotriethylsilane (1.72 mL, 10.2 mmol) was added and the solution was stirred for another 30 min at room temperature. The reaction was quenched by addition of water (20 mL) while cooling. The organic layer was separated and the aqueous layer was extracted with THF (2 x 40mL). The combined organic layer was washed with saturated brine (50 mL), dried with sodium sulfate and the solvent was removed in vacuo. The crude product was purified by flash chromatographie (silica; eluent: hexane/ethyl acetate/triethylamine, 100:10:1), to give 1.81g (88 %) of the 6,6'-bis(triethylsilylmethyl)-2,2'-bipyridine.

<sup>1</sup>H NMR (400 MHz, CDCl<sub>3</sub>): δ = 0.60 (q, 12H, J = 8.1 Hz), 0.98 (t, 18H, J = 8.1 Hz), 2.43(s, 4H), 6.96 (d, 2H, J = 8.1 Hz), 7.59 (t, 2H, J = 8.1 Hz), 8.15 (d, 2H, J = 8.1).

**6,6'-bis(chloromethyl)-2,2'-bipyridine (20):**Formula: C<sub>12</sub>H<sub>10</sub>Cl<sub>2</sub>N<sub>2</sub>

Molecular weight: 252.02



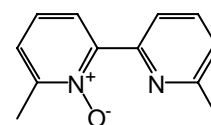
To a solution of 6,6'-bis(triethylsilylmethyl)-2,2'-bipyridine (4.3 mmol, 1.78 g) and Cl<sub>3</sub>CCCl<sub>3</sub> (8.6 mmol, 2.026 g) in 150 ml dry DMF under inert gas atmosphere anhydrous CsF (8.6 mmol, 1.31 g) was added. The reaction mixture was stirred at room temperature for six hours. The reaction mixture was poured into a mixture of EtOAc and H<sub>2</sub>O (200 ml each), the organic layer was separated and the aqueous layer was extracted three times with 100 ml EtOAc each. The combined organic fractions were dried over Na<sub>2</sub>SO<sub>4</sub>. Filtration and evaporation of the solvent gave a yellowish product which was purified by washing with cold toluene to yield a white solid (0.88 g, 78 %).

<sup>1</sup>H NMR (400 MHz, CDCl<sub>3</sub>): δ = 4.75 (s, 4H, H-7, 7'), 7.50 (d, 2H, J=8.1, H-5, 5'), 7.85 (t, 2H, J=7.6, H-4, 4'), 8.39 (d, 2H, J=8.1, H-3, 3').

<sup>13</sup>C NMR (100 MHz, CDCl<sub>3</sub>): 47.33, 120.89, 123.27, 138.35, 155.74, 156.49.

**6,6'-Dimethyl-2,2'-bipyridine N-oxide (21):**Formula: C<sub>12</sub>H<sub>12</sub>N<sub>2</sub>O

Molecular weight: 200.24



6,6'-Dimethyl-2,2'-bipyridine (1.5 g, 8.14 mmol) was dissolved in CHCl<sub>3</sub> (12 mL) and was cooled in an ice-bath. To this mixture, *m*-chloroperbenzoic acid (77%, 2.0 g, 8.95 mmol) in CHCl<sub>3</sub> (30 mL) was added dropwise over 3 hours. The reaction was kept at 0 °C during the addition after which it was brought to room temperature and stirred for 1 hour. The reaction mixture was then washed with a saturated NaHCO<sub>3</sub> solution and then with water. The combined organic layers were dried with Na<sub>2</sub>SO<sub>4</sub>, the solvent removed, and the product dried on the pump. The resulting yellowish solid was treated with diethyl ether to remove the di-*N*-

oxide as an insoluble solid. The product was purified via column chromatography (Al<sub>2</sub>O<sub>3</sub>, ethyl acetate: methanol, 4:1) to yield the desired product as a white solid (1.13g, 69%)<sup>[4]</sup>.

**<sup>1</sup>H NMR** (400 MHz, CDCl<sub>3</sub>): δ = 2.07 (s, 3H), 2.54 (s, 3H), 7.28 (d, 1H, J = 7.5 Hz), 7.48 (t, 1H, J = 7.6 Hz), 7.61 (d, 1H, J = 7.8 Hz), 7.80 (t, 1H, J = 7.8 Hz), 7.88 (d, 1H, J = 8.8 Hz), 8.17 (d, 1H, J = 7.9 Hz)

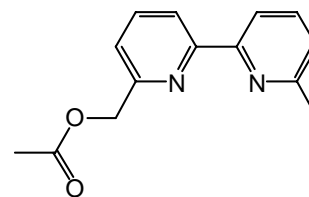
**<sup>13</sup>C NMR** (100 MHz, CDCl<sub>3</sub>): δ = 18.33, 24.52, 122.37, 123.51, 124.77, 125.52, 125.58, 136.20, 147.60, 149.62, 149.67, 157.90.

**ESI-MS** *m/z*: 201.1 ([M + H]<sup>+</sup>)

**6-(Acetoxymethyl)-6'-methyl-2,2'-bipyridine (22):**

Formula: C<sub>14</sub>H<sub>14</sub>N<sub>2</sub>O<sub>2</sub>

Molecular weight: 242.27



6,6'-Dimethyl-2,2'-bipyridine-*N*-oxide (700 mg, 3.50 mmol) was dissolved in freshly distilled acetic anhydride (10 mL) and brought to reflux for 15 minutes. The dark brown reaction solution was then evaporated and the product dried on the high vacuum pump. It was purified by column chromatography (Al<sub>2</sub>O<sub>3</sub>, dichloromethane:petroleum spirits 40-60 °C, 1:1) to give a beige solid (595 mg, 71%)<sup>[4]</sup>.

**<sup>1</sup>H NMR** (400 MHz, CDCl<sub>3</sub>): δ = 2.12 (s, 3H), 2.56 (s, 3H), 5.25 (s, 2H), 7.09 (d, 1H, J = 7.6 Hz), 7.28 (d, 1H, J = 7.6 Hz), 7.61 (t, 1H, J = 7.6 Hz), 7.74 (t, 1H, J = 7.6 Hz), 8.16 (d, 1H, J = 8.0), 8.30 (d, 1H, J = 8.0 Hz).

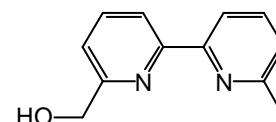
**<sup>13</sup>C NMR** (100 MHz, CDCl<sub>3</sub>): δ = 21.01, 24.67, 67.08, 118.26, 120.17, 121.30, 123.40, 137.06, 137.52, 155.23, 155.26, 156.12, 157.86, 170.68.

**ESI-MS** *m/z*: 243.0 ([M + H]<sup>+</sup>)



**6-(Hydroxymethyl)-6'-methyl-2,2'-bipyridine (23):**Formula: C<sub>12</sub>H<sub>12</sub>N<sub>2</sub>O

Molecular weight: 200.24



Absolute ethanol (10 mL) was added to a mixture of 6-(acetoxymethyl)-6'-methyl-2,2'-bipyridine (860 mg, 3.58 mmol) and anhydrous K<sub>2</sub>CO<sub>3</sub> (980 mg, 7.1 mmol). The reaction mixture was stirred at room temperature for 24 hours and was then filtered through celite. The filtrate was evaporated and the product dried on the pump, yielding the desired product as a beige solid (705 mg, 98%)<sup>[4]</sup>.

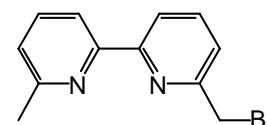
<sup>1</sup>H NMR (400 MHz, CDCl<sub>3</sub>): δ = 2.62 (s, 3H), 4.81 (s, 2H), 7.17 (d, 1H, J = 7.6 Hz), 7.22 (d, 1H, J = 7.6 Hz), 7.69 (t, 1H, J = 8.0 Hz), 7.79 (t, 1H, J = 8.0), 8.18 (d, 1H, J = 7.6 Hz), 8.32 (d, 1H, J = 7.6 Hz)

<sup>13</sup>C NMR (100 MHz, CDCl<sub>3</sub>): 24.84, 64.01, 118.23, 119.94, 120.39, 123.64, 137.24, 137.76, 155.22, 155.34, 158.21, 158.26.

ESI-MS *m/z*: 201.0 ([M + H]<sup>+</sup>)

**6-(Bromomethyl)-6'-methyl-2, 2'-bipyridine (24):**Formula: C<sub>12</sub>H<sub>11</sub>BrN<sub>2</sub>

Molecular weight: 263.13



6-(Hydroxymethyl)-6'-methyl-2,2'-bipyridine (150 mg, 0.75 mmol) was brought to reflux in hydrobromic acid (2 mL) for 2 hours. The reaction mixture was then neutralized with 6M NaOH to give a precipitate. After cooling the mixture in an ice-bath, the precipitate was filtered and washed (15 mL x 5) with water to yield the desired product as a beige solid (128 mg, 65%)<sup>[6]</sup>.

**<sup>1</sup>H NMR** (400 MHz, CDCl<sub>3</sub>): δ = 2.65 (s, 3H), 4.63 (s, 2H), 7.18 (d, 1H, J = 7.6 Hz), 7.45 (d, 1H, J = 7.5 Hz), 7.72 (t, 1H, J = 7.6 Hz), 7.80 (t, 1H, J = 7.6 Hz), 8.24 (d, 1H, J = 7.6 Hz), 8.35 (d, 1H, J = 8.1 Hz).

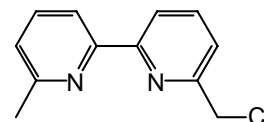
**<sup>13</sup>C NMR** (100 MHz, CDCl<sub>3</sub>): 24.79, 34.49, 118.84, 120.74, 123.59, 123.86, 137.64, 138.13, 155.23, 156.17, 156.48, 158.11.

**ESI-MS** *m/z*: 265.3 ([M + H]<sup>+</sup>).

**6-(Chloromethyl)-6'-methyl-2, 2'-bipyridine (25):**

Formula: C<sub>12</sub>H<sub>11</sub>ClN<sub>2</sub>

Molecular weight: 218.16



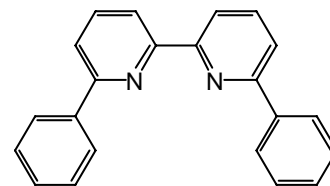
To a stirred solution of 6-(hydroxymethyl)-6'-methyl-2,2'-bipyridine (250 mg, 1.25 mmol) in CHCl<sub>3</sub> (25 mL) was added PCl<sub>3</sub> (2 mL). The mixture was refluxed for 2h and then concentrated in vacuo to afford an oil, which was neutralized with aqueous Na<sub>2</sub>CO<sub>3</sub> (30%) and extracted with CH<sub>2</sub>Cl<sub>2</sub> (3 x 20 mL), dried with anhydrous MgSO<sub>4</sub> and concentrated in vacuo to give the desired compound (149 mg, 54%).

**<sup>1</sup>H NMR** (400 MHz, CDCl<sub>3</sub>): δ = 2.67 (s, 3H), 4.74 (s, 2H), 7.19 (d, 1H, J = 7.6 Hz), 7.49 (d, 1H, J = 7.6 Hz), 7.73 (t, 1H, J = 7.6 Hz, J = 8.1 Hz), 7.84 (t, 1H, J = 7.6 Hz, J = 8.1 Hz), 8.23 (d, 1H, J = 8.1 Hz), 8.41 (d, 1H, J = 8.1 Hz).

**<sup>13</sup>C NMR** (100 MHz, CDCl<sub>3</sub>): 24.72, 47.35, 119.12, 121.09, 123.13, 124.16, 138.09, 138.35, 155.19, 155.73, 156.51, 158.18.

**6, 6'-Diphenyl-2, 2'-bipyridine**Formula: C<sub>22</sub>H<sub>16</sub>N<sub>2</sub>

Molecular weight: 308.13



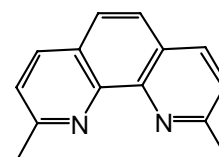
To a cool (-78 °C) solution of 2,2'-bipyridine (6.0 g, 0.038 mol) in dry THF (200 mL) was added phenyllithium (2 M, 38 mL, 0.076 mol). The reaction was kept at -78 °C for 1 hour after which it was allowed to reach room temperature for an additional hour. The reaction mixture was then brought to reflux for 3 hours after which the PhLi was quenched with ice which resulted in the formation of a yellow precipitate. The mixture was condensed and the product was extracted using dichloromethane/water. The organic layer was dried with magnesium sulfate and manganese dioxide was then added (100 g) and the mixture was stirred for 1.5 hours. The mixture was then filtered through celite and the product was condensed. The final product was found to be a white powder (8.5 g, 72%).

<sup>1</sup>H NMR (400 MHz, CDCl<sub>3</sub>): δ =7.46 (t, 4H, J = 7.6), 7.53 (t, 4H, J = 8.1), 7.79 (d, 2H, J = 8.1), 7.92 (t, 2H, J = 7.6), 8.19 (d, 2H, J = 8.6), 8.62 (d, 2H, J = 8.1).

<sup>13</sup>C NMR (100 MHz, CDCl<sub>3</sub>): 119.83, 120.58, 127.24, 129.02, 129.27, 137.86, 139.71, 156.22, 156.60.

**2,9-Dimethyl-1,10-phenanthroline (1):**Formula: C<sub>14</sub>H<sub>12</sub>N<sub>2</sub>

Molecular weight: 208.10



To a cool (-78 °C) solution of 1,10-phenanthroline (6.0 g, 0.038 mol) in dry THF (200 mL) was added methyllithium (1.6 M, 100 mL, 0.16 mol). The reaction was kept at -78 °C for 1 hour after which it was allowed to reach room temperature for an additional hour. The reaction mixture was then brought to reflux for 3 hours after which the MeLi was quenched with ice which resulted in the formation of a yellow precipitate. The mixture was condensed

and the product was extracted using dichloromethane/water. The organic layer was dried with magnesium sulfate and manganese dioxide was then added (100 g) and the mixture was stirred for 1.5 hours. The mixture was then filtered through celite and the product was condensed. The final product was found to be a beige solid (7.05 g, 88%)<sup>[3]</sup>.

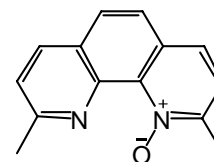
**<sup>1</sup>H NMR** (400 MHz, CDCl<sub>3</sub>):  $\delta$  = 2.62 (s, 6H, 2,9-phenCH<sub>3</sub>), 7.14 (d, 2H, J = 7.8 Hz), 7.67 (t, 2H, J = 7.8 Hz), 8.17 (d, 2H, J = 7.8 Hz)

**ESI-MS** *m/z*: 185.0 ([M + H]<sup>+</sup>)

### 2,9-Dimethyl-1,10-phenanthroline *N*-oxide (9):

Formula: C<sub>14</sub>H<sub>12</sub>N<sub>2</sub>O

Molecular weight: 204.09



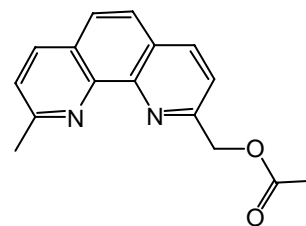
2,9-Dimethyl-1,10-phenanthroline (1.5 g, 8.14 mmol) was dissolved in acetic acid (28 mL) and heated to 75 °C. Then 30% hydrogen peroxide (4.36 mL, 0.04 mol) was added. After 3.5 h reflux, the mixture was cooled and added to a sodium carbonate solution (30 g in 270 mL of water). The resulting mixture was stirred for 30 min and then extracted with chloroform, dried, and evaporated, (yielding 4.75 g, 92%)<sup>[7]</sup>.

**<sup>1</sup>H NMR** (400 MHz, CDCl<sub>3</sub>):  $\delta$  = 2.51 (s, 3H, 2-phenCH<sub>3</sub>), 2.68 (s, 3H, 9-phenCH<sub>3</sub>), 7.21 (d, 1H, J = 8.6, 3-phenH), 7.22 (d, 1H, J = 8.1, 8-phenH), 7.31 (d, 1H, J = 8.6, 4-phenH), 7.33 (d, 1H, J = 8.1, 5-phenH), 7.38 (d, 1H, J = 8.6, 6-phenH), 7.80 (d, 1H, J = 8.1, 7-phenH).

**<sup>13</sup>C NMR** (100 MHz, CDCl<sub>3</sub>):  $\delta$  = 18.86, 25.38, 122.80, 123.17, 123.37, 124.89, 126.30, 127.24, 131.06, 135.37, 137.04, 141.39, 149.46, 157.87.

**2-(Acetoxymethyl)-9-methyl-1,10-phenanthroline (10):**Formula: C<sub>16</sub>H<sub>14</sub>N<sub>2</sub>O<sub>2</sub>

Molecular weight: 266.11



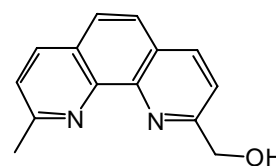
6,6'-Dimethyl-2,2'-bipyridine-*N*-oxide (700 mg, 3.50 mmol) was dissolved in freshly distilled acetic anhydride (10 mL) and brought to reflux for 15 minutes. The dark brown reaction solution was then evaporated and the product dried on the high vacuum pump. It was purified by column chromatography (Al<sub>2</sub>O<sub>3</sub>, dichloromethane:petroleum spirits 40-60 °C, 1:1, R<sub>f</sub> = 0.34) to give a beige solid (595 mg, 71%).<sup>[7]</sup>

<sup>1</sup>H NMR (400 MHz, CDCl<sub>3</sub>): δ = 2.19 (s, 3H, CO<sub>2</sub>CH<sub>3</sub>), 2.92 (s, 3H, 9-phenCH<sub>3</sub>), 5.63 (s, 2H, 2-phenCH<sub>2</sub>), 7.48 (d, 1H, J = 8.3, 3-phenH), 7.66 (d, 1H, J = 8.3, 8-phenH), 7.72 (s, 2H, 5,6-phenH), 8.10 (d, 1H, J = 8.3, 4-phenH), 8.23 (d, 1H, J = 8.3, 7-phenH).

<sup>13</sup>C NMR (100 MHz, CDCl<sub>3</sub>): δ = 20.92, 25.76, 67.73, 120.83, 123.74, 125.23, 126.48, 126.86, 127.98, 136.29, 136.92, 145.02, 145.15, 156.32, 159.56, 170.62.

**2-(Hydroxymethyl)-9-methyl-1,10-phenanthroline (11):**Formula: C<sub>14</sub>H<sub>12</sub>N<sub>2</sub>O

Molecular weight: 204.09



Absolute ethanol (10 mL) was added to a mixture of 2-(acetoxymethyl)-9-methyl-1,10-phenanthroline (860 mg, 3.58 mmol) and anhydrous K<sub>2</sub>CO<sub>3</sub> (980 mg, 7.1 mmol). The reaction mixture was stirred at room temperature for 24 hours and was then filtered through celite. The filtrate was evaporated and the product dried on the pump, yielding the desired product as a beige solid (705 mg, 98%)<sup>[7]</sup>.

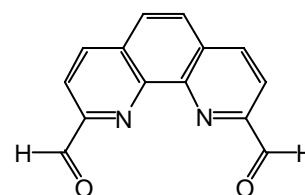
**$^1\text{H}$  NMR** (400 MHz,  $\text{CDCl}_3$ ):  $\delta$  = 2.89 (s, 3H, 9-phen $\text{CH}_3$ ), 5.13 (s, 2H, 2-phen $\text{CH}_2$ ), 7.46 (d, 1H,  $J$  = 8.1, 8-phenH), 7.64 (d, 1H,  $J$  = 8.1, 3-phenH), 7.70 (s, 2H, 5,6-phenH), 8.11 (d, 1H,  $J$  = 8.1, 7-phenH), 8.17 (d, 1H,  $J$  = 8.1, 4-phenH).

**$^{13}\text{C}$  NMR** (100 MHz,  $\text{CDCl}_3$ ): 25.82, 65.95, 120.81, 124.16, 125.89, 126.32, 127.30, 128.22, 136.91, 137.13, 144.85, 145.34, 159.70, 160.08.

**1,10-Phenanthroline-2, 9-dicarboxaldehyde (2):**

Formula:  $\text{C}_{14}\text{H}_8\text{N}_2\text{O}_2$

Molecular weight: 236.06



A mixture of 2,9-Dimethyl-1,10-phenanthroline (3.0 g, 13.8 mmol) and selenium dioxide (8.75g, 78.9 mmol) in dioxan containing 4% water (200 mL) was heated under reflux for 2 hours and then filtered through celite while hot. The dialdehyde (2.4 g, 73.5%) separated from the cold filtrate as yellow powder <sup>[8]</sup>.

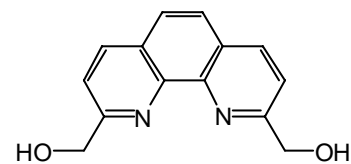
**$^1\text{H}$  NMR** (400 MHz,  $\text{DMSO-d}_6$ ):  $\delta$  = 8.26 (s, 2H, 5,6-phenH), 8.30 (d, 2H,  $J$ = 8.5, 3,8-phenH), 8.77 (d, 2H,  $J$ =8.7, 4,7-phenH), 10.30 (s, 2H, CHO).

**$^{13}\text{C}$  NMR** (100 MHz,  $\text{DMSO-d}_6$ ): 120.14, 129.28, 131.47, 138.45, 145.25, 152.20, 193.74.

**ESI-MS**  $m/z$ : 236.0 ( $[\text{M} + \text{H}]^+$ )

**2,9-Bis(hydroxymethyl)-1,10-phenanthroline (4):**Formula: C<sub>14</sub>H<sub>12</sub>N<sub>2</sub>O<sub>2</sub>

Molecular weight: 240.09



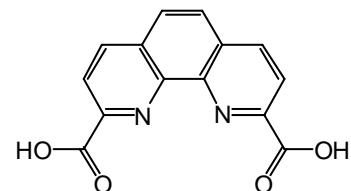
A solution of 1,10-Phenanthroline-2,9-dicarboxaldehyde (0.5 g) and sodium borohydride (0.1 g) in ethanol (50 mL) was heated under reflux for 2 hours. The mixture was then concentrated, and the residue recrystallized from water to give the dialcohol (0.35 g, 68%) as yellow needles <sup>[8]</sup>.

<sup>1</sup>H NMR (400 MHz, DMSO-d<sub>6</sub>): 4.86 (s, 4H, 2,9-phenCH<sub>2</sub>), 7.85 (d, 2H, J=8.1, 3,8-phenH), 7.91 (s, 2H, 5,6-phenH), 8.46 (d, 2H, J=8.6, 4,7-phenH).

<sup>13</sup>C NMR (100 MHz, DMSO-d<sub>6</sub>): 66.76, 121.10, 126.77, 128.34, 137.61, 145.19, 163.04.

**1,10-Phenanthroline-2,9-dicarboxylic acid (3):**Formula: C<sub>14</sub>H<sub>8</sub>N<sub>2</sub>O<sub>4</sub>

Molecular weight: 268.05



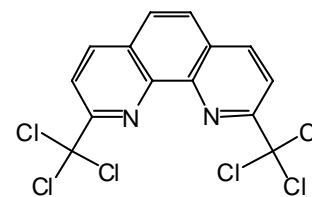
1.0 g (4.24 mmol) of 1,10-phenanthroline-2,9-dicarbaldehyde in 115 mL of 60% nitric acid (HNO<sub>3</sub>) was heated to reflux for 4 h. The mixture was cooled and poured onto ice. The precipitated solid was filtered and was washed with water to give 1.08 g (96%) of the desired compound <sup>[8]</sup>.

<sup>1</sup>H NMR (400 MHz, DMSO-d<sub>6</sub>): 8.20 (s, 2H, 5,6-phenH), 8.43 (d, 2H, J=8.3, 3,8-phenH), 8.76 (d, 2H, J= 8.3, 4,7-phenH).

<sup>13</sup>C NMR (100 MHz, DMSO): 123.86, 128.75, 130.78, 138.28, 145.25, 147.86, 166.68.

**2, 9-Bis(Trichloromethyl)-1,10-phenanthroline:**Formula: C<sub>14</sub>H<sub>6</sub>Cl<sub>6</sub>N<sub>2</sub>

Molecular weight: 411.87



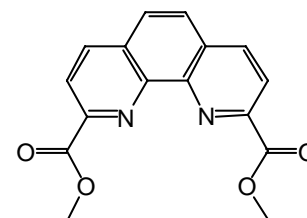
A mixture of 2,9-bis (methyl)-1,10-phenanthroline (3.0 g, 13.8 mmol), *N*-chlorosuccinimide (12 g, 90 mmol), 3-chloroperbenzoic acid (15 mg) in CCl<sub>4</sub> (100 mL) was stirred and heated to reflux for 12h. The mixture was then cooled and concentrated to give a solid which was dissolved in CHCl<sub>3</sub> and washed with saturated Na<sub>2</sub>CO<sub>3</sub> solution, dried over anhydrous MgSO<sub>4</sub>, filtered concentrated and dried in vacuum to give the desired compound as a yellow solid (5.6 g, 98%).

<sup>1</sup>H NMR (400 MHz, DMSO-d<sub>6</sub>): δ = 8.25 (s, 2H, 5,6-phenH), 8.49 (d, J=8.48, 2H, 3,8-phenH), 8.84 (d, J=8.67, 2H, 4,7-phenH).

<sup>13</sup>C NMR (100 MHz, DMSO-d<sub>6</sub>): 98.09, 119.93, 128.07, 129.44, 139.44, 142.63, 156.69.

**1,10-Phenanthroline-2,9-dicarboxylic acid dimethyl ester :**Formula: C<sub>16</sub>H<sub>12</sub>N<sub>2</sub>O<sub>4</sub>

Molecular weight: 296.08



A mixture of 2, 9-Bis(Trichloromethyl)-1,10-phenanthroline (3.0 g, 7.22 mmol) and concentrated H<sub>2</sub>SO<sub>4</sub> (1.5 mL) was heated to 90°C for 2h. After cooling the mixture, CH<sub>3</sub>OH (3.5 mL) was added with rapid stirring and the solution refluxed for 1h. The solution was cooled and neutralized cautiously with a saturated aq. Na<sub>2</sub>CO<sub>3</sub> solution and filtered to give the desired compound. This crude product was purified by recrystallisation from methanol to give the 1,10-phenanthroline-2,9-dicarboxylic acid dimethyl ester as yellow plates (3.5 g, 84%).

<sup>1</sup>H NMR (400 MHz, DMSO-d<sub>6</sub>): δ = 4.04 (s, 6H, COOCH<sub>3</sub>), 8.23 (s, 2H, 5,6-phenH), 8.44 (d, J=8.29, 2H, 3,8-phenH), 8.77 (d, J=8.29, 2H, 4,7-phenH).

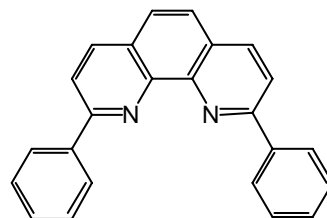


$^{13}\text{C}$  NMR (100 MHz, DMSO- $d_6$ ): 52.74, 123.68, 128.52, 130.57, 138.12, 144.95, 147.56, 165.43.

### 2,9-Diphenyl-1,10-phenanthroline:

Formula:  $\text{C}_{24}\text{H}_{16}\text{N}_2$

Molecular weight: 332.13



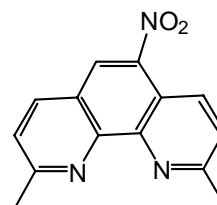
To a cool ( $-78\text{ }^\circ\text{C}$ ) solution of 1,10-phenanthroline (6.0 g, 0.038 mol) in dry THF (200 mL) was added phenyllithium (2 M, 35 mL, 0.076 mol). The reaction was kept at  $-78\text{ }^\circ\text{C}$  for 1 hour after which it was allowed to reach room temperature for an additional hour. The reaction mixture was then brought to reflux for 3 hours after which the PhLi was quenched with ice which resulted in the formation of a yellow precipitate. The mixture was condensed and the product was extracted using dichloromethane/water. The organic layer was dried with magnesium sulfate and manganese dioxide was then added (100 g) and the mixture was stirred for 1.5 hours. The mixture was then filtered through celite and the product was condensed. The final product was found to be a white powder (7.05 g, 56%).

$^1\text{H}$  NMR (250 MHz,  $(\text{CD}_3)_2\text{SO}$ ):  $\delta$  = 7.1 (br s, 4H), 7.42 (d, 4H,  $J$  = 8.4 Hz), 7.60 (d, 2H,  $J$  = 8.4 Hz), 8.00 (d, 2H,  $J$  = 8.03 Hz), 8.57 (d, 2H,  $J$  = 8.7 Hz).

### 5-Nitro-2,9-dimethyl-1,10-phenanthroline

Formula:  $\text{C}_{14}\text{H}_{11}\text{N}_3\text{O}_2$

Molecular weight: 253.26



A mixture of 2,9-dimethyl-1,10-phenanthroline (5.0 g, 23 mmol), 75 mL sulphuric acid and 40 mL of nitric acid was heated at 120 degrees for two hours. The yellow solution was poured

onto 150 g of crushed ice. After filtering, the white solid was washed with ether (3x20 ml) and dried under vacuum (2.30 g, 40%).

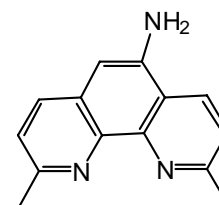
**<sup>1</sup>H NMR** (400 MHz, (DMSO-d<sub>6</sub>): δ = 3.00 (s, 3H), 3.08 (s, 3H), 8.14 (d, 1H, J=9.1), 8.21 (d, 1H, J = 8.6), 9.10 (t, 2H, J = 9.1), 9.19 (s, 1H).

**<sup>13</sup>C NMR** (100 MHz, DMSO-d<sub>6</sub>): 23.79, 24.24, 120.65, 125.76, 125.87, 128.47, 128.58, 136.81, 139.12, 139.86, 144.37, 144.50, 161.54, 163.21.

### 5-Amino-2,9-dimethyl-1,10-phenanthroline

Formula: C<sub>14</sub>H<sub>13</sub>N<sub>3</sub>

Molecular weight: 223.28

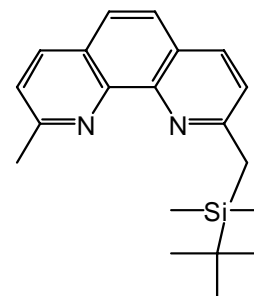


To a solution of 5-nitro-2,9-dimethyl-1,10-phenanthroline (5.0 g; 7.897 mmol) in absolute ethanol (100 ml) was added Pd/C (5%; 1 g; 9.4 mmol). Hydrazine hydrate (1.23 g; 39.5 mmol; 1.23 ml) was then added dropwise. The solution was refluxed for four hours. The solution was filtered to remove the palladium. The filtrate was then evaporated at reduced pressure. The resulting yellow solid was washed with ether (3x20 ml) and dried under vacuum (1.60 g; 91%).

**<sup>1</sup>H NMR** (250 MHz, (CD<sub>3</sub>)<sub>2</sub>SO): δ = 2.68 (s, 3H, 9-phenCH<sub>3</sub>), 2.74 (s, 3H, 2-phenCH<sub>3</sub>), 6.80 (s, 1H, , 6-phenH), 7.1 (br s, 2H, NH<sub>2</sub>) 7.42 (d, 1H, J = 8.4 Hz), 7.60 (d, 1H, J = 8.4 Hz), 8.00 (d, 1H, J = 8.03 Hz), 8.57 (d, 1H, J = 8.7 Hz).

**2-Methyl-9-(tert-butyldimethylsilyl)methyl)-1,10-phenanthroline:**Formula: C<sub>20</sub>H<sub>26</sub>N<sub>2</sub>Si

Molecular weight: 322.19

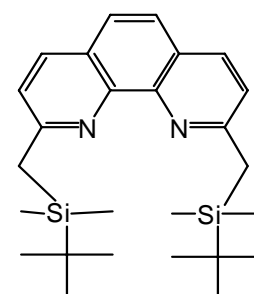


A solution of neocuproine (4.14 g, 20.0 mmol) in dry tetrahydrofuran was cooled to 0°C under argon. A 2M solution in THF of lithium diisopropylamide (12.5 mL, 25 mmol) was then added dropwise. The cooling bath was removed and the solution was stirred for 1h. A solution of tert-butylchlorodimethylsilane (3.01 g, 20 mmol) in dry tetrahydrofuran was slowly added at room temperature and the mixture was stirred for another 30 min. The reaction was quenched by addition of water (30 mL) while cooling. More water (30 mL) was added, the organic layer separated and the aqueous layer was extracted with dichloromethane (2x30 mL). Solvent was removed and the residue was filtered through basic alumina (eluent: dichloromethane). After removal of the solvent in vacuo, the white powder was dry in vacuo to give the desired compound (3.93 g, 61%).

<sup>1</sup>H NMR (250 MHz, CDCl<sub>3</sub>): δ = 0.03 (s, 6H), 0.96 (s, 9H), 2.81 (s, 2H), 2.90 (s, 3H), 7.31 (d, 2H, J=8.37), 7.44 (d, 2H, J = 8.37 Hz), 7.64 (s, 2H), 8.03 (d, 2H, J = 8.37 Hz).

**2,9-(tert-butyldimethylsilyl)methyl)-1,10-phenanthroline:**Formula: C<sub>26</sub>H<sub>40</sub>N<sub>2</sub>Si<sub>2</sub>

Molecular weight: 436.26



A solution of neocuproine (4.14 g, 20.0 mmol) in dry tetrahydrofuran was cooled to 0°C under argon. A 2M solution in THF of lithium diisopropylamide (60 mL, 120 mmol) was then

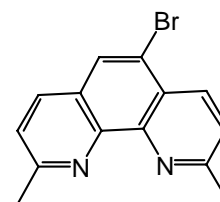
added dropwise. The cooling bath was removed and the solution was stirred for 1h. a solution of tet-butylchlorodimethylsilane (6.18 g, 41.0 mmol) in dry tetrahydrofuran was slowly added at room temperature and the mixture was stirred for another 30 min. The reaction was quenched by addition of water (30 mL) while cooling. More water (30 mL) was added, the organic layer separated and the aqueous layer was extracted with dichloromethane (2x30 mL). Solvent was removed and the residue was filtered through basic alumina (eluent: dichloromethane). After removal of the solvent in vacuo, the white powder was dry in vacuo to give the desired compound (8.1 g, 92%)<sup>[9]</sup>.

**<sup>1</sup>H NMR** (250 MHz, CDCl<sub>3</sub>):  $\delta$  = -0.02 (s, 12H, -Si(CH<sub>3</sub>)<sub>2</sub>), 0.93 (s, - 18H, -C(CH<sub>3</sub>)<sub>3</sub>), 2.76 (s, 4H, 2,9-phenCH<sub>2</sub>), 7.22 (d, 2H, J=8.4, 3,8-phenH), 7.50 (s, 2H, 5,6-phenH), 7.92 (d, 2H, J = 8.03 Hz, 4,7-phenH).

### 5-Bromo-2,9-dimethyl-1,10-phenanthroline:

Formula: C<sub>14</sub>H<sub>11</sub>Br N<sub>2</sub>

Molecular weight: 287.16

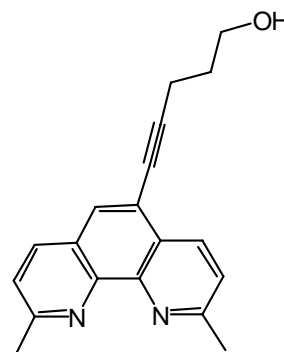


Concentrated hydrochloric acid (10 mL) was added to a solution of 5-bromo-2-methyl-9-(*tert*-butyldimethylsilyl)methyl-1,10-phenanthroline (0.4 g, 1.24 mmol) in acetone (25 mL) and the reaction was stirred overnight at room temperature. 2M NaOH was added until the solution was basic, and the precipitate was filtered off, washed with water and dried in vacuo to give the compound (0.26 g, 73%).

**<sup>1</sup>H NMR** (250 MHz, CDCl<sub>3</sub>):  $\delta$  = 2.93 (s, 3H, 9-phenCH<sub>3</sub>), 2.97 (s, 3H, 2-phenCH<sub>3</sub>), 7.49 (d, 1H, J = 8.4 Hz, 8-phenH), 7.58 (d, 1H, J = 8.4 Hz, 3-phenH), 8.03 (s, 1H, 6-phenH), 8.06 (s, 1H, 7-phenH), 8.54 (d, 1H, J = 8.4 Hz, 4-phenH).

**6-(2,9-Dimethyl-1,10-phenanthroline-5-yl)hex-5-yn-1-ol:**Formula: C<sub>20</sub>H<sub>20</sub>N<sub>2</sub>O

Molecular weight: 304.16

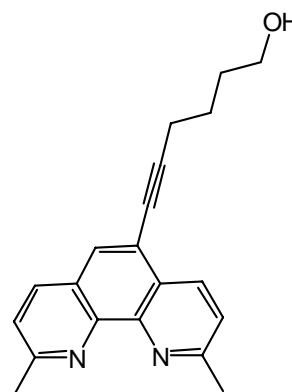


To a stirred solution of 5-bromo-2,9-dimethyl-1,10-phenanthroline (555 mg, 1.93 mmol) and hex-5-ynol (350 mg, 3.57 mmol) in pyrrolidine (7.5 ml), [Pd(PPh<sub>3</sub>)<sub>4</sub>] (115 mg, 0.1 mmol) was added. The reaction mixture was heated to 70°C and stirred overnight. After this period there was no starting material. The reaction mixture was dissolved in 2M HCl (5 ml), and this solution was extracted with CH<sub>2</sub>Cl<sub>2</sub> (50 ml x 4). Then the aqueous phase was basified with K<sub>2</sub>CO<sub>3</sub> to pH 10 and extracted with CH<sub>2</sub>Cl<sub>2</sub> (50 ml x 4). The organic extracts were dried with K<sub>2</sub>CO<sub>3</sub> and the solvent was removed under reduced pressure. An orange solid was obtained (432 mg, 78%).

**<sup>1</sup>H NMR** (250 MHz, CDCl<sub>3</sub>): δ = 1.78 (m, 4H), 2.59 (m, 2H), 2.89 (s, 3H), 2.91 (s, 3H), 3.72 (m, 2H), 7.43 (d, 1H, J = 8.0 Hz), 7.50 (d, 1H, J = 8.4 Hz), 7.81 (s, 1H), 8.00 (d, 1H, J=8.4), 8.55 (d, 1H, J = 8.4 Hz).

**5-(2, 9-dimethyl-1,10-phenanthroline-5-yl) pent-4-yn-1-ol:**Formula: C<sub>19</sub>H<sub>18</sub>N<sub>2</sub>O

Molecular weight: 290.14

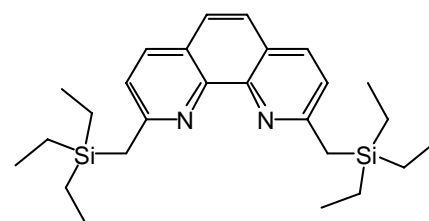


To a stirred solution of 5-bromo-2,9-dimethyl-1,10-phenanthroline (555 mg, 1.93 mmol) and pent-4-ynol (285 mg, 3.39 mmol) in pyrrolidine (7.5 ml), [Pd(PPh<sub>3</sub>)<sub>4</sub>] (115 mg, 0.1 mmol) was added. The reaction mixture was heated to 70°C and stirred over night. After this period there was no starting material. The reaction mixture was dissolved in 2M HCl (5 ml), and this solution was extracted with CH<sub>2</sub>Cl<sub>2</sub> (50 ml x 4). Then the aqueous phase was basified with K<sub>2</sub>CO<sub>3</sub> to pH 10 and extracted with CH<sub>2</sub>Cl<sub>2</sub> (50 ml x 4). The organic extracts were dried with K<sub>2</sub>CO<sub>3</sub>, and the solvent was removed under reduced pressure. An orange solid was obtained (448 mg, 80%).

<sup>1</sup>H NMR (250 MHz, CDCl<sub>3</sub>): δ = 1.89 (q, 2H), 2.63 (t, 2H, J=7.0), 2.87 (s, 3H), 2.88 (s, 3H), 3.83 (t, 2H, J=6.2), 7.37 (d, 1H, J = 8.4 Hz), 7.41 (d, 1H, J = 8.4 Hz), 7.67 (s, 1H), 7.92 (d, 1H, J=8.4), 8.43 (d, 1H, J = 8.4 Hz).

**2,9-Bis[(triethylsilyl)methyl]-1,10-phenanthroline (7):**Formula: C<sub>26</sub>H<sub>40</sub>N<sub>2</sub>Si<sub>2</sub>

Molecular weight: 436.78



A solution of 2,9-dimethyl-1,10-phenanthroline (1.04 g, 5.0 mmol) in dry THF (30 mL) was cooled to 0°C under nitrogen. A 2M solution in THF of lithium diisopropylamide (15 mL, 30.0 mmol) was added quickly, the cooling was removed and the reaction mixture was

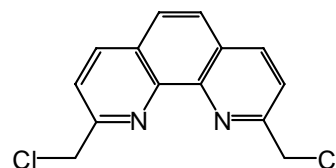
stirred for 1h at room temperature. Chlorotriethylsilane (1.72 mL, 10.2 mmol) was added and the solution was stirred for another 30 min at room temperature. The reaction was quenched by addition of water (20 mL) while cooling. The organic layer was separated and the aqueous layer was extracted with THF (2 x 40mL). The combined organic layer was washed with saturated brine (50 mL), dried with sodium sulfate and the solvent was removed in vacuo. The crude product was purified by flash chromatographie (silica; eluent: hexane/ethyl acetate/triethylamine, 100:10:1), to give the 2,9-bis[(triethylsilyl)methyl]-1,10-phenanthroline (1.87 g, 88%)<sup>[10]</sup>.

**<sup>1</sup>H NMR** (400 MHz, CDCl<sub>3</sub>):  $\delta$  = 0.64 (q, 12H, J = 8.6), 0.96 (t, 18H, J = 8.1), 2.80 (s, 4H), 7.28 (d, 2H, J = 8.1), 7.58 (s, 2H, J = 8.1), 7.98 (d, 2H, J = 8.1).

### 2,9-Di(chloromethyl)-1,10-phenanthroline (6):

Formula: C<sub>14</sub>H<sub>10</sub>Cl<sub>2</sub> N<sub>2</sub>

Molecular weight: 276.02



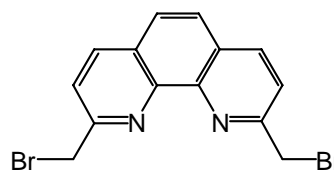
To a solution of 2,9-bis[(triethylsilyl)methyl]-1,10-phenanthroline (4.3 mmol, 1.87 g) and Cl<sub>3</sub>CCl<sub>3</sub> (8.6 mmol, 2.026 g) in 150 ml dry DMF under inert gas atmosphere anhydrous CsF (8.6 mmol, 1.306 g) was added. The reaction mixture was stirred at room temperature for six hours. The reaction mixture was poured into a mixture of EtOAc and H<sub>2</sub>O (200 ml each), the organic layer was separated and the aqueous layer was extracted three times with 100 ml EtOAc. The combined organic fractions were dried over Na<sub>2</sub>SO<sub>4</sub>. Filtration and evaporation of the solvent gave a yellowish product which was purified by washing with cold toluene to yield a white solid (0.65 g, 55 %).

**<sup>1</sup>H NMR** (400 MHz, CDCl<sub>3</sub>):  $\delta$  = 4.96 (s, 4H, 2,9-phenCH<sub>2</sub>), 7.82 (s, 2H, 5,6-phenH), 7.94 (d, 2H, J = 8.6, 3,8-phenH), 8.31 (d, 2H, 8.6, 4,7-phenH).

**<sup>13</sup>C NMR** (100 MHz, CDCl<sub>3</sub>):  $\delta$  = 47.95, 122.99, 127.09, 128.70, 137.92, 145.11, 157.92.

**2,9-Di(bromomethyl)-1,10-phenanthroline (5):**Formula: C<sub>14</sub>H<sub>10</sub>Br<sub>2</sub> N<sub>2</sub>

Molecular weight: 363.92

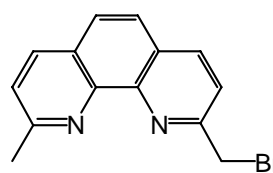


A solution of 2,9-bis(hydroxymethyl)-1,10-phenanthroline (0.5g, 2.08 mmol) was brought to reflux in hydrobromic acid (2 mL) for 2 hours. The reaction mixture was then neutralized with 2 M NaOH to give a precipitate. After cooling the mixture in an ice-bath, the precipitate was filtered and washed (15 mL x 5) with water to yield the desired product as yellow solid (292 mg, 40%)<sup>[6]</sup>.

<sup>1</sup>H NMR (400 MHz, CDCl<sub>3</sub>): δ = 4.97 (s, 4H, 2,9-phenCH<sub>2</sub>), 7.82 (s, 2H, 5,6-phenH), 7.92 (d, 2H, J = 8.1, 3,8-phenH), 8.28 (d, 2H, J = 8.4, 4,7-phenH).

**2-Bromomethyl-9-methyl-1,10-phenanthroline (13):**Formula: C<sub>14</sub>H<sub>11</sub>Br N<sub>2</sub>

Molecular weight: 286.01



A solution of 2-(hydroxymethyl)-9-methyl-1,10-phenanthroline (0.5 g, 2.45 mmol) was brought to reflux in hydrobromic acid (2 mL) for 2 hours. The reaction mixture was then neutralized with 2 M NaOH to give a precipitate. After cooling the mixture in an ice-bath, the precipitate was filtered and washed (15 mL x 5) with water to yield the desired product as yellow solid (385 mg, 55%)<sup>[6]</sup>.



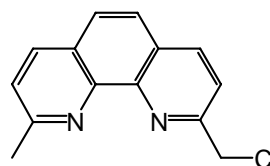
**$^1\text{H}$  NMR** (400 MHz,  $\text{CDCl}_3$ ):  $\delta = 2.80$  (s, 3H), 5.06 (s, 2H), 7.34 (d, 1H,  $J = 8.1$ ), 7.51 (t, 3H,  $J = 8.3$ ), 7.97 (t, 2H,  $J = 8.6$ ).

**$^{13}\text{C}$  NMR** (100 MHz,  $\text{CDCl}_3$ ):  $\delta = 24.94$ , 65.33, 103.63, 120.14, 123.46, 125.18, 125.44, 126.53, 127.38, 136.27, 144.06, 144.56, 158.90, 160.45.

**2-Chloromethyl-9-methyl-1,10-phenanthroline (12):**

Formula:  $\text{C}_{14}\text{H}_{11}\text{Cl N}_2$

Molecular weight: 242.06



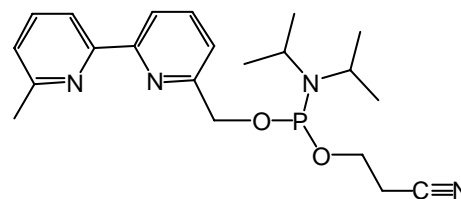
To a stirred solution of 2-hydroxymethyl-9-methyl-1,10-phenanthroline (450 mg, 2.2 mmol) in  $\text{CHCl}_3$  (25 mL) was added  $\text{PCl}_3$  (2 mL). The mixture was refluxed for 2h and then concentrated in vacuo to afford an oil, which was neutralized with aqueous  $\text{Na}_2\text{CO}_3$  (30%) and extracted with  $\text{CH}_2\text{Cl}_2$  (3 x 20 mL), dried with anhydrous  $\text{MgSO}_4$  and concentrated in vacuo to give the desired compound (261 mg, 55%).

**$^1\text{H}$  NMR** (400 MHz,  $\text{CDCl}_3$ ):  $\delta = 2.95$  (s, 3H, 9-phen $\text{CH}_3$ ), 4.97 (s, 2H, 2-phen $\text{CH}_2$ ), 7.55 (d, 1H,  $J = 8.3$ , 8-phenH), 7.74 (q, 2H,  $J = 8.8$ ,  $J = 8.6$ , 5,6-phenH), 7.84 (d, 1H,  $J = 8.1$ , 3-phenH), 8.23 (d, 1H,  $J = 8.1$ , 7-phenH), 8.24 (d, 1H,  $J = 8.3$ , 4-phenH).

**$^{13}\text{C}$  NMR** (100 MHz,  $\text{CDCl}_3$ ):  $\delta = 25.55$ , 47.76, 123.02, 124.72, 126.16, 127.06, 127.55, 128.57, 137.80, 138.10, 144.08, 144.39, 157.59, 159.81.

**6-phosphoramidite-6'-methyl-2, 2'-bipyridine (37):**Formula: C<sub>21</sub>H<sub>29</sub>N<sub>4</sub>O<sub>2</sub>P

Molecular weight: 400.20



Diisopropylammonium cyanoethoxyphosphite (360 mg, 1.2 mmol) was added to a mixture of 6-(Hydroxymethyl)-6'-methyl-2,2'-bipyridine (200 mg, 1 mmol) and diisopropylammonium tetrazolide (171 mg, 1 mmol) in dry CH<sub>2</sub>Cl<sub>2</sub> (10 mL) under a nitrogen atmosphere. The mixture was stirred at r.t. for 1 hour. Evaporation of the solvent gave a light brown oil, which was purified by flash chromatography (hexane/ EtOAc 2:1 + 2% Et<sub>3</sub>N) to afford the desired compound (280 mg, 70%).

**<sup>1</sup>H NMR** (300 MHz, CD<sub>3</sub>CN): δ = 1.26 (m, 12H), 2.61 (s, 3H), 2.73 (m, 2H), 2.77 (m, 2H), 3.95 (m, 2H), 4.91 (m, 2H), 7.30 (d, J=7.72, 1H), 7.56 (d, J=7.72, 1H), 7.82 (t, J=7.73, 1H), 7.95 (t, J=7.73, 1H), 8.33 (d, J=7.53, 1H), 8.36 (d, J=7.92, 1H).

**<sup>13</sup>C NMR** (75 MHz, CD<sub>3</sub>CN): 20.37, 20.45, 21.80, 22.39, 24.58, 24.63, 24.73, 43.19, 43.35, 47.32, 47.38, 58.52, 48.78, 66.32, 118.18, 119.64, 120.61, 123.19, 137.00, 137.42, 155.62.

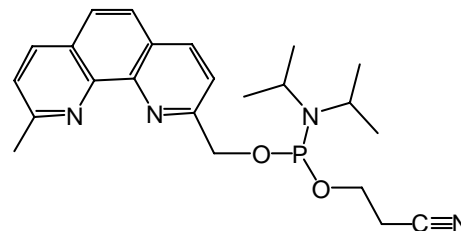
**<sup>31</sup>P NMR** (121.5 MHz, CD<sub>3</sub>CN): 148.71

**ESI-MS** (positive mode): *m/z*=401

**Diisopropyl-phosphoramidous acid 2-cyano-ethyl ester 9-methyl-1,10-phenanthroline-2-ylmethyl ester (38).**

Formula: C<sub>23</sub>H<sub>29</sub>N<sub>4</sub>O<sub>2</sub>P

Molecular weight: 424.20



A mixture of 2-(hydroxymethyl)-9-methyl-1,10-phenanthroline (114 mg, 0.67 mmol) and diisopropylammonium terazolide (114 mg, 0.67 mmol) is co-evaporated in dry CH<sub>2</sub>Cl<sub>2</sub> (2 x 1 mL). Dichloromethane (6 mL) and diisopropylammonium cyanoethoxyphosphine (242 mg, 0.8 mmol) is added under nitrogen atmosphere and the mixture was stirred at r.t. The reaction showed a complete conversion of 2-(Hydroxymethyl)-9-methyl-1,10-phenanthroline into the phosphoramidite within 1 hour. The product was purified by flash column chromatography utilising hexane/EtOAc (1:2) + Et<sub>3</sub>N as eluant to afford pure desired compound (214 mg, 75%).

<sup>1</sup>H NMR (300 MHz, DMSO): δ = 1.08-1.25 (m, 12H), 2.64 (t, J=6.4, 3H), 2.87 (s, 3H), 3.42-3.57 (m, 2H), 3.63-3.71 (m, 3H), 3.82-3.94 (m, 2H), 5.08-5.27 (m, 2H), 7.45 (d, J=8.29, 1H), 7.68 (s, 2H), 7.85 (d, J=8.29, 1H), 8.09 (d, J=8.29, 1H), 8.22 (d, J=8.45, 1H).

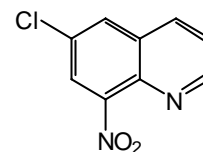
<sup>13</sup>C NMR (75 MHz, CDCl<sub>3</sub>): 20.38, 21.76, 22.39, 24.66, 25.96, 43.24, 47.31, 58.62, 120.45, 125.57, 126.02, 136.33, 136.83.

<sup>31</sup>P NMR (121.5 MHz, CD<sub>3</sub>CN): 149.11

**6-chloro-8-nitroquinoline (11):**

Formula: C<sub>9</sub>H<sub>5</sub>ClN<sub>2</sub>O<sub>2</sub>

Molecular weight: 208.00



A mixture of 4-chloro-2-nitroaniline (5.0 g, 29 mmol), arsenic pentoxide (4.0 g, 17.4 mmol), H<sub>2</sub>SO<sub>4</sub> (6 mL) and H<sub>2</sub>O (2 mL) was heated to 100°C. Glycerol (7 mL) was then added at such a rate that the temperature did not exceed 140°C. After 2 hours of reaction, the mixture was poured into water, neutralized with NaOH and the precipitate extracted with hot toluene. Recrystallisation from toluene affords the desired quinoline (5.0 g, 83%)<sup>[11]</sup>.

<sup>1</sup>H NMR (300 MHz, DMSO): δ = 7.73 (q, J=4.1, 1H), 8.42 (s, 1H), 8.45 (s, 1H), 8.49 (d, J=8.85, 1H), 8.99 (d, J=4.16, 1H).

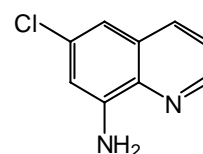
<sup>13</sup>C NMR (75 MHz, DMSO): 123.96, 124.57, 129.64, 130.05, 130.92, 136.32, 137.29, 153.50.

ESI-MS (positive mode): *m/z*=208 ([M + H]<sup>+</sup>).

### 6-chloro-quinolin-8-ylamine:

Formula: C<sub>9</sub>H<sub>7</sub>ClN<sub>2</sub>

Molecular weight: 178.03



A solution of 6-chloro-8-nitro-quinoline (1 g, 4.8 mmol) and Pd/C (0.1 g) in MeOH (25 mL) under an H<sub>2</sub> atmosphere was stirred at r.t for 3 hours. The mixture was then filtered on celite. The residue obtained after evaporation of methanol was recrystallised using petroleum ether to afford the 6-chloro-quinolin-8-ylamine (0.6 g, 68%).

<sup>1</sup>H NMR (300 MHz, CDCl<sub>3</sub>): δ =5.02 (s, 2H, NH<sub>2</sub>), 6.78 (s, 1H), 7.03 (s, 1H), 7.28-7.32 (q, J=4.23, 1H), 7.90 (d, J=8.28, 1H), 8.64 (d, J=4.15, 1H).

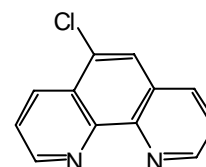
$^{13}\text{C}$  NMR (250 MHz,  $\text{CDCl}_3$ ): 110.17, 114.33, 120.09, 122.30, 129.30, 133.13, 135.14, 144.00, 147.38.

ESI-MS (positive mode):  $m/z=178$  ( $[\text{M} + \text{H}]^+$ ).

**5-chloro-1,10 phenanthroline :**

Formula:  $\text{C}_{12}\text{H}_7\text{ClN}_2$

Molecular weight: 214.03



8-Amino-6-chloroquinoline (470 mg, 2.6 mmol), arsenic pentoxide (363 mg, 1.6 mmol),  $\text{H}_2\text{SO}_4$  (600 mL) and  $\text{H}_2\text{O}$  (200  $\mu\text{L}$ ) was heated to  $100^\circ\text{C}$ . The mixture was then treated with glycerol (672  $\mu\text{L}$ , 9 mmol) at such a rate that the temperature did not exceed  $140^\circ\text{C}$ . Heating was continued at this temperature for 4 hours. The mixture was then poured in water, made alkaline and the precipitate extracted with hot toluene. Recrystallisation from toluene affords the 5-chloro-1,10 phenanthroline (364 mg, 65%).

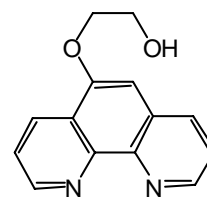
$^1\text{H}$  NMR (300 MHz,  $\text{CDCl}_3$ ):  $\delta$  =7.50-7.54 (q,  $J=4.33$ , 1H), 7.86-7.95 (m, 2H), 8.12 (d,  $J=8.47$ , 1H), 9.00 (d,  $J=4.34$ , 1H).

$^{13}\text{C}$  NMR (75 MHz,  $\text{CDCl}_3$ ): 123.66, 124.71, 129.63, 130.41, 133.29, 135.23, 149.51, 150.92, 152.76.

ESI-MS (positive mode):  $m/z=214$  ( $[\text{M} + \text{H}]^+$ ).

**2-(1,10-phenanthrolin-5-yloxy)ethanol :**Formula: C<sub>14</sub>H<sub>12</sub>N<sub>2</sub>O<sub>2</sub>

Molecular weight: 240.09

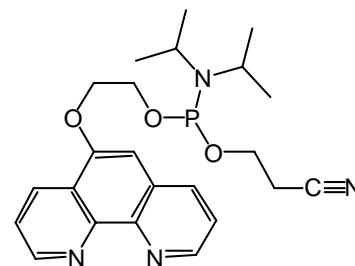


To stirred suspension of powdered KOH (250 mg) in dry DMSO (4 mL) at 80°C, ethane-1,2-diol (58 mg, 0.9 mmol) was added. After 1 hour, 5-chloro-1,10-phenanthroline (200 mg, 0.9 mmol) was added by portions and the reaction was continued for 5 hours at 70°C. The mixture was poured into distilled water and extracted with dichloromethane to afford the desired compound (121 mg, 54%).

<sup>1</sup>H NMR (300 MHz, CDCl<sub>3</sub>): δ = 4.04 (t, J=4.53, 2H), 4.30 (t, J=4.53, 2H), 7.50-7.54 (q, J=4.33, 2H), 7.86-7.95 (m, 1H), 8.62 (d, J=8.67, 1H), 9.01 (d, J=4.15, 1H).

**Diisopropyl-phosphoramidous acid 2-cyano-ethyl ester 2-(1,10-phenanthrolin-5-yloxy)-ethyl ester :**Formula: C<sub>23</sub>H<sub>29</sub>N<sub>4</sub>O<sub>3</sub>P

Molecular weight: 440.20



Diisopropylammonium cyanoethoxyphosphine (165 mg, 0.55 mmol) was added to a mixture of 2-(1,10-phenanthrolin-5-yloxy)ethanol (110 mg, 0.46 mmol) and diisopropylammonium tetrazolide (78.5 mg, 0.46 mmol) in dry CH<sub>2</sub>Cl<sub>2</sub> (5 mL) under nitrogen atmosphere. The mixture was stirred at r.t. and followed by TLC (hexane/ EtOAc 1:2 + 2% Et<sub>3</sub>N) without any work-up, to afford the phosphoramidite (128 mg, 64%).

<sup>1</sup>H NMR (300 MHz, CD<sub>3</sub>CN): δ = 1.20 (m, 12H), 2.66 (t, J=5.65, 2H), 3.59 (m, 2H), 3.53-3.61 (m, 3H), 3.72-3.83 (m, 3H), 4.04-4.13 (m, 2H), 4.49-4.52 (m, 2H), 7.76 (dd, J<sub>1</sub>=4.14, J<sub>2</sub>=4.52, 1H), 8.22 (s, 1H), 8.84 (dd, J<sub>1</sub>=1.51, J<sub>2</sub>=6.97, 1H), 9.04 (m, 1H).

$^{13}\text{C}$  NMR (75 MHz,  $\text{CD}_3\text{CN}$ ): 25.37, 29.10, 29.20, 48.08, 48.24, 49.69, 63.53, 63.79, 68.06, 68.29, 80.38, 80.48, 122.62, 128.76, 130.02, 137.02, 158.16.

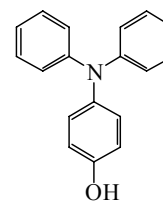
$^{31}\text{P}$  NMR (121.5 MHz,  $\text{CD}_3\text{CN}$ ): 148.43

ESI-MS (positive mode):  $m/z=441$

**4-(*N,N*-Diphenylamino)phenol (26):**

Formula:  $\text{C}_{18}\text{H}_{15}\text{NO}$

Molecular weight: 261.12

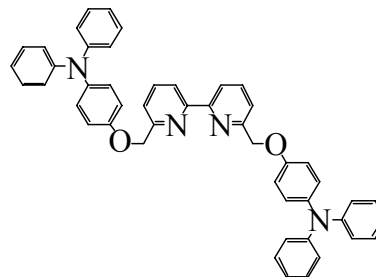


4-Methoxytriphenylamine (3.0 g, 10.89 mmol) was dissolved in 100 mL of  $\text{CH}_2\text{Cl}_2$  at 0 °C under nitrogen, to which was added 22 mL of a solution of boron tribromide (1.0 M) in  $\text{CH}_2\text{Cl}_2$ . The mixture was stirred at 0 °C for 24 h, after which the mixture was washed thoroughly with distilled water. The product, obtained by evaporating  $\text{CH}_2\text{Cl}_2$ , was pure enough to use in the next steps. The yield was 2.11 g (73 %).

$^1\text{H}$  NMR ( $\text{CDCl}_3$ ):  $\delta$  7.21 (m, 4H), 7.07 (m, 6H), 6.92 (t,  $J=7.11$  Hz, 2H), 6.83 (d,  $J=8.90$  Hz, 2H), 5.67 (s, 1H).

**6,6'-Bis(4-(*N,N*-diphenylamino)phenoxy)methyl)-2,2'-bipyridine (27) :**Formula: C<sub>48</sub>H<sub>38</sub>N<sub>4</sub>O<sub>2</sub>

Molecular weight: 702.30



This reaction was carried out in sealed microwave process vials at 180 °C for 30 minutes in acetonitrile. The reaction involved 1 equivalent of the 6,6'-bis(chloromethyl)-2,2'-bipyridine (100 mg, 0.39 mmol) and 2.1 equivalents of the 4-(*N,N*-diphenylamino)phenol (215 mg, 0.82 mmol) in the presence of 10 equivalents of K<sub>2</sub>CO<sub>3</sub>. After the reaction the vessel was allowed to cool and the residue taken up with CH<sub>2</sub>Cl<sub>2</sub> washed with water dried and filtered. The impure solids were then recrystallised from CH<sub>2</sub>Cl<sub>2</sub>/Et<sub>2</sub>O mixtures to yield pure off white solid. The yield was 116 mg (42%).

<sup>1</sup>H NMR (CDCl<sub>3</sub>, 400 MHz) δ = 8.34 (d, 2H, J = 7.9 Hz), 7.86 (t, 2H, J = 7.6 Hz), 7.6 (d, 2H, J = 7.56 Hz), 7.21 (t, 8H, J = 7.4 Hz), 7.09-7.03 (m, 12H), 6.98-6.94 (m, 8 H), 5.28 (s, 4H).

<sup>13</sup>C NMR (125 MHz, CDCl<sub>3</sub>) δ = 157.0, 155.6, 155.1, 148.2, 141.4, 137.8, 129.2, 127.2, 123.2, 122.1, 121.4, 120.2, 155.9, 71.3.

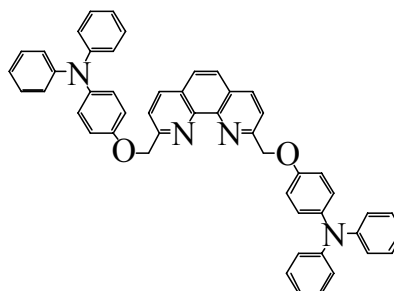
ES-MS: *m/z* 703 [M + H<sup>+</sup>]

**Anal. Calcd:** For C<sub>48</sub>H<sub>38</sub>N<sub>4</sub>O<sub>2</sub>·3HBr: C, 53.02; H, 3.10; N, 5.38; found: C, 52.84; H, 3.29; N, 5.66%.



**2,9-bis(4-(*N,N*-diphenylamino)phenoxy)methyl)-1,10-phenanthroline (28) :**Formula: C<sub>50</sub>H<sub>38</sub>N<sub>4</sub>O<sub>2</sub>

Molecular weight: 726.30



This reaction was carried out in sealed microwave process vials at 180 °C for 30 minutes in acetonitrile. The reaction involved 1 equivalent of the 2,9-bis(chloromethyl)-1,10-phenanthroline (100 mg, 0.36 mmol) and 2.1 equivalents of the 4-(*N,N*-diphenylamino)phenol (197 mg, 0.76 mmol) in the presence of 10 equivalents of K<sub>2</sub>CO<sub>3</sub>. After the reaction the vessel was allowed to cool and the residue taken up with CH<sub>2</sub>Cl<sub>2</sub> washed with water dried and filtered. The impure solids were then recrystallised from CH<sub>2</sub>Cl<sub>2</sub>-Et<sub>2</sub>O mixtures to yield pure off white solid. The yield was 178 mg (68%).

<sup>1</sup>H NMR (CDCl<sub>3</sub>, 400 MHz) δ = 8.33 (d, 2H, J = 8.3 Hz), 7.99 (d, 2H, J = 8.3Hz), 7.83 (s, 2H), 7.21 (m, 7H), 7.02 (m, 21H), 7.23 (m, 5H), 5.59 (s, 4H).

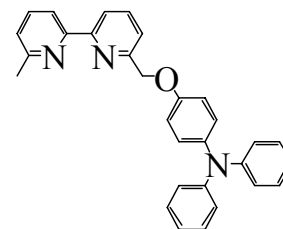
<sup>13</sup>C-NMR (CDCl<sub>3</sub>, 100 MHz): δ = 158.8, 155.3, 148.5, 145.5, 141.7, 137.5, 129.5, 127.5, 126.7, 123.4, 123.1, 122.3, 121.3, 116.1, 71.9.

MS (ESI+): *m/z* 727.1

Anal. Calcd for C<sub>50</sub>H<sub>38</sub>N<sub>4</sub>O<sub>2</sub>: C, 82.62; H, 5.27; N, 7.71; found: C, 82.02; H, 5.66; N, 6.02%.

**6-(4-(*N,N*-Diphenylamino)phoxymethyl)-6'-methyl-2,2'-bipyridine (29) :**Formula: C<sub>30</sub>H<sub>25</sub>N<sub>3</sub>O

Molecular weight: 443.20



This experiment was carried out in sealed microwave process vials at 180 °C for 30 minutes in acetonitrile. The reaction involved 1 equivalent of the 6-(chloromethyl)-6'-methyl-2,2'-bipyridine (100 mg, 0.48 mmol) and 1.1 equivalents of the 4-(*N,N*-Diphenylamino)phenol (139 mg, 0.53 mmol) in the presence of 10 equivalents of K<sub>2</sub>CO<sub>3</sub>. After the reaction the vessel was allowed to cool and the residue taken up with CH<sub>2</sub>Cl<sub>2</sub> washed with water dried and filtered. The impure solids were then recrystallised from CH<sub>2</sub>Cl<sub>2</sub>/Et<sub>2</sub>O mixtures to yield pure off white solids. The yield was 96 mg (45%).

<sup>1</sup>H NMR (CDCl<sub>3</sub>, 400 MHz) δ = 8.44 (d, 1H, J = 7.7 Hz), 8.26 (d, 1H, J = 7.6 Hz), 7.90 (t, 1H, J = 7.9 Hz), 7.78 (t, 1H, J = 7.9 Hz), 7.60 (d, 1H, J = 7.7 Hz), 7.23 (m, 5H), 7.09 (m, 6 H), 7.00 (m, 4H) 5.30 (s, 2H), 2.73 (s, 3H).

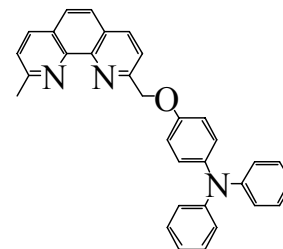
<sup>13</sup>C-NMR (CDCl<sub>3</sub>, 100 MHz): δ = 157.8, 156.9, 155.0, 154.9, 148.1, 141.2, 137.7, 129.3, 129.1, 127.1, 123.7, 123.0, 122.7, 121.9, 121.3, 120.4, 118.7, 115.7, 71.1, 24.2.

MS (ESI+): *m/z* 444.5 [M + H<sup>+</sup>].

**Anal. Calcd** for C<sub>30</sub>H<sub>25</sub>N<sub>3</sub>O: C, 81.24; H, 5.68; N, 9.47; found: C, 80.04; H, 5.68; N, 9.32%.

**2-(4-(*N,N*-Diphenylamino)phenoxy)methyl)-9-methyl-1,10-phenanthroline (30) :**Formula: C<sub>32</sub>H<sub>25</sub>N<sub>3</sub>O

Molecular weight: 467.20



This experiment was carried out in sealed microwave process vials at 180 °C for 30 minutes in acetonitrile. The reaction involved 1 equivalent of 2-Chloromethyl-9-methyl-1,10-phenanthroline (100 mg, 0.41 mmol) and 1.1 equivalents of the 4-(*N,N*-Diphenylamino)phenol (120 mg, 0.46 mmol) in the presence of 10 equivalents of K<sub>2</sub>CO<sub>3</sub>. After the reaction the vessel was allowed to cool and the residue taken up with CH<sub>2</sub>Cl<sub>2</sub> washed with water dried and filtered. The impure solids were then recrystallised from CH<sub>2</sub>Cl<sub>2</sub>/Et<sub>2</sub>O mixtures to yield pure off white solids. The yield was 159 mg (83%).

<sup>1</sup>H NMR (CDCl<sub>3</sub>, 400 MHz) δ = 8.29 (d, 1H, J = 8.6 Hz), 8.17 (d, 1H, J = 8.1 Hz), 7.94 (d, 1H, J = 8.6 Hz), 7.76 (s, 1H), 7.53 (d, 1H, J = 8.1 Hz), 7.20 (m, 4H), 7.05 (m, 4H), 6.95 (m, 6H) 5.45 (s, 2H), 2.94 (s, 3H).

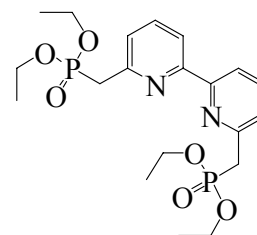
<sup>13</sup>C-NMR (CDCl<sub>3</sub>, 100 MHz): δ = 160.0, 158.7, 155.3, 148.5, 145.6, 145.3, 141.6, 137.4, 137.0, 129.5, 129.4, 128.4, 127.5, 127.4, 126.6, 126.0, 124.4, 123.5, 122.3, 121.0, 116.1, 71.6.

MS (ESI<sup>+</sup>): *m/z* 468.5 [M + H<sup>+</sup>].

Anal. Calcd for C<sub>32</sub>H<sub>25</sub>N<sub>3</sub>O: C, 82.20; H, 5.39; N, 8.99; found: C, 81.22; H, 5.55; N, 7.80 %.

**6,6'-Bis(diethylphosphonomethyl)-2,2'-bipyridine (31) :**Formula: C<sub>20</sub>H<sub>30</sub>N<sub>2</sub>O<sub>6</sub>P<sub>2</sub>

Molecular weight: 456.16



A solution 6-6'-bis(chloromethyl)-2,2'-bipyridine 1.92 g, 7.60 mmol) and triethylphosphite (5 mL, 0.29 mol) was heated at 80 °C for 6 h. The solution was then allowed to cool to room temperature, and triethylphosphite were removed under reduced pressure. The oily brown residue was taken up with pentane (20 mL). The residue was redissolved in CH<sub>2</sub>Cl<sub>2</sub> and purified by column chromatography. The fractions containing the pure product were combined and evaporated to dryness to give a white solid (3.12 g, 90 %).

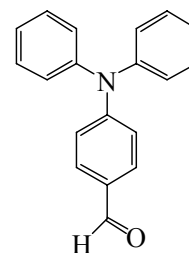
<sup>1</sup>H NMR (CDCl<sub>3</sub>, 400 MHz) δ = 1.24 (t, J = 7.1 Hz, 12 H, CH<sub>3</sub>), 3.48 (d, J = 22.0 Hz, 4 H, ), 4.14 (m, 8 H), 7.36 (m, 2 H), 7.74 (t, J = 7.8 Hz, 2 H), 8.327.36 (m, 2 H).

<sup>13</sup>C-NMR (CDCl<sub>3</sub>, 100 MHz): δ = 155.8, 152.5, 137.7, 124.7, 119.0, 62.6, 37.7, 36.7, 16.7.

<sup>31</sup>P-NMR (CDCl<sub>3</sub>, 400 MHz): δ = 22.17.

**4-Formyltriphenylamine (32) :**Formula: C<sub>19</sub>H<sub>15</sub>NO

Molecular weight: 273.12



Triphenylamine (4.0 g, 16.3 mmol) was dissolved in 20 mL DMF. POCl<sub>3</sub> (7.6 mL, 81.5 mmol) was added dropwise to the mixture at 0°C. As the temperature rose to room temperature, the mixture changed to a clear bright red solution. The reaction was heated to 145°C for an addition 2 h. After cooling, the mixture was poured in an ice-bath with stirring

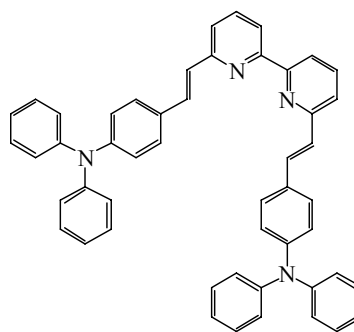
and later neutralized with sodium carbonate. Pale yellow solids were collected by filtering and recrystallized in ethanol (2.94 g, 66%).

$^1\text{H NMR}$  ( $\text{CDCl}_3$ )  $\delta$  = 7.00 (d,  $J$  = 8.9, 2H), 7.30–7.36 (t,  $J$  = 7.8, 4H), 7.15–7.18 (m, 6H), 7.67 (d,  $J$  = 8.9, 2H), 9.79 (s, 1H).

**6,6'-Bis(2-(4-(*N,N*-diphenylamino)phenyl)ethenyl)-2,2'-bipyridine (33) :**

Formula:  $\text{C}_{50}\text{H}_{38}\text{N}_4$

Molecular weight: 694.31



Potassium tertbutoxide (243 mg, 2.15 mmol) was added to a solution of [*N,N*-(4-formyltriphenylamine (1.03 g, 1.9 mmol) and 2,2'-bis(diethylphosphonomethyl)-2,2'-bipyridine (365 mg, 0.85 mmol) in THF (30 mL). The reaction mixture was stirred for 2 h at room temperature. After addition of water (10 mL), THF was removed under reduced pressure, and the aqueous residue was extracted with  $\text{CH}_2\text{Cl}_2$  (3x30 mL). The collected organic layers were washed with brine (30 mL) and water (50 mL), dried over magnesium sulfate, and filtered. After evaporation of the solvent, precipitation from  $\text{CH}_2\text{Cl}_2$ /pentane obtained an orange powder. The yield was 319 mg, (54%).

$^1\text{H NMR}$  ( $\text{CDCl}_3$ , 400 MHz)  $\delta$  = 8.42 (d, 2H,  $J$  = 7.6 Hz), 7.81 (t, 2H,  $J$  = 7.6 Hz), 7.32 (d, 2H,  $J$  = 15.9 Hz), 7.50 (d, 4H,  $J$  = 7.6 Hz), 7.39 (d, 2 H,  $J$  = 7.6 Hz), 7.28 (m, 8 H), 7.13 (m, 10H), 7.07 (m, 8H).

$^{13}\text{C-NMR}$  ( $\text{CDCl}_3$ , 100 MHz):  $\delta$  = 156.3, 155.6, 148.3, 147.8, 137.7, 132.6, 131.1, 129.7, 128.4, 126.8, 125.1, 123.6, 123.5, 122.2, 119.7.

**MS (FAB):**  $m/z$  694 [ $\text{M} + \text{H}^+$ ].

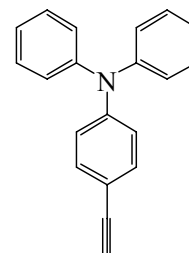
**Anal. Calcd** for: C<sub>50</sub>H<sub>38</sub>N<sub>4</sub>: C, 86.42; H, 5.51; N, 8.06; found: C, 82.84; H, 5.49; N, 8.97%.

**UV-VIS** (CH<sub>3</sub>CN):  $\lambda$ /nm ( $\epsilon$ /M<sup>-1</sup> cm<sup>-1</sup>) 299 (108000), 389 (189425).

**4-(Ethynylphenyl)diphenylamine (32) :**

Formula: C<sub>20</sub>H<sub>15</sub>N

Molecular weight: 269.12



A three necked round bottomed flask was charged with 4-bromobenzenediphenyl amine (3.24 g, 10 mmol), trimethylsilylacetylene (1.70 mL, 12 mmol), [Pd(PhCN)<sub>2</sub>Cl<sub>2</sub>] (115 mg, 0.06 mmol), and CuI (7.64 mg, 0.04 mmol). Then 20 mL toluene, P(*t*-Bu)<sub>3</sub> (0.8 mL of a 0.4 M solution in hexane, 0.16 mmol), and triethylamine (4 mL) were added via syringe. The reaction mixture was stirred at rt for 15 h, diluted with Et<sub>2</sub>O, filtered over celite. The solvent was removed in vacuo, and the crude product was placed in a round-bottom flask and dissolved in 30 mL of CH<sub>2</sub>Cl<sub>2</sub>. The flask was cooled to 0 °C, and a 1 M tetrabutylammonium fluoride solution in THF (15 mL, 15 mmol) was added via syringe. The reaction mixture was stirred for 2 h at 0 °C and successively absorbed onto silica. Chromatography on silica gel (hexane / CH<sub>2</sub>Cl<sub>2</sub> = 93/7) gave 1.52 g (56%).

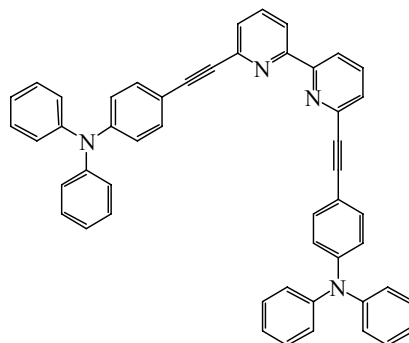
<sup>1</sup>H NMR (CDCl<sub>3</sub>):  $\delta$  = 7.33 (m, 6H), 7.05 (m, 6H), 6.90 (m, 2H), 3.08 (s, 1H).

<sup>13</sup>C NMR (CDCl<sub>3</sub>):  $\delta$  = 147.1, 140.4, 132.4, 129.3, 123.5, 122.2, 116.2, 84.6, 78.4.

**6,6'-Bis(4-(*N,N*-diphenylamino)phenylethynyl)-2,2'-bipyridine (36) :**

Formula: C<sub>50</sub>H<sub>34</sub>N<sub>4</sub>

Molecular weight: 690.28



To a mixture of 6,6'-dibromo-2,2'-dipyridyl (0.16 g, 0.32 mmol), CuI (9.6 mg, 0.05 mmol), triphenylphosphine (0.768 mg, 0.03 mmol) and [Pd(PPh<sub>3</sub>)<sub>2</sub>Cl<sub>2</sub>] (7.44 mg, 0.01 mmol) was added triethylamine (10 mL) under N<sub>2</sub>. (4-Ethynylphenyl)diphenylamine (0.19 g, 0.7 mmol) was introduced portion wise, and the reaction mixture was allowed to stir at room temperature overnight after which the reaction was quenched by pouring over distilled water. The aqueous layer was extracted with CH<sub>2</sub>Cl<sub>2</sub>, and the combined organic phases were dried and concentrated. The residue was chromatographed on silica gel (elution with 1:1 CH<sub>2</sub>Cl<sub>2</sub>/hexane) to provide a yellow solid (94 mg, 42%).

<sup>1</sup>H NMR (CDCl<sub>3</sub>, 400 MHz) δ = 8.44 (d, 2H, J= 8.1 Hz), 7.79 (t, 2H, J= 7.8 Hz), 7.54 (d, 2H, J= 8.6Hz), 7.45 (d, 4H, J= 8.6 Hz), 7.28 (m, 10 H), 7.14 (m, 7H), 7.09 (m, 3H), 7.02 (m, 4H).

<sup>13</sup>C-NMR (CDCl<sub>3</sub>, 100 MHz): δ = 156.3, 148.9, 147.4, 143.5, 137.4, 133.4, 129.8, 127.7, 125.6, 124.2, 122.1, 120.8, 115.1, 90.0, 88.7.

**MS (FAB):** *m/z* 690

**Anal. Calcd** for: C<sub>50</sub>H<sub>34</sub>N<sub>4</sub>CH<sub>2</sub>Cl<sub>2</sub>: C, 78.96; H, 4.68; N, 7.22; found: C, 75.84; H, 5.49; N, 7.88%.

**UV-VIS** (CH<sub>3</sub>CN): λ/nm (ε/M<sup>-1</sup> cm<sup>-1</sup>) : 245 (27754), 296 (35414), 369 (66457).

## 6.2.2 Copper(I) complexes: synthesis and characterisation

*General method for  $[CuL_2]^+$  complexes:*

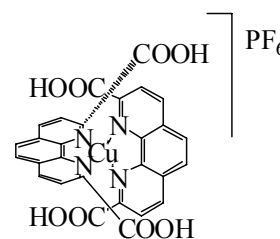
A solution of 1 equivalent of  $[Cu(MeCN)_4][PF_6]$  in degassed acetonitrile (2 mL) was treated with 1 equivalent of the 1,10-phenanthroline or 2,2'-bipyridine ligand and the mixture ultrasonicated for 1h at room temperature. The mixtures turned dark red instantaneously, indicating the formation of the complexes. The complete dissolution of the ligand marked the end of complexation. Any unreacted  $[Cu(MeCN)_4][PF_6]$  was removed by filtration over celite. The solvent was concentrated in vacuo.

### **Bis[1-10-Phenanthroline-2,9-dicarboxylic acid]copper(I) hexafluorophosphate:**

Formula:  $C_{28}H_{16}CuF_6N_4O_8P$

Molecular weight: 744.96

The yield was 50 mg (42%).



$^1H$  NMR (400 MHz, DMSO):  $\delta$  = 8.20 (s, 4H), 8.40 (d, 4H,  $J=8.08$ ), 8.72 (d, 4H,  $J = 8.08$ ).

$^{13}C$  NMR (100 MHz, DMSO): 124.28, 129.25, 131.33, 138.98, 145.60, 149.14, 167.12.

MS (MALDI-TOF+):  $m/z$  : 743 [M].

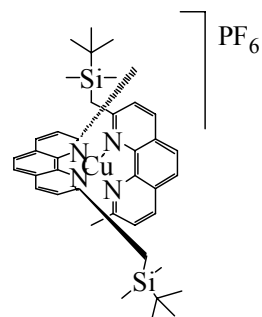
**Anal. Calcd:** For  $C_{28}H_{15.75}N_4O_8CuP_{0.75}F_{4.5}$ ; C: 47.47, H: 2.24, N: 7.91 **Found:** C: 47.02, H: 3.15, N: 8.79.



**Bis[2-dimethyl-9-(tert-butyl-dimethylsilyl)methyl]-1,10-phenanthroline]copper(I) hexafluorophosphate:**

Formula:  $C_{40}H_{52}N_4CuPF_6Si_2$

Molecular weight: 853.56



The yield was 81mg (87%).

$^1H$  NMR (250 MHz,  $CD_3CN$ ):  $\delta$  = -0.65 (s, 6H), -0.09 (s, 6H), 0.15 (s, 18H), 2.14 (s, 4H), 2.49 (s, 6H), 7.66 (d, 2H,  $J$  = 8.4 Hz), 7.82 (d, 2H,  $J$  = 8.4 Hz), 8.04 (s, 2H), 8.49 (d, 2H,  $J$  = 8.4 Hz), 8.55 (d, 2H,  $J$  = 8.4 Hz).

$^{13}C$  NMR (100 MHz,  $CD_3CN$ ):  $\delta$  = -7.35, -6.59, 25.02, 25.74, 28.02, 125.53, 125.61, 126.07, 126.44, 127.34, 128.17, 137.04, 137.64, 143.43, 143.73, 158.29, 162.43.

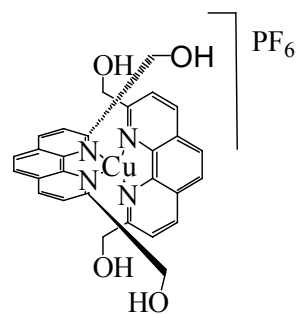
MS (MALDI-TOF+):  $m/z$ : 708 [M -  $PF_6$ ]

**Anal. Calcd:** For  $C_{40}H_{52}N_4CuPF_6Si_2$ ; C: 56.29, H: 6.14, N: 6.56 **Found:** C: 56.54, H: 6.10, N: 6.39.

**Bis[2,9-Bis(hydroxymethyl)-1,10-phenanthroline]copper(I) hexafluorophosphate:**

Formula:  $C_{28}H_{24}N_4O_4CuPF_6$

Molecular weight: 689.03



The yield was 42 mg (47%).

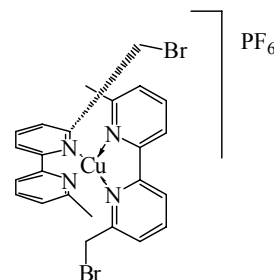
$^{13}C$  NMR (100 MHz, DMSO):  $\delta$  = 65.07, 123.29, 127.29, 128.96, 138.94, 142.77, 162.09.

**Anal. Calcd:** For  $C_{28}H_{24}N_4O_4CuPF_6$ ; C: 48.81, H: 3.51, N: 8.13 **Found:** C: 45.47, H: 4.70, N: 4.20.

**Bis[6-(Bromomethyl)-6'-methyl-2,2'-bipyridine]copper(I) hexafluorophosphate:**

Formula:  $C_{24}H_{22}N_4Br_2CuPF_6$

Molecular weight: 734.78



The yield was 81mg (98%).

**$^1H$  NMR** (400 MHz,  $CD_3CN$ ):  $\delta$  = 2.29 (s, 6H), 4.36 (s, 4H), 7.54 (d, 2H,  $J$  = 5.1 Hz), 7.75 (d, 2H,  $J$  = 5.6 Hz), 8.06 (t, 2H,  $J$  = 7.1 Hz), 8.16 (t, 2H,  $J$  = 7.8 Hz), 8.32 (d, 2H,  $J$  = 6.6 Hz), 8.41 (d, 2H,  $J$  = 7.1 Hz).

**$^{13}C$  NMR** (100 MHz,  $CD_3CN$ ):  $\delta$  = 25.06, 34.27, 120.19, 122.21, 126.83, 139.00, 140.01, 151.47, 153.28, 156.40, 158.43.

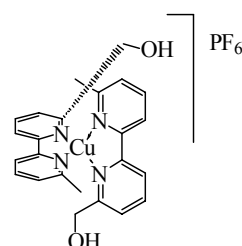
**MS (MALDI-TOF+):**  $m/z$ : 590 [M- $PF_6$ ].

**Anal. Calcd:** For  $C_{24}H_{22}N_4Br_2CuPF_6$ ; C: 39.23, H: 3.02, N: 7.63 **Found:** C: 39.29, H: 3.07, N: 7.60.

**Bis[6-(Hydroxymethyl)-6'-methyl-2,2'-bipyridine]copper(I) hexafluorophosphate:**

Formula:  $C_{24}H_{24}N_4O_2CuPF_6$

Molecular weight: 608.99



The yield was 88 mg (96 %).

**<sup>1</sup>H NMR** (400 MHz, CD<sub>3</sub>CN):  $\delta$  = 2.19 (s, 6H), 4.26 (s, 4H), 7.51 (d, 2H, J = 7.6), 7.75 (d, 2H, 7.8), 8.04 (t, 2H, J = 7.8), 8.16 (t, 2H, J = 7.8), 8.31 (d, 2H, 8.1), 8.34 (d, 2H, J = 8.1).

**<sup>13</sup>C NMR** (100 MHz, CD<sub>3</sub>CN):  $\delta$  = 24.66, 64.67, 119.99, 120.96, 123.24, 126.38, 138.94, 139.29, 151.70, 151.95, 158.06, 160.90.

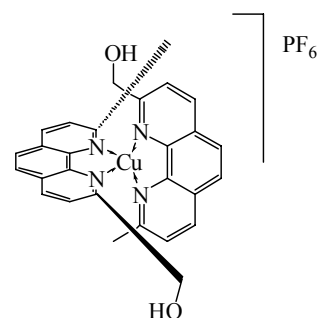
**MS (MALDI-TOF+):**  $m/z$ : 464 [M - PF<sub>6</sub>].

**Anal. Calcd:** For C<sub>24</sub>H<sub>24</sub>N<sub>4</sub>O<sub>2</sub>CuPF<sub>6</sub>; C: 47.33, H: 3.97, N: 9.20 **Found:** C: 44.83, H: 3.76, N: 8.60.

**Bis[2-(Hydroxymethyl)-9-methyl-1,10-phenanthroline]copper(I) hexafluorophosphate:**

Formula: C<sub>28</sub>H<sub>24</sub>N<sub>4</sub>O<sub>2</sub>CuPF<sub>6</sub>

Molecular weight: 657.03



The yield was 56 mg (84%).

**<sup>1</sup>H NMR** (400 MHz, CD<sub>3</sub>CN):  $\delta$  = 2.39 (s, 6H), 3.46 (br, 2H), 4.45 (s, 4H), 7.84 (d, 2H, J = 8.1), 8.10 (d, 2H, J = 8.1), 8.14 (s, 4H), 8.60 (d, 2H, J = 8.1), 8.72 (d, 2H, J = 8.1).

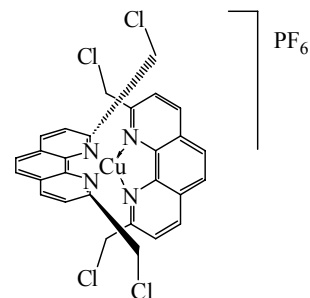
**<sup>13</sup>C NMR** (100 MHz, CD<sub>3</sub>CN):  $\delta$  = 25.40, 65.30, 122.77, 126.10, 126.38, 126.73, 128.06, 128.91, 137.69, 138.15, 143.26, 143.33, 158.82, 161.26.

**Anal. Calcd:** For C<sub>28</sub>H<sub>24</sub>N<sub>4</sub>O<sub>2</sub>CuPF<sub>6</sub>; C: 51.19, H: 3.68, N: 8.53 **Found:** C: 50.71, H: 3.69, N: 8.48.

**Bis[6,6'-di(chloromethyl)-1,10-phenanthroline]copper(I) hexafluorophosphate:**Formula:  $C_{28}H_{20}Cl_4CuF_6N_4P$ 

Molecular weight: 762.81

The yield was 104 mg (94%).



$^1H$  NMR (400 MHz,  $CD_3CN$ ):  $\delta$  = 4.61 (s, 8H), 8.13 (d, 4H,  $J$  = 8.1), 8.27 (s, 4H), 8.81 (d, 4H,  $J$  = 8.6).

$^{13}C$  NMR (100 MHz,  $CD_3CN$ ):  $\delta$  = 47.54, 125.83, 127.71, 129.74, 139.54, 143.71, 156.25.

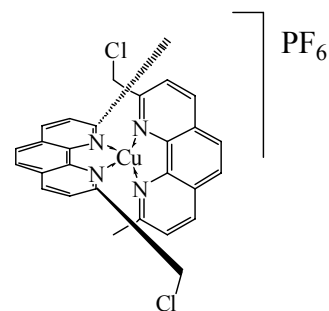
MS (MALDI-TOF+) :  $m/z$  : 656 [ $M - PF_6 + K^+$ ]

**Anal. Calcd:** For  $C_{28}H_{20}Cl_4CuF_6N_4P$ ; C: 44.09, H: 2.64, N: 7.34 **Found:** C: 43.70, H: 2.84, N: 7.04.

**Bis[2-Chloromethyl-9-methyl-1,10-phenanthroline]copper(I) hexafluorophosphate:**Formula:  $C_{28}H_{22}Cl_2CuF_6N_4P$ 

Molecular weight: 693.92

The yield was 85 mg (87%).

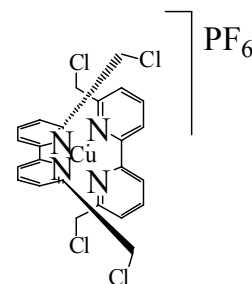


**Anal. Calcd:** For  $C_{28}H_{22}Cl_2CuF_6N_4P$ ; C: 48.46, H: 3.20, N: 8.07 **Found:** C: 48.75, H: 3.42, N: 7.90.

**Bis[6,6'-bis(chloromethyl)-2,2'-bipyridine]copper(I) hexafluorophosphate:**Formula:  $C_{24}H_{20}Cl_4CuF_6N_4P$ 

Molecular weight: 714.76

The yield was 76 mg (92%).

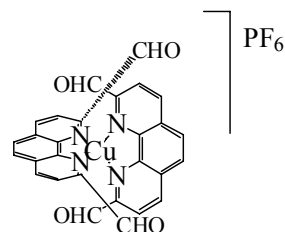


**Anal. Calcd:** For  $C_{24}H_{20}N_4Cl_4CuPF_6$ ; C: 40.33, H: 2.82, N: 7.84 **Found:** C: 40.43, H: 2.78, N: 7.85.

**Bis[1-10-Phenanthroline-2,9-dicarboxaldehyde]copper(I) hexafluorophosphate:**Formula:  $C_{28}H_{16}CuF_6N_4O_4P$ 

Molecular weight: 680.96

The yield was 47 mg (57%).



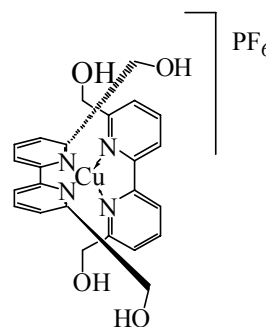
$^1H$  NMR (400 MHz,  $CD_3CN$ ):  $\delta$  = 8.39 (s, 4H), 8.44 (d, 4H,  $J$  = 8.4), 8.93 (d, 4H,  $J$  = 8.4), 9.99 (d, 4H).

**MS (MALDI-TOF+):**  $m/z$ : 536 [M -  $PF_6$ ].

**Anal. Calcd:** For  $C_{28}H_{16}N_4O_4CuPF_6 \cdot 2.5H_2O$ ; C: 46.32, H: 2.92, N: 7.72 **Found:** C: 46.10, H: 2.95, N: 7.69.

**Bis[6,6'-Bis(hydroxymethyl)-2,2'-bipyridine]copper(I) hexafluorophosphate:**Formula:  $C_{24}H_{24}CuF_6N_4O_4P$ 

Molecular weight: 640.99



The yield was 78 mg (87%).

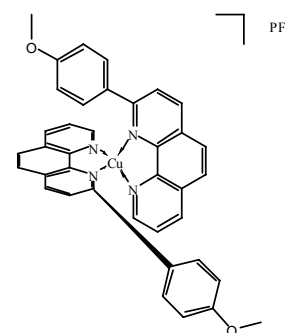
$^1\text{H NMR}$  (400 MHz, MeOD):  $\delta = 4.25$  (s, 8H), 7.80 (d, 4H,  $J = 7.3$ ), 8.20 (t, 4H,  $J = 7.4$ ), 8.49 (d, 4H,  $J = 7.7$ ).

$^{13}\text{C NMR}$  (100 MHz, MeOD):  $\delta = 66.33, 122.54, 124.79, 140.98, 153.20, 162.39$ .

**MS (MALDI-TOF+):**  $m/z$ : 496 [M – PF<sub>6</sub>]

**Bis[2-(p-anisyl)-1,10-phenanthroline] copper(I) hexafluorophosphate:**Formula:  $C_{38}H_{28}CuF_6N_4O_2P$ 

Molecular weight: 780.12



$^1\text{H NMR}$  (400 MHz,  $\text{CD}_3\text{CN}$ ):  $\delta = 9.09$  (d br, 2H), 8.67 (d, 2H,  $J = 7.6$ ), 8.40 (d, 2H,  $J = 8.1$ ), 8.01 (m, 6H), 7.79 (d, 2H,  $J = 8.1$ ), 7.16 (d br, 4H), 5.87 (d br, 4H), 3.40 (s, 6H).

$^{13}\text{C NMR}$  (100 MHz,  $\text{CD}_3\text{CN}$ ):  $\delta = 160.2, 157.1, 149.5, 144.1, 143.8, 137.3, 137.2, 131.9, 130.0, 129.2, 127.8, 127.0, 126.4, 125.6, 117.7, 112.6, 55.0$ .

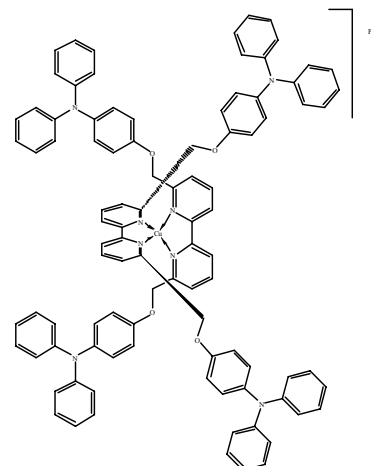
**MS (MALDI-TOF+):**  $m/z$ : 636 [M – PF<sub>6</sub>]

**Anal. Calcd** for:  $C_{38}H_{28}CuF_6N_4O_2P$ : C 58.43, H 3.61, N 7.17; **found**: C 58.20, H 3.78, N 6.92.

**Bis[6,6'-Bis(4-(*N,N*-diphenylamino)phenoxy)methyl)-2,2'-bipyridine]copper(I)  
hexafluorophosphate:**

Formula: C<sub>96</sub>H<sub>76</sub>CuF<sub>6</sub>N<sub>8</sub>O<sub>4</sub>P

Molecular weight: 1612.49



A solution of [Cu(MeCN)<sub>4</sub>][PF<sub>6</sub>] (10.7 mg, 0.028 mmol) in degassed acetonitrile (2mL) was treated 4,4'-(2,2'-bipyridine-6,6'-diylbis(methylene))bis(oxy)bis(*N,N*-diphenylaniline) (40 mg, 0.057 mmol) and the mixture ultrasonicated for 1h at room temperature. The mixture turned dark red instantaneously, indicating the formation of the complex. The complete dissolution of the ligand marked the end of complexation. Any unreacted [Cu(MeCN)<sub>4</sub>][PF<sub>6</sub>] removed by filtration over celite. The solvent was concentrated in vacuo.

<sup>1</sup>H NMR (CDCl<sub>3</sub>, 400 MHz) δ = 8.45 (d, 4H, J = 7.41 Hz), 8.17 (t, 4H, J = 7.89 Hz), 7.88 (d, 4H, J = 7.72 Hz), 7.26-7.23 (m, 18H), 6.98 (t, 2H, J = 1.10 Hz), 6.97 (t, 4H, J = 0.95 Hz), 6.95 (t, 2H, J = 1.10 Hz), 6.90-6.89 (m, 16H), 6.74 (d, 8H, J = 8.99 Hz), 6.36 (d, 8H, J = 9.14 Hz), 4.95 (s, 8H).

<sup>13</sup>C-NMR (CDCl<sub>3</sub>, 100 MHz): δ = 155.3, 154.2, 151.7, 148.0, 141.1, 139.4, 129.2, 126.8, 126.0, 122.8, 122.2, 121.7, 114.7, 70.7.

MS (ESI<sup>+</sup>): 1469 [M – PF<sub>6</sub>].

**Anal. Calcd** for: C<sub>96</sub>H<sub>76</sub>CuF<sub>6</sub>N<sub>8</sub>O<sub>4</sub>P: C 71.43, H 4.75, N 6.94; **found**: C 68.26, H 4.56, N 6.76.

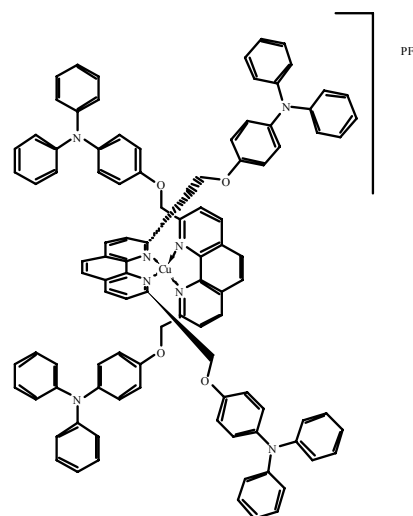
UV-VIS (CH<sub>3</sub>CN): λ/nm (ε/M<sup>-1</sup>cm<sup>-1</sup>): 300 (120101), 450 (4573).



**Bis[2,9-bis(4-(*N,N*-diphenylamino)phenoxy)methyl)-1,10-phenanthroline]copper(I)  
hexafluorophosphate:**

Formula:  $C_{100}H_{76}CuF_6N_8O_4P$

Molecular weight: 1660.49



A solution of  $[Cu(MeCN)_4][PF_6]$  (10.35g, 0.0275mol) in degassed acetonitrile (2mL) was treated 1,10-phenanthroline-2,9-diylbis(methylene)bis(oxy)bis(*N,N*-diphenylaniline) (40 mg, 0.055mmol) and the mixture ultrasonicated for 1h at room temperature. The mixture turned dark red instantaneously, indicating the formation of the complex. The complete dissolution of the ligand marked the end of complexation. Any unreacted  $[Cu(MeCN)_4][PF_6]$  removed by filtration over celite. The solvent was concentrated in vacuo. The yield was 39.72 mg (87%).

$^1H$  NMR ( $CDCl_3$ , 400 MHz)  $\delta$  = 8.44 (d, 4H,  $J$  = 8.7 Hz), 7.96 (m, 8H), 7.22 (m, 18 H), 6.93 (m, 22H), 6.64 (d, 8 H,  $J$  = 8.8 Hz), 6.14 (d, 8 H,  $J$  = 9.1), 4.96, (s, 8H).

$^{13}C$ -NMR ( $CDCl_3$ , 100 MHz):  $\delta$  = 156.3, 154.0, 148.3, 143.3, 141.7, 138.2, 129.5, 129.2, 127.2, 126.9, 125.3, 123.4, 122.6, 115.0, 71.6.

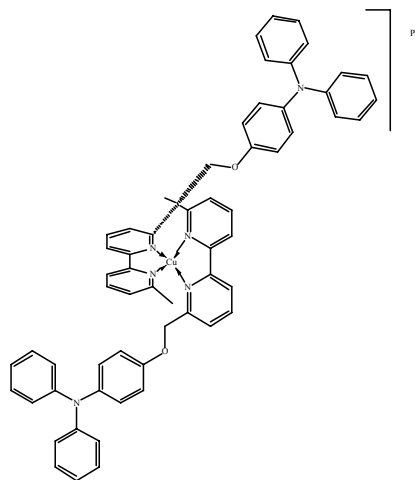
MS (ESI+): 1517  $[M - PF_6]$ .

**Anal. Calcd** for:  $C_{103}H_{84}CuF_6N_8O_4P$ : C, 72.50; H, 4.96; N, 6.57; **found**: C 68.26, H 4.56, N 6.76.

**Bis[6-(4-(*N,N*-Diphenylamino)phenoxy)methyl)-6'-methyl-2,2'-bipyridine]copper(I)  
hexafluorophosphate:**

Formula: C<sub>60</sub>H<sub>50</sub>CuF<sub>6</sub>N<sub>6</sub>O<sub>2</sub>P

Molecular weight: 1094.29



A solution of [Cu(MeCN)<sub>4</sub>][PF<sub>6</sub>] (17 mg, 0.045 mmol) in degassed acetonitrile (2mL) was 4-((6'-methyl-2,2'-bipyridin-6-yl)methoxy)-*N,N*-diphenylanile (40 mg, 0.09 mmol) and the mixture ultrasonicated for 1h at room temperature. The mixture turned dark red instantaneously, indicating the formation of the complex. The complete dissolution of the ligand marked the end of complexation. Any unreacted [Cu(MeCN)<sub>4</sub>][PF<sub>6</sub>] removed by filtration over celite. The solvent was concentrated in vacuo. The yield was 38.90 mg (79%).

<sup>1</sup>H NMR (CDCl<sub>3</sub> 400 MHz) δ = 8.25 (d, 2H, J = 8.0 Hz), 8.15 (d, 2H, J = 7.9 Hz), 8.07 (d, 2H, J = 7.9 Hz), 7.95 (d, 2H, J = 7.9 Hz), 7.70 (d, 2H, J = 7.6 Hz), 7.43 (d, 2H, J = 7.6 Hz), 7.22 (m, 14 H), 6.96 (m, 14H), 6.82 (d, 4H, J = 8.8 Hz), 6.27 (d, 4H, J = 8.8 Hz), 4.70 (s, 4H), 2.29 (s, 6H).

<sup>13</sup>C-NMR (CDCl<sub>3</sub>, 100 MHz): δ 157.5, 155.1, 153.7, 152.1, 150.9, 147.9, 141.5, 139.3, 138.7, 129.2, 126.8, 126.4, 125.2, 123.1, 122.3, 121.6, 119.7, 114.6, 70.4, 25.5.

MS (ESI+): 949 [M – PF<sub>6</sub>].

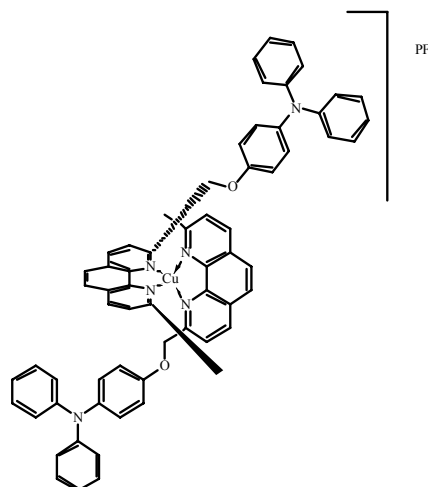
Anal. Calcd for: C<sub>67</sub>H<sub>58</sub>CuF<sub>6</sub>N<sub>6</sub>O<sub>2</sub>P: C, 67.75; H, 4.92; N, 7.08; found: pending

UV-VIS (CH<sub>3</sub>CN): λ/nm (ε/M<sup>-1</sup>cm<sup>-1</sup>) 301 (77622), 450 (6382).

**Bis[2-(4-(*N,N*-Diphenylamino)phoxymethyl)-9-methyl-1,10-phenanthroline]copper(I) hexafluorophosphate:**

Formula: C<sub>64</sub>H<sub>50</sub>CuF<sub>6</sub>N<sub>6</sub>O<sub>2</sub>P

Molecular weight: 1142.29



A solution of [Cu(MeCN)<sub>4</sub>][PF<sub>6</sub>] (17 mg, 0.045 mmol) in degassed acetonitrile (2mL) was added to 2-(4-(*N,N*-Diphenylamino)phoxymethyl)-9-methyl-1,10-phenanthroline (42 mg, 0.09 mmol) and the mixture ultrasonicated for 1h at room temperature. The mixture turned dark red instantaneously, indicating the formation of the complex. The complete dissolution of the ligand marked the end of complexation. Any unreacted [Cu(MeCN)<sub>4</sub>][PF<sub>6</sub>] removed by filtration over celite. The solvent was concentrated in vacuo. The yield was 45.23 mg (88%).

<sup>1</sup>H NMR (CDCl<sub>3</sub>, 400 MHz) δ = 8.53 (d, 2H, J = 8.4 Hz), 8.44 (d, 2H, J = 8.4 Hz), 7.99 (m, 6H), 7.77 (d, 2H, J = 8.4 Hz), 7.22 (m, 8H), 6.93 (m, 12H), 6.67 (d, 4 H, J = 8.8), 6.10 (d, 4H, J = 9.1), 4.83 (s, 4H), 2.55 (s, 6H).

<sup>13</sup>C-NMR (CDCl<sub>3</sub>, 100 MHz): δ 158.8, 155.8, 154.0, 148.3, 143.6, 143.2, 141.8, 138.5, 137.9, 129.6, 129.3, 128.1, 127.6, 126.9, 126.6, 126.4, 124.6, 123.5, 122.7, 114.9, 71.3, 26.7.

MS (ESI<sup>+</sup>): 998 [M – PF<sub>6</sub>].

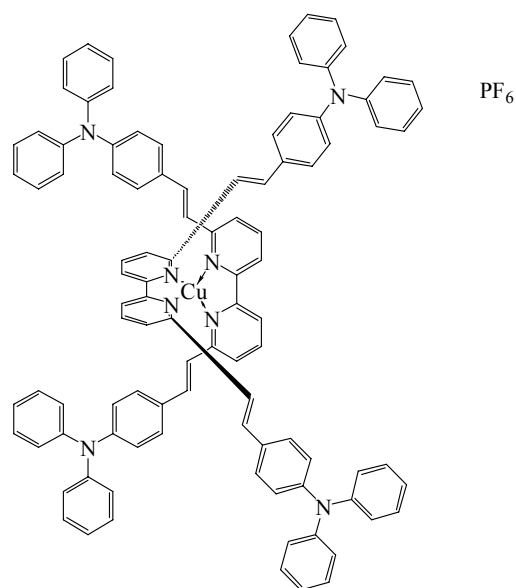
Anal. Calcd for: C<sub>67</sub>H<sub>58</sub>CuF<sub>6</sub>N<sub>6</sub>O<sub>2</sub>P: C, 67.75; H, 4.92; N, 7.08; found: pending

UV-VIS (CH<sub>3</sub>CN): λ/nm (ε/M<sup>-1</sup>cm<sup>-1</sup>) 301 (77622), 450 (6382).

**Bis[6,6'-Bis(2-(4-(*N,N*-diphenylamino)phenyl)ethenyl)-2,2'-bipyridine]copper(I)  
hexafluorophosphate:**

Formula: C<sub>100</sub>H<sub>76</sub>CuF<sub>6</sub>N<sub>8</sub>P

Molecular weight: 1596.51



A solution of [Cu(MeCN)<sub>4</sub>][PF<sub>6</sub>] (16.2 mg, 0.04 mmol) in degassed acetonitrile (2mL) was treated with Bis(ethene-2,1-diyl)bis(*N,N*-diphenylaniline)-(2,2'-bipyridine-6,6'-diyl) (60 mg, 0.086 mmol) and the mixture ultrasonicated for 1h at room temperature. The mixture turned dark red instantaneously, indicating the formation of the complex. The complete dissolution of the ligand marked the end of complexation. Any unreacted [Cu(MeCN)<sub>4</sub>][PF<sub>6</sub>] removed by filtration over celite. The solvent was concentrated in vacuo. The yield was 51 mg (80 %).

<sup>1</sup>H NMR (CDCl<sub>3</sub> 400 MHz) δ = 7.87 (m, 8H), 7.73 (d, 4H, J= 7.3 Hz), 7.29 (m, 18H), 7.10 (m, 26H), 6.77 (m, 12 H), 6.06 (m, 8 H).

<sup>13</sup>C-NMR (CDCl<sub>3</sub>, 100 MHz): δ = 155.8, 152.4, 149.1, 147.4, 138.2, 135.2, 129.8, 129.0, 128.1, 125.3, 125.0, 124.2, 122.6, 122.5, 120.1.

MS (ESI+): 1452 [M – PF<sub>6</sub>]

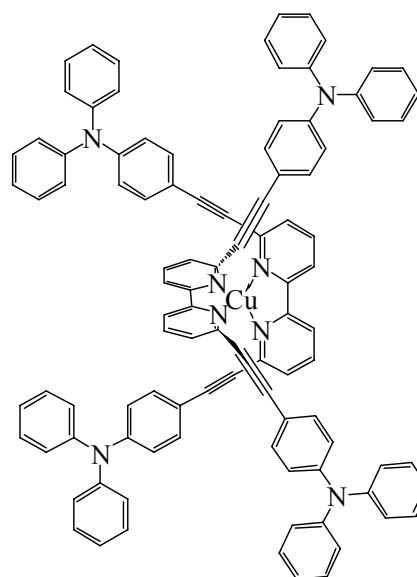
**Anal. Calcd** for: C<sub>100</sub>H<sub>76</sub>CuF<sub>6</sub>N<sub>8</sub>P: C, 75.15; H, 4.79; N, 7.01; **found**: C, 76.22; H, 5.06; N, 6.37.

UV-VIS (CH<sub>3</sub>CN): λ/nm (ε/M<sup>-1</sup>cm<sup>-1</sup>) 299 (180500) 398 (231750).

**Bis[6,6'-Bis(4-(*N,N*-diphenylamino)phenylethynyl)-2,2'-bipyridine]copper(I)  
hexafluorophosphate:**

Formula: C<sub>100</sub>H<sub>68</sub>CuF<sub>6</sub>N<sub>8</sub>P

Molecular weight: 1590.20



A solution of [Cu(MeCN)<sub>4</sub>][PF<sub>6</sub>] (21.8 mg, 0.05 mmol) in degassed acetonitrile (2mL) was treated with 4,4'-(2,2'-bipyridine-6,6'-diylbis(ethyne-2,1-diyl))bis(*N,N*-diphenylaniline) (80 mg, 0.12 mmol) and the mixture ultrasonicated for 1h at room temperature. The mixture turned dark red instantaneously, indicating the formation of the complex. The complete dissolution of the ligand marked the end of complexation. Any unreacted [Cu(MeCN)<sub>4</sub>][PF<sub>6</sub>] removed by filtration over celite. The solvent was concentrated in vacuo. The yield was 67 mg (85 %).

<sup>1</sup>H NMR (CDCl<sub>3</sub>, 400 MHz) δ = 8.37 (d, 4H, J= 9.1 Hz), 8.08 (t, 4H, J= 8.1 Hz), 7.82 (d, 4H, J= 8.6 Hz), 7.38 (m, 16H), 7.17 (m, 8 H), 7.09 (m, 16 H), 6.75 (m, 8 H), 6.66 (m, 8 H).

<sup>13</sup>C-NMR (CDCl<sub>3</sub>, 100 MHz): δ = 152.2, 149.5, 147.1, 142.0, 138.3, 132.7, 130.1, 129.3, 125.8, 124.7, 121.7, 121.1, 113.1, 93.7, 87.0.

MS (ESI<sup>+</sup>): 1445 [M – PF<sub>6</sub>].

Anal. Calcd for: C<sub>100</sub>H<sub>68</sub>CuF<sub>6</sub>N<sub>8</sub>P: C, 75.53; H, 4.31; N, 7.05; C, 73.61; H, 4.27; N, 7.64.

UV-VIS (CH<sub>3</sub>CN): λ/nm (ε/M<sup>-1</sup>cm<sup>-1</sup>): 297 (102052), 383 (115415).

## 6.3 Characterisation of oligonucleotides

**This part was carried out by Dr Gabian Bianké in the group of Prof. Dr. Robert Häner at the University of Bern.**

### 6.3.1 Synthesis and purification of oligonucleotides

Oligonucleotides were synthesized on a 392 *DNA/RNA* Synthesizer (Applied Biosystems) according to standard phosphoramidite solid-phase chemistry. The 5'-conjugated oligonucleotide sequences were extended from the 3'-end using normal nucleoside phosphoramidites whereas the 3'-conjugated oligonucleotide sequences were developed from the 5'-end using reverse nucleoside phosphoramidites. The nucleoside phosphoramidites were purchased from *Transgenomic* (Glasgow G20 OUA, Scotland) and the universal solid support used for the reverse synthesis was from *Glen/Research* (Sterling, Virginia, USA). The solvents ( $\text{CH}_3\text{CN}$  and  $\text{CH}_2\text{Cl}_2$ ) were of analytical grade from *proligo GmbH* (Hamburg) and reagents (3% TCA/  $\text{CH}_2\text{Cl}_2$  deblock solution, 30mg/ml activator solution, oxidising solution, capping solutions A and B) used for the synthesis were from *Transgenomic* (Glasgow G20 OUA, Scotland). Standard synthetic procedure ("trityl-off" mode) and standard condition (i.e. a coupling time of 90 sec) were used to incorporate the phosphoramidite building blocks **37** and **38** into oligonucleotide sequences. Detachment of the oligonucleotides from the solid support and deprotection after the synthesis was performed using standard procedures (conc.  $\text{NH}_3$  solution, 55°C, 16 h), followed by filtration through a *spritzenfilter* (nylon, 0.17 mm/0.45  $\mu\text{m}$ , *Semadeni AG*).

All crude oligonucleotides were purified by ion-exchange HPLC, using Tricorn column Source 15Q 4.6/100PE - 15  $\mu\text{m}$  from *Amersham Biosciences* (Freiburg, Germany). The following buffers were used :

Buffer A : 20mM  $\text{Na}_2\text{HPO}_4$  in miliQ-H<sub>2</sub>O, pH11.5 (degassed)

Buffer B : 20mM  $\text{Na}_2\text{HPO}_4$  in miliQ-H<sub>2</sub>O + 2M NaCl, pH 11.5 (degassed)

The collected basic fractions were first neutralised with 30  $\mu\text{l}$  of acetic acid (0.1 M) per ml of collected fraction and desalted over *Sep-Pak* cartridges (Waters, Milford, USA) following the loading procedure described below.

10 ml of acetonitrile

10 ml of buffer A (0.1 M triethylammonium acetate)

Neutralised solution of oligonucleotide to be in desalted in 0.3 M triethylammonium acetate

10 ml of buffer A

10 ml mQ-H<sub>2</sub>O

4-5 ml elution buffer B (CH<sub>3</sub>CN/H<sub>2</sub>O 1:1)

The ODs of the purified oligonucleotides were measured at 260 nm with a NanoDrop ND-1000 spectrophotometer, and the masses determined by electrospray mass spectroscopy: *VG Platform* single quadrupole ESI-MS.

### 6.3.2 Analysis

If not otherwise indicated, all experiments were carried out under the following conditions: oligonucleotide concentration 1.5  $\mu$ M; 10 mM phosphate buffer, pH = 7.5 (23°C); 100 mM NaCl.

For experiments with metal salts, 1 mM stock solutions (in miliQ-H<sub>2</sub>O) of the following salts were used: ZnCl<sub>2</sub>; CuCl<sub>2</sub>·2H<sub>2</sub>O; [Cu(CH<sub>3</sub>CN)<sub>4</sub>][PF<sub>6</sub>]. The latter was prepared as described in the literature. The solution of [Cu(CH<sub>3</sub>CN)<sub>4</sub>][PF<sub>6</sub>] was always freshly prepared and argon bubbled through it for at least 10 min to avoid rapid oxidation of Cu(I) in to Cu(II). This procedure was also used to degas the buffers or solution used in all the experiments involving copper(I) species.

#### *UV Melting Experiments :*

These were performed using a *Varan Cary 3e UV/VIS* spectrophotometer equipped with a *Peltier* block temperature-controller and *Varan WinUV* software to determine the melting curves at 260 nm. A heating-cooling-heating cycle in the temperature range of 0-90°C or 20-90°C was applied with a temperature gradient of 0.5°C/min. To avoid H<sub>2</sub>O condensation on the UV cells at temperatures <20°C, the cell compartment was flushed with N<sub>2</sub>. Data were collected and analysed with *Kaleidagraph* software from *Synergy Software*. T<sub>m</sub> values were determined as the maximum of the first derivative of the melting curve.

### *Circular Dichroism:*

CD experiments were performed using a *Jasco J-715* spectropolarimeter with a 150W Xe high-pressure lamp. A *Jasco PDF-350S-Peltier* unit, coupled with a *Colora K5* ultrathermostat, controlled the temperature of the cell holder. The temperature was determined directly in the sample. The phosphate buffer was used as blank. For the measurement parameters, we used 0.5  $\mu$ L for the step resolution, 50 nm/min for the scan speed, 1nm for the band width, 50 mdeg for the sensibility and 3 scans for the accumulation. The CD spectra are given in mdeg from 210 to 320 nm.

### *Non-denaturing polyacrylamide gel electrophoresis*

*Pharmacia Biotech*, Power supply EPS 3500 XL, Mini-PROTEAN 3 electrophoresis module, 10.1 x 7.3 cm (W x L) glass plates and x 0.5 mm spacer from *Bio-Rad Laboratories Hercules*, CA, were used. Prior to use, the plates were siliconized with SIGMACOTE from Sigma.

20% polyacrylamide gel : 5ml 40% acrylamide-bis (19:1) solution , from *SERMA*  
 1ml TB-buffer 10 x (tris-Borate 0.9 M)  
 4 ml (qsp) mQ H<sub>2</sub>O  
 pH 7.0

A total of 64  $\mu$ l of ammonium peroxydisulfate (10% in mQ H<sub>2</sub>O) and 5  $\mu$ l of *N,N,N'*-tetramethylethylenediamine (TEMED) were added to this solution. The gel was then poured and polymerized. TB-buffer 1x was used as electrophoresis running buffer. For each single strand oligonucleotide, the loading concentration was 450 pmol/ $\mu$ l. The concentration of the oligonucleotide was 450 pmol/ $\mu$ l of loading sample. The quantity of oligonucleotides were pipetted in an Eppendorff and dried under speed vacuum and taken up in 10 $\mu$ l of loading buffer ((1 g glycerol + 1 ml 10 x TB-buffer + 9 ml mili-Q H<sub>2</sub>O). Before loading, the samples were first equilibrated by heating to 90°C for 5 min, cooling slowly to r.t. and then to 0°C for 5 min. As migration markers, xylocyanol and bromophenol blue were used. The gel was run using the following parameters : TB 1x - buffer, 10 mA, 1W, 32V, 3 h.

To visualise the bands of migration, the gel was stained with *stains all*.



## 6.4 References

- [1] Puglisi, A., Benaglia, M., Roncan, G., *Eur. J. Org. Chem.*, **2003**, 8, 1552.
- [2] Cassol, T. M., Demnitz, F. W. J., Navarro, M., d. Neves, E. A., *Tetrahedron Lett.*, **2000**, 41, 8203.
- [3] Shaul, M., Cohen, Y., *J. Org. Chem.*, **1999**, 64, 9358.
- [4] Schubert, U. S., Newkome, G. R., Goldel, A., Pemp, A., Kersten, J. L., Eisenbach, C. D., *Heterocycles*, **1998**, 48, 2141.
- [5] Schubert, U. S., Kersten, J. L., Pemp, A. E., Eisenbach, C. D., Newkome, G. R., *Eur. J. Org. Chem.*, **1998**, 2573.
- [6] Harding, M. M., Koert, U., Lehn, J. M., Marquis-Rigault, A., Piguet, C., Siegel, J., *Helv. Chim. Acta*, **1991**, 74, 594.
- [7] Newkome, G. R., Theriot, K. J., Gupta, V. K., Fronczek, F. R., Baker, G. R., *J. Org. Chem.*, **1989**, 54, 1766.
- [8] Chandler, J. C., Deady, L. W., Reiss, J. A., *J. Heterocyclic chem.*, **1981**, 18, 599.
- [9] Eggert, J. P. W., Lüning, U., Näther, C., *Eur. J. Org. Chem.*, **2005**, 1107.
- [10] Eggert, J. P. W., Harrowfield, J., Lüning, U., Skelton, B. W., White, A. H., Löffler, F., Konrad, S., *Eur. J. Org. Chem.*, **2005**, 1348.
- [11] Mosher, H. S., Yanko, W. H., Whitmore, F. C., *Org. Synth.*, **1947**, 27, 48.

## Appendices

### Crystal data and structure refinement for 6,6'-bis(2-(4-(*N,N*-diphenylamino)phenyl)ethynyl)-2,2'-bipyridine 36.

Table 1. Crystal data and structure refinement for 6,6'-bis(2-(4-(*N,N*-diphenylamino)phenyl)ethynyl)-2,2'-bipyridine 36.

Identification code	ValC-K6L	
Empirical formula	C <sub>50</sub> H <sub>34</sub> N <sub>4</sub>	
Formula weight	690.85	
Temperature	173 K	
Wavelength	0.71073 Å	
Crystal system	Triclinic	
Space group	P -1	
Unit cell dimensions	a = 8.1157(4) Å	α = 82.377(3)°.
	b = 9.1308(5) Å	β = 85.144(3)°.
	c = 13.5638(9) Å	γ = 66.419(3)°.
Volume	912.49(9) Å <sup>3</sup>	
Z	1	
Density (calculated)	1.257 Mg/m <sup>3</sup>	
Absorption coefficient	0.074 mm <sup>-1</sup>	
F(000)	362	
Crystal size	0.27 x 0.13 x 0.13 mm <sup>3</sup>	
Theta range for data collection	2.448 to 27.469°.	
Index ranges	-10 ≤ h ≤ 10, -11 ≤ k ≤ 11, -17 ≤ l ≤ 17	
Reflections collected	7698	
Independent reflections	4161 [R(int) = 0.050]	
Completeness to theta = 27.469°	99.5 %	
Absorption correction	Semi-empirical from equivalents	
Max. and min. transmission	0.99 and 0.99	
Refinement method	Full-matrix least-squares on F <sup>2</sup>	
Data / restraints / parameters	2477 / 0 / 244	
Goodness-of-fit on F <sup>2</sup>	1.1441	
Final R indices [I > 2σ(I)]	R1 = 0.0677, wR2 = 0.0544	
R indices (all data)	R1 = 0.1250, wR2 = 0.0791	
Largest diff. peak and hole	0.27 and -0.23 e.Å <sup>-3</sup>	

Table 2. Atomic coordinates ( $\times 10^4$ ) and equivalent isotropic displacement parameters ( $\text{\AA}^2 \times 10^3$ ) or 6,6'-bis(2-(4-(*N,N*-diphenylamino)phenyl)ethynyl)-2,2'-bipyridine **36**.  $U(\text{eq})$  is defined as one third of the trace of the orthogonalized  $U_{ij}$  tensor.

	x	y	z	$U(\text{eq})$
C(1)	224(2)	5717(2)	4886(1)	34
C(2)	-789(3)	7026(2)	4232(1)	42
C(3)	-290(3)	8315(3)	4030(2)	49
C(4)	1189(3)	8269(3)	4490(2)	47
C(5)	2122(3)	6936(2)	5134(1)	39
C(6)	3644(3)	6882(3)	5638(2)	42
C(7)	4878(3)	6898(2)	6052(1)	42
C(8)	6341(2)	6882(2)	6577(1)	38
C(9)	6784(3)	8222(2)	6495(2)	43
C(10)	8187(3)	8206(3)	7006(2)	43
C(11)	9206(2)	6857(2)	7636(1)	34
C(12)	8762(3)	5515(2)	7715(1)	38
C(13)	7357(3)	5533(2)	7193(1)	40
C(14)	10818(3)	8257(2)	8341(1)	37
C(15)	9359(3)	9581(2)	8634(2)	44
C(16)	9587(3)	10948(3)	8810(2)	48
C(17)	11280(3)	10986(2)	8726(2)	46
C(18)	12729(3)	9668(2)	8444(2)	44
C(19)	12512(3)	8312(2)	8259(2)	41
C(20)	12005(3)	5329(2)	8518(1)	37
C(21)	12268(3)	4952(2)	9526(2)	45
C(22)	13620(3)	3526(3)	9885(2)	48
C(23)	14714(3)	2481(2)	9232(2)	47
C(24)	14452(3)	2854(3)	8220(2)	45
C(25)	13105(3)	4278(2)	7859(2)	40
N(1)	1655(2)	5668(2)	5340(1)	36
N(8)	10620(2)	6830(2)	8165(1)	39

Table 3. Bond lengths [Å] and angles [°] for 6,6'-bis(2-(4-(*N,N*-diphenylamino)phenyl)ethynyl)-2,2'-bipyridine **36**.

C(1)-C(1)#1	1.483(4)	C(14)-C(15)	1.387(3)
C(1)-C(2)	1.395(3)	C(14)-C(19)	1.390(3)
C(1)-N(1)	1.342(2)	C(14)-N(8)	1.427(2)
C(2)-C(3)	1.379(3)	C(15)-C(16)	1.385(3)
C(2)-H(21)	0.957	C(15)-H(151)	0.960
C(3)-C(4)	1.383(3)	C(16)-C(17)	1.383(3)
C(3)-H(31)	0.959	C(16)-H(161)	0.963
C(4)-C(5)	1.383(3)	C(17)-C(18)	1.376(3)
C(4)-H(41)	0.960	C(17)-H(171)	0.960
C(5)-C(6)	1.442(3)	C(18)-C(19)	1.375(3)
C(5)-N(1)	1.345(2)	C(18)-H(181)	0.969
C(6)-C(7)	1.195(3)	C(19)-H(191)	0.965
C(7)-C(8)	1.430(3)	C(20)-C(21)	1.378(3)
C(8)-C(9)	1.396(3)	C(20)-C(25)	1.387(3)
C(8)-C(13)	1.388(3)	C(20)-N(8)	1.434(2)
C(9)-C(10)	1.377(3)	C(21)-C(22)	1.384(3)
C(9)-H(91)	0.965	C(21)-H(211)	0.972
C(10)-C(11)	1.399(3)	C(22)-C(23)	1.378(3)
C(10)-H(101)	0.964	C(22)-H(221)	0.967
C(11)-C(12)	1.397(3)	C(23)-C(24)	1.383(3)
C(11)-N(8)	1.395(2)	C(23)-H(231)	0.962
C(12)-C(13)	1.386(3)	C(24)-C(25)	1.382(3)
C(12)-H(121)	0.965	C(24)-H(241)	0.956
C(13)-H(131)	0.971	C(25)-H(251)	0.952
C(1)#1-C(1)-C(2)	121.3(2)	C(3)-C(4)-H(41)	120.9
C(1)#1-C(1)-N(1)	116.0(2)	C(5)-C(4)-H(41)	120.0
C(2)-C(1)-N(1)	122.73(18)	C(4)-C(5)-C(6)	119.92(18)
C(1)-C(2)-C(3)	118.89(19)	C(4)-C(5)-N(1)	122.92(17)
C(1)-C(2)-H(21)	120.0	C(6)-C(5)-N(1)	117.14(17)
C(3)-C(2)-H(21)	121.1	C(5)-C(6)-C(7)	177.6(2)
C(2)-C(3)-C(4)	118.76(19)	C(6)-C(7)-C(8)	177.9(2)
C(2)-C(3)-H(31)	120.8	C(7)-C(8)-C(9)	121.24(18)
C(4)-C(3)-H(31)	120.4	C(7)-C(8)-C(13)	120.86(18)
C(3)-C(4)-C(5)	119.1(2)	C(9)-C(8)-C(13)	117.89(17)
		C(8)-C(9)-C(10)	121.09(18)

C(8)-C(9)-H(91)	120.0	C(17)-C(18)-H(181)	119.6
C(10)-C(9)-H(91)	118.9	C(19)-C(18)-H(181)	119.7
C(9)-C(10)-C(11)	121.35(18)	C(14)-C(19)-C(18)	120.56(19)
C(9)-C(10)-H(101)	120.5	C(14)-C(19)-H(191)	118.7
C(11)-C(10)-H(101)	118.1	C(18)-C(19)-H(191)	120.7
C(10)-C(11)-C(12)	117.44(17)	C(21)-C(20)-C(25)	119.86(18)
C(10)-C(11)-N(8)	121.89(17)	C(21)-C(20)-N(8)	119.17(17)
C(12)-C(11)-N(8)	120.67(17)	C(25)-C(20)-N(8)	120.95(17)
C(11)-C(12)-C(13)	121.01(18)	C(20)-C(21)-C(22)	120.4(2)
C(11)-C(12)-H(121)	119.1	C(20)-C(21)-H(211)	119.9
C(13)-C(12)-H(121)	119.9	C(22)-C(21)-H(211)	119.7
C(8)-C(13)-C(12)	121.21(18)	C(21)-C(22)-C(23)	119.82(19)
C(8)-C(13)-H(131)	119.0	C(21)-C(22)-H(221)	120.3
C(12)-C(13)-H(131)	119.8	C(23)-C(22)-H(221)	119.9
C(15)-C(14)-C(19)	118.75(18)	C(22)-C(23)-C(24)	119.97(19)
C(15)-C(14)-N(8)	121.34(18)	C(22)-C(23)-H(231)	120.8
C(19)-C(14)-N(8)	119.85(17)	C(24)-C(23)-H(231)	119.2
C(14)-C(15)-C(16)	120.30(19)	C(23)-C(24)-C(25)	120.30(19)
C(14)-C(15)-H(151)	119.6	C(23)-C(24)-H(241)	120.1
C(16)-C(15)-H(151)	120.1	C(25)-C(24)-H(241)	119.6
C(15)-C(16)-C(17)	120.3(2)	C(20)-C(25)-C(24)	119.68(18)
C(15)-C(16)-H(161)	119.5	C(20)-C(25)-H(251)	119.0
C(17)-C(16)-H(161)	120.2	C(24)-C(25)-H(251)	121.3
C(16)-C(17)-C(18)	119.39(19)	C(5)-N(1)-C(1)	117.56(16)
C(16)-C(17)-H(171)	120.8	C(20)-N(8)-C(14)	116.91(14)
C(18)-C(17)-H(171)	119.8	C(20)-N(8)-C(11)	120.27(15)
C(17)-C(18)-C(19)	120.65(19)	C(14)-N(8)-C(11)	
22.75(15)			

Symmetry transformations used to generate equivalent atoms: #1 -x,-y+1,-z+1

**Crystal data and structure refinement for Bis[6,6'-Bis(4-(N,N-diphenylamino)phenoxy)methyl)-2,2'-bipyridine]copper(I) hexafluorophosphate.**

Table 1. Crystal data and structure refinement for Bis[6,6'-Bis(4-(N,N-diphenylamino)phenoxy)methyl)-2,2'-bipyridine]copper(I) hexafluorophosphate.

Identification code	ValC-Cu1K1PF6	
Empirical formula	C100 H86 Cu1 F6 N8 O5 P1	
Formula weight	1688.34	
Temperature	173 K	
Wavelength	0.71073 Å	
Crystal system	Triclinic	
Space group	P -1	
Unit cell dimensions	a = 14.8634(2) Å	$\alpha = 105.1880(6)^\circ$
	b = 15.3994(2) Å	$\beta = 95.8722(8)^\circ$
	c = 19.9945(3) Å	$\gamma = 92.3113(8)^\circ$
Volume	4382.71(11) Å <sup>3</sup>	
Z	2	
Density (calculated)	1.279 Mg/m <sup>3</sup>	
Absorption coefficient	0.339 mm <sup>-1</sup>	
F(000)	1760	
Crystal size	0.50 x 0.10 x 0.07 mm <sup>3</sup>	
Theta range for data collection	1.949 to 26.391°.	
Index ranges	-17<=h<=18, -19<=k<=19, -25<=l<=25	
Reflections collected	34274	
Independent reflections	17922 [R(int) = 0.022]	
Completeness to theta = 26.391°	99.8 %	
Absorption correction	Semi-empirical from equivalents	
Max. and min. transmission	0.98 and 0.97	
Refinement method	Full-matrix least-squares on F <sup>2</sup>	
Data / restraints / parameters	11882 / 300 / 1186	

Goodness-of-fit on $F^2$	1.1008
Final R indices [ $I > 2\sigma(I)$ ]	$R1 = 0.0613$ , $wR2 = 0.0729$
R indices (all data)	$R1 = 0.0946$ , $wR2 = 0.1005$
Largest diff. peak and hole	0.77 and -0.44 $e.\text{\AA}^{-3}$

Table 2. Atomic coordinates ( $\times 10^4$ ) and equivalent isotropic displacement parameters ( $\text{\AA}^2 \times 10^3$ ) for Bis[6,6'-Bis(4-(*N,N*-diphenylamino)phenoxy)methyl]-2,2'-bipyridine]copper(I) hexafluorophosphate.

U(eq) is defined as one third of the trace of the orthogonalized  $U_{ij}$  tensor.

	<b>x</b>	<b>y</b>	<b>z</b>	<b>U(eq)</b>
Cu(1)	4671(1)	2106(1)	8012(1)	41
N(1)	5493(3)	5897(3)	6190(2)	83
N(2)	5503(2)	1179(2)	7506(1)	46
N(3)	4179(2)	981(1)	8246(1)	37
N(4)	630(2)	5093(2)	8909(2)	53
N(5)	8404(2)	-1100(2)	9023(1)	51
N(6)	5227(2)	3224(2)	8766(1)	38
N(7)	4052(2)	3079(2)	7652(1)	41
N(8)	969(3)	-620(4)	3860(2)	119
O(1)	5683(2)	2476(2)	6643(1)	72
O(2)	2592(1)	2024(1)	8376(1)	43
O(3)	6722(1)	2050(1)	8959(1)	47
O(4)	2288(2)	1973(2)	6343(1)	66
C(7)	6146(3)	6245(3)	5867(2)	75
C(8)	6130(5)	7134(4)	5814(3)	100
C(9)	6767(8)	7492(5)	5506(4)	135
C(10)	7440(6)	6979(7)	5247(4)	126
C(11)	7501(4)	6108(5)	5302(3)	109
C(12)	6831(3)	5744(4)	5613(3)	82
C(13)	5561(3)	5029(3)	6326(2)	72
C(14)	6197(3)	4890(3)	6832(2)	77
C(15)	6272(3)	4052(3)	6955(2)	73
C(16)	5685(3)	3329(3)	6567(2)	68
C(17)	5031(3)	3470(4)	6067(2)	81

C(18)	4972(3)	4300(4)	5946(2)	83
C(19)	6358(2)	2302(3)	7140(2)	64
C(20)	6194(2)	1346(3)	7163(2)	56
C(21)	6746(3)	658(4)	6875(2)	77
C(22)	6580(3)	-196(3)	6945(3)	81
C(23)	5886(2)	-365(3)	7296(2)	68
C(24)	5349(2)	340(2)	7578(2)	46
C(25)	4613(2)	233(2)	7994(2)	44
C(26)	4394(3)	-576(2)	8144(2)	64
C(27)	3719(3)	-619(2)	8558(3)	74
C(28)	3267(3)	146(2)	8816(2)	58
C(29)	3524(2)	933(2)	8653(2)	41
C(30)	3102(2)	1799(2)	8946(2)	43
C(31)	2159(2)	2806(2)	8541(2)	40
C(32)	1550(2)	2941(2)	8014(2)	47
C(33)	1054(2)	3699(2)	8135(2)	49
C(34)	1160(2)	4316(2)	8783(2)	47
C(35)	1770(2)	4186(2)	9302(2)	49
C(36)	2276(2)	3434(2)	9189(2)	45
C(37)	1084(2)	5946(2)	9008(2)	43
C(38)	795(2)	6712(2)	9461(2)	50
C(39)	1258(2)	7545(2)	9572(2)	54
C(40)	1998(2)	7640(2)	9241(2)	60
C(41)	2299(2)	6889(3)	8800(2)	61
C(42)	1847(2)	6044(2)	8681(2)	54
C(43)	-325(2)	4949(2)	8846(2)	46
C(44)	-711(2)	4217(2)	9024(2)	52
C(45)	-1639(2)	4040(3)	8939(2)	61
C(46)	-2199(2)	4598(3)	8686(2)	66
C(47)	-1830(2)	5345(3)	8529(2)	66
C(48)	-893(2)	5519(2)	8598(2)	58
C(49)	8562(3)	-1759(2)	8418(2)	53
C(50)	7891(3)	-2042(3)	7866(2)	70
C(51)	8061(4)	-2691(3)	7262(2)	91
C(52)	8904(5)	-3050(3)	7226(3)	96
C(53)	9565(4)	-2772(3)	7772(3)	82



C(54)	9410(3)	-2116(2)	8364(2)	62
C(55)	8763(2)	-1128(2)	9694(2)	44
C(56)	8991(2)	-333(2)	10215(2)	50
C(57)	9330(2)	-356(3)	10882(2)	60
C(58)	9457(2)	-1169(3)	11036(2)	60
C(59)	9240(2)	-1957(2)	10522(2)	51
C(60)	8883(2)	-1947(2)	9858(2)	48
C(61)	7906(2)	-340(2)	8955(2)	45
C(62)	7146(2)	-147(2)	9296(2)	45
C(63)	6720(2)	641(2)	9303(2)	45
C(64)	7062(2)	1238(2)	8964(2)	42
C(65)	7798(2)	1021(2)	8589(2)	48
C(66)	8217(2)	234(2)	8588(2)	49
C(67)	6056(2)	2351(2)	9423(2)	43
C(68)	5815(2)	3245(2)	9328(2)	41
C(69)	6196(2)	4048(2)	9782(2)	48
C(70)	5958(2)	4849(2)	9652(2)	53
C(71)	5353(2)	4834(2)	9082(2)	50
C(72)	4995(2)	4011(2)	8645(2)	41
C(73)	4326(2)	3930(2)	8027(2)	44
C(74)	4005(2)	4681(2)	7839(2)	57
C(75)	3377(3)	4548(3)	7262(2)	69
C(76)	3087(3)	3691(3)	6881(2)	64
C(77)	3441(2)	2965(2)	7088(2)	50
C(78)	3189(2)	2013(3)	6671(2)	59
C(79)	2019(3)	1307(3)	5741(2)	68
C(80)	1141(3)	1365(3)	5438(2)	73
C(81)	810(3)	721(4)	4828(2)	89
C(82)	1332(3)	26(4)	4506(2)	99
C(83)	2182(3)	4(4)	4812(3)	109
C(84)	2521(3)	626(4)	5435(2)	85
C(85)	1108(3)	-1575(5)	3742(3)	109
C(86)	1045(4)	-2097(5)	3040(3)	145
C(87)	1196(3)	-3004(5)	2914(3)	129
C(88)	1393(5)	-3425(6)	3440(4)	155
C(89)	1457(5)	-2876(5)	4097(4)	153

C(90)	1313(5)	-1967(5)	4270(4)	129
C(91)	355(4)	-280(5)	3422(2)	126
C(92)	601(6)	483(5)	3229(3)	159
C(93)	-25(6)	847(6)	2842(4)	173
C(94)	-905(6)	457(5)	2632(3)	161
C(95)	-1150(5)	-314(4)	2809(3)	133
C(96)	-526(4)	-677(4)	3194(2)	111
P(1)	4367(1)	2526(1)	10928(1)	53
F(1)	4175(2)	3444(2)	11469(1)	86
F(2)	4546(2)	1613(2)	10385(2)	95
F(3)	5415(2)	2741(3)	11179(2)	119
F(4)	3321(2)	2332(2)	10682(1)	82
F(5)	4469(2)	3045(1)	10340(1)	76
F(6)	4271(2)	2011(2)	11515(1)	75
C(204)	5000	0	5000	150
C(201)	3581(13)	-1102(13)	6010(10)	164
C(202)	4241(12)	-1180(8)	5486(10)	154
O(203)	4350(5)	-259(6)	5410(5)	122
C(205)	5056(11)	905(8)	4873(10)	157
C(206)	129(9)	7147(10)	5615(7)	120
C(207)	821(10)	6883(9)	6098(8)	99
O(208)	531(4)	5964(5)	6115(3)	87
C(209)	1195(9)	5658(11)	6578(9)	104
C(210)	761(9)	4843(10)	6693(9)	127
C(257)	288(17)	6166(12)	5435(7)	100
C(259)	574(17)	4975(8)	5987(9)	106
C(101)	4677(3)	6329(3)	6320(2)	97
C(102)	4418(6)	6540(6)	6985(5)	73
C(103)	3682(4)	7039(3)	7131(3)	115
C(104)	3273(8)	7376(7)	6588(5)	128
C(105)	3509(7)	7222(7)	5907(6)	130
C(106)	4257(6)	6700(6)	5787(5)	107
C(2)	4530(7)	6771(5)	6989(5)	75
C(4)	2917(6)	6833(5)	6664(5)	99
C(5)	3060(6)	6384(5)	5995(5)	102
C(6)	3902(5)	6101(5)	5831(5)	91

Table 3. Bond lengths [Å] and angles [°] for Bis[6,6'-Bis(4-(*N,N*-diphenylamino)phenoxy)methyl)-2,2'-bipyridine]copper(I) hexafluorophosphate.

Cu(1)-N(2)	2.058(3)	C(7)-C(8)	1.401(7)
Cu(1)-N(3)	2.036(2)	C(7)-C(12)	1.362(7)
Cu(1)-N(6)	2.047(2)	C(8)-C(9)	1.355(11)
Cu(1)-N(7)	2.037(2)	C(8)-H(81)	0.959
N(1)-C(7)	1.383(6)	C(9)-C(10)	1.360(11)
N(1)-C(13)	1.437(6)	C(9)-H(91)	0.960
N(1)-C(101)	1.422(6)	C(10)-C(11)	1.379(11)
N(2)-C(20)	1.344(4)	C(10)-H(101)	0.961
N(2)-C(24)	1.349(4)	C(11)-C(12)	1.399(7)
N(3)-C(25)	1.349(3)	C(11)-H(111)	0.960
N(3)-C(29)	1.343(4)	C(12)-H(121)	0.960
N(4)-C(34)	1.440(4)	C(13)-C(14)	1.378(6)
N(4)-C(37)	1.408(4)	C(13)-C(18)	1.393(6)
N(4)-C(43)	1.416(4)	C(14)-C(15)	1.383(6)
N(5)-C(49)	1.408(4)	C(14)-H(141)	0.960
N(5)-C(55)	1.404(4)	C(15)-C(16)	1.390(6)
N(5)-C(61)	1.439(4)	C(15)-H(151)	0.960
N(6)-C(68)	1.343(4)	C(16)-C(17)	1.388(6)
N(6)-C(72)	1.349(4)	C(17)-C(18)	1.367(7)
N(7)-C(73)	1.350(4)	C(17)-H(171)	0.960
N(7)-C(77)	1.342(4)	C(18)-H(181)	0.960
N(8)-C(82)	1.445(6)	C(19)-C(20)	1.495(6)
N(8)-C(85)	1.454(9)	C(19)-H(191)	0.960
N(8)-C(91)	1.411(9)	C(19)-H(192)	0.960
O(1)-C(16)	1.361(5)	C(20)-C(21)	1.405(6)
O(1)-C(19)	1.422(5)	C(21)-C(22)	1.374(7)
O(2)-C(30)	1.430(4)	C(21)-H(211)	0.960
O(2)-C(31)	1.368(3)	C(22)-C(23)	1.359(6)
O(3)-C(64)	1.369(3)	C(22)-H(221)	0.960
O(3)-C(67)	1.433(4)	C(23)-C(24)	1.405(4)
O(4)-C(78)	1.422(4)	C(23)-H(231)	0.960
O(4)-C(79)	1.372(4)	C(24)-C(25)	1.470(5)

C(25)-C(26)	1.389(5)	C(45)-H(451)	0.960
C(26)-C(27)	1.374(6)	C(46)-C(47)	1.377(6)
C(26)-H(261)	0.960	C(46)-H(461)	0.960
C(27)-C(28)	1.387(5)	C(47)-C(48)	1.393(5)
C(27)-H(271)	0.960	C(47)-H(471)	0.960
C(28)-C(29)	1.383(4)	C(48)-H(481)	0.960
C(28)-H(281)	0.960	C(49)-C(50)	1.375(6)
C(29)-C(30)	1.499(4)	C(49)-C(54)	1.398(5)
C(30)-H(301)	0.960	C(50)-C(51)	1.403(6)
C(30)-H(302)	0.960	C(50)-H(501)	0.960
C(31)-C(32)	1.381(4)	C(51)-C(52)	1.391(8)
C(31)-C(36)	1.389(4)	C(51)-H(511)	0.960
C(32)-C(33)	1.387(4)	C(52)-C(53)	1.357(8)
C(32)-H(321)	0.960	C(52)-H(521)	0.960
C(33)-C(34)	1.381(5)	C(53)-C(54)	1.387(6)
C(33)-H(331)	0.960	C(53)-H(531)	0.960
C(34)-C(35)	1.367(5)	C(54)-H(541)	0.960
C(35)-C(36)	1.389(4)	C(55)-C(56)	1.388(5)
C(35)-H(351)	0.960	C(55)-C(60)	1.396(4)
C(36)-H(361)	0.960	C(56)-C(57)	1.388(5)
C(37)-C(38)	1.398(4)	C(56)-H(561)	0.960
C(37)-C(42)	1.388(5)	C(57)-C(58)	1.380(5)
C(38)-C(39)	1.385(5)	C(57)-H(571)	0.960
C(38)-H(381)	0.960	C(58)-C(59)	1.372(5)
C(39)-C(40)	1.362(5)	C(58)-H(581)	0.960
C(39)-H(391)	0.960	C(59)-C(60)	1.383(5)
C(40)-C(41)	1.380(6)	C(59)-H(591)	0.960
C(40)-H(401)	0.960	C(60)-H(601)	0.960
C(41)-C(42)	1.390(5)	C(61)-C(62)	1.381(5)
C(41)-H(411)	0.960	C(61)-C(66)	1.382(5)
C(42)-H(421)	0.960	C(62)-C(63)	1.389(4)
C(43)-C(44)	1.388(5)	C(62)-H(621)	0.960
C(43)-C(48)	1.391(5)	C(63)-C(64)	1.386(4)
C(44)-C(45)	1.379(5)	C(63)-H(631)	0.960
C(44)-H(441)	0.960	C(64)-C(65)	1.391(4)
C(45)-C(46)	1.374(6)	C(65)-C(66)	1.385(4)

C(65)-H(651)	0.960	C(86)-H(861)	0.962
C(66)-H(661)	0.960	C(87)-C(88)	1.387(8)
C(67)-C(68)	1.491(4)	C(87)-H(871)	0.960
C(67)-H(671)	0.960	C(88)-C(89)	1.354(7)
C(67)-H(672)	0.960	C(88)-H(881)	0.960
C(68)-C(69)	1.387(4)	C(89)-C(90)	1.383(7)
C(69)-C(70)	1.377(5)	C(89)-H(891)	0.960
C(69)-H(691)	0.960	C(90)-H(901)	0.960
C(70)-C(71)	1.374(5)	C(91)-C(92)	1.376(7)
C(70)-H(701)	0.960	C(91)-C(96)	1.401(6)
C(71)-C(72)	1.387(4)	C(92)-C(93)	1.379(8)
C(71)-H(711)	0.960	C(92)-H(921)	0.960
C(72)-C(73)	1.479(4)	C(93)-C(94)	1.393(8)
C(73)-C(74)	1.393(4)	C(93)-H(931)	0.960
C(74)-C(75)	1.374(6)	C(94)-C(95)	1.371(7)
C(74)-H(741)	0.960	C(94)-H(941)	0.962
C(75)-C(76)	1.366(6)	C(95)-C(96)	1.374(7)
C(75)-H(751)	0.960	C(95)-H(951)	0.961
C(76)-C(77)	1.394(5)	C(96)-H(961)	0.960
C(76)-H(761)	0.960	P(1)-F(1)	1.594(2)
C(77)-C(78)	1.496(5)	P(1)-F(2)	1.587(2)
C(78)-H(781)	0.960	P(1)-F(3)	1.581(3)
C(78)-H(782)	0.960	P(1)-F(4)	1.574(2)
C(79)-C(80)	1.397(6)	P(1)-F(5)	1.602(2)
C(79)-C(84)	1.361(7)	P(1)-F(6)	1.592(2)
C(80)-C(81)	1.385(6)	C(204)-O(203)	1.438(7)
C(80)-H(801)	0.960	C(204)-C(205)	1.481(9)
C(81)-C(82)	1.404(8)	C(204)-H(2041)	0.960
C(81)-H(811)	0.960	C(204)-H(2042)	0.960
C(82)-C(83)	1.352(8)	C(201)-C(202)	1.493(9)
C(83)-C(84)	1.390(6)	C(201)-H(2011)	0.961
C(83)-H(831)	0.960	C(201)-H(2012)	0.959
C(84)-H(841)	0.960	C(201)-H(2013)	0.957
C(85)-C(86)	1.414(6)	C(202)-O(203)	1.470(9)
C(85)-C(90)	1.363(7)	C(202)-H(2021)	0.962
C(86)-C(87)	1.385(8)	C(202)-H(2022)	0.962

O(203)-H(2051)#1	1.069	C(210)-H(2603)	0.961
C(205)-H(2051)	0.961	C(257)-H(2571)	0.961
C(205)-H(2052)	0.958	C(257)-H(2572)	0.960
C(205)-H(2053)	0.961	C(259)-H(2591)	0.960
C(206)-C(207)	1.481(9)	C(259)-H(2592)	0.958
C(206)-C(257)	1.492(10)	C(101)-C(102)	1.383(8)
C(206)-H(2061)	0.960	C(101)-C(106)	1.436(8)
C(206)-H(2062)	0.958	C(101)-C(2)	1.377(8)
C(206)-H(2063)	0.961	C(101)-C(6)	1.401(7)
C(206)-H(2561)	0.960	C(102)-C(103)	1.374(9)
C(206)-H(2562)	0.961	C(102)-H(1021)	0.960
C(206)-H(2563)	0.958	C(103)-C(104)	1.415(9)
C(207)-O(208)	1.472(9)	C(103)-C(2)	1.376(9)
C(207)-H(2071)	0.959	C(103)-C(4)	1.366(8)
C(207)-H(2072)	0.962	C(103)-H(31)	0.960
O(208)-C(209)	1.461(9)	C(103)-H(1031)	0.960
O(208)-C(257)	1.486(10)	C(104)-C(105)	1.404(9)
O(208)-C(259)	1.483(10)	C(104)-H(1041)	0.961
C(209)-C(210)	1.470(9)	C(105)-C(106)	1.403(9)
C(209)-H(2091)	0.958	C(105)-H(1051)	0.960
C(209)-H(2092)	0.961	C(106)-H(1061)	0.960
C(210)-C(259)	1.479(10)	C(2)-H(21)	0.960
C(210)-H(2101)	0.961	C(4)-C(5)	1.377(8)
C(210)-H(2102)	0.961	C(4)-H(41)	0.960
C(210)-H(2103)	0.958	C(5)-C(6)	1.384(8)
C(210)-H(2601)	0.959	C(5)-H(51)	0.960
C(210)-H(2602)	0.962	C(6)-H(61)	0.960
N(2)-Cu(1)-N(3)	80.10(10)	C(13)-N(1)-C(101)	117.2(4)
N(2)-Cu(1)-N(6)	119.66(10)	Cu(1)-N(2)-C(20)	126.6(2)
N(3)-Cu(1)-N(6)	122.31(10)	Cu(1)-N(2)-C(24)	114.2(2)
N(2)-Cu(1)-N(7)	127.46(10)	C(20)-N(2)-C(24)	119.1(3)
N(3)-Cu(1)-N(7)	132.45(9)	Cu(1)-N(3)-C(25)	114.6(2)
N(6)-Cu(1)-N(7)	80.59(10)	Cu(1)-N(3)-C(29)	126.75(18)
C(7)-N(1)-C(13)	121.2(4)	C(25)-N(3)-C(29)	118.5(2)
C(7)-N(1)-C(101)	121.2(4)	C(34)-N(4)-C(37)	118.0(2)

C(34)-N(4)-C(43)	118.2(2)	N(1)-C(13)-C(14)	121.7(4)
C(37)-N(4)-C(43)	123.5(2)	N(1)-C(13)-C(18)	120.3(4)
C(49)-N(5)-C(55)	122.3(3)	C(14)-C(13)-C(18)	118.0(4)
C(49)-N(5)-C(61)	119.3(3)	C(13)-C(14)-C(15)	121.7(4)
C(55)-N(5)-C(61)	118.3(3)	C(13)-C(14)-H(141)	119.145
Cu(1)-N(6)-C(68)	127.18(19)	C(15)-C(14)-H(141)	119.131
Cu(1)-N(6)-C(72)	114.01(19)	C(14)-C(15)-C(16)	119.6(4)
C(68)-N(6)-C(72)	118.7(2)	C(14)-C(15)-H(151)	120.212
Cu(1)-N(7)-C(73)	114.1(2)	C(16)-C(15)-H(151)	120.220
Cu(1)-N(7)-C(77)	127.7(2)	C(15)-C(16)-O(1)	125.2(4)
C(73)-N(7)-C(77)	118.1(3)	C(15)-C(16)-C(17)	118.9(4)
C(82)-N(8)-C(85)	121.1(6)	O(1)-C(16)-C(17)	115.9(4)
C(82)-N(8)-C(91)	114.9(6)	C(16)-C(17)-C(18)	120.8(4)
C(85)-N(8)-C(91)	123.0(4)	C(16)-C(17)-H(171)	119.567
C(16)-O(1)-C(19)	117.3(3)	C(18)-C(17)-H(171)	119.600
C(30)-O(2)-C(31)	115.9(2)	C(13)-C(18)-C(17)	120.9(4)
C(64)-O(3)-C(67)	116.5(2)	C(13)-C(18)-H(181)	119.551
C(78)-O(4)-C(79)	118.9(3)	C(17)-C(18)-H(181)	119.527
N(1)-C(7)-C(8)	120.4(5)	O(1)-C(19)-C(20)	108.1(3)
N(1)-C(7)-C(12)	121.0(4)	O(1)-C(19)-H(191)	109.832
C(8)-C(7)-C(12)	118.6(5)	C(20)-C(19)-H(191)	109.828
C(7)-C(8)-C(9)	121.5(7)	O(1)-C(19)-H(192)	109.829
C(7)-C(8)-H(81)	119.232	C(20)-C(19)-H(192)	109.813
C(9)-C(8)-H(81)	119.272	H(191)-C(19)-H(192)	109.459
C(8)-C(9)-C(10)	119.1(6)	C(19)-C(20)-N(2)	116.2(3)
C(8)-C(9)-H(91)	120.453	C(19)-C(20)-C(21)	122.9(3)
C(10)-C(9)-H(91)	120.417	N(2)-C(20)-C(21)	120.8(4)
C(9)-C(10)-C(11)	121.7(6)	C(20)-C(21)-C(22)	119.8(4)
C(9)-C(10)-H(101)	119.173	C(20)-C(21)-H(211)	120.096
C(11)-C(10)-H(101)	119.104	C(22)-C(21)-H(211)	120.122
C(10)-C(11)-C(12)	118.4(7)	C(21)-C(22)-C(23)	119.5(3)
C(10)-C(11)-H(111)	120.795	C(21)-C(22)-H(221)	120.262
C(12)-C(11)-H(111)	120.782	C(23)-C(22)-H(221)	120.224
C(11)-C(12)-C(7)	120.6(5)	C(22)-C(23)-C(24)	119.1(4)
C(11)-C(12)-H(121)	119.708	C(22)-C(23)-H(231)	120.440
C(7)-C(12)-H(121)	119.704	C(24)-C(23)-H(231)	120.431

C(23)-C(24)-N(2)	121.7(3)	C(34)-C(35)-C(36)	120.8(3)
C(23)-C(24)-C(25)	123.0(3)	C(34)-C(35)-H(351)	119.601
N(2)-C(24)-C(25)	115.3(2)	C(36)-C(35)-H(351)	119.589
C(24)-C(25)-N(3)	115.8(3)	C(35)-C(36)-C(31)	119.5(3)
C(24)-C(25)-C(26)	122.6(3)	C(35)-C(36)-H(361)	120.268
N(3)-C(25)-C(26)	121.6(3)	C(31)-C(36)-H(361)	120.263
C(25)-C(26)-C(27)	119.5(3)	N(4)-C(37)-C(38)	120.7(3)
C(25)-C(26)-H(261)	120.253	N(4)-C(37)-C(42)	121.0(3)
C(27)-C(26)-H(261)	120.253	C(38)-C(37)-C(42)	118.3(3)
C(26)-C(27)-C(28)	119.2(3)	C(37)-C(38)-C(39)	120.4(3)
C(26)-C(27)-H(271)	120.406	C(37)-C(38)-H(381)	119.782
C(28)-C(27)-H(271)	120.393	C(39)-C(38)-H(381)	119.780
C(27)-C(28)-C(29)	118.5(3)	C(38)-C(39)-C(40)	121.0(3)
C(27)-C(28)-H(281)	120.762	C(38)-C(39)-H(391)	119.511
C(29)-C(28)-H(281)	120.766	C(40)-C(39)-H(391)	119.505
C(28)-C(29)-N(3)	122.8(3)	C(39)-C(40)-C(41)	119.3(3)
C(28)-C(29)-C(30)	121.4(3)	C(39)-C(40)-H(401)	120.356
N(3)-C(29)-C(30)	115.8(3)	C(41)-C(40)-H(401)	120.356
C(29)-C(30)-O(2)	107.3(2)	C(40)-C(41)-C(42)	120.8(3)
C(29)-C(30)-H(301)	110.019	C(40)-C(41)-H(411)	119.574
O(2)-C(30)-H(301)	110.027	C(42)-C(41)-H(411)	119.610
C(29)-C(30)-H(302)	110.027	C(41)-C(42)-C(37)	120.2(3)
O(2)-C(30)-H(302)	110.027	C(41)-C(42)-H(421)	119.923
H(301)-C(30)-H(302)	109.458	C(37)-C(42)-H(421)	119.920
O(2)-C(31)-C(32)	115.4(2)	N(4)-C(43)-C(44)	119.9(3)
O(2)-C(31)-C(36)	124.8(3)	N(4)-C(43)-C(48)	121.4(3)
C(32)-C(31)-C(36)	119.8(3)	C(44)-C(43)-C(48)	118.8(3)
C(31)-C(32)-C(33)	119.9(3)	C(43)-C(44)-C(45)	120.9(3)
C(31)-C(32)-H(321)	120.023	C(43)-C(44)-H(441)	119.545
C(33)-C(32)-H(321)	120.035	C(45)-C(44)-H(441)	119.560
C(32)-C(33)-C(34)	120.3(3)	C(44)-C(45)-C(46)	120.3(3)
C(32)-C(33)-H(331)	119.850	C(44)-C(45)-H(451)	119.854
C(34)-C(33)-H(331)	119.876	C(46)-C(45)-H(451)	119.842
N(4)-C(34)-C(33)	120.0(3)	C(45)-C(46)-C(47)	119.6(3)
N(4)-C(34)-C(35)	120.3(3)	C(45)-C(46)-H(461)	120.194
C(33)-C(34)-C(35)	119.7(3)	C(47)-C(46)-H(461)	120.195



C(46)-C(47)-C(48)	120.6(3)	C(58)-C(59)-C(60)	120.8(3)
C(46)-C(47)-H(471)	119.685	C(58)-C(59)-H(591)	119.568
C(48)-C(47)-H(471)	119.706	C(60)-C(59)-H(591)	119.584
C(47)-C(48)-C(43)	119.8(3)	C(55)-C(60)-C(59)	120.3(3)
C(47)-C(48)-H(481)	120.114	C(55)-C(60)-H(601)	119.828
C(43)-C(48)-H(481)	120.120	C(59)-C(60)-H(601)	119.826
N(5)-C(49)-C(50)	120.4(3)	N(5)-C(61)-C(62)	119.9(3)
N(5)-C(49)-C(54)	120.4(3)	N(5)-C(61)-C(66)	120.3(3)
C(50)-C(49)-C(54)	119.2(3)	C(62)-C(61)-C(66)	119.6(3)
C(49)-C(50)-C(51)	119.8(4)	C(61)-C(62)-C(63)	120.6(3)
C(49)-C(50)-H(501)	120.078	C(61)-C(62)-H(621)	119.714
C(51)-C(50)-H(501)	120.110	C(63)-C(62)-H(621)	119.721
C(50)-C(51)-C(52)	120.0(5)	C(62)-C(63)-C(64)	119.6(3)
C(50)-C(51)-H(511)	120.035	C(62)-C(63)-H(631)	120.224
C(52)-C(51)-H(511)	120.011	C(64)-C(63)-H(631)	120.225
C(51)-C(52)-C(53)	120.2(4)	C(63)-C(64)-O(3)	124.7(3)
C(51)-C(52)-H(521)	119.917	C(63)-C(64)-C(65)	119.9(3)
C(53)-C(52)-H(521)	119.845	O(3)-C(64)-C(65)	115.4(3)
C(52)-C(53)-C(54)	120.1(5)	C(64)-C(65)-C(66)	119.8(3)
C(52)-C(53)-H(531)	119.933	C(64)-C(65)-H(651)	120.079
C(54)-C(53)-H(531)	119.944	C(66)-C(65)-H(651)	120.096
C(49)-C(54)-C(53)	120.6(4)	C(65)-C(66)-C(61)	120.4(3)
C(49)-C(54)-H(541)	119.651	C(65)-C(66)-H(661)	119.822
C(53)-C(54)-H(541)	119.702	C(61)-C(66)-H(661)	119.827
N(5)-C(55)-C(56)	120.1(3)	O(3)-C(67)-C(68)	105.8(2)
N(5)-C(55)-C(60)	121.4(3)	O(3)-C(67)-H(671)	110.378
C(56)-C(55)-C(60)	118.5(3)	C(68)-C(67)-H(671)	110.371
C(55)-C(56)-C(57)	120.3(3)	O(3)-C(67)-H(672)	110.372
C(55)-C(56)-H(561)	119.827	C(68)-C(67)-H(672)	110.371
C(57)-C(56)-H(561)	119.826	H(671)-C(67)-H(672)	109.466
C(56)-C(57)-C(58)	120.6(3)	C(67)-C(68)-N(6)	115.9(2)
C(56)-C(57)-H(571)	119.687	C(67)-C(68)-C(69)	121.9(3)
C(58)-C(57)-H(571)	119.685	N(6)-C(68)-C(69)	122.2(3)
C(57)-C(58)-C(59)	119.3(3)	C(68)-C(69)-C(70)	118.7(3)
C(57)-C(58)-H(581)	120.373	C(68)-C(69)-H(691)	120.650
C(59)-C(58)-H(581)	120.355	C(70)-C(69)-H(691)	120.668

C(69)-C(70)-C(71)	119.5(3)	C(80)-C(81)-C(82)	122.0(4)
C(69)-C(70)-H(701)	120.232	C(80)-C(81)-H(811)	119.020
C(71)-C(70)-H(701)	120.237	C(82)-C(81)-H(811)	118.975
C(70)-C(71)-C(72)	119.3(3)	N(8)-C(82)-C(81)	120.3(5)
C(70)-C(71)-H(711)	120.375	N(8)-C(82)-C(83)	122.1(6)
C(72)-C(71)-H(711)	120.367	C(81)-C(82)-C(83)	117.5(4)
C(71)-C(72)-N(6)	121.6(3)	C(82)-C(83)-C(84)	121.6(5)
C(71)-C(72)-C(73)	123.0(3)	C(82)-C(83)-H(831)	119.218
N(6)-C(72)-C(73)	115.4(2)	C(84)-C(83)-H(831)	119.188
C(72)-C(73)-N(7)	115.6(2)	C(83)-C(84)-C(79)	120.7(5)
C(72)-C(73)-C(74)	122.3(3)	C(83)-C(84)-H(841)	119.650
N(7)-C(73)-C(74)	122.1(3)	C(79)-C(84)-H(841)	119.642
C(73)-C(74)-C(75)	118.7(3)	N(8)-C(85)-C(86)	116.9(7)
C(73)-C(74)-H(741)	120.681	N(8)-C(85)-C(90)	123.0(5)
C(75)-C(74)-H(741)	120.659	C(86)-C(85)-C(90)	120.1(7)
C(74)-C(75)-C(76)	119.9(3)	C(85)-C(86)-C(87)	118.0(7)
C(74)-C(75)-H(751)	120.037	C(85)-C(86)-H(861)	120.976
C(76)-C(75)-H(751)	120.070	C(87)-C(86)-H(861)	121.016
C(75)-C(76)-C(77)	118.9(3)	C(86)-C(87)-C(88)	123.3(6)
C(75)-C(76)-H(761)	120.535	C(86)-C(87)-H(871)	118.361
C(77)-C(76)-H(761)	120.554	C(88)-C(87)-H(871)	118.364
C(76)-C(77)-N(7)	122.3(3)	C(87)-C(88)-C(89)	115.1(8)
C(76)-C(77)-C(78)	121.4(3)	C(87)-C(88)-H(881)	122.473
N(7)-C(77)-C(78)	116.2(3)	C(89)-C(88)-H(881)	122.474
C(77)-C(78)-O(4)	107.9(3)	C(88)-C(89)-C(90)	125.5(9)
C(77)-C(78)-H(781)	109.867	C(88)-C(89)-H(891)	117.228
O(4)-C(78)-H(781)	109.870	C(90)-C(89)-H(891)	117.256
C(77)-C(78)-H(782)	109.873	C(89)-C(90)-C(85)	118.0(7)
O(4)-C(78)-H(782)	109.880	C(89)-C(90)-H(901)	120.946
H(781)-C(78)-H(782)	109.463	C(85)-C(90)-H(901)	121.005
O(4)-C(79)-C(80)	114.2(4)	N(8)-C(91)-C(92)	120.1(5)
O(4)-C(79)-C(84)	126.1(4)	N(8)-C(91)-C(96)	121.8(5)
C(80)-C(79)-C(84)	119.7(4)	C(92)-C(91)-C(96)	118.1(7)
C(79)-C(80)-C(81)	118.4(5)	C(91)-C(92)-C(93)	119.7(6)
C(79)-C(80)-H(801)	120.813	C(91)-C(92)-H(921)	120.195
C(81)-C(80)-H(801)	120.785	C(93)-C(92)-H(921)	120.122

C(92)-C(93)-C(94)	121.7(7)	C(202)-C(201)-H(2013)	109.384
C(92)-C(93)-H(931)	119.183	H(2011)-C(201)-H(2013)	109.639
C(94)-C(93)-H(931)	119.140	H(2012)-C(201)-H(2013)	109.798
C(93)-C(94)-C(95)	119.0(7)	C(201)-C(202)-O(203)	103.4(12)
C(93)-C(94)-H(941)	120.497	C(201)-C(202)-H(2021)	111.227
C(95)-C(94)-H(941)	120.495	O(203)-C(202)-H(2021)	110.881
C(94)-C(95)-C(96)	119.3(6)	C(201)-C(202)-H(2022)	111.169
C(94)-C(95)-H(951)	120.348	O(203)-C(202)-H(2022)	110.891
C(96)-C(95)-H(951)	120.348	H(2021)-C(202)-H(2022)	109.189
C(91)-C(96)-C(95)	122.2(6)	C(202)-O(203)-C(204)	122.6(9)
C(91)-C(96)-H(961)	118.900	C(204)-C(205)-H(2051)	109.381
C(95)-C(96)-H(961)	118.899	C(204)-C(205)-H(2052)	109.593
F(1)-P(1)-F(2)	179.28(18)	H(2051)-C(205)-H(2052)	109.512
F(1)-P(1)-F(3)	89.07(19)	C(204)-C(205)-H(2053)	109.441
F(2)-P(1)-F(3)	91.61(19)	H(2051)-C(205)-H(2053)	109.306
F(1)-P(1)-F(4)	90.04(16)	H(2052)-C(205)-H(2053)	109.594
F(2)-P(1)-F(4)	89.28(16)	C(207)-C(206)-H(2061)	109.398
F(3)-P(1)-F(4)	178.97(19)	C(207)-C(206)-H(2062)	109.476
F(1)-P(1)-F(5)	90.65(13)	H(2061)-C(206)-H(2062)	109.669
F(2)-P(1)-F(5)	89.13(14)	C(207)-C(206)-H(2063)	109.379
F(3)-P(1)-F(5)	89.24(17)	H(2061)-C(206)-H(2063)	109.351
F(4)-P(1)-F(5)	90.24(14)	H(2062)-C(206)-H(2063)	109.553
F(1)-P(1)-F(6)	89.40(13)	C(257)-C(206)-H(2561)	109.359
F(2)-P(1)-F(6)	90.82(14)	C(257)-C(206)-H(2562)	109.335
F(3)-P(1)-F(6)	90.51(17)	C(257)-C(206)-H(2563)	109.500
F(4)-P(1)-F(6)	90.01(14)	H(2061)-C(206)-H(2563)	101.285
F(5)-P(1)-F(6)	179.75(15)	H(2561)-C(206)-H(2562)	109.373
O(203)-C(204)-C(205)	122.6(7)	H(2561)-C(206)-H(2563)	109.652
O(203)-C(204)-H(2041)	106.079	H(2562)-C(206)-H(2563)	109.608
O(203)-C(204)-H(2042)	106.084	C(206)-C(207)-O(208)	106.4(10)
C(205)-C(204)-H(2041)	106.064	C(206)-C(207)-H(2071)	110.311
C(205)-C(204)-H(2042)	106.162	O(208)-C(207)-H(2071)	110.294
H(2041)-C(204)-H(2042)	109.467	C(206)-C(207)-H(2072)	110.256
C(202)-C(201)-H(2011)	109.216	O(208)-C(207)-H(2072)	110.092
C(202)-C(201)-H(2012)	109.288	H(2071)-C(207)-H(2072)	109.415
H(2011)-C(201)-H(2012)	109.500	C(207)-O(208)-C(209)	109.1(9)

C(257)-O(208)-C(259)	108.3(11)	N(1)-C(101)-C(106)	117.3(6)
O(208)-C(209)-C(210)	105.6(10)	C(102)-C(101)-C(106)	121.6(7)
O(208)-C(209)-H(2091)	110.499	N(1)-C(101)-C(2)	120.6(6)
C(210)-C(209)-H(2091)	110.633	C(106)-C(101)-C(2)	114.7(7)
O(208)-C(209)-H(2092)	110.306	N(1)-C(101)-C(6)	121.1(5)
C(210)-C(209)-H(2092)	110.285	C(102)-C(101)-C(6)	109.2(7)
H(2091)-C(209)-H(2092)	109.510	C(2)-C(101)-C(6)	115.6(7)
C(209)-C(210)-H(2101)	109.409	C(101)-C(102)-C(103)	120.1(8)
C(209)-C(210)-H(2102)	109.326	C(101)-C(102)-H(1021)	119.953
C(259)-C(210)-H(2102)	104.827	C(103)-C(102)-H(1021)	119.962
H(2101)-C(210)-H(2102)	109.302	C(102)-C(103)-C(104)	116.4(8)
C(209)-C(210)-H(2103)	109.673	C(104)-C(103)-C(2)	110.0(8)
H(2101)-C(210)-H(2103)	109.591	C(102)-C(103)-C(4)	118.4(7)
H(2102)-C(210)-H(2103)	109.525	C(2)-C(103)-C(4)	125.0(7)
C(259)-C(210)-H(2601)	109.620	C(102)-C(103)-H(31)	121.743
H(2102)-C(210)-H(2601)	104.364	C(104)-C(103)-H(31)	114.837
C(209)-C(210)-H(2602)	103.728	C(2)-C(103)-H(31)	117.515
C(259)-C(210)-H(2602)	109.552	C(4)-C(103)-H(31)	117.493
H(2101)-C(210)-H(2602)	105.119	C(102)-C(103)-H(1031)	121.814
C(259)-C(210)-H(2603)	109.502	C(104)-C(103)-H(1031)	121.784
H(2601)-C(210)-H(2602)	109.399	C(2)-C(103)-H(1031)	126.009
H(2601)-C(210)-H(2603)	109.478	C(4)-C(103)-H(1031)	103.976
H(2602)-C(210)-H(2603)	109.277	C(103)-C(104)-C(105)	127.2(11)
C(206)-C(257)-O(208)	105.1(11)	C(103)-C(104)-H(1041)	116.415
C(206)-C(257)-H(2571)	110.651	C(105)-C(104)-H(1041)	116.370
O(208)-C(257)-H(2571)	110.482	C(104)-C(105)-C(106)	113.7(11)
C(206)-C(257)-H(2572)	110.577	C(104)-C(105)-H(1051)	123.185
O(208)-C(257)-H(2572)	110.551	C(106)-C(105)-H(1051)	123.106
H(2571)-C(257)-H(2572)	109.390	C(101)-C(106)-C(105)	120.6(9)
O(208)-C(259)-C(210)	103.9(11)	C(101)-C(106)-H(1061)	119.699
O(208)-C(259)-H(2591)	110.797	C(105)-C(106)-H(1061)	119.720
C(210)-C(259)-H(2591)	110.651	C(101)-C(2)-C(103)	120.4(8)
O(208)-C(259)-H(2592)	110.959	C(101)-C(2)-H(21)	119.802
C(210)-C(259)-H(2592)	110.781	C(103)-C(2)-H(21)	119.813
H(2591)-C(259)-H(2592)	109.606	C(103)-C(4)-C(5)	114.5(8)
N(1)-C(101)-C(102)	119.7(6)	C(103)-C(4)-H(41)	122.767

C(5)-C(4)-H(41)	122.739	C(101)-C(6)-C(5)	121.9(8)
C(4)-C(5)-C(6)	122.1(9)	C(101)-C(6)-H(61)	119.063
C(4)-C(5)-H(51)	118.982	C(5)-C(6)-H(61)	119.068
C(6)-C(5)-H(51)	118.911		

Symmetry transformations used to generate equivalent atoms:

#1 -x+1,-y,-z+1

**Crystal data and structure refinement for Bis[6-(4-(*N,N*-Diphenylamino)phenoxy)methyl)-6'-methyl-2,2'-bipyridine]copper(I) hexafluorophosphate.**

Table 1. Crystal data and structure refinement for Bis[6-(4-(*N,N*-Diphenylamino)phenoxy)methyl)-6'-methyl-2,2'-bipyridine]copper(I) hexafluorophosphate.

Identification code	ValC-K5_173k	
Empirical formula	C <sub>60</sub> H <sub>50</sub> Cu <sub>1</sub> F <sub>6</sub> N <sub>6</sub> O <sub>2</sub> P <sub>1</sub>	
Formula weight	1095.60	
Temperature	173 K	
Wavelength	0.71073 Å	
Crystal system	Orthorhombic	
Space group	P c a n	
Unit cell dimensions	a = 10.9516(2) Å	α = 90°
	b = 16.2294(3) Å	β = 90°
	c = 29.4099(7) Å	γ = 90°
Volume	5227.25(18) Å <sup>3</sup>	
Z	4	
Density (calculated)	1.392 Mg/m <sup>3</sup>	
Absorption coefficient	0.521 mm <sup>-1</sup>	
F(000)	2264	
Crystal size	0.31 x 0.20 x 0.05 mm <sup>3</sup>	
Theta range for data collection	1.869 to 27.477°.	
Index ranges	-14 ≤ h ≤ 14, -20 ≤ k ≤ 21, -38 ≤ l ≤ 38	
Reflections collected	35240	
Independent reflections	5967 [R(int) = 0.067]	
Completeness to theta = 27.477°	99.5 %	

Absorption correction	Semi-empirical from equivalents
Max. and min. transmission	0.97 and 0.90
Refinement method	Full-matrix least-squares on F <sup>2</sup>
Data / restraints / parameters	5904 / 96 / 344
Goodness-of-fit on F <sup>2</sup>	1.0623
Final R indices [I > 2σ(I)]	R1 = 0.0415, wR2 = 0.1015
R indices (all data)	R1 = 0.0858, wR2 = 0.1493
Largest diff. peak and hole	0.44 and -0.46 e.Å <sup>-3</sup>

Table 2. Atomic coordinates (x 10<sup>4</sup>) and equivalent isotropic displacement parameters (Å<sup>2</sup>x 10<sup>3</sup>) for Bis[6-(4-(*N,N*-Diphenylamino)phenoxy)methyl]-6'-methyl-2,2'-bipyridine]copper(I) hexafluorophosphate  
U(eq) is defined as one third of the trace of the orthogonalized Uij tensor.

	<b>x</b>	<b>y</b>	<b>z</b>	<b>U(eq)</b>
C(1)	3976(3)	4982(2)	8226(1)	66
C(2)	4402(3)	5840(2)	8138(1)	55
C(3)	3876(4)	6526(3)	8345(1)	69
C(4)	4312(4)	7294(3)	8243(2)	76
C(5)	5272(4)	7387(2)	7944(1)	66
C(6)	5757(3)	6684(2)	7744(1)	48
C(7)	6742(3)	6713(2)	7399(1)	48
C(8)	7353(4)	7434(2)	7278(1)	63
C(9)	8218(4)	7412(3)	6942(2)	75
C(10)	8442(4)	6678(2)	6718(1)	65
C(11)	7809(3)	5979(2)	6850(1)	50
C(12)	7942(3)	5184(2)	6594(1)	52
C(13)	6782(3)	4468(2)	6023(1)	54
C(14)	7642(4)	3854(2)	5982(1)	58
C(15)	7405(4)	3182(2)	5699(1)	65
C(16)	6313(4)	3113(2)	5468(1)	61
C(17)	5442(4)	3738(2)	5514(1)	65
C(18)	5695(4)	4413(2)	5782(1)	65
C(19)	6297(4)	1614(2)	5346(1)	75
C(20)	6075(4)	1409(3)	5795(2)	75
C(21)	6286(5)	608(3)	5948(2)	89

C(22)	6763(7)	35(3)	5651(2)	124
C(23)	7018(8)	235(3)	5206(2)	138
C(24)	6768(7)	1021(3)	5053(2)	117
C(25)	5520(4)	2553(2)	4755(1)	61
C(26)	4606(5)	2077(4)	4593(2)	107
C(27)	4058(5)	2267(4)	4170(2)	112
C(28)	4468(5)	2908(3)	3924(2)	90
C(29)	5421(6)	3352(3)	4084(2)	106
C(30)	5912(5)	3191(3)	4491(1)	87
N(1)	5323(2)	5925(2)	7842(1)	46
N(2)	6992(2)	5987(1)	7192(1)	43
N(3)	6067(4)	2419(2)	5184(1)	78
Cu(1)	6154(1)	5000	7500	48
P(1)	719(1)	5000	7500	56
F(3)	1747(2)	5633(1)	7663(1)	80
O(1)	6915(2)	5157(1)	6290(1)	62
F(5)	-315(2)	4371(2)	7338(1)	83
F(1)	726(2)	5418(2)	7009(1)	83

Table 3. Bond lengths [Å] and angles [°] for Bis[6-(4-(*N,N*-Diphenylamino)phenoxy)methyl)-6'-methyl-2,2'-bipyridine]copper(I) hexafluorophosphate

C(1)-C(2)	1.492(5)	C(7)-C(8)	1.395(5)
C(1)-H(11)	0.986	C(7)-N(2)	1.355(4)
C(1)-H(12)	0.977	C(8)-C(9)	1.369(6)
C(1)-H(13)	0.999	C(8)-H(81)	0.933
C(2)-C(3)	1.394(5)	C(9)-C(10)	1.383(6)
C(2)-N(1)	1.339(4)	C(9)-H(91)	0.962
C(3)-C(4)	1.368(6)	C(10)-C(11)	1.384(5)
C(3)-H(31)	0.970	C(10)-H(101)	0.959
C(4)-C(5)	1.379(6)	C(11)-C(12)	1.501(4)
C(4)-H(41)	0.940	C(11)-N(2)	1.346(4)
C(5)-C(6)	1.388(5)	C(12)-O(1)	1.438(4)
C(5)-H(51)	0.943	C(12)-H(121)	0.992
C(6)-C(7)	1.482(5)	C(12)-H(122)	0.996
C(6)-N(1)	1.352(4)	C(13)-C(14)	1.377(5)

C(13)-C(18)	1.389(5)	C(24)-H(241)	0.960
C(13)-O(1)	1.374(4)	C(25)-C(26)	1.351(5)
C(14)-C(15)	1.396(5)	C(25)-C(30)	1.363(5)
C(14)-H(141)	0.967	C(25)-N(3)	1.415(5)
C(15)-C(16)	1.380(6)	C(26)-C(27)	1.415(6)
C(15)-H(151)	0.962	C(26)-H(261)	0.945
C(16)-C(17)	1.400(5)	C(27)-C(28)	1.344(6)
C(16)-N(3)	1.428(5)	C(27)-H(271)	0.946
C(17)-C(18)	1.377(5)	C(28)-C(29)	1.352(6)
C(17)-H(171)	0.978	C(28)-H(281)	0.945
C(18)-H(181)	0.948	C(29)-C(30)	1.339(6)
C(19)-C(20)	1.384(5)	C(29)-H(291)	0.973
C(19)-C(24)	1.391(6)	C(30)-H(301)	0.968
C(19)-N(3)	1.413(5)	N(1)-Cu(1)	2.023(2)
C(20)-C(21)	1.396(5)	N(2)-Cu(1)	2.057(3)
C(20)-H(201)	0.986	P(1)-F(3)#1	1.598(2)
C(21)-C(22)	1.378(6)	P(1)-F(5)#1	1.596(2)
C(21)-H(211)	0.959	P(1)-F(1)#1	1.595(2)
C(22)-C(23)	1.377(7)	P(1)-F(3)	1.598(2)
C(22)-H(221)	0.974	P(1)-F(5)	1.596(2)
C(23)-C(24)	1.381(6)	P(1)-F(1)	1.595(2)
C(23)-H(231)	0.949		
C(2)-C(1)-H(11)	113.3	C(3)-C(4)-H(41)	120.1
C(2)-C(1)-H(12)	110.9	C(5)-C(4)-H(41)	119.5
H(11)-C(1)-H(12)	104.9	C(4)-C(5)-C(6)	118.1(4)
C(2)-C(1)-H(13)	113.1	C(4)-C(5)-H(51)	121.9
H(11)-C(1)-H(13)	107.5	C(6)-C(5)-H(51)	120.0
H(12)-C(1)-H(13)	106.5	C(5)-C(6)-C(7)	122.8(3)
C(1)-C(2)-C(3)	122.7(4)	C(5)-C(6)-N(1)	121.6(3)
C(1)-C(2)-N(1)	116.4(3)	C(7)-C(6)-N(1)	115.5(3)
C(3)-C(2)-N(1)	120.9(3)	C(6)-C(7)-C(8)	123.4(3)
C(2)-C(3)-C(4)	119.1(4)	C(6)-C(7)-N(2)	115.3(3)
C(2)-C(3)-H(31)	118.4	C(8)-C(7)-N(2)	121.3(3)
C(4)-C(3)-H(31)	122.5	C(7)-C(8)-C(9)	119.6(3)
C(3)-C(4)-C(5)	120.4(4)	C(7)-C(8)-H(81)	119.5



C(9)-C(8)-H(81)	120.9	C(24)-C(19)-N(3)	119.8(4)
C(8)-C(9)-C(10)	119.3(4)	C(19)-C(20)-C(21)	120.1(5)
C(8)-C(9)-H(91)	120.9	C(19)-C(20)-H(201)	117.7
C(10)-C(9)-H(91)	119.8	C(21)-C(20)-H(201)	122.2
C(9)-C(10)-C(11)	118.9(4)	C(20)-C(21)-C(22)	119.1(5)
C(9)-C(10)-H(101)	120.9	C(20)-C(21)-H(211)	118.2
C(11)-C(10)-H(101)	120.2	C(22)-C(21)-H(211)	122.7
C(10)-C(11)-C(12)	121.0(3)	C(21)-C(22)-C(23)	121.4(5)
C(10)-C(11)-N(2)	122.3(3)	C(21)-C(22)-H(221)	119.7
C(12)-C(11)-N(2)	116.6(3)	C(23)-C(22)-H(221)	118.8
C(11)-C(12)-O(1)	105.3(3)	C(22)-C(23)-C(24)	119.2(5)
C(11)-C(12)-H(121)	113.1	C(22)-C(23)-H(231)	118.2
O(1)-C(12)-H(121)	108.5	C(24)-C(23)-H(231)	122.7
C(11)-C(12)-H(122)	109.5	C(19)-C(24)-C(23)	120.7(5)
O(1)-C(12)-H(122)	108.7	C(19)-C(24)-H(241)	121.2
H(121)-C(12)-H(122)	111.5	C(23)-C(24)-H(241)	118.1
C(14)-C(13)-C(18)	119.7(3)	C(26)-C(25)-C(30)	117.9(4)
C(14)-C(13)-O(1)	124.6(3)	C(26)-C(25)-N(3)	122.6(4)
C(18)-C(13)-O(1)	115.8(3)	C(30)-C(25)-N(3)	119.5(4)
C(13)-C(14)-C(15)	119.4(4)	C(25)-C(26)-C(27)	119.9(5)
C(13)-C(14)-H(141)	119.6	C(25)-C(26)-H(261)	118.9
C(15)-C(14)-H(141)	121.0	C(27)-C(26)-H(261)	121.2
C(14)-C(15)-C(16)	121.2(3)	C(26)-C(27)-C(28)	120.0(5)
C(14)-C(15)-H(151)	119.7	C(26)-C(27)-H(271)	120.9
C(16)-C(15)-H(151)	119.1	C(28)-C(27)-H(271)	119.0
C(15)-C(16)-C(17)	119.0(3)	C(27)-C(28)-C(29)	118.9(4)
C(15)-C(16)-N(3)	121.0(3)	C(27)-C(28)-H(281)	120.3
C(17)-C(16)-N(3)	120.0(4)	C(29)-C(28)-H(281)	120.9
C(16)-C(17)-C(18)	119.6(4)	C(28)-C(29)-C(30)	121.1(5)
C(16)-C(17)-H(171)	120.4	C(28)-C(29)-H(291)	119.7
C(18)-C(17)-H(171)	120.0	C(30)-C(29)-H(291)	119.2
C(13)-C(18)-C(17)	121.1(4)	C(25)-C(30)-C(29)	122.1(5)
C(13)-C(18)-H(181)	119.9	C(25)-C(30)-H(301)	120.9
C(17)-C(18)-H(181)	119.0	C(29)-C(30)-H(301)	117.1
C(20)-C(19)-C(24)	119.4(4)	C(6)-N(1)-C(2)	119.8(3)
C(20)-C(19)-N(3)	120.8(4)	C(6)-N(1)-Cu(1)	114.4(2)

C(2)-N(1)-Cu(1)	125.9(2)	F(5)#1-P(1)-F(1)#1	90.35(14)
C(7)-N(2)-C(11)	118.6(3)	F(3)#1-P(1)-F(3)	90.40(19)
C(7)-N(2)-Cu(1)	112.9(2)	F(5)#1-P(1)-F(3)	89.97(13)
C(11)-N(2)-Cu(1)	128.2(2)	F(1)#1-P(1)-F(3)	89.98(14)
C(16)-N(3)-C(25)	118.7(3)	F(3)#1-P(1)-F(5)	89.97(13)
C(16)-N(3)-C(19)	119.9(3)	F(5)#1-P(1)-F(5)	89.7(2)
C(25)-N(3)-C(19)	121.2(3)	F(1)#1-P(1)-F(5)	90.06(14)
N(2)-Cu(1)-N(2)#1	126.96(15)	F(3)-P(1)-F(5)	179.63(15)
N(2)-Cu(1)-N(1)#1	124.02(10)	F(3)#1-P(1)-F(1)	89.98(14)
N(2)#1-Cu(1)-N(1)#1	80.92(10)	F(5)#1-P(1)-F(1)	90.06(14)
N(2)-Cu(1)-N(1)	80.92(10)	F(1)#1-P(1)-F(1)	179.4(2)
N(2)#1-Cu(1)-N(1)	124.02(10)	F(3)-P(1)-F(1)	89.62(14)
N(1)#1-Cu(1)-N(1)	126.56(15)	F(5)-P(1)-F(1)	90.35(14)
F(3)#1-P(1)-F(5)#1	179.63(15)	C(12)-O(1)-C(13)	117.5(3)
F(3)#1-P(1)-F(1)#1	89.62(14)		

Symmetry transformations used to generate equivalent atoms:

#1  $x, -y+1, -z+3/2$

### **Crystal data and structure refinement for Bis[2-(4-Methoxyphenyl)-1,10-phenanthroline]copper(I) hexafluorophosphate.**

Table 1. Crystal data and structure refinement for Bis[2-(4-Methoxyphenyl)-1,10-phenanthroline]copper(I) hexafluorophosphate.

Identification code	chaurinCuHe	
Empirical formula	C <sub>38</sub> H <sub>28</sub> Cu <sub>1</sub> F <sub>6</sub> N <sub>4</sub> O <sub>2</sub> P <sub>1</sub>	
Formula weight	781.17	
Temperature	173 K	
Wavelength	0.71073 Å	
Crystal system	Triclinic	
Space group	P -1	
Unit cell dimensions	a = 10.1491(3) Å	$\alpha = 71.8196(16)^\circ$
	b = 11.4654(3) Å	$\beta = 82.5003(13)^\circ$
	c = 15.1523(4) Å	$\gamma = 82.8793(17)^\circ$
Volume	1654.33(8) Å <sup>3</sup>	

Z	2
Density (calculated)	1.568 Mg/m <sup>3</sup>
Absorption coefficient	0.785 mm <sup>-1</sup>
F(000)	796
Crystal size	0.28 x 0.22 x 0.04 mm <sup>3</sup>
Theta range for data collection	2.364 to 27.486°.
Index ranges	-13<=h<=13, -13<=k<=14, -19<=l<=19
Reflections collected	14503
Independent reflections	7534 [R(int) = 0.016]
Completeness to theta = 26.936°	99.9 %
Absorption correction	Semi-empirical from equivalents
Max. and min. transmission	0.97 and 0.84
Refinement method	Full-matrix least-squares on F <sup>2</sup>
Data / restraints / parameters	5304 / 784 / 523
Goodness-of-fit on F <sup>2</sup>	1.1024
Final R indices [I>2sigma(I)]	R1 = 0.0382, wR2 = 0.0447
R indices (all data)	R1 = 0.0602, wR2 = 0.0602
Largest diff. peak and hole	0.36 and -0.39 e.Å <sup>-3</sup>

Table 2. Atomic coordinates (x 10<sup>4</sup>) and equivalent isotropic displacement parameters (Å<sup>2</sup>x 10<sup>3</sup>) for Bis[2-(4-Methoxyphenyl)-1,10-phenanthroline]copper(I) hexafluorophosphate.

U(eq) is defined as one third of the trace of the orthogonalized Uij tensor.

	x	y	z	U(eq)
Cu(1)	4858(1)	6322(1)	7493(1)	40
N(1)	6243(2)	5857(2)	8394(1)	40
N(2)	3691(2)	6797(2)	8605(1)	34
N(3)	4330(2)	5612(2)	6555(1)	41
N(4)	4460(2)	7981(2)	6445(1)	36
C(1)	7489(2)	5372(2)	8300(2)	48
C(2)	8404(3)	5221(3)	8957(2)	57
C(3)	8019(3)	5588(2)	9726(2)	53
C(4)	6698(3)	6101(2)	9865(2)	45
C(5)	5840(2)	6203(2)	9180(2)	37

C(6)	6210(3)	6532(2)	10648(2)	52
C(7)	4951(3)	7049(2)	10733(2)	50
C(8)	4049(3)	7174(2)	10047(2)	43
C(9)	4484(2)	6728(2)	9280(2)	37
C(10)	2740(3)	7735(2)	10091(2)	48
C(11)	1962(3)	7850(2)	9393(2)	47
C(12)	2460(2)	7354(2)	8657(2)	38
C(13)	1612(2)	7453(2)	7908(2)	38
C(14)	1479(2)	6445(2)	7613(2)	39
C(15)	685(2)	6534(2)	6911(2)	43
C(16)	36(2)	7669(2)	6480(2)	46
C(17)	173(2)	8692(2)	6754(2)	49
C(18)	935(2)	8587(2)	7469(2)	44
C(19)	-909(3)	6867(3)	5450(2)	68
C(20)	4274(3)	4439(2)	6606(2)	51
C(21)	3725(3)	4075(3)	5944(2)	61
C(22)	3205(3)	4958(3)	5208(2)	59
C(23)	3228(3)	6208(3)	5123(2)	50
C(24)	3822(2)	6495(2)	5813(2)	41
C(25)	2652(3)	7195(3)	4396(2)	57
C(26)	2615(3)	8376(3)	4388(2)	56
C(27)	3181(2)	8698(2)	5096(2)	46
C(28)	3842(2)	7758(2)	5775(2)	39
C(29)	3074(3)	9894(2)	5169(2)	50
C(30)	3641(3)	10113(2)	5867(2)	48
C(31)	4370(2)	9136(2)	6490(2)	39
C(32)	5058(2)	9345(2)	7222(2)	38
C(33)	6340(2)	8809(2)	7390(2)	39
C(34)	6988(2)	8965(2)	8094(2)	43
C(35)	6315(3)	9637(2)	8660(2)	45
C(36)	5027(3)	10171(2)	8506(2)	51
C(37)	4409(3)	10047(2)	7784(2)	46
C(38)	8159(3)	9285(3)	9574(2)	63
O(1)	-762(2)	7877(2)	5776(2)	63
O(2)	6832(2)	9810(2)	9394(1)	60
P(1)	376(1)	2478(1)	7559(1)	55

F(1)	-757(7)	1803(7)	7443(6)	124
F(2)	1624(8)	3066(8)	7751(5)	112
F(3)	-128(9)	3699(6)	6905(5)	107
F(4)	996(6)	1169(5)	8264(4)	72
F(5)	-377(9)	2753(8)	8439(5)	149
F(6)	1303(8)	2088(7)	6778(4)	115
F(11)	-161(5)	1684(3)	7004(3)	97
F(12)	791(6)	3348(4)	8062(4)	123
F(13)	304(5)	3628(4)	6614(3)	90
F(14)	330(5)	1374(4)	8458(3)	115
F(15)	-1150(4)	2904(5)	7788(3)	126
F(16)	1798(4)	2117(5)	7239(5)	164

Table 3. Bond lengths [ $\text{\AA}$ ] and angles [ $^{\circ}$ ] for Bis[2-(4-Methoxyphenyl)-1,10-phenanthroline]copper(I) hexafluorophosphate.

Cu(1)-N(1)	1.9959(19)	C(5)-C(9)	1.441(3)
Cu(1)-N(2)	2.1046(18)	C(6)-C(7)	1.348(4)
Cu(1)-N(3)	1.9999(19)	C(6)-H(61)	1.000
Cu(1)-N(4)	2.0968(18)	C(7)-C(8)	1.435(3)
N(1)-C(1)	1.326(3)	C(7)-H(71)	1.000
N(1)-C(5)	1.367(3)	C(8)-C(9)	1.411(3)
N(2)-C(9)	1.359(3)	C(8)-C(10)	1.405(4)
N(2)-C(12)	1.335(3)	C(10)-C(11)	1.364(4)
N(3)-C(20)	1.331(3)	C(10)-H(101)	1.000
N(3)-C(24)	1.366(3)	C(11)-C(12)	1.415(3)
N(4)-C(28)	1.363(3)	C(11)-H(111)	1.000
N(4)-C(31)	1.338(3)	C(12)-C(13)	1.481(3)
C(1)-C(2)	1.406(4)	C(13)-C(14)	1.389(3)
C(1)-H(11)	1.000	C(13)-C(18)	1.401(3)
C(2)-C(3)	1.354(4)	C(14)-C(15)	1.388(3)
C(2)-H(21)	1.000	C(14)-H(141)	1.000
C(3)-C(4)	1.413(4)	C(15)-C(16)	1.387(4)
C(3)-H(31)	1.000	C(15)-H(151)	1.000
C(4)-C(5)	1.408(3)	C(16)-C(17)	1.388(4)
C(4)-C(6)	1.432(4)	C(16)-O(1)	1.367(3)

C(17)-C(18)	1.378(3)	C(32)-C(33)	1.388(3)
C(17)-H(171)	1.000	C(32)-C(37)	1.399(3)
C(18)-H(181)	1.000	C(33)-C(34)	1.390(3)
C(19)-O(1)	1.424(4)	C(33)-H(331)	1.000
C(19)-H(191)	1.000	C(34)-C(35)	1.386(4)
C(19)-H(192)	1.000	C(34)-H(341)	1.000
C(19)-H(193)	1.000	C(35)-C(36)	1.389(4)
C(20)-C(21)	1.399(4)	C(35)-O(2)	1.367(3)
C(20)-H(201)	1.000	C(36)-C(37)	1.381(4)
C(21)-C(22)	1.365(4)	C(36)-H(361)	1.000
C(21)-H(211)	1.000	C(37)-H(371)	1.000
C(22)-C(23)	1.401(4)	C(38)-O(2)	1.429(4)
C(22)-H(221)	1.000	C(38)-H(381)	1.000
C(23)-C(24)	1.411(3)	C(38)-H(382)	1.000
C(23)-C(25)	1.437(4)	C(38)-H(383)	1.000
C(24)-C(28)	1.434(3)	P(1)-F(1)	1.521(5)
C(25)-C(26)	1.347(4)	P(1)-F(2)	1.605(5)
C(25)-H(251)	1.000	P(1)-F(3)	1.514(6)
C(26)-C(27)	1.441(4)	P(1)-F(4)	1.652(5)
C(26)-H(261)	1.000	P(1)-F(5)	1.548(5)
C(27)-C(28)	1.407(3)	P(1)-F(6)	1.556(5)
C(27)-C(29)	1.399(4)	P(1)-F(11)	1.599(3)
C(29)-C(30)	1.369(4)	P(1)-F(12)	1.553(4)
C(29)-H(291)	1.000	P(1)-F(13)	1.619(4)
C(30)-C(31)	1.418(3)	P(1)-F(14)	1.543(3)
C(30)-H(301)	1.000	P(1)-F(15)	1.593(3)
C(31)-C(32)	1.479(3)	P(1)-F(16)	1.511(3)
N(1)-Cu(1)-N(2)	82.23(7)	C(1)-N(1)-C(5)	117.5(2)
N(1)-Cu(1)-N(3)	135.21(8)	Cu(1)-N(2)-C(9)	109.23(14)
N(2)-Cu(1)-N(3)	129.67(7)	Cu(1)-N(2)-C(12)	131.00(15)
N(1)-Cu(1)-N(4)	129.85(7)	C(9)-N(2)-C(12)	118.17(19)
N(2)-Cu(1)-N(4)	97.58(7)	Cu(1)-N(3)-C(20)	129.48(17)
N(3)-Cu(1)-N(4)	81.96(7)	Cu(1)-N(3)-C(24)	112.55(15)
Cu(1)-N(1)-C(1)	129.53(17)	C(20)-N(3)-C(24)	117.5(2)
Cu(1)-N(1)-C(5)	112.69(15)	Cu(1)-N(4)-C(28)	109.46(14)

Cu(1)-N(4)-C(31)	128.82(15)	C(11)-C(12)-C(13)	120.0(2)
C(28)-N(4)-C(31)	118.46(19)	N(2)-C(12)-C(13)	117.94(19)
N(1)-C(1)-C(2)	123.1(3)	C(12)-C(13)-C(14)	121.57(19)
N(1)-C(1)-H(11)	118.441	C(12)-C(13)-C(18)	120.0(2)
C(2)-C(1)-H(11)	118.420	C(14)-C(13)-C(18)	118.4(2)
C(1)-C(2)-C(3)	119.6(3)	C(13)-C(14)-C(15)	121.7(2)
C(1)-C(2)-H(21)	120.181	C(13)-C(14)-H(141)	119.141
C(3)-C(2)-H(21)	120.225	C(15)-C(14)-H(141)	119.129
C(2)-C(3)-C(4)	119.6(2)	C(14)-C(15)-C(16)	118.8(2)
C(2)-C(3)-H(31)	120.210	C(14)-C(15)-H(151)	120.579
C(4)-C(3)-H(31)	120.229	C(16)-C(15)-H(151)	120.609
C(3)-C(4)-C(5)	117.2(2)	C(15)-C(16)-C(17)	120.3(2)
C(3)-C(4)-C(6)	123.5(2)	C(15)-C(16)-O(1)	124.3(2)
C(5)-C(4)-C(6)	119.3(2)	C(17)-C(16)-O(1)	115.3(2)
C(4)-C(5)-N(1)	122.9(2)	C(16)-C(17)-C(18)	120.4(2)
C(4)-C(5)-C(9)	119.8(2)	C(16)-C(17)-H(171)	119.824
N(1)-C(5)-C(9)	117.27(19)	C(18)-C(17)-H(171)	119.781
C(4)-C(6)-C(7)	121.1(2)	C(13)-C(18)-C(17)	120.3(2)
C(4)-C(6)-H(61)	119.443	C(13)-C(18)-H(181)	119.851
C(7)-C(6)-H(61)	119.463	C(17)-C(18)-H(181)	119.841
C(6)-C(7)-C(8)	121.2(2)	O(1)-C(19)-H(191)	109.492
C(6)-C(7)-H(71)	119.402	O(1)-C(19)-H(192)	109.482
C(8)-C(7)-H(71)	119.386	H(191)-C(19)-H(192)	109.476
C(7)-C(8)-C(9)	119.2(2)	O(1)-C(19)-H(193)	109.426
C(7)-C(8)-C(10)	123.4(2)	H(191)-C(19)-H(193)	109.476
C(9)-C(8)-C(10)	117.4(2)	H(192)-C(19)-H(193)	109.476
C(5)-C(9)-C(8)	119.3(2)	N(3)-C(20)-C(21)	123.4(3)
C(5)-C(9)-N(2)	117.60(19)	N(3)-C(20)-H(201)	118.293
C(8)-C(9)-N(2)	123.0(2)	C(21)-C(20)-H(201)	118.312
C(8)-C(10)-C(11)	119.5(2)	C(20)-C(21)-C(22)	119.0(3)
C(8)-C(10)-H(101)	120.241	C(20)-C(21)-H(211)	120.498
C(11)-C(10)-H(101)	120.209	C(22)-C(21)-H(211)	120.509
C(10)-C(11)-C(12)	119.7(2)	C(21)-C(22)-C(23)	120.0(2)
C(10)-C(11)-H(111)	120.141	C(21)-C(22)-H(221)	119.973
C(12)-C(11)-H(111)	120.146	C(23)-C(22)-H(221)	119.981
C(11)-C(12)-N(2)	122.1(2)	C(22)-C(23)-C(24)	117.3(3)

C(22)-C(23)-C(25)	123.7(2)	C(34)-C(35)-O(2)	124.0(2)
C(24)-C(23)-C(25)	119.0(2)	C(36)-C(35)-O(2)	115.6(2)
C(23)-C(24)-N(3)	122.7(2)	C(35)-C(36)-C(37)	120.3(2)
C(23)-C(24)-C(28)	119.7(2)	C(35)-C(36)-H(361)	119.837
N(3)-C(24)-C(28)	117.5(2)	C(37)-C(36)-H(361)	119.856
C(23)-C(25)-C(26)	121.1(2)	C(32)-C(37)-C(36)	120.2(2)
C(23)-C(25)-H(251)	119.423	C(32)-C(37)-H(371)	119.902
C(26)-C(25)-H(251)	119.458	C(36)-C(37)-H(371)	119.897
C(25)-C(26)-C(27)	121.2(2)	O(2)-C(38)-H(381)	109.541
C(25)-C(26)-H(261)	119.370	O(2)-C(38)-H(382)	109.372
C(27)-C(26)-H(261)	119.405	H(381)-C(38)-H(382)	109.475
C(26)-C(27)-C(28)	118.7(2)	O(2)-C(38)-H(383)	109.487
C(26)-C(27)-C(29)	123.7(2)	H(381)-C(38)-H(383)	109.476
C(28)-C(27)-C(29)	117.6(2)	H(382)-C(38)-H(383)	109.476
C(24)-C(28)-C(27)	119.9(2)	C(19)-O(1)-C(16)	117.7(2)
C(24)-C(28)-N(4)	117.1(2)	C(38)-O(2)-C(35)	117.7(2)
C(27)-C(28)-N(4)	122.9(2)	F(1)-P(1)-F(2)	174.4(4)
C(27)-C(29)-C(30)	119.6(2)	F(1)-P(1)-F(3)	93.7(4)
C(27)-C(29)-H(291)	120.185	F(2)-P(1)-F(3)	91.9(4)
C(30)-C(29)-H(291)	120.176	F(1)-P(1)-F(4)	88.8(3)
C(29)-C(30)-C(31)	119.7(2)	F(2)-P(1)-F(4)	85.7(3)
C(29)-C(30)-H(301)	120.129	F(3)-P(1)-F(4)	177.3(4)
C(31)-C(30)-H(301)	120.126	F(1)-P(1)-F(5)	92.3(4)
C(30)-C(31)-N(4)	121.5(2)	F(2)-P(1)-F(5)	87.3(4)
C(30)-C(31)-C(32)	121.5(2)	F(3)-P(1)-F(5)	93.6(4)
N(4)-C(31)-C(32)	116.98(19)	F(4)-P(1)-F(5)	87.3(3)
C(31)-C(32)-C(33)	120.7(2)	F(1)-P(1)-F(6)	92.1(4)
C(31)-C(32)-C(37)	120.6(2)	F(2)-P(1)-F(6)	87.6(4)
C(33)-C(32)-C(37)	118.7(2)	F(3)-P(1)-F(6)	94.0(4)
C(32)-C(33)-C(34)	121.5(2)	F(4)-P(1)-F(6)	84.9(3)
C(32)-C(33)-H(331)	119.240	F(5)-P(1)-F(6)	171.0(4)
C(34)-C(33)-H(331)	119.269	F(11)-P(1)-F(12)	174.5(2)
C(33)-C(34)-C(35)	118.9(2)	F(11)-P(1)-F(13)	87.0(2)
C(33)-C(34)-H(341)	120.532	F(12)-P(1)-F(13)	89.2(2)
C(35)-C(34)-H(341)	120.527	F(11)-P(1)-F(14)	90.6(2)
C(34)-C(35)-C(36)	120.3(2)	F(12)-P(1)-F(14)	93.0(2)



F(13)-P(1)-F(14)	175.6(3)	F(11)-P(1)-F(16)	90.3(3)
F(11)-P(1)-F(15)	86.2(2)	F(12)-P(1)-F(16)	93.7(3)
F(12)-P(1)-F(15)	89.5(3)	F(13)-P(1)-F(16)	89.9(2)
F(13)-P(1)-F(15)	85.2(2)	F(14)-P(1)-F(16)	93.8(3)
F(14)-P(1)-F(15)	90.9(2)	F(15)-P(1)-F(16)	174.2(3)

**Crystal data and structure refinement for Bis[2-dimethyl-9-(tert-butyldimethylsilyl)methyl]-1-10-phenanthroline]copper(I) hexafluorophosphate.**

Table 1. Crystal data and structure refinement for Bis[2-dimethyl-9-(tert-butyldimethylsilyl)methyl]-1-10-phenanthroline]copper(I) hexafluorophosphate.

Identification code	ValC_TBDMS	
Empirical formula	C <sub>41</sub> H <sub>54</sub> Cl <sub>2</sub> Cu <sub>1</sub> F <sub>3.20</sub> N <sub>4</sub> O <sub>1.40</sub> P <sub>1</sub> Si <sub>2</sub>	
Formula weight	907.70	
Temperature	173 K	
Wavelength	0.71073 Å	
Crystal system	Triclinic	
Space group	P -1	
Unit cell dimensions	a = 12.7104(2) Å	α = 94.7535(6)°
	b = 13.3937(2) Å	β = 112.0157(6)°
	c = 15.5455(2) Å	γ = 109.8909(7)°
Volume	2238.90(6) Å <sup>3</sup>	
Z	2	
Density (calculated)	1.346 Mg/m <sup>3</sup>	
Absorption coefficient	0.747 mm <sup>-1</sup>	
F(000)	948.000	
Crystal size	0.29 x 0.28 x 0.16 mm <sup>3</sup>	
Theta range for data collection	1.456 to 27.867°.	
Index ranges	-16 ≤ h ≤ 16, -17 ≤ k ≤ 17, -20 ≤ l ≤ 20	
Reflections collected	21157	
Independent reflections	10656 [R(int) = 0.014]	
Completeness to theta = 27.867°	99.9 %	
Absorption correction	Semi-empirical from equivalents	

Max. and min. transmission	0.89 and 0.89
Refinement method	Full-matrix least-squares on F <sup>2</sup>
Data / restraints / parameters	7781 / 1100 / 586
Goodness-of-fit on F <sup>2</sup>	1.0135
Final R indices [I>2sigma(I)]	R1 = 0.0510, wR2 = 0.0497
R indices (all data)	R1 = 0.0650, wR2 = 0.0574
Largest diff. peak and hole	0.85 and -1.61 e.Å <sup>-3</sup>

Table 2. Atomic coordinates (x 10<sup>4</sup>) and equivalent isotropic displacement parameters (Å<sup>2</sup>x 10<sup>3</sup>) for Bis[2-dimethyl-9-(tert-butyldimethylsilyl)methyl]-1-10-phenanthroline]copper(I) hexafluorophosphate.

U(eq) is defined as one third of the trace of the orthogonalized U<sup>ij</sup> tensor.

	x	y	z	U(eq)
Cu(1)	4174(1)	3363(1)	2467(1)	33
N(1)	5519(2)	2932(2)	3352(1)	35
N(2)	3268(2)	2661(1)	3242(1)	31
N(3)	4823(2)	4929(1)	2311(1)	34
N(4)	3246(2)	3023(1)	1011(1)	31
C(1)	7026(2)	3678(3)	2721(2)	57
C(2)	6645(2)	3125(2)	3421(2)	45
C(3)	7478(3)	2807(3)	4123(2)	63
C(4)	7110(3)	2272(3)	4730(2)	66
C(5)	5924(3)	2055(2)	4677(2)	47
C(6)	5157(2)	2421(2)	3982(1)	35
C(7)	5457(3)	1479(2)	5278(2)	58
C(8)	4308(3)	1290(2)	5194(2)	56
C(9)	3515(3)	1674(2)	4501(2)	43
C(10)	3950(2)	2251(2)	3909(1)	34
C(11)	2300(3)	1484(2)	4365(2)	51
C(12)	1612(2)	1877(2)	3691(2)	48
C(13)	2118(2)	2478(2)	3131(2)	36
C(14)	1397(2)	2951(2)	2421(2)	41
C(15)	3095(2)	5260(2)	3720(2)	52
C(16)	587(3)	4040(2)	3722(2)	53

C(17)	697(2)	4876(2)	1945(2)	47
C(18)	1434(3)	5124(3)	1347(2)	70
C(19)	-639(3)	4050(3)	1301(2)	67
C(20)	660(5)	5934(3)	2349(3)	81
C(21)	6176(2)	5782(2)	3990(2)	51
C(22)	5640(2)	5853(2)	2970(2)	41
C(23)	5992(2)	6866(2)	2723(2)	51
C(24)	5500(2)	6911(2)	1783(2)	51
C(25)	4653(2)	5946(2)	1078(2)	41
C(26)	4346(2)	4969(2)	1374(2)	34
C(27)	4097(2)	5917(2)	77(2)	49
C(28)	3293(2)	4967(2)	-568(2)	49
C(29)	2963(2)	3953(2)	-288(2)	40
C(30)	3497(2)	3952(2)	683(1)	33
C(31)	2126(2)	2943(2)	-937(2)	50
C(32)	1855(2)	2008(2)	-604(2)	50
C(33)	2428(2)	2070(2)	385(2)	38
C(34)	2153(2)	1068(2)	760(2)	42
C(35)	4611(4)	1043(3)	898(4)	88
C(36)	2160(6)	-583(4)	-719(3)	102
C(37)	2823(3)	-849(2)	1322(2)	54
C(38)	3480(6)	-277(4)	2376(2)	99
C(39)	1435(4)	-1502(3)	1066(4)	84
C(40)	3374(4)	-1649(3)	1121(3)	74
C(41)	113(4)	1601(3)	6114(3)	76
Si(1)	1446(1)	4300(1)	2962(1)	37
Si(2)	2950(1)	156(1)	554(1)	43
Cl(1)	-776(1)	1360(1)	6764(1)	62
Cl(2)	747(1)	2998(1)	6137(1)	85
P(1)	7802(1)	261(1)	3132(1)	85
F(1)	7760(9)	-639(8)	3690(8)	91
F(2)	7885(13)	1293(9)	2630(8)	96
F(3)	8891(8)	1270(7)	3984(7)	98
F(4)	6643(7)	-432(7)	2188(7)	102
F(5)	6725(10)	377(9)	3427(8)	108
F(6)	8715(8)	30(8)	2787(6)	87

F(11)	8139(7)	-262(6)	4022(4)	102
F(12)	8048(5)	-643(4)	2590(3)	62
O(1)	6632(6)	39(6)	2726(6)	132
O(2)	8566(5)	1192(4)	3268(5)	82
F(21)	9236(10)	596(9)	3983(7)	79
F(22)	7379(10)	46(8)	3889(8)	73
O(21)	7448(11)	-677(12)	2477(10)	92
O(22)	7598(12)	1269(16)	2742(10)	79

Table 3. Bond lengths [Å] and angles [°] for Bis[2-dimethyl-9-(tert-butyl dimethylsilyl)methyl]-1-10-phenanthroline]copper(I) hexafluorophosphate.

Cu(1)-N(1)	2.0471(16)	C(7)-H(71)	0.970
Cu(1)-N(2)	2.0388(16)	C(8)-C(9)	1.439(4)
Cu(1)-N(3)	2.0481(17)	C(8)-H(81)	0.970
Cu(1)-N(4)	2.0455(16)	C(9)-C(10)	1.399(3)
N(1)-C(2)	1.325(3)	C(9)-C(11)	1.405(4)
N(1)-C(6)	1.369(3)	C(11)-C(12)	1.363(4)
N(2)-C(10)	1.368(3)	C(11)-H(111)	0.970
N(2)-C(13)	1.337(3)	C(12)-C(13)	1.415(3)
N(3)-C(22)	1.333(3)	C(12)-H(121)	0.970
N(3)-C(26)	1.366(3)	C(13)-C(14)	1.486(3)
N(4)-C(30)	1.365(2)	C(14)-Si(1)	1.901(2)
N(4)-C(33)	1.337(3)	C(14)-H(141)	0.970
C(1)-C(2)	1.500(4)	C(14)-H(142)	0.970
C(1)-H(11)	0.970	C(15)-Si(1)	1.871(3)
C(1)-H(12)	0.970	C(15)-H(151)	0.970
C(1)-H(13)	0.970	C(15)-H(152)	0.970
C(2)-C(3)	1.417(3)	C(15)-H(153)	0.970
C(3)-C(4)	1.357(5)	C(16)-Si(1)	1.867(2)
C(3)-H(31)	0.970	C(16)-H(161)	0.970
C(4)-C(5)	1.403(4)	C(16)-H(162)	0.970
C(4)-H(41)	0.970	C(16)-H(163)	0.970
C(5)-C(6)	1.407(3)	C(17)-C(18)	1.532(4)
C(5)-C(7)	1.430(4)	C(17)-C(19)	1.541(4)
C(6)-C(10)	1.430(3)	C(17)-C(20)	1.525(4)
C(7)-C(8)	1.346(5)	C(17)-Si(1)	1.890(2)

C(18)-H(181)	0.970	C(35)-H(351)	0.970
C(18)-H(182)	0.970	C(35)-H(352)	0.970
C(18)-H(183)	0.970	C(35)-H(353)	0.970
C(19)-H(191)	0.970	C(36)-Si(2)	1.847(4)
C(19)-H(192)	0.970	C(36)-H(361)	0.970
C(19)-H(193)	0.970	C(36)-H(362)	0.970
C(20)-H(201)	0.970	C(36)-H(363)	0.970
C(20)-H(202)	0.970	C(37)-C(38)	1.517(5)
C(20)-H(203)	0.970	C(37)-C(39)	1.549(5)
C(21)-C(22)	1.499(4)	C(37)-C(40)	1.535(4)
C(21)-H(211)	0.970	C(37)-Si(2)	1.878(3)
C(21)-H(212)	0.970	C(38)-H(381)	0.970
C(21)-H(213)	0.970	C(38)-H(382)	0.970
C(22)-C(23)	1.411(3)	C(38)-H(383)	0.970
C(23)-C(24)	1.373(4)	C(39)-H(391)	0.970
C(23)-H(231)	0.970	C(39)-H(392)	0.970
C(24)-C(25)	1.401(4)	C(39)-H(393)	0.970
C(24)-H(241)	0.970	C(40)-H(401)	0.970
C(25)-C(26)	1.402(3)	C(40)-H(402)	0.970
C(25)-C(27)	1.438(4)	C(40)-H(403)	0.970
C(26)-C(30)	1.436(3)	C(41)-Cl(1)	1.750(4)
C(27)-C(28)	1.342(4)	C(41)-Cl(2)	1.759(4)
C(27)-H(271)	0.970	C(41)-H(411)	0.970
C(28)-C(29)	1.435(3)	C(41)-H(412)	0.970
C(28)-H(281)	0.970	P(1)-F(1)	1.540(9)
C(29)-C(30)	1.405(3)	P(1)-F(2)	1.634(11)
C(29)-C(31)	1.404(4)	P(1)-F(3)	1.597(8)
C(31)-C(32)	1.379(4)	P(1)-F(4)	1.552(8)
C(31)-H(311)	0.970	P(1)-F(5)	1.646(8)
C(32)-C(33)	1.414(3)	P(1)-F(6)	1.553(7)
C(32)-H(321)	0.970	P(1)-F(11)	1.584(7)
C(33)-C(34)	1.492(3)	P(1)-F(12)	1.600(4)
C(34)-Si(2)	1.909(2)	P(1)-O(1)	1.289(7)
C(34)-H(341)	0.970	P(1)-O(2)	1.233(5)
C(34)-H(342)	0.970	P(1)-F(21)	1.677(11)
C(35)-Si(2)	1.870(4)	P(1)-F(22)	1.477(9)

P(1)-O(21)	1.370(17)	P(1)-O(22)	1.59(2)
N(1)-Cu(1)-N(2)	82.55(7)	C(4)-C(5)-C(7)	123.7(2)
N(1)-Cu(1)-N(3)	114.13(7)	C(6)-C(5)-C(7)	118.8(2)
N(2)-Cu(1)-N(3)	132.76(7)	C(5)-C(6)-N(1)	122.1(2)
N(1)-Cu(1)-N(4)	132.57(7)	C(5)-C(6)-C(10)	120.1(2)
N(2)-Cu(1)-N(4)	119.80(7)	N(1)-C(6)-C(10)	117.82(17)
N(3)-Cu(1)-N(4)	82.24(7)	C(5)-C(7)-C(8)	121.3(2)
Cu(1)-N(1)-C(2)	130.01(15)	C(5)-C(7)-H(71)	119.399
Cu(1)-N(1)-C(6)	110.87(13)	C(8)-C(7)-H(71)	119.330
C(2)-N(1)-C(6)	119.01(18)	C(7)-C(8)-C(9)	120.9(2)
Cu(1)-N(2)-C(10)	111.47(13)	C(7)-C(8)-H(81)	119.513
Cu(1)-N(2)-C(13)	129.63(14)	C(9)-C(8)-H(81)	119.570
C(10)-N(2)-C(13)	118.63(17)	C(8)-C(9)-C(10)	119.2(2)
Cu(1)-N(3)-C(22)	129.59(15)	C(8)-C(9)-C(11)	123.6(2)
Cu(1)-N(3)-C(26)	111.64(14)	C(10)-C(9)-C(11)	117.2(2)
C(22)-N(3)-C(26)	118.73(18)	C(6)-C(10)-C(9)	119.62(19)
Cu(1)-N(4)-C(30)	111.35(13)	C(6)-C(10)-N(2)	117.21(17)
Cu(1)-N(4)-C(33)	129.72(14)	C(9)-C(10)-N(2)	123.2(2)
C(30)-N(4)-C(33)	118.84(17)	C(9)-C(11)-C(12)	119.7(2)
C(2)-C(1)-H(11)	109.478	C(9)-C(11)-H(111)	120.195
C(2)-C(1)-H(12)	109.423	C(12)-C(11)-H(111)	120.068
H(11)-C(1)-H(12)	109.476	C(11)-C(12)-C(13)	120.3(2)
C(2)-C(1)-H(13)	109.499	C(11)-C(12)-H(121)	119.839
H(11)-C(1)-H(13)	109.476	C(13)-C(12)-H(121)	119.846
H(12)-C(1)-H(13)	109.476	C(12)-C(13)-N(2)	121.0(2)
C(1)-C(2)-N(1)	118.4(2)	C(12)-C(13)-C(14)	120.9(2)
C(1)-C(2)-C(3)	119.8(2)	N(2)-C(13)-C(14)	118.11(18)
N(1)-C(2)-C(3)	121.7(2)	C(13)-C(14)-Si(1)	113.89(15)
C(2)-C(3)-C(4)	119.5(3)	C(13)-C(14)-H(141)	108.308
C(2)-C(3)-H(31)	120.245	Si(1)-C(14)-H(141)	108.306
C(4)-C(3)-H(31)	120.273	C(13)-C(14)-H(142)	108.426
C(3)-C(4)-C(5)	120.2(2)	Si(1)-C(14)-H(142)	108.386
C(3)-C(4)-H(41)	119.869	H(141)-C(14)-H(142)	109.467
C(5)-C(4)-H(41)	119.942	Si(1)-C(15)-H(151)	109.426
C(4)-C(5)-C(6)	117.4(2)	Si(1)-C(15)-H(152)	109.516

H(151)-C(15)-H(152)	109.476	H(211)-C(21)-H(212)	109.476
Si(1)-C(15)-H(153)	109.458	C(22)-C(21)-H(213)	109.607
H(151)-C(15)-H(153)	109.476	H(211)-C(21)-H(213)	109.476
H(152)-C(15)-H(153)	109.476	H(212)-C(21)-H(213)	109.476
Si(1)-C(16)-H(161)	109.395	C(21)-C(22)-N(3)	117.7(2)
Si(1)-C(16)-H(162)	109.475	C(21)-C(22)-C(23)	120.8(2)
H(161)-C(16)-H(162)	109.476	N(3)-C(22)-C(23)	121.5(2)
Si(1)-C(16)-H(163)	109.529	C(22)-C(23)-C(24)	119.8(2)
H(161)-C(16)-H(163)	109.476	C(22)-C(23)-H(231)	120.057
H(162)-C(16)-H(163)	109.476	C(24)-C(23)-H(231)	120.107
C(18)-C(17)-C(19)	109.3(3)	C(23)-C(24)-C(25)	119.5(2)
C(18)-C(17)-C(20)	108.7(3)	C(23)-C(24)-H(241)	120.208
C(19)-C(17)-C(20)	108.8(3)	C(25)-C(24)-H(241)	120.309
C(18)-C(17)-Si(1)	110.72(18)	C(24)-C(25)-C(26)	117.6(2)
C(19)-C(17)-Si(1)	109.90(19)	C(24)-C(25)-C(27)	123.2(2)
C(20)-C(17)-Si(1)	109.4(2)	C(26)-C(25)-C(27)	119.1(2)
C(17)-C(18)-H(181)	109.687	C(25)-C(26)-N(3)	122.7(2)
C(17)-C(18)-H(182)	109.182	C(25)-C(26)-C(30)	120.24(19)
H(181)-C(18)-H(182)	109.476	N(3)-C(26)-C(30)	117.02(17)
C(17)-C(18)-H(183)	109.531	C(25)-C(27)-C(28)	120.6(2)
H(181)-C(18)-H(183)	109.476	C(25)-C(27)-H(271)	119.637
H(182)-C(18)-H(183)	109.476	C(28)-C(27)-H(271)	119.737
C(17)-C(19)-H(191)	109.301	C(27)-C(28)-C(29)	121.6(2)
C(17)-C(19)-H(192)	109.430	C(27)-C(28)-H(281)	119.214
H(191)-C(19)-H(192)	109.476	C(29)-C(28)-H(281)	119.215
C(17)-C(19)-H(193)	109.669	C(28)-C(29)-C(30)	119.3(2)
H(191)-C(19)-H(193)	109.476	C(28)-C(29)-C(31)	123.5(2)
H(192)-C(19)-H(193)	109.476	C(30)-C(29)-C(31)	117.3(2)
C(17)-C(20)-H(201)	109.688	C(26)-C(30)-C(29)	119.14(19)
C(17)-C(20)-H(202)	109.288	C(26)-C(30)-N(4)	117.75(17)
H(201)-C(20)-H(202)	109.476	C(29)-C(30)-N(4)	123.1(2)
C(17)-C(20)-H(203)	109.424	C(29)-C(31)-C(32)	119.6(2)
H(201)-C(20)-H(203)	109.476	C(29)-C(31)-H(311)	120.242
H(202)-C(20)-H(203)	109.476	C(32)-C(31)-H(311)	120.156
C(22)-C(21)-H(211)	109.269	C(31)-C(32)-C(33)	119.9(2)
C(22)-C(21)-H(212)	109.524	C(31)-C(32)-H(321)	120.018

C(33)-C(32)-H(321)	120.053	H(391)-C(39)-H(392)	109.476
C(32)-C(33)-N(4)	121.2(2)	C(37)-C(39)-H(393)	109.533
C(32)-C(33)-C(34)	120.8(2)	H(391)-C(39)-H(393)	109.476
N(4)-C(33)-C(34)	117.96(18)	H(392)-C(39)-H(393)	109.476
C(33)-C(34)-Si(2)	114.38(16)	C(37)-C(40)-H(401)	109.635
C(33)-C(34)-H(341)	108.168	C(37)-C(40)-H(402)	109.425
Si(2)-C(34)-H(341)	108.251	H(401)-C(40)-H(402)	109.476
C(33)-C(34)-H(342)	108.287	C(37)-C(40)-H(403)	109.339
Si(2)-C(34)-H(342)	108.222	H(401)-C(40)-H(403)	109.476
H(341)-C(34)-H(342)	109.467	H(402)-C(40)-H(403)	109.476
Si(2)-C(35)-H(351)	109.784	Cl(1)-C(41)-Cl(2)	111.27(19)
Si(2)-C(35)-H(352)	109.384	Cl(1)-C(41)-H(411)	108.914
H(351)-C(35)-H(352)	109.476	Cl(2)-C(41)-H(411)	108.922
Si(2)-C(35)-H(353)	109.231	Cl(1)-C(41)-H(412)	109.109
H(351)-C(35)-H(353)	109.476	Cl(2)-C(41)-H(412)	109.135
H(352)-C(35)-H(353)	109.476	H(411)-C(41)-H(412)	109.467
Si(2)-C(36)-H(361)	109.371	C(14)-Si(1)-C(17)	107.70(11)
Si(2)-C(36)-H(362)	109.521	C(14)-Si(1)-C(15)	109.26(11)
H(361)-C(36)-H(362)	109.476	C(17)-Si(1)-C(15)	110.61(13)
Si(2)-C(36)-H(363)	109.509	C(14)-Si(1)-C(16)	108.76(12)
H(361)-C(36)-H(363)	109.476	C(17)-Si(1)-C(16)	111.10(11)
H(362)-C(36)-H(363)	109.476	C(15)-Si(1)-C(16)	109.36(13)
C(38)-C(37)-C(39)	108.2(3)	C(34)-Si(2)-C(37)	107.99(12)
C(38)-C(37)-C(40)	109.9(3)	C(34)-Si(2)-C(35)	108.28(13)
C(39)-C(37)-C(40)	108.9(3)	C(37)-Si(2)-C(35)	110.68(19)
C(38)-C(37)-Si(2)	111.6(2)	C(34)-Si(2)-C(36)	109.10(19)
C(39)-C(37)-Si(2)	108.8(2)	C(37)-Si(2)-C(36)	109.81(17)
C(40)-C(37)-Si(2)	109.4(2)	C(35)-Si(2)-C(36)	110.9(3)
C(37)-C(38)-H(381)	109.497	F(1)-P(1)-F(2)	174.8(6)
C(37)-C(38)-H(382)	109.272	F(1)-P(1)-F(3)	98.2(5)
H(381)-C(38)-H(382)	109.476	F(2)-P(1)-F(3)	77.4(5)
C(37)-C(38)-H(383)	109.630	F(1)-P(1)-F(4)	97.8(5)
H(381)-C(38)-H(383)	109.476	F(2)-P(1)-F(4)	86.2(5)
H(382)-C(38)-H(383)	109.476	F(3)-P(1)-F(4)	162.4(5)
C(37)-C(39)-H(391)	109.219	F(1)-P(1)-F(5)	85.2(5)
C(37)-C(39)-H(392)	109.648	F(2)-P(1)-F(5)	92.3(5)



F(3)-P(1)-F(5)	93.2(5)	F(11)-P(1)-O(2)	113.6(4)
F(4)-P(1)-F(5)	81.0(5)	F(12)-P(1)-O(2)	111.6(3)
F(1)-P(1)-F(6)	92.5(5)	O(1)-P(1)-O(2)	120.3(5)
F(2)-P(1)-F(6)	90.4(5)	F(21)-P(1)-F(22)	86.4(5)
F(3)-P(1)-F(6)	92.6(5)	F(21)-P(1)-O(21)	110.1(5)
F(4)-P(1)-F(6)	93.8(5)	F(22)-P(1)-O(21)	112.6(4)
F(5)-P(1)-F(6)	173.9(5)	F(21)-P(1)-O(22)	113.2(4)
F(11)-P(1)-F(12)	87.1(3)	F(22)-P(1)-O(22)	112.4(4)
F(11)-P(1)-O(1)	111.3(4)	O(21)-P(1)-O(22)	117.9(7)
F(12)-P(1)-O(1)	107.9(4)		

### Crystal data and structure refinement for 1,10-Phenanthroline-2,9-dicarboxylic acid.

Table 1. Crystal data and structure refinement for 1,10-Phenanthroline-2,9-dicarboxylic acid.

Identification code	ValC-421	
Empirical formula	C <sub>17</sub> H <sub>17</sub> N <sub>3</sub> O <sub>6</sub>	
Formula weight	359.34	
Temperature	173 K	
Wavelength	0.71073 Å	
Crystal system	Monoclinic	
Space group	P 1 21/a 1	
Unit cell dimensions	a = 6.9434(4) Å	α = 90°
	b = 23.8950(8) Å	β = 92.0269(19)°
	c = 10.1897(5) Å	γ = 90°
Volume	1689.54(14) Å <sup>3</sup>	
Z	4	
Density (calculated)	1.413 Mg/m <sup>3</sup>	
Absorption coefficient	0.109 mm <sup>-1</sup>	
F(000)	752	
Crystal size	0.22 x 0.14 x 0.02 mm <sup>3</sup>	
Theta range for data collection	2.000 to 26.007°.	
Index ranges	-8 ≤ h ≤ 8, 0 ≤ k ≤ 29, 0 ≤ l ≤ 12	
Reflections collected	10144	
Independent reflections	3317 [R(int) = 0.000]	
Completeness to theta = 26.007°	99.7 %	

Absorption correction	Semi-empirical from equivalents
Max. and min. transmission	1.00 and 0.98
Refinement method	Full-matrix least-squares on $F^2$
Data / restraints / parameters	2364 / 0 / 236
Goodness-of-fit on $F^2$	0.8166
Final R indices [ $I > 2\sigma(I)$ ]	$R_1 = 0.0757$ , $wR_2 = 0.0533$
R indices (all data)	$R_1 = 0.1025$ , $wR_2 = 0.0660$
Largest diff. peak and hole	0.40 and -0.42 e. $\text{\AA}^{-3}$

Table 2. Atomic coordinates ( $\times 10^4$ ) and equivalent isotropic displacement parameters ( $\text{\AA}^2 \times 10^3$ ) for 1,10-Phenanthroline-2,9-dicarboxylic acid.

U(eq) is defined as one third of the trace of the orthogonalized  $U_{ij}$  tensor.

	<b>x</b>	<b>y</b>	<b>z</b>	<b>U(eq)</b>
C(1)	6405(4)	6571(1)	9033(3)	35
C(2)	5795(4)	7019(1)	8074(3)	32
C(3)	5887(4)	7587(1)	8416(3)	36
C(4)	5414(4)	7975(1)	7468(3)	38
C(5)	4840(4)	7800(1)	6207(3)	33
C(6)	4330(4)	8187(1)	5180(3)	37
C(7)	3762(4)	8006(1)	3972(3)	39
C(8)	3667(4)	7418(1)	3676(3)	33
C(9)	3093(4)	7221(1)	2429(3)	40
C(10)	3010(4)	6656(1)	2201(3)	40
C(11)	3543(4)	6290(1)	3220(3)	33
C(12)	3469(4)	5672(1)	2962(3)	36
C(13)	4155(4)	7018(1)	4652(3)	30
C(14)	4749(3)	7217(1)	5953(3)	30
C(16)	7727(4)	5479(1)	11308(3)	43
C(17)	8761(5)	5069(2)	13387(3)	55
C(18)	8228(6)	4485(1)	11407(4)	65
O(1)	6751(3)	6747(1)	10224(2)	50
O(2)	6624(4)	6089(1)	8704(2)	58
O(3)	2954(4)	5487(1)	1901(2)	52
O(4)	3973(3)	5372(1)	3978(2)	43
O(5)	7712(4)	5967(1)	11754(2)	53
O(6)	3576(3)	4324(1)	3809(2)	45
N(1)	5235(3)	6835(1)	6888(2)	30
N(2)	4096(3)	6461(1)	4426(2)	31
N(3)	8188(4)	5037(1)	11999(2)	43

Table 3. Bond lengths [ $\text{\AA}$ ] and angles [ $^\circ$ ] for 1,10-Phenanthroline-2,9-dicarboxylic acid.

C(1)-C(2)	1.501(4)	C(1)-O(1)	1.299(3)
-----------	----------	-----------	----------

C(1)-O(2)	1.211(3)	C(12)-O(3)	1.210(3)
C(2)-C(3)	1.402(3)	C(12)-O(4)	1.298(3)
C(2)-N(1)	1.331(3)	C(13)-C(14)	1.454(4)
C(3)-C(4)	1.371(4)	C(13)-N(2)	1.351(3)
C(3)-H(31)	0.943	C(14)-N(1)	1.353(3)
C(4)-C(5)	1.396(4)	C(16)-O(5)	1.253(3)
C(4)-H(41)	0.944	C(16)-N(3)	1.301(4)
C(5)-C(6)	1.432(4)	C(16)-H(221)	0.926
C(5)-C(14)	1.419(3)	C(17)-N(3)	1.458(4)
C(6)-C(7)	1.350(4)	C(17)-H(251)	0.962
C(6)-H(61)	0.947	C(17)-H(252)	0.953
C(7)-C(8)	1.439(3)	C(17)-H(253)	0.952
C(7)-H(71)	0.951	C(18)-N(3)	1.451(4)
C(8)-C(9)	1.400(4)	C(18)-H(151)	0.968
C(8)-C(13)	1.412(3)	C(18)-H(152)	0.980
C(9)-C(10)	1.371(4)	C(18)-H(153)	0.972
C(9)-H(91)	0.949	O(1)-H(1)	0.840
C(10)-C(11)	1.397(4)	O(4)-H(4)	0.839
C(10)-H(101)	0.918	O(6)-H(6)	0.838
C(11)-C(12)	1.501(4)	O(6)-H(7)	0.833
C(11)-N(2)	1.338(3)		
C(2)-C(1)-O(1)	114.6(2)	C(6)-C(5)-C(14)	119.5(3)
C(2)-C(1)-O(2)	122.3(2)	C(5)-C(6)-C(7)	121.1(2)
O(1)-C(1)-O(2)	123.0(3)	C(5)-C(6)-H(61)	118.9
C(1)-C(2)-C(3)	121.3(2)	C(7)-C(6)-H(61)	119.9
C(1)-C(2)-N(1)	114.9(2)	C(6)-C(7)-C(8)	120.9(2)
C(3)-C(2)-N(1)	123.7(2)	C(6)-C(7)-H(71)	120.8
C(2)-C(3)-C(4)	118.2(2)	C(8)-C(7)-H(71)	118.3
C(2)-C(3)-H(31)	120.3	C(7)-C(8)-C(9)	121.8(2)
C(4)-C(3)-H(31)	121.5	C(7)-C(8)-C(13)	120.4(2)
C(3)-C(4)-C(5)	119.9(2)	C(9)-C(8)-C(13)	117.8(2)
C(3)-C(4)-H(41)	119.7	C(8)-C(9)-C(10)	119.5(2)
C(5)-C(4)-H(41)	120.4	C(8)-C(9)-H(91)	118.3
C(4)-C(5)-C(6)	122.3(2)	C(10)-C(9)-H(91)	122.2
C(4)-C(5)-C(14)	118.2(2)	C(9)-C(10)-C(11)	118.8(3)

C(9)-C(10)-H(101)	123.0	H(251)-C(17)-H(252)	109.2
C(11)-C(10)-H(101)	118.2	N(3)-C(17)-H(253)	110.7
C(10)-C(11)-C(12)	118.6(2)	H(251)-C(17)-H(253)	110.5
C(10)-C(11)-N(2)	123.5(2)	H(252)-C(17)-H(253)	109.8
C(12)-C(11)-N(2)	117.9(2)	N(3)-C(18)-H(151)	110.6
C(11)-C(12)-O(3)	121.6(2)	N(3)-C(18)-H(152)	108.9
C(11)-C(12)-O(4)	113.4(2)	H(151)-C(18)-H(152)	109.7
O(3)-C(12)-O(4)	124.9(3)	N(3)-C(18)-H(153)	109.2
C(8)-C(13)-C(14)	118.3(2)	H(151)-C(18)-H(153)	108.3
C(8)-C(13)-N(2)	122.8(2)	H(152)-C(18)-H(153)	110.2
C(14)-C(13)-N(2)	118.9(2)	C(1)-O(1)-H(1)	109.5
C(13)-C(14)-C(5)	119.8(2)	C(12)-O(4)-H(4)	109.9
C(13)-C(14)-N(1)	118.5(2)	H(6)-O(6)-H(7)	105.8
C(5)-C(14)-N(1)	121.7(2)	C(14)-N(1)-C(2)	118.3(2)
O(5)-C(16)-N(3)	124.3(3)	C(13)-N(2)-C(11)	117.6(2)
O(5)-C(16)-H(221)	118.4	C(17)-N(3)-C(18)	116.2(3)
N(3)-C(16)-H(221)	117.3	C(17)-N(3)-C(16)	122.5(3)
N(3)-C(17)-H(251)	109.6	C(18)-N(3)-C(16)	121.3(3)
N(3)-C(17)-H(252)	107.0		

**Crystal data and structure refinement for Bis[6,6'-Bis(hydroxymethyl)-2,2'-bipyridine]copper(I) hexafluorophosphate.**

Table 1. Crystal data and structure refinement for Bis[6,6'-Bis(hydroxymethyl)-2,2'-bipyridine]copper(I) hexafluorophosphate.

Identification code	CRYSTALS_cif	
Empirical formula	C <sub>24</sub> H <sub>22</sub> Cu <sub>1</sub> F <sub>6</sub> N <sub>4</sub> O <sub>2</sub> P <sub>1</sub>	
Formula weight	606.97	
Temperature	173 K	
Wavelength	0.71073 Å	
Crystal system	Monoclinic	
Space group	P 1 21/a 1	
Unit cell dimensions	a = 8.97880(10) Å	α = 90°
	b = 22.3034(3) Å	β = 94.1642(7)°
	c = 12.74790(10) Å	γ = 90°
Volume	2546.13(5) Å <sup>3</sup>	

Z	4
Density (calculated)	1.583 Mg/m <sup>3</sup>
Absorption coefficient	0.995 mm <sup>-1</sup>
F(000)	1232
Crystal size	0.19 x 0.15 x 0.11 mm <sup>3</sup>
Theta range for data collection	1.602 to 27.901°.
Index ranges	-11<=h<=11, -29<=k<=29, -16<=l<=16
Reflections collected	23557
Independent reflections	6081 [R(int) = 0.027]
Completeness to theta = 27.901°	100.0 %
Absorption correction	Semi-empirical from equivalents
Max. and min. transmission	0.90 and 0.86
Refinement method	Full-matrix least-squares on F <sup>2</sup>
Data / restraints / parameters	3848 / 196 / 361
Goodness-of-fit on F <sup>2</sup>	1.1808
Final R indices [I>2sigma(I)]	R1 = 0.0593, wR2 = 0.0709
R indices (all data)	R1 = 0.0828, wR2 = 0.0924
Largest diff. peak and hole	0.74 and -0.59 e.Å <sup>-3</sup>

Table 2. Atomic coordinates (x 10<sup>4</sup>) and equivalent isotropic displacement parameters (Å<sup>2</sup>x 10<sup>3</sup>) for Bis[6,6'-Bis(hydroxymethyl)-2,2'-bipyridine]copper(I) hexafluorophosphate.

U(eq) is defined as one third of the trace of the orthogonalized U<sub>ij</sub> tensor.

	x	y	z	U(eq)
Cu(1)	6090(1)	6262(1)	2172(1)	54
P(1)	10956(1)	6307(1)	7175(1)	61
F(1)	9914(5)	5792(2)	7514(3)	111
F(2)	11917(5)	6855(2)	6825(3)	110
F(3)	11417(5)	6443(2)	8353(2)	131
F(4)	10465(6)	6208(2)	5977(3)	128
F(5)	9613(5)	6761(2)	7253(4)	134
F(6)	12277(5)	5873(2)	7052(4)	152
N(1)	5952(3)	6539(2)	657(2)	46
N(2)	8220(4)	6065(2)	1826(3)	51
N(3)	5428(3)	6696(2)	3444(2)	47

N(4)	4934(4)	5582(2)	2819(2)	53
C(1)	3435(5)	6900(3)	721(4)	75
C(2)	4804(4)	6821(2)	133(3)	54
C(3)	4891(5)	7021(2)	-893(3)	60
C(4)	6201(5)	6936(2)	-1382(3)	59
C(5)	7366(5)	6645(2)	-853(3)	53
C(6)	7216(4)	6449(2)	168(3)	45
C(7)	8439(4)	6135(2)	800(3)	48
C(8)	9688(5)	5917(2)	359(4)	66
C(9)	10765(5)	5625(3)	1004(5)	78
C(10)	10569(5)	5564(2)	2054(4)	69
C(11)	9285(5)	5785(2)	2448(3)	62
C(12)	8946(7)	5709(3)	3579(4)	96
C(13)	6529(6)	7635(2)	2941(4)	75
C(14)	5718(5)	7266(2)	3706(3)	59
C(15)	5277(6)	7513(3)	4633(4)	74
C(16)	4515(6)	7153(3)	5307(4)	79
C(17)	4196(5)	6569(2)	5028(3)	64
C(18)	4657(4)	6347(2)	4090(3)	48
C(19)	4355(4)	5726(2)	3726(3)	49
C(20)	3541(5)	5314(2)	4272(3)	60
C(21)	3326(6)	4751(2)	3877(4)	72
C(22)	3931(6)	4598(2)	2961(4)	77
C(23)	4741(6)	5022(2)	2433(3)	69
C(24)	5483(9)	4923(3)	1426(4)	103
O(1)	9953(12)	5395(6)	4241(7)	176
O(2)	5460(17)	7809(9)	2119(13)	105
O(3)	5491(9)	4368(2)	977(5)	115
O(4)	2072(13)	7100(7)	259(12)	117

Table 3. Bond lengths [ $\text{\AA}$ ] and angles [ $^\circ$ ] for Bis[6,6'-Bis(hydroxymethyl)-2,2'-bipyridine]copper(I) hexafluorophosphate.

Cu(1)-N(1)	2.023(3)	Cu(1)-N(4)	2.045(4)
Cu(1)-N(2)	2.042(3)	P(1)-F(1)	1.562(3)
Cu(1)-N(3)	2.014(3)	P(1)-F(2)	1.577(3)

P(1)-F(3)	1.559(3)	C(10)-C(11)	1.382(7)
P(1)-F(4)	1.573(3)	C(10)-H(101)	1.015
P(1)-F(5)	1.583(4)	C(11)-C(12)	1.505(6)
P(1)-F(6)	1.548(4)	C(12)-O(1)	1.382(7)
N(1)-C(2)	1.343(5)	C(12)-H(121)	1.015
N(1)-C(6)	1.350(5)	C(12)-H(122)	1.024
N(2)-C(7)	1.346(5)	C(13)-C(14)	1.504(5)
N(2)-C(11)	1.350(5)	C(13)-O(2)	1.422(10)
N(3)-C(14)	1.337(6)	C(13)-H(131)	1.013
N(3)-C(18)	1.358(5)	C(13)-H(132)	1.018
N(4)-C(19)	1.341(5)	C(13)-H(133)	0.986
N(4)-C(23)	1.348(6)	C(14)-C(15)	1.387(6)
C(1)-C(2)	1.496(5)	C(15)-C(16)	1.392(7)
C(1)-O(4)	1.392(9)	C(15)-H(151)	1.013
C(1)-H(11)	1.015	C(16)-C(17)	1.375(8)
C(1)-H(12)	1.005	C(16)-H(161)	1.016
C(1)-H(13)	0.996	C(17)-C(18)	1.386(5)
C(2)-C(3)	1.390(5)	C(17)-H(171)	1.023
C(3)-C(4)	1.384(6)	C(18)-C(19)	1.479(6)
C(3)-H(31)	1.015	C(19)-C(20)	1.391(6)
C(4)-C(5)	1.366(6)	C(20)-C(21)	1.361(7)
C(4)-H(41)	1.011	C(20)-H(201)	1.033
C(5)-C(6)	1.388(5)	C(21)-C(22)	1.367(8)
C(5)-H(51)	1.011	C(21)-H(211)	1.019
C(6)-C(7)	1.490(5)	C(22)-C(23)	1.396(8)
C(7)-C(8)	1.379(6)	C(22)-H(221)	1.027
C(8)-C(9)	1.385(7)	C(23)-C(24)	1.505(7)
C(8)-H(81)	1.010	C(24)-O(3)	1.365(7)
C(9)-C(10)	1.369(8)	C(24)-H(241)	1.044
C(9)-H(91)	1.012	C(24)-H(242)	1.016
N(1)-Cu(1)-N(2)	81.52(12)	N(3)-Cu(1)-N(4)	81.02(13)
N(1)-Cu(1)-N(3)	128.38(13)	F(1)-P(1)-F(2)	176.3(3)
N(2)-Cu(1)-N(3)	127.83(13)	F(1)-P(1)-F(3)	89.9(2)
N(1)-Cu(1)-N(4)	127.86(13)	F(2)-P(1)-F(3)	90.6(2)
N(2)-Cu(1)-N(4)	115.97(14)	F(1)-P(1)-F(4)	91.9(2)



F(2)-P(1)-F(4)	87.5(2)	C(4)-C(3)-H(31)	120.6
F(3)-P(1)-F(4)	176.9(3)	C(3)-C(4)-C(5)	119.2(4)
F(1)-P(1)-F(5)	88.7(2)	C(3)-C(4)-H(41)	120.1
F(2)-P(1)-F(5)	87.6(2)	C(5)-C(4)-H(41)	120.6
F(3)-P(1)-F(5)	88.0(3)	C(4)-C(5)-C(6)	119.3(4)
F(4)-P(1)-F(5)	89.5(3)	C(4)-C(5)-H(51)	120.9
F(1)-P(1)-F(6)	92.7(3)	C(6)-C(5)-H(51)	119.8
F(2)-P(1)-F(6)	91.0(2)	C(5)-C(6)-N(1)	121.9(4)
F(3)-P(1)-F(6)	93.8(3)	C(5)-C(6)-C(7)	122.5(3)
F(4)-P(1)-F(6)	88.7(3)	N(1)-C(6)-C(7)	115.5(3)
F(5)-P(1)-F(6)	177.7(2)	C(6)-C(7)-N(2)	115.2(3)
Cu(1)-N(1)-C(2)	127.6(2)	C(6)-C(7)-C(8)	122.3(4)
Cu(1)-N(1)-C(6)	113.7(2)	N(2)-C(7)-C(8)	122.4(4)
C(2)-N(1)-C(6)	118.7(3)	C(7)-C(8)-C(9)	118.5(4)
Cu(1)-N(2)-C(7)	113.0(2)	C(7)-C(8)-H(81)	121.2
Cu(1)-N(2)-C(11)	127.4(3)	C(9)-C(8)-H(81)	120.4
C(7)-N(2)-C(11)	118.5(3)	C(8)-C(9)-C(10)	119.6(4)
Cu(1)-N(3)-C(14)	126.5(3)	C(8)-C(9)-H(91)	120.1
Cu(1)-N(3)-C(18)	114.0(3)	C(10)-C(9)-H(91)	120.3
C(14)-N(3)-C(18)	119.5(3)	C(9)-C(10)-C(11)	119.3(4)
Cu(1)-N(4)-C(19)	114.2(3)	C(9)-C(10)-H(101)	119.6
Cu(1)-N(4)-C(23)	126.5(3)	C(11)-C(10)-H(101)	121.1
C(19)-N(4)-C(23)	119.3(4)	C(10)-C(11)-N(2)	121.7(4)
C(2)-C(1)-O(4)	123.7(8)	C(10)-C(11)-C(12)	122.7(4)
C(2)-C(1)-H(11)	109.8	N(2)-C(11)-C(12)	115.5(4)
O(4)-C(1)-H(11)	125.7	C(11)-C(12)-O(1)	118.2(6)
C(2)-C(1)-H(12)	110.2	C(11)-C(12)-H(121)	108.5
H(11)-C(1)-H(12)	107.9	O(1)-C(12)-H(121)	109.5
C(2)-C(1)-H(13)	110.9	C(11)-C(12)-H(122)	108.0
H(11)-C(1)-H(13)	108.6	O(1)-C(12)-H(122)	105.5
H(12)-C(1)-H(13)	109.4	H(121)-C(12)-H(122)	106.5
C(1)-C(2)-N(1)	115.8(3)	C(14)-C(13)-O(2)	107.1(8)
C(1)-C(2)-C(3)	122.5(4)	C(14)-C(13)-H(131)	109.6
N(1)-C(2)-C(3)	121.7(4)	C(14)-C(13)-H(132)	109.7
C(2)-C(3)-C(4)	119.2(4)	H(131)-C(13)-H(132)	107.1
C(2)-C(3)-H(31)	120.3	C(14)-C(13)-H(133)	111.5

H(131)-C(13)-H(133)	109.6	N(4)-C(19)-C(20)	121.6(4)
H(132)-C(13)-H(133)	109.2	C(19)-C(20)-C(21)	119.4(4)
C(13)-C(14)-N(3)	117.0(4)	C(19)-C(20)-H(201)	119.4
C(13)-C(14)-C(15)	121.1(4)	C(21)-C(20)-H(201)	121.2
N(3)-C(14)-C(15)	121.9(4)	C(20)-C(21)-C(22)	119.4(5)
C(14)-C(15)-C(16)	118.7(5)	C(20)-C(21)-H(211)	120.7
C(14)-C(15)-H(151)	120.7	C(22)-C(21)-H(211)	119.9
C(16)-C(15)-H(151)	120.6	C(21)-C(22)-C(23)	119.7(5)
C(15)-C(16)-C(17)	119.3(4)	C(21)-C(22)-H(221)	120.1
C(15)-C(16)-H(161)	120.0	C(23)-C(22)-H(221)	120.1
C(17)-C(16)-H(161)	120.7	C(22)-C(23)-N(4)	120.6(4)
C(16)-C(17)-C(18)	119.6(4)	C(22)-C(23)-C(24)	126.2(5)
C(16)-C(17)-H(171)	120.7	N(4)-C(23)-C(24)	113.2(5)
C(18)-C(17)-H(171)	119.7	C(23)-C(24)-O(3)	120.5(6)
C(17)-C(18)-N(3)	121.0(4)	C(23)-C(24)-H(241)	107.9
C(17)-C(18)-C(19)	123.1(4)	O(3)-C(24)-H(241)	105.7
N(3)-C(18)-C(19)	115.9(3)	C(23)-C(24)-H(242)	109.3
C(18)-C(19)-N(4)	114.9(3)	O(3)-C(24)-H(242)	107.6
C(18)-C(19)-C(20)	123.5(4)	H(241)-C(24)-H(242)	104.9

Crystal data and structure refinement for Bis[6,6'-di(chloromethyl)-1,10-phenanthroline]copper(I) hexafluorophosphate.

Table 1. Crystal data and structure refinement for Bis[6,6'-di(chloromethyl)-1,10-phenanthroline]copper(I) hexafluorophosphate.

Identification code	ValC-Cl	
Empirical formula	C <sub>28</sub> H <sub>20</sub> Cl <sub>4</sub> Cu <sub>1</sub> F <sub>6</sub> N <sub>4</sub> P <sub>1</sub>	
Formula weight	762.81	
Temperature	173 K	
Wavelength	0.71073 Å	
Crystal system	Monoclinic	
Space group	P 1 21/a 1	
Unit cell dimensions	a = 10.1292(2) Å	α = 90°
	b = 18.6376(3) Å	β = 93.9892(9)°

	$c = 15.6042(3) \text{ \AA}$	$\gamma = 90^\circ$
Volume	2938.69(9) $\text{\AA}^3$	
Z	4	
Density (calculated)	1.724 $\text{Mg/m}^3$	
Absorption coefficient	1.228 $\text{mm}^{-1}$	
F(000)	1528	
Crystal size	0.35 x 0.14 x 0.04 $\text{mm}^3$	
Theta range for data collection	1.704 to 27.072°.	
Index ranges	-12 ≤ h ≤ 12, -23 ≤ k ≤ 23, -19 ≤ l ≤ 19	
Reflections collected	24207	
Independent reflections	6439 [R(int) = 0.041]	
Completeness to theta = 27.072°	99.7 %	
Absorption correction	Semi-empirical from equivalents	
Max. and min. transmission	0.95 and 0.84	
Refinement method	Full-matrix least-squares on F <sup>2</sup>	
Data / restraints / parameters	4166 / 568 / 415	
Goodness-of-fit on F <sup>2</sup>	1.1266	
Final R indices [I > 2σ(I)]	R1 = 0.0415, wR2 = 0.0362	
R indices (all data)	R1 = 0.0623, wR2 = 0.0441	
Largest diff. peak and hole	0.60 and -0.37 $\text{e.\AA}^{-3}$	

Table 2. Atomic coordinates ( $\times 10^4$ ) and equivalent isotropic displacement parameters ( $\text{\AA}^2 \times 10^3$ ) for Bis[6,6'-di(chloromethyl)-1,10-phenanthroline]copper(I) hexafluorophosphate. U(eq) is defined as one third of the trace of the orthogonalized U<sub>ij</sub> tensor.

	<b>x</b>	<b>y</b>	<b>z</b>	<b>U(eq)</b>
Cu(1)	7066(1)	4152(1)	2653(1)	41
N(1)	5659(2)	4860(1)	2178(2)	39
N(2)	6361(2)	3563(1)	1617(2)	40
N(3)	9018(2)	4418(1)	2862(2)	37
N(4)	7340(2)	3795(1)	3893(2)	41
C(1)	4983(3)	4601(2)	1468(2)	41
C(2)	5364(3)	3916(2)	1156(2)	42
C(3)	6106(4)	5765(2)	3253(2)	59
C(4)	5338(3)	5503(2)	2464(2)	47

C(5)	4314(4)	5916(2)	2061(3)	63
C(6)	3638(3)	5659(2)	1351(3)	64
C(7)	3942(3)	4988(2)	1026(2)	54
C(8)	3277(4)	4672(3)	284(2)	69
C(9)	3642(4)	4031(3)	-14(2)	70
C(10)	4714(3)	3630(2)	405(2)	56
C(11)	5163(4)	2961(2)	120(2)	68
C(12)	6162(4)	2621(2)	576(3)	66
C(13)	6746(3)	2931(2)	1334(2)	51
C(14)	7854(4)	2580(2)	1863(3)	66
C(15)	9488(3)	4260(2)	3678(2)	40
C(16)	8590(3)	3928(2)	4226(2)	42
C(17)	9292(3)	4883(2)	1445(2)	52
C(18)	9839(3)	4716(2)	2338(2)	45
C(19)	11155(3)	4884(2)	2609(3)	60
C(20)	11626(3)	4732(2)	3420(3)	64
C(21)	10798(3)	4407(2)	3990(2)	52
C(22)	11201(4)	4210(2)	4860(2)	67
C(23)	10374(4)	3899(2)	5370(2)	68
C(24)	9028(4)	3737(2)	5081(2)	56
C(25)	8123(4)	3393(2)	5570(2)	69
C(26)	6883(4)	3256(2)	5230(2)	66
C(27)	6507(3)	3468(2)	4382(2)	52
C(28)	5175(4)	3340(2)	3956(3)	70
P(1)	1031(1)	3092(1)	7952(1)	68
F(1)	537(3)	3407(1)	8831(1)	88
F(2)	1563(4)	2793(1)	7092(1)	116
F(3)	1891(3)	2514(1)	8475(2)	85
F(4)	174(4)	3677(2)	7435(2)	143
F(5)	2221(3)	3643(2)	8045(2)	124
F(6)	-148(3)	2546(2)	7897(3)	132
Cl(1)	5350(1)	5413(1)	4165(1)	72
Cl(3)	9524(1)	4136(1)	747(1)	64
Cl(2)	7535(2)	1671(1)	2123(1)	76
Cl(4)	5325(2)	2484(1)	3458(1)	73
Cl(20)	6985(4)	2006(2)	2558(3)	85

Cl(40)                      3896(3)              3008(2)              4419(2)              85  
 Table 3. Bond lengths [Å] and angles [°] for Bis[6,6'-di(chloromethyl)-1,10-phenanthroline]copper(I) hexafluorophosphate.

Cu(1)-N(1)	2.043(2)	C(12)-C(13)	1.409(5)
Cu(1)-N(2)	2.042(2)	C(12)-H(121)	0.970
Cu(1)-N(3)	2.042(2)	C(13)-C(14)	1.497(5)
Cu(1)-N(4)	2.046(2)	C(14)-Cl(2)	1.776(4)
N(1)-C(1)	1.351(4)	C(14)-Cl(20)	1.797(5)
N(1)-C(4)	1.328(4)	C(14)-H(141)	0.967
N(2)-C(2)	1.367(4)	C(14)-H(142)	0.972
N(2)-C(13)	1.326(4)	C(14)-H(143)	0.968
N(3)-C(15)	1.360(3)	C(14)-H(144)	0.972
N(3)-C(18)	1.328(4)	C(15)-C(16)	1.432(4)
N(4)-C(16)	1.358(4)	C(15)-C(21)	1.409(4)
N(4)-C(27)	1.325(4)	C(16)-C(24)	1.420(4)
C(1)-C(2)	1.429(4)	C(17)-C(18)	1.496(4)
C(1)-C(7)	1.417(4)	C(17)-Cl(3)	1.794(3)
C(2)-C(10)	1.407(4)	C(17)-H(171)	0.970
C(3)-C(4)	1.491(5)	C(17)-H(172)	0.972
C(3)-Cl(1)	1.787(4)	C(18)-C(19)	1.405(4)
C(3)-H(31)	0.969	C(19)-C(20)	1.350(5)
C(3)-H(32)	0.970	C(19)-H(191)	0.970
C(4)-C(5)	1.405(5)	C(20)-C(21)	1.403(5)
C(5)-C(6)	1.350(6)	C(20)-H(201)	0.970
C(5)-H(51)	0.971	C(21)-C(22)	1.438(5)
C(6)-C(7)	1.393(6)	C(22)-C(23)	1.327(6)
C(6)-H(61)	0.970	C(22)-H(221)	0.969
C(7)-C(8)	1.426(5)	C(23)-C(24)	1.439(5)
C(8)-C(9)	1.344(6)	C(23)-H(231)	0.970
C(8)-H(81)	0.967	C(24)-C(25)	1.390(5)
C(9)-C(10)	1.437(6)	C(25)-C(26)	1.353(6)
C(9)-H(91)	0.970	C(25)-H(251)	0.971
C(10)-C(11)	1.410(6)	C(26)-C(27)	1.409(5)
C(11)-C(12)	1.353(6)	C(26)-H(261)	0.973
C(11)-H(111)	0.970	C(27)-C(28)	1.481(5)

C(28)-Cl(4)	1.785(4)	P(1)-F(1)	1.604(2)
C(28)-Cl(40)	1.647(4)	P(1)-F(2)	1.582(3)
C(28)-H(281)	0.968	P(1)-F(3)	1.577(2)
C(28)-H(282)	0.971	P(1)-F(4)	1.579(3)
C(28)-H(283)	0.969	P(1)-F(5)	1.584(3)
C(28)-H(284)	0.974	P(1)-F(6)	1.566(3)
N(1)-Cu(1)-N(2)	82.13(10)	H(31)-C(3)-H(32)	109.5
N(1)-Cu(1)-N(3)	123.00(9)	C(3)-C(4)-N(1)	116.6(3)
N(2)-Cu(1)-N(3)	122.53(9)	C(3)-C(4)-C(5)	121.1(3)
N(1)-Cu(1)-N(4)	126.77(9)	N(1)-C(4)-C(5)	122.3(3)
N(2)-Cu(1)-N(4)	126.18(10)	C(4)-C(5)-C(6)	119.4(3)
N(3)-Cu(1)-N(4)	82.08(9)	C(4)-C(5)-H(51)	120.2
Cu(1)-N(1)-C(1)	111.59(19)	C(6)-C(5)-H(51)	120.4
Cu(1)-N(1)-C(4)	129.9(2)	C(5)-C(6)-C(7)	120.3(3)
C(1)-N(1)-C(4)	118.5(3)	C(5)-C(6)-H(61)	119.7
Cu(1)-N(2)-C(2)	111.30(19)	C(7)-C(6)-H(61)	120.0
Cu(1)-N(2)-C(13)	130.3(2)	C(1)-C(7)-C(6)	117.2(3)
C(2)-N(2)-C(13)	118.4(3)	C(1)-C(7)-C(8)	118.6(4)
Cu(1)-N(3)-C(15)	111.65(18)	C(6)-C(7)-C(8)	124.2(3)
Cu(1)-N(3)-C(18)	130.1(2)	C(7)-C(8)-C(9)	121.5(3)
C(15)-N(3)-C(18)	118.2(2)	C(7)-C(8)-H(81)	119.4
Cu(1)-N(4)-C(16)	111.36(19)	C(9)-C(8)-H(81)	119.1
Cu(1)-N(4)-C(27)	130.1(2)	C(8)-C(9)-C(10)	121.5(3)
C(16)-N(4)-C(27)	118.5(3)	C(8)-C(9)-H(91)	119.3
N(1)-C(1)-C(2)	117.7(2)	C(10)-C(9)-H(91)	119.3
N(1)-C(1)-C(7)	122.3(3)	C(9)-C(10)-C(2)	118.5(4)
C(2)-C(1)-C(7)	119.9(3)	C(9)-C(10)-C(11)	124.4(3)
C(1)-C(2)-N(2)	117.2(2)	C(2)-C(10)-C(11)	117.0(3)
C(1)-C(2)-C(10)	120.0(3)	C(10)-C(11)-C(12)	119.6(3)
N(2)-C(2)-C(10)	122.8(3)	C(10)-C(11)-H(111)	119.9
C(4)-C(3)-Cl(1)	108.0(2)	C(12)-C(11)-H(111)	120.5
C(4)-C(3)-H(31)	109.9	C(11)-C(12)-C(13)	120.3(3)
Cl(1)-C(3)-H(31)	109.8	C(11)-C(12)-H(121)	119.7
C(4)-C(3)-H(32)	109.9	C(13)-C(12)-H(121)	120.0
Cl(1)-C(3)-H(32)	109.8	C(12)-C(13)-N(2)	121.8(3)

C(12)-C(13)-C(14)	122.6(3)	C(15)-C(21)-C(20)	117.1(3)
N(2)-C(13)-C(14)	115.5(3)	C(15)-C(21)-C(22)	118.4(3)
C(13)-C(14)-Cl(2)	113.7(3)	C(20)-C(21)-C(22)	124.5(3)
C(13)-C(14)-Cl(20)	102.3(3)	C(21)-C(22)-C(23)	121.9(3)
C(13)-C(14)-H(141)	108.5	C(21)-C(22)-H(221)	119.1
Cl(2)-C(14)-H(141)	108.6	C(23)-C(22)-H(221)	119.1
C(13)-C(14)-H(142)	108.1	C(22)-C(23)-C(24)	121.8(3)
Cl(2)-C(14)-H(142)	108.4	C(22)-C(23)-H(231)	119.1
H(141)-C(14)-H(142)	109.6	C(24)-C(23)-H(231)	119.1
C(13)-C(14)-H(143)	111.2	C(23)-C(24)-C(16)	118.0(3)
Cl(20)-C(14)-H(143)	111.6	C(23)-C(24)-C(25)	124.8(3)
C(13)-C(14)-H(144)	110.9	C(16)-C(24)-C(25)	117.2(3)
Cl(20)-C(14)-H(144)	111.2	C(24)-C(25)-C(26)	120.1(3)
H(143)-C(14)-H(144)	109.5	C(24)-C(25)-H(251)	119.7
N(3)-C(15)-C(16)	117.2(2)	C(26)-C(25)-H(251)	120.2
N(3)-C(15)-C(21)	122.8(3)	C(25)-C(26)-C(27)	119.9(3)
C(16)-C(15)-C(21)	119.9(3)	C(25)-C(26)-H(261)	120.3
C(15)-C(16)-N(4)	117.6(2)	C(27)-C(26)-H(261)	119.8
C(15)-C(16)-C(24)	120.0(3)	C(26)-C(27)-N(4)	122.0(3)
N(4)-C(16)-C(24)	122.4(3)	C(26)-C(27)-C(28)	123.7(3)
Cu(1)-C(16)-C(24)	164.5(2)	N(4)-C(27)-C(28)	114.3(3)
C(18)-C(17)-Cl(3)	110.4(2)	C(27)-C(28)-Cl(4)	103.7(3)
C(18)-C(17)-H(171)	109.4	C(27)-C(28)-Cl(40)	125.7(3)
Cl(3)-C(17)-H(171)	109.2	C(27)-C(28)-H(281)	111.1
C(18)-C(17)-H(172)	109.3	Cl(4)-C(28)-H(281)	110.8
Cl(3)-C(17)-H(172)	109.1	C(27)-C(28)-H(282)	110.9
H(171)-C(17)-H(172)	109.3	Cl(4)-C(28)-H(282)	110.6
C(17)-C(18)-N(3)	116.9(3)	Cl(40)-C(28)-H(282)	114.4
C(17)-C(18)-C(19)	121.1(3)	H(281)-C(28)-H(282)	109.6
N(3)-C(18)-C(19)	122.0(3)	C(27)-C(28)-H(283)	105.4
C(18)-C(19)-C(20)	120.1(3)	Cl(40)-C(28)-H(283)	105.3
C(18)-C(19)-H(191)	119.9	C(27)-C(28)-H(284)	105.4
C(20)-C(19)-H(191)	120.1	Cl(40)-C(28)-H(284)	105.2
C(19)-C(20)-C(21)	119.8(3)	H(281)-C(28)-H(284)	129.9
C(19)-C(20)-H(201)	120.3	H(283)-C(28)-H(284)	109.2
C(21)-C(20)-H(201)	119.9	F(1)-P(1)-F(2)	178.13(19)

F(1)-P(1)-F(3)	90.09(13)	F(3)-P(1)-F(5)	90.34(18)
F(2)-P(1)-F(3)	89.39(15)	F(4)-P(1)-F(5)	89.2(2)
F(1)-P(1)-F(4)	89.52(15)	F(1)-P(1)-F(6)	90.15(18)
F(2)-P(1)-F(4)	90.99(16)	F(2)-P(1)-F(6)	91.63(19)
F(3)-P(1)-F(4)	179.43(16)	F(3)-P(1)-F(6)	88.66(15)
F(1)-P(1)-F(5)	87.97(15)	F(4)-P(1)-F(6)	91.8(2)
F(2)-P(1)-F(5)	90.24(18)	F(5)-P(1)-F(6)	177.9(2)

**Crystal data and structure refinement for Bis[6,6'-bis(chloromethyl)-2,2'-bipyridine]copper(I) hexafluorophosphate.**

Table 1. Crystal data and structure refinement for Bis[6,6'-bis(chloromethyl)-2,2'-bipyridine]copper(I) hexafluorophosphate.

Identification code	ValC-CuClPF6	
Empirical formula	C <sub>24</sub> H <sub>20</sub> Cl <sub>4</sub> Cu <sub>1</sub> F <sub>6</sub> N <sub>4</sub> P <sub>1</sub>	
Formula weight	714.77	
Temperature	173 K	
Wavelength	0.71073 Å	
Crystal system	Monoclinic	
Space group	P 1 21/n 1	
Unit cell dimensions	a = 12.4844(3) Å	α = 90°
	b = 14.0092(2) Å	β = 100.7204(10)°
	c = 16.1422(3) Å	γ = 90°
Volume	2773.94(9) Å <sup>3</sup>	
Z	4	
Density (calculated)	1.711 Mg/m <sup>3</sup>	
Absorption coefficient	1.295 mm <sup>-1</sup>	
F(000)	1432	
Crystal size	0.43 x 0.20 x 0.06 mm <sup>3</sup>	
Theta range for data collection	1.900 to 27.454°.	
Index ranges	-16 ≤ h ≤ 16, -17 ≤ k ≤ 18, -20 ≤ l ≤ 20	
Reflections collected	22346	
Independent reflections	6333 [R(int) = 0.039]	
Completeness to theta = 27.454°	100.0 %	
Absorption correction	Semi-empirical from equivalents	



Max. and min. transmission	0.93 and 0.77
Refinement method	Full-matrix least-squares on $F^2$
Data / restraints / parameters	4194 / 120 / 415
Goodness-of-fit on $F^2$	1.2823
Final R indices [ $I > 2\sigma(I)$ ]	R1 = 0.0460, wR2 = 0.0546
R indices (all data)	R1 = 0.0729, wR2 = 0.0753
Largest diff. peak and hole	0.83 and -0.72 e.Å <sup>-3</sup>

Table 2. Atomic coordinates ( $\times 10^4$ ) and equivalent isotropic displacement parameters ( $\text{Å}^2 \times 10^3$ ) for Bis[6,6'-bis(chloromethyl)-2,2'-bipyridine]copper(I) hexafluorophosphate.  $U(\text{eq})$  is defined as one third of the trace of the orthogonalized  $U^{ij}$  tensor.

	<b>x</b>	<b>y</b>	<b>z</b>	<b>U(eq)</b>
Cu(1)	7071(1)	1597(1)	3624(1)	39
N(1)	7866(2)	1901(2)	2676(2)	37
N(2)	5915(3)	1153(2)	2648(2)	39
N(3)	7673(2)	876(2)	4688(2)	39
N(4)	6745(2)	2584(2)	4460(2)	38
C(1)	9459(3)	2509(3)	3616(3)	50
C(2)	8874(3)	2258(3)	2746(2)	40
C(3)	9360(3)	2404(3)	2050(3)	48
C(4)	8779(4)	2201(3)	1270(3)	55
C(5)	7739(4)	1842(3)	1188(2)	49
C(6)	7300(3)	1695(3)	1904(2)	39
C(7)	6182(3)	1308(3)	1885(2)	41
C(8)	5458(4)	1126(3)	1140(3)	52
C(9)	4438(4)	771(4)	1187(3)	62
C(10)	4172(4)	595(3)	1965(3)	58
C(11)	4925(3)	803(3)	2691(3)	45
C(12)	4681(4)	650(3)	3546(3)	52
C(13)	8211(4)	-450(3)	3928(3)	64
C(14)	8107(3)	-2(3)	4752(3)	48
C(15)	8406(4)	-451(4)	5527(3)	61
C(16)	8257(4)	21(4)	6242(3)	66
C(17)	7828(4)	920(4)	6183(3)	57

C(18)	7522(3)	1338(3)	5396(2)	42
C(19)	7038(3)	2299(3)	5270(2)	42
C(20)	6895(4)	2893(4)	5924(3)	56
C(21)	6459(4)	3791(4)	5736(3)	65
C(22)	6186(3)	4088(3)	4915(3)	56
C(23)	6327(3)	3459(3)	4281(3)	45
C(24)	6022(4)	3661(3)	3357(3)	52
Cl(1)	9043(1)	3685(1)	3871(1)	72
Cl(2)	5192(1)	-486(1)	3956(1)	64
Cl(3)	5708(1)	4871(1)	3097(1)	81
Cl(4)	9271(1)	-1320(1)	4029(1)	71
P(1)	2825(1)	3113(1)	3624(1)	54
F(1)	2048(5)	2274(6)	3145(4)	100
F(2)	3602(6)	3800(5)	4135(6)	115
F(3)	2312(9)	3809(6)	2972(4)	132
F(4)	3324(8)	2279(5)	4284(4)	106
F(5)	1944(5)	3280(6)	4187(4)	78
F(6)	3694(7)	2799(7)	3077(6)	87
F(11)	2425(7)	2258(5)	3989(6)	123
F(12)	3198(5)	4124(4)	3248(4)	71
F(13)	1791(4)	3231(6)	2898(4)	84
F(14)	3867(5)	3183(8)	4306(4)	111
F(15)	2196(6)	3785(5)	4197(4)	86
F(16)	3437(7)	2594(6)	3003(5)	75

Table 3. Bond lengths [Å] and angles [°] for Bis[6,6'-bis(chloromethyl)-2,2'-bipyridine]copper(I) hexafluorophosphate.

Cu(1)-N(1)	2.018(3)	N(3)-C(14)	1.341(5)
Cu(1)-N(2)	2.026(3)	N(3)-C(18)	1.356(5)
Cu(1)-N(3)	2.014(3)	N(4)-C(19)	1.351(5)
Cu(1)-N(4)	2.026(3)	N(4)-C(23)	1.342(5)
N(1)-C(2)	1.340(5)	C(1)-C(2)	1.498(5)
N(1)-C(6)	1.345(5)	C(1)-Cl(1)	1.798(5)
N(2)-C(7)	1.352(5)	C(1)-H(11)	0.968
N(2)-C(11)	1.343(5)	C(1)-H(12)	0.976

C(2)-C(3)	1.388(5)	C(16)-H(161)	0.942
C(3)-C(4)	1.362(6)	C(17)-C(18)	1.386(6)
C(3)-H(31)	0.945	C(17)-H(171)	0.949
C(4)-C(5)	1.376(6)	C(18)-C(19)	1.474(6)
C(4)-H(41)	0.933	C(19)-C(20)	1.381(6)
C(5)-C(6)	1.383(5)	C(20)-C(21)	1.382(8)
C(5)-H(51)	0.944	C(20)-H(201)	0.949
C(6)-C(7)	1.492(5)	C(21)-C(22)	1.370(8)
C(7)-C(8)	1.388(5)	C(21)-H(211)	0.936
C(8)-C(9)	1.382(7)	C(22)-C(23)	1.386(6)
C(8)-H(81)	0.953	C(22)-H(221)	0.947
C(9)-C(10)	1.378(7)	C(23)-C(24)	1.496(6)
C(9)-H(91)	0.937	C(24)-Cl(3)	1.773(4)
C(10)-C(11)	1.391(6)	C(24)-H(241)	0.978
C(10)-H(101)	0.936	C(24)-H(242)	0.980
C(11)-C(12)	1.482(6)	P(1)-F(1)	1.625(5)
C(12)-Cl(2)	1.795(4)	P(1)-F(2)	1.500(6)
C(12)-H(121)	0.977	P(1)-F(3)	1.489(6)
C(12)-H(122)	0.969	P(1)-F(4)	1.625(5)
C(13)-C(14)	1.498(7)	P(1)-F(5)	1.569(5)
C(13)-Cl(4)	1.784(5)	P(1)-F(6)	1.583(6)
C(13)-H(131)	0.974	P(1)-F(11)	1.462(5)
C(13)-H(132)	0.975	P(1)-F(12)	1.643(5)
C(14)-C(15)	1.388(6)	P(1)-F(13)	1.582(5)
C(15)-C(16)	1.373(8)	P(1)-F(14)	1.543(5)
C(15)-H(151)	0.940	P(1)-F(15)	1.622(6)
C(16)-C(17)	1.366(8)	P(1)-F(16)	1.551(6)
N(1)-Cu(1)-N(2)	81.66(12)	C(2)-N(1)-C(6)	118.8(3)
N(1)-Cu(1)-N(3)	126.47(12)	Cu(1)-N(2)-C(7)	113.4(2)
N(2)-Cu(1)-N(3)	127.47(12)	Cu(1)-N(2)-C(11)	126.9(3)
N(1)-Cu(1)-N(4)	123.29(12)	C(7)-N(2)-C(11)	119.5(3)
N(2)-Cu(1)-N(4)	121.68(12)	Cu(1)-N(3)-C(14)	127.4(3)
N(3)-Cu(1)-N(4)	82.15(13)	Cu(1)-N(3)-C(18)	113.0(3)
Cu(1)-N(1)-C(2)	127.0(2)	C(14)-N(3)-C(18)	119.4(3)
Cu(1)-N(1)-C(6)	114.2(2)	Cu(1)-N(4)-C(19)	113.0(3)

Cu(1)-N(4)-C(23)	126.7(3)	C(10)-C(11)-N(2)	121.1(4)
C(19)-N(4)-C(23)	120.2(3)	C(10)-C(11)-C(12)	122.0(4)
C(2)-C(1)-Cl(1)	108.6(3)	N(2)-C(11)-C(12)	116.9(4)
C(2)-C(1)-H(11)	111.5	C(11)-C(12)-Cl(2)	110.5(3)
Cl(1)-C(1)-H(11)	108.0	C(11)-C(12)-H(121)	109.4
C(2)-C(1)-H(12)	110.6	Cl(2)-C(12)-H(121)	109.0
Cl(1)-C(1)-H(12)	108.0	C(11)-C(12)-H(122)	109.3
H(11)-C(1)-H(12)	110.0	Cl(2)-C(12)-H(122)	108.5
C(1)-C(2)-N(1)	116.9(3)	H(121)-C(12)-H(122)	110.1
C(1)-C(2)-C(3)	120.9(3)	C(14)-C(13)-Cl(4)	112.9(4)
N(1)-C(2)-C(3)	122.1(3)	C(14)-C(13)-H(131)	109.5
C(2)-C(3)-C(4)	118.7(4)	Cl(4)-C(13)-H(131)	106.1
C(2)-C(3)-H(31)	120.3	C(14)-C(13)-H(132)	110.2
C(4)-C(3)-H(31)	121.0	Cl(4)-C(13)-H(132)	108.5
C(3)-C(4)-C(5)	119.7(4)	H(131)-C(13)-H(132)	109.5
C(3)-C(4)-H(41)	120.7	C(13)-C(14)-N(3)	114.6(4)
C(5)-C(4)-H(41)	119.6	C(13)-C(14)-C(15)	123.9(4)
C(4)-C(5)-C(6)	119.2(4)	N(3)-C(14)-C(15)	121.5(4)
C(4)-C(5)-H(51)	121.2	C(14)-C(15)-C(16)	119.0(5)
C(6)-C(5)-H(51)	119.6	C(14)-C(15)-H(151)	119.9
C(5)-C(6)-N(1)	121.4(4)	C(16)-C(15)-H(151)	121.1
C(5)-C(6)-Cu(1)	161.6(3)	C(15)-C(16)-C(17)	119.8(4)
C(5)-C(6)-C(7)	123.5(3)	C(15)-C(16)-H(161)	120.2
N(1)-C(6)-C(7)	115.1(3)	C(17)-C(16)-H(161)	120.0
C(6)-C(7)-N(2)	115.4(3)	C(16)-C(17)-C(18)	119.4(4)
C(6)-C(7)-C(8)	122.8(4)	C(16)-C(17)-H(171)	120.4
N(2)-C(7)-C(8)	121.9(4)	C(18)-C(17)-H(171)	120.2
C(7)-C(8)-C(9)	118.5(4)	C(17)-C(18)-N(3)	120.9(4)
C(7)-C(8)-H(81)	120.7	C(17)-C(18)-C(19)	123.2(4)
C(9)-C(8)-H(81)	120.8	N(3)-C(18)-C(19)	116.0(3)
C(8)-C(9)-C(10)	119.7(4)	C(18)-C(19)-N(4)	115.7(3)
C(8)-C(9)-H(91)	119.7	C(18)-C(19)-C(20)	123.6(4)
C(10)-C(9)-H(91)	120.6	N(4)-C(19)-C(20)	120.7(4)
C(9)-C(10)-C(11)	119.4(4)	Cu(1)-C(19)-C(20)	161.7(3)
C(9)-C(10)-H(101)	121.5	C(19)-C(20)-C(21)	118.9(4)
C(11)-C(10)-H(101)	119.1	C(19)-C(20)-H(201)	120.4

C(21)-C(20)-H(201)	120.8	F(2)-P(1)-F(5)	92.1(4)
C(20)-C(21)-C(22)	120.4(4)	F(3)-P(1)-F(5)	93.2(4)
C(20)-C(21)-H(211)	119.9	F(4)-P(1)-F(5)	87.3(4)
C(22)-C(21)-H(211)	119.7	F(1)-P(1)-F(6)	86.8(4)
C(21)-C(22)-C(23)	118.6(4)	F(2)-P(1)-F(6)	92.5(4)
C(21)-C(22)-H(221)	121.8	F(3)-P(1)-F(6)	92.1(4)
C(23)-C(22)-H(221)	119.7	F(4)-P(1)-F(6)	86.9(4)
C(22)-C(23)-N(4)	121.2(4)	F(5)-P(1)-F(6)	172.5(5)
C(22)-C(23)-C(24)	124.9(4)	F(11)-P(1)-F(12)	175.2(4)
N(4)-C(23)-C(24)	113.8(3)	F(11)-P(1)-F(13)	95.3(4)
C(23)-C(24)-Cl(3)	114.9(3)	F(12)-P(1)-F(13)	83.4(3)
C(23)-C(24)-H(241)	109.2	F(11)-P(1)-F(14)	94.1(4)
Cl(3)-C(24)-H(241)	105.5	F(12)-P(1)-F(14)	87.0(4)
C(23)-C(24)-H(242)	109.5	F(13)-P(1)-F(14)	170.0(5)
Cl(3)-C(24)-H(242)	106.2	F(11)-P(1)-F(15)	90.5(4)
H(241)-C(24)-H(242)	111.5	F(12)-P(1)-F(15)	84.8(3)
F(1)-P(1)-F(2)	173.4(5)	F(13)-P(1)-F(15)	87.0(3)
F(1)-P(1)-F(3)	89.8(4)	F(14)-P(1)-F(15)	89.5(4)
F(2)-P(1)-F(3)	96.7(5)	F(11)-P(1)-F(16)	97.1(4)
F(1)-P(1)-F(4)	85.1(4)	F(12)-P(1)-F(16)	87.5(4)
F(2)-P(1)-F(4)	88.3(4)	F(13)-P(1)-F(16)	90.1(4)
F(3)-P(1)-F(4)	174.9(5)	F(14)-P(1)-F(16)	92.2(4)
F(1)-P(1)-F(5)	87.9(3)	F(15)-P(1)-F(16)	172.1(4)

**Crystal data and structure refinement for 6-(Bromomethyl)-6'-methyl-2, 2'-bipyridine.**

Table 1. Crystal data and structure refinement for 6-(Bromomethyl)-6'-methyl-2, 2'-bipyridine.

Identification code	CRYSTALS_cif	
Empirical formula	C12 H11 Br1 N2	
Formula weight	263.14	
Temperature	173 K	
Wavelength	0.71073 Å	
Crystal system	Monoclinic	
Space group	P 1 21/c 1	
Unit cell dimensions	a = 6.58310(10) Å	$\alpha = 90^\circ$

	$b = 24.6674(4) \text{ \AA}$	$\beta = 111.4355(9)^\circ$
	$c = 7.23630(10) \text{ \AA}$	$\gamma = 90^\circ$
Volume	$1093.81(3) \text{ \AA}^3$	
Z	4	
Density (calculated)	$1.598 \text{ Mg/m}^3$	
Absorption coefficient	$3.724 \text{ mm}^{-1}$	
F(000)	528	
Crystal size	$0.23 \times 0.22 \times 0.11 \text{ mm}^3$	
Theta range for data collection	1.651 to 29.945°.	
Index ranges	$-9 \leq h \leq 9, -34 \leq k \leq 34, -10 \leq l \leq 10$	
Reflections collected	11682	
Independent reflections	3163 [R(int) = 0.024]	
Completeness to theta = 29.945°	100.0 %	
Absorption correction	Semi-empirical from equivalents	
Max. and min. transmission	0.66 and 0.44	
Refinement method	Full-matrix least-squares on F <sup>2</sup>	
Data / restraints / parameters	2324 / 0 / 136	
Goodness-of-fit on F <sup>2</sup>	1.0547	
Final R indices [I > 2σ(I)]	R1 = 0.0260, wR2 = 0.0254	
R indices (all data)	R1 = 0.0351, wR2 = 0.0295	
Largest diff. peak and hole	0.24 and -0.79 e.Å <sup>-3</sup>	

Table 2. Atomic coordinates ( $\times 10^4$ ) and equivalent isotropic displacement parameters ( $\text{\AA}^2 \times 10^3$ ) for 6-(Bromomethyl)-6'-methyl-2, 2'-bipyridine.

U(eq) is defined as one third of the trace of the orthogonalized  $U^{ij}$  tensor.

	x	y	z	U(eq)
Br(1)	-1639(1)	5016(1)	2055(1)	36
N(1)	1451(2)	6103(1)	4964(2)	25
N(2)	4796(2)	6656(1)	9734(2)	27
C(1)	-382(3)	5715(1)	1722(2)	30
C(2)	1673(2)	5826(1)	3462(2)	26
C(3)	3679(3)	5648(1)	3454(3)	31
C(4)	5539(3)	5761(1)	5094(3)	34
C(5)	5331(3)	6045(1)	6661(2)	30

C(6)	3272(2)	6210(1)	6555(2)	24
C(7)	2968(2)	6507(1)	8221(2)	23
C(8)	887(3)	6612(1)	8214(2)	29
C(9)	695(3)	6875(1)	9830(3)	33
C(10)	2557(3)	7034(1)	11378(3)	33
C(11)	4584(3)	6917(1)	11274(2)	30
C(12)	6663(3)	7080(1)	12914(3)	43

Table 3. Bond lengths [Å] and angles [°] for 6-(Bromomethyl)-6'-methyl-2, 2'-bipyridine.

Br(1)-C(1)	1.9651(17)	C(5)-H(51)	0.937
N(1)-C(2)	1.336(2)	C(6)-C(7)	1.485(2)
N(1)-C(6)	1.3503(19)	C(7)-C(8)	1.393(2)
N(2)-C(7)	1.3491(19)	C(8)-C(9)	1.384(2)
N(2)-C(11)	1.338(2)	C(8)-H(81)	0.923
C(1)-C(2)	1.499(2)	C(9)-C(10)	1.381(3)
C(1)-H(11)	0.969	C(9)-H(91)	0.928
C(1)-H(12)	0.988	C(10)-C(11)	1.394(2)
C(2)-C(3)	1.395(2)	C(10)-H(101)	0.942
C(3)-C(4)	1.387(2)	C(11)-C(12)	1.502(2)
C(3)-H(31)	0.953	C(12)-H(121)	0.960
C(4)-C(5)	1.381(2)	C(12)-H(122)	0.950
C(4)-H(41)	0.974	C(12)-H(123)	0.955
C(5)-C(6)	1.390(2)		
C(2)-N(1)-C(6)	117.82(13)	C(2)-C(3)-C(4)	118.28(15)
C(7)-N(2)-C(11)	118.31(14)	C(2)-C(3)-H(31)	119.7
Br(1)-C(1)-C(2)	110.38(11)	C(4)-C(3)-H(31)	122.0
Br(1)-C(1)-H(11)	108.6	C(3)-C(4)-C(5)	118.89(15)
C(2)-C(1)-H(11)	111.1	C(3)-C(4)-H(41)	118.9
Br(1)-C(1)-H(12)	105.9	C(5)-C(4)-H(41)	122.2
C(2)-C(1)-H(12)	111.4	C(4)-C(5)-C(6)	119.37(14)
H(11)-C(1)-H(12)	109.2	C(4)-C(5)-H(51)	121.6
C(1)-C(2)-N(1)	116.33(14)	C(6)-C(5)-H(51)	119.1
C(1)-C(2)-C(3)	120.29(15)	C(5)-C(6)-N(1)	122.26(14)
N(1)-C(2)-C(3)	123.38(14)	C(5)-C(6)-C(7)	121.14(13)

N(1)-C(6)-C(7)	116.59(13)	C(9)-C(10)-H(101)	121.8
C(6)-C(7)-N(2)	116.69(13)	C(11)-C(10)-H(101)	119.4
C(6)-C(7)-C(8)	120.84(14)	C(10)-C(11)-N(2)	122.53(15)
N(2)-C(7)-C(8)	122.46(14)	C(10)-C(11)-C(12)	121.11(16)
C(7)-C(8)-C(9)	118.54(15)	N(2)-C(11)-C(12)	116.36(16)
C(7)-C(8)-H(81)	120.3	C(11)-C(12)-H(121)	114.0
C(9)-C(8)-H(81)	121.1	C(11)-C(12)-H(122)	110.8
C(8)-C(9)-C(10)	119.36(16)	H(121)-C(12)-H(122)	107.6
C(8)-C(9)-H(91)	118.9	C(11)-C(12)-H(123)	112.7
C(10)-C(9)-H(91)	121.7	H(121)-C(12)-H(123)	104.7
C(9)-C(10)-C(11)	118.79(15)	H(122)-C(12)-H(123)	106.7

### **Crystal data and structure refinement for 2,9-Di(chloromethyl)-1,10-phenanthroline.**

Table 1. Crystal data and structure refinement for 2,9-Di(chloromethyl)-1,10-phenanthroline.

Identification code	ValC-074l	
Empirical formula	C <sub>14</sub> H <sub>12</sub> Cl <sub>2</sub> N <sub>2</sub> O <sub>1</sub>	
Formula weight	295.17	
Temperature	173 K	
Wavelength	0.71073 Å	
Crystal system	Orthorhombic	
Space group	P 21 21 21	
Unit cell dimensions	a = 4.605(2) Å	α = 90°
	b = 16.575(7) Å	β = 90°
	c = 17.134(6) Å	γ = 90°
Volume	1307.9(9) Å <sup>3</sup>	
Z	4	
Density (calculated)	1.499 Mg/m <sup>3</sup>	
Absorption coefficient	0.488 mm <sup>-1</sup>	
F(000)	608	
Crystal size	0.40 x 0.06 x 0.04 mm <sup>3</sup>	
Theta range for data collection	3.420 to 25.301°.	
Index ranges	-4 ≤ h ≤ 5, -16 ≤ k ≤ 19, -19 ≤ l ≤ 20	
Reflections collected	4685	
Independent reflections	2195 [R(int) = 0.069]	



Completeness to $\theta = 25.301^\circ$	95.0 %
Absorption correction	Semi-empirical from equivalents
Max. and min. transmission	0.98 and 0.97
Refinement method	Full-matrix least-squares on $F^2$
Data / restraints / parameters	1668 / 0 / 173
Goodness-of-fit on $F^2$	1.0751
Final R indices [ $I > 2\sigma(I)$ ]	$R1 = 0.0974$ , $wR2 = 0.0829$
R indices (all data)	$R1 = 0.1271$ , $wR2 = 0.1266$
Absolute structure parameter	0.0(2)
Largest diff. peak and hole	0.82 and -0.63 $e.\text{\AA}^{-3}$

Table 2. Atomic coordinates ( $\times 10^4$ ) and equivalent isotropic displacement parameters ( $\text{\AA}^2 \times 10^3$ ) for 2,9-Di(chloromethyl)-1,10-phenanthroline.

$U(\text{eq})$  is defined as one third of the trace of the orthogonalized  $U_{ij}$  tensor.

	<b>x</b>	<b>y</b>	<b>z</b>	<b>U(eq)</b>
Cl(1)	11767(6)	9346(1)	3964(1)	79
Cl(2)	3570(7)	4703(1)	4400(1)	85
N(1)	10089(14)	7639(3)	2957(3)	49
N(2)	5917(13)	6464(3)	3200(3)	47
C(1)	13560(20)	8521(4)	3547(4)	62
C(2)	12004(16)	8213(4)	2846(4)	47
C(3)	12719(16)	8510(4)	2101(4)	49
C(4)	11418(18)	8179(4)	1473(4)	49
C(5)	9466(16)	7561(4)	1555(4)	47
C(6)	8085(19)	7138(5)	925(4)	57
C(7)	6188(19)	6532(5)	1034(4)	61
C(8)	5327(17)	6291(4)	1803(4)	49
C(9)	3304(18)	5686(4)	1948(4)	55
C(10)	2576(16)	5491(4)	2688(5)	57
C(11)	3986(15)	5910(4)	3308(4)	42
C(12)	3240(20)	5748(4)	4139(4)	59
C(13)	6658(17)	6673(4)	2451(4)	46
C(14)	8754(16)	7305(4)	2334(4)	44
O(1)	8415(14)	7225(3)	4662(3)	66

Table 3. Bond lengths [Å] and angles [°] for 2,9-Di(chloromethyl)-1,10-phenanthroline.

Cl(1)-C(1)	1.750(8)	C(6)-C(7)	1.344(11)
Cl(2)-C(12)	1.795(7)	C(6)-H(61)	0.925
N(1)-C(2)	1.311(9)	C(7)-C(8)	1.432(11)
N(1)-C(14)	1.351(9)	C(7)-H(71)	0.929
N(2)-C(11)	1.292(8)	C(8)-C(9)	1.392(10)
N(2)-C(13)	1.372(9)	C(8)-C(13)	1.417(9)
C(1)-C(2)	1.488(11)	C(9)-C(10)	1.351(11)
C(1)-H(11)	0.965	C(9)-H(91)	0.932
C(1)-H(12)	0.969	C(10)-C(11)	1.426(10)
C(2)-C(3)	1.407(9)	C(10)-H(101)	0.934
C(3)-C(4)	1.350(10)	C(11)-C(12)	1.489(10)
C(3)-H(31)	0.924	C(12)-H(121)	0.969
C(4)-C(5)	1.370(10)	C(12)-H(122)	0.964
C(4)-H(41)	0.928	C(13)-C(14)	1.438(10)
C(5)-C(6)	1.436(10)	O(1)-H(1)	0.827
C(5)-C(14)	1.439(9)	O(1)-H(2)	0.829
C(2)-N(1)-C(14)	119.3(6)	C(5)-C(4)-H(41)	119.7
C(11)-N(2)-C(13)	119.0(6)	C(4)-C(5)-C(6)	125.3(7)
Cl(1)-C(1)-C(2)	111.8(6)	C(4)-C(5)-C(14)	117.8(6)
Cl(1)-C(1)-H(11)	107.9	C(6)-C(5)-C(14)	116.9(7)
C(2)-C(1)-H(11)	108.8	C(5)-C(6)-C(7)	123.2(7)
Cl(1)-C(1)-H(12)	109.2	C(5)-C(6)-H(61)	118.1
C(2)-C(1)-H(12)	109.6	C(7)-C(6)-H(61)	118.7
H(11)-C(1)-H(12)	109.5	C(6)-C(7)-C(8)	121.1(7)
C(1)-C(2)-N(1)	117.1(6)	C(6)-C(7)-H(71)	119.5
C(1)-C(2)-C(3)	119.9(6)	C(8)-C(7)-H(71)	119.3
N(1)-C(2)-C(3)	122.9(7)	C(7)-C(8)-C(9)	123.4(7)
C(2)-C(3)-C(4)	118.5(7)	C(7)-C(8)-C(13)	118.4(7)
C(2)-C(3)-H(31)	121.2	C(9)-C(8)-C(13)	118.1(7)
C(4)-C(3)-H(31)	120.2	C(8)-C(9)-C(10)	120.4(7)
C(3)-C(4)-C(5)	120.9(7)	C(8)-C(9)-H(91)	119.9
C(3)-C(4)-H(41)	119.4	C(10)-C(9)-H(91)	119.7

C(9)-C(10)-C(11)	118.1(7)	Cl(2)-C(12)-H(122)	108.1
C(9)-C(10)-H(101)	122.1	H(121)-C(12)-H(122)	109.6
C(11)-C(10)-H(101)	119.9	C(8)-C(13)-N(2)	120.8(7)
C(10)-C(11)-N(2)	123.5(7)	C(8)-C(13)-C(14)	120.4(6)
C(10)-C(11)-C(12)	121.3(6)	N(2)-C(13)-C(14)	118.7(6)
N(2)-C(11)-C(12)	115.2(6)	C(5)-C(14)-C(13)	119.8(6)
C(11)-C(12)-Cl(2)	113.1(5)	C(5)-C(14)-N(1)	120.6(7)
C(11)-C(12)-H(121)	108.9	C(13)-C(14)-N(1)	119.6(6)
Cl(2)-C(12)-H(121)	108.3	H(1)-O(1)-H(2)	113.1
C(11)-C(12)-H(122)	108.8		

### Crystal data and structure refinement for 2,9-di(anisyl)-1,10-phenanthroline.

Table 1. Crystal data and structure refinement for 2,9-di(anisyl)-1,10-phenanthroline.

Identification code	CRYSTALS_cif	
Empirical formula	C <sub>26.33</sub> H <sub>20.67</sub> Cl <sub>0.67</sub> N <sub>2</sub> O <sub>2</sub>	
Formula weight	420.77	
Temperature	173 K	
Wavelength	0.71073 Å	
Crystal system	Hexagonal	
Space group	P 61	
Unit cell dimensions	a = 17.5578(3) Å	α = 90°
	b = 17.5578(3) Å	β = 90°
	c = 12.0266(2) Å	γ = 120°
Volume	3210.80(9) Å <sup>3</sup>	
Z	6	
Density (calculated)	1.306 Mg/m <sup>3</sup>	
Absorption coefficient	0.163 mm <sup>-1</sup>	
F(000)	1320.000	
Crystal size	0.18 x 0.15 x 0.13 mm <sup>3</sup>	
Theta range for data collection	1.339 to 27.471°.	
Index ranges	-20 ≤ h ≤ 19, -22 ≤ k ≤ 22, -14 ≤ l ≤ 15	
Reflections collected	15149	
Independent reflections	4845 [R(int) = 0.046]	
Completeness to theta = 27.471°	99.8 %	

Absorption correction	Semi-empirical from equivalents
Max. and min. transmission	0.98 and 0.98
Refinement method	Full-matrix least-squares on $F^2$
Data / restraints / parameters	3310 / 18 / 299
Goodness-of-fit on $F^2$	1.1107
Final R indices [ $I > 2\sigma(I)$ ]	R1 = 0.0432, wR2 = 0.0498
R indices (all data)	R1 = 0.0673, wR2 = 0.0652
Absolute structure parameter	0.07(18)
Largest diff. peak and hole	0.47 and -0.21 e.Å <sup>-3</sup>

Table 2. Atomic coordinates ( $\times 10^4$ ) and equivalent isotropic displacement parameters ( $\text{Å}^2 \times 10^3$ ) for 2,9-di(anisyl)-1,10-phenanthroline.

U(eq) is defined as one third of the trace of the orthogonalized  $U^{ij}$  tensor.

	<b>x</b>	<b>y</b>	<b>z</b>	<b>U(eq)</b>
C(1)	4760(2)	5622(1)	-106(2)	32
C(2)	4683(2)	5331(2)	-1215(2)	41
C(3)	5384(2)	5347(2)	-1729(2)	42
C(4)	6175(2)	5646(2)	-1137(2)	38
C(5)	6198(2)	5921(1)	-34(2)	32
C(6)	6927(2)	5659(2)	-1614(2)	46
C(7)	7653(2)	5897(2)	-1005(2)	48
C(8)	6998(2)	6212(1)	621(2)	34
C(9)	7703(2)	6168(2)	130(2)	40
C(10)	8426(2)	6367(2)	822(2)	49
C(11)	8431(2)	6601(2)	1894(2)	46
C(12)	7719(2)	6673(2)	2308(2)	37
C(13)	4009(1)	5621(1)	465(2)	32
C(14)	4146(2)	6205(2)	1318(2)	37
C(15)	3451(2)	6210(2)	1857(2)	40
C(16)	2594(2)	5612(2)	1545(2)	37
C(17)	2446(2)	5026(2)	684(2)	38
C(18)	3146(2)	5035(2)	149(2)	35
C(19)	1987(2)	6073(2)	2985(2)	53
C(20)	7689(2)	6945(2)	3475(2)	38

C(21)	8404(2)	7258(2)	4183(2)	46
C(22)	8356(2)	7474(2)	5280(2)	48
C(23)	7570(2)	7364(2)	5692(2)	44
C(24)	6839(2)	7041(2)	4999(2)	44
C(25)	6903(2)	6848(2)	3906(2)	41
C(26)	8183(2)	7896(2)	7496(3)	67
N(1)	5498(1)	5911(1)	476(2)	32
N(2)	7018(1)	6477(1)	1681(2)	34
O(1)	1863(1)	5541(1)	2039(2)	46
O(2)	7444(1)	7545(1)	6766(2)	56
C(31)	9281(6)	9570(5)	1074(8)	78
Cl(31)	8703(2)	8544(2)	529(2)	69
Cl(32)	9954(3)	10285(3)	171(5)	128

Table 3. Bond lengths [Å] and angles [°] for 2,9-di(anisyl)-1,10-phenanthroline.

C(1)-C(2)	1.411(3)	C(11)-C(12)	1.409(3)
C(1)-C(13)	1.487(3)	C(11)-H(111)	0.927
C(1)-N(1)	1.329(3)	C(12)-C(20)	1.492(3)
C(2)-C(3)	1.366(4)	C(12)-N(2)	1.334(3)
C(2)-H(21)	0.935	C(13)-C(14)	1.383(3)
C(3)-C(4)	1.408(4)	C(13)-C(18)	1.393(3)
C(3)-H(31)	0.930	C(14)-C(15)	1.386(3)
C(4)-C(5)	1.405(3)	C(14)-H(141)	0.930
C(4)-C(6)	1.429(3)	C(15)-C(16)	1.388(3)
C(5)-C(8)	1.461(3)	C(15)-H(151)	0.923
C(5)-N(1)	1.366(3)	C(16)-C(17)	1.389(4)
C(6)-C(7)	1.343(4)	C(16)-O(1)	1.362(3)
C(6)-H(61)	0.946	C(17)-C(18)	1.380(3)
C(7)-C(9)	1.434(4)	C(17)-H(171)	0.936
C(7)-H(71)	0.937	C(18)-H(181)	0.938
C(8)-C(9)	1.409(3)	C(19)-O(1)	1.418(3)
C(8)-N(2)	1.351(3)	C(19)-H(191)	0.964
C(9)-C(10)	1.408(4)	C(19)-H(192)	0.975
C(10)-C(11)	1.351(4)	C(19)-H(193)	0.974
C(10)-H(101)	0.945	C(20)-C(21)	1.382(4)

C(20)-C(25)	1.403(3)	C(25)-H(251)	0.940
C(21)-C(22)	1.388(4)	C(26)-O(2)	1.427(4)
C(21)-H(211)	0.927	C(26)-H(261)	0.954
C(22)-C(23)	1.385(4)	C(26)-H(262)	0.981
C(22)-H(221)	0.949	C(26)-H(263)	0.984
C(23)-C(24)	1.392(4)	C(31)-Cl(31)	1.695(7)
C(23)-O(2)	1.374(3)	C(31)-Cl(32)	1.633(8)
C(24)-C(25)	1.376(4)	C(31)-H(311)	1.000
C(24)-H(241)	0.941	C(31)-H(312)	1.000
C(2)-C(1)-C(13)	120.7(2)	C(8)-C(9)-C(10)	116.5(2)
C(2)-C(1)-N(1)	122.4(2)	C(9)-C(10)-C(11)	120.5(2)
C(13)-C(1)-N(1)	116.88(18)	C(9)-C(10)-H(101)	118.9
C(1)-C(2)-C(3)	119.8(2)	C(11)-C(10)-H(101)	120.6
C(1)-C(2)-H(21)	120.1	C(10)-C(11)-C(12)	119.6(2)
C(3)-C(2)-H(21)	120.0	C(10)-C(11)-H(111)	120.7
C(2)-C(3)-C(4)	119.3(2)	C(12)-C(11)-H(111)	119.8
C(2)-C(3)-H(31)	119.6	C(11)-C(12)-C(20)	122.4(2)
C(4)-C(3)-H(31)	121.0	C(11)-C(12)-N(2)	121.5(2)
C(3)-C(4)-C(5)	117.3(2)	C(20)-C(12)-N(2)	116.0(2)
C(3)-C(4)-C(6)	122.3(2)	C(1)-C(13)-C(14)	121.0(2)
C(5)-C(4)-C(6)	120.4(2)	C(1)-C(13)-C(18)	120.8(2)
C(4)-C(5)-C(8)	119.1(2)	C(14)-C(13)-C(18)	118.1(2)
C(4)-C(5)-N(1)	123.2(2)	C(13)-C(14)-C(15)	121.6(2)
C(8)-C(5)-N(1)	117.6(2)	C(13)-C(14)-H(141)	118.1
C(4)-C(6)-C(7)	120.8(2)	C(15)-C(14)-H(141)	120.3
C(4)-C(6)-H(61)	119.8	C(14)-C(15)-C(16)	119.6(2)
C(7)-C(6)-H(61)	119.4	C(14)-C(15)-H(151)	120.7
C(6)-C(7)-C(9)	120.9(2)	C(16)-C(15)-H(151)	119.8
C(6)-C(7)-H(71)	120.5	C(15)-C(16)-C(17)	119.5(2)
C(9)-C(7)-H(71)	118.6	C(15)-C(16)-O(1)	124.5(2)
C(5)-C(8)-C(9)	118.2(2)	C(17)-C(16)-O(1)	116.0(2)
C(5)-C(8)-N(2)	119.0(2)	C(16)-C(17)-C(18)	120.2(2)
C(9)-C(8)-N(2)	122.8(2)	C(16)-C(17)-H(171)	119.9
C(7)-C(9)-C(8)	120.5(2)	C(18)-C(17)-H(171)	119.9
C(7)-C(9)-C(10)	122.9(2)	C(13)-C(18)-C(17)	121.0(2)

C(13)-C(18)-H(181)	119.2	C(23)-C(24)-H(241)	119.5
C(17)-C(18)-H(181)	119.8	C(25)-C(24)-H(241)	120.5
O(1)-C(19)-H(191)	109.9	C(20)-C(25)-C(24)	121.3(2)
O(1)-C(19)-H(192)	108.7	C(20)-C(25)-H(251)	119.3
H(191)-C(19)-H(192)	109.9	C(24)-C(25)-H(251)	119.4
O(1)-C(19)-H(193)	108.9	O(2)-C(26)-H(261)	108.5
H(191)-C(19)-H(193)	110.5	O(2)-C(26)-H(262)	111.3
H(192)-C(19)-H(193)	109.0	H(261)-C(26)-H(262)	109.0
C(12)-C(20)-C(21)	122.4(2)	O(2)-C(26)-H(263)	109.5
C(12)-C(20)-C(25)	119.9(2)	H(261)-C(26)-H(263)	108.8
C(21)-C(20)-C(25)	117.6(2)	H(262)-C(26)-H(263)	109.7
C(20)-C(21)-C(22)	121.8(2)	C(5)-N(1)-C(1)	117.88(18)
C(20)-C(21)-H(211)	119.6	C(8)-N(2)-C(12)	118.98(19)
C(22)-C(21)-H(211)	118.5	C(19)-O(1)-C(16)	117.5(2)
C(21)-C(22)-C(23)	119.6(2)	C(26)-O(2)-C(23)	117.5(2)
C(21)-C(22)-H(221)	119.3	Cl(31)-C(31)-Cl(32)	112.2(5)
C(23)-C(22)-H(221)	121.1	Cl(31)-C(31)-H(311)	107.9
C(22)-C(23)-C(24)	119.6(2)	Cl(32)-C(31)-H(311)	108.8
C(22)-C(23)-O(2)	124.6(2)	Cl(31)-C(31)-H(312)	109.2
C(24)-C(23)-O(2)	115.8(2)	Cl(32)-C(31)-H(312)	109.3
C(23)-C(24)-C(25)	120.1(2)	H(311)-C(31)-H(312)	109.5

**Crystal data and structure refinement for 6,6'-Bis(2-(4-(*N,N*-diphenylamino)phenyl)ethenyl)-2,2'-bipyridine.**

Table 1. Crystal data and structure refinement for 6,6'-Bis(2-(4-(*N,N*-diphenylamino)phenyl)ethenyl)-2,2'-bipyridine.

Identification code	ValC-K2Ligand_173k	
Empirical formula	C <sub>50</sub> H <sub>38</sub> N <sub>4</sub>	
Formula weight	694.88	
Temperature	173 K	
Wavelength	0.71073 Å	
Crystal system	Orthorhombic	
Space group	P b c a	
Unit cell dimensions	a = 9.0171(5) Å	α = 90°

	$b = 15.4471(8) \text{ \AA}$	$\beta = 90^\circ$
	$c = 26.8697(16) \text{ \AA}$	$\gamma = 90^\circ$
Volume	$3742.6(4) \text{ \AA}^3$	
Z	4	
Density (calculated)	$1.233 \text{ Mg/m}^3$	
Absorption coefficient	$0.072 \text{ mm}^{-1}$	
F(000)	1464	
Crystal size	$0.33 \times 0.25 \times 0.07 \text{ mm}^3$	
Theta range for data collection	$1.516$ to $25.360^\circ$ .	
Index ranges	$-10 \leq h \leq 10$ , $-13 \leq k \leq 18$ , $-31 \leq l \leq 32$	
Reflections collected	15084	
Independent reflections	3418 [R(int) = 0.093]	
Completeness to theta = $25.360^\circ$	99.5 %	
Absorption correction	Semi-empirical from equivalents	
Max. and min. transmission	0.99 and 0.98	
Refinement method	Full-matrix least-squares on $F^2$	
Data / restraints / parameters	2457 / 0 / 245	
Goodness-of-fit on $F^2$	1.0202	
Final R indices [ $I > 2\sigma(I)$ ]	$R1 = 0.1048$ , $wR2 = 0.1154$	
R indices (all data)	$R1 = 0.1303$ , $wR2 = 0.1333$	
Extinction coefficient	426.673	
Largest diff. peak and hole	$0.72$ and $-0.38 \text{ e.\AA}^{-3}$	

Table 2. Atomic coordinates ( $\times 10^4$ ) and equivalent isotropic displacement parameters ( $\text{\AA}^2 \times 10^3$ ) for 6,6'-Bis(2-(4-(*N,N*-diphenylamino)phenyl)ethenyl)-2,2'-bipyridine.

U(eq) is defined as one third of the trace of the orthogonalized  $U_{ij}$  tensor.

	<b>x</b>	<b>y</b>	<b>z</b>	<b>U(eq)</b>
N(1)	-391(4)	5723(2)	1877(1)	36
N(2)	-725(3)	1016(2)	223(1)	31
C(1)	-69(5)	6503(2)	1622(1)	34
C(2)	-660(4)	7288(2)	1775(2)	37
C(3)	-328(5)	8045(2)	1523(2)	40
C(4)	542(5)	8029(3)	1103(2)	50
C(5)	1121(6)	7243(3)	946(2)	50



C(6)	822(5)	6487(3)	1196(2)	41
C(7)	-296(4)	5701(2)	2409(1)	31
C(8)	-1213(4)	5152(2)	2677(1)	34
C(9)	-1134(5)	5128(3)	3194(2)	40
C(10)	-149(4)	5660(2)	3447(1)	35
C(11)	764(4)	6203(3)	3179(2)	38
C(12)	706(5)	6229(2)	2664(1)	36
C(13)	-541(4)	4930(2)	1616(1)	32
C(14)	-1481(4)	4894(2)	1196(1)	32
C(15)	-1623(4)	4130(2)	935(1)	31
C(16)	-822(4)	3389(2)	1062(1)	29
C(17)	115(4)	3435(2)	1482(1)	32
C(18)	227(4)	4190(2)	1750(1)	35
C(19)	-901(4)	2578(2)	782(1)	32
C(20)	-1977(4)	2325(2)	473(1)	32
C(21)	-1972(4)	1488(2)	207(1)	28
C(22)	-3226(4)	1222(2)	-50(1)	35
C(23)	-3193(4)	431(2)	-294(1)	36
C(24)	-1926(4)	-56(2)	-276(1)	32
C(25)	-706(4)	246(2)	-14(1)	28

Table 3. Bond lengths [ $\text{\AA}$ ] and angles [ $^\circ$ ] for 6,6'-Bis(2-(4-(*N,N*-diphenylamino)phenyl)ethenyl)-2,2'-bipyridine.

N(1)-C(1)	1.416(4)	C(4)-H(41)	0.946
N(1)-C(7)	1.430(4)	C(5)-C(6)	1.373(6)
N(1)-C(13)	1.418(4)	C(5)-H(51)	0.925
N(2)-C(21)	1.341(5)	C(6)-H(61)	0.927
N(2)-C(25)	1.349(4)	C(7)-C(8)	1.387(5)
C(1)-C(2)	1.387(5)	C(7)-C(12)	1.397(5)
C(1)-C(6)	1.400(6)	C(8)-C(9)	1.389(5)
C(2)-C(3)	1.383(5)	C(8)-H(81)	0.939
C(2)-H(21)	0.936	C(9)-C(10)	1.388(6)
C(3)-C(4)	1.375(6)	C(9)-H(91)	0.937
C(3)-H(31)	0.952	C(10)-C(11)	1.379(5)
C(4)-C(5)	1.387(7)	C(10)-H(101)	0.941

C(11)-C(12)	1.384(5)	C(18)-H(181)	0.929
C(11)-H(111)	0.944	C(19)-C(20)	1.337(5)
C(12)-H(121)	0.935	C(19)-H(191)	0.943
C(13)-C(14)	1.413(5)	C(20)-C(21)	1.477(5)
C(13)-C(18)	1.385(5)	C(20)-H(201)	0.949
C(14)-C(15)	1.377(5)	C(21)-C(22)	1.387(5)
C(14)-H(141)	0.945	C(22)-C(23)	1.386(5)
C(15)-C(16)	1.396(5)	C(22)-H(221)	0.934
C(15)-H(151)	0.929	C(23)-C(24)	1.369(5)
C(16)-C(17)	1.412(5)	C(23)-H(231)	0.934
C(16)-C(19)	1.461(5)	C(24)-C(25)	1.387(5)
C(17)-C(18)	1.373(5)	C(24)-H(241)	0.941
C(17)-H(171)	0.937	C(25)-C(25)#1	1.486(7)
C(1)-N(1)-C(7)	119.4(3)	N(1)-C(7)-C(8)	119.9(3)
C(1)-N(1)-C(13)	120.9(3)	N(1)-C(7)-C(12)	121.0(3)
C(7)-N(1)-C(13)	118.6(3)	C(8)-C(7)-C(12)	119.1(3)
C(21)-N(2)-C(25)	118.3(3)	C(7)-C(8)-C(9)	120.3(3)
N(1)-C(1)-C(2)	121.4(3)	C(7)-C(8)-H(81)	119.2
N(1)-C(1)-C(6)	120.0(3)	C(9)-C(8)-H(81)	120.4
C(2)-C(1)-C(6)	118.6(3)	C(8)-C(9)-C(10)	120.4(4)
C(1)-C(2)-C(3)	120.7(4)	C(8)-C(9)-H(91)	119.9
C(1)-C(2)-H(21)	119.1	C(10)-C(9)-H(91)	119.6
C(3)-C(2)-H(21)	120.2	C(9)-C(10)-C(11)	119.1(3)
C(2)-C(3)-C(4)	120.7(4)	C(9)-C(10)-H(101)	120.4
C(2)-C(3)-H(31)	118.2	C(11)-C(10)-H(101)	120.5
C(4)-C(3)-H(31)	121.1	C(10)-C(11)-C(12)	121.1(4)
C(3)-C(4)-C(5)	118.6(4)	C(10)-C(11)-H(111)	119.2
C(3)-C(4)-H(41)	120.5	C(12)-C(11)-H(111)	119.7
C(5)-C(4)-H(41)	120.8	C(7)-C(12)-C(11)	119.9(3)
C(4)-C(5)-C(6)	121.5(4)	C(7)-C(12)-H(121)	119.4
C(4)-C(5)-H(51)	119.7	C(11)-C(12)-H(121)	120.7
C(6)-C(5)-H(51)	118.9	N(1)-C(13)-C(14)	119.2(3)
C(1)-C(6)-C(5)	119.8(4)	N(1)-C(13)-C(18)	122.5(3)
C(1)-C(6)-H(61)	120.1	C(14)-C(13)-C(18)	118.3(3)
C(5)-C(6)-H(61)	120.1	C(13)-C(14)-C(15)	119.7(3)

C(13)-C(14)-H(141)	119.8	C(19)-C(20)-H(201)	118.1
C(15)-C(14)-H(141)	120.5	C(21)-C(20)-H(201)	118.2
C(14)-C(15)-C(16)	122.1(3)	C(20)-C(21)-N(2)	117.5(3)
C(14)-C(15)-H(151)	119.3	C(20)-C(21)-C(22)	119.9(3)
C(16)-C(15)-H(151)	118.6	N(2)-C(21)-C(22)	122.6(3)
C(15)-C(16)-C(17)	117.5(3)	C(21)-C(22)-C(23)	118.6(3)
C(15)-C(16)-C(19)	123.6(3)	C(21)-C(22)-H(221)	120.2
C(17)-C(16)-C(19)	118.9(3)	C(23)-C(22)-H(221)	121.2
C(16)-C(17)-C(18)	120.4(3)	C(22)-C(23)-C(24)	119.0(3)
C(16)-C(17)-H(171)	120.2	C(22)-C(23)-H(231)	119.8
C(18)-C(17)-H(171)	119.4	C(24)-C(23)-H(231)	121.2
C(13)-C(18)-C(17)	121.9(3)	C(23)-C(24)-C(25)	119.6(3)
C(13)-C(18)-H(181)	118.0	C(23)-C(24)-H(241)	120.6
C(17)-C(18)-H(181)	120.1	C(25)-C(24)-H(241)	119.8
C(16)-C(19)-C(20)	127.3(3)	C(25)#1-C(25)-C(24)	122.2(4)
C(16)-C(19)-H(191)	115.9	C(25)#1-C(25)-N(2)	116.0(4)
C(20)-C(19)-H(191)	116.8	C(24)-C(25)-N(2)	121.8(3)
C(19)-C(20)-C(21)	123.7(3)		

Symmetry transformations used to generate equivalent atoms:

#1 -x,-y,-z

**Crystal data and structure refinement for Bis[6,6'-Bis(2-(4-(*N,N*-diphenylamino)phenyl)ethenyl)-2,2'-bipyridine]copper(I) hexafluorophosphate.**

Table 1. Crystal data and structure refinement for Bis[6,6'-Bis(2-(4-(*N,N*-diphenylamino)phenyl)ethenyl)-2,2'-bipyridine]copper(I) hexafluorophosphate.

Identification code	ValC-K2Komplex	
Empirical formula	C104 H86 Cu1 F6 N8 O1 P1	
Formula weight	1672.39	
Temperature	173 K	
Wavelength	0.71073 Å	
Crystal system	Tetragonal	
Space group	P 4/n	
Unit cell dimensions	a = 15.1300(10) Å	$\alpha = 90^\circ$

	$b = 15.1300(10) \text{ \AA}$	$\beta = 90^\circ$
	$c = 18.2421(9) \text{ \AA}$	$\gamma = 90^\circ$
Volume	$4175.9(4) \text{ \AA}^3$	
Z	2	
Density (calculated)	$1.330 \text{ Mg/m}^3$	
Absorption coefficient	$0.351 \text{ mm}^{-1}$	
F(000)	1744.000	
Crystal size	$0.52 \times 0.28 \times 0.04 \text{ mm}^3$	
Theta range for data collection	$3.211$ to $27.007^\circ$ .	
Index ranges	$-16 \leq h \leq 17$ , $-19 \leq k \leq 19$ , $-23 \leq l \leq 23$	
Reflections collected	48153	
Independent reflections	4581 [R(int) = 0.072]	
Completeness to theta = $27.007^\circ$	99.7 %	
Absorption correction	Semi-empirical from equivalents	
Max. and min. transmission	0.99 and 0.90	
Refinement method	Full-matrix least-squares on $F^2$	
Data / restraints / parameters	3433 / 551 / 324	
Goodness-of-fit on $F^2$	1.1596	
Final R indices [I > 2 $\sigma$ (I)]	R1 = 0.0419, wR2 = 0.0425	
R indices (all data)	R1 = 0.0593, wR2 = 0.0487	
Largest diff. peak and hole	0.51 and -0.50 e. $\text{\AA}^{-3}$	

Table 2. Atomic coordinates ( $\times 10^4$ ) and equivalent isotropic displacement parameters ( $\text{\AA}^2 \times 10^3$ ) for Bis[6,6'-Bis(2-(4-(*N,N*-diphenylamino)phenyl)ethenyl)-2,2'-bipyridine]copper(I) hexafluorophosphate.

U(eq) is defined as one third of the trace of the orthogonalized Uij tensor.

	<b>x</b>	<b>y</b>	<b>z</b>	<b>U(eq)</b>
Cu(1)	2500	7500	5000	26
N(1)	-414(1)	4896(1)	8041(1)	38
N(2)	1683(1)	7191(1)	4148(1)	26
C(1)	-1197(1)	4625(1)	8394(1)	35
C(2)	-1203(1)	3839(1)	8794(1)	39
C(3)	-1970(2)	3578(2)	9144(1)	51
C(4)	-2727(1)	4071(2)	9102(1)	59

C(5)	-2721(1)	4852(2)	8713(1)	56
C(6)	-1955(1)	5134(2)	8360(1)	47
C(7)	416(1)	4690(1)	8374(1)	33
C(8)	1077(1)	4276(1)	7978(1)	37
C(9)	1871(1)	4065(1)	8311(1)	42
C(10)	2011(1)	4264(1)	9042(1)	45
C(11)	1356(1)	4679(2)	9437(1)	46
C(12)	560(1)	4898(1)	9106(1)	38
C(13)	-420(1)	5313(1)	7347(1)	32
C(14)	-1057(1)	5123(1)	6817(1)	36
C(15)	-1004(1)	5505(1)	6127(1)	36
C(16)	-319(1)	6071(1)	5941(1)	33
C(17)	290(1)	6290(1)	6491(1)	35
C(18)	242(1)	5917(1)	7178(1)	35
C(19)	-197(1)	6388(1)	5186(1)	34
C(20)	568(1)	6696(1)	4946(1)	35
C(21)	831(1)	6963(1)	4211(1)	29
C(22)	268(1)	6963(1)	3597(1)	35
C(23)	621(1)	7168(1)	2923(1)	36
C(24)	1503(1)	7368(1)	2854(1)	31
C(25)	2028(1)	7382(1)	3482(1)	26
P(1)	2500	2500	6212(1)	38
F(1)	1963(2)	3392(2)	6213(3)	102
F(3)	1873(4)	2160(4)	5617(4)	101
F(4)	3107(4)	2844(6)	6844(4)	112
F(5)	2500	2500	7032(8)	72
F(6)	2500	2500	5347(8)	80
C(51)	2390(20)	2823(8)	3187(5)	67
C(52)	2536(14)	2121(5)	2586(4)	73
O(53)	2500(1)	2500(1)	1905(2)	85
C(54)	2482(17)	1965(6)	1277(5)	112
C(55)	2500	2500	602(5)	120
C(60)	2500	2500	3973(9)	75
C(61)	2390(20)	2823(8)	3187(5)	67
O(62)	2536(14)	2121(5)	2586(4)	73
C(63)	2500(1)	2500(1)	1905(2)	85

C(64) 2482(17) 1965(6) 1277(5) 112  
 Table 3. Bond lengths [Å] and angles [°] for Bis[6,6'-Bis(2-(4-(*N,N*-diphenylamino)phenyl)ethenyl)-2,2'-bipyridine]copper(I) hexafluorophosphate.

Cu(1)-N(2)	2.0401(13)	C(13)-C(18)	1.390(3)
Cu(1)-N(2)#1	2.0401(13)	C(14)-C(15)	1.387(2)
Cu(1)-N(2)#2	2.0401(13)	C(14)-H(141)	0.955
Cu(1)-N(2)#3	2.0401(13)	C(15)-C(16)	1.387(2)
N(1)-C(1)	1.408(2)	C(15)-H(151)	0.941
N(1)-C(7)	1.429(2)	C(16)-C(17)	1.402(2)
N(1)-C(13)	1.416(2)	C(16)-C(19)	1.469(2)
N(2)-C(21)	1.339(2)	C(17)-C(18)	1.376(2)
N(2)-C(25)	1.3540(19)	C(17)-H(171)	0.973
C(1)-C(2)	1.394(3)	C(18)-H(181)	0.954
C(1)-C(6)	1.384(3)	C(19)-C(20)	1.323(3)
C(2)-C(3)	1.382(3)	C(19)-H(191)	0.965
C(2)-H(21)	0.950	C(20)-C(21)	1.456(2)
C(3)-C(4)	1.370(4)	C(20)-H(201)	0.972
C(3)-H(31)	0.940	C(21)-C(22)	1.408(2)
C(4)-C(5)	1.378(4)	C(22)-C(23)	1.376(2)
C(4)-H(41)	0.954	C(22)-H(221)	0.972
C(5)-C(6)	1.393(3)	C(23)-C(24)	1.374(3)
C(5)-H(51)	0.974	C(23)-H(231)	0.940
C(6)-H(61)	0.952	C(24)-C(25)	1.394(2)
C(7)-C(8)	1.383(3)	C(24)-H(241)	0.948
C(7)-C(12)	1.389(2)	C(25)-C(25)#1	1.473(3)
C(8)-C(9)	1.385(3)	P(1)-F(1)#4	1.574(2)
C(8)-H(81)	0.968	P(1)-F(1)#5	1.574(2)
C(9)-C(10)	1.384(3)	P(1)-F(1)#6	1.574(2)
C(9)-H(91)	0.961	P(1)-F(4)#6	1.564(5)
C(10)-C(11)	1.377(3)	P(1)-F(4)#5	1.564(5)
C(10)-H(101)	0.968	P(1)-F(4)#4	1.564(5)
C(11)-C(12)	1.388(3)	P(1)-F(3)#5	1.531(4)
C(11)-H(111)	0.942	P(1)-F(3)#4	1.531(4)
C(12)-H(121)	0.975	P(1)-F(3)#6	1.531(4)
C(13)-C(14)	1.394(2)	P(1)-F(1)	1.574(2)

P(1)-F(3)	1.531(4)	C(55)-H(553)	0.970
P(1)-F(4)	1.564(5)	C(60)-C(61)	1.524(15)
P(1)-F(5)	1.495(15)	C(60)-H(601)	0.969
P(1)-F(6)	1.578(15)	C(60)-H(602)	0.970
C(51)-C(52)	1.543(10)	C(60)-H(603)	0.970
C(51)-H(511)	0.971	C(61)-O(62)	1.543(10)
C(51)-H(512)	0.952	C(61)-H(511)	0.971
C(51)-H(513)	0.989	C(61)-H(512)	0.952
C(52)-H(521)	0.974	C(61)-H(513)	0.989
C(52)-H(522)	0.964	O(62)-H(521)	0.974
C(52)-O(53)	1.369(8)	O(62)-H(522)	0.964
O(53)-C(54)	1.403(10)	O(62)-C(63)	1.369(8)
O(53)-H(631)	0.970	C(63)-C(64)	1.403(10)
O(53)-H(632)	0.970	C(63)-H(631)	0.970
C(54)-C(55)	1.474(11)	C(63)-H(632)	0.970
C(54)-H(541)	0.970	C(64)-H(541)	0.970
C(54)-H(542)	0.968	C(64)-H(542)	0.968
C(55)-H(551)	0.970	C(64)-H(641)	0.975
C(55)-H(552)	0.970		
N(2)#1-Cu(1)-N(2)#2	125.49(4)	C(1)-C(2)-H(21)	119.1
N(2)#1-Cu(1)-N(2)#3	125.49(4)	C(3)-C(2)-H(21)	121.4
N(2)#2-Cu(1)-N(2)#3	80.73(7)	C(2)-C(3)-C(4)	121.3(2)
N(2)#1-Cu(1)-N(2)	80.73(7)	C(2)-C(3)-H(31)	118.3
N(2)#2-Cu(1)-N(2)	125.49(4)	C(4)-C(3)-H(31)	120.3
N(2)#3-Cu(1)-N(2)	125.49(4)	C(3)-C(4)-C(5)	119.39(19)
C(1)-N(1)-C(7)	118.78(14)	C(3)-C(4)-H(41)	119.7
C(1)-N(1)-C(13)	122.25(14)	C(5)-C(4)-H(41)	120.9
C(7)-N(1)-C(13)	118.84(14)	C(4)-C(5)-C(6)	120.4(2)
Cu(1)-N(2)-C(21)	125.22(10)	C(4)-C(5)-H(51)	120.9
Cu(1)-N(2)-C(25)	113.70(11)	C(6)-C(5)-H(51)	118.8
C(21)-N(2)-C(25)	120.17(13)	C(5)-C(6)-C(1)	119.9(2)
N(1)-C(1)-C(2)	119.55(17)	C(5)-C(6)-H(61)	120.7
N(1)-C(1)-C(6)	120.96(17)	C(1)-C(6)-H(61)	119.4
C(2)-C(1)-C(6)	119.49(17)	N(1)-C(7)-C(8)	120.82(16)
C(1)-C(2)-C(3)	119.4(2)	N(1)-C(7)-C(12)	119.78(16)

C(8)-C(7)-C(12)	119.39(17)	C(20)-C(19)-H(191)	120.1
C(7)-C(8)-C(9)	120.18(18)	C(19)-C(20)-C(21)	129.94(16)
C(7)-C(8)-H(81)	119.4	C(19)-C(20)-H(201)	116.0
C(9)-C(8)-H(81)	120.5	C(21)-C(20)-H(201)	114.0
C(8)-C(9)-C(10)	120.41(19)	C(20)-C(21)-N(2)	114.43(14)
C(8)-C(9)-H(91)	120.2	C(20)-C(21)-C(22)	124.55(16)
C(10)-C(9)-H(91)	119.4	N(2)-C(21)-C(22)	120.99(15)
C(9)-C(10)-C(11)	119.53(18)	C(21)-C(22)-C(23)	118.38(17)
C(9)-C(10)-H(101)	119.7	C(21)-C(22)-H(221)	119.9
C(11)-C(10)-H(101)	120.7	C(23)-C(22)-H(221)	121.7
C(10)-C(11)-C(12)	120.39(19)	C(22)-C(23)-C(24)	120.60(15)
C(10)-C(11)-H(111)	120.8	C(22)-C(23)-H(231)	119.2
C(12)-C(11)-H(111)	118.8	C(24)-C(23)-H(231)	120.2
C(7)-C(12)-C(11)	120.08(19)	C(23)-C(24)-C(25)	118.76(15)
C(7)-C(12)-H(121)	119.2	C(23)-C(24)-H(241)	120.8
C(11)-C(12)-H(121)	120.7	C(25)-C(24)-H(241)	120.4
N(1)-C(13)-C(14)	122.17(16)	C(25)#1-C(25)-C(24)	123.81(10)
N(1)-C(13)-C(18)	119.13(15)	C(25)#1-C(25)-N(2)	115.17(9)
C(14)-C(13)-C(18)	118.68(15)	C(24)-C(25)-N(2)	121.00(16)
C(13)-C(14)-C(15)	120.21(16)	F(1)#4-P(1)-F(1)#5	90.000
C(13)-C(14)-H(141)	119.8	F(1)#4-P(1)-F(1)#6	90.000(7)
C(15)-C(14)-H(141)	120.0	F(1)#5-P(1)-F(1)#6	179.9(4)
C(14)-C(15)-C(16)	121.48(16)	F(1)#5-P(1)-F(4)#6	88.9(4)
C(14)-C(15)-H(151)	120.2	F(1)#6-P(1)-F(4)#6	91.0(3)
C(16)-C(15)-H(151)	118.3	F(1)#5-P(1)-F(4)#5	91.0(3)
C(15)-C(16)-C(17)	117.48(15)	F(1)#6-P(1)-F(4)#5	88.9(4)
C(15)-C(16)-C(19)	121.65(15)	F(4)#6-P(1)-F(4)#5	84.9(7)
C(17)-C(16)-C(19)	120.75(15)	F(1)#4-P(1)-F(4)#4	91.0(3)
C(16)-C(17)-C(18)	121.35(16)	F(1)#5-P(1)-F(3)#5	88.2(3)
C(16)-C(17)-H(171)	119.7	F(1)#6-P(1)-F(3)#5	91.9(3)
C(18)-C(17)-H(171)	119.0	F(4)#6-P(1)-F(3)#5	92.7(4)
C(13)-C(18)-C(17)	120.62(16)	F(4)#5-P(1)-F(3)#5	177.5(5)
C(13)-C(18)-H(181)	120.0	F(1)#4-P(1)-F(3)#4	88.2(3)
C(17)-C(18)-H(181)	119.3	F(1)#5-P(1)-F(3)#6	91.9(3)
C(16)-C(19)-C(20)	122.34(16)	F(1)#6-P(1)-F(3)#6	88.2(3)
C(16)-C(19)-H(191)	117.6	F(4)#6-P(1)-F(3)#6	177.5(5)



F(4)#5-P(1)-F(3)#6	92.7(4)	H(521)-C(52)-H(522)	109.6
F(1)#4-P(1)-F(1)	179.9(4)	H(521)-C(52)-O(53)	108.6
F(1)#5-P(1)-F(1)	90.000	H(522)-C(52)-O(53)	109.2
F(1)#6-P(1)-F(1)	90.000(7)	C(54)-O(53)-C(52)	120.0(5)
F(1)#4-P(1)-F(3)	91.9(3)	O(53)-C(54)-C(55)	111.4(7)
F(1)#4-P(1)-F(4)	88.9(4)	O(53)-C(54)-H(541)	109.2
F(1)#4-P(1)-F(5)	90.0(2)	O(53)-C(54)-H(542)	109.4
F(1)#5-P(1)-F(5)	90.0(2)	C(55)-C(54)-H(541)	108.5
F(1)#6-P(1)-F(5)	90.0(2)	C(55)-C(54)-H(542)	108.7
F(1)#4-P(1)-F(6)	90.0(2)	H(541)-C(54)-H(542)	109.6
F(1)#5-P(1)-F(6)	90.0(2)	C(54)-C(55)-H(551)	109.5
F(1)#6-P(1)-F(6)	90.0(2)	C(54)-C(55)-H(552)	109.4
F(3)#5-P(1)-F(3)#6	89.7(7)	C(54)-C(55)-H(553)	109.4
F(4)#4-P(1)-F(1)	88.9(4)	H(551)-C(55)-H(552)	109.5
F(3)#4-P(1)-F(1)	91.9(3)	H(551)-C(55)-H(553)	109.5
F(4)#4-P(1)-F(3)	92.7(4)	H(552)-C(55)-H(553)	109.5
F(3)#4-P(1)-F(3)	89.7(7)	C(61)-C(60)-H(601)	109.5
F(1)-P(1)-F(3)	88.2(3)	C(61)-C(60)-H(602)	108.6
F(4)#4-P(1)-F(4)	84.9(7)	H(601)-C(60)-H(602)	109.6
F(3)#4-P(1)-F(4)	92.7(4)	C(61)-C(60)-H(603)	110.1
F(1)-P(1)-F(4)	91.0(3)	H(601)-C(60)-H(603)	109.6
F(1)-P(1)-F(5)	90.0(2)	H(602)-C(60)-H(603)	109.5
F(1)-P(1)-F(6)	90.0(2)	C(60)-C(61)-O(62)	115.6(6)
F(3)-P(1)-F(4)	177.5(5)	C(60)-C(61)-H(512)	102.4
F(5)-P(1)-F(6)	179.993	C(60)-C(61)-H(513)	110.0
F(3)#6-F(3)-F(3)#5	90.000	O(62)-C(61)-H(511)	109.3
F(4)#5-F(4)-F(4)#6	90.000	O(62)-C(61)-H(512)	110.9
C(52)-C(51)-H(511)	109.3	H(511)-C(61)-H(512)	111.0
C(52)-C(51)-H(512)	110.9	O(62)-C(61)-H(513)	108.3
C(52)-C(51)-H(513)	108.3	H(511)-C(61)-H(513)	107.9
H(511)-C(51)-H(512)	111.0	H(512)-C(61)-H(513)	109.4
H(511)-C(51)-H(513)	107.9	C(61)-O(62)-C(63)	110.6(5)
H(512)-C(51)-H(513)	109.4	C(64)-C(63)-H(631)	106.7
C(51)-C(52)-H(521)	108.4	C(64)-C(63)-H(632)	106.6
C(51)-C(52)-H(522)	110.4	H(631)-C(63)-H(632)	109.4
C(51)-C(52)-O(53)	110.6(5)	C(64)-C(63)-O(62)	120.0(5)

H(631)-C(63)-O(62)	107.1
H(632)-C(63)-O(62)	106.7
C(63)-C(64)-H(541)	109.2
C(63)-C(64)-H(542)	109.4
C(63)-C(64)-H(641)	109.5
H(541)-C(64)-H(542)	109.6
H(541)-C(64)-H(641)	112.6
H(542)-C(64)-H(641)	106.6

Symmetry transformations used to generate equivalent atoms:

#1  $-x+1/2, -y+3/2, z$  #2  $-y+1, x+1/2, -z+1$

#3  $y-1/2, -x+1, -z+1$

#4  $-x+1/2, -y+1/2, z$  #5  $-y+1/2, x, z$  #6  $y, -x+1/2, z$

## Valérie Chaurin

Address:	ZI Saint Severin 28220 Cloyes sur le Loir France	Date of Birth:	3rd October 1978
		Nationality:	French
		Marital Status:	Single
Email:	chaurin_valerie@yahoo.fr		

### Education

2003-2007: PhD in chemistry with Prof. Edwin Constable, University of Basel, Basel, Switzerland. "*Multifunctional oligopyridines for application in biological and materials chemistry*".

2002-2003: DEA in Molecular Chemistry (French equivalent of master's degree, specialising in organic chemistry), University Rennes I, Rennes, France.

2001-2002: Licence and Maitrise, Chemistry (French equivalent of BSc Degree), University Rennes I, Rennes, France.

### Training and Work Experience

2006-2007: Mentoring program "women in industry", NOVARTIS / University of Basel, Basel, Switzerland.

Mar-Sept 2003: Industrial experience, organic chemistry, **BAYER CROPSCIENCE**, Frankfurt, Germany.  
*Total synthesis of a new herbicide. Investigation of new structures for improved selectivity.*

Sep 2002-Feb 2003: Project work in organometallic chemistry (Prof. Pierre Dixneuf), University of Rennes I, Rennes, France.  
*Synthesis of innovative Ruthenium complexes for heavy- metal trapping.*

Apr-Aug 2002: Industrial experience, combinatorial chemistry, **MERCK AG**, Darmstadt, Germany.  
*Parallel synthesis in medicinal chemistry; Petasis reaction, Suzuki coupling, Acylation.*

Jun-Sep 2001: Industrial experience, organometallic chemistry, **BASF AG**, Ludwigshafen, Germany. *Synthesis of Phosphorus ligands.*

## Skills

Languages: French (mother tongue), English (fluent), German (fluent)

Computing: MS Office Suite, Origin, SciFinder, ISIS Draw, Beilstein, ChemOffice, MestRe-C

Driving licence: Category B

## Publications

### **The aryl-phen and phen-phen embraces – new supramolecular motifs.**

Edwin C. Constable, Valérie Chaurin, Catherine E. Housecroft, Markus Neuburger, Silvia Schaffner, *CrystEngComm*, **2008**, *10*, 1063-1069.

### **Quantification of single-stranded nucleic acid and oligonucleotide interactions with metal ions by affinity capillary electrophoresis Part II.**

Alexandra R. Stettler, Valérie Chaurin, Edwin C. Constable, Catherine E. Housecroft, Maria A. Schwarz, *Electrophoreses*, **2008**, *29*, 3342-3348.

### **Quantification of single-stranded nucleic acid and oligonucleotide interactions with metal ions by affinity capillary electrophoresis Part I.**

Alexandra R. Stettler, Valérie Chaurin, Edwin C. Constable, Catherine E. Housecroft, Maria A. Schwarz, *Journal of Biological Inorganic Chemistry*, **2007**, *12*, 194-203.

### **What is the coordination number of copper (II) in metallosupramolecular chemistry?**

Valérie Chaurin, Edwin C. Constable, Catherine E. Housecroft, *New Journal of Chemistry*, **2006**, *30*, 1740-1744.

### **Copper Complex-Assisted DNA Hybridization.**

Gapian Bianké, Valérie Chaurin, Maxim Egorov, Jacques Lebreton, Catherine E. Housecroft, Edwin C. Constable, Robert Häner, *Bioconjugate Chemistry*, **2006**, *17*, 1441-1446.

### **In-Strand Metallated Nucleic Acids – Novel Bioinorganic Constructs.**

Edwin C. Constable, Valérie Chaurin, Catherine E. Housecroft, Amina Wirth, *Chimia*, **2005**, *59*, 832-835.

## **Oral Presentations**

- Aug 2006: 1st European Chemistry Congress, Budapest, Hungary.  
*Use of Oligonucleotide-Metal Conjugates for the detection of DNA.*
- Feb 2006: Swiss Young Chemists' Association Snow Symposium, Grindelwald, Switzerland.  
*Use of Oligonucleotide-Metal Conjugates for the detection of DNA.*
- Oct 2005: Swiss Chemical Society Fall Meeting 2005, Lausanne, Switzerland.  
*Use of Oligonucleotide-Metal Conjugates for the detection of DNA.*

## **Posters**

- Aug 2006: 1st European Chemistry Congress, Budapest, Hungary.  
*Syntheses and spectroscopic studies of a novel Cu(I) complex with a new triarylamine 2,2' – bipyridine ligand.*
- Aug 2006: 1st European Chemistry Congress, Budapest, Hungary.  
*Use of Oligonucleotide-Metal Conjugates for the detection of DNA.*
- Oct 2005: Swiss Chemical Society Fall Meeting 2005, Lausanne, Switzerland.  
*Use of Oligonucleotide-Metal Conjugates for the detection of DNA.*
- Aug 2005: Congrès SFC Eurochem 2005, Nancy, France.  
*Oligonucleotide-Arrays: Use of Oligonucleotide-Metal Conjugates for the detection of DNA*
- Oct 2004: Swiss Chemical Society Fall Meeting 2004, Lausanne, Switzerland.  
*Cooperative Stabilization of Nucleic Acid Duplex mediated by Metal Coordinating Ligand Complexes, Conjugated to Oligonucleotides.*

